Processes and mechanisms of slow mass movement in a small catchment in wearable, n. England

Daniel Nial Mills Donoghue

Processes and Mechanisms of Slow Mass Movement in a small catchment in Weardale, N. England

A thesis presented for the degree of

Doctor of Philosophy

by

Daniel Nial Mills Donoghue

University of Durham
Department of Geography
July 1988

To Mum and Dad

A colour infrared aerial image of the study area

When you can measure what you are speaking about and express it in numbers, you know something about it; but when you cannot express it in numbers, your knowledge is of a meager, unsatisfactory kind. (Attr.) Lord Kelvin 1824-1907

DECLARATION

The work contained in this thesis has not been submitted elsewhere for any other degree or qualification and that unless otherwise referenced it is the author's own work.

STATEMENT OF COPYRIGHT

ACKNOWLEDGEMENTS

Many people gave help and encouragement during the preparation of this thesis.

From the Department of Geography: Ewan Anderson, Francis Bell, Marlene Crichton, Dave Cowton, Nicholas Cox, Ian Dennison, Joan Dorril, Ian Evans, Andrew Hudspeth and Simon Hook.

From the Department of Geological Engineering: Alan Swan and the late Roy Taylor.

I am very grateful to all those mentioned for technical and practical assistance. Special thanks go to Karen Bell for expertly typing the manuscript, Elizabeth Roberts for cartographic assistance, Khalil Rashidian for many valuable discussions and Charles Donoghue for help with fieldwork. I, however, not they, am responsible for what is written.

LIST OF FIGURES

LIST OF TABLES

Abstract

This thesis investigates sediment transport by slow mass movement within a small upland catchment area near Stanhope in Weardale, N. England. In the field, emphasis is placed on measurements of the rate and spatial distribution of mass movement; in the laboratory, a possible mechanism for slow movement has been investigated in several controlled experiments.

A review of the literature on slow mass movement processes indicates that there is considerable confusion over terminology. Terms such as **creep**, **slow mass flow** and **soil slip** imply that the mechanism of movement is known, whereas they are usually intended to be descriptive. An alternative classification of movement is suggested which separates description, knowledge of mechanism and knowledge of the domain in which a process operates. The term **slow mass movement** (S.M.M) is used throughout this thesis to refer to downslope displacement of soil particles at a rate expressed in mm^2/yr but whose mechanism of movement is not necessarily known.

A fieldwork programme was established to measure superficial slow mass movement rates in an upland catchment area for a period of two years. Data were recorded from seventy $1m^2$ measurement plots at monthly intervals. Each plot contained four instruments recording mass movement, thus allowing comparison within as well as between plots. The experimental design allows analysis of the effects of slope angle, vegetation type and soil texture on movement patterns and rates. The general

aim is to develop an understanding of how S.M.M. relates to physical and ecological variables in an upland catchment area and to assess its importance as an erosional process.

The instruments used are techniques, or modifications of techniques which have been described and used successfully by several previous researchers. These include Anderson's Tubes, Anderson's Inclinometer Pegs and Young's Pits. Measurements were also taken of water table levels and of the shear strength of soils at all plots at regular intervals in order to assess how the mechanical properties of soils may change in situ, over short time periods. These changes are related to the temporal patterns of S.M.M.

Associated with rapid mass movements such as landslides and mudflows are slowly deforming soil masses. Several slopes within the catchment area appear to be exhibiting slow deformation. The mechanism of this process has been analysed by simulating the normal and shear forces imposed upon the soil mass in a stress-controlled, undrained, direct shear test. From this test the value of the yield stress of the soil can be derived: this is the maximum shear stress the soil can withstand without undergoing continuous deformation. By comparing the yield stress with the predicted shear stress occurring in a natural slope it is possible to determine, according to a slope stability equation, whether continuous deformation could occur and at what rate it could proceed.

The apparatus was used to determine the contribution that the natural soil structure and plant rootlets make towards strength during slow deformation. Previous analyses have measured either root tensile strength or root permeated soil shear strength. Neither of these techniques is suitable because in the former case the frictional and apparent

cohesive strengths of the soil are ignored and in the latter case the forces imposed during testing far exceed those actually encountered in the field.

The creep-shear test allows the tensile and shear components of strength to be combined with realistic shear stresses because the slow rates of strain which occur during testing allow roots to stretch along the zone of failure causing a tensile stress to build up in the roots, thus increasing the apparent cohesion of the soil.

The research described in this thesis concentrates on substantiating and amending previous ideas on the rate of slow mass movement, its temporal persistence and on variables which control its action. The investigation is based upon both empirical and theoretical methods with field observations being compared with the results from laboratory experiments and also with theoretical ideas being analysed using data collected from a field experiment.

Chapter 1

Introduction

Contents

1.1 Introduction

Soil particles on hillslopes are constantly subjected to electrochemical and mechanical stresses which, under the constant force of gravity, tend to induce downslope displacement. This thesis investigates the physical processes of slow mass displacement of soil particles on natural hillslopes. Slope failure processes are not considered in detail except where slow mass movement precedes rapid failure. The distinction between *slow* and *rapid* mass movement is vague since few studies have related measured movement rates to movement mechanism. However, slow mass movement measurements from hillslope soils have commonly been obtained by recording observations over several years (Anderson 1977; Ivernova 1964; Young 1978).

Generally speaking, displacement or translation of material from any given point in a soil mass rarely exceeds 50 mm per year and is usually considerably less. Such linear rates contrast with observed rates of landslide, rockfall, mud flow and debris flow events which are commonly an order of magnitude greater (Saunders and Young 1983).

Slow movement of materials, particularly crystalline solids, is often termed *creep*. In the engineering literature the term *creep* refers specifically to time dependent crystalline deformation (Feltham 1976). In the earth sciences such processes have been used to describe the behaviour of rock, snow and ice (Haefeli 1965; Weertman 1957). The term *creep* is avoided here as a descriptive term for slow mass movement of superficial soils since it implies a pattern of behaviour that has never been demonstrated for hillslope soils.

Another basic distinction must be made between superficial movement and that which occurs at depths beyond the influence of seasonal

climatic fluctuation (Terzaghi 1953). Such a simple division may not always exist since groundwater fluctuations may cause seasonal variations in pore water pressures deep within soil masses. This thesis, however, only considers superficial soil masses with a maximum depth to bedrock of 2.5m and so no comparison is made between deep and superficial movement processes.

Such superficial slow mass movement (S.M.M.) will be affected by fluctuations of temperature and moisture within the soil. This dependence is examined at one location and therefore for one set of climatic conditions. It is fully recognised that geographical variation of climate will account for considerable variation in the observed rates and perhaps in the mechanism of S.M.M. but the emphasis of this study is on quantifying the effect of controlling variables at a location where these variables can be measured and monitored precisely. Furthermore, very few previous studies have attempted to test hypotheses of movement mechanism by empirical means, yet it is only a clear understanding of underlying process mechanics that will allow confident prediction. Therefore, by the collection of suitable empirical data, this thesis aims to answer questions relating to the mechanisms of S.M.M. and the variables which control its action.

1.2 Mechanisms of movement

Four distinct mechanisms have been proposed to explain S.M.M.: **expansion and contraction with net downslope movement** (Moseley 1869; Davison 1888, 1889; Young 1958, Kirkby 1963, 1967; Washburn 1967), **viscous flow** (Jeffreys 1922; Allen 1982), **pure shear** (Ter Stepanian 1957) and **particulate diffusion** (Culling 1963, 1965).

All, singly or in combination, are theoretically appealing and plausi-

ble but few studies have attempted to distinguish between these mechanisms. It is generally recognised, however, that expansion and contraction forces caused by the freezing and thawing of pore water are primarily responsible for soil movement in periglacial environments, particularly in the processes of frost creep and gelifluction (Harris 1981; Washburn 1967). The work of Hutchinson and Brunsden (1975) has shown that the process of mudflowing can be successfully modelled by a viscous flow mechanism but the general applicability of such a model is disputed and its relevance to other slope phenomena such as solifluction or temperate S.M.M. has rarely been investigated.

Soil displacement resulting from the formation of distinct planes of failure is perhaps the best documented mechanism of mass movement, yet it has been shown to be extremely complex (Casagrande 1936; Chandler 1972; Skempton 1953; Terzaghi 1950).

All hillslope soils are subjected to shear stresses. Intergranular readjustments only occur when grain to grain bonds are ruptured and surface friction forces overcome persistent concentration of shear stress, which results in the formation of distinct areas of shear failure and quiescent areas exhibiting no intergranular strain. The mechanism of pure shear describes deformation (of a soil mass) without rotation of individual particles.

Evidence supporting this mechanism of S.M.M. comes from strain records in boreholes (Kojan 1968; Swanson and Swanston 1977) and visible shear planes from excavated slopes (Chandler and Pook 1971).

A novel approach in thinking about slope development came from Culling (1963, 1965) who proposed a model of particulate diffusion in granular soils characterised by a random and a downslope component when particles are subjected to natural disruptive forces. This model has not been widely accepted in soil mechanics literature due to a lack of

empirical and experimental evidence. There is clearly a need to establish experiments capable of testing Culling's theory.

1.3 Landform Association

Many earth surface processes produce distinctive or unique landforms which may be erosional or depositional in character. Several landforms have been causally linked with S.M.M.: however, such associations have rarely been tested against geomorphometric and sedimentological data. For example, many researchers have proposed that on temperate slopes micro-forms such as terracettes or micro scarps result from slope movements, just as there is a clear relationship between periglacial landforms and periglacial mass movement processes. S.M.M. has also been associated with *bulging slopes* which are thought to indicate imminent rapid slope failure. As yet such evidence of transient morphological change is restricted to laboratory simulation experiments (Saito, 1965).

Classical theories of landscape development have invoked S.M.M. as a process capable of producing the convex upper component typical of slope profiles in temperate latitudes (Davis 1892; Gilbert 1909). This is because, unlike water, the erosive power of mass movement need not increase with distance from the watershed as the catchment size increases. Clearly it is important to establish a database incorporating information on the spatial distribution of movement and its controlling variables in order to test slope development models which incorporate S.M.M.

Many of the landform associations suggested have been disputed, usually on the grounds that they cannot be uniquely attributed to S.M.M.; however, very few attempts have been made to relate empirical measurements of slope movement to geomorphometric variables. Very little attention has been given to correlating soil texture and fabric structure

to movement rates.

1.4 Theoretical approach

The overall strategy of this research has been to provide a quantitative assessment of the importance of S.M.M. on hillslopes in a humid temperate climate. A detailed knowledge of erosion processes is important because little can be said about past or future adjustments to landforms until the rates, variables and mechanisms controlling earth surface processes are known.

Until recently individual processes have rarely been studied in isolation; rather the combined effects of all processes were lumped into single estimates of degradation in the form of gross sediment budgets. Such studies have been severely criticised for non representative sampling in both space and time because the underlying assumption that all areas of a catchment contribute equally to the budget seems unreasonable (Trimble, 1965). Also the effects of individual processes cannot be easily isolated. Large disparities in budget contribution both spatially and by process in small upland catchments support Trimble's view (Dietrich and Dunne 1978; Lehre 1982; Rapp 1960).

The approach taken has been to identify the key variables controlling erosion by field and laboratory experimentation in order to produce a predictive model. Such a model must be based upon the fundamental properties of soil particles and their behaviour when subjected to chemical, electrical and mechanical forces. The success of empirically tested models derived from known mechanical principles is ably demonstrated by the work of Bagnold (1956, 1966) on aeolian and fluvial transport of cohesionless sand.

1.5 Research methods

Unlike many branches of physical science geomorphology is not exclusively experimental and thus the adoption of such a methodology in the study of earth surface processes and landforms requires care. Contemporary models of hillslope processes are principally derived from an inductive, empirical approach encompassing a variety of measurement procedures and geographical locations. The criteria by which research hypotheses are tested will therefore depend upon the context within which the experimental results were obtained and the inexorable variation of human interpretation (Waddington 1977). Of immediate concern to the study of hillslope processes is the question; Can experiments be devised which test the validity of a movement mechanism or distinguish between rival conjectured mechanisms? Commonly geomorphological experimentation is limited by practical restrictions on the form of data which may be collected in the field. This problem is compounded when predictions from competing hypotheses overlap.

Although many of the ideas and methods used in this research are adopted from established theories any shortcomings in the application of these theories to slope processes would not justify their rejection but rather a re-assessment of the context of their use. For example the derivation of rheological models and the use of rheological principles supplements the application of Newtonian mechanics to strain behaviour in soils. In this case empirical information is needed to supplement classical theory. Therefore, S.M.M. research cannot be a purely deductive operation.

Popper's principle that powerful hypotheses or theories should produce a dialogue of conjecture and refutation between testable and often

unexpected predictions remains the most respected description of scientific method (Medawar and Medawar 1985). Therefore, despite the uncertainties surrounding refutation, and the possibilities that parallel or corresponding hypotheses may appear inseparable (Lakatos 1978), Popper's model implies that the most powerful ideas will win through given an array of multiple working hypotheses.

In broad terms this thesis takes two directions.

First, the mechanisms of S.M.M. proposed by previous researchers are viewed as competing working hypotheses and are assessed both theoretically and empirically.

Second, extensive field measurement undertaken in an upland catchment area assesses the spatial and temporal continuity of the processes within a recognisable hydrological system. In addition the experimental design allowed the hypothesed relationships of S.M.M. with slope gradient, vegetation cover and soil properties to be tested quantitatively.

These directions have been achieved by the integration of field and laboratory measurement, and laboratory experimentation.

1.5.1 Field measurement

Field observation of slope processes has a very long history dating back to early Greek philosophers. Quantitative measurement has only recently become widely adopted. The advent of techniques for making precise measurements of process rates has allowed results obtained by different researchers to be compared quantitatively. This stimulated Leopold, Wolman and Miller (1964) into advocating that a large data base of empirical field process data be established with which to test models and theories. Quite apart from implicitly accepting inductive modelling, this suggestion assumes consistency in the measurement technique used and the physical domain of process studied. Further, notation

and definitions must be clearly established and should be unambiguous. To date no such consensus exists, and, since no single model of movement mechanism is available against which to test a large data base, each research programme must tailor its field measurement requirements individually.

Each of the following factors plays an important role in the final results obtained from any measurement programme:

(i) Geographical extent of study area,

(ii) temporal extent of study period,

(iii) physical domain of study,

(iv) measurement techniques employed,

(v) experimental design.

First, the geographical extent of the study area is related to the required level of spatial detail and the practical limitations of instrument insertion and mutual interference.

In the absence of correlative morphological features S.M.M. has been assumed to occur ubiquitously over space varying only in rate of activity and depth of operation. The field observations from detailed process studies by Kirkby (1963), Evans (1974), Anderson (1977), Finlayson (1976) and Rashidian (1984) all support this assertion at the scale of first order drainage basins. A first order drainage basin is also used in this study not just for continuity but because it contains a broad range of landform, soil and vegetation type within a limited and clearly defined topographic unit. It also provides a convenient open system in terms of inputs, outputs and internal mass and energy transfer within which to model the influence of S.M.M. processes.

Two aspects of time are important in S.M.M. research. First, long observation periods will be required when rates are slow and levels of random variation or disturbance are high. Second, the choice of time

interval between measurement depends upon the temporal continuity of the process, for example an infrequent event should be observed on several occasions in order to substantiate knowledge of rates and durations.

With regard to the length of observation period then clearly the longer the better. However, instrument imprecision may be reduced which offsets the problem to some extent. The problem of temporal sampling is unresolved.

Anderson and Cox (1986) have shown that short term, even diurnal, variability exists although the contribution of short term fluctuation to long term trend could not be adequately assessed. This problem is not pursued further in this thesis because it requires continuous monitoring of movement in the field for further investigation.

The domain of operation of a process must be recognised and clearly defined if instruments are to be designed which measure the required rather than extraneous variables. Erosion pins, used extensively by Rapp (1960), Leopold, Wolman and Miller (1964) and Schumm (1964), provide an example of a simple yet ambiguous technique to measure surface lowering because surface to pin head height is affected by depositional as well as erosional processes. Due consideration must be given to the interaction and interdependency of processes within any given spatial domain.

Formal experimental design has often been very weak in geomorphological field measurement; it appears that most investigations have been exploratory rather than formal. Ahnert (1980) and Church (1984) distinguish between field measurement and field experimentation on the grounds that the latter must be formulated to test specific hypotheses. In practice such a distinction is less obvious for experimentation in the classical sense involves holding certain variables constant while monitoring other variables in a system where all energy exchanges are accounted for. Such conditions are usually impossible to find or arrange in the field.

It is possible to control certain key variables in the field using suitable research designs. For example, the effect of slope angle is often accounted for in runoff and rainsplash plot experiments where treatment is applied to several plots at identical slope angles then repeated for different slope angles, as in classical trial experiments (Quansah, 1981).

Techniques for the monitoring of S.M.M. have been documented and reviewed by Anderson and Finlayson (1975) and Statham (1981) and are reassessed with recent additions in Chapter 3. Choice of the most suitable instrument for the scope and purpose of research is of paramount importance for this ultimately controls the precision and accuracy of the data obtained.

Instruments selected must be suited to the process domain in question. Instrument accuracy should be known, and ideally all possible sources of error documented and quantified. Any field calibration procedures should also be carefully documented.

Many instruments designed to measure S.M.M. are buried markers which may not accurately reflect the behaviour of undisturbed soil particles due to emplacement disturbance or the presence of inertial or drag forces on the instruments. Anderson and Cox (1978) provide a quantitative assessment of six instruments which provides the basis of the instrument selection for this thesis.

1.5.2 Laboratory investigation

Laboratory investigation is here divided into two distinct categories.

1. Quantitative assessment of soil properties.
2. Simulation experiments.

First, accurate measurement of many geomorphological variables can only be achieved in the laboratory. This brings advantages of pre-

cise, repeatable measurements but also disadvantages because many soil testing procedures involve destructive sampling which pose problems of analysing seasonal variation in soil properties. If sample collection be attempted during data collection the effect of disturbance which may involve a delayed response will be difficult to detect. Ideally soil sampling should only occur at the termination of research in order to minimise measurement error. Where possible soil properties should be monitored using non-destructive sampling methods.

Laboratory techniques in geomorphology are expanding rapidly. Many are capable of providing much useful information on S.M.M. of sampled soils and sediments. These include:

(i) geotechnical tests of soil consistency,strength and rheological behaviour,

(ii) microscopical analysis of thin sections,

(iii) scanning electron microscopy of soil fabrics and

(iv) palaeobotanic analysis of organic inclusions especially pollen and wood samples.

Second, simulation studies provide an extremely important role in hypothesis testing by allowing the reconstruction of field conditions often with space scaled down and time speeded up (Thornes 1979). Such an approach is very valuable in S.M.M. research because no great scale changes are necessary in either space or time (Kirkby 1963,1967). Major problems can be encountered, however, in attempting to reconstruct field conditions in the laboratory particularly with hydrological and biological variables. Simulation experiments with the extremes of possible field conditions can provide valuable insights into the range of possible process responses and may form the empirical basis of a predictive model.

Chapter 2

Previous research

Contents

2.1 Introduction

Modern geomorphological research on hillslopes is primarily directed towards field measurement, laboratory experimentation and theoretical modelling of degradational processes. Studies involving detailed field measurement and experimentation have been notably successful in determining rates of operation and isolating controlling variables for individual hillslope processes (Mosley 1981).

Recently slow mass movement has been the focus of considerable quantitative research from geomorphologists. This has involved work on measurement techniques (Finlayson 1977; Young 1978; Anderson and Cox 1978; Auzet 1981), investigations of factors which influence S.M.M. in the field (Finlayson 1977; Anderson and Cox 1984, 1986) and theoretical modelling (Culling 1981, 1983a, 1983b, 1983c; Kirkby 1982). Engineering geologists are becoming increasingly aware of the important role slow deformation plays in consolidation and failure phenomena on many natural slopes other than the well documented sensitive clays (Mitchell 1976; Pusch 1979; Morgenstern 1981). In addition a great deal of recent research has been directed towards fundamental aspects of soil behaviour such as its response to thermal stress (Demars and Charles 1982), phase changes in pore fluids (Konrad and Morgenstern, 1980), changes in pore fluid chemistry (Carson 1979) and stresses induced by surface vegetation. Clearly these studies are of direct relevance to the understanding of near surface mass movement phenomena.

Despite the wealth of recent empirical data on slow mass movement processes, technological improvements in data collection and soil testing procedures, and several novel approaches to mass movement modelling, no attempt has been made to collate these recent advances.

Previous reviews by Kirkby (1963), Carson and Kirkby (1972), Young (1972) and Anderson (1977) have not been comprehensive nor have they been able to provide a quantitative appraisal of instrument performance and measurement practices and procedures.

2.2 Aims

This review is intended to provide a comprehensive survey and critique of geomorphological research on slow mass movement of soils on temperate hillslopes, the environment of the author's field research.

To date there has been no systematic survey of the mechanical and geotechnical aproaches to slow mass movement despite recognition of this work by geomorphologists (Carson and Kirkby 1972; Statham 1977). This work is particularly relevant to movement processes in soils which possess a dominantly clay matrix where rheological behaviour is complex and theoretical models based upon discrete particles appear inadequate.

The task of identifying general mechanisms from individual case studies is problematic. Many studies which claim to describe mass movement phenonema are based on qualitative and sometimes speculative evidence such as the displacement of walls, trees and other structures cannot be uniquely attributed to S.M.M. On the other

hand, some quantitative studies have used crude methods of data collection and too few possess a systematic research design.

Despite such problems research is discussed according to the mode of behaviour envisaged by each author with a view to encouraging the development of general theories of slow mass movement.

It is also intended to clarify inconsistencies in terminology and notation between researchers which are particularly prevalent due to the multidisciplinary nature of the subject.

2.3 Sources

The majority of articles referred to are written in English, French or German; fortunately much Soviet, Romanian and Polish work has been either translated or published in English. Unpublished references include recent conference papers, theses and personal discussions.

Geological and geotechnical publications have been critically selected to include only the most substantial contributions relevant to natural hillslopes. These have been drawn from six principal sources; Bulletin of the Geological Society of America. Canadian Geotechnical Journal, Geotechnical Engineering, Geotechnique, Journal of the Geotechnical Engineering Division of the American Society of Civil Engineers, and the proceedings of several specialist conferences.

2.4 Early Ideas

2.4.1 The Growth of Fluvialism

Mankind has long been interested in processes of mass movement of hillslopes. From earliest times references are made to rapid and catastrophic processes such as rockfalls, landslips and avalanches. However, widespread recognition of slow mass movement processes or indeed any slow acting or small scale geomorphological event did not occur until the late nineteenth century when the uniformitarian ideas of James Hutton (1726-97) and John Playfair (1748-1819) had gained worldwide acceptance by earth scientists and, perhaps for the first time, provided the stimulus for studying the less dramatic geological processes. Hutton's concept of geological time, succinctly summarised in his famous phrase *...no vestige of a beginning, no prospect of an end*, attested to the belief that the incessant and prolonged operation of fluvial processes was the primary mechanism for continental degradation. Hutton and his immediate uniformitarian followers Charles Lyell (1797-1875) in Britain and James Dwight Dana in the United States of America thus provided the conceptual platform from which began the systematic and detailed scientific study of the processes of degradation on hillslopes.

It is ironic that one of the first scientific discussions of slow mass movement of geological material was made by Abraham Gottlob

Werner (1749-1817), a contemporary of Hutton and a bitter opponent of uniformitarianism. Werner claimed that the bedding structures of the oldest rocks resulted from the slumping and flowing of volcanic deposits while they were still in a plastic state. Werner's ideas, widely accepted at the time, particularly in Germany, were very successful in explaining the structure of volcanic regions and forsighted when modern knowledge of dilatant creep in rock is considered.

Notable early studies of fluvial processes are described by Chorley, Dunn and Beckinsale (1964) and Chandler (1982) to which further reference may be made.

2.4.2 Early Theory

Henry Moseley, a clergyman and amateur scientist, produced a quantitative model invoking non-isotropic expansion and contraction of an inclined but otherwise uniform body due to the action of gravitational force aiding downward expansion or contraction but retarding upward expansion or contraction (Moseley 1869). The result of continued cycles of expansion and contraction, induced by heating and cooling for example, was a gradual downslope motion proportional to slope gradient:

$$\frac{a \cdot \epsilon \cdot \Delta t \cdot tan\theta}{\mu}$$

a = length of body ϵ = coefficient of expansion

μ = coefficient of friction between body slope

θ = slope angle t temperature rise

Equation 2 (1)

Moseley tested his model by observing the rate of motion of a piece of detached lead sheeting on Bristol Cathedral roof. Although the experimental verification of the model was hardly exhaustive this deductive approach was rare in the geological sciences at the time and the physical basis of the model remains unchallenged today.

Several of Moseley's contemporaries, including Lesley (1856), Anstead (1871), Mallet and Fuchs, made passing reference to the existence of slow mass movement processes on soil-covered hillslopes. For example Lesley, an American exploratory geologist (1856 p35), noted *..all soils slide .. in fact the whole surface of all hills have been in slow but perpetual movement downward from the beginning, so that in the present day the soil or weathered broken edge of any stratum overlies the strata below it, while it is itself covered by the soil of some stratum above it. On slight slopes this translation of material has gone to no great distance, but on slopes of 20° or 30° the smut of a given coal bed has probably been drawn out in a long knife-like wedge, the edge of which is to be seen many yards below its proper place.* What is not clear from the writings of these researchers is how much importance they attributed to slow soil movement as an agent in sculpturing the landscape.

C Wyville Thomson (1877) described features he termed *stone rivers* on the hillslopes of East Falkland Island. His proposed mechanism for the transportation of large quartzite blocks from resistant strata to valley sides and floor is a gradual creeping of a fine soil matrix with the larger blocks entrained within it. When the fines are somehow washed out or eroded away the characteristic stone stream features persist. Thomson (1877, p360) stated *It seems to me self*

evident that whenever there is a slope, be it ever so gentle, the soil cap must be in motion, be the motion ever so slow .. James Geikie (1877, p 397) commenting on Thomson's proposed mechanism argued that *the soil cap being .. acted upon by frost, is forced to move downslope, a movement which is of course aided by a vis a tergo, the weight of the descending mass.* Geikie thus supported the principle but he doubted that the process was geomorphologically significant compared with fluvial erosion on hillslopes. He compared Thomson's Falkland *stone rivers* with *earth glaciers* described by a Dr Haydon in the Rocky Mountains of the USA and also noted that Robert Mallet and Theodor Fuchs had previously proposed the same mechanism for soil cap motion. P.S. Abraham (1877) also commented on Thomson's 1877 paper, noting similar features in the Hartz Mountains and offering an alternative mechanism. He proposes that weathering of tors results in rockfall and subsequent downslope deposition. Direct comparison of features is impossible due to the lack of morphological evidence. Abraham also appears to have been one of the first people to attribute outcrop curvature to surficial soil movement, *...although the slope of the hill is not high, the constant weight of the super-incumbent earth and rubbish, bearing downwards for ages, would, it seems to me, be enough to cause such a result* (Abraham 1877, p431).

2.4.3 Geomorphological literature - early ideas

The term **soil creep** was used by W.M. Davis to denote the slow mass movement of soils, supposedly responsible for the upper convexity of the hillslope profiles he observed throughout temperate lat-

itudes. Davis's (1892) paper represents one of the earliest deductive approaches to the study of hillslope processes through his hypothesed creep mechanism for explaining the convexity of drainage divides. Although Davis never addressed himself to testing his hypothesis empirically, he challenged existing ideas on hillslope erosion processes, stimulating discussion, and later a considerable amount of empirical research.

Of similar historical interest is an important paper by Beeby Thompson (1896-97) which considers the physical and chemical principles of the denudation of clay slopes of the Upper Lias in Northamptonshire. Thompson summarises his discussion of the creeping of superficial material thus: .. *clay slopes that are only intermittently wetted are subject to a surface creep through expansion and contraction, also to further denudation and slipping when thoroughly wetted because of the greater separation of the particles and the fluid lubricant between them, both of which actions tend to bring hillsides to the angle of repose of soaked clay.* By contrast with Davis's, and later Gilbert's deductive approach, Thompson presents a clear and cogent argument for the existence of denudation by superficial creep from empirical observations and mechanical reasoning. For example, Thompson describes the mechanism of desiccation creep in some detail paying particular attention to the ability of clays to absorb and retain moisture through the sequence of wetting and drying phases; clearly he was well aware of the regulating effect that antecedent moisture content would have on the wetting of a clay mass following a prolonged period of desiccation. Thompson cites comparative measurements made of the shrinkage of natural and fired clay bricks to support his observations

and claims Lias clay shrinkage of 20% is possible. In addition to this early experimental evidence some consideration is given to mechanical and stratigraphic ideas. In particular, the concept of a geomorphic threshold is implicit in the following quotations: .. *gravity alone will tend to reduce the angle of slope, when it happens to be greater than the angle of repose of soaked clay, though vegetation may have a great retarding influence on this* and .... *the greater coefficient of friction of merely damp clay may delay the movement, so as to render it more spasmodic.*

R.J. Chandler (1982) in drawing attention to Thompson's perspicacious contribution to the study of slope processes attributes the first description of **desiccation creep** to Thompson. However, G.K. Gilbert (1909), in a similar expository which, attributes the first scientific description of this process to Davis (1892). It is of no particular significance who was first to publish an account of the desiccation creep process but what is important is that early workers realised the significance of the apparently stationary process of freezing and thawing, heating and cooling and wetting and drying as mechanisms for both downslope displacement of particles and .. providing sites for the initiation of rills and gullies.

The experimental work of Charles Davison (1888, 1889), which is based upon Moseley's original model of particle movement, is the first deductive study of insolation creep. Davison's (1888) work was far sighted; he first undertook to replicate the results of Moseley, using clay bricks, then sandstone flags. On finding close agreement with Moseley he attempted to analyse the model further by varying several important parameters such as particle size coefficient of expansion

(particle type). temperature range, and slope angle. Despite the lack of replication in his experiments, Davison took careful measurements paying considerable attention to detail. He noted that movement rates were particularly sensitive to rapid rates of change of temperature and changes in the coefficient of friction between particle and base.

Davison obtained rates of movement for insolation rock creep of 0.004 cm - 1.52 cm per year on a 30^{o} slope, so clearly the process was very effective. However, Davison notes that fabric shape will greatly reduce overall rates by constricting movement and increasing interparticle friction.

By the late 19th century, Quaternary geologists were beginning to recognise unusual stratigraphy and fabric shapes in unlithified diamictons in the margins of known ice cap limits. Kerr (1881) attributed such a deposit to the action of frost or frost creep, primarily because of the sorted nature of the material and the downslope orientation of large clasts.

Davison (1889) attempted to simulate this hypothetical process experimentally by subjecting a variety of soil types to several freeze-thaw cycles and measuring the displacement of marked particles. Displacement was observed to be directly proportional to the number of freeze-thaw events but explaining a depth-movement decay curve in terms of the depth of frost penetration proved difficult. Davison was particularly concerned that observed depths of frost penetration in temperate and alpine climates were insufficient to explain the sorting and stratigraphy of deep deposits such as those described by Kerr(1881).

2.5 Geomorphological studies of S.M.M.

The experimental work of Charles Davison marks an important progression whereby hypotheses are tested by experiments. The continuation of experimental research in geomorphology can be traced with particular reference to mass movement of slopes in periglacial environments (Andersson 1906; Lozinski 1912). At this time, insolation creep (frost creep) and slow viscous flow were considered the most likely mechanisms for the observed downslope movement of soils. However, further research has revealed a much more complex picture.

Terzaghi, who so influenced soil mechanics by recognising the importance of pore water pressures in defining the effective stress of a soil, recognised that slow displacement by internal shear may occur in soil masses in response to gradual increases in stress. A similar mechanism of crystalline shearing was thought to occur in rock masses, and M. Lugeon described this process as early as 1922 in the eastern European Alps. Shear failures in shallow soil masses have been described by many researchers, particularly by Chandler (1972). Such deformation may only result in translational displacement of a few cm and the movement can mimic solifluction or slow flow. However, it is the result of failure about a discrete shear plane, asociated with high positive pore water pressure. For example, within the periglacial environment, Morgenstern (1981) and others have studied the process of displacement associated with ice lenses near the freezing front. Within a temperate environment, Iverson (1986) has quantified the patterns of shear displacement at the base of landslides which exhibit unsteady, nonuniform motion. Shear processes are still poorly understood because of the difficulty of collecting precise empirical data. In

particular, shallow soil masses have received little attention outside of periglacial regions.

A fourth class of mechanism, particulate diffusion, was proposed by Culling (1963) to account for S.M.M. in granular soils. Culling's theory describes the natural disturbance of particles as a type of Brownian motion in which slope gradient introduces a downslope component to an otherwise random displacement pattern. He assumes that particles behave independently of each other and that the grain size distribution of the soil governs its susceptibility to movement. The theory describes the physical forces promoting motion in very general terms through equations for drift and diffusion components. The soil itself is described in only one dimension. Recent empirical research by Flavell (1986) undertakes to test predicted changes in soil porosity downslope of a barrier which partially impedes S.M.M. Her results do indicate increased packing upslope of the barrier but this could be due to a variety of other processes. The theory requires further empirical support as well as discussion of the origin of fabric shape and the behaviour to the process at different soil depths.

Several attempts have been made to clarify the various theories of S.M.M. and their physical effects. These accounts fall into two groups, the lumpers and the splitters.

2.5.1 Splitters

Classifications of mass movement phenomena are often based on the morphology of landform which results from their action despite the fact that similar landforms can result from different processes of

movement. For example, Hutchinson (1968), in a widely referenced classification scheme, separates periglacial processes on the basis of their landform assemblage alone. Carson and Kirkby (1972) attempt to reconcile this problem of arbitrary classification by splitting all mass movements into a threefold scheme of slide, flow and heave processes, regulated by moisture content (figure 2.1). Although theoretically appealing, this scheme is based upon very specific definitions of slide, flow and heave and is thus not exhaustive. Variables which tend to promote shearing or sliding will not necessarily be inversely correlated with those tending to promote viscous flow. For example, the shear strength of sand will increase with increasing moisture content until dilatancy, associated with positive pore water pressures, causing either flow or shear to occur depending on other factors such as the magnitude and rate of build-up of stress. It is also difficult to imagine a situation in which soil heaving occurs independently of forces which restrict particulate shearing, bearing in mind the granulometric and hydraulic parameters which regulate frost heaving.

Other researches have proposed a variety of schemes to encompass both mechanisms of movement and the landforms which result from that movement. Sharpe (1938) differentiates processes into sliding and flowing, Varnes (1958) includes falls, slides, flows, and combinations of these, and Varnes (1975) adds topples and lateral spreads in his 1958 scheme (figure 2.2). Despite the appealing simplicity of the classification schemes there is no unequivocal empirical evidence to characterise S.M.M. as the simple flow phenomenon often envisaged or that movement proceeds in a similar fashion in all soil types. The classifications of Varnes and Hutchinson are further subdivided according

Figure 2.1 Classification of mass movement processes (after Carson and Kirkby 1972)

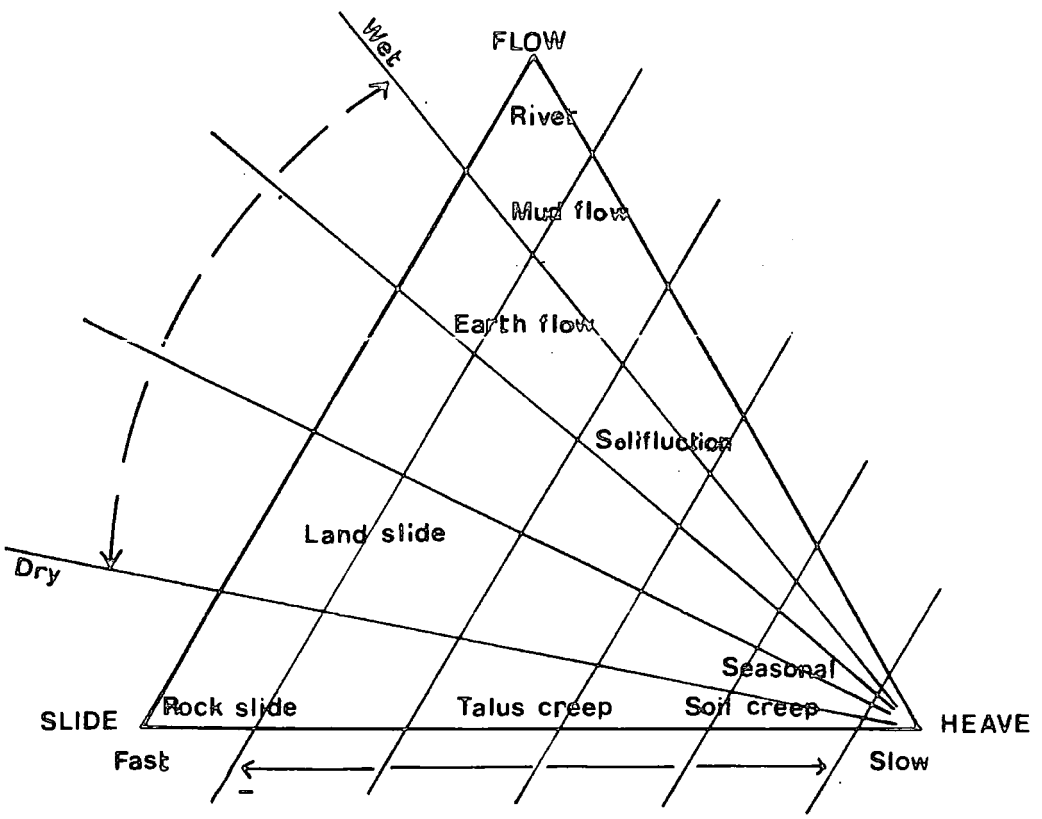

igure 2.2 Classification of mass movement processes (after Sharpe 1938, Varnes 1958, 1975)

Table Classification of Sharpe (1938)

	Nature and Rate of Movement	GLACIAL TRANSPORT	With Increasing Ice Content ⟵ Rock or Soil ⟶ With Increasing Water Content			FLUVIAL TRANSPORT
FLOW	imperceptible		SOLIFLUCTION	CREEP (ROCK CREEP SOIL CREEP)	SOLIFLUCTION	
FLOW	slow to rapid		DEBRIS AVALANCHE		EARTH FLOW MUD FLOW DEBRIS AVALANCHE	
SLIDE	slow to rapid			SLUMP DEBRIS-SLIDE DEBRIS-FALL ROCKSLIDE ROCK FALL		

Table Classification of Varnes (1958)

Type of Movement	Type of Material			
	Bedrock		Soils	
FALLS	ROCKFALL		SOILFALL	
SLIDES few units	rotational SLUMP	planar BLOCK SLUMP	planar BLOCK GLIDE	rotational BLOCK SLUMP
SLIDES many units		ROCKSLIDE	DEBRIS SLIDE	FAILURE BY LATERAL SPREADING
	All Unconsolidated			
	rock fragments	sand or silt	mixed	mostly plastic
FLOWS dry	ROCK FRAGMENT FLOW	SAND RUN	LOESS FLOW	
FLOWS			RAPID EARTHFLOW	DEBRIS AVALANCHE / SLOW EARTHFLOW
FLOWS wet			SAND OR SILT FLOW	DEBRIS FLOW / MUDFLOW
COMPLEX	Combinations of Materials or Type of Movement			

Table Classification of Varnes (1975)

Type of Movement			Type of Material		
			Bedrock	Soils — coarse	Soils — fine
FALLS			ROCKFALL	DEBRIS FALL	EARTH FALL
TOPPLES			ROCK TOPPLE	" TOPPLE	" TOPPLE
SLIDES	rotational	few units	" SLUMP	" SLUMP	" SLUMP
SLIDES	translational	few units	" BLOCK GLIDE	" BLOCK GLIDE	" BLOCK GLIDE
SLIDES	translational	many units	" SLIDE	" SLIDE	" SLIDE
LATERAL SPREAD			" SPREAD	" SPREAD	" SPREAD
FLOWS			" FLOW (deep creep)	" FLOW (soil creep)	" FLOW
COMPLEX			Combination of 2 or more types		

to material type and Sharpe also considers the effect of increasing moisture and ice content on mechanism of movement. However, the schemes could equally well have been divided on other parameters, stress state, or degree of consolidation, for example.

There seems little purpose in classifying processes unless there be a mechanical reason for doing so. Otherwise an infinite number of somewhat arbitrary divisions will exist, many of which may have no physical basis.

2.5.2 Lumpers

Several periglacial geomorphologists have pointed out the naivete of simple mass movement classifications. Dylik (1967) suggests that a continuum exists between slow and rapid movement processes. He proposes that moisture status regulates the pathway of the process where the potential for S.M.M. is a property of the soil matrix but the execution of that potential is a function of the local moisture conditions. This idea is similar to J. Ross Mackay's hypothesis for moisture regulation of pingo development (Mackay 1981).

Another method of integrating processes is to base research on measurements of sediment transport where the effects of individual processes are combined. McRoberts and Morgenstern (1974) suggest, rather unhelpfully, that separation of the effects of flow, frost creep, and consolidation is impossible in the field and consequently, they argue, any such distinction is of little practical relevance.

A further approach to resolving geomorphological ideas on S.M.M. has been to characterise their action, either individually or collectively,

by mathematical models. Examples of models relating to slow viscous flow are given by Allen (1982), Brunner et al.(1975), Jeffrey (1922), Johnson (1970) and Scheidegger (1970). Models of a more general nature have been suggested by Culling (1963) and Kirkby (1967). These and others have been reviewed by Cox (1979) in which criticism is made where no plausible process mechanism is suggested.

On the other hand Allen (1982), Culling (1963), Jeffrey (1922) and Johnson (1970) proposed models of movement which, in principle, can be tested experimentally. However, very few studies have sought to test theoretical predictions in the field and so no consensus emerges from geomorphological studies of S.M.M. so far. In addition, most empirical studies of S.M.M. fail to entertain more than one working hypothesis for movement so that mechanisms cannot distinguished from the data. This has resulted in a ruling hypothesis that S.M.M. is a flow process although there is a lack of empirical evidence to support this.

It is clear that despite minor geographical variations, the fundamental physical parameter controlling mass movement phenomena, gravitational acceleration, is effectively ubiquitous and constant and so mass movement can only vary according to the energetics of the geomorphic system in question and the rheological properties of mass withinthat system.

Rheology has rarely been considered by geomorphologists, with the obvious exception of those concerned with glacial physics, yet the intrinsic behaviour of material when stressed, which is ignored in classical Newtonian mechanics, must be of paramount importance to the understanding of slow soil deformation.

2.6 Geotechnical studies of S.M.M.

Geotechnical studies of soils are often applied to specific practical problems. Many soils exhibit creep either naturally or during consolidation. Safe loading stresses are normally determined by laboratory study of rates of deformation (Mitchell, Campenella and Singh 1968).

Fleming and Johnson (1975) were among the first soil engineers to study in situ creep. They confined their interest to a silty clay soil around San Francisco, USA, the movement of which seemed responsible for much structural damage. Their results show a significant positive cross correlation between moisture content and movement. They also suggested that a log-linear relationship exists between displacement and time.

This is a significant result for two reasons. First it implies that creep does not occur continususly in the field under a constant applied stress, and if continuous movement be observed then other environmental factors are involved. Secondly the relationship observed may be similar to that of high temperature creep. A longer study time will be necessary to determine if microfabric alteration would eventually lead to softening and extended displacement or failure.

Morgenstern (1981) reviews recent research on slow soil determination in a permafrost environment. Results show a good correlation between ice-rich segments of the material and high creep rates. It is also noted that lateral movements due to settlement when measured in the field are not easily distinguished from creep movements.

Morgenstern's laboratory results indicate that a power law summarises the stress-strain relationship of deformation in an ice rich soil.

Pusch and Feltham (1980) propose a stochastic model of creep behaviour in soils based on the assumption that creep is dependent upon stress and temperature; thermally activated slip being the most likely rate-determining process. The model is stochastic in the sense that it views the soil as a heterogeneous material with a variety of (possible) energy barriers to be overcome in a random order.

Earlier rate process theories (Singh and Mitchell 1968; Pusch 1979) are based on the assumption that all energy barriers are of the same type.

In the tests which they describe, pore-water pressures are ignored because these pressures should remain constant during undrained tests. The physical model proposed by Pusch (1979), and Pusch and Feltham (1980) was derived from analysis of the microstructure of an illite clay deposit, using scanning electron micrographs to identify structures associated with stress induced deformation.

In a clay the formation and movement of domains lead to the formation of rigid structural units, thus increasing internal friction. The formation of new inter-aggregate bonds increases shear resistance. The redistribution of microstresses into more concentrated areas produces an increased strain rate.

From analyses of several types of clay the research shows that the linear stress-strain relationship only holds for moderate stresses. At higher stresses an exponential function is more appropriate.

Pusch and Feltham further argue that the success of their isothermal model provides a solid basis for further systematic studies of

rate-determining processes.

2.7 Terminology

Sharpe (1938) terms S.M.M. a flow process regulated by moisture or ice content without presenting evidence why this need be so. Parizek and Woodruff (1965) criticize Sharpe for ambiguity and for being all encompassing. They note that slow flowage is not a mechanism which has been substantiated by observation or by experiment. They also criticize Sharpe, rather unfairly, for distinguishing processes by their rate when rates are difficult to measure in the short term. The alternative given is a division into perceptible and imperceptible movement according to observability. This suggestion regresses from precise definitions of the mechanism of the movement process. Parizek and Woodruff (1965) define S.M.M. as slope melt *..downslope gravitative transportation of surface and subsurface materials deemed imperceptible because of small displacement, slow movement or quantity of material moved.* Here ideas such as perceptibility and observability take precedence over mechanism of movement and the precise description of the depth at which movement occurs and the rate at which it occurs. The fact that this scheme has not been widely adopted suggests that it is neither workable nor desirable.

Terms for S.M.M. introduced by Terzaghi (1953) divide movement according to its temporal persistence (Seasonal creep - continuous creep). In a strict engineering sense the term creep refers to a time dependent process and this leads to some confusion in the literature.

In order to clarify and simplify description of mass movement in soils, the following terms are suggested.

1. Mass displacement - to refer to a process which may operate at any depth in the soil when its rate, direction and mechanisms are unknown.
2. Superficial slow mass movement - to refer to a process whose rate and depth of operation are known but whose mechanism is unknown.
3. Slow mass movement - to refer to a process whose rate is known but whose depth of operation is unknown, as is its mechanism.

These terms offer useful descriptions of process rates and the depth of movement if known, but they specifically exclude any implication of mechanism. If detailed research leads to an understanding of the underlying mechanism of movement, then this should be stated according to the mechanical or biotic forces involved.

Chapter 3

Measurement techniques

Contents

3.1 Measuring slow mass movement

Techniques for measuring slow mass movement can be classified into those which possess a fixed reference point and those which indicate relative changes in movement. In addition some techniques attempt to characterise a movement-depth profile by the burying and re-excavating of markers. Such a technique, however, can only be used once and it gives no indication of the pattern of movement through time. The simplest method of monitoring mass movement is by careful survey of surface markers but obviously this gives no indication of the movement depth profile (Rudberg 1958; Schumm 1966). Techniques described in the literature are reviewed in some detail by Auzet(1985), Anderson (1977), Anderson and Finlayson (1975), Rashidian (1984) and Selby (1966).

3.1.1. Displacement-depth measurement through time

Several researchers have designed instruments which are capable of measuring changes in the mass movement velocity profile through time (Williams 1962; Selby 1968; Sugden 1973; Troeh 1975; Finlayson 1977; Rashidian 1984 and Auzet 1985). The systems employed by Selby and by Troeh are simple extensiometers: markers at prescribed depths are connected to a fixed position by wires which extend to measure strain. This approach yields a partial velocity profile which is accurate to 0.1 mm/yr according to Selby (1968). However, it does cause considerable disturbance to the site when installed and it is assumed that the markers move in sympathy with the soil and do not affect movement. The techniques described by Williams, Sugden,

Mercier and Geissert, and Auzet measure the deformation of a thin, wide, flexible object inserted into the ground with its wide side perpendicular to the expected direction of movement. Measurements are made from strain gauges responding to the flexure of the strip. The problem is that of knowing in what *plane* the deformation is occurring. If the gauge is a flat strip with its *easy* axis of bending in the direction of the incipient deformation then the strain gauge readings are proportional to the local radius of curvature. Integration of those data gives the shape of deformed gauge. If, however, the direction of movement is unknown then two gauges set at 90^o round from each other would be required to define the local plane of bending and the curvature of that plane. If the deflections in the two directions are y and z with x measured down the gauge then the strain measurements are proportional to dy/dx and dz/dx and the data would need to be integrated twice to give y and z. Pairs of strain gauges would have to be attached to a flexible probe, perhaps circular in section, at intervals apart which would depend on the anticipated form of the movement depth curve.

The approach is attractive as a continuous measurement device but the interpretation of the profile does cause some difficulties because each point on the profile is not independent of its neighbour. For example, the hypothetical profile shown in figure 3.1 could result from a depth decay function or equally well from a discrete shear zone near the top of the profile. The form of the flexure is more a function of the behaviour of a spring than of the behaviour of soil particles. In addition, because the strip behaves as a spring it will impede movement in direct proportion to the magnitude of flexure provided that it is fixed at top or bottom. If the likely magnitude and direction of mass movement to be measured are known then strain

igure 3.1 Hypothetical displacement - depth profiles.

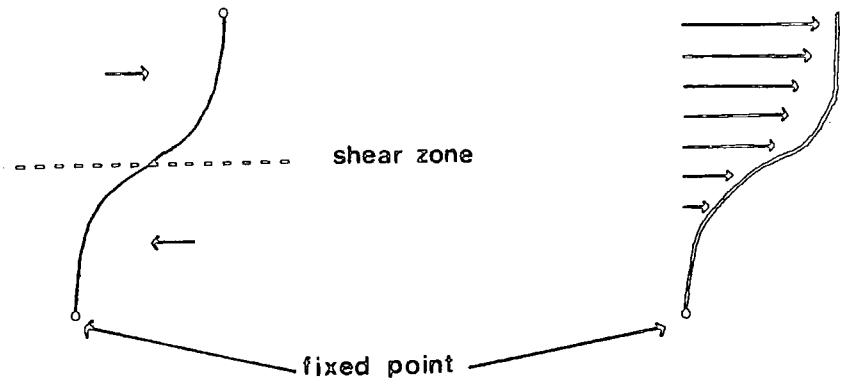

igure 3.2 Four-point displacement - depth profile (after Finlayson 1976)

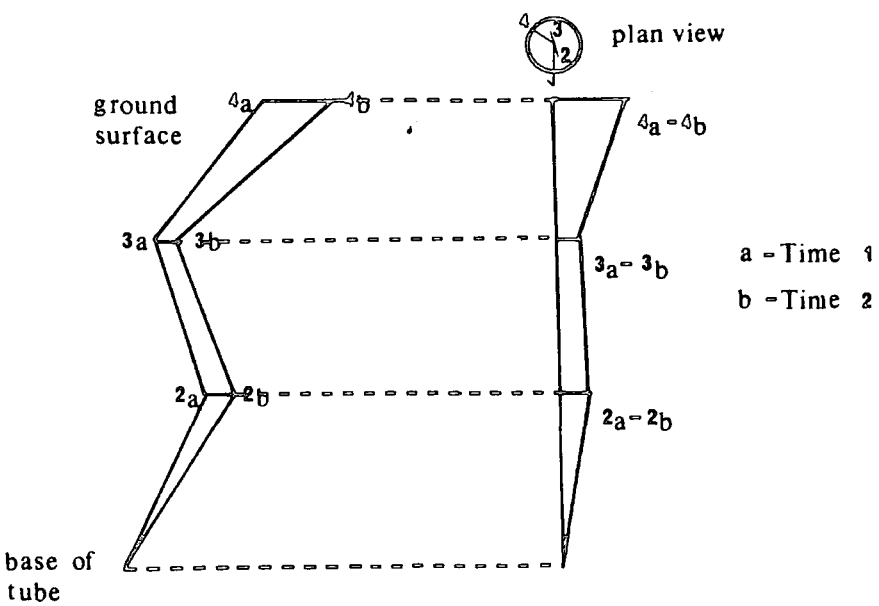

Displacement/depth curve

(after Finlayson 1976)

gauge data can be interpreted correctly and will provide very precise strain measurements.

Analogous techniques are commonly used in the practice of civil engineering. It is usual to insert flexible piping into a borehole and measure resultant deformation by inserting an inclinometer to different depths within the pipe. Fleming (1973) applies a simple inclinometer system to measurement of a silty clay soil in the San Francisco Bay area. Fleming found that operational difficulties such as variation in the tiltmeter alignment, electrical drifting of the strain gauges and imperfect zeroing of the gauges reduced the precision of the system to 3 minutes of arc. Finlayson and Osmaston (1977) describe an optical device which measures the deformation of a flexible tube to an accuracy of 0.025 mm/m. This device was used by Finlayson in a study of slow mass movement in a catchment area in the Mendip Hills. The results provided a simple 4 point displacement-depth curve with the direction as well as the magnitude of movement at each of the points (figure 3.2).

Rashidian (1984,1986) presents a novel method for acquiring a displacement depth profile using markers emplaced to differing depths in small adjacent boreholes. The displacement of each marker is observed independently to provide an estimate of the displacement-depth profile (figure 3.3).

3.1.2. Once only displacement-depth measurement

Techniques for obtaining a single displacement-depth profile using buried markers have been widely used to measure seasonal solifluction in arctic environments. The best known method uses the emplacement of a length of dowling cut into short lengths perpendicular to the slope,(Rudberg 1964). The technique has been adopted by several

Figure 3.3 Rashidian's method for estimating displacement - depth profiles

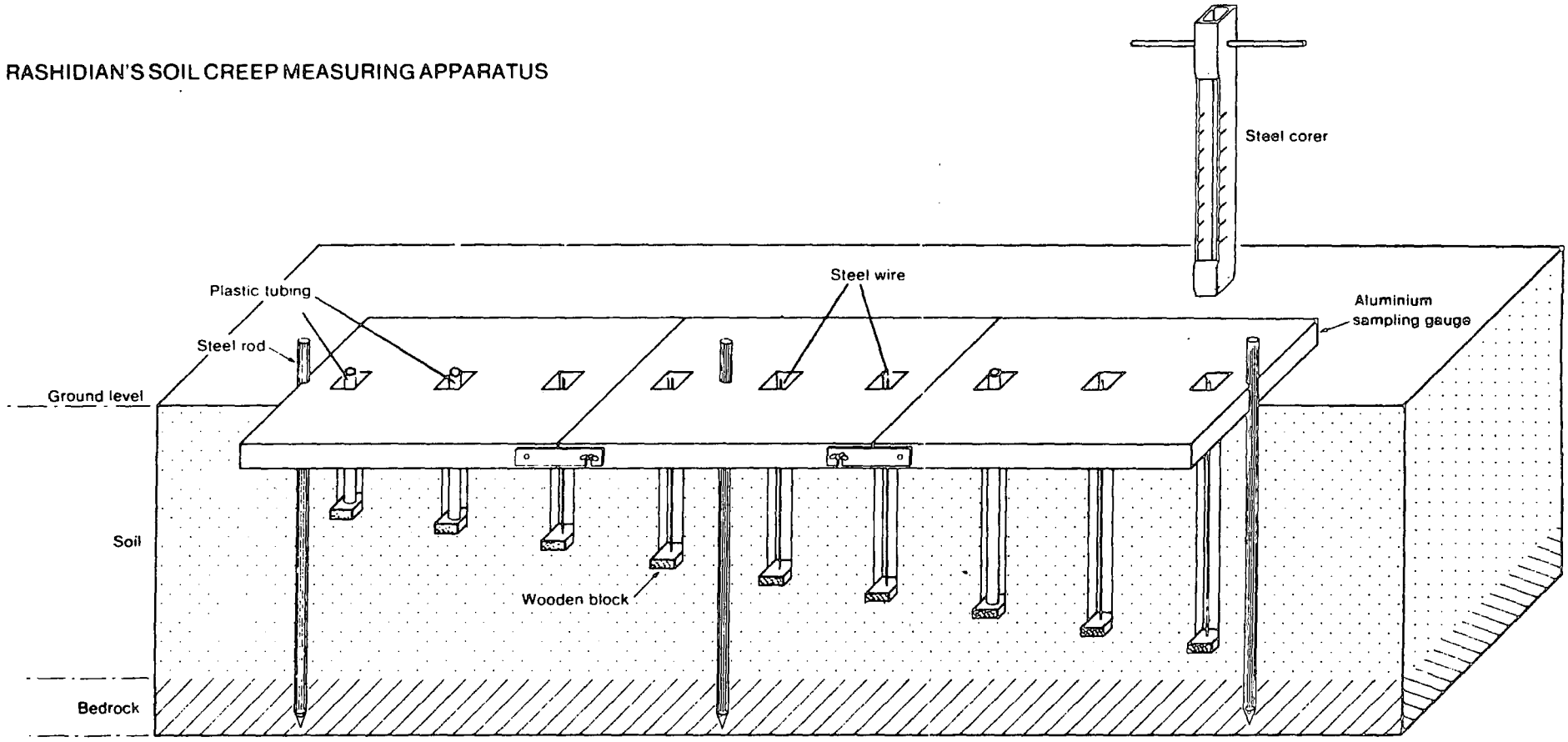

researchers and used to measure slow mass movement in other environments (Rapp 1960; Jahn 1979; Emmett and Leopold 1965; Young 1960).

Young (1960) proposed the vertical emplacement of small wires into the side of a pit dug into the hillslope (figure 3.4). This method of measurement assumes that the pins will reflect the movement of soil particles surrounding them and that a stable reference point exists at the base of the profile. If the pins are accurately positioned, both vertical and horizontal displacement can be detected. Young (1978) notes that the technique is most satisfactory for long term studies. Excavation of pits installed for 10 years showed a distinct pattern of downward vertical displacement of the pins. Young suggests that this may be due to the effects of chemical as well as physical erosion.

Other techniques have been suggested for displacement/depth profile measurement using columns of coloured sand, glass beads and plastic pellets (Rudberg 1964). All these methods can be criticised for disturbing the soil during their insertion and for the fact that they allow only a single measurement to be taken. On the other hand, displacement/depth profiles are required in order to measure the total volume of soil transported past any given plane. By convention mass movement rates are expressed as the integrated area under the displacement/depth curve over an arbitrary width of slope per year. Finlayson (1976) expressed volumetric movement in units of $cm^3/cm/year$.

3.1.3 Relative displacement through time

Instruments in this category include Anderson's Tubes, which can measure mass displacement relative to a fixed reference point, and other inclinometer techniques which have no fixed reference. Both

Figure 3.4

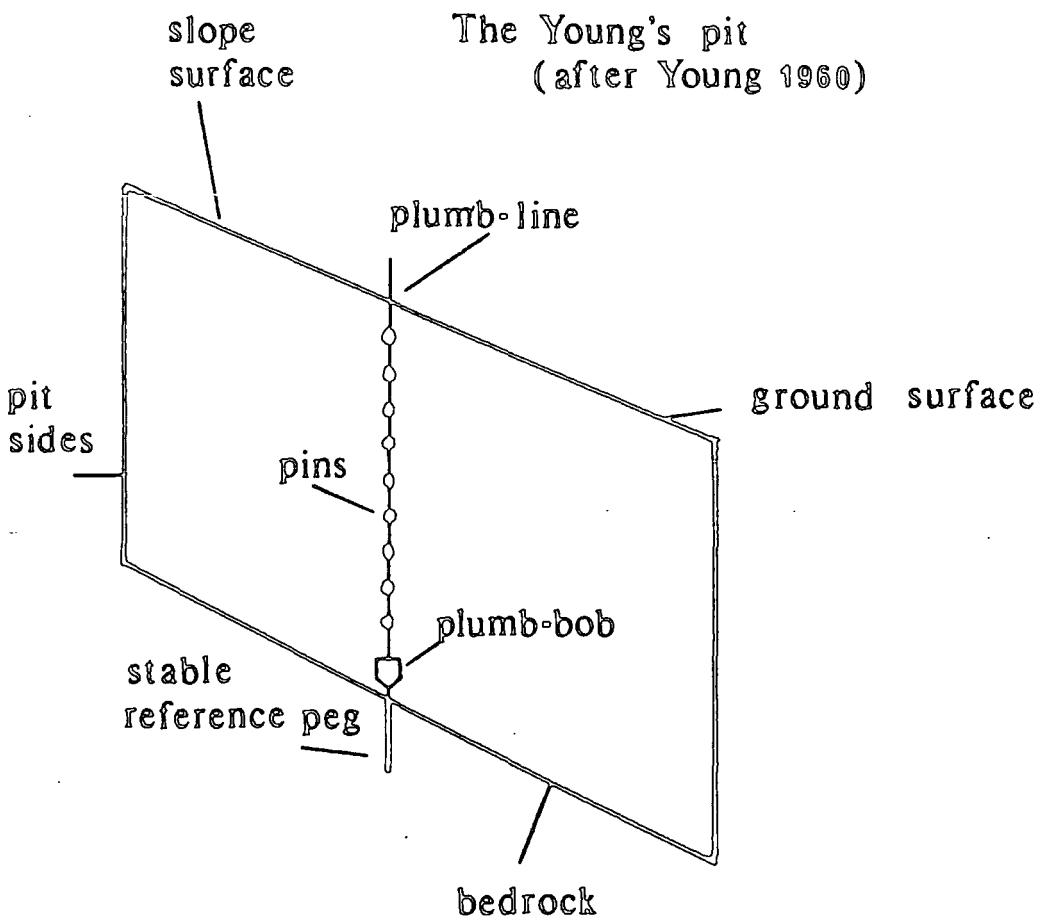
slope surface
The Young's pit (after Young 1960)
plumb-line
pit sides
ground surface
pins
plumb-bob
stable reference peg
bedrock

Anderson's Tubes and Inclinometer Pegs are rigid in the vertical or depth dimension and so they give only a relative volumetric measurement. The advantages of these techniques are:

(i) simplicity of design, operation and installation,

(ii) low cost and so ease of replication,

(iii) rapid measurement time allowing temporal changes to be monitored for many sites,

(iv) lack of ground disturbance on installation.

Inclinometer Pegs have been used extensively by previous researchers. Kirkby (1963) designed a T-peg with graduated spirit level as the measurement device. Evans (1974) used a similar T-bar modified from Kirkby's design to allow measurements to be taken in two orthogonal directions. The pegs used by both Kirkby and Evans were long, narrow metal rods. The Kirkby T-peg was 0.25 inch square steel rod 9 or 15 inches long with an adjustment mechanism as the top of the T. Anderson (1977) designed an inclinometer which allows angular readings to be obtained from wooden or aluminium pegs 1 cm^2 in section. Readings are obtained by inserting hard wood pegs vertically into the soil and fitting the inclinometer gently over the peg. The inclinometer tilt is adjusted by turning a graduated thread to pivot a spirit level (see figure 3.5). When the level lies horizontally the number of turns on the graduated thread can be directly converted to angle of tilt. The method assumes that the base of the peg is its pivot point. Since this is uncertain Anderson suggests inserting pegs to three sensible depths and comparing the results.

Other inclinometer devices have been used by Plantema (1953), Kallstenius and Bergau (1961), Morland (1978) and Kaiser (1980).

Anderson's Tubes, designed and used by Anderson(1977)measure the absolute displacement of a solid tube, inserted vertically into the

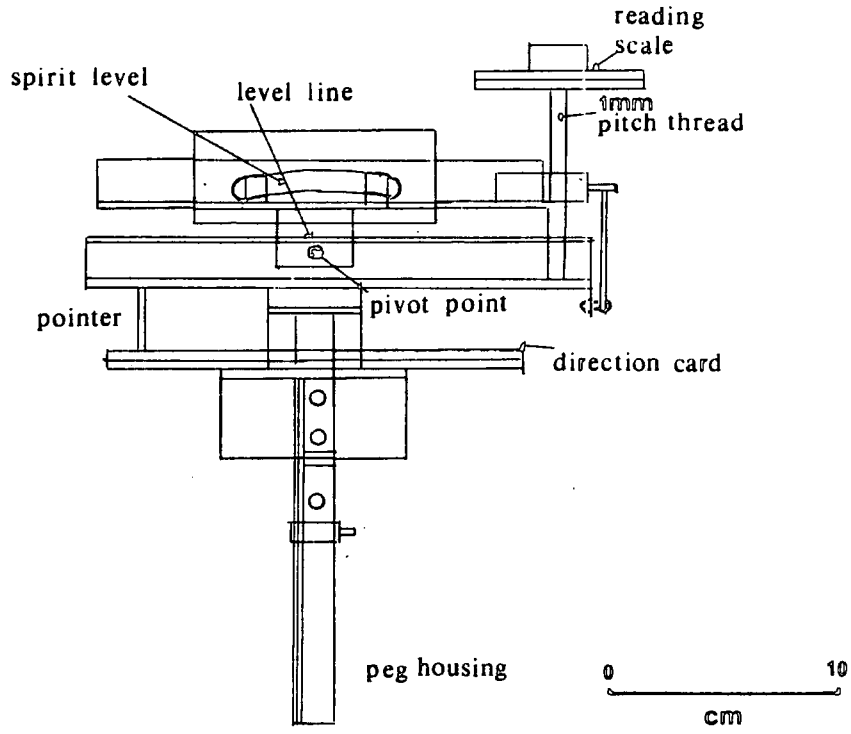

Figure 3.5 Anderson's Inclinometer
(after Anderson 1977)

Figure 3.6 Anderson's Tube.

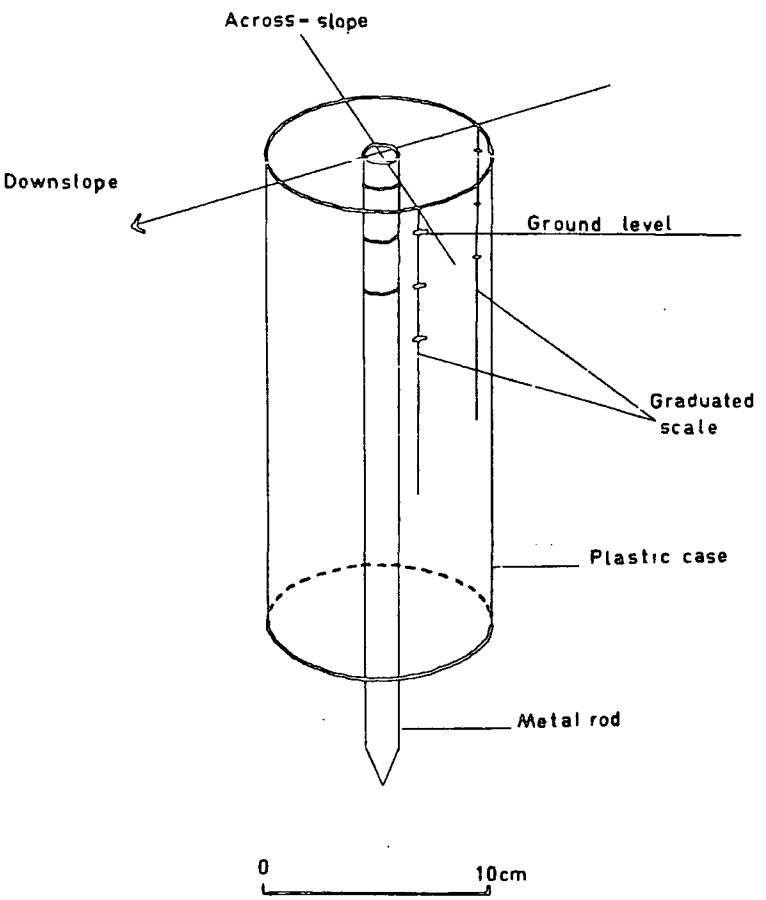

slope, relative to a fixed central metal stake (see figure 3.6). The technique measures relative mass movement, however, because it approximates the displacement/depth profile as linear.

3.2. Instrument selection

The field experiment requirements for S.M.M. data include (i) large numbers of sample sites, (ii) a volumetric measurement of S.M.M. and (iii) details of the displacement-depth profile. The large number of sample sites necessitated the adoption of simple instruments which could be widely replicated and still be easily compared. In addition it was important that measurements could be made at different time periods in order to assess movement trends. Consequently three techniques were chosen.

1. Anderson's tubes - absolute displacement
2. Inclinometer pegs - relative displacement
3. Young's pits - displacement-depth profile

These three devices yield complementary information on S.M.M. and are simple in design and easy to replicate. All three approaches make assumptions about the nature of the process but Anderson and Cox (1978) used these instruments in conjunction with dowelling pillars and Cassidy's tubes and found, in a two way factorial study, that differences between plots were much greater than differences among instruments at each plot. They also found that Anderson's Tubes, Inclinometer Pegs, and Young's Pits gave the most consistent results.

These techniques are ideal for assessing the effect of vegetation type and slope angle on the relative rate of soil mass movement. Following the example of Anderson (1977) the instruments have been

located in $1m^2$ sample plots in which the soil and environmental variables that may govern the process of movement are assumed to be constant.

The Anderson's Tubes and Inclinometer Pegs may be read at any time throughout the study while the Young's pits are excavated at the end of the study. It is important to analyse the temporal pattern of movement because a single measurement might represent a wild observation if the pattern of movement fluctuates. The presence of fluctuations could not be detected without close temporal sampling.

3.3. Sample selection

Table 3.1 illustrates the structure of a bi-factorial design which incorporates four slope gradient classes and four vegetation groupings. These samples were derived from the hillslope profile elements constructed from slope profile data described in Chapter 4. Samples were allocated by replacement random sampling of elements for each category until five elements filled each cell category. An additional ten sites were then allocated at random to any cell since it was envisaged that some sites would be disturbed during the course of the experiment.

An initial sample size of 80 sites was chosen based on the results of previous researchers who found that a small number of sample sites severely limited the statistical analysis of the data (Anderson, 1977; Rashidian, 1984). The sample size was also based on the number of sites which could be measured in a day. This sample gives a reasonable replication for each category in the design, thereby allowing wild observations to be detected. A larger sample size would have given given greater logistical problems.

Table 3·1 Sampling design of measurement plots

Slope angle classes (degrees)	Vegetation groupings			
	Juncus	Nardus	Pteridium	Heath
0-10	7	6 (6)	5* (5)	3*
11-20	(6) 5*	5	7	5
21-30	5 (5)	4*	5 (5)	1*
> 30	(7) 5*	6‡	+	+
Total	22	21	17	9

Slope angle classes (degrees)	Total
0-10	21
11-20	22
21-30	15
> 30	11
Total	69

\+ Cells incomplete due to lack of suitable field locations

* Cells incomplete due to site disturbance during measurement period

‡ Two sites in this cell partly disturbed during measurement period

( ) Original sample size

3.4. Instrument layout

Each of the chosen hillslope elements (5m) was located in the field. Then a 1 m^2 plot was located on an area of straight slope with homogenous vegetation cover. Each plot was subdivided into 9 equal 0.2 m^2 sub-plots using a quadrat as shown in figure 3.7. The following instruments were located at random into the 9 available sub-plots.

(i) 1 Anderson's Tube

(ii) 3 Inclinometer Pegs

(iii) 1 Young's Pit

(iv) 1 water table level inspection pipe.

The random allocation of instruments to plots ensures that no systematic bias in instrument performance occurs as a result of mutual interference. The design of the quadrat ensures that instruments are not located less than 0.3 m apart.

3.5. Installation

3.5.1. Inclinometer Pegs

Pegs were constructed from Ramin, a hard wood, that does not swell in contact with moisture and is very resistant to rotting. Three lengths of pegs were used 0.05 m, 0.10 m and 0.15 m into the ground with each peg protruding 0.05 m at the surface for measurement purposes. The peg was inserted into the ground by being pushed firmly at a constant rate with an inserter which has a housing similar to that

Figure 3.7

Instrument layout within plot

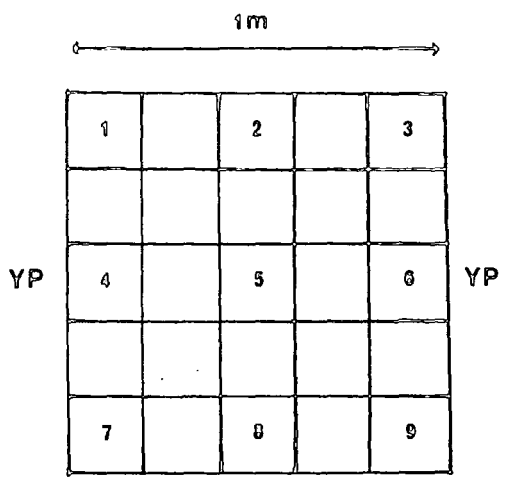

1 - 9 Instrument locations

YP Young's pit location

Figure 3.8 Inclinometer peg measurement

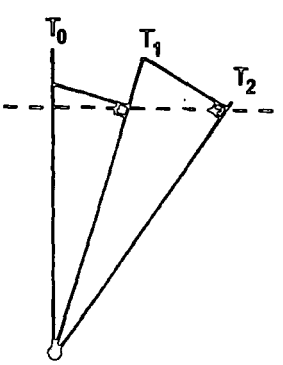

of the inclinometer. A reading was then taken to check the datum but the peg was left to settle for one month before the measurement program started.

3.5.2. Anderson's Tubes

These were constructed from rigid 10 cm diameter plastic piping cut to a height of 30 cm. The lower edge of the tube was sharpened to ease insertion into the soil and marks were fashioned on the inside of the tube at 5 cm intervals on two orthogonal long axes of the tube. These marks were carefully positioned and machined to allow the callipers to be positioned exactly on the measurement position at each time of reading. This was particularly important because without an exact sized recess the callipers could not be positioned accurately at the lowest position when the tube was installed in the soil, particularly if the ground water table was above the measured depth.

To install the tube, a 0.5 m corer was constructed. This had a 0.1 m outside diameter and was used to construct a 0.30 m deep hole in which a tube could be carefully inserted. The soil sample from the cover was then kept and used for analysing the physical and granulometric properties of the site. The tube itself was installed with the measurement axes facing upslope and across slope. The central measurement rod, constructed of toughened steel coated with anti-corrosive paint, was then inserted to a depth of 0.5 m. Each tube was designed to protrude 0.02 m above the ground surface to avoid it being infilled by surface wash, but for further protection a lid was also fitted.

3.5.3. Young's Pit

The procedure for installing markers described by Young (1960) was closely followed. First a narrow pit 0.5 m long by 0.4 m deep was excavated in the downslope direction. Then a perspex marker was positioned vertically within the pit and its position marked at the base with two metal pegs. Small 0.03 m lengths of welding rod were then inserted into the side of the pit at 0.01 m intervals through the correct positions in the perspex. The perspex was then removed and the rods pushed flush with the side of the pit before the pit was carefully refilled and a surface location marker installed.

3.6 Instrument measurement

3.6.1. Inclinometer Pegs

The tilt of each peg is measured along the axis parallel to the gradient of the slope. The inclinometer instrument is placed over the peg and clamped until firm. The adjustment screw is positioned 100mm from the pivot point of the peg and has a pitch of 1mm. The angle of tilt can can be calculated as $0^{o}\ 48'$ for each revolution of the measurement screw. If the peg is assumed to pivot at its base, and the base is stationary then the angle is converted into a volumetric measure using the cosine rule.

This method assumes that very high tilt angles are not encountered; otherwise the volume of soil moved would be underestimated if a right-angled triangle is assumed. This effect is shown in figure 3.8.

3.6.2. Anderson's Tubes

Anderson (1977) measured movement of the tube by reading the distance from the edge of the tube to the central rod at four cardinal points near the top and a further four points near the base. The position of the tube could then be plotted on a circular diagram and the overlay of subsequent diagrams allowed displacement to be plotted. In this study three orthogonal sets of measurements were taken at 0.05 m intervals from the top of the tube. If three readings are taken then a measurement error can be spotted by mental arithmetic in the field. This also indicates the level of precision to which measurements can be taken.

If the two measurement axes are labelled x and y with z indicating depth, then figure 3.9 illustrates how the results could be misinterpreted.

The direction of maximum displacement θ is calculated from:

$$cos\theta = \frac{\delta y}{(\delta x^2 + \delta y^2)^{\frac{1}{2}}}$$

A volumetric measurement was derived by calculating a least-squares fit to the 3 displacement measurements, then extrapolating that function to the zero movement axis to derive the depth at which the tube pivots. A FORTRAN program for this calculation is listed in Appendix A.

3.7 Summary of S.M.M. instrumentation

At each of the sample plots one Anderson's Tube, three Inclinometer Pegs and one water table inspection standpipe were installed. A Young's pit was installed at one site in each of the slope angle and

Figure 3.9 Anderson's Tube measurement.

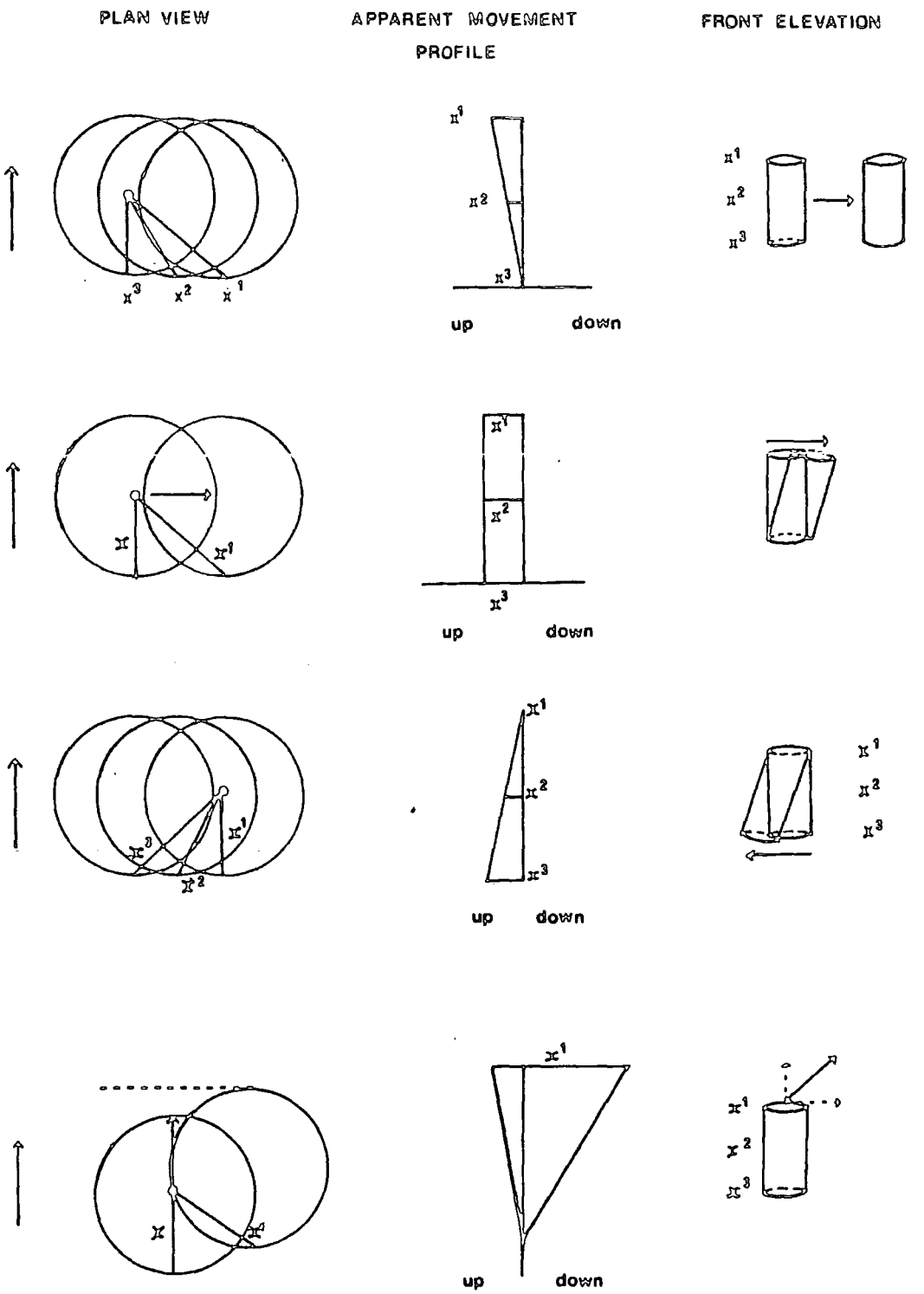

vegetation cover classes listed in table 3.1. During the period of the field experiment six Anderson's Tubes were vandalised and could not be replaced due to excessive site disturbance. Twenty-two of the 207 inclinometer pegs were disturbed and profiles from 2 of the 14 Young's Pits could not be reconstructed because pins could not be accurately relocated.

All the measurements were taken by the same operator, myself, and so operator variance is likely to be negligible. A reading was taken for each instrument at every plot in turn over a two day period at monthly intervals. The plots were always re-visited in the same order.

It is recognised that the instruments chosen will only yield information on the relative differences in S.M.M. among the different plots. However, the replication of different instruments in the same plot allows quantitative comparison of the consistency of results among the different instruments. Furthermore, each slope angle and vegetation class is represented by up to five plots and so the consistency of each instrument can be compared within the class.

The remaining difficulties of measuring absolute mass movement rates are not addressed in this thesis. The principal difficulty is to find an instrument capable of detecting subsurface displacement of soil particles without affecting the process by its presence. The disturbance of the soil fabric by installing buried markers is particularly unsatisfactory. The Anderson's tube and inclinometer peg cause the least installation disturbance of all the techniques examined. The results of this research can be directly compared with those of Anderson (1977) and Rashidian (1984) because these studies used the same type of instruments to measure S.M.M. in upland catchment areas.

3.8 Physical measurements of soil properties

Samples of soil were collected during the installation of Anderson's tubes at each experimental plot and from these granulometric and engineering properties have been derived in the laboratory. Previous researchers have emphasized the importance of correlation analysis in identifying the physical properties of the soil which influence S.M.M. (Evans 1974; Anderson 1977; Rashidian 1984; Auzet 1985).

3.8.1 Particle size analysis

The particle size distribution for each site was derived by following the test procedures BS-1377 described fully in British Standard (1975). Each sample was air dried then oven dried at 110^{o} C for 24 hours before being dry sieved using a stack to trap particles at 2000, 1180, 600, 212 and 63 μm. This divides the sample into coarse, medium and find sand, leaving silt and clay as the remainder.

Particles less than 63 μm were sized using hydrometer analysis BS-1377 test 7(D). This method was chosen because it allows rapid analysis of the large number of samples. The technique measures the density of a fluid in which particles are suspended. It is assumed that the fluid density is proportional to the percentage of particles in suspension and that particles fall out of suspension according to their diameter at a rate governed by Stokes' law. The density measurements were made using a mercury hydrometer and 1000 cm^3 measuring cylinder. Details of the hydrometer calibration for this analysis are given in appendix B.

Method

A 50 g sample is pre-treated with 150 ml of 30 % hydrogen peroxide and allowed to stand overnight in order to decompose any organic matter in the sample. The mixture is then filtered through a Buchner funnel before being transferred to an oven, dried at 100° C for 24 hours and re-weighed. 20 ml of sodium hexametaphosphate was added to the sample as a dispersing agent for the colloidal fraction and the mixture agitated in a drum mixer overnight to ensure thorough mixing. The suspension was then transferred to a 1000 cm^3 measuring cylinder and made up to 1000 cm^3 with distilled water. The cylinders were placed in a water bath to ensure a constant temperature of 20° C. Each cylinder was stoppered, re-mixed then the suspension left to settle. Readings of the density of the suspension were taken after the following prescribed time intervals.

Reading	Time elapsed
1	30 seconds
2	1 minute
3	2 minutes
4	4 minutes
5	30 minutes
6	1 hour
7	2 hours
8	4 hours
9	8 hours

The percentage of the total sample left in suspension can then be calculated from the nomographic chart published for test BS-1377 in British Standard (1975).

A typical cumulative particle size distribution is shown in figure 3.10. This shows, for example, that site 1/2 is a sandy silt with over 60

Figure 3.10 A cumulative particle size distribution for site 1/2.

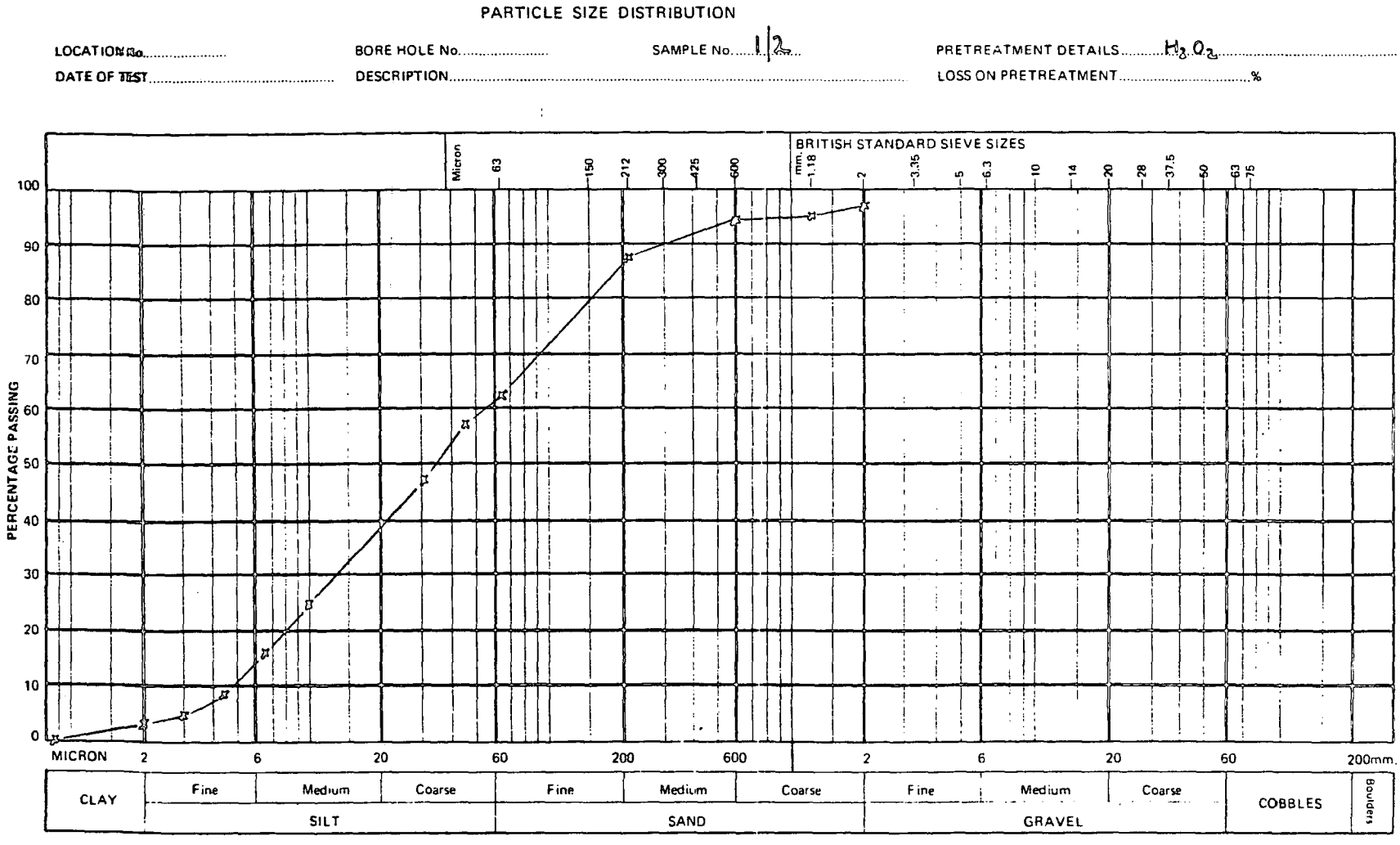

Figure 3.11

Particle size range for all sites.

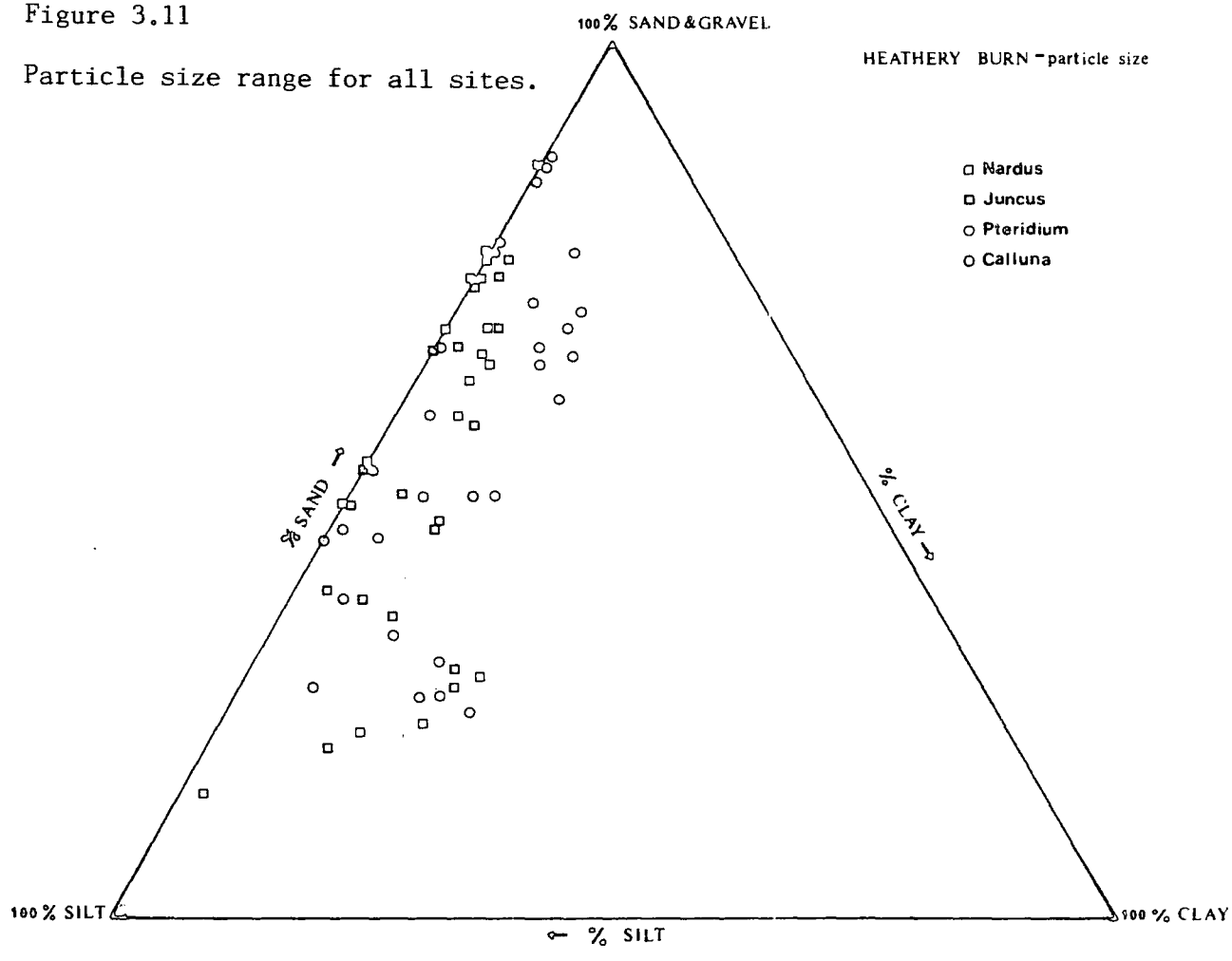

% of the sample consisting of silt and clay sized particles. Figure 3.11 summarises the sand, silt and clay particle size percentages for all sites and the cumulative distributions for all sites are given in appendix 2. Sites 1/1, 2/1, 2/3, 4/1, 5/2 and 6/2 have been omitted from this analysis because of the high organic matter content at each site. In each case only a few grammes of mineral material were recovered after the sample was treated with 30 % hydrogen peroxide.

3.8.2. Index tests of soil consistency

Measures of soil consistency describe how a soil may react to externally imposed forces. Practical test procedures can be derived to assess the influence of moisture on the mechanical behaviour of the soil. Soils can exhibit behaviour that can be classified into several rheological states according to its granulometric constituents and its moisture status.

Atterberg derived indices describing the moisture content of a soil as it passed from a solid to a plastic then to a viscous liquid state. These measures are collectively known as soil limit tests.

(i) Flocculation limit - mass wetness at which a soil suspension in transformed from a liquid to a semi-liquid state with an appreciable increase in volume.

(ii) Liquid limit - mass wetness at which the soil-water system changes from a viscous liquid to a plastic body.

(iii) Plastic limit - mass wetness at which the soil stiffens from a plastic to a semi-rigid and friable state.

(iv) Shrinkage limit -mass wetness at which the soil changes from a semi-rigid to a rigid solid with no additional change in specific volume as drying proceeds.

Figure 3.12 illustrates the nature of the limit tests.

Figure 3.12

Relationship between soil volume and moisture content

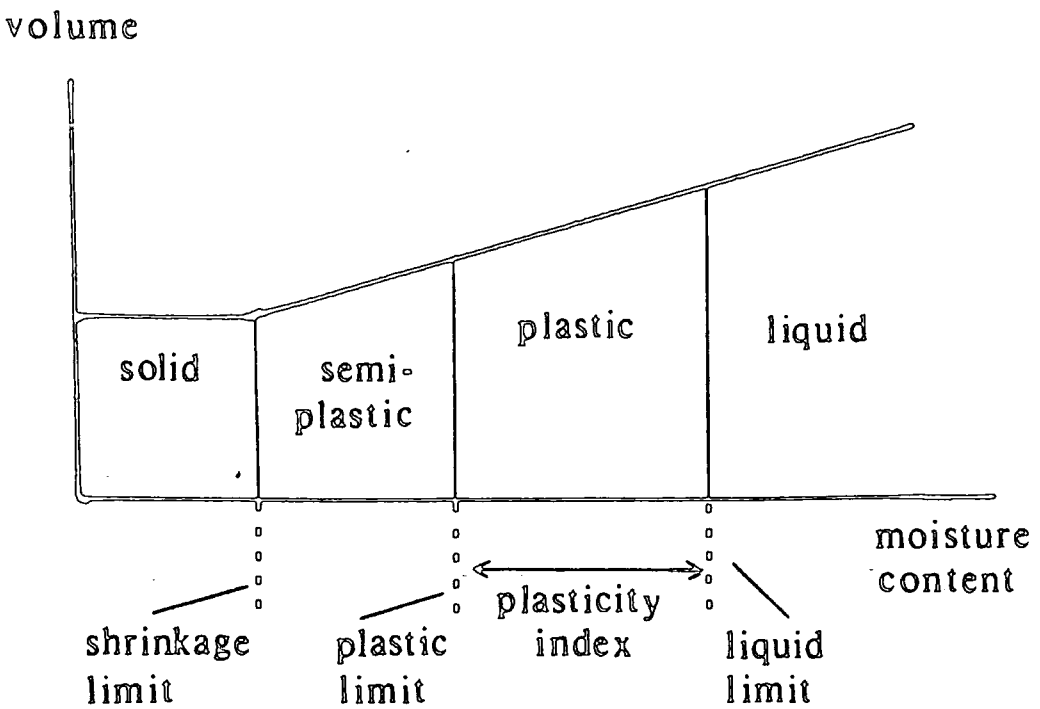

These tests have been widely adopted in the engineering description of soils for they provide a simple measure of soil consistency which can be interpreted easily. In addition, a further index can be derived.

(i) Plasticity index (Casagrande 1932). P.I. = liquid limit - plastic limit. This is a measure of potential plasticity and has been shown to depend on the nature and content of clay and organic matter in a soil.

The plastic limit, and derived indices which relate to it, are of particular importance to the study of S.M.M. because it is the transition from a brittle to a plastic state that may promote downslope movement. The plastic limit is an important criterion in agricultural soil management (Archer 1975) and in civil engineering it has been shown to be related to drained internal frictional angle.

Two methods of testing exist: the Casagrande (1932) method and the drop-cone penetrometer method of Campbell (1976). A number of studies have been made to compare the techniques and results show that the Casagrande method gives poor reproducibility and the methods yield slightly different results (Sherwood 1970; Davidson 1983; Moon and White 1985).

The drop cone penetrometer, unlike the Casagrande method, is not subjective and is determined using a range of moisture contents. In addition Campbell (1976) suggests that the minimum of the moisture/cone penetration curve indicates a physical change in the state of the soil which is a better indication of the plastic limit than the Casagrande plastic limit (brittle-plastic). The plastic limit as determined by the fall cone penetrometer corresponds to the maximum soil compaction (Campbell *et al.* 1980) and is therefore an important result. An important relationship exists between cone penetration and the shear strength of cohesive soils (Skempton and Northey 1952) and

Wood and Wroth (1978) and Wood (1985) suggest that soils with water contents close their liquid limits have unique shear strength (1.57 kN/m^2) as determined by the British Standard test in British Standard (1975).

Test procedure

The soil is pre-treated to pass through a 425 μm BS test sieve and equilibrated with water for 24 hours. The soil is then placed in a test cup and a 30^o cone of mass 80 g is dropped from rest into the soil with the tip of the cone just in contact with the soil surface. The penetration is recorded and the moisture content calculated. The test is then repeated with a range of moisture contents until a curve is derived (see fig 3.13). The liquid limit corresponds to the moisture content of a cone penetration of 20 mm and the liquid limit is the minimum of the curve.

The soil samples were not pre-treated other than by air drying and dry sieving. Where possible the aim was to test the behaviour of the natural soil. However, samples from sites 1/1, 2/3, 3/4, 4/1 and 6/2 could not be tested due to excessive organic content. The samples will also differ from the *in situ* soil due to their lack of compaction. In order to assess this effect two samples, one organic and one mineral, were tested using artificial compaction. The organic sample showed a small difference in liquid limit but the mineral soil showed no significant difference between the standard samples and sample compacted with a 350g weight. Plastic limits remain unaffected by compaction (see figure 3.14).

Figure 3.15 shows the soil index values for the Heathery Burn samples. Liquid limit values for most samples lie in the range from 40% to 80% but sites with high organic matter contents give exceptionally

Figure 3.13 Typical liquid limit test curves

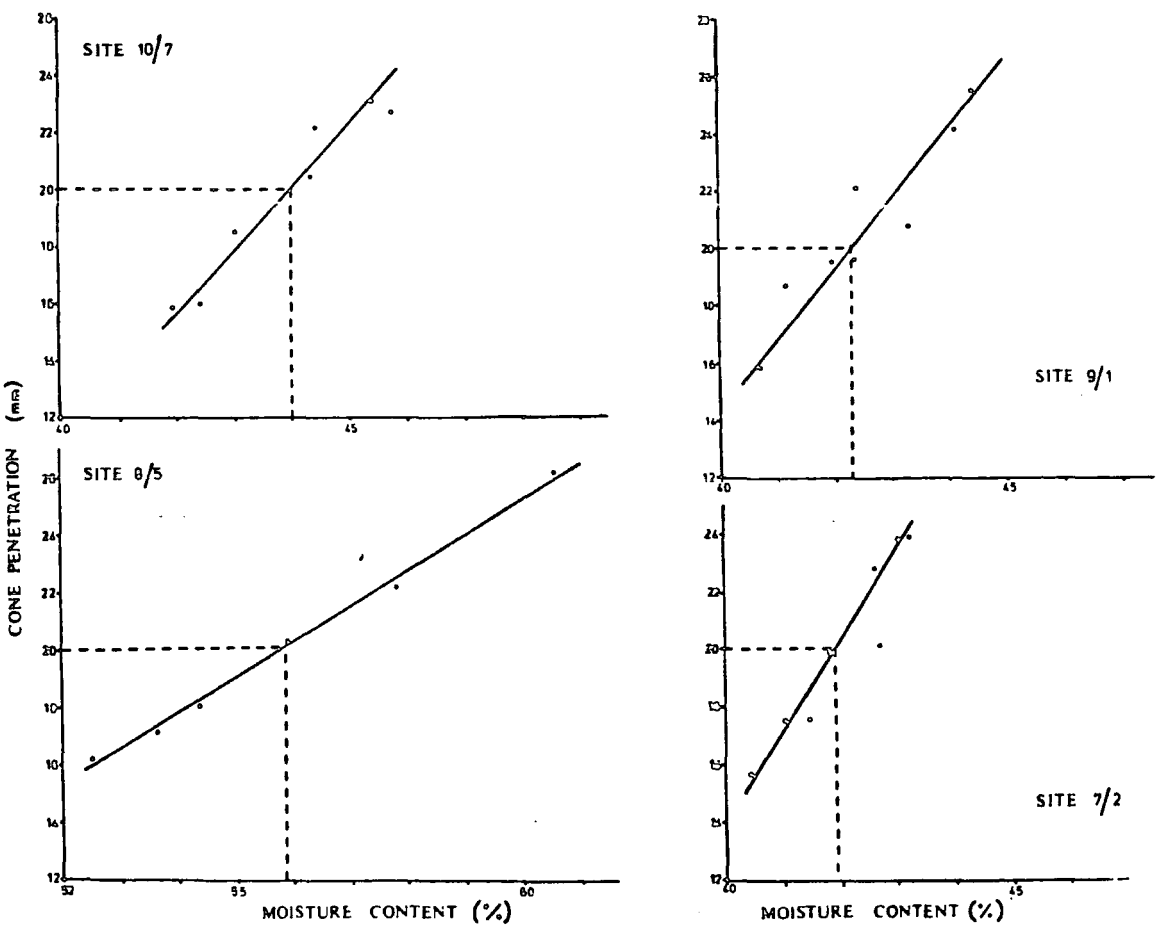

Figure 3.14 Plastic limit determination from drop-cone penetrometer.

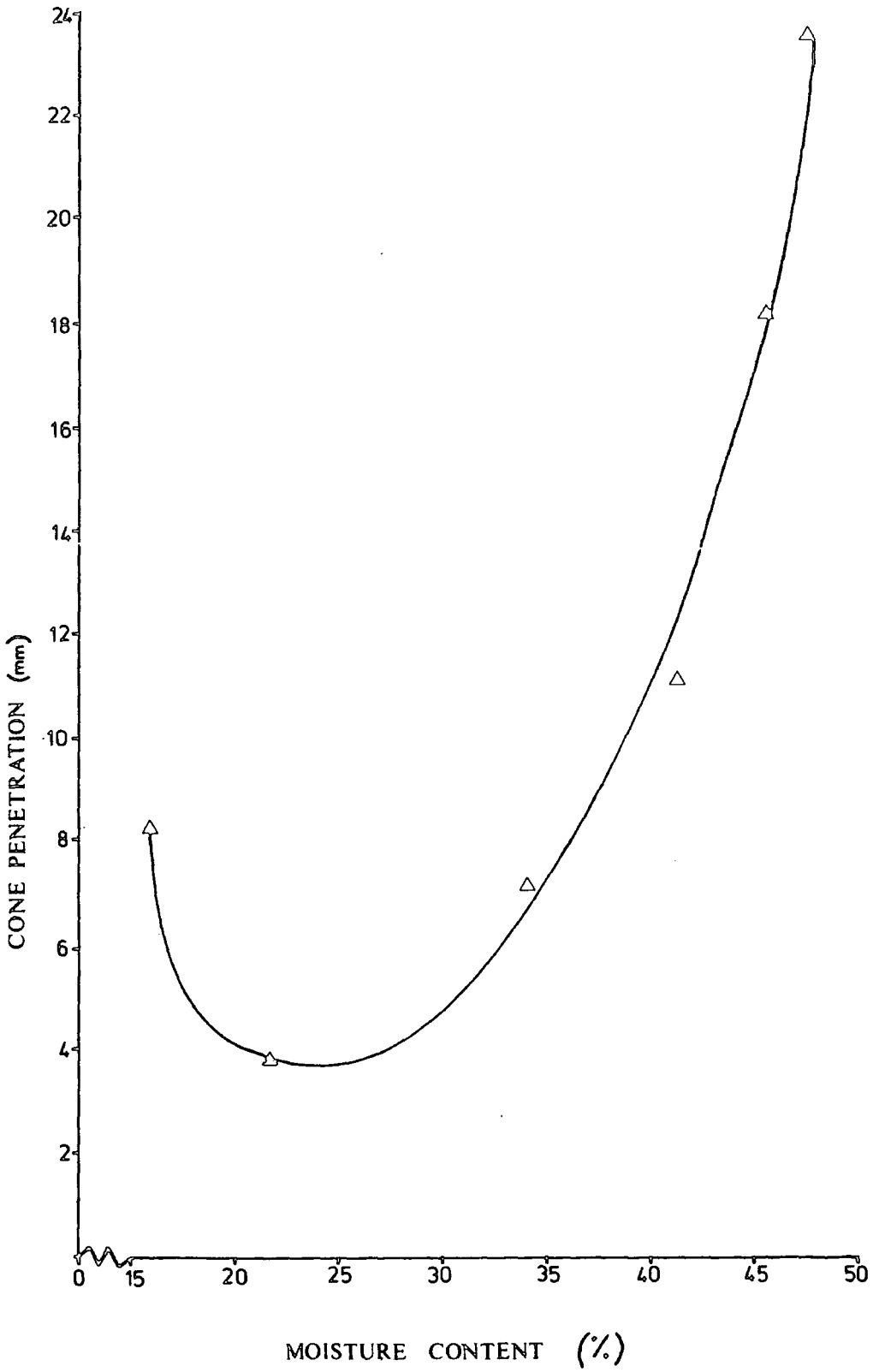

high limits. Site 5/2 and 2/6 yield results which appear anomalous.

3.8.3 Soil strength characteristics

The strength of soil is usually expressed as the maximum force which can be exerted on a soil body without causing the body to fail. The strength of a soil is particularly affected by its textural characteristics, moisture status and the direction and rate in which it is stressed. In order to relate strength characteristics to S.M.M. in the field it was decided to measure strength *in situ* using a portable shear vane testing method. This approach measures the torque required to shear a column of soil using a vane with a width to height ratio of 4:1. The test does not measure ϕ' ,the internal friction, of the soil but it gives a rapid measure of relative shear strength in the field. It is also capable of measuring multiple readings to obtain a depth profile without extracting the vane.

Perhaps most importantly a field based technique allows soil strength to be monitored through time and so a measure of the range of a soil's strength can be derived.

Test procedure

The instrument used in this study was a GEONOR field inspection vane (Geonor 1975) see figure 3.16. The instrument consisted of a handle with opposing calibrated springs attached to a dial. A medium-sized vane 4 cm x 1 cm was attached to the instrument and the shear strength of the soil measured by slowly rotating the vane in the soil sample until the reading on the dial became constant. The test was then repeated three times and the average reading calculated.

Shear strengths measured in kN/m^2 were then derived from the

following equations.

$$T = C\pi(\frac{1}{2}d^2h + \frac{1}{3}d^3)$$

$$C = \frac{3T}{28\pi r^3}$$

T = Torque required to shear soil (kN/m^2)

h = Height of vane blade

d = Width of vane blade

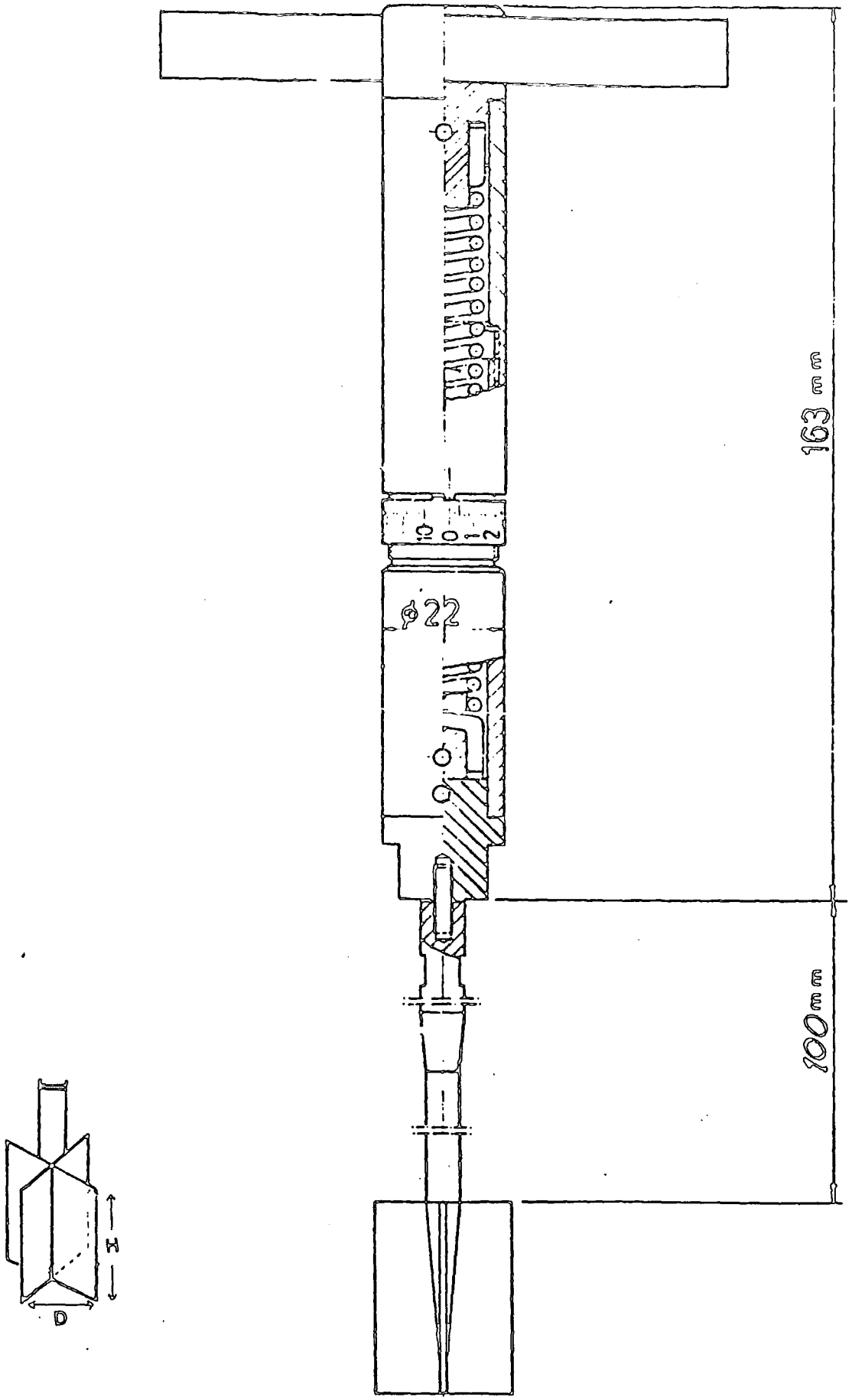

Figure 3.15 Geonor field inspection vane.

Chapter 4

Contents

Catchment area study

4.1 Aims

The drainage basin is the fundamental spatial unit for the study of fluvial processes. The understanding of water and sediment dynamics within this open system is a continuing challenge and this thesis aims to provide a quantitative appraisal of the importance of slow mass movement (S.M.M.) processes in sediment transport on hillslopes within a first-order catchment. It also seeks to test hypotheses about controlling variables and temporal patterns of S.M.M.: many geomorphologists consider ubiquity and continuity of operation to be fundamental characteristics of S.M.M. and these tenets have yet to be challenged.

Despite attempts to relate sediment mobility to catchment variables, such as hydraulic radius, channel gradient and stream order, the interaction between the drainage network and basin slope processes remains obscure.

Intuitively, one would expect the relationship between channel gradient and adjacent hillslope gradient to govern sediment delivery processes and rates from slopes; however, such interdependence is often not evident at the level of the individual stream (Carter and Chorley, 1961). Richards (1982) suggests that this may reflect the ability of streams to adjust in their cross sections, as well as in their gradients, to maximise sediment transport capacity, and also the dependence of sediment entrainment upon stream power, which is a function of both gradient and discharge.

In order to relate channel form and hillslope form, detailed process measurements need to be made within an individual drainage basin. Slow mass movement measurements have rarely been available in sufficient quantity

or quality from first-order catchments to test the assertions of Carter and Chorley (1961) and Richards (1982).

Many models of slope processes have assumed that S.M.M. rate is proportional to some function of slope angle and many studies of sediment budgets have averaged the effect of S.M.M. over space: both these actions have the effect of minimising any observed relationship between channel and hillslope form, in terms of adjustment to sediment transport capacity.

The first-order drainage basin is also a convenient physical representation of a cascading sediment system, in which the spatial pattern of sediment transport can be identified and monitored relatively easily, and so it offers several practical advantages over a more widely dispersed study. First, it allows close spatial sampling of slope and soil units, thereby providing the necessary replication of instrument sites on such units that would be needed in order to isolate controlling variables in an experimental framework. Second, a standard spatial unit of measurement (drainage basin order) enables broad comparisons to be made between different erosion or transportation processes within catchments and comparison of similar process rates between catchments. Third, it is recognised that sediment storage within small catchments is poorly documented. However, storage sites such as swales, terraces and lochans provide a wealth of palaeoenvironmental data which may be used to date erosion events or to document the nature of sediment movement paths in catchments.

It is important to be able to estimate parameters associated with the physical structure of a drainage basin which will influence any given geomorphological process for useful, quantitative-geomorphological models are built from the marriage of appropriate geomorphometric variables and accurate empirical process measurements: the first-order catchment provides a

suitable spatial framework for both empirical process and geomorphometric measurement.

The selection of an individual catchment immediately introduces selection bias as the particular combination of environmental conditions and landforms at any one site is likely to be unique. For this study a location was sought which embodied as diverse a set of slope facets as possible in order to sample the likely range of S.M.M. process rates in situ and yet have enough variability (as well as measurement site replication) to allow an experimental treatment of the data where certain variables are held constant while others vary widely. For example, measurement plots located on slope facets of similar inclination may exhibit a wide variety of soil moisture conditions, even for soils with similar structure and particle size composition, and so slope angle can be controlled for; in this way the influence of key variables such as the moisture status of soil on S.M.M. can be assessed quasi-experimentally in the field.

Five factors were considered in detail when selecting the experimental catchment:

1. Environmental variability,
2. Catchment size,
3. Land use,
4. Accessibility,
5. Availability of secondary data sources.

A central tenet of geomorphological research is relating process to form, and so the cornerstone of the field research design is the identification of geomorphometric variables which may be used either singly or in combination to predict S.M.M. Slope gradient, slope curvature in profile and slope curvature in plan seem to be the most important, as these relate directly to the

pore water pressures and stresses found in hillslope soils. Variation of these factors is caused by changes in environmental variables such as geological setting, soil type, vegetation phenology, slope drainage, aspect.

In the first instance a catchment was chosen which displayed diversity in such variables before detailed geomorphometric surveying was used for the fine tuning of experimental design. The other four selection criteria are essentially practical requirements of field-based measurement and experimental studies. The catchment should be large enough to allow a large number of instrument stations to be located without mutual interference, yet should be small enough to allow all the major hillslope facets to be sampled and the spatial distribution of the process in the catchment to be mapped. It is assumed unless otherwise stated that this study relates to natural rather than disturbed or cultivated soils: enclosed pasture and arable land are omitted altogether. It was fortuitous, and fortunate, that several rain gauges were in the close vicinity of one particularly suitable catchment, thereby reducing some of the task of secondary data collection.

The chosen catchment is located in Weardale, Northern England, at national grid reference NY 84 990 415 and is locally termed Heathery Burn (figure 4.1). It is a first-order catchment which faces predominantly S.W. and it has an altitudinal range of 275 m to 430 m. Valley-side slopes are soil covered to a minimum depth of 25 cm and alluvial and colluvial valley-bottom fill extends to a maximum depth of 3.5 m below ground surface in isolated localities. The catchment also provides a suitably wide variety of soil types, vegetation phenology and bedrock types within the relatively small area of 35 ha.

The following two sections in this chapter describe the physical setting and geological history of the catchment as well as its morphology and geomor-

Figure 4.1
Heathery Burn Catchment Area

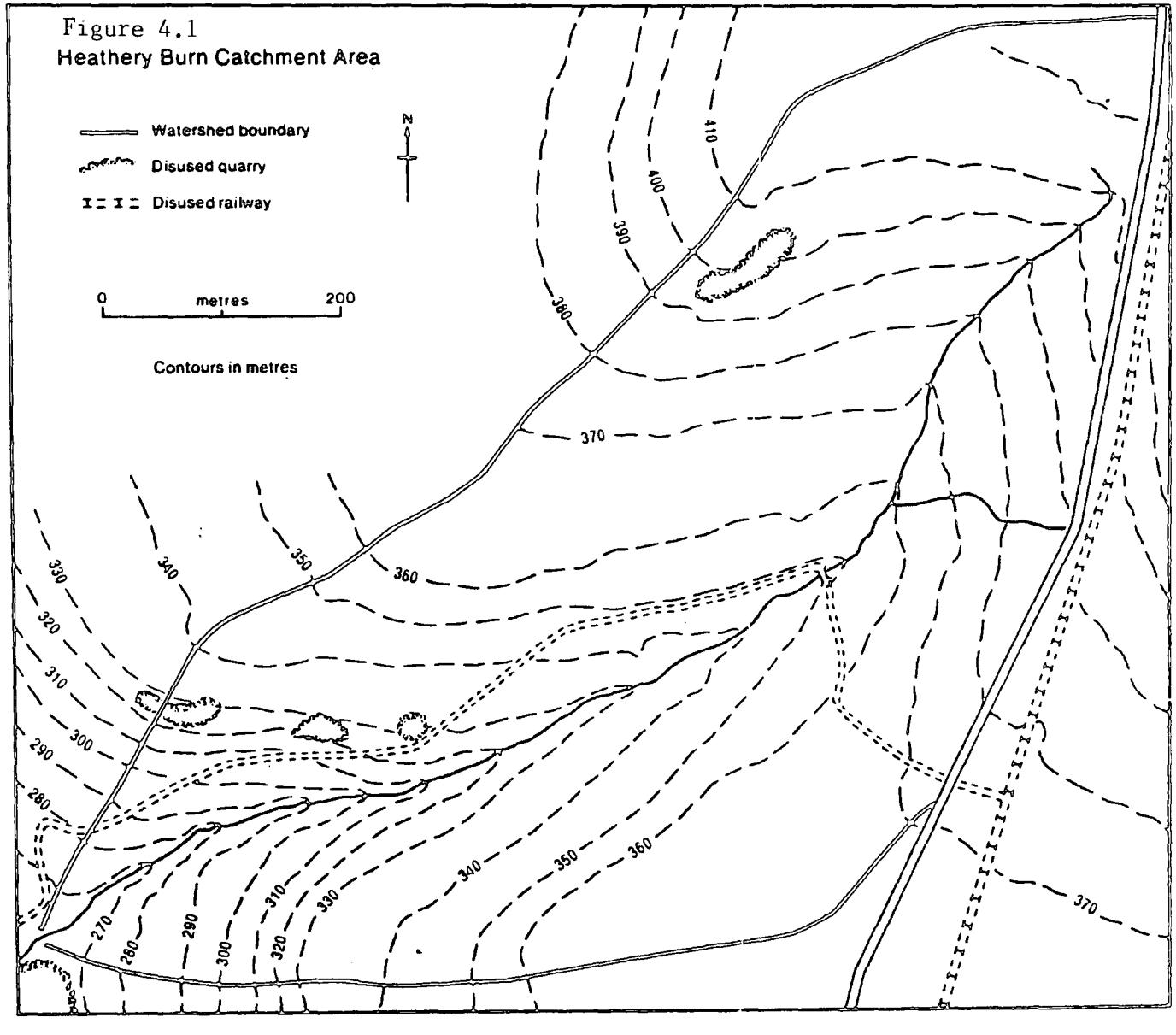

phometry. The fourth section describes the experimental design for S.M.M. instrumention and measurement and it outlines the inherent assumptions, biases and possible sources of error associated with geomorphological experimentation in the field.

4.2 Physical setting and geological history

Heathery Burn catchment is located on the east flank of the Pennine anticline on Carboniferous sedimentary rocks. The structural geology of the site is dominated by the post-Hercynian development of the Alston block which resulted in the intrusion of granitic sills and extensive local mineralisation. Uplift of the Alston block horst is strongly associated with isostatic adjustment due to the presence of low density Devonian granite at the base of the Carboniferous sediments. The typical cyclothem stratigraphy observed in this area may be explained in part by isostatic controls over sedimentary environments and processes (Johnson, 1967).

The stratigraphy in this basin (figure 4.2) consists of rocks from the Upper Limestone Group of the Carboniferous Limestone series (Dunham, 1946). At its confluence with Stanhope Burn, Heathery Burn dissects the Great Limestone which is the basal member of the Upper Limestone Group (figure 4.2). The sequence is completed by rhythmic alternations of shale, sandstone and limestone, capped by a succession of thick sandstone sills intercalated with thin shale beds in the uppermost parts of the basin. Such a succession is typical of the Upper Limestone Group (Dunham, 1946) and reflects a series of alternations between marine and deltaic depositionary environments. Where sandstone strata outcrop cross-bedding is well formed

Figure 4.2

Stratigraphic section of Weardale cyclothem

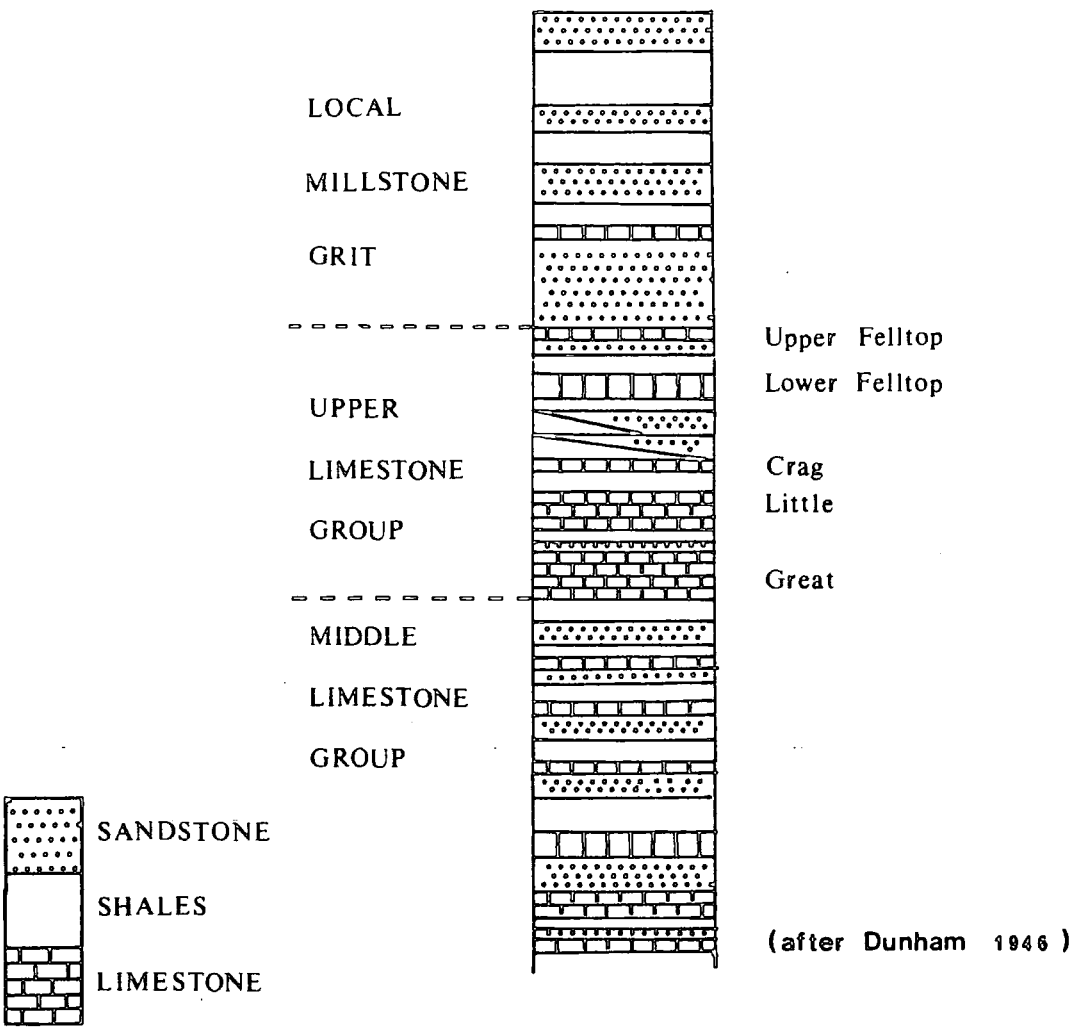

and clearly visible and at one site channels can be identified from the sedimentary sequence and from the presence of coarse pebbly lag deposits.

Resistant sandstone sills, which have a gentle north-south regional dip of 5°, give the surface topography a characteristic stepped appearance where adjacent less resistant strata have been eroded more intensely. To some extent, however, the solid geology is obscured by soil, colluvium, alluvium and glacially-derived deposits.

At a regional scale Pleistocene glaciations have certainly contributed to the erosional development of the Pennine Dales, through the action of ice abrasion and plucking, and fluvial erosion by glacial meltwater, yet the lack of dramatic landforms of glacial erosion suggests that ice was locally derived and restricted in its effect to minor resculpturing of the uplifted palimpsest of the Tertiary peneplain (Trotter 1929).

No firm evidence has been found in Upper Weardale for pre-Devensian glacial advances although Atkinson (1968) suggested that the lower boulder clay of County Durham may represent a pre-late-Devensian till or a late-Devensian stadial deposit.

In upper Weardale lodgement till is found in isolated parts of the valley floor and is certainly of late-Devensian age (Falconer, 1970). Such till deposits contain clasts of local sedimentary rock types in a sandy clay matrix: no exotic erratics were found in this till by Howse (1889), Dwerryhouse (1902) or Falconer (1970). Only Atkinson (1968) cites an example of a Lake District erratic found in north-west Weardale at an altitude of 2200 feet (670 metres). The former evidence, together with the lack of distinctive erosional features on the interfluves and the lack of till on interfluves and valley hillslopes, led to the conclusion that Weardale contained only local ice and possibly only a valley glacier during the last glacial maximum (Dwerryhouse,

1902; Raistrick, 1931).

Vincent (1969) and Falconer (1970) argue against this model from sedimentological analysis of the local deposits. Re-mapping of glacial meltwater channels in this study supports their argument.

Vincent attributes a subglacial origin to coarse diamicton deposits lying on the South Tyne-Wear watershed. Clast orientations within these deposits indicate active ice movement from the north-west, that is, from the South Tyne to the Wear. The distribution of diamicton deposits was shown to be heavily influenced by topography (Vincent, 1969; Falconer, 1970).

Several researchers have considered the distribution and genesis of glacial meltwater channel features in North East England (Dwerryhouse 1902; Kendall 1902; Raistrick 1931; Maling 1955; Peel 1949. 1956; Sissons 1960; Clapperton 1966; Vincent 1969 and Burgess and Holliday, 1979).

Despite this research, Weardale has never received detailed analysis. Figure 4.3 shows a number of newly mapped features found in central and upper Weardale. Although many channels are small-scale features, only a few metres deep and a few hundred metres long, their location and distribution are inconsistent with the valley glacier hypothesis of Dwerryhouse (1902). The altitudes of channels A, B and C (figure 4.3), which are major features, are particularly significant as each bisects or lies close to a major interfluve. Channels A and B have humped long profiles and intermittent courses which strongly suggest a sub-glacial origin: that is, a *Nye* channel cut into bedrock by meltwater under high hydrostatic pressure (Nye 1973). The origin of channel C is more controversial as this has been disturbed by 18th and 19th century activity: however, it displays many characteristics of a Nye channel.

A recent reappraisal of subglacial meltwater hydrology and erosion by Hallet (1979) suggests that many Nye channels form under active ice rather

Figure 4.3 Glacial meltwater channels in Northern England

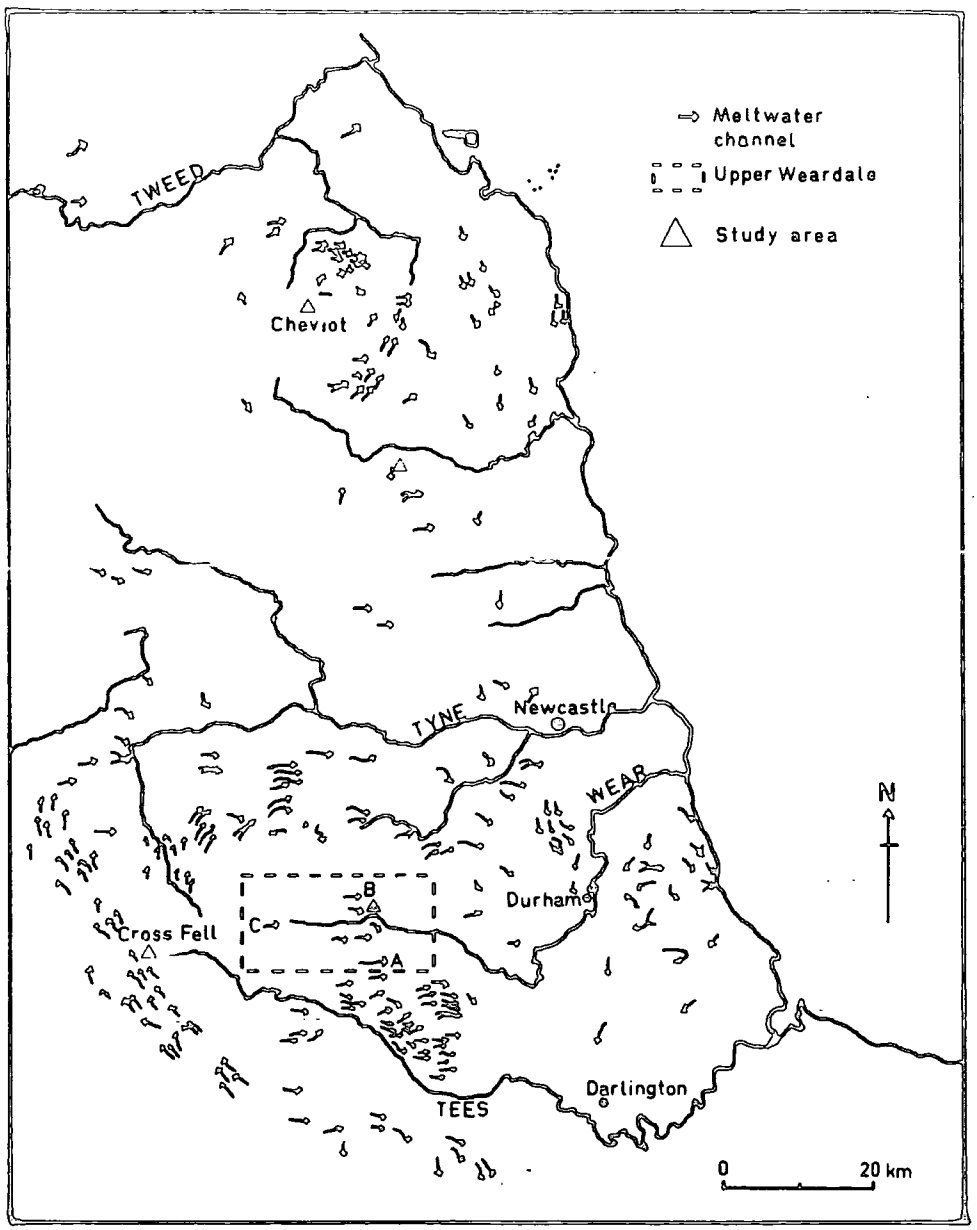

than during deglaciation, the prevailing hypothesis. Such a model, if correct, would help to explain the otherwise anomalous topographic location of these channels. Other smaller meltwater channels in Weardale are best developed on the lee (east) side of ridges which lie transverse to the line of the main Wear Valley indicating strong topographic control over channel formation. A similar topographic effect was observed by Clapperton (1966) for channel distribution in the Cheviot massif and surrounding area.

The meltwater channel evidence indicates complete inundation of the Wear Valley by active ice flowing with a west to east surface gradient at some period during the Pleistocene. Dating of channels is not possible, but the freshness of many channels suggests a late-Devensian origin.

The superficial deposits of Weardale have been mapped in detail by Maling (1955), Atkinson (1968) and Falconer (1970) and can be broadly classified into glacial till, solifluctate, soils derived from colluviation or weathering and unconsolidated debris derived from mining activity. According to Atkinson (1968) the pedology of upper Weardale can largely be explained in terms of the distribution of parent materials. The upland regolith often shows a stratified morphology with an upper layer of coarse sub-angular clasts of Carboniferous sandstone, a second layer of fine sandy loam which grades into a third layer of coarse angular material towards the bedrock (Atkinson, 1968). Such stratification is evident for deposits in the Heathery Burn catchment area as well as in other areas of Weardale. This probably arises from intensive cryoturbation processes during the late glacial and early Flandrian periods. The particle size distribution of this material falls within the range for frost susceptibility suggested by Corte (1963) (see Falconer 1970).

The glacially derived diamicton is the dominant superficial deposit in the Heathery Burn catchment area. Hillslope colluvium, swale fills and soil pro-

files are derived or developed from this material. In a few places weathered sandstone and mining spoil provide the parent materials for soil development. The general uniformity of parent material explains why soil development is closely related to the moisture status of the site. Using the terminology of the soil classification of England and Wales (Avery, 1980), well drained sites have developed as Humoferric podzols or Acid Brown earths whereas poorly drained sites have developed as Stagnopodzols, Stagnohumic gley soils and surface water gley soils.

The distribution of surface vegetation within the catchment is clearly related to the moisture status of the soils and so also related to the distribution of soil types. The vegetation distribution has been classified into four broad groups with associated species.

1 Calluna heath. *Calluna vulgaris, Eriophorum vaginatum, Poa pratensis, Erica tetralix.*

2 Nardus grassland: *Nardus stricta, poa pratensis. Poa augustinfolia, other grasses.*

3 Bracken heath: *Pteridium aquilinum, various mosses and lichens.*

4 Juncus bog: *Juncus squarrosus, Juncus effusus, Sphagnum rubellum, Sphagnum recurvum, various mosses and liverworts.*

This vegetation suite, representing an open upland heath environment on acid soils, is typical of much of the Pennine uplands.

Palaeoecological studies using pollen analysis have been undertaken by several researchers at eight sites within an 8 km radius of the catchment (Raistrick and Blackburn, 1931; Roberts, Turner and Ward, 1970; Hodgson, 1974; Turner and Hodgson, 1979, 1981). However, only pollen diagrams from Fortherley Moss and Pow Hill cover the whole of the Flandrian period and these show several unusual features departing significantly from the pattern

described by Godwin (1940).

There appears to have been a long pioneer phase dominated by *Betula* and hardy shrubs before climatic amelioration allowed the introduction of *Pinus* followed by *Quercus* and *Alnus* after approximately 7000 years B.P. (Turner and Hodgson, 1981). The Pow Hill diagram indicates that *Pinus* persisted in upland areas until the Iron age in marked contrast to the rest of Britain. Extensive evidence suggests that a dramatic change from a woodland environment to one dominated by the heathland and grassland taxa of today occurred within the late Iron age or Roman periods, 300 B.C. to 200 A.D. (Turner 1979).

The untypical nature of the vegetation history of this locality when compared with other sites in northern England suggests that thin acid podzolic soils have persisted since late Flandrian I. The exposed location of the Pow Hill and neighbouring sites implies that much of the input has been transported from the surrounding region, perhaps a few kilometres in extent. Small bogs such as that at Bollihope common are more likely to have collected locally derived pollen rain (Roberts, Turner and Ward 1970).

Present-day ecological change in the Heathery Burn catchment area is associated with land use practices. The principal land use is as open pasture for sheep. Unenclosed land is designated common grazing and used by several farms. Enclosed land is owned by one farm but is still used as unimproved pasture. Upper heathland is extensively used for grouse breeding and shooting.

Land management practices here include open ditch field drainage, periodic and restricted burning of the *Calluna* heath, enclosure and road maintenance. The drainage of wetland is seen as an important step towards increasing the productivity of the land both for grouse nesting sites and for

the provision of better quality grazing. Both burning and drainage have dramatically increased abiotic transfer of organic and inorganic materials within the catchment. The effects of such practices on S.M.M. and on the sediment budget of the catchment will be discussed later.

Artefacts of former mineral mining can be seen in the lower part of the catchment area; Stanhope Burn mine produced lead ore and fluorspar before closing in 1983.

Local mineral veins have been mined at periodic intervals since the Bronze age (Smith, 1923). The first documentary evidence dates from the 12th century but the heyday of mining activity in the Durham Dales was during the 19th century when galena, fluorspar and barytes were all extracted. The disused Stanhope to Edmondbyers railway, which bounds the catchment on the north-east, and associated sandstone quarrying date from this period. Apart from the obvious disruption to slopes and superficial soils and sediments, mining activity has caused localised ecological disturbance through the pollution of soils by toxic metals such as lead, cadmium and arsenic. Atkinson (1968) also notes the effects that lead and manganese presence can have on soil profile development.

The climate at Stanhope is temperate maritime with a mean annual rainfall of 950 mm, a mean annual temperature of 7.5° C and a range of mean monthly windspeeds of 6.0 to 16.2 $m.s^{-1}$. Northumbrian Water Authority manage five rainfall stations within 5 km of the catchment: those at Stanhope and Waskerly 3 represent the lower and upper altitudinal extremes. The monthly rainfall figures are summarised by box plots in figure 4.4. The box plot divisions represent the maxima, minima, median and upper and lower quartiles of the data. At Stanhope the ten-year monthly medians show rainfall levels to be relatively constant throughout the year: levels

Figure 4.4

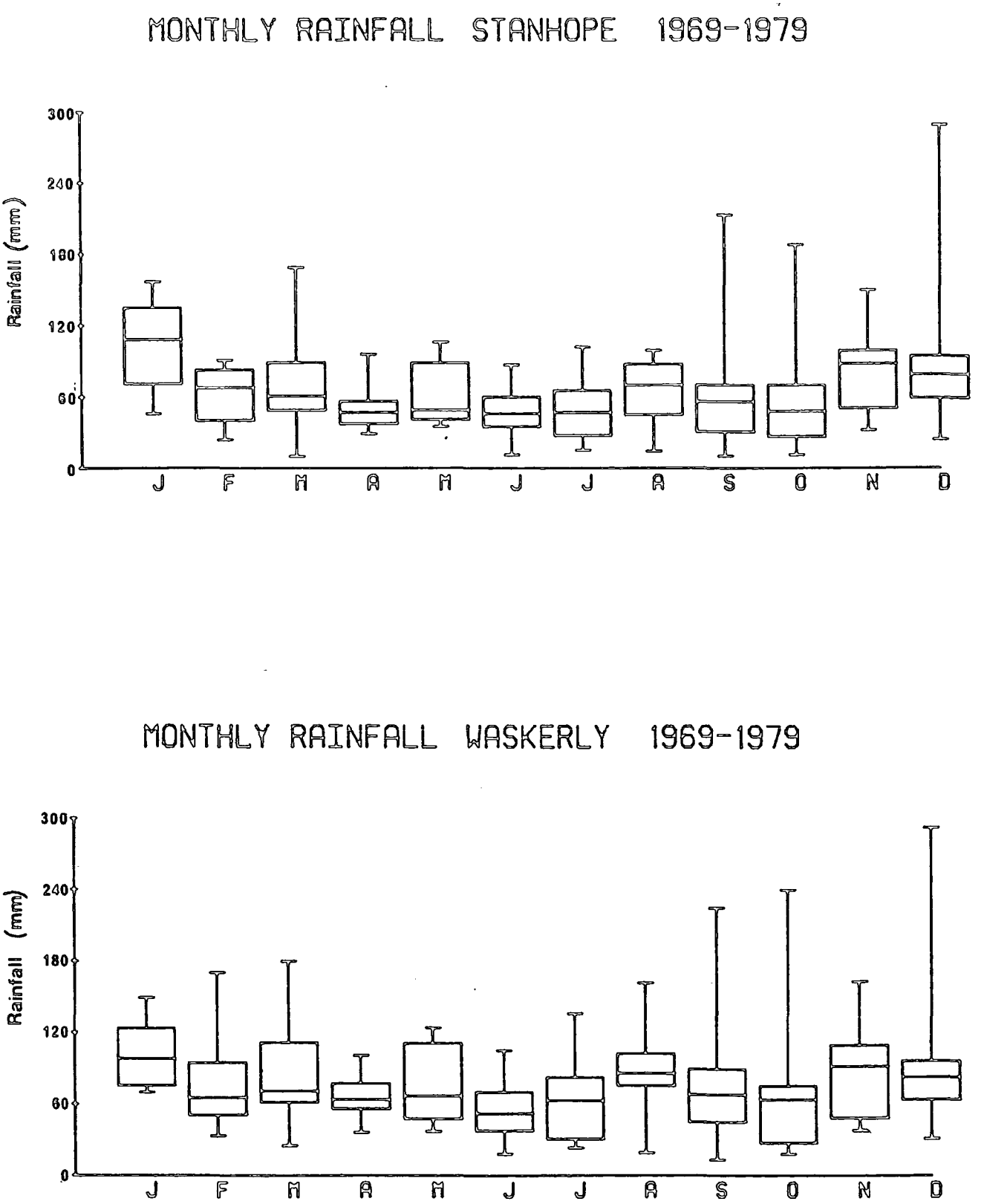
MONTHLY RAINFALL STANHOPE 1969-1979
Rainfall (mm)
300
240
180
120
60
0
J
F
M
A
M
J
J
A
S
O
N
D
MONTHLY RAINFALL WASKERLY 1969-1979
Rainfall (mm)
300
240
180
120
60
0
J
F
M
A
M
J
J
A
S
O
N
D

are marginally higher at Waskerly 3 and the inter-quartile range shows a slight increase in annual variability. The months of September, October and December show the greatest variability with several very wet months at both sites. A considerable proportion of the measured precipitation in January, February and March can fall as snow.

Interrelationships between precipitation, soil moisture and S.M.M. processes will be discussed further in Chapter 7.

Data on air and soil temperatures or windspeed are not available for the immediate vicinity; the nearest meteorological stations are at Durham (altitude 101m), 32 km away, Moor House (altitude 555m), 17 km away, and Widdybank Fell (altitude 521m), 13 km away.

4.3 Geo-morphometry

Geomorphometric data was collected for the catchment area from Ordnance Survey 1:10,000 maps and from a detailed slope profile survey. Information about the range and distribution of hillslope gradients forms an integral part of the experimental design and so a method was required for selecting representative measurement sites within the basin. Two methods of analysing morphometric data were employed -

(i) construction and interpretation of an altitude matrix constructed from 1:10,000 map data and

(ii) field survey of hillslope profiles using a hand held level and tape.

4.3.1. Altitude matrix data

An altitude matrix, which is a regular grid of height data, required accurate maps which have a suitable contour interval to allow precise interpolation of heights when the intersections of the matrix grid do not lie on a known height. The most accurate maps of the catchment are 1977 OS 1:10,000 which have photogrammetrically surveyed contours at 10 m intervals. The map scale and contour interval were such that 50 m was the minimum grid cell size that could be accurately interpolated. The matrix generated from the OS map consisted of 23 rows and 29 columns within which 256 points lay within the catchment area. The data were analysed using a series of morphometric programs developed by Evans (1980). This software produces descriptive statistics for geomorphometric variables.

Table 4.1 shows the statistics for estimated altitude, gradient and slope curvature in both plan and profile. The statistics for gradient and curvature are generated from calculations of the first and second derivatives respectively of the sample points and their eight nearest neighbours.

The catchment area consists of a relatively open moor in its upper part and is deeply incised by the river channel in its lower part. This is reflected in the distribution of the altitude data indicated by the negatively skewed histogram, figure 4.5. The standard deviation value of 48.24 m indicates a wide spread of altitudes for so small a catchment. Figure 4.6 shows a line printer map of the height data.

The height data clearly indicate that the terrain is stepped; this is partly due to class intervals chosen for the map but it does also reflect structural control of the basin form.

The data for slope gradients show a range from 0 to 21^{o} which indicates the minimum range of the data because of the coarse sampling of the height

Table 4.1 Summary statistics and correlation coefficients for altitude matrix data.

HEATHERY BURN Weardale
NO. OF ROWS= 23

STATISTICS FOR 253 POINTS WITH NON ZERO GRADIENT

	EST.ALT.	GRADIENT	PROFC	PLANC
MEAN	377.836	9.243	0.362	-14.637
SDEV	48.241	4.050	9.996	81.105
SKEW	-0.344	0.782	-0.302	-3.376
KURT	-0.544	0.691	1.680	19.291
MAX	464.333	21.243	32.377	215.230
MIN	253.111	0.854	-37.339	-654.555

VECTOR MEAN ASPECT ANGLE 210.462
VECTOR STRENGTH(PROPORTION) 0.691
GRADIENT WEIGHTED VECTOR MEAN ASPECT ANGLE 209.565
GRADIENT WEIGHTED VECTOR STRENGTH(PROPORTION) 0.665

CORRELATION COEFFS

	EST.ALT.	GRADIENT	PROFC	PLANC
EST.ALT.	1.000	-0.573	0.136	0.239
GRADIENT	-0.573	1.000	0.085	0.064
PROFC	0.136	0.085	1.000	0.234
PLANC	0.239	0.064	0.234	1.000

STATISTICS INCLUDING ZERO GRADIENT POINTS
EST ALT AND GRADIENT FOR ALL 256 POINTS
PROFC AND PLANC FOR 256 NON ZERO AND PLAIN POINTS
WHERE PLANC IS TAKEN AS 0.0 FOR PLAIN POINTS

	EST.ALT.	GRADIENT	PROFC	PLANC
MEAN	378.495	9.134	0.357	-14.466
SDEV	48.337	4.148	9.937	80.642
SKEW	-0.360	0.668	-0.302	-3.401
KURT	-0.552	0.672	1.735	19.568

Figure 4.5 Histogram of altitude data.

```
<HISTO VAR=1 INTERVAL=(250)/10.>


HISTOGRAM

MIDPOINT    COUNT FOR 1.CALCALT  (EACH X= 1)

 250.00         1 +X
 260.00         3 +XXX
 270.00         1 +X
 280.00         7 +XXXXXXX
 290.00         4 +XXXX
 300.00         7 +XXXXXXX
 310.00         2 +XX
 320.00         6 +XXXXXX
 330.00        11 +XXXXXXXXXXX
 340.00        16 +XXXXXXXXXXXXXXXX
 350.00        22 +XXXXXXXXXXXXXXXXXXXXX
 360.00        28 +XXXXXXXXXXXXXXXXXXXXXXXXXXXX
 370.00        18 +XXXXXXXXXXXXXXXXXX
 380.00        13 +XXXXXXXXXXXXX
 390.00        15 +XXXXXXXXXXXXXXX
 400.00        12 +XXXXXXXXXXXX
 410.00        13 +XXXXXXXXXXXXX
 420.00        19 +XXXXXXXXXXXXXXXXXXX
 430.00        29 +XXXXXXXXXXXXXXXXXXXXXXXXXXXXX
 440.00        11 +XXXXXXXXXXX
 450.00         7 +XXXXXXX
 460.00         8 +XXXXXXXX

 TOTAL        253  (INTERVAL WIDTH= 10.000)
```

Figure 4.6

Heathery Burn – Weardale

Altitude

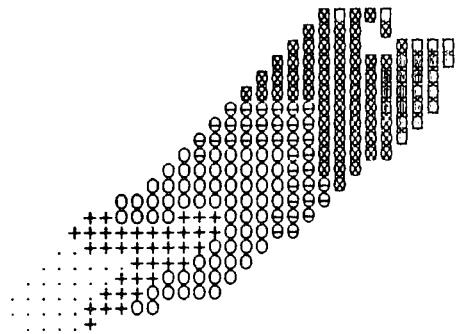

In metres

436
407
378
349
320
252

Gradient

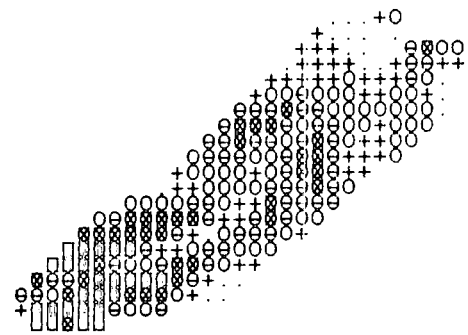

In degrees

14·0
11·6
9·2
6·8
4·4
0·0

Aspect

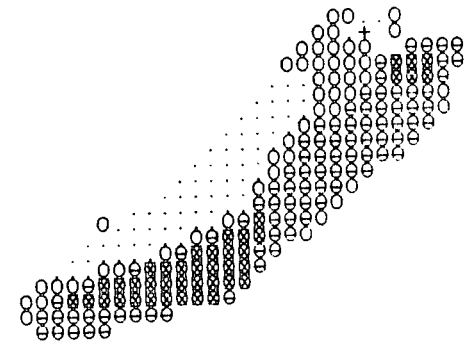

N
NW
W
SW
SE
S

Figure 4.7 Histogram of gradient data.

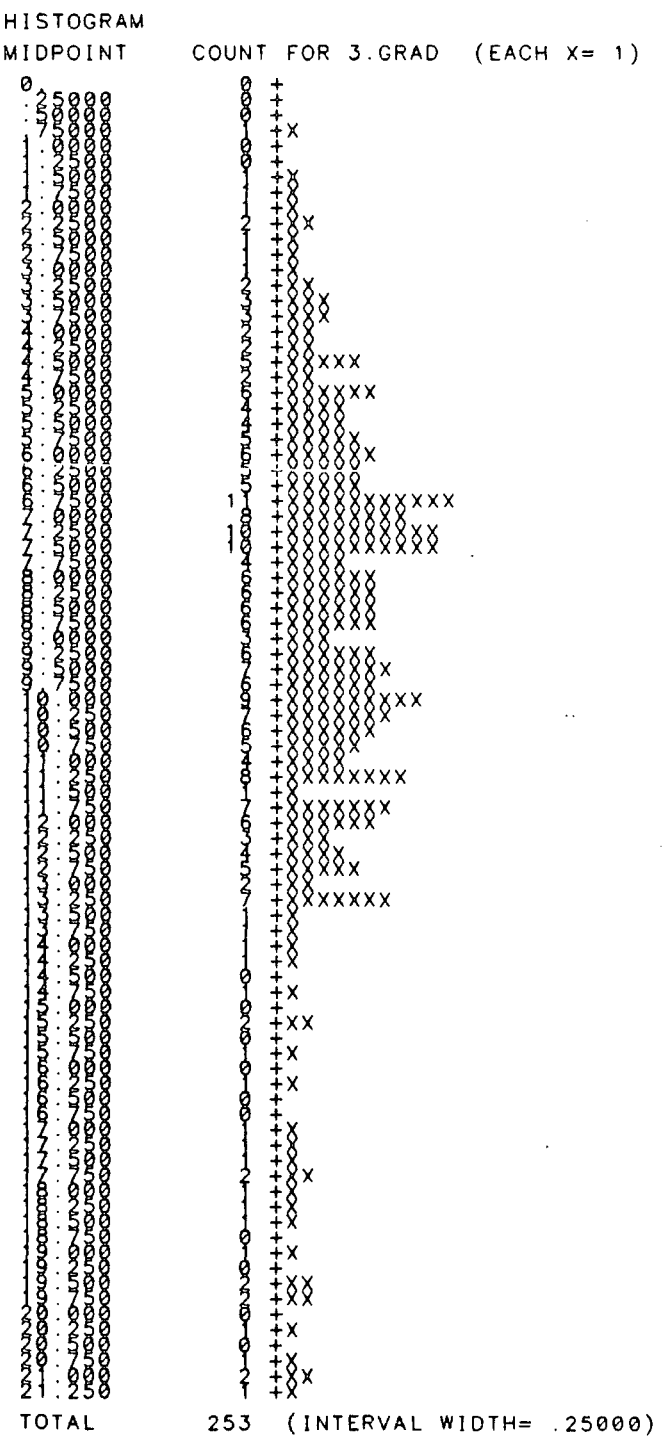

Figure 4.8 Histogram of aspect data.

```
HISTOGRAM

MIDPOINT    COUNT FOR 2.ASPECT  (EACH X= 1)

 0.           0 +
 8.0000       0 +
 16.000       0 +
 24.000       0 +
 32.000       0 +
 40.000       0 +
 48.000       0 +
 56.000       0 +
 64.000       0 +
 72.000       0 +
 80.000       0 +
 88.000       0 +
 96.000       0 +
 104.00       0 +
 112.00       0 +
 120.00       0 +
 128.00       0 +
 136.00       0 +
 144.00       0 +
 152.00       1 +X
 160.00       3 +XXX
 168.00      17 +XXXXXXXXXXXXXXXXX
 176.00      14 +XXXXXXXXXXXXXX
 184.00      14 +XXXXXXXXXXXXXX
 192.00      15 +XXXXXXXXXXXXXXX
 200.00      10 +XXXXXXXXXX
 208.00      12 +XXXXXXXXXXXX
 216.00      12 +XXXXXXXXXXXX
 224.00       8 +XXXXXXXX
 232.00       2 +XX
 240.00       9 +XXXXXXXXX
 248.00      10 +XXXXXXXXXX
 256.00      40 +XXXXXXXXXXXXXXXXXXXXXXXXXXXXXXXXXXXXXXXX
 264.00      18 +XXXXXXXXXXXXXXXXXX
 272.00       8 +XXXXXXXX
 280.00       9 +XXXXXXXXX
 288.00       9 +XXXXXXXXX
 296.00       9 +XXXXXXXXX
 304.00       8 +XXXXXXXX
 312.00       6 +XXXXXX
 320.00      14 +XXXXXXXXXXXXXX
 328.00       5 +XXXXX
 336.00       0 +
 344.00       0 +
 352.00       0 +
 360.00       0 +

 TOTAL      253  (INTERVAL WIDTH= 8.0000)
```

Figure 4.9 Histogram of profile curvature.

```
HISTOGRAM

MIDPOINT    COUNT FOR 4.PROFC  (EACH X= 1)

-54.000        0 +
-52.000        0 +
-50.000        0 +
-48.000        0 +
-46.000        0 +
-44.000        0 +
-42.000        0 +
-40.000        0 +
-38.000        1 +X
-36.000        1 +X
-34.000        1 +X
-32.000        0 +
-30.000        0 +
-28.000        0 +
-26.000        0 +
-24.000        0 +
-22.000        3 +XXX
-20.000        4 +XXXX
-18.000        3 +XXX
-16.000        3 +XXX
-14.000        7 +XXXXXXX
-12.000        4 +XXXX
-10.000        3 +XXX
-8.0000       12 +XXXXXXXXXXXX
-6.0000       18 +XXXXXXXXXXXXXXXXXX
-4.0000       21 +XXXXXXXXXXXXXXXXXXXXX
-2.0000       26 +XXXXXXXXXXXXXXXXXXXXXXXXX
 0.           32 +XXXXXXXXXXXXXXXXXXXXXXXXXXXXXXXX
 2.0000       29 +XXXXXXXXXXXXXXXXXXXXXXXXXXXXX
 4.0000       17 +XXXXXXXXXXXXXXXXX
 6.0000       16 +XXXXXXXXXXXXXXXX
 8.0000       12 +XXXXXXXXXXXX
 10.000        3 +XXX
 12.000       14 +XXXXXXXXXXXXXX
 14.000        8 +XXXXXXXX
 16.000        3 +XXX
 18.000        2 +XX
 20.000        4 +XXXX
 22.000        2 +XX
 24.000        1 +X
 26.000        2 +XX
 28.000        0 +
 30.000        0 +
 32.000        1 +X
 34.000        0 +
 36.000        0 +
 38.000        0 +
 40.000        0 +
 42.000        0 +
 44.000        0 +
 46.000        0 +
 48.000        0 +
 50.000        0 +
 52.000        0 +
 54.000        0 +

 TOTAL       253  (INTERVAL WIDTH= 2.0000)
```

Figure 4.10

Heathery Burn - Weardale

Plan Convexity

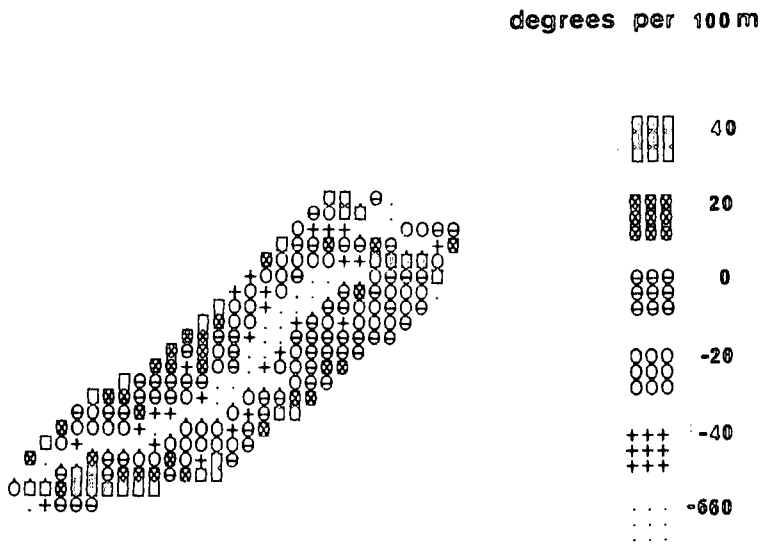

Heathery Burn - Weardale

Profile Convexity

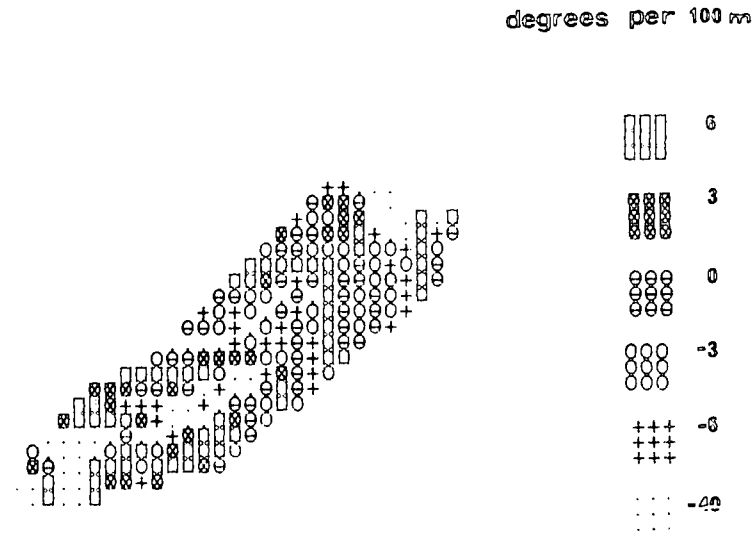

Figure 4.11 Histogram of plan curvature.

```
HISTOGRAM

MIDPOINT    COUNT FOR 5.PLANC  (EACH X= 1)

-540.00        0 +
-520.00        0 +
-500.00        0 +
-480.00        0 +
-460.00        0 +
-440.00        0 +
-420.00        1 +X
-400.00        1 +X
-380.00        0 +
-360.00        0 +
-340.00        0 +
-320.00        0 +
-300.00        0 +
-280.00        2 +XX
-260.00        2 +XX
-240.00        0 +
-220.00        2 +XX
-200.00        1 +X
 180.00        0 +
-160.00        1 +X
-140.00        3 +XXX
-120.00        4 +XXXX
-100.00        4 +XXXX
-80.000        4 +XXXX
-60.000       11 +XXXXXXXXXXX
-40.000       19 +XXXXXXXXXXXXXXXXXXX
-20.000       43 +XXXXXXXXXXXXXXXXXXXXXXXXXXXXXXXXXXXXXXXXXXX
 0.           68 +XXXXXXXXXXXXXXXXXXXXXXXXXXXXXXXXXXXXXXXXXXXXXXXXXXXXXXXXXXXXXXXXXXXXXXXXXXX
 20.000       45 +XXXXXXXXXXXXXXXXXXXXXXXXXXXXXXXXXXXXXXXXXXX
 40.000       19 +XXXXXXXXXXXXXXXXXXX
 60.000       11 +XXXXXXXXXXX
 80.000        5 +XXXXX
 100.00        4 +XXXX
 120.00        0 +
 140.00        1 +X
 160.00        0 +
 180.00        0 +
 200.00        0 +
 220.00        1 +X
 240.00        0 +
 260.00        0 +
 280.00        0 +
 300.00        0 +
 320.00        0 +
 340.00        0 +
 360.00        0 +
 380.00        0 +
 400.00        0 +
 420.00        0 +
 440.00        0 +
 460.00        0 +
 480.00        0 +
 500.00        0 +
 520.00        0 +
 540.00        0 +

               1 < -540.00
TOTAL        253  (INTERVAL WIDTH= 20.000)
```

data. The histogram of figure 4.7 shows a distribution which is positively skewed by a few large gradient values. The map of gradient (figure 4.6) shows the steep slopes to be concentrated in the lower incised part of the catchment area and along the outcrops of sandstone benches.

Aspect displays a rectangular square distribution between about 160^o and 330^o, as seen in figure 4.8. The vector mean aspect angle is 210.5^o indicating a predominantly SW facing catchment area. This statistic can be misleading as it is a geometric rather than an arithmetic mean and may be biased by gradient since very flat surfaces have a weak aspect and very steep slopes have a strong aspect.

Evans (1980) proposes a gradient weighted vector mean aspect angle as a solution to this bias. For Heathery Burn this correction is unimportant due to the apparently narrow range of gradient values. The gradient weighted vector mean aspect is 209.56^o. Figure 4.6 further emphasises the dominant south-westerly aspect of the hillslopes.

The values of profile and plan curvature are expressed in degrees per 100 m. The distribution of profile curvature data in figure 4.9 displays almost perfect symmetry between convexity and concavity as indicated by mean and skewness values close to zero. Like the gradient data, the range of the profile curvatures will be a minimum estimate because of the crude 50 m sampling interval between data points.

However, the map of profile curvature (figure 4.10), shows an interesting spatial pattern where a transition from convexity to concavity downslope is often interrupted by *benches* of high profile convexity. These show a strong spatial correlation with sandstone outcrops and emphasise the importance of the underlying geology in determining basin form.

Plan curvature of the slopes is almost symmetrically distributed about

zero, that is a slope rectilinear in plan. The values are clustered about zero, hence the height kurtosis value of 19.29; the ~~second~~ third moment statistic of skewness is influenced by several outlying data values which are spatially distributed adjacent to the stream channel (see figure 4.11 and table 4.1).

The map of plan convexity, figure 4.10, shows the wide distribution of slopes which are almost rectilinear in plan. The slopes adjacent to the stream channel show the highest negative curvature and those near the catchment area boundary show the highest values of positive curvature and seem to be associated with small spurs.

The principal aim of the field experiments is to establish the relationship between S.M.M. and hillslope gradient given that all other factors are equal. Clearly the variables of aspect, profile curvature and plan curvature are likely to influence the relationship by their effects upon water and sediment pathways for example. Therefore, it is important that sample units be located, as far as is possible, on rectilinear slopes so that inter-site comparison is simplified by omitting compounding variables where possible.

A measure of the interrelationship between geomorphometric variables is given by the correlation matrix shown in table 4.1. The strongest relationship, -0.57 between gradient and altitude, reflects the pattern of channel incision in the lower part of the catchment especially where the stream channel has eroded weak shale bands in the Yoredale cyclothem. Consequently, sampling units for steep slopes are likely to be located in the lower part of the basin, irrespective of the sampling scheme used. Surprisingly the correlation between profile curvature and gradient is very weak (0.08), also the correlation plan curvature and gradient is very weak (0.06), suggesting that the steepest slopes are in fact straight slopes. The correlations of slope curvature with altitude are positive but weak. This reinforces the pattern

indicated by figures 4.6 and 4.10 where points with high negative curvature are predominantly located in the lower part of the catchment area.

The altitude matrix analysis yielded much useful background information about basin form and the spatial distribution of slope properties; however, this could not easily be correlated with details of soil type, soil moisture status and vegetation cover which are also essential variables in sampling unit selection. In addition, a visual inspection of the catchment area clearly indicated that the grid size of 50 m of the altitude matrix and the neighbourhood method of gradient and curvature calculation grossly underestimated the range of these variables. Therefore, a slope profile survey was undertaken in order to derive more detailed information.

4.3.2. Slope profile survey

The methods used for constructing the profiles conformed to the recommendations of Young (1974), Pitty (1966) and Cox (1981). A baseline was drawn along the stream channel within the catchment area and pairs of profile origins were located at approximately 200 m intervals regularly along the baseline. The only purpose sampling criterion was that of avoiding plan convex or plan concave slopes. This systematic sample was designed to collect detailed information about a large number of slope stations that are straight in plan and profile which may be used to direct the field experiment sampling unit selection.

The profile data were collected using a Suunto hand held inclinometer, a 50 m tape measure and two ranging poles. The ground surface length was fixed as 5 m, thereby ensuring that a large number of elements would be sampled for each profile while the 5 m length of each station seemed a sensible

compromise between local undulations and the observed rate of change of gradient in the field. Each profile was measured from a fixed stake located adjacent to the channel and extended upslope towards the divide following the maximum gradient path. The profiles were terminated according to the cut-off procedure suggested by Pitty (1966) whereby the profile continues until the measured slope angle equals that of the slope of the divide. For each profile station a record was made of gradient, vegetation type and percentage cover, soil type and a categorical assessment of soil moisture status. Ten profiles were measured and in total information was collected at 458 stations. Table 4.2 shows the frequencies of hillslope stations in six vegetation classes. The moss class is a sub-division of the *Juncus* dominated bog group; the other grasses class is a sub-division of the *Nardus* dominated grassland group. Otherwise the constituents of each vegetation class are those described on page 84.

Figure 4.12 shows the location of each of the ten profiles within the catchment area and figures 4.13 - 4.17 show the form of each of the ten hillslope profiles with the approximate extent of vegetation distribution marked. Note that each profile contains sections where similar gradient and vegetation cover persist for several measurement stations. These station values can usefully be combined and be termed profile elements, after Cox (1978), where gradient is constant, profile curvature is minimal and vegetation type (and so soil type) is homogenous. The construction of hillslope elements classifies the hillslope profile data into a sub-set which is suitable for S.M.M. field experiments on geomorphometric criteria.

Table 4.3 gives the summary statistics from the slope profile survey. Clearly the profile station data display a wider range of hillslope gradients than was indicated by the altitude matrix analysis. An important question

Table 4.2

Frequency of hillslope profile stations in each vegetation class

Profile	Juncus	Moss	Nardus	Grass	Pteridium	Heath	Total
1	8	-	-	1	12	30	51
2	6	1	6	3	3	11	30
3	-	6	5	16	17	17	61
4	-	13	1	3	6	14	37
5	8	-	17	9	3	21	58
6	8	-	-	-	6	39	53
7	1	-	8	12	8	11	40
8	1	1	17	2	8	13	42
9	2	-	5	15	-	24	46
10	-	6	15	19	-	-	40
Total	34	27	74	80	63	180	458

Figure 4.12 Location of hillslope profiles.

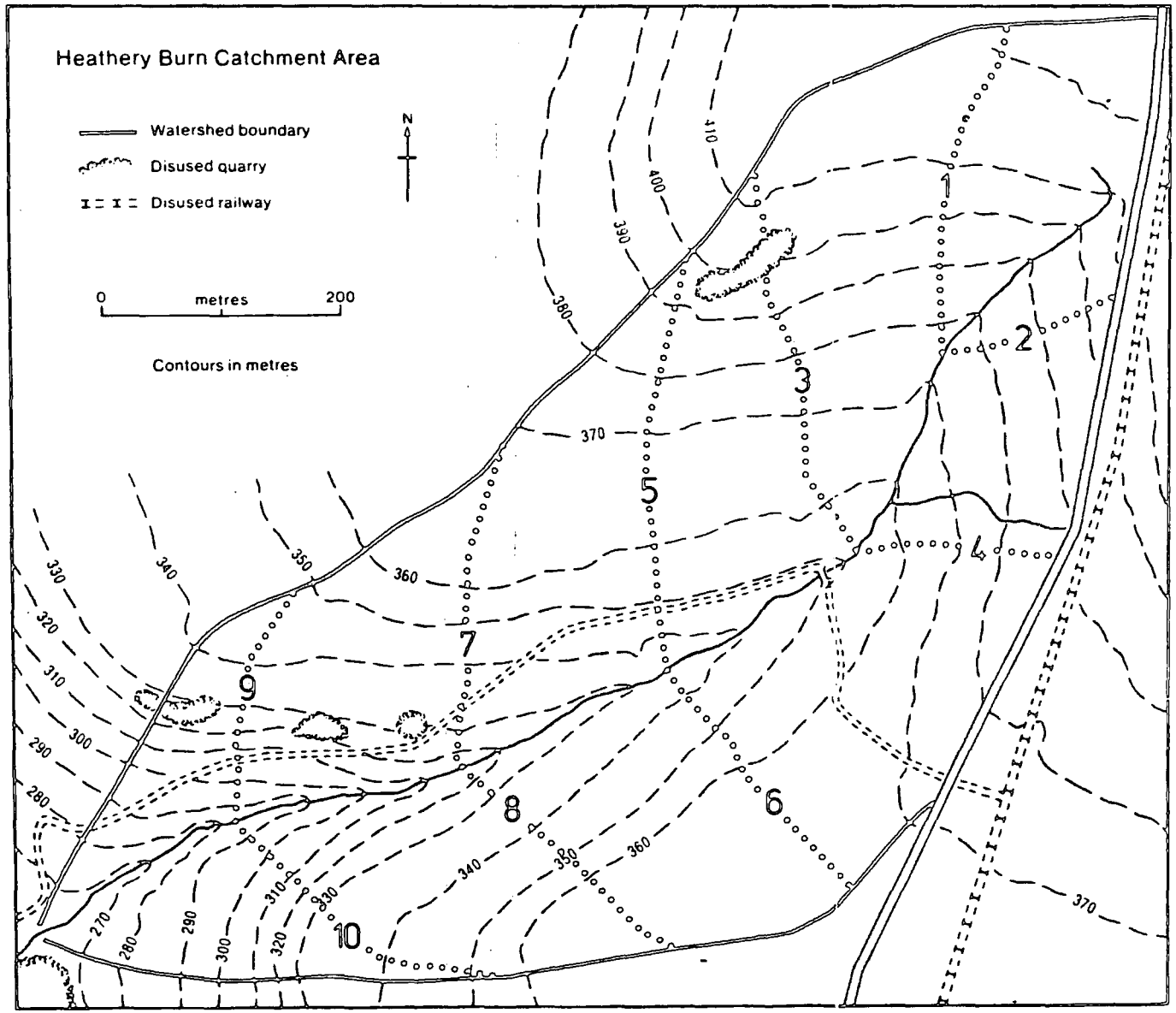

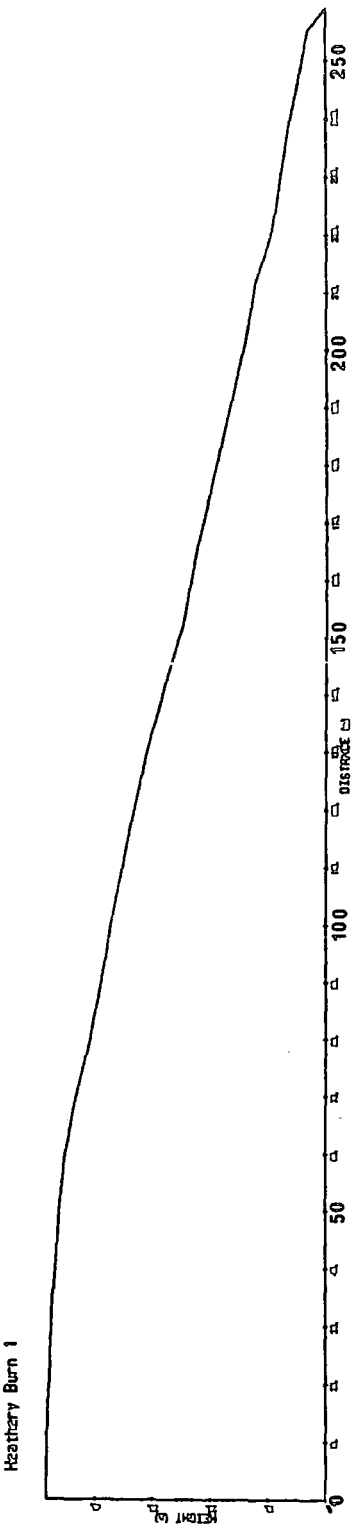

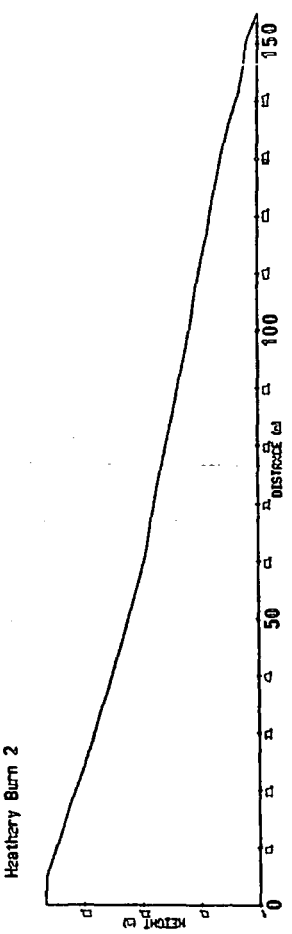

Figure 4.13 Hillslope profiles.

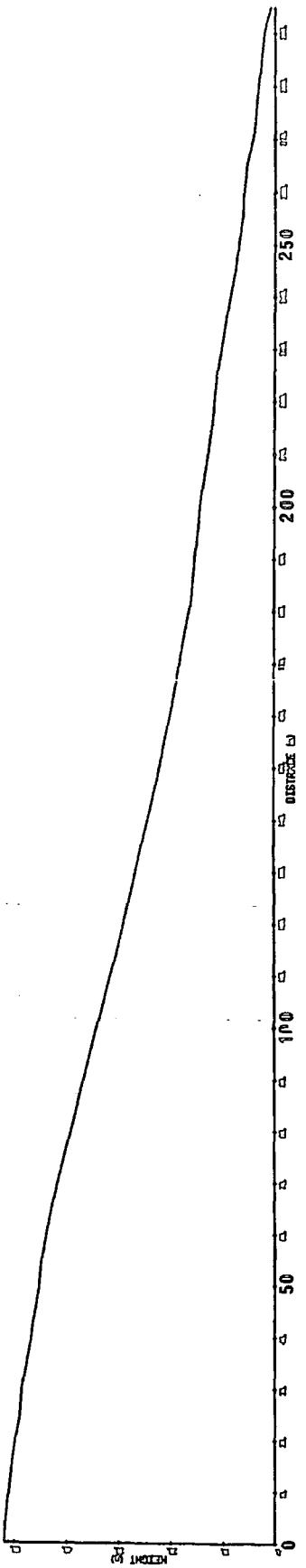

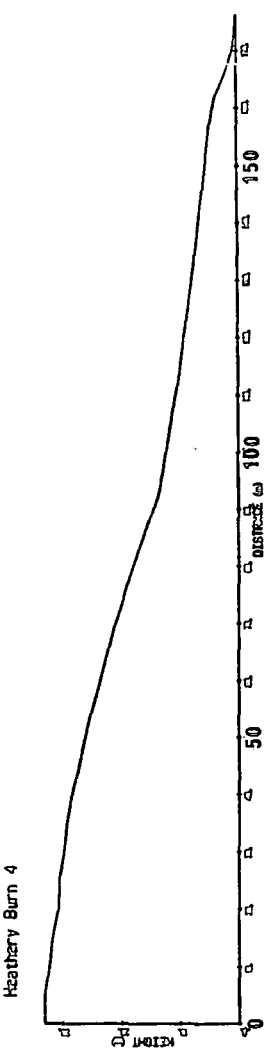

Figure 4.14 Hillslope profiles.

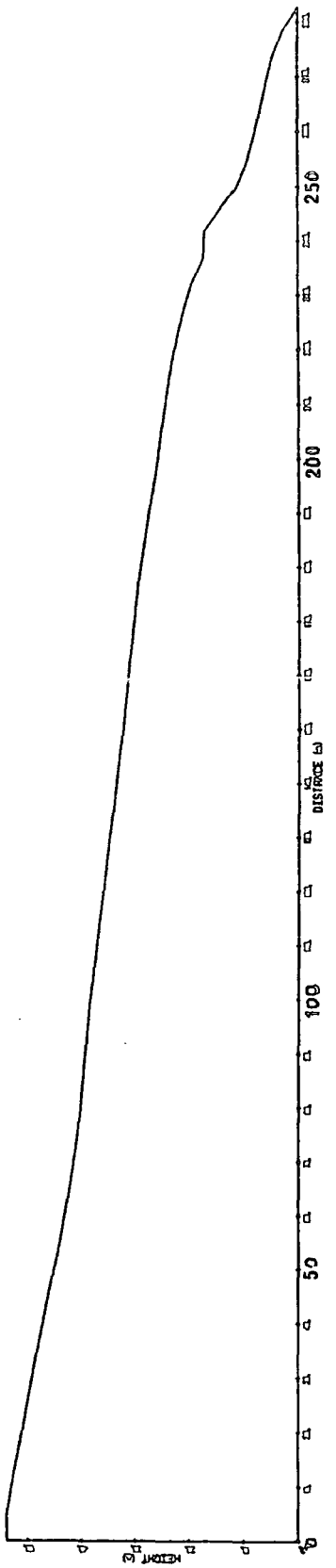

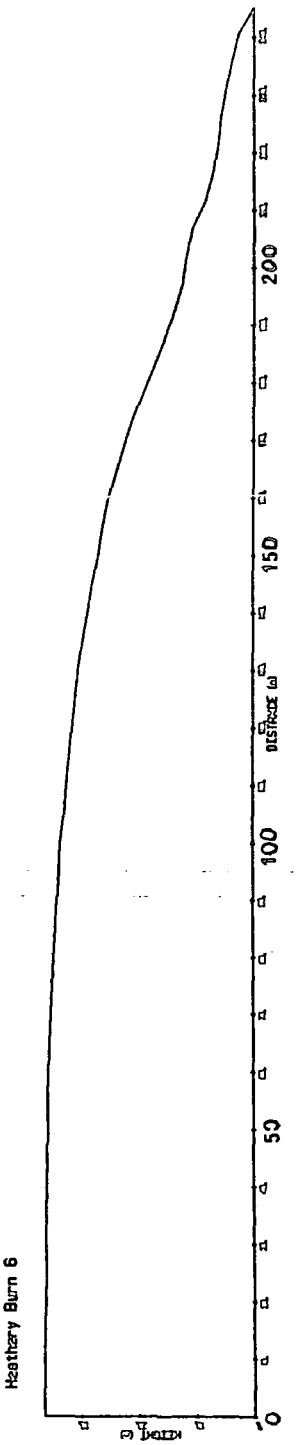

Figure 4.15 Hillslope profiles.

Figure 4.16 Hillslope profiles.

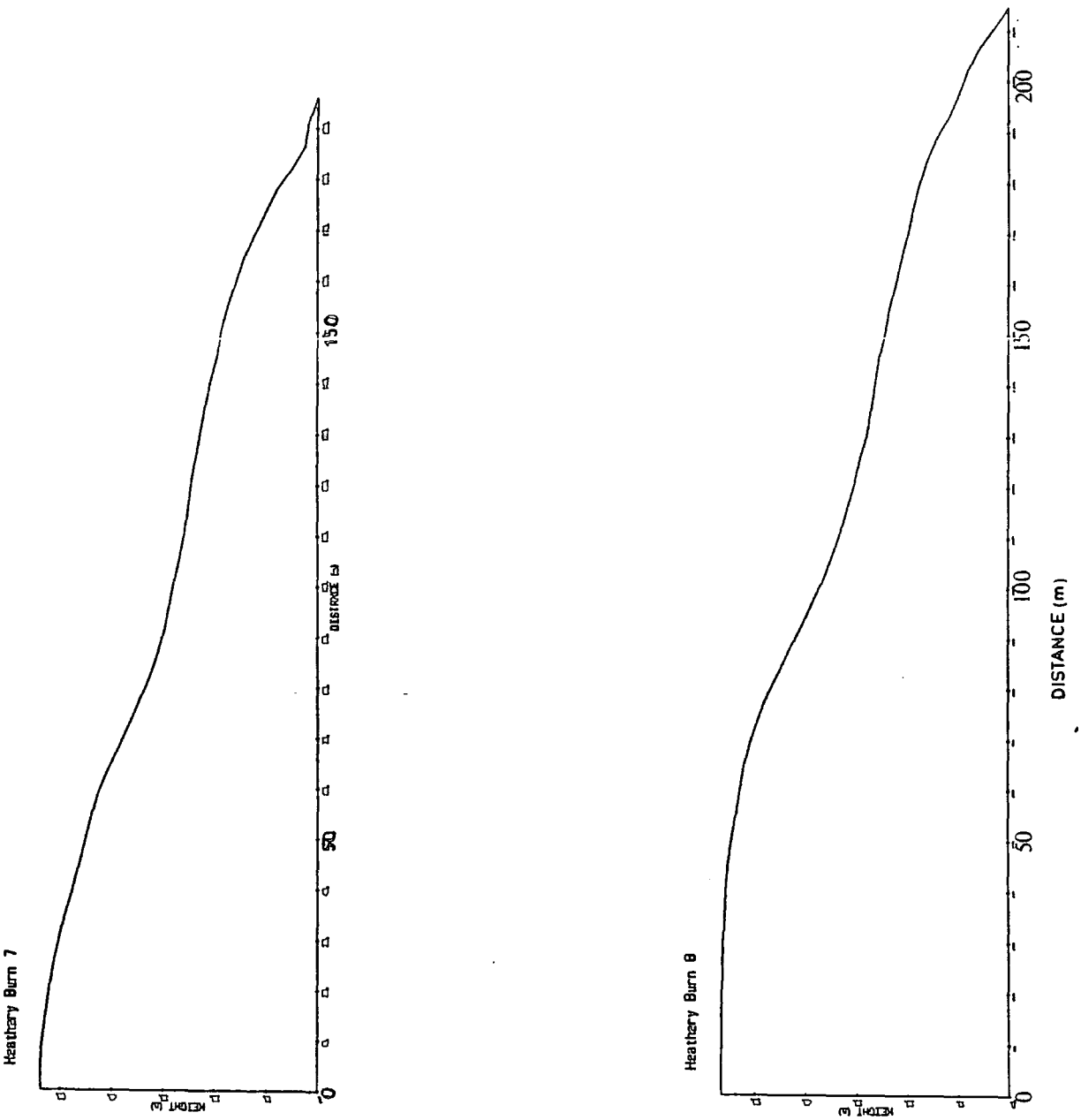

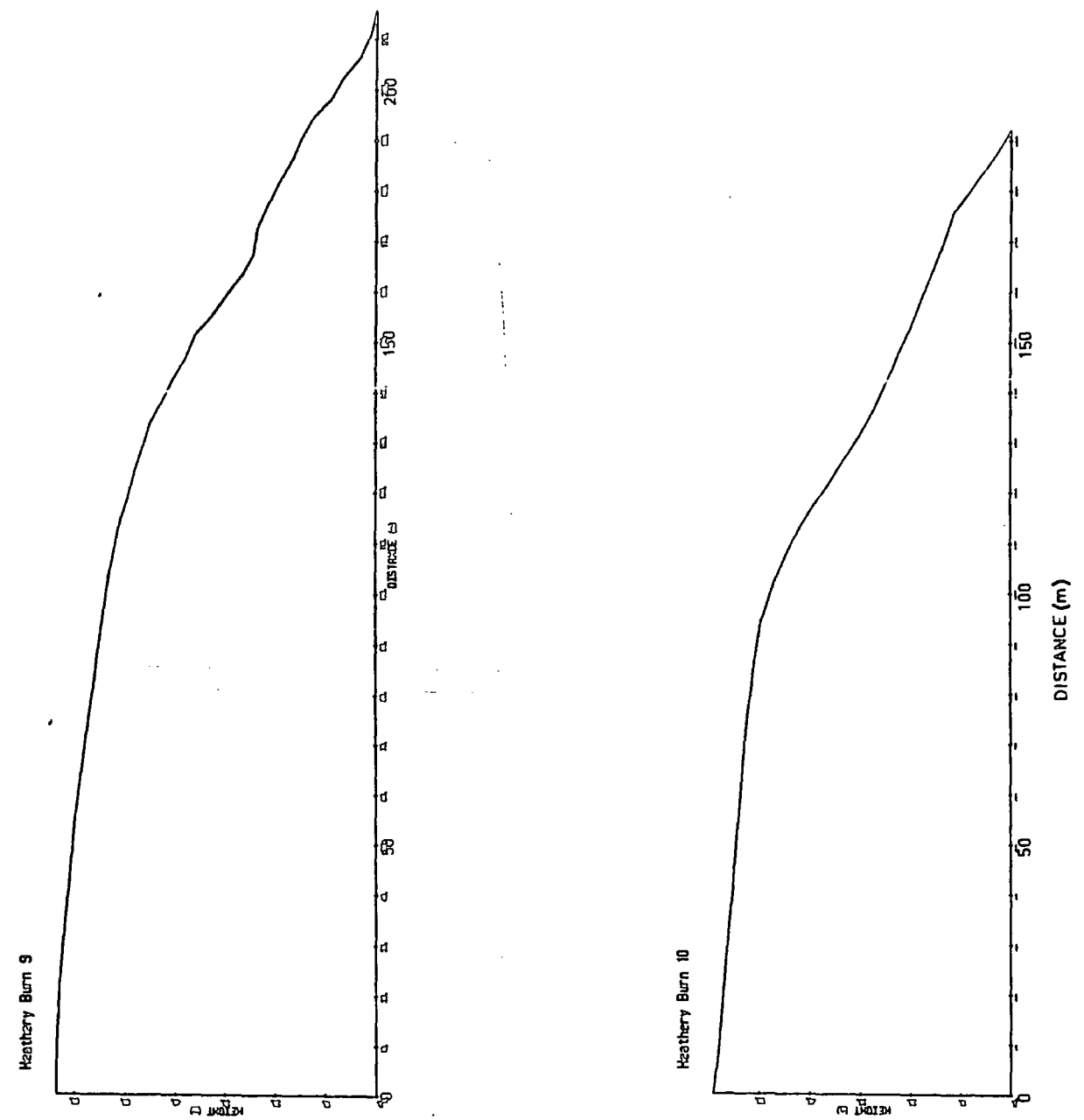

Figure 4.17 Hillslope profiles.

Table 4.3 Summary statistics for slope profile survey

Profile	Max	Min	Mean	Median	N
1	18.0	0.0	10.6	11.0	53
2	22.0	1.0	13.3	13.0	32
3	15.5	3.5	9.8	10.0	61
4	23.0	0.5	10.7	9.75	36
5	36.5	0.0	10.8	9.25	58
6	27.5	0.0	8.5	8.0	50
7	35.5	0.0	15.3	14.5	41
8	37.0	0.0	14.7	13.5	45
9	40.5	0.0	16.4	18.0	46
10	37.5	4.0	17.1	19.0	41

is, *do the data from the 10 profiles adequately represent the range of slopes present within the basin?* It is unlikely that the measurement of central tendency of gradient is an accurate statistic for the catchment area as a whole since much of this area comprises relatively low gradient heathland which has not been sampled heavily. Figure 4.13 clearly shows that the steepest slopes are located on the profiles in the lower part of the basin area, as was indicated by the altitude matrix analysis. Because the profiles are sited regularly along the channel length they will account in part for the spatial division of the hillslope gradients within the catchment area. An important aim of the field experiment is to understand the behaviour patterns of S.M.M. processes over a wide range of slope gradient and environmental conditions. Therefore, an important aspect of the sampling procedure should be to sample the extreme conditions as heavily as the typical conditions, in spite of the difference in their frequency of occurrence. For example, a random sample of field locations in the Heathery Burn catchment area would produce an experiment where the majority of sites displayed very similar conditions and would therefore not satisfy the original aims of the experiment.

Profile elements were constructed from adjoining station measurements with similar vegetation and slope characteristics. The table 4.4 shows the frequencies of hillslope elements for each profile. A variety of quantitative methods have been proposed for profile segmentation including *best units analysis* (Young 1971) and a linear regression method (Ongley 1970). However, these techniques are directed towards quantitative description of hillslope form rather than quantitative assessment of sampling units, therefore, the criteria used for selecting elements are different. For example, the length of measured segments is not important since lengths of zero profile curvature can be found within the length of two adjoining station measurements of

equal gradient.

Each angle was measured to an assumed accuracy of 0.5^o; however, it is difficult to measure angles precisely using a hand held inclinometer. A value of 1.5^o was set for comparing gradient measurements during segment allocation. Although seemingly arbitrary the 1.5^o tolerance value was a practical necessity to avoid an excessive number of sampling units (segments) being generated.

Table 4.4

Frequency of slope elements of similar vegetation and slope characteristics constructed from station measurements for each hillslope profile.

Profile	Stations	Elements
1	51	11
2	30	10
3	61	13
4	37	12
5	58	19
6	53	12
7	40	16
8	42	18
9	46	18
10	40	12
Total	458	141

Table 4.5 Frequencies of hillslope elements for each profile (subdivided by vegetation type).

Slope Elements	Slope Profile 1	2	3	4	5	6	7	8	9	10
1	J3	J2	J3	J2‡	J7‡	J7‡	J4	N8	J3	N7*
2	J2‡	J4‡	P2+	J3‡	J4	J3	O2	J6	J5*	N8
3	P4‡	J3‡	N2‡	J5‡	J3‡	J2‡	O6	N5	J8*	N7+
4	P2‡	N3+	J2‡	J2	J4‡	J3	P6‡	N6‡	J6	N4
5	H3‡	H2	P3‡	P2‡	J5	P6	P6‡	N5‡	J9	N5‡
6	P3‡	P3‡	H3	P4‡	O8	P2	O2	N4	O6	N6
7	P4	J3‡	H3‡	H3	O1	P4‡	N2‡	N3	O5	N7
8	P3	H3	H3	H1	N5	P5‡	N2‡	P2	O6	N6
9	H3	H4‡	H2‡	H3	N4	P2‡	H3	J2‡	O2	N4
10	H2	H4	H1	H2‡	N3	H4	P4	P4	H6	O2
11	H1		H3	H2	N2	H3	P5	N4‡	H8	O1
12			H2	H1	H2	H2	O5	P5‡	H5	O2
13			H1		N2	H1	O3	H6‡	H6	
14					H2		H3+	H5	H4	
15					N2		O2	H3	N4‡	
16					J2		O1	H2	N3‡	
17					H2			H1	H2	
18					P3			H1	H1	
19					H2					
20										
Total	11	10	13	12	19	13	16	18	18	12
Sample	5	7	7	6	10	6	6	6	8	8

‡ - 1 plot
\+ - 2 plots
* - 3 plots

Chapter 5

Process Mechanisms

Contents

5.1 Introduction

Four physical mechanisms have been postulated to produce slow mass movement (S.M.M.) on transport-limited hillslope soils: *Pure shear* (Ter-Stepanian 1957; Kirkby 1963, 1967), *viscous flow* (Sharpe 1938; Sharpe and Dosch 1942; Varnes 1958, 1975; Scheidegger 1970), *expansion and contraction* of particles with net downslope settlement (Moseley 1869; Davison 1888, 1889; Young 1963; Kirkby 1963, 1967) and *particulate diffusion* of granular materials (Culling 1963, 1965, 1983a, 1983b). All of these mechanisms, singly or in combination, are theoretically appealing and plausible, but few researchers have attempted to distinguish among them by analysis of field measurements or by experimentation.

In this chapter the physical basis of each mechanism is briefly described and a summary is given of empirical evidence that has been cited in its support. It is assumed that macroscopic downslope movement of soil particles results from the action of physical rather than surface (electrical) forces since surface forces are restricted to colloids with specific surfaces greater than 25 m^2/g (Mitchell 1976). Physical forces may be defined in terms of the stress state within a soil mass and this will depend upon a large number of compositional and environmental factors such as mineralogy, shape and size distribution of particles, nature of absorbed cations, pore water composition, confining pressure, fabric shape and availability of water and so on. Indeed, because natural soils are subject to a wide variety of changing environmental conditions and because it is difficult to estimate physical parameters relating to *in situ* soil behaviour, general physico-chemical theories relating compositional and environmental variables do not

help to explain the details of S.M.M. mechanism. It is perhaps not surprising that no single mechanism has been universally accepted as responsible for S.M.M. given the wide range of soil composition and environmental conditions that have been studied. Further, there seems no reason to assume that a single mechanism exists or that any mechanism or combination of mechanisms is temporally or spatially persistent.

5.2 Pure Shear

Pure shear describes deformation of a soil mass along a plane or narrow zone, without significant rotation of individual particles, by the action of a deviatoric (shear) stress. The mechanical analysis of deformable bodies is termed rheology. Such analysis disregards the internal reactions of bodies to forces acting on them. For any given applied force the reaction of a body can be characterised in terms of its relative deformation or strain, that is the ratio of its deformation to its initial dimensions. The effect of a force in causing deformation is directly related to its magnitude and inversely related to the area over which it acts. The ratio of force to area is called stress. When a force is perpendicular to the area on which it acts it produces a normal stress ($\sigma = F/A$); when the direction of the force is not perpendicular to the area on which it acts it causes a deviatoric or shearing stress ($\tau = F/A$). Also important in determining the behaviour of materials is the rate of change of stress and the time dependence of strain. Indeed, the stress-strain-time relationships of a material fully describe its rheological character. Soils invariably exhibit complex rheological properties ranging from elastic to plastic behaviour. A perfectly elastic solid when subject to stress deforms instantly, retains its new form

while the stress remains constant, and then returns to its original form when the stress is released. A perfectly plastic solid on the other hand deforms progressively when stressed and retains its deformed shape when the stress is released.

Empirical analysis of the stress-strain-time behaviour of natural soil masses has shown that they often exhibit progressive deformation under a constant pressure, that is to say they creep (Singh and Mitchell 1968). The rate of strain or creep depends on the ability of the material to relieve stress gradually through internal structural adjustments.

All hillslope soils are subjected to shear stresses. However, inter-granular readjustments only occur when grain-to-grain bonds are ruptured and the surface friction forces are overcome. A persistent shear stress may result in the formation of distinct planes or zones of shear failure and areas exhibiting no inter-granular strain. A number of researchers have attempted to describe progressive failure of hillslope soils as a time dependent pure shear process (Singh and Mitchell 1968; Pusch and Feltham 1980). Mitchell (1976) states that progressive strain rates are controlled by the viscous resistance of the soil structure. That is, the soil skeleton controls the frictional resistance to a shearing stress, pore water pressures are assumed to have reached an equilibrium state and so high effective stresses do not develop.

Progressive or creep behaviour can pose considerable problems for engineers who need to predict the effect that increases of stress will have on the stability of the material. Empirical evidence for progressive failure of soils as a pure shear process has come from controlled laboratory testing under known effective stress conditions using triaxial or direct shear testing apparatus.

A simple shearing mechanism may be produced using stress con-

trolled direct shear apparatus suitably modified for the low normal and shear forces that apply in shallow soil masses. Such apparatus has been used by Goldstein and Ter-Stepanian (1957), Singh and Mitchell (1968) and Andersland and Douglas (1970) to investigate stress-strain-time behaviour of soils. Waldron *et al.*(1983) used similar testing apparatus to investigate the behaviour of root permeated soils: Nixon (1982) and Morgenstern (1981) used the same approach in the investigation of fine-grained permafrost soils.

Singh and Mitchell (1968) described the strain behaviour they observed for San Francisco Bay clays in terms of rate process theory. That is, particles are constrained from movement relative to each other by virtue of energy barriers separating adjacent equilibrium positions. Normally barriers are crossed with equal frequency in all directions and there is no overall change in particle distribution. However, if a directional potential such as a shear stress exists then barrier heights become distorted and the force of activation increases in the direction of that potential (Singh and Mitchell 1968). This model is borrowed from the study of deformation of crystalline solids where rate process theory describes creep as a stress dependent thermally activated process (Feltham 1968).

Detailed examination of the structural changes which occur in silty clay soils when they are sheared has provided valuable empirical support for the energy barrier model of progressive failure (Pusch 1979). Pusch provides micro-morphological evidence from transmission electron micrographs of natural, soft illitic clays that shearing between aggregates occurs at stress levels higher than about two thirds of the maximum deviatoric stress. The micrographs reveal a complex, heterogeneous, fabric structure where clay particles tend to aggregate and displacement occurs between these aggregates. Pusch and Feltham

(1980) regard progressive failure as a stick-slip process where stresses are built up and released at recognised domains within the silt-clay structure of the soil. The failure of the soil can be modelled as a rate process where there is a range of energy barriers whose distribution within the soil mass is random.

5.3 Viscous flow

A fluid is a substance that deforms continuously when subjected to a shear stress and so in special circumstances a slowly deforming solid, like a soil, may be regarded as a viscous fluid. A flow model is characterised by the effective viscosity of the fluid, the velocity gradient of the flow, and the deviatoric stress level. However, unlike Newtonian fluids, soils rarely behave elastically and so non-linear flow models must be derived empirically. Resistance within flowing material is generated by the collision of particles across the surface of shearing, thus inhibiting slippage. The frictional component of flow transferred through a plane of shear is proportional to the velocity gradient. The applicability of a flow model to describe the mechanism of S.M.M. of superficial soils is uncertain because very few empirical velocity-depth profiles are available for analysis and hardly any trace the development of that profile through time.

Rheological analogue models have been postulated to describe flow processes within landslides and mudflows. Goldstein and Ter Stepanian (1957), Yen (1969) and Savage and Chleborad (1982) use a Bingham type (elastic, visco-plastic) model to describe two stage strain observations within rotational landslides.

Empirical support for viscous flow mechanisms for S.M.M. is derived from stress-strain-time observations during laboratory testing of

materials. Allen (1982) postulates that analysis of soil fabric shape may provide an insight into its genesis. For example, Lindsay (1968) has shown that clast orientations and distributions within debris flow deposits indicate a rapid, turbulent, surging flow of the silt and clay matrix. Boulton (1967) has also shown that strong clast orientation is a typical feature of glacial flow fills. The theoretical basis of relating fabric shape to flow conditions is provided in a seminal paper by Jeffrey (1922) whose theory quantitatively relates fluid viscosity, flow velocity and ellipsoidal particle size. Jeffrey's theory reinforces perfect fluid theory stating that particles tend to adopt that motion which, of all possible motions, corresponds to the least dissipation of energy. In practice both prolate and oblate spheroids immersed in a fluid in laminar motion will set themselves with their longest axis perpendicular to the plane of undisturbed motion of the fluid. This result was confirmed experimentally by Taylor (1922) who noted that particles take a long time to reach their final orientation and that oblate spheroids settle down to a stable position four times as quickly as prolate spheroids. Gay (1966, 1968) extended Jeffrey's equations of motions to particles deformed by pure shear; in this case the particle's long axis will align parallel to flow only after an indefinitely large strain. It is not known in precise detail how collisions between particles in highly viscous fluids affect these models (Manley, Arlov and Mason 1955).

Fabric shape, however, has rarely been used in this context and yet it provides a method of distinguishing between materials deposited by turbulent and laminar processes. It is not known if S.M.M. is capable of producing a secondary, characteristic, deformational fabric with oblate spheroid particles which is quantitatively different from a primary appositional fabric. Problems could arise if a soil mass

were to possess a secondary fabric stronger than the fabric which would result from the action of S.M.M.: this would be the case with solifluction deposits and glacial lodgement and flow fills.

Strong fabric shapes in soils subjected to persistent slow mass movement have been reported by Yogashita and Morris (1979) where the primary isotropic fabric of waterlogged unconsolidated sands was rotated towards the plane of shear. Mills (1983) attributes strong fabric orientations of 2 to 10 cm clasts in silty colluvial soils to slow mass movement. Strong fabric shapes have also been reported for clasts suspended in active and relict solifluction deposits.

Both viscous flow and pure shear processes should produce strong secondary fabric shapes, but estimations of movement rates, material viscosity and paricle size distribution are required before theoretical predictions can be made. It seems likely that several necessary conditions of the Jeffrey and Gay theories, such as uniform velocity gradient and neutral buoyancy of particles, will not be met by slowly moving soil masses. The Reynolds number governs the minimum particle size fraction that will be affected by the flow and, in theory, only silt and clay size fractions should be affected by flows with rates of 1 mm to 5 mm per year.

5.4 Volume change behaviour

The repeated action of forces which cause volume changes in soil masses, in soil pore fluids, and in gases will tend to produce a net downslope movement of particles on hillslopes. This occurs simply because expansion and contraction are inhibited by gravity in an upslope direction and assisted by gravity in a downslope direction (Moseley 1869; Davison 1888; Tamburi 1974). Such processes will be most

effective at or close to the soil surface where there will be large variations in pore moisture content and soil temperature. Terzaghi (1950) termed such processes *seasonal creep* and Scheidegger (1970) termed them *skin creep*. Soil volume change induced by freezing of pore fluids may be considerable in frost-susceptible soils where ice lenses or ice needles can form. Washburn (1967) presents a comprehensive model of frost heaving, resettlement and gelifluction in a periglacial environment. Detailed reviews of frost creep processes induced by volume change behaviour can be found in Benedict (1976) and Harris (1981). The thermally controlled displacement of dry rocks by expansion and settlement has been described in mechanical terms by Scheidegger (1970). Quantitative empirical evidence for this process has been presented by Schumm (1964) and by Tamburi (1974).

By controlled laboratory experimentation on several rock types, Tamburi identified a complex relationship between particle volume, temperature flux from particle to surface and effective stress. Threshold stresses exist for given particle volumes and rock types (Tamburi 1974).

Kirkby (1967) noted that expansion and contraction cycles associated with repetitive changes in soil moisture cause a *sigmoid* movement of soil particles. The movement is not restricted to superficial particles but also occurs at depth although no clear movement-depth pattern was observed. Kojan (1967) states that shear failure of soil particle bonds must accompany volume changes for downhill strain to occur, a situation which would require the temporary reduction of shear strength on expansion. This mechanism is quite distinct from that proposed by Moseley and it is particularly effective in partly saturated soils, with an open metastable structure, in the presence of a high shearing stress (Barden, Madedor and Sides 1969).

Campanella and Mitchell (1968) note that soil volume changes induced by temperature cycling cause variation in the voids ratio of normally consolidated soils. This has the effect of altering the frictional resistance between particles. Demars and Charles (1982) have shown, however, that volume changes may contain a permanent and transient component that is independent of effective confining stress for a normally consolidated soil. Permanent voids ratio reduction is directly related to soil plasticity. However, the initial temperature cycle removes most of the irreversible volume change and thereafter temperature cycles of the same order of magnitude produce no further permanent volume changes. These results have important implications for laboratory testing and simulation studies of natural hillslope soils.

5.5 Diffusion

A novel approach in thinking about S.M.M. came from Culling (1963, 1965) who proposed a diffusion model for granular soils characterised by random and downslope components for particles subjected to all natural disruptive forces. Such forces, whether internally or externally generated, cause particles to be displaced into adjacent free voids in the soil structure. This process requires particles to behave independently of neighbours and movement is controlled by local stress and inter-particle bond distribution, providing that suitable recipient voids are available to accept particle translation. The translation of particles between adjacent voids may be transient or permanent, movement being analogous to Brownian motion but on a macroscopic level (Culling 1963).

Culling (1981) proposes an empirical test of his model which in-

volves constructing a voids or particle density map for a plane of soil surrounding a circular barrier inserted into a diffusive flow. Culling's model predicts that a steady state pattern will eventually develop around the barrier that is uniquely associated with diffusive flow. Flavell (1986) has produced such a voids map for a plane of soil upslope and downslope of a circular barrier in a sandy soil. As discussed in Chapter 2 the results are supportive of Culling's model. However, many factors are likely to complicate an ideal behaviour pattern such as fabric shape constraints, diagenesis of soil particles, knowledge of past stress conditions, and the presence of tensiometric or dilating forces which may be locally important.

5.6 Summary

Quantitative evidence with which to test predictions from the S.M.M. mechanisms outlined may be obtained from field instruments, sedimentological investigation and laboratory simulation experiments.

Direct observation of sub-surface movement is not possible because of the particulate level and slow rate of the process. However, indirect evidence is supplied by the tilting, translation, or deformation of buried markers of various designs (Anderson and Finlayson 1975).

Such evidence describes the cumulative effect of many particles acting as a physical barrier of arbitrary dimensions. This may or may not reflect the true nature of the process because of instrument inertia or drag or because of local disruptions of soil microstructure and the resultant effect upon the through-flow of water around the barrier.

If the marker's coefficient of thermal conductivity differs markedly from that of the undisturbed soil then it may not respond in sympathy with heat exchanges which stimulate soil movement. Despite these limitations, field instruments, if suitably replicated for a given experimental design, will provide important information about spatial and temporal patterns of S.M.M. which may be analysed statistically and which may give an insight into the process mechanism. Results from such a programme of field instrumentation are presented in Chapter 7.

Sedimentological evidence for S.M.M based upon fabric shape relies on the ability to test the *Jeffrey/Gay* theory of viscous fluid flow. This introduces considerable practical difficulties as analysis requires stereo-optical or stereoscopic scanning electron microscopy, which involves complex sampling and preparation techniques that could dis-

rupt the fabric. A brief discussion of attempts to analyse fabric shape using scanning electron microscopy is given in Chapter 8.

Experiments which simulate S.M.M. hold the most promise in the understanding of its mechanism. Key variables may be analysed quantitatively and controlled independently. At present such external control has only been achieved in the laboratory and even then full control over the stress and hydrological state of a soil mass is difficult to achieve.

A simple shearing mechanism may be simulated using stress controlled direct shear testing apparatus suitably modified for the low normal and shear stresses encountered in shallow soil masses. Full details of the design and analysis of this shearing test which attempts to separate the effects of pure shear and viscous flow mechanisms are presented in Chapter 6.

Chapter 6

Laboratory simulation of slow mass movement

Contents

6.1 Aims

Laboratory experiments were undertaken to investigate the behaviour of natural and remoulded soils when subjected to levels of shear stress that would occur naturally. A procedure was designed to test whether direct shearing is an effective cause of mass movement or whether other forces must act in conjunction with a shearing force in order to promote instability. This is achieved by testing soil samples that are known from field measurement to exhibit high rates of mass movement. In situ effective stresses for each sample are re-created in the laboratory from field measurements of water table levels and slope geometry. The soil sample is then subjected to the simulated effective stress conditions and its strain behaviour monitored and compared with that measured in the field.

The same laboratory procedure is also designed to determine accurately the level of shear stress at which a sample deforms at a constant rate and the stress level at which it fails. These are important mechanical parameters which are difficult to estimate from conventional direct shear or triaxial tests. A number of reseachers have described apparatus for investigating stress-strain-time behaviour of soils (Goldstein and Ter-Stepanian 1957; Singh and Mitchell 1968; Andersland and Douglas 1970), and the equipment described in this chapter for shear testing has been modified from their basic designs.

The testing procedure also aims to quantify the effect that soil fabric and plant root permeation have on the shearing strength of the soil. Waldron *et al.* (1983) describe the use of direct shear apparatus to investigate the behaviour of root permeated soils at constant stress levels. In the case of Weardale soils, plant roots permeate to below the

depth of measured mass movement and so a method of soil strength testing which quantifies root effects is essential.

6.2 Definitions of terminology

The terms used in this chapter conform to the conventions of soil mechanics; however, there are a few minor departures and so each term is defined to avoid ambiguity.

Materials can be subjected to shearing, tensile and compressive forces which may result in changes to both shape and volume. The reaction of a body to an applied force can be characterised in terms of the ratio of its deformation to its initial dimensions.

$$\epsilon = \frac{\delta L}{L}$$

ϵ = longtitudinal strain L = length of body in given plane

Equation 6 (1)

ϵ may be positive, indicating compression, or negative, indicating tension. Strain may also be defined as an angular deformation, the simplest case being:

$$\epsilon = \frac{u}{h} = tan\theta$$

Equation 6 (2)

The expression for strain is a ratio of lengths and thus dimensionless, being expressed as percentage of change to original dimension.

The effect of a force in causing deformation is directly related to its magnitude and inversely related to the area over which it acts. A force per unit area is termed a stress. When a stress is perpendicular to the area on which it acts it is termed a normal stress -

$$\sigma = \lim_{\delta A \to 0} \frac{\delta F}{\delta A}$$

F = force

A = area

Equation 6 (3)

When a force is applied in a direction other than perpendicular to the area on which it acts it causes a shearing stress.

$$\tau = - \lim_{\delta A \to 0} \frac{\delta F}{\delta A}$$

Equation 6 (4)

Also important in describing deformation is the rate of change of stress and the time dependence of strain. This is defined as the time rate of elongation or strain rate -

$$\dot{\epsilon} = \frac{\delta \epsilon}{\delta t} = \frac{1}{L} \cdot \frac{\delta \Delta L}{\delta t}$$

ΔL = elongation

L = original length

t = time

Equation 6 (5)

The stress-strain-time relationships of a material determine its rheological character. Rheology is concerned with describing the mechanics of deformable bodies which in the case of soils corresponds to analysing the degree to which a soil exhibits ideally elastic or plastic deformation. An elastic solid deforms instantly when stressed, retains its form while stress remains constant, then returns to to its original form when stress is released. Ideally elastic behaviour is analogous to that of a spring, as defined by Hooke's law, and is represented rheologically as a Hookeian spring.

FIG 6·1

The property of a body to deform progressively when stressed and retain the deformed shape when the stress is released is termed plasticity. An ideally plastic deformation exhibits a positive relationship between stress and rate of strain. However, the coefficient of proportionality is not a true constant but a function of the yield strength of the material and the rate of strain (Mitchell 1976).

Ideally plastic deformation is analogous to a piston being pushed through a fluid of constant viscosity at a rate proportional to the stress. This is defined rheologically as a dashpot or Newtonian body.

FIG 6·2

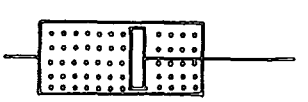

Real soils, however, rarely exhibit ideal behaviour, mainly because they are non-isotropic materials. They commonly deform elastically until some critical point at which elasticity gives way to plastic behaviour.

The experiments described in this chapter are designed to measure the stress-strain parameters at which soils undergo progressive deformation under a constant stress level. Several researchers have described progressive behaviour of soils by a rheological model which incorporates both elastic and plastic components, termed a Kelvin body.

FIG 6·3

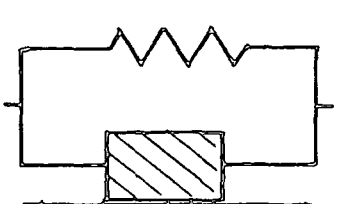

A more widely held view is that a soil will deform plastically once a critical yield stress has been attained. A yield stress is defined rheologically as a Saint-Venant friction block. Singh and Mitchell (1968) suggested that a rheological model incorporating plastic and yielding elements corresponded well with empirical stress-strain-time experiments on non-sensitive silty clay soils. The model is represented as a Bingham body and described thus:

FIG 6·4

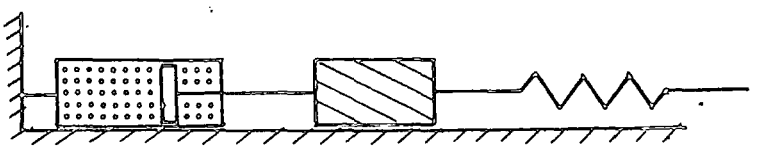

According to Mitchell (1976) time dependent shear strains develop at a rate controlled by the viscous resistance of the soil structure. That viscosity would be defined as the reciprocal of the stress-strain rate relationship of a Bingham body. More generally, the rate of progressive deformation depends on the ability of the soil to relieve stress gradually through internal structural adjustments.

If slow mass movement can indeed be described by a rheological model of progressive shear deformation then the level of yield stress and effective viscosity must be empirically determined from a linear strain rate-stress plot for each soil.

6.3 Background

Experiments which simulate S.M.M. are valuable in the understanding of movement mechanism by quantifying the effect of key variables which may be controlled independently. At present such external control has only been achieved in the laboratory since accurate reconstruction of the stress and hydrological states of a soil

mass is difficult to produce. Young (1958) and Kirkby (1963) both monitored movement of small wires embedded in a soil block which was artificially subjected to wetting and drying cycles. In both of these experiments slope angle was kept constant and so the effects of shearing stresses and hydrologically induced stresses cannot be separated, particularly when factors such as the rate of wetting and drying are not varied. Their initial simulation experiments lacked a control which is essential to ensure that the treatment effects are not induced fortuitously. Corresponding experimental work on thermal displacements of single or loose rocks by Davison (1888) and Tamburi (1974) demonstrated the value of isolating treatment effects in quantifying processes and in being able to compare observed results with theoretical predictions. For example Tamburi (1974) notes that theoretical models, such as that of Scheidegger (1970), had not accounted for the influence of static friction in producing a movement threshold.

The importance of static friction was clearly demonstrated in a precisely formulated experiment and an empirical coefficient could be determined for different rock types.

In the case of slow mass movement, a simple, planar, shearing process may be simulated in the laboratory using stress controlled direct shear testing apparatus suitably modified for the low normal and shear stresses that act on shallow soil masses. Shear strength of granular soils is commonly determined using strain controlled direct shear apparatus. In such a test a soil sample is held within a split box which is subjected to both an arbitrary normal load and a shearing stress produced by extending the top half of the box at a constant rate. The lower half of the box is attached to a calibrated proving ring that measures the increase in shear stress within the sample until it fails. This test is then repeated for various incremental increases in

normal load until a curve of failure points can be plotted for various normal loads and peak or residual shearing stresses; see figure 6.5.

The test is termed strain controlled because the outcome of the test is often dependent upon the rate and magnitude of stress applied to the sample. However, it is well known that the behaviour of many soils varies with the rate at which stress is applied to them and that some soils fail when subjected to quite a low shear stress for a long time period (Mitchell 1976) .In order to study the behaviour of soils under realistic stress conditions, stress controlled direct shear testing may be substituted for strain controlled testing. In the stress controlled test the lower half of the shear box is fixed to an immobile plate and the shearing force is applied only to the upper half of the box. A normal force is also applied in order to simulate vertical or geostatic stress. Once a shearing force is induced the vertical and linear patterns of strain are observed, through time, from linear motion transducers. Shearing forces are incremented in order to produce a stress-strain-time graph (see figure 6.6) and to measure the stress at which continuous motion will be initiated (yield stress). Such time dependent motion, often termed secondary creep, results in fabric rearrangements which may cause a loss of strength (Mitchell 1976). This test has several advantages over the strain controlled procedure. For example,

(i) it is likely to give a better estimate of yield strength for soils which deform in a ductile fashion,

(ii) the testing procedure is equally suitable for both brittle and ductile materials providing that strain rates are slow enough to allow pore water pressures to dissipate during testing,

(iii) it can usefully simulate the *in situ* effective stress state of a sample and so has a role in stability prediction.

Figure 6.5 Typical plot for strain controlled, direct shear testing.

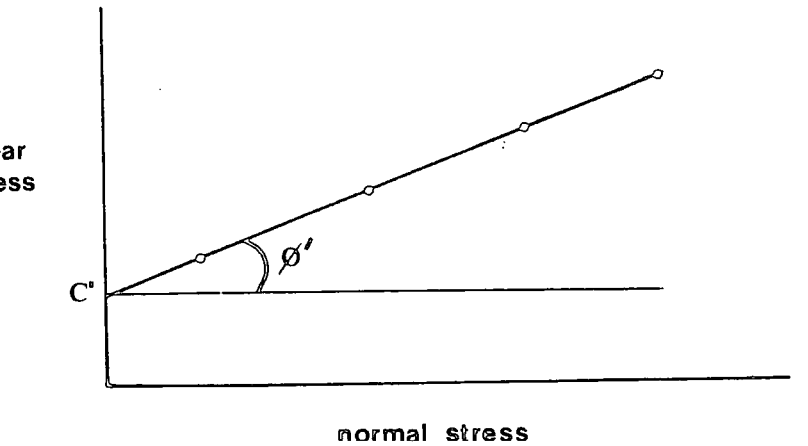

Figure 6.6 Stress-strain-time plot for stress-controlled shear testing.

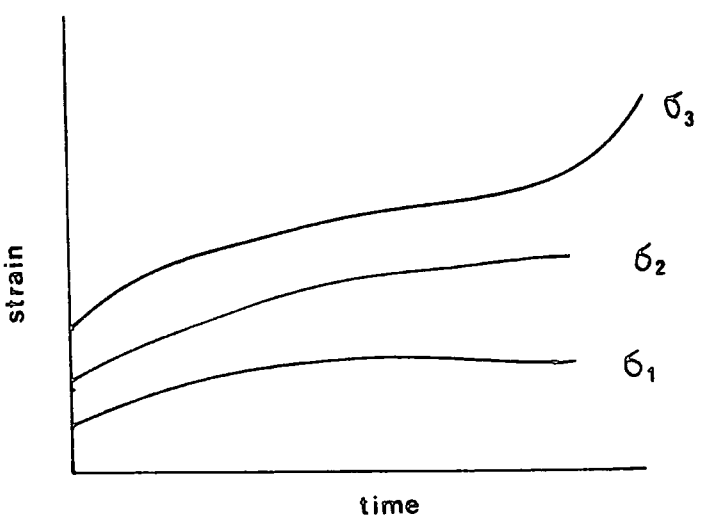

The apparatus used in the following experimental procedure is shown in figure 6.7. The shear box and stand were purpose built for stress controlled testing. The box itself is larger than a standard 60 cm x 60 cm x 6 cm box to give a large shear surface in order to minimise the chance of strain behaviour being influenced by anomalous soil structure in the shear zone. The box was enclosed within a watertight collar in order that the sample should remain saturated throughout the test if required.

The normal force, provided by weights mounted on a travelling hanger, was applied to the centre of the top plate of the shear box. This plate was shaped to allow equal spread of load over the top surface area of the sample during testing. Within the box itself the sample was held in place by two ridged brass plates with a ridge pitch of 5 mm. The plates were solid and non-porous, because drainage was not permitted through the top and base of the sample since the testing procedure was to be undrained. Normally undrained direct shear testing results in a rapid build up of positive pore water pressures within saturated or moist samples. However, with stress controlled testing the pore pressures have adequate time to dissipate during testing and so drainage need not be provided. This greatly simplifies the procedure because pore water pressures need not be artificially controlled.

The shear box, collar and hanger were mounted on a rigid steel frame and fixed to a stable base for the duration of the tests.

Normal and shear forces are applied to the sample by applying mass, in increments, to the hanger and pulley system shown in figure 6.7. The shear stress for soil of thickness z and unit weight γ on a slope of angle θ can be calculated from:

Figure 6.7 Apparatus for stress-controlled shear testing.

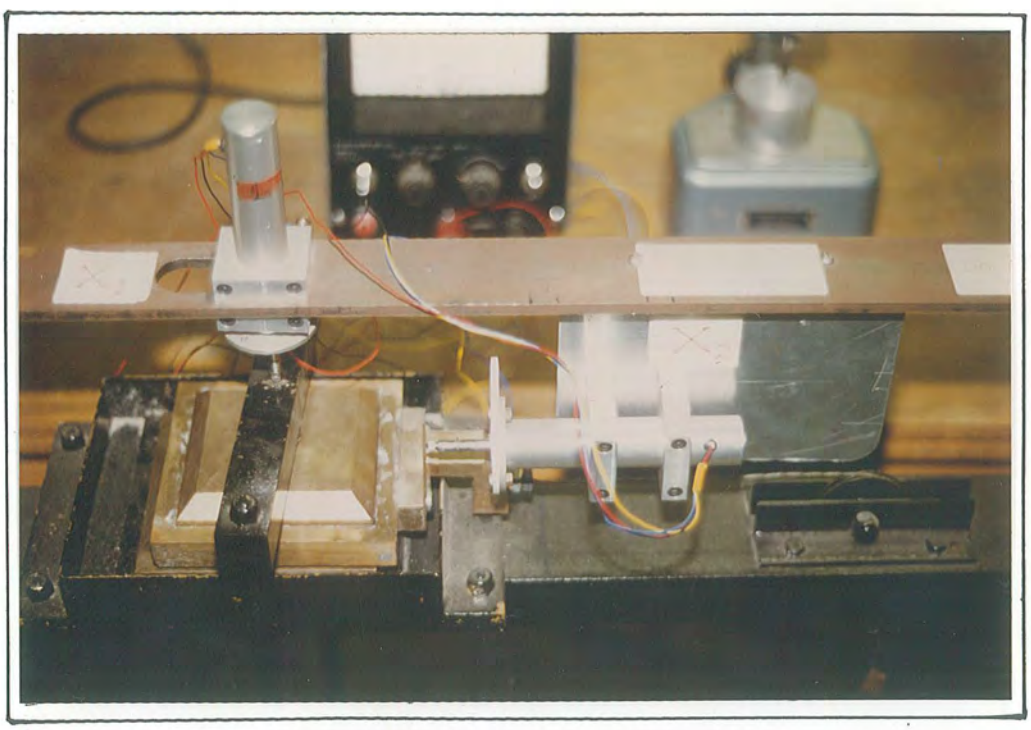

$$\tau = \gamma_s \cdot z \cdot sin\theta cos\theta$$

Equation 6 (6)

and the effective normal stress from:

$$\sigma = (\sigma_v - u)cos^2\theta$$

$$\sigma_v = \int_0^z \gamma_s dz'$$

Equation 6 (7)

where σ is the total vertical geostatic stress, z = depth, and u the pore water pressure. Such stresses are an order of magnitude lower than those commonly encountered in direct shear tests (σ not normally exceeding 50 kN/m^2) and are imposed upon undisturbed soil samples. In order to maintain known effective stress conditions during testing, fully saturated samples are used in an undrained test which proceeds so slowly that pore water pressures have sufficient time to dissipate. Long time intervals are required for each test because very low, but nevertheless significant, strain rates can be expected in the direction of shear. Strain rates measured in the field vary from 0.5 mm/year to 5.0 mm/year in any one plane. Because of these very low rates an accurate linear motion transducer system is needed to detect changes in strain at an hourly timescale.

This instrument has a travelling arm whose position relative to its casing produces a variable resistance to an electric current. Therefore, its output voltage is directly proportional to the displacement of the arm provided there is stabilized input voltage. A transducer was mounted on the shear box frame to measure both displacement of the top plate of the box (vertical consolidation) and horizontal displacement of the top half of the box relative to the fixed bottom part. Each transducer was connected to a stabilized input voltage

and a chart recorder to monitor accurately output voltage, and so displacement, accurately through time. Figures 6.8 and 6.9 show the voltage to displacement calibrations for the two measurement scales used during the testing. Both instruments showed excellent linearity, thus allowing a simple calibration to be derived.

Transducer X1 $D = 1.25(\text{mV})$ (X 10 scale)

Transducer X2 $D = 1.45(\text{mV})$ (X 10 scale)

D = displacement in $\text{m}.10^{-4}$

The strength of the calibration relationships, calculated from ten measured points, were *X1* : 99.6 % of variance explained and *X2* : 97.2 % of variance explained. The best fit lines were not forced through the origin because the transducer is likely to be least accurate at the extremes of its range. Both instruments, however, seem very accurate over the intended range of measurement.

6.4 Experimental Procedure

Testing proceeds by applying a predetermined normal force to a fully saturated or air dry specimen of dimensions 10 cm x 10 cm x 2.5 cm. The normal force is usually identical to that of the soil sample's *in situ* effective normal stress. The sample consolidates when the normal load is applied. This is monitored until movement ceases or is reduced to a rate of 0.01 mm/hour or less. A shear force is then added in small increments until the required *in situ* shear stress level of the sample is reached. The response of the soil is plotted as a graph of strain against time for each level of shear stress. Shear stress levels must be increased in small increments because a large static force added instantly represents an unrealistic rate of stress application which may induce failure prematurely. A gradual build-up which allows the soil to absorb the stress fully at each level alleviates this problem. Once

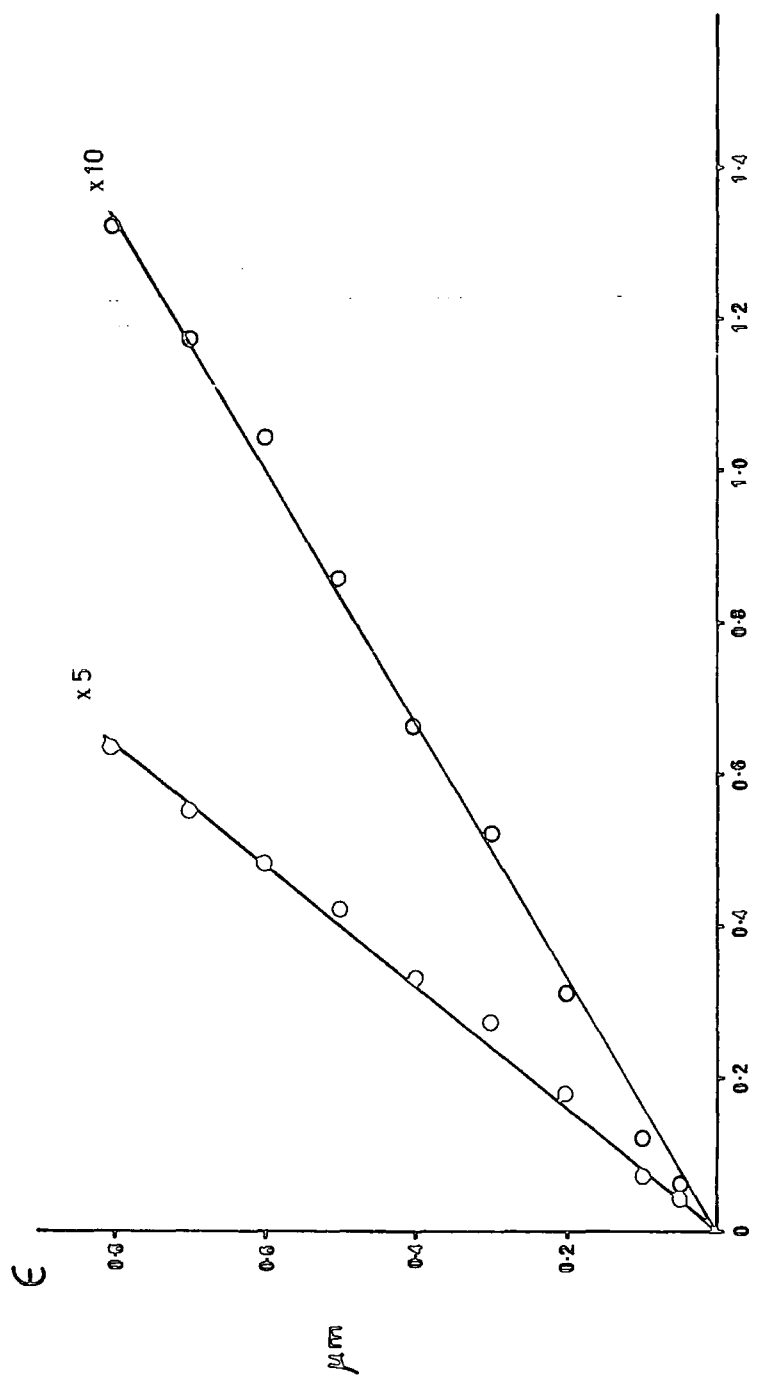

Figure 6.8
Consolidation probe transducer calibration X_1

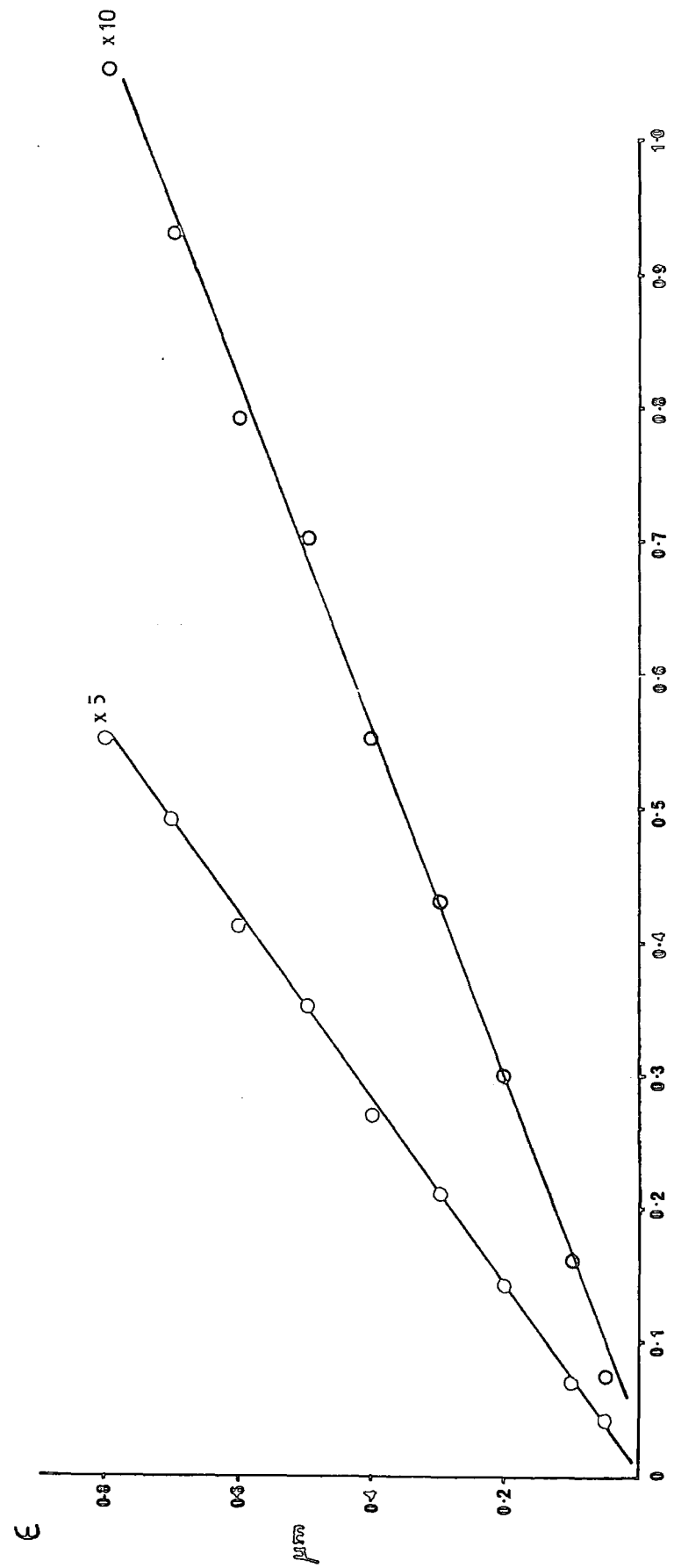

Figure 6.9

Linear strain probe transducer calibration X_2

the target shear stress is reached and studied the test may continue by further addition of stress in order to determine the yield stress value and the peak shear strength.

A simulation run for each level of effective normal stress aims to identify the equilibrium state, in terms of stress-strain behaviour, for every applied shear stress value. Four equilibrium states are possible as shown in fig 6.10:

(i) no strain

(ii) primary creep (initial extension followed by recovery)

(iii) secondary creep (time-dependent strain)

(iv) tertiary creep (acceleration of strain to failure).

No strain will occur if the deviatoric stress is less than the modulus of rigidity of the solid structure when its behaviour resembles that of a brittle solid.

Primary creep shows initial rapid extension followed by an asymptotic recovery pathway typical of deviatoric stresses below the yield and failure thresholds. Initial rapid strain occurs on loading as the rate of stress application is instantaneously very high. This does not seriously disrupt the test provided that the stress increments are small compared with the maximum deviatoric stress. The recovery phase represents an increase in soil strength analogous to work hardening in ductile solids (Tabor 1979; Pusch and Feltham 1980). The rearrangement of soil fabric (Oda 1977) and internal electro-chemical bond restructuring (Pusch 1979) may account for this apparent strength increase in soils.

The stress state at which a constant rate of movement occurs represents the critical yield stress for S.M.M. which can then be compared with the known shear stress calculated from the field location. Experimentally induced strain rates may be compared with observations

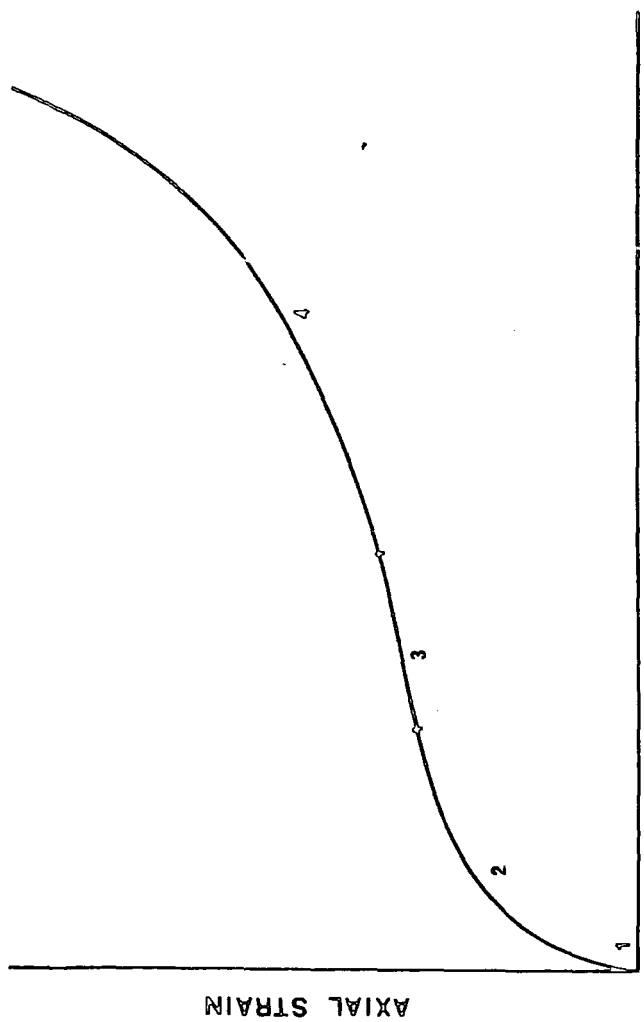

Figure 6.10 Equilibrium states for a creeping material.

of strain obtained from field instruments; similar strain rates would support (although not prove) the hypothesis that mechanisms in the field and in the laboratory were the same.

Tertiary creep represents the phase of soil failure. In a brittle solid the shear stress value at which tertiary creep occurs would represent the peak shear strength. Therefore, the difference between the two is a measure of the susceptibility of the soil to S.M.M.

6.5 Experimental results

Experiments were carried out on samples of three soil types collected undisturbed from the Heathery Burn catchment for which monthly S.M.M. records are available for an eighteen month period. The soil properties for the three soil samples are detailed in table 6.1. These sites were chosen because of the high rates of S.M.M. that were measured in the field at these sites, all of which showed a strong consistent linear trend of movement through time. The samples also span an interesting range of consistency, from a sensitive silty sand to two insensitive clay silty sands which have very different index properties despite their similarity in particle size.

Figure 6.11 shows a summary stress-strain-time diagram for sample A (site 2/1) in its undisturbed state with the direction of shearing orientated to the maximum gradient vector of the site. At low levels of shear stress, the sample deforms rapidly before reaching a point where no strain is apparent with time.

This is often defined as a terminal strain (Lohnes and Handy 1968), analogous to the path of a primary creep curve where fabric rearrangements result in apparent strengthening. This sample begins to show signs of constant, then accelerating, deformation with a shear stress level of 10 kN/m^2 but then undergoes a phase of decelerating

Figure 6.11 Stress-strain-time diagram for sample 2/1 (undisturbed).

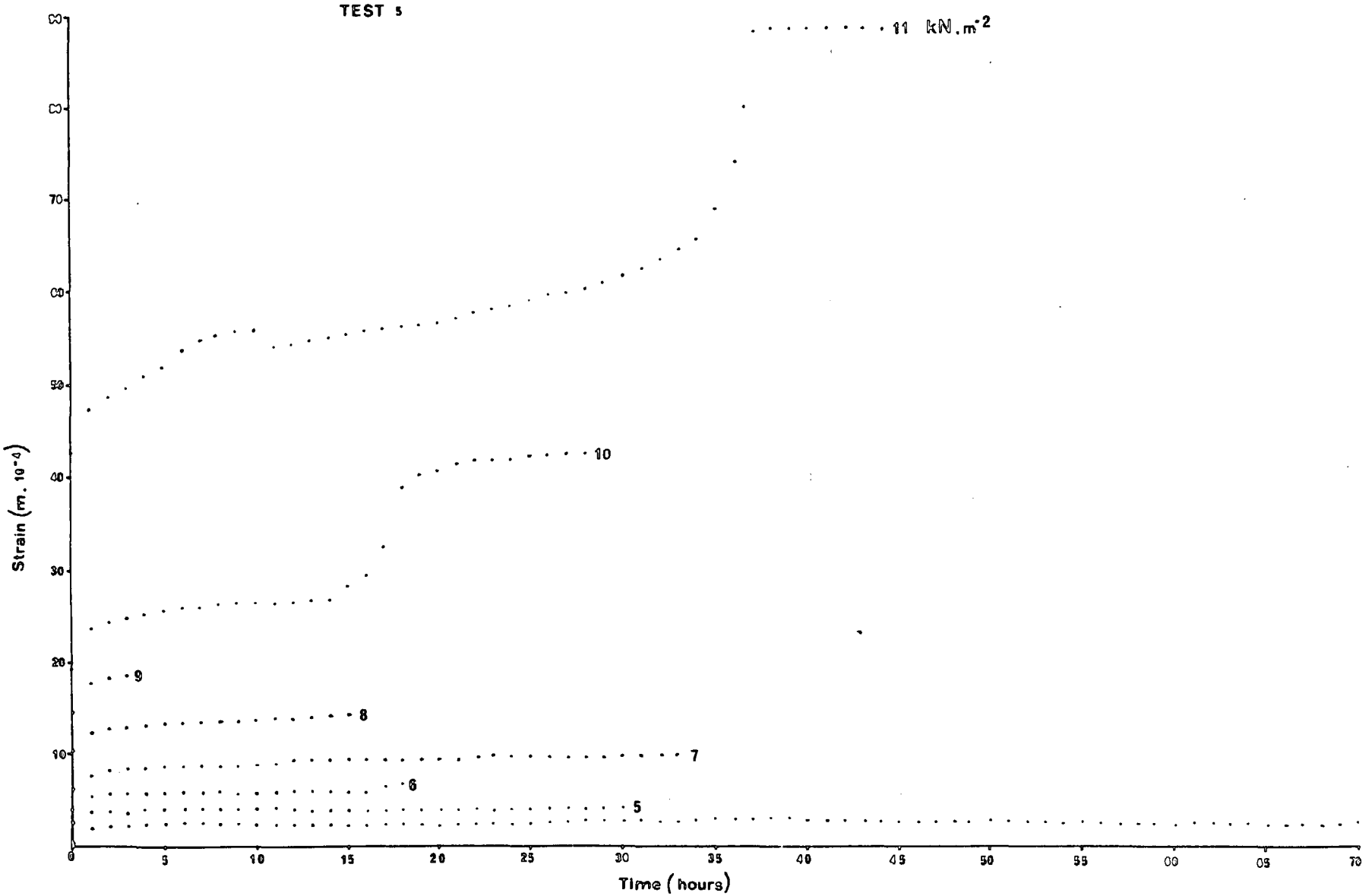

strain and recovery after 18 hours. A phase of constant, then accelerating rate of strain leading to failure is finally exhibited when the shear stress level reaches 11 kN/m^2. Figures 6.12 and 6.13 show the stress-strain-time plots for samples B (site 4/4) and C (site 2/6) in an undisturbed state. These samples show less erratic displacement patterns in the primary creep phase but both show a sudden, sharp transition to secondary then tertiary creep before failure.

Figures 6.14 , 6.15 and 6.16 show the stress-strain-time curves for each of the samples tested after remoulding, that is a total disruption of the original soil fabric and a removal of inclusions such as plant rootlets and macrofossils. Each of these curves shows a smooth primary phase followed by a sudden transition to an accelerating strain rate and failure. The level of stress that each of the remoulded samples can withstand is significantly reduced, see table 6.2. This result emphasises the importance of the primary soil fabric and rootlets in contributing to shear strength.

Among others, Goldstein and Ter-Stepanian (1957) and Singh and Mitchell (1968) have suggested that soils which behave as ductile solids display a linear strain rate stress relationship. When strain rate is plotted against stress levels the reciprocal of the gradient of the relationship is the plastic viscosity of the soil (Lohnes and Handy 1968). Singh and Mitchell (1968) first postulated that creep behaviour of soils corresponds rheologically to a Bingham body.

Figures 6.17-6.22 show strain rate plotted against stress for each of the soil samples in their undisturbed and remoulded forms. Each of the remoulded samples shows a clear linear relationship but the small number of stress increments which could be added to samples B and C means that the relationship is rather imprecisely defined. Lohnes and Handy (1968), Singh and Mitchell (1968) and Mitchell

Figure 6.12 Stress-strain-time diagram for sample 4/4 (undisturbed).

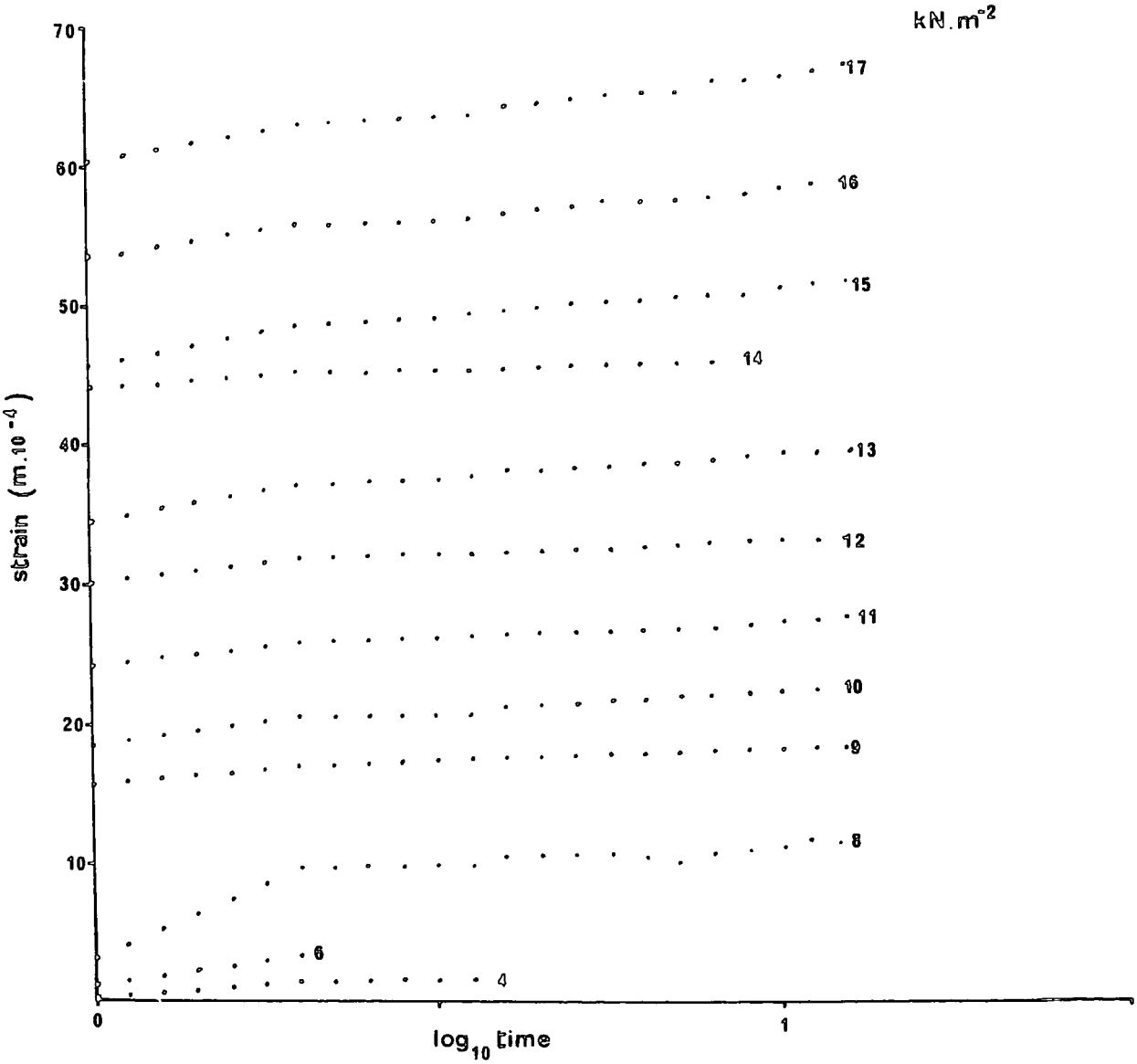

Figure 6.13 Stress-strain-time diagram for sample 2/6 (undisturbed).

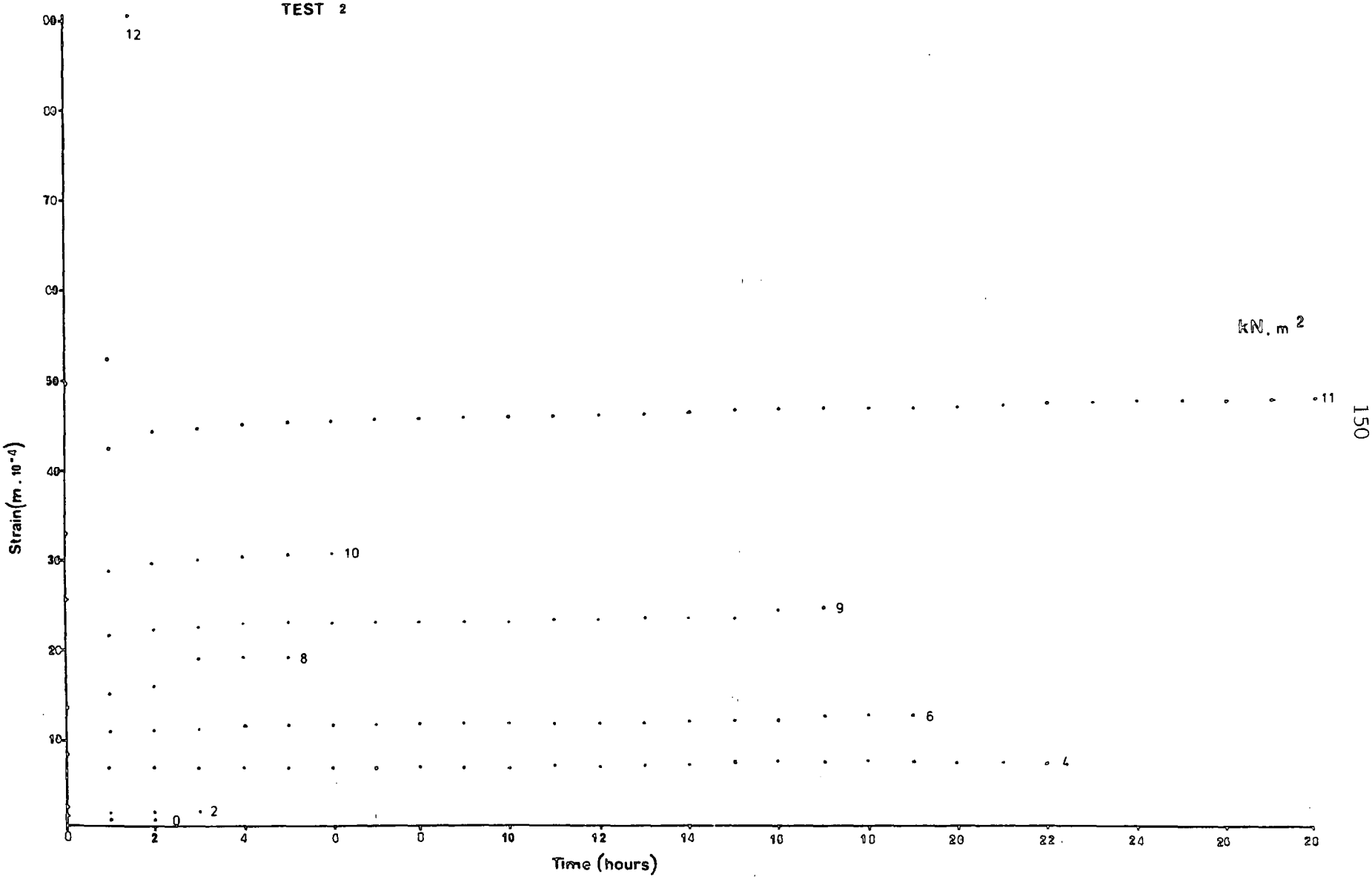

Figure 6.14 Stress-strain-time diagram for sample 2/1 (remoulded).

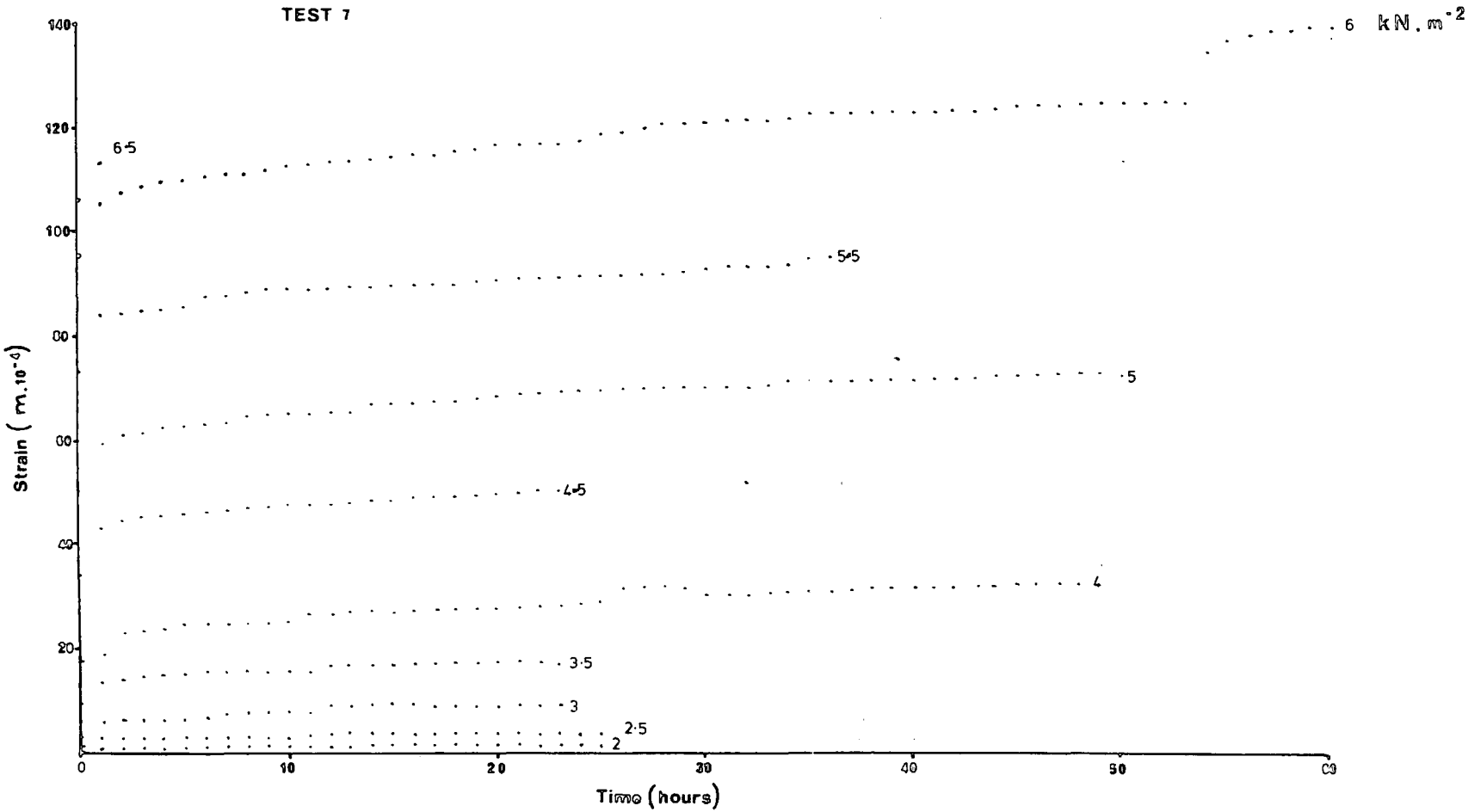

Figure 6.15 Stress-strain-time diagram for sample 4/4 (remoulded).

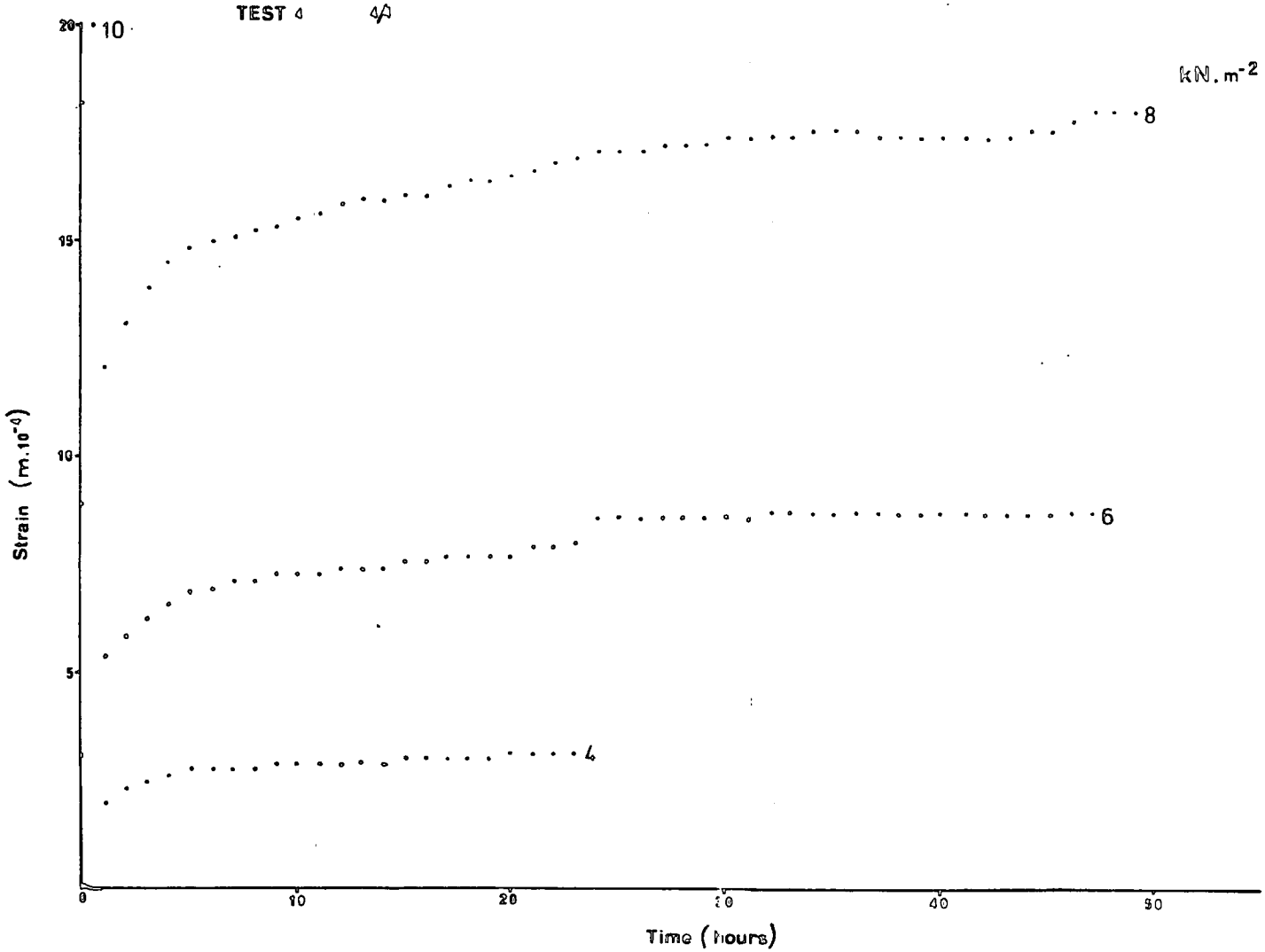

Figure 6.16 Stress-strain-time diagram for sample 2/6 (remoulded).

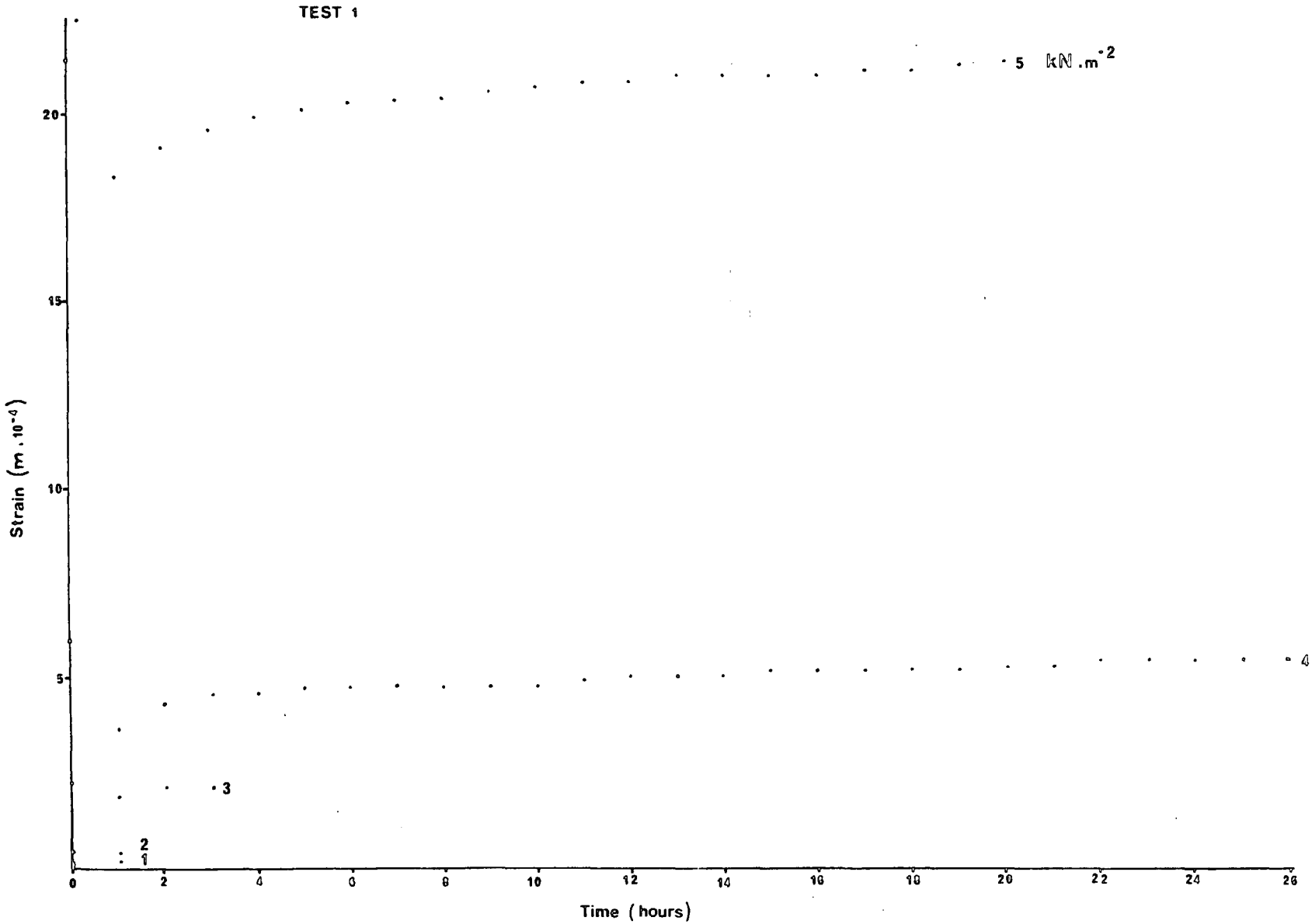

Figure 6.17 Strain rate against stress for sample 2/6 (undisturbed).

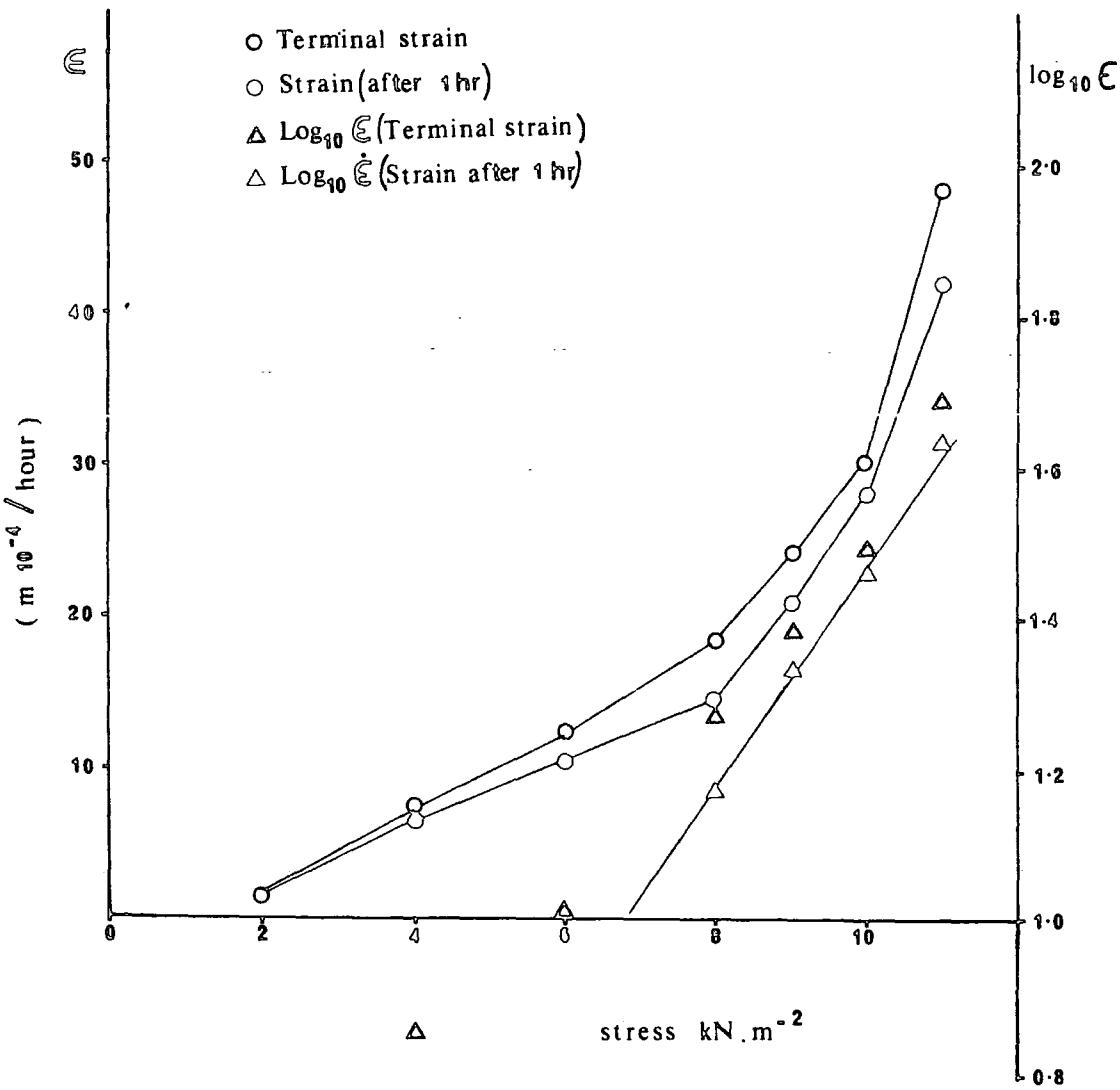

Figure 6.18 Strain rate against stress for sample 2/6 (remoulded).

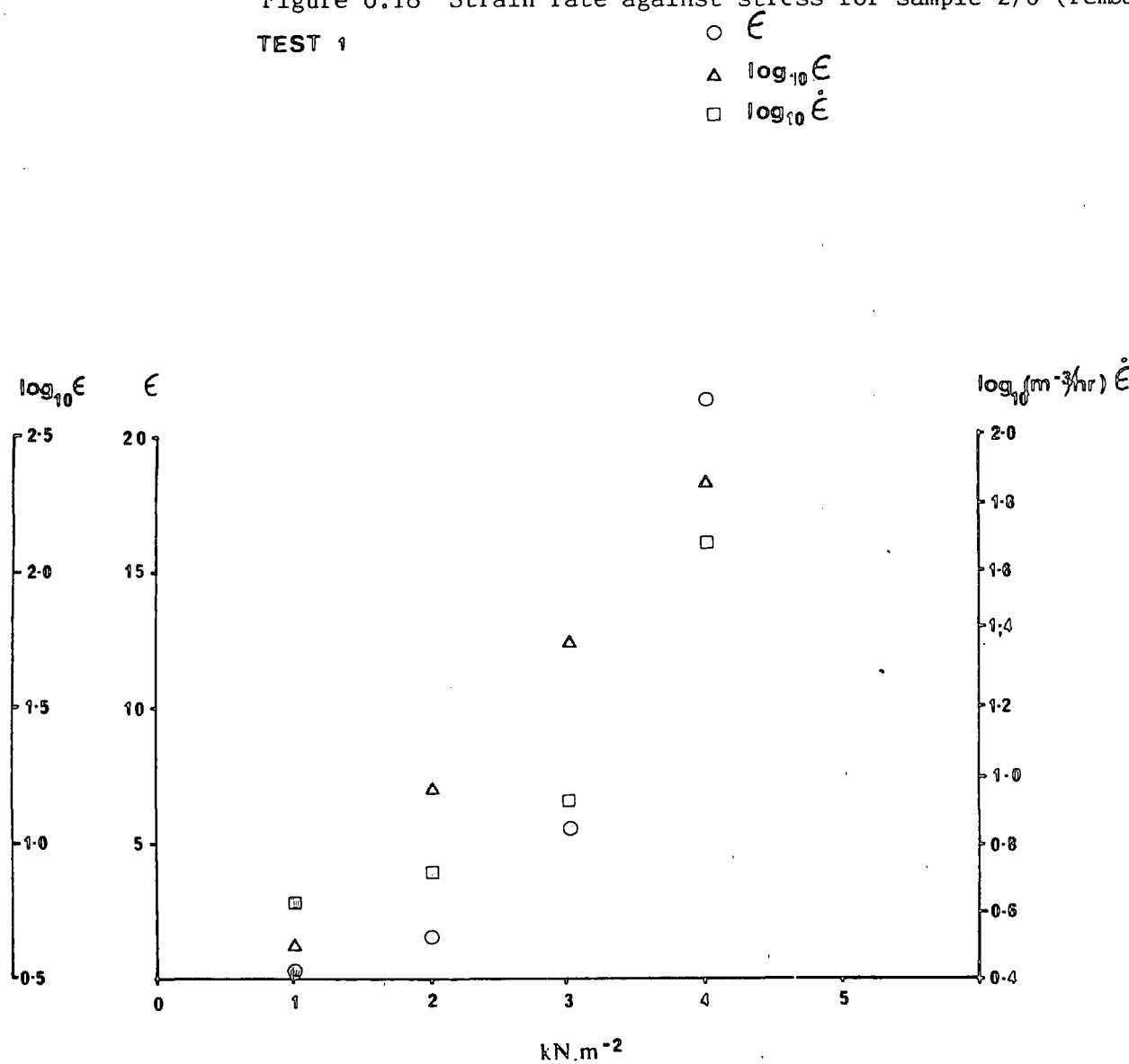

Figure 6.19 Strain rate against stress for sample 4/4 (undisturbed).

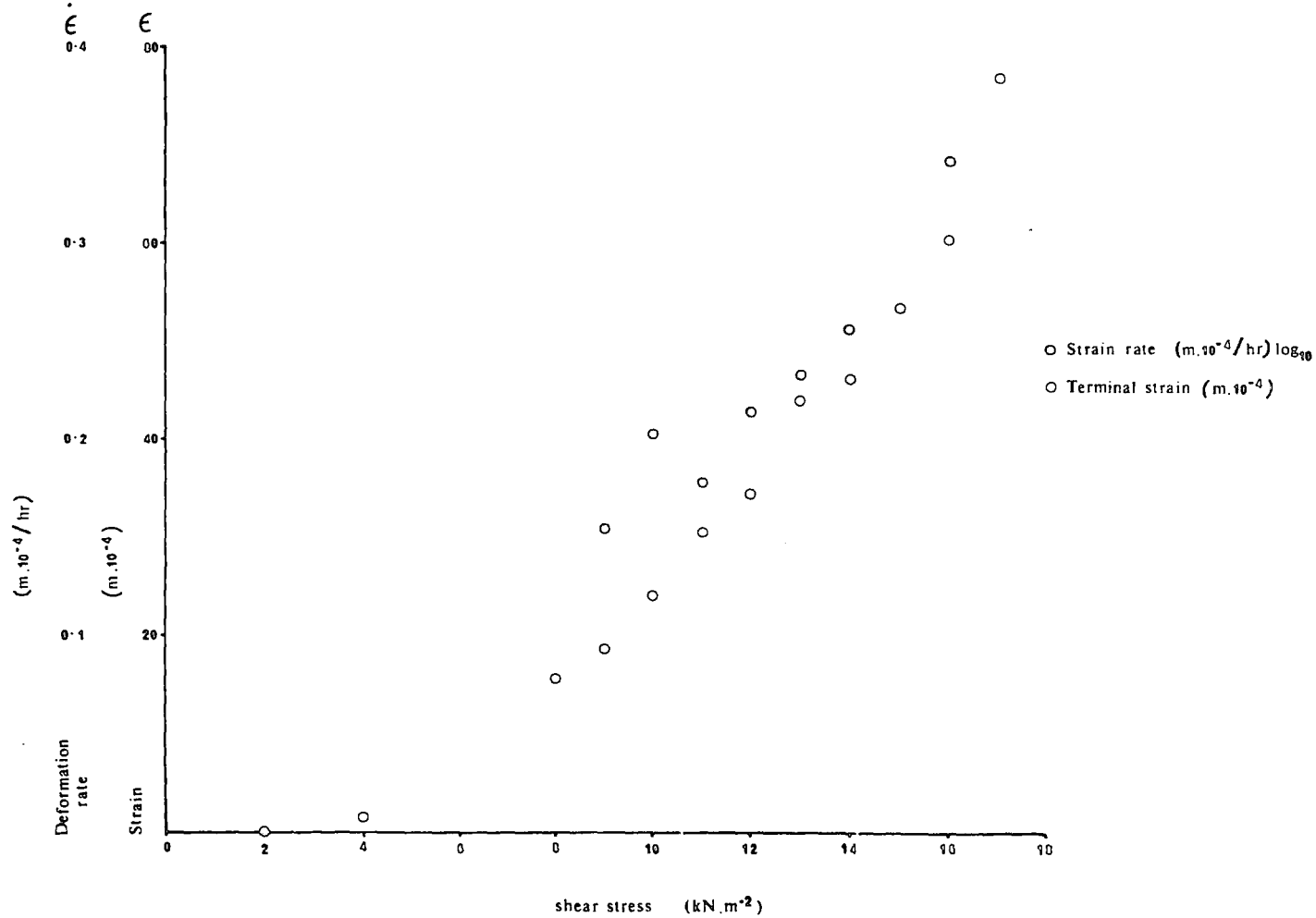

Figure 6.20 Strain rate against stress for sample 4/4 (remoulded).

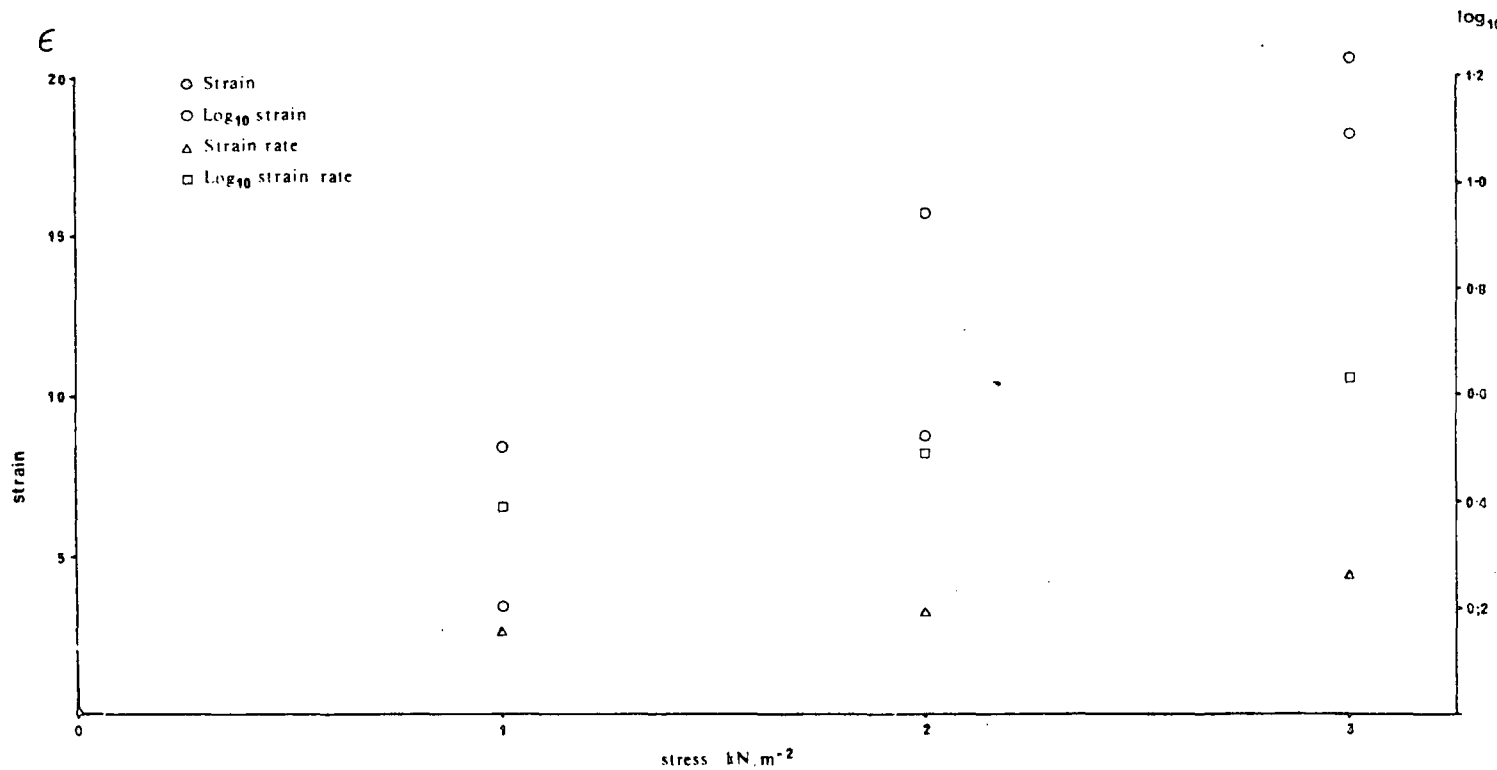

Figure 6.21 Strain rate against stress for sample 2/1 (undisturbed).

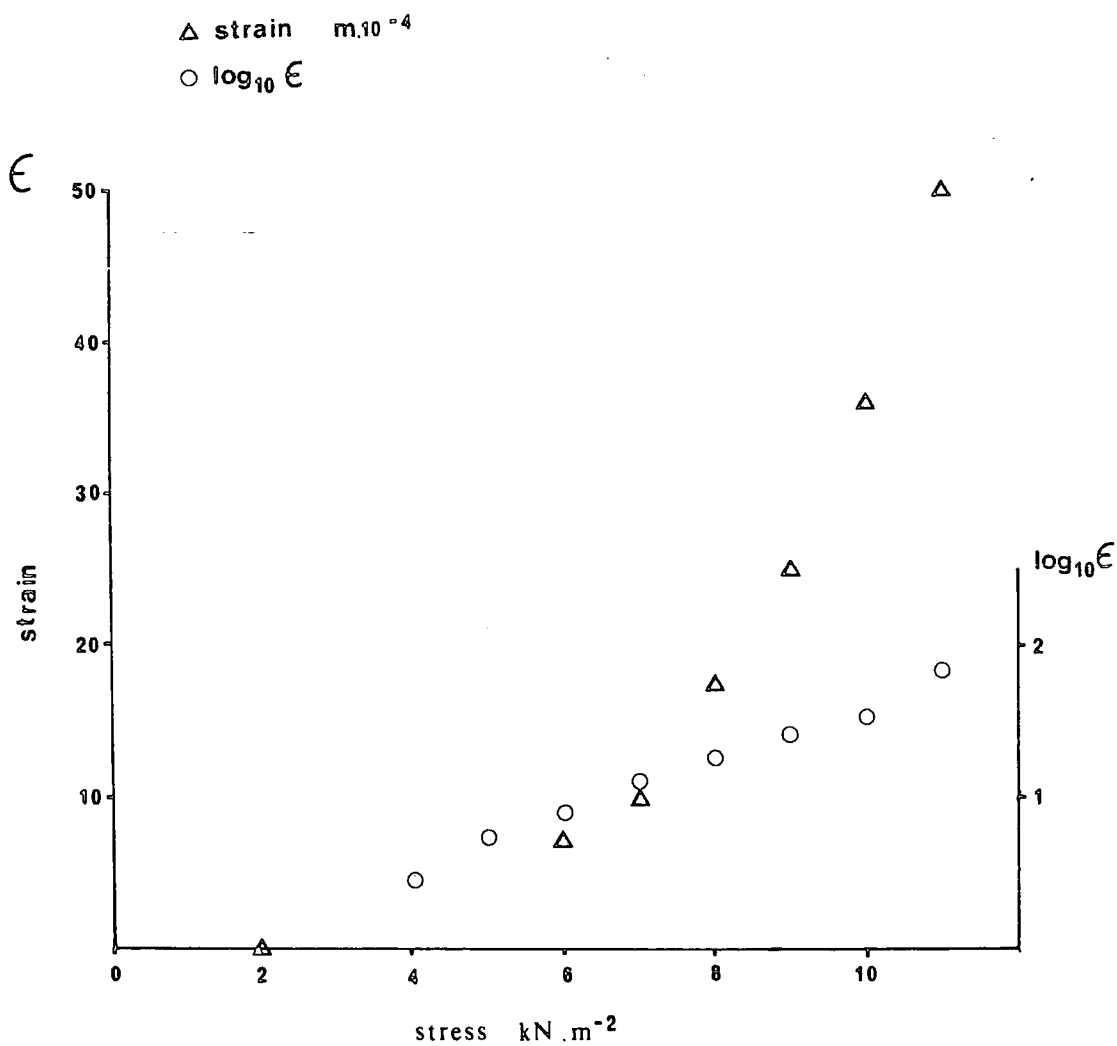

Figure 6.22 Strain rate against stress for sample 2/1 (remoulded).

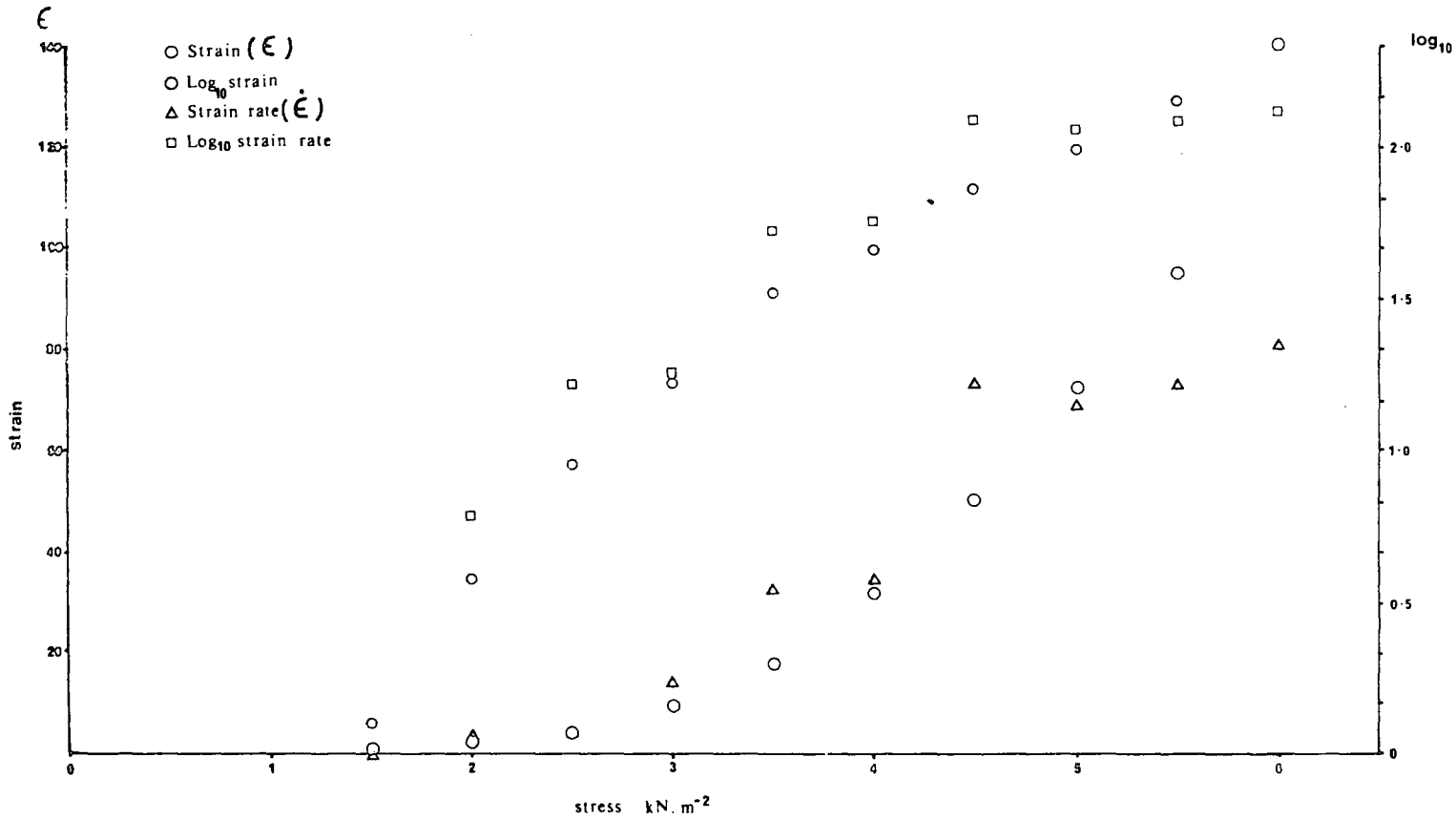

(1976) suggest that extrapolation of the relationships through the x-axis defines the yield stress of the material. This would be analogous to the force required to initiate movement of a St-Venant friction block in a rheological model. Indeed the remoulded soil curves correspond well to that suggested for a Bingham body.

The undisturbed samples appear more complex. Each of the soils does exhibit a linear strain rate-stress pattern at high stress levels but at lower stress levels the linear fit does not seem appropriate. Indeed both samples A and B both appear to possess a clear break in the slope of the line, perhaps suggesting a threshold of movement behaviour. This may be due to the presence of true cohesion in these soils due to mineral cementation, electrostatic attraction between closely spaced particles or surface adhesion of particles. As testing proceeds and large fabric readjustments occur such forces will become negligible and a purely frictional response to stress will resume (Mitchell 1976).

Plotting strain rate against time at each successive stress increment allows evaluation of the stress level at which a dynamic equilibrium is reached. Figure 6.23 shows the plot for soil A. It is interesting to note that strain rate at the yield stress level of 12.0 kN/m^2 displays a fluctuating pattern which dampens with time to a steady rate of 1.0 %/hour until failure occurs after 34 hours. Since there is an initial recovery phase of six to eight hours followed by several oscillations of period approximately four hours it would be unwise to apply load increments at a greater frequency than once per thirty six hours. One of the problems with this testing procedure is the inability to increase deviatoric stress on a continuous (rather than incremental) scale and thus perhaps the critical stress value being sought may be missed because of sudden failure following loading. This difficulty is encountered whatever the apparatus used and is dependent on the

Figure 6.23 Strain rate against time for sample 2/6 (undisturbed).

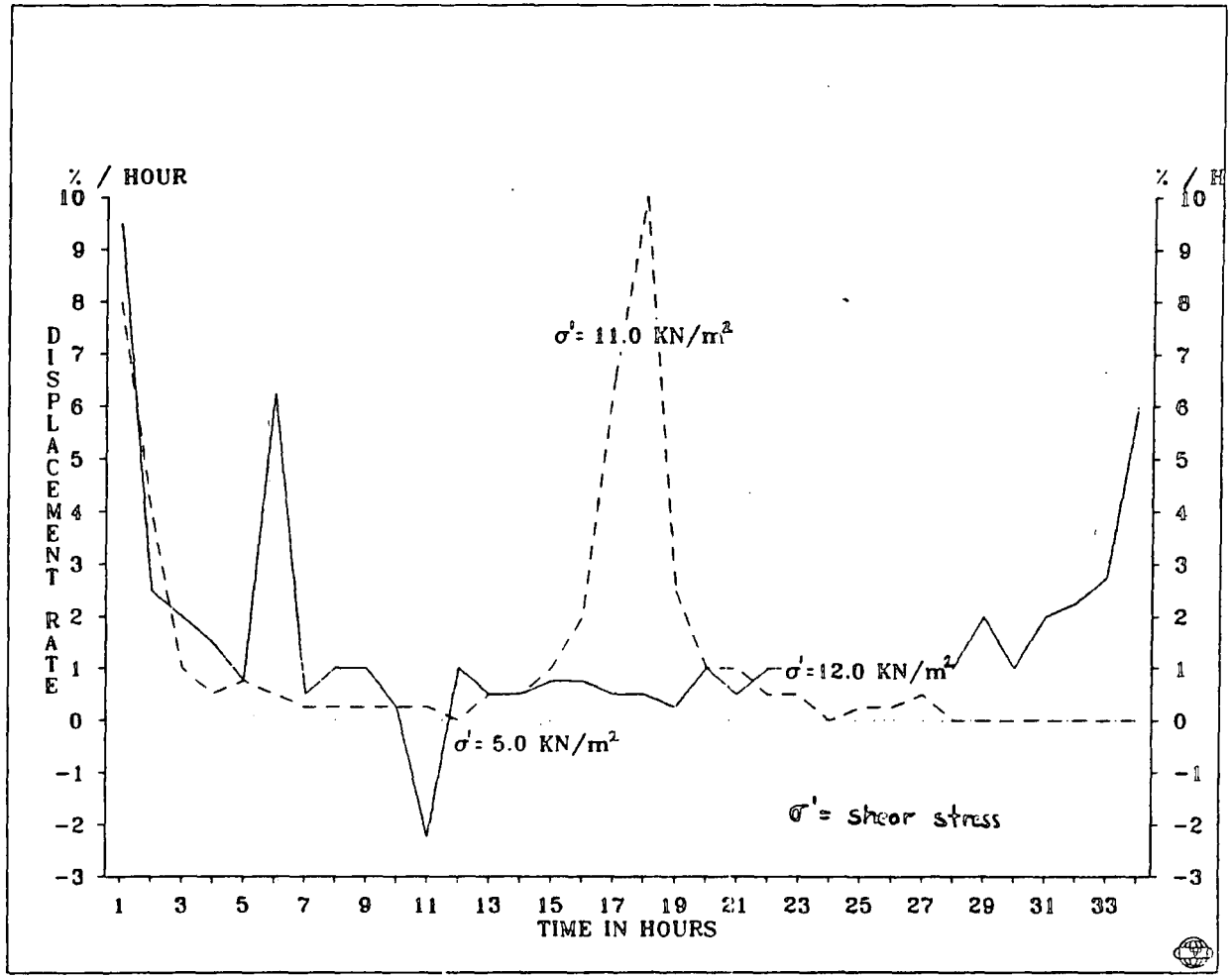

magnitude of the stress increase at each loading, the sensitivity of the soil and the stress history of the soil. In practice shallow soils which have not been overconsolidated pose little difficulty because the range of stresses between the yield and peak levels represent a transition of behaviour rather than a sharp threshold.

The peak shear stress values obtained from this test procedure are consistently lower than those obtained from shear vane apparatus or conventional strain controlled direct shear testing (table 6.2). In the case of S.M.M. studies involving low effective stress levels this is mainly due to the inherent unsuitability of tests which employ

(i) a high rate of stress application

(ii) inappropriate level of shearing stress

(iii) small area of shear surface

iv) inappropriate orientation of shear surface.

Additional variability may be introduced because of non-identical samples, variable drainage conditions during testing and differences in sample pre-treatment. However, the similarity between values obtained from direct shear testing and field vane testing would appear to indicate that the latter factors exert a minimal influence. The similarity of test procedure between stress and strain controlled direct shear testing, and the differing results, would strongly indicate that the rate of stress application during testing and the level of applied stress are crucial. As the stress controlled apparatus is designed to simulate realistic stress levels and strain rates the results obtained will be more reliable indicators of stability thresholds than those obtained from other conventional geotechnical procedures.

Table 6.2 also shows yield stress values to be consistently less than peak stress values in all soil types studied although in soil B whose shear strength has a high frictional component, the difference is not

TABLE 6·1

Soil Physical properties

	A	B	C
% Sand	60	54	84
% Silt	25	32	12
% Clay	15	14	4
Liquid limit (%)	65.50	98.57	71.12
Plastic limit (%)	48.38	72.62	51.75
Plasticity index (%)	17.12	25.95	19.37
Dry density (Mg/m^3)	1.83	1.91	1.95
pH	4.9	4.5	5.1
Loss on ignition (%)	12.88	10.65	3.44
Saturated moisture %	74.77	66.42	57.38

TABLE 6·2

A comparison of geotechnical procedures

		Sites		
		A	B	C
Stress controlled test	τ_p	12.0	13.0	18.0
	τ_y	11.0	12.5	17.0
	τ_r	5.0	7.0	17.0
	$\Delta\tau_{(pr)}$	7.0	6.0	1.0
	Φ'_p	28.0	35.0	42.0
	Φ'_r	29.0	35.0	42.0
Strain controlled test	τ_p	15.0	22.7	27.9
	τ_y	11.6	14.1	25.4
	$\Delta\tau_{(pr)}$	3.4	8.6	2.5
	Φ'_p	31.0	36.0	42.0
	Φ'_r	30.0	36.5	40.5
Field shear vane	τ_p	15.69	21.90	26.15

τ – Shear strength (kN/m^2)
Φ' – Internal friction (degrees)
p – Peak
y – Yield
r – Remoulded

TABLE 6·3 A comparison of predicted yield stress levels, actual field stress levels and observed movement rates for three test soils.

Site	Predicted yield stress (kN/m^2)		Actual field stress (kN/m^2)	Observed movement (cm^2/year)	
	Undisturbed	Remoulded		AT	IP
A	11.0	5.0	2.72	6.00	11.05
B	12.5	7.0	2.12	7.25	7.50
C	17.0	17.0	1.21	5.55	8.30

AT – ANDERSON's tube, IP – Inclinometer peg.

significant. This confirms that all soils studied exhibit the potential for S.M.M.

From table 6.3 it can be seen that the shear stress thresholds needed to initiate S.M.M. in all three samples by far exceed the simulated naturally occurring shear stresses corresponding to each soil type indicating that samples should not exhibit S.M.M. from a shearing mechanism. Data from Anderson's tubes and inclinometer pegs (Anderson and Finlayson 1975) indicate that significant movement does occur at each site suggesting that the simple model of the soil undergoing slow confined shearing does not provide a full explanation of the mechanism. The test, however, provides a valuable method of testing this hypothesis quantitatively.

Results from the remoulded samples show that the presence of plant rootlets, fabric shape, and soil structure contribute significantly to the yield and peak shear strength of soils A and B.

Clearly vegetation type and soil structure exert important controls over S.M.M. by the addition of apparent cohesion to the soil matrix. Root type, depth of penetration and spatial pattern of root system are of particular importance. Waldron *et al.* (1983) note that alfalfa (herbaceous) rootlets can increase apparent soil cohesion by up to 50 % which is in broad agreement with the results in table 6.3. Soils A and B have loss on ignition values of 12.88 % and 10.65 % respectively, and are densely permeated by long penetrating *Juncus squarrosus* roots. On the other hand soil C has a loss on ignition value of 3.44%. and is sparsely permeated with a shallow network of fine fibrous roots. These differences may explain why the apparent cohesion varies so significantly among soil types despite similarities in the angle of internal friction.

The testing procedures described are particularly appropriate for

assessing how plant roots affect shear strength for two reasons. First, the slow rate of the test allows the roots to strain in tension rather than be sheared rapidly; and secondly, roots are tested over the range of stresses which would be encountered in the field. Tensional straining of roots is important as the lignin in the root's cell wall only displays longitudinal strength. (Waldron *et al.* 1983).

6.6 Comparing experimental results with field observations

The stress controlled direct shear test can be used to predict movement rate in the field if movement is parallel to the ground slope surface once the strain rate-stress relationship has been established.

Consider the balance of forces used to solve a conventional planar stability problem where a shear stress and shear strength are defined thus:

shear stress $= \gamma_s \cdot z \cdot sin\theta cos\theta$

and

shear strength $= c' + z.cos^2\theta(\gamma_s - \gamma_w)\tan\phi'$

c' = effective cohesion,

γ_s = unit weight of soil,

γ_w = unit weight of water,

ϕ' = angle of internal friction.

θ = slope angle Equation 6 (8) During progressive failure effective cohesion is reduced to zero by definition and the angle of internal friction is replaced by the apparent viscosity of the soil as measured from different shear to normal stress ratios. Therefore at instability the $\frac{\tau}{\sigma_n}$ ratio will correspond to a given rate of movement.

The relationship can be rearranged to solve for an equivalent slope

angle for any given $\frac{\tau}{\sigma_n}$ ratio.

If

$$\frac{\sigma_n}{\tau} = 1$$

Equation 6 (9)

then

$$\frac{\gamma_s \cdot z \cdot cos\theta sin\theta}{z \cdot cos^2\theta(\gamma_s - \gamma_w)} = 1$$

Equation 6 (10)

$$\Rightarrow \quad \frac{sin\theta \cdot \gamma_s}{cos\theta(\gamma_s - \gamma_w)} = \frac{\tau}{\sigma_n}$$

Equation 6 (11)

$$\Rightarrow \quad tan\theta = \frac{\tau}{\sigma_n} \cdot \frac{\gamma_s - \gamma_w}{\gamma_s}$$

Equation 6 (12)

Therefore for any given soil with zero pore water pressure an equivalent slope angle can be defined for each normal to shear stress ratio at any point leading up to instability. Table 6.4 shows this equivalent slope angle plotted for soil sample A (undisturbed) for a number of shear stress levels. The pattern indicates that slow strain is predicted for low slope angles; however, that movement is very small, less than 1 mm/year for the actual slope angle of the site the sample was derived from. This result assumes that the sample will exhibit a time dependent movement at all stress levels above the yield stress as defined by extrapolating the curve of strain rate versus stress. The previous comparative analysis between measured shear strength, or critical stress in this case, where a tertiary creep curve was observed, makes no such assumption and probably equates better to actual behaviour. However, the strain rate-stress relationship of a ductile soil

Table 6.4 Equivalent slope angles

θ	τ	σ_n	$\frac{\tau}{\sigma_n}$
5^o	86.8	496.2	0.175
10^o	171.0	484.9	0.35
15^o	250.0	466.5	0.54
20^o	321.4	441.5	0.73
25^o	383.0	410.7	0.93
30^o	433.0	375.0	1.15
35^o	469.8	335.5	1.40
40^o	492.4	293.4	1.68

has many practical applications and further work is required in order to establish how the relationship varies with soil consistency and fabric.

6.7 Summary

The stress controlled direct-shear testing procedure has allowed the thresholds of initial soil yielding (yield stress) and final soil failure (critical stress) to be identified for levels of stress appropriate to the samples' undisturbed field state. Since none of the samples has been overconsolidated this gives good results which incorporate the effects of primary soil fabric and rootlet inclusion within the samples. Shear strength values obtained from conventional strain controlled testing consistently give higher values for shear strength which are likely to be too high due to the lack of consideration of root and fabric effects.

The simulation experiments described above are a first attempt to model shear movement by reconstructing the intrinsic stress state of the soil. Although these preliminary results are restricted to the recogntion of a simple threshold this is nevertheless a valuable first step in predictive modelling. Further progress should be made by controlled alteration of soil moisture properties, and by subjection to differing levels of thermal disturbance during testing.

Chapter 7

Field experimental data

Contents

7.1 Experimental design

The field experiment described attempts to test two general hypotheses; first, that S.M.M. rate or activity is positively associated with hillslope gradient (other factors being equal), and second, that vegetation and moisture status strongly influence S.M.M. activity. This forms the basis of a bi-factorial experiment in which the interaction between gradient and vegetation may be analysed for its effect upon S.M.M. rate.

In simple mechanical terms, gradient is thought to influence S.M.M. because the force acting upon a body at rest on an inclined plane, in the direction of that plane, is proportional to $m.g.sin.\theta$. In addition, within a soil mass, shear stress is a function of slope gradient.

$$\text{Shear stress} = \gamma_s \cdot z \cdot sin\theta cos\theta$$

Equation 7 (1)

Several researchers have proposed equations to describe the transport of colluvium on hillslopes where movement rate is expressed as a function of slope angle.

$$C(z) = k_s sin\beta \int_z^{\infty} M(z') \cdot dz'$$

Equation 7 (2)

The effect of vegetation cover in modifying S.M.M. has been widely reported from empirical studies. However, the precise mechanism by which movement is affected is not well understood. Anderson and Cox (1984)

attribute widely varying observations of S.M.M. in a catchment area to differences in soil moisture and soil texture, which were in turn associated with major changes in surface vegetation cover. In their analysis, the vegetation cover was selected as a surrogate variable for the combined influence of moisture and soil consistency on mass movement. The importance of plant rootlets in increasing a soil's resistance to deformation was demonstrated in Chapter 6 in the context of a direct shearing force. However, rootlets may also disrupt and weaken the soil fabric through particle mixing and by the transmission of forces exerted from above ground level through the roots. The structure and morphology of the root system will be important as will be seasonal changes in root growth and decay and moisture availability.

Measurements of S.M.M. made by previous researchers have never revealed a strong association with gradient (Young 1959; Kirkby 1963; Evans 1974; Anderson 1977; Rashidian 1984; Auzet 1985). Finlayson (1976) attributes this weak relationship to the disrupting influence of other biological and pedological forces. Several factors mitigate against this relationship being observed easily.

(i) Fewer measurements have been made on steep slopes, such as those with angles greater than 30^{o}, than gentler slopes.

(ii) Those measurements made on steep slopes are likely to have sampled soils which persist there because of high resistance and efficient drainage. Whereas, within slow moving soils (by definition) there cannot be such an adjustment between gradient and resistance of the soil.

(iii) The mechanical behaviour of the soil is influenced by the profile and plan geometry of the slope as well as a local measure of gradient. Very few researchers have attempted to sample a consistent set of slope facets, such as straight slope elements, which would simplify analysis.

(iv) The process of measuring S.M.M. is rather imprecise and most

field based results contain a striking number of unusual or wild observations. Unfortunately, the presence of even a few wild observations has an extremely adverse effect on a least-squares correlation calculation. In addition, experience seems to show that steep slopes show the widest scatter of results (Anderson 1977; Finlayson 1976).

Other important sources of bias in S.M.M. field movement and experimentation include measurement bias from the instrument used or from the human interpretation of the instrument reading, and most insidious of all, bias resulting from unfortunate sampling schemes.

Some of these problems can be overcome through the careful choice of measurement techniques, instrument replication, random sampling within treatment categories, and finally through the comparison of results with exogenous data from a similar experiment.

Analysis of the resulting data must account for the possible influence of a few unreliable results. Therefore, an estimate of central tendency, based on the median rather than the mean, is extremely useful because of the resistance of the median to the influence of a wild observation.

The temporal pattern of S.M.M. events is very poorly understood because very few studies have been sustained for long periods at close sampling intervals. Also, previous studies may have been biased towards visibly active sites.

A consideration of temporal behaviour has been introduced into this study for both theoretical and practical reasons. Many theoretical statements about S.M.M. assume the process to be temporally persistent; however, Anderson and Cox (1986) demonstrate that rapidly fluctuating climatic variables do influence mass movement. Regular monitoring is required in order that seasonal effects may be detected thereby ensuring that an annual movement rate is a meaningful measure.

7.2 Factorial experiment

7.2.1 One-way analysis of variance

Table 7.1 shows S.M.M. data for three depths of inclinometer pegs and for Anderson's tubes. Mass movement is expressed as an annual volumetric measure for the inclinometer peg data and as annual linear (surface) and volumetric movement for Anderson's tube data (to allow comparison of the two measures).

In the first instance a simple hypothesis test should reveal if mean movement rates differ significantly in each slope and vegetation category. Table 7.2 shows that for 15 cm pegs only the *Nardus* group has a mean which is significantly different from the other vegetation groups and that all groups have very high standard deviations. An inspection of the residual variation for each vegetation class figure 7.1 indicates a wide scatter of data, particularly in the *Juncus* group. The 10 cm peg data show slightly better separation among the vegetation groups but the *Nardus* and *Pteridium* groups overlap considerably. Five cm peg data separate more clearly but the standard deviations for each class remain large compared with the mean movement rates themselves.

Table 7.3 shows results from ANOVA of Inclinometer peg data separated by slope angle class. Fifteen cm peg data appears to show no division according to slope class, however, the 10 cm and 5 cm data do show evidence of class means increasing with slope angle, although the results are not significant at the 0.05 ~~confidence~~ level.

Similar analysis of the Anderson's Tube data, table 7.4 and table 7.5, again indicates a confused pattern where there is a large variation of movement rates present within each vegetation and slope category. The mean movement rates for Anderson's Tubes and Inclinometer Pegs show a weak positive association with slope angle. The vegetation groups show

little agreement with the model except that the *Nardus* group consistently shows the lowest movement rates and often has the lowest variability.

Inspection of plots of residuals from the analysis of variance shows that several wild or extreme observations are present in the data. Figure 7.2 demonstrates these clearly for the *Nardus* and *Pteridium* group with Anderson's Tube volumetric data.

The failure to reject the null hypothesis in all the analyses of variance may be in part due to the influence of a few unreliable readings in each of the data sets.

Since slope and vegetation factors cannot be uniquely attributed to explain S.M.M. rates their combined influence is assessed in a two-way analysis.

Table 7.1 Summary statistics for S.M.M. instruments.

	N	N*	MEAN	MEDIAN	TRMEAN	STDEV	SEMEAN	MIN	MAX
IP 15	59	10	136.3	115.5	126.1	133.0	17.3	-292.4	761.4
IP 10	57	12	99.0	78.6	92.5	116.7	15.5	-181.3	459.3
IP 5	62	7	39.99	28.70	37.36	43.79	5.56	-56.68	209.21
AT LIN	50	19	0.977	0.644	0.891	0.849	0.120	0.127	3.263
AT VOL	51	18	121.1	78.9	108.6	119.4	16.7	2.6	479.2

Table 7.2 ANOVA Inclinometer data with vegetation group.

ANALYSIS OF VARIANCE ON IP 15

SOURCE	DF	SS	MS	F
VEG GRP	3	349627	116542	2.60
ERROR	55	2461235	44750	
TOTAL	58	2810862		

LEVEL		N	MEAN	STDEV
J	1	17	299.8	310.9
N	2	18	113.7	173.5
Pt	3	16	269.3	147.6
C	4	8	232.0	104.5

POOLED STDEV = 211.5

INDIVIDUAL 95 PCT CI'S FOR MEAN
BASED ON POOLED STDEV

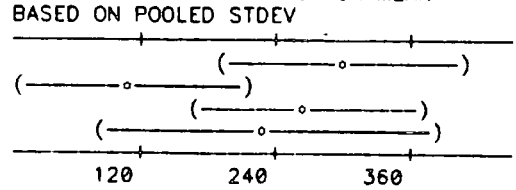

ANALYSIS OF VARIANCE ON IP 10

SOURCE	DF	SS	MS	F
VEG GRP	3	441349	147116	4.73
ERROR	53	1648212	31098	
TOTAL	56	2089561		

LEVEL		N	MEAN	STDEV
J	1	16	301.6	247.1
N	2	17	97.4	77.9
Pt	3	15	100.0	207.4
C	4	9	150.6	64.5

POOLED STDEV = 176.3

INDIVIDUAL 95 PCT CI'S FOR MEAN
BASED ON POOLED STDEV

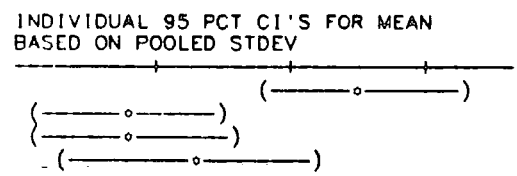

ANALYSIS OF VARIANCE ON IP 5

SOURCE	DF	SS	MS	F
VEG GRP	3	55592	18531	4.06
ERROR	58	264720	4564	
TOTAL	61	320312		

LEVEL		N	MEAN	STDEV
J	1	18	104.87	92.23
N	2	20	32.31	58.09
Pt	3	16	76.26	57.39
C	4	8	43.59	30.72

POOLED STDEV = 67.56

INDIVIDUAL 95 PCT CI'S FOR MEAN
BASED ON POOLED STDEV

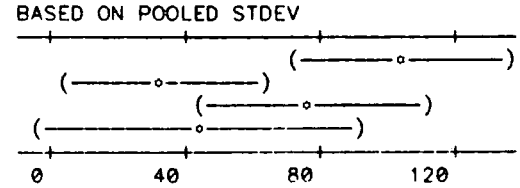

Table 7.3 ANOVA Inclinometer data with slope group.

ANALYSIS OF VARIANCE ON IP 15

SOURCE	DF	SS	MS	F
SLOP GRP	3	96897	32299	0.65
ERROR	55	2713966	49345	
TOTAL	58	2810862		

LEVEL		N	MEAN	STDEV
0-10	1	19	171.7	93.5
11-20	2	18	264.4	206.5
21-30	3	12	259.7	121.4
> 30	4	10	217.1	430 7

POOLED STDEV = 222.1

INDIVIDUAL 95 PCT CI'S FOR MEAN
BASED ON POOLED STDEV

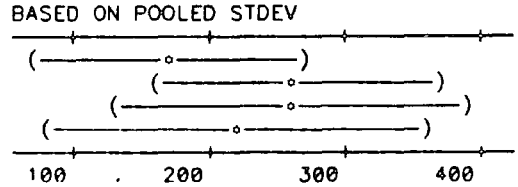

ANALYSIS OF VARIANCE ON IP 10

SOURCE	DF	SS	MS	F
SLOP GRP	3	324540	108180	3.25
ERROR	53	1765021	33302	
TOTAL	56	2089561		

LEVEL		N	MEAN	STDEV
0-10	1	16	85.0	99.5
11-20	2	18	173.9	176.6
21-30	3	13	134.6	232.8
> 30	4	10	309.5	220.1

POOLED STDEV = 182.5

INDIVIDUAL 95 PCT CI'S FOR MEAN
BASED ON POOLED STDEV

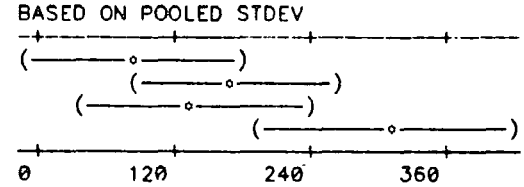

ANALYSIS OF VARIANCE ON IP 5

SOURCE	DF	SS	MS	F
SLOP GRP	3	25572	8524	1.68
ERROR	58	294740	5082	
TOTAL	61	320312		

LEVEL		N	MEAN	STDEV
0-10	1	20	45 88	46.42
11-20	2	20	57.14	41.04
21-30	3	12	94.38	72.01
> 30	4	10	90.98	135 30

POOLED STDEV = 71 29

INDIVIDUAL 95 PCT CI'S FOR MEAN
BASED ON POOLED STDEV

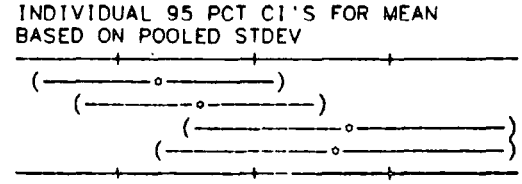

Table 7.4 ANOVA Anderson's Tube with vegetation groups.

ANALYSIS OF VARIANCE ON AT LIN

SOURCE	DF	SS	MS	F
VEG GRP	3	0.2872	0.0957	3.72
ERROR	49	1.2620	0.0258	
TOTAL	52	1.5492		

	LEVEL	N	MEAN	STDEV
J	1	17	0.2706	0.2083
N	2	13	0.0957	0.0718
M	3	15	0.2041	0.1847
C	4	8	0.1032	0.0632

POOLED STDEV = 0.1605

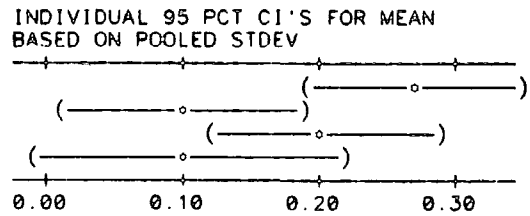

ANALYSIS OF VARIANCE ON AT VOL

SOURCE	DF	SS	MS	F
SLOP GRP	3	4450	1483	1.28
ERROR	50	57854	1157	
TOTAL	53	62304		

	LEVEL	N	MEAN	STDEV
J	1	17	13.95	17.88
N	2	19	35.07	49.32
M	3	9	26.70	18.86
C	4	9	32.99	27.61

POOLED STDEV = 34.02

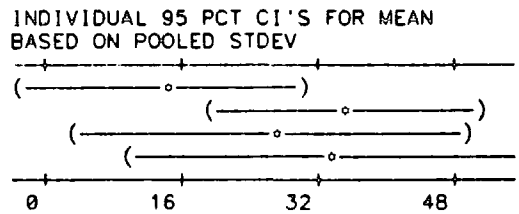

Table 7.5 ANOVA Anderson's Tube with slope group.

ANALYSIS OF VARIANCE ON AT LIN

SOURCE	DF	SS	MS	F
SLOP GRP	3	0.2074	0.0691	2.53
ERROR	49	1.3417	0.0274	
TOTAL	52	1.5492		

	LEVEL	N	MEAN	STDEV
0-10	1	17	0.1058	0.1076
11-20	2	18	0.2149	0.2107
21-30	3	9	0.1706	0.1069
>30	4	9	0.2810	0.1970

POOLED STDEV = 0.1655

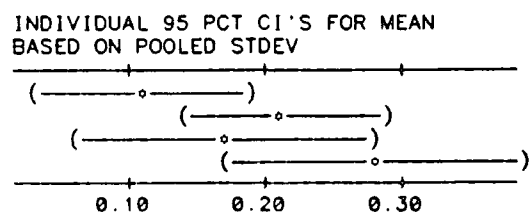

ANALYSIS OF VARIANCE ON AT VOL

SOURCE	DF	SS	MS	F
VEG GRP	3	4026	1342	1.15
ERROR	50	58278	1166	
TOTAL	53	62304		

	LEVEL	N	MEAN	STDEV
0-10	1	17	32.21	25.86
11-20	2	13	23.53	36.80
21-30	3	15	33.49	46.99
>30	4	9	9.42	7.17

POOLED STDEV = 34.14

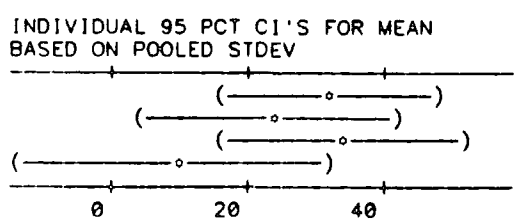

Figure 7.1

PLOT OF RESIDUALS AGAINST VEGETATION CLASS - 15 cm peg data

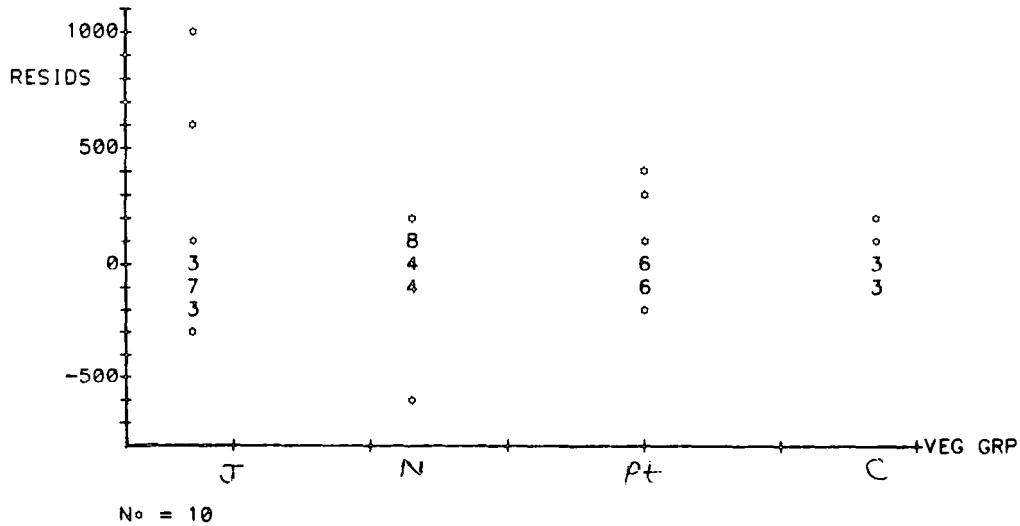

Figure 7.2

RESIDUALS AGAINST VEGETATION GROUP - Anderson's Tube data

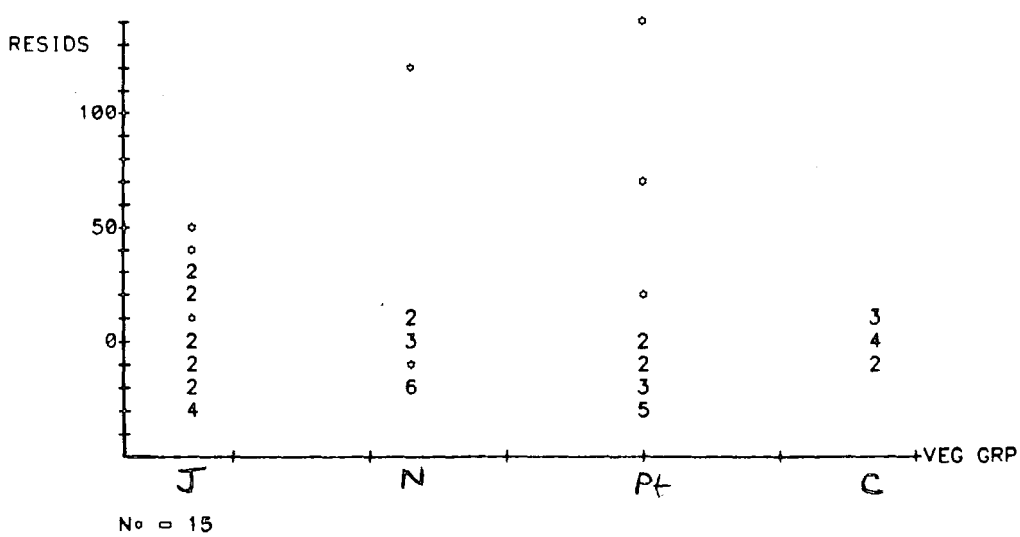

7.2.2 Two-way tables

Table 7.6 shows the distribution of measurement plots in each of the slope angle and vegetation classes, previously described. The experiment is designed to investigate the effect of varying one factor while the other remains constant. In this case the factors vary simultaneously and so the various combinations of slope and vegetation grouping would allow interaction effects to be seen. The underlying hypothesis supposes that the factors (slope angle and vegetation group) are additive in their effect on S.M.M.

$$y_{ij} = \mu + \alpha_i + \beta_j + \epsilon_{ij}$$

y_{ij} = actual mass movement rate.

μ = typical value.

α_i = slope effect.

β_j = vegetation effect.

ϵ_{ij} = residual common to both factors.

Equation 7 (3)

A method for analysing two-way tables using medians uses an algorithm suggested by Tukey (1977) in which row and column medians are repeatedly subtracted from entries in the table until each row and column median is equal to zero. This process is termed median polish because of its iterative nature; however, it is similar to a two-way analysis of

Table 7.6 Sampling design of measurement plots

Slope angle classes (degrees)	Vegetation groupings				
	Juncus	Nardus	Pteridium	Heath	Total
0-10	7	6 (6)	5* (5)	3*	21
11-20	(6) 5*	5	7	5	22
21-30	5 (5)	4*	5	(5) 1*	15
> 30	(7) 5*	6‡	+	+	11
Total	22	21	17	9	69

+ Cells incomplete due to lack of suitable field locations

* Cells incomplete due to site disturbance during measurement period

‡ Two sites in this cell partly disturbed during measurement period

( ) Original sample size

variance which is based on the comparison of row and column means.

A median polish analysis proceeds by fitting a linear model to the data so that the sum of absolute residuals is as small as possible (Hoaglin *et al.* 1983).

$$SAR = \sum_{i=1}^{n} |x_i - c|$$

Where $c = med\{x_1, ..., x_n\}$

SAR = sum of absolute residuals.

The technique is attractive because of its resistance to untrustworthy values and its simplicity of calculation. On the other hand the presence of missing cells in the table requires a greater number of iterations to yield a fit whereby row and column medians are near zero. Also, the fit is to a small degree dependent upon the row or column order in which median subtraction is initiated. Although other methods of fitting exist, median polish is an established technique which neatly summarizes the effect of factors in a two-way table and focuses attention on residual patterns (Velleman and Hoaglin 1981).

For consistency, the following analyses were all carried out using the computer implementation of median polish in the MINITAB statistical package (Ryan *et al.* 1982). Calculations carried out by hand showed that six iterations gave a good fit in the presence of two missing cells in the table.

7.2.3 Median polish results

A summary of the annual mass movement rate for each instrument is given in tables 7.7 to 7.11. Each of the cells may be summarised by

Table 7.7 Two-way table for 15 cm inclinometer peg data.

ROWS: SLOP GRP COLUMNS: VEG GRP

	1	2	3	4
1	95.18	102.01	169.93	88.35
	74.81	27.19	122.37	88.35
	244.74	33.96	81.58	122.37
	95.18	67.98	176.76	
	122.37	0.00	108.77	
	149.57			
2	81.58	115.54	380.71	251.51
	95.18	6.77	115.54	81.58
	67.98	67.98	224.32	217.55
	523.45	122.37	163.16	122.37
			142.74	
			95.18	
	1	2	3	4
3	183.59	156.39	346.75	149.57
	129.14	81.58	135.97	
		203.95	47.62	
		156.39	122.37	
			169.93	
4	108.77	115.54	--	--
	190.36	-292.36	--	--
	761.42	61.16	--	--
	169.99	108.77	--	--
	-13.60	102.01	--	--

CELL CONTENTS --
IP 15:DATA

Table 7.8 Two-way table for 10 cm inclinometer peg data.

ROWS: SLOP GRP COLUMNS: VEG GRP

	1	2	3	4
1	148.05	111.80	102.73	39.28
	48.34	-9.06	27.19	63.45
	33.24	78.56	48.34	99.71
	-120.86	75.54		
		42.30		
		33.24		
2	214.53	93.67	416.97	148.05
	57.41	-6.04	99.71	81.58
	84.60	21.15	57.41	102.73
	232.66		69.50	36.26
			-78.56	120.86
			138.99	
	1	2	3	4
3	163.16	78.56	51.37	126.90
	459.27	18.13	9.06	
		126.90	69.50	
		60.43	51.37	
			24.17	
			-181.29	
4	226.61	60.43	--	--
	344.45	102.73	--	--
	220.57	129.93	--	--
	235.68	-18.13	--	--
	138.99		--	--
	429.06		--	--

CELL CONTENTS --
IP 10:DATA

Table 7.9 Two-way table for 5 cm inclinometer peg data.

ROWS: SLOP GRP COLUMNS: VEG GRP

	1	2	3	4
1	28.704	92.942	28.704	14.382
	14.382	4.532	24.172	1.511
	-9.790	4.532	58.920	52.091
	79.285	27.194	15.833	
	53.662	47.619	15.833	
		-4.532		
		4.532		
2	40.791	8.339	51.366	28.704
	11.361	67.199	69.495	42.301
	33.962	-12.811	20.425	45.323
	20.425	69.495	77.834	16.618
		18.915	54.387	
		17.404	9.065	
	1	2	3	4
3	41.576	21.876	58.920	9.790
	87.624	48.344	40.791	
	129.200	34.747	41.576	
			20.425	
			149.565	
4	130.651	27.919	--	--
	102.007	-56.684	--	--
	209.210	1.511	--	--
	79.345	-32.512	--	--
	88.349		--	--
	0.000		--	--

CELL CONTENTS --
IP 5:DATA

Table 7.10 Two-way table for Anderson's tube linear data.

ROWS: SLOP GRP COLUMNS: VEG GRP

	1	2	3	4
1	0.6164	1.1844	0.6768	0.3988
	0.1873	0.1269	0.3203	0.1994
	2.8100	0.5439	0.2175	0.5318
	0.4834	0.5137	0.4593	
		0.2478		
2	1.0696	0.3565	0.4411	1.4322
	0.1692	0.1269	2.3930	0.3868
	0.9367	1.6921	0.1692	0.8521
	1.9942	0.7554	1.5228	0.4955
	1	2	3	4
3	0.1329	0.5137	2.1151	0.6949
			0.9790	
			1.6316	
			0.8400	
			1.6981	
			0.6708	
4	2.6831	0.3807	--	--
	1.6679	0.5318	--	--
	0.7614	0.5439	--	--
	2.2238		--	--
	3.2270		--	--
	3.2632		--	--

CELL CONTENTS --
AT LIN:DATA

Table 7.11 Two-way table for Anderson's tube volumetric.

ROWS: SLOP GRP COLUMNS: VEG GRP

	1	2	3	4
1	75.54	195.46	57.14	37.46
	9.67	3.93	10.64	2.82
	375.42	172.54	14.80	37.75
	240.61	167.91	16.17	
	6.97	8.13		
2	73.20	140.22	71.95	140.42
	305.48	2.60	186.20	97.88
	26.69	29.16	39.29	45.98
	167.16			41.70
	107.29			19.88
	1	2	3	4
3	365.60	44.56	313.66	88.33
			133.70	
			197.66	
			164.17	
			104.27	
			40.20	
4	307.54	37.23	--	--
	119.92	78.92	--	--
	29.32	122.37	--	--
	195.14		--	--
	424.64		--	--
	479.24		--	--

CELL CONTENTS --
AT VOL:DATA

a mean or a median statistic; however, it is obvious that a number of classes appear to contain one or more anomalous values which suggests the use of medians as a resistant summary measure. In addition, the *Juncus* and *Calluna* classes contain only a single measurement in two cases and so these results must be viewed with caution.

The results from each instrument are presented as a separate median polish analysis; however, data from Young's pits are not included because too many results are missing from each cell. The data that were successfully recovered from this instrument are presented in the analysis of movement-depth profiles in Chapter 8.

Table 7.12 gives details of a median polish for 15 cm Inclinometer peg data. Note that the original data matrix contains two missing entries from slope class 4, for vegetation groups *Pteridium* and *Calluna*. No data were sampled for these classes. The additive linear model is summarised by the table of fitted values and the success of this summary is indicated by the table of residuals and vegetation and slope effects. These may be interpreted as:

S.M.M. = typical value + slope effect + vegetation effect + residual where,

slope effect = row effect

vegetation effect = column effect

residual = remainder after subtracting row and column medians from the data.

The model accounts for 50.71% of the total variation in the data.

Table 7.12 Median-polish results for 15 cm IP.

ROWS: SLOPE COLUMNS: VEG

	1	2	3	4
1	108.77	33.96	122.37	88.35
2	88.38	91.76	152.95	169.96
3	156.36	156.39	135.97	149.57
4	169.99	102.01	—	—

CELL CONTENTS —
PEGS L:DATA

ROWS: SLOPE COLUMNS: VEG

	1	2	3	4
1	4.255	-15.314	5.963	-5.117
2	-52.681	5.947	0.000	39.954
3	-4.255	51.019	-36.540	0.000
4	6.793	-5.947	—	—

CELL CONTENTS —
RESIDUAL:DATA

ROWS: SLOPE COLUMNS: VEG

	1	2	3	4
1	104.52	49.28	116.41	93.47
2	141.06	85.82	152.95	130.01
3	160.62	105.38	172.51	149.57
4	163.20	107.95	—	—

CELL CONTENTS —
FIT:DATA

ROW	ROW EFF
1	-46.3198
2	-9.7792
3	9.7794
4	12.3581

COL EFF			
5.5267	-49.7170	17.4160	-5.5267

TABLE MEDIAN 145.313

$$\sum |S.M.M. - med_t| = 474.28$$

$$\sum |\epsilon| = 233.78$$

med_t = table median

ϵ = residual values

Slope class 1 and *Nardus* vegetation display large negative effects but otherwise both factors show effects of similar magnitude. A closer inspection of the residuals reveals no obvious pattern although there are large residuals in all the vegetation groups, figure 7.3. A plot of fitted data against slope class reveals a clearer pattern, figure 7.4. Here, the additive model distinguishes *Nardus* vegetation from the other groups in terms of the absolute magnitude of S.M.M. for each slope class. The relative response of all the groups is, however, similar with S.M.M. rates increasing linearly with slope angle. The plot of fitted data against vegetation group, figure 7.5, shows that the *Nardus* group accounts for most of the variability in the vegetation effects.

Table 7.13 summarises the results from the 10 cm inclinometer peg data. In this case the linear model explains 52.32% of total variation.

$$\sum |S.M.M. - med_t| = 839.72$$

$$\sum |\epsilon| = 400.35$$

For *Pteridium* and *Calluna* vegetation classes the slope effects are significantly larger than vegetation effects: however, the *Juncus* and *Nardus* classes contain large vegetation effects and some very large residuals. Four large residuals are particularly obvious from figure 7.6; the largest are associated with the *Juncus* class. Otherwise, the data fit the model

Figure 7.3 Median polish for 15 cm Inclinometer Pegs - residual against fit.

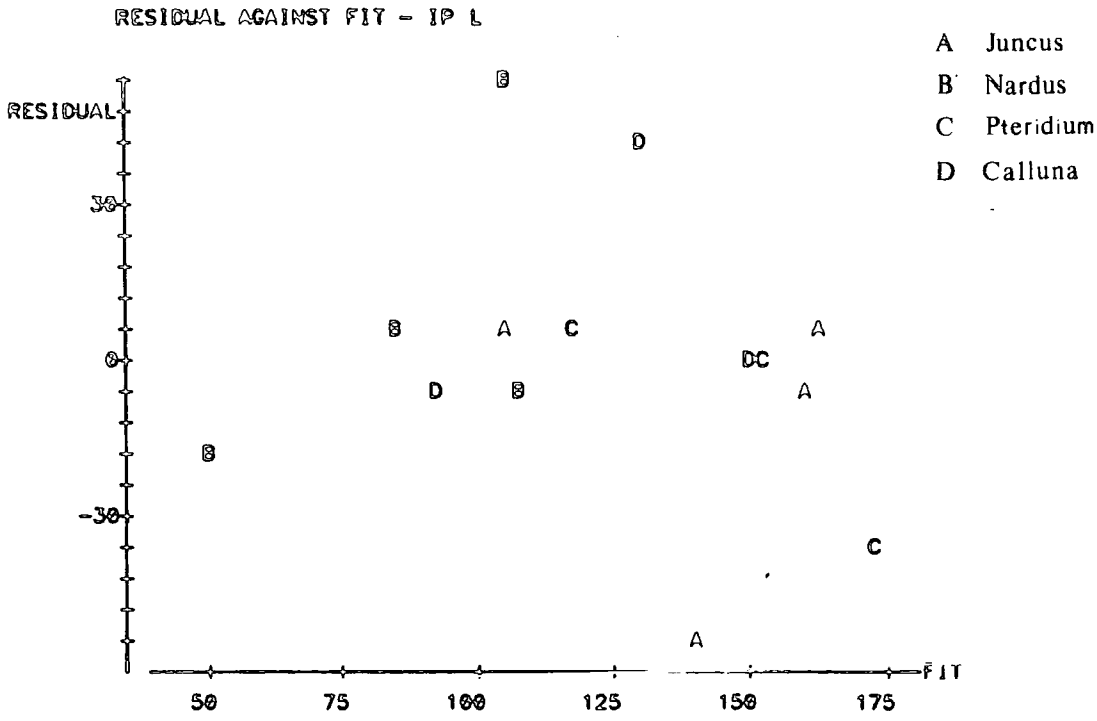

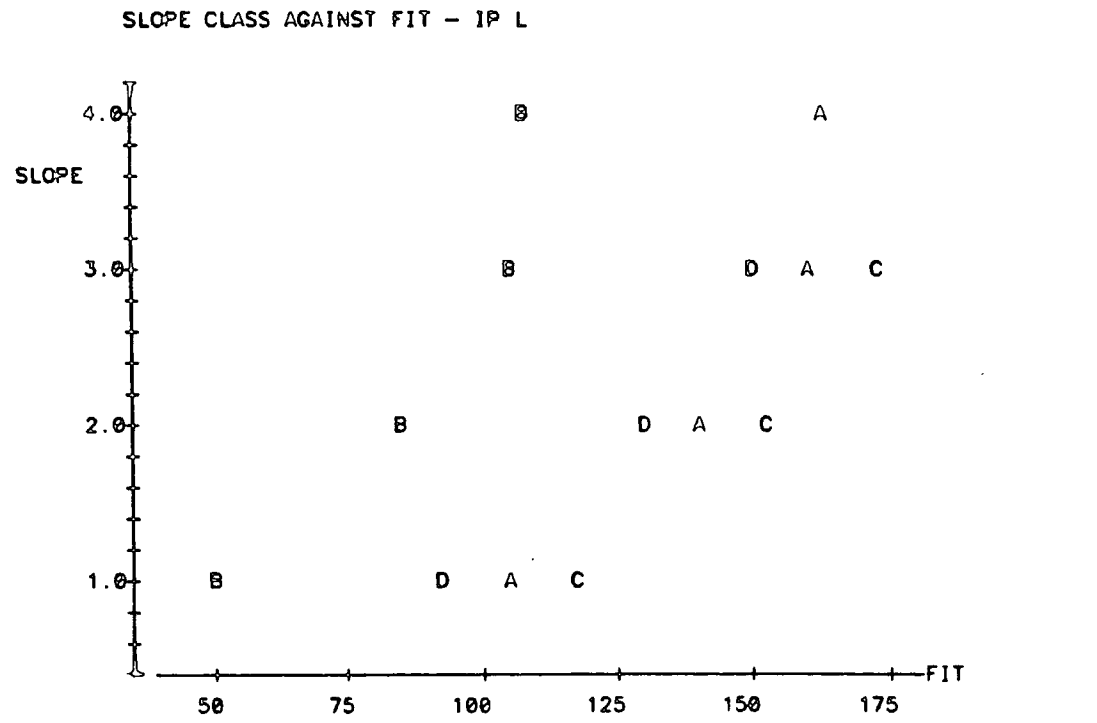

Figure 7.4 Median polish for 15 cm Inclinometer pegs - slope class against fit.

Table 7.13 Median-polish results for 10 cm IP.

ROWS: SLOPE COLUMNS: VEG

	1	2	3	4
1	40.79	58.92	48.34	63.45
2	149.57	21.15	84.60	102.73
3	311.22	69.50	37.77	126.90
4	231.15	81.58	—	—

CELL CONTENTS —
PEGS M:DATA

ROWS: SLOPE COLUMNS: VEG

	1	2	3	4
1	-87.246	62.649	0.000	0.000
2	-8.734	-5.382	5.996	9.017
3	115.337	5.382	-78.418	-4.391
4	8.734	-9.065	—	—

CELL CONTENTS —
RESIDUAL:DATA

ROWS: SLOPE COLUMNS: VEG

	1	2	3	4
1	128.04	-3.73	48.34	63.45
2	158.30	26.53	78.61	93.71
3	195.88	64.11	116.19	131.29
4	222.41	90.65	—	—

CELL CONTENTS —
FIT:DATA

ROW	ROW EFF	COL EFF
1	-49.0525	72.1388
2	-18.7901	-59.6278
3	18.7901	-7.5538
4	45.3228	7.5538

COL EFF

72.1388	-59.6278	-7.5538	7.5538

TABLE MEDIAN 104.951

Figure 7.5 Median polish for 15 cm Inclinometer Pegs - vegetation class against fit.

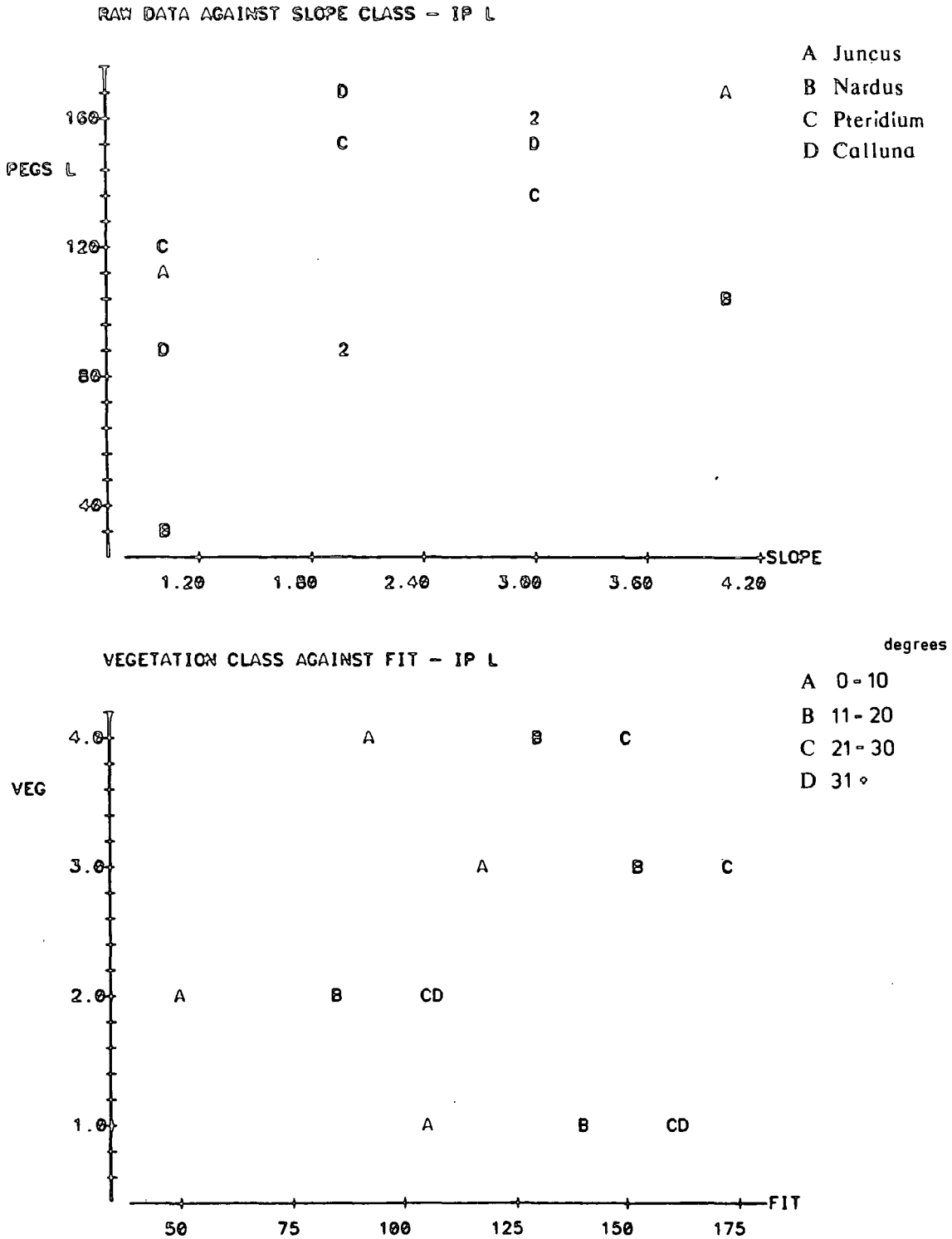

Figure 7.6 Median polish for 10 cm Inclinometer Pegs - residual against fit.

Histogram of RESIDUAL N = 14

Midpoint	Count	
-80	2	oo
-60	0	
-40	0	
-20	0	
0	10	oooooooooo
20	0	
40	0	
60	1	o
80	0	
100	0	
120	1	o

A Juncus
B Nardus
C Pteridium
D Calluna

RESIDUAL AGAINST FIT - IP M

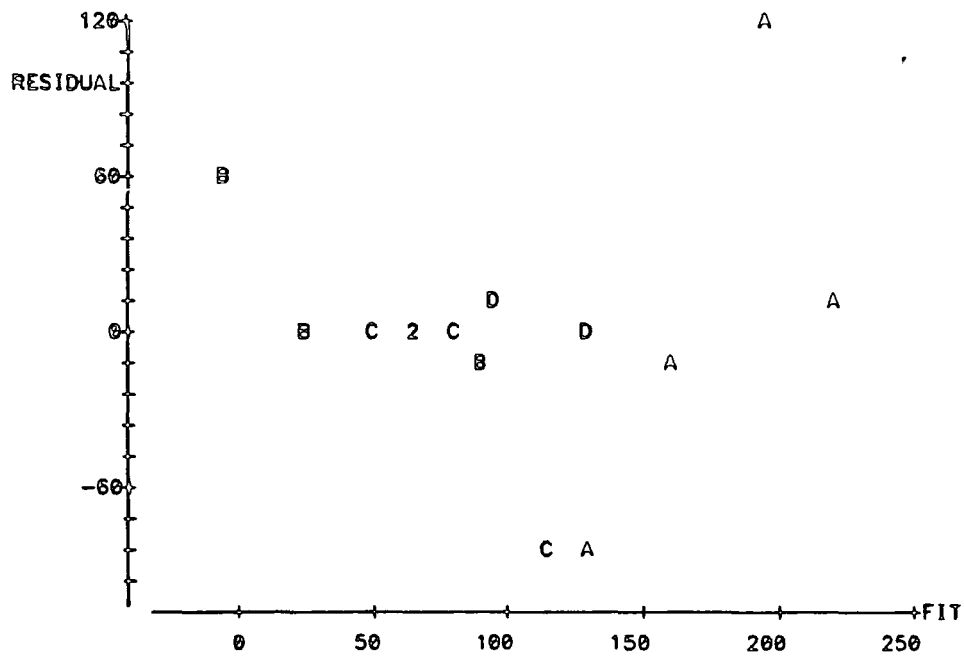

very well. Figures 7.7 and 7.8 summarise the general pattern with rates increasing linearly with slope angle within each vegetation class and with the overall magnitude of S.M.M. differing considerably among vegetation classes. *Juncus* class shows the highest rates of movement and *Nardus* shows the lowest.

The linear additive model explains 47.1% of the variation in the 5 cm Inclinometer peg data.

$$\sum |S.M.M. - med_l| = 296.989$$

$$\sum |\epsilon| = 157.121$$

With this data, no clear pattern emerges from inspection of the slope and vegetation effects, table 7.14. The model does not fit the *Juncus* or the *Calluna* classes readily, and these show large residuals in figure 7.9. The general trend of a positive linear relationship between S.M.M. and slope class still emerges but differences among the vegetation classes are less pronounced than in the two other Inclinometer peg data sets, see figure 7.10 and figure 7.11.

A plot of fitted data against actual data shows which values differ from the predicted additive model, see figure 7.11. The typical rate recorded from 5 cm pegs is much lower than that of 10 cm and 15 cm pegs which suggests that movement is inhibited in the upper part of the soil profile in the region where plant roots are most dense. Movement must be occurring beneath the pivot points of the 5 cm pegs and, to a lesser extent, beneath the 10 cm pegs. A summary movement - depth profile can be constructed from the 178 Inclinometer pegs using the typical values extracted from the median polish analysis. If 40.8 mm^2/yr typifies the contribution of the upper 5 cm of the soil then this can be subtracted from the 10 cm peg result of 104.9 mm^2/yr to give an idea of the amount of movement that the lower 10 cm of the profile contributes.

Figure 7.7 Median polish for 10 cm Inclinometer Pegs - slope class against fit.

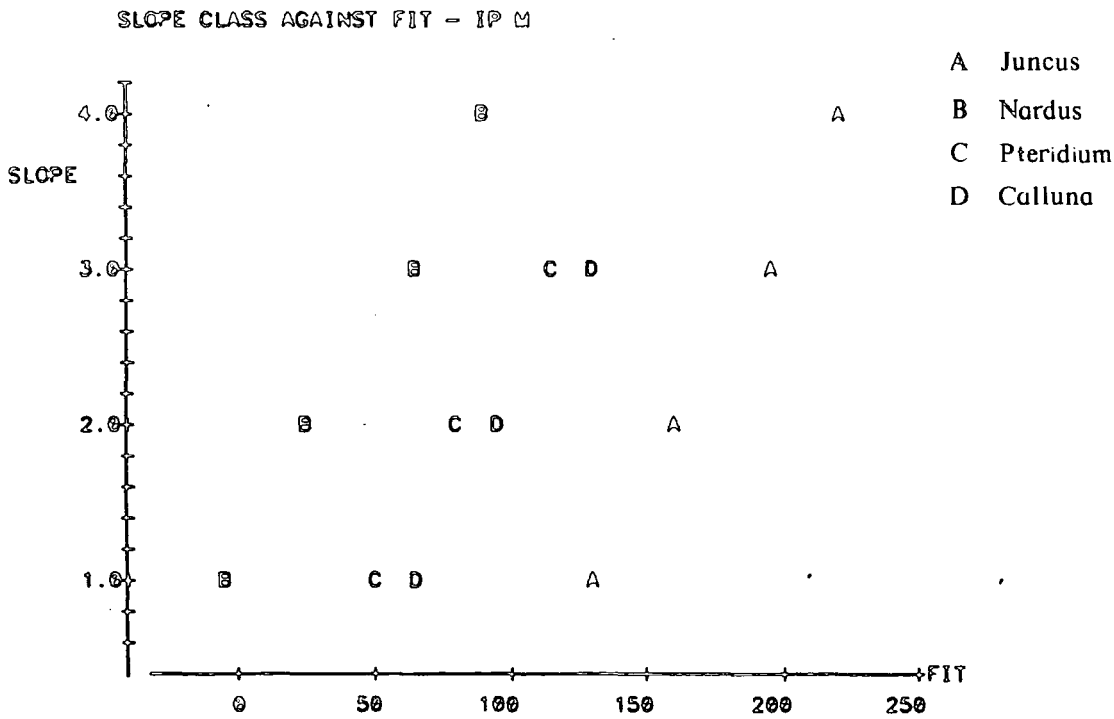

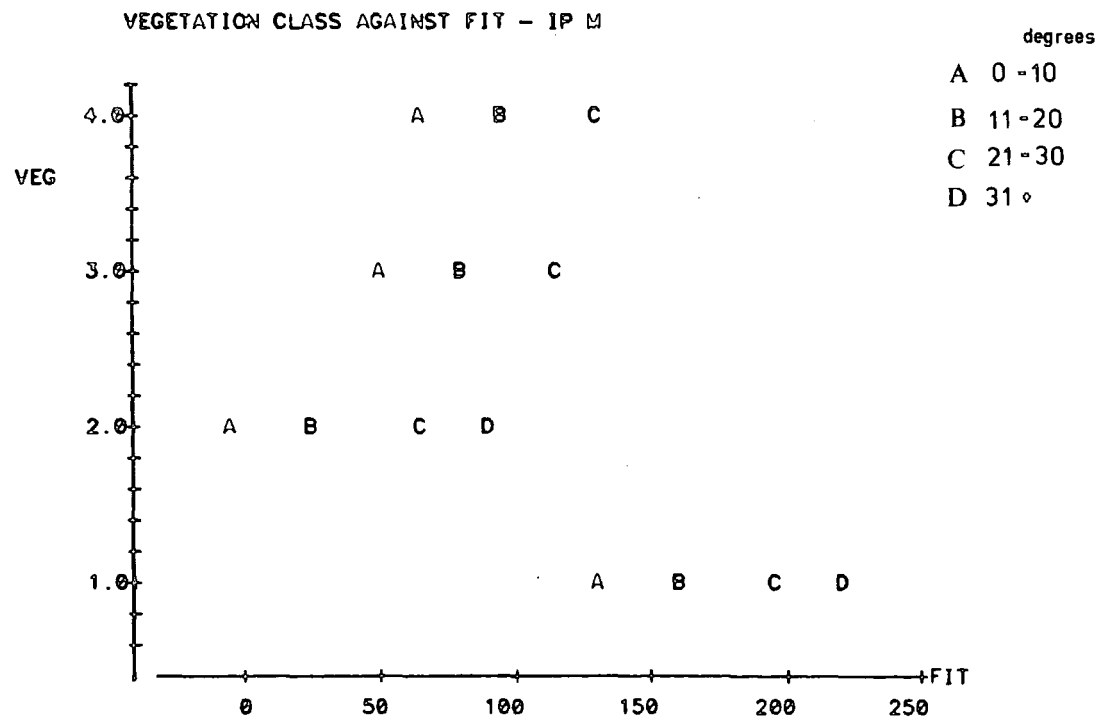

Figure 7.8 Median polish for 10 cm Inclinometer Pegs - vegetation class against fit.

Table 7.14 Median-polish results for 5 cm IP.

ROWS: SLOPE COLUMNS: VEG

	1	2	3	4
1	28.704	4.532	24.172	14.382
2	27.194	18.159	52.877	35.503
3	87.624	34.747	41.576	0.790
4	95.178	27.919	—	—

CELL CONTENTS —
PEGS S:DATA

ROWS: SLOPE COLUMNS: VEG

	1	2	3	4
1	-13.753	2.342	0.000	0.000
2	-33.574	-2.342	10.394	2.810
3	20.421	7.811	-7.342	-29.339
4	13.753	-13.240	—	—

CELL CONTENTS —
RESIDUAL:DATA

ROWS: SLOPE COLUMNS: VEG

	1	2	3	4
1	42.457	2.191	24.172	14.382
2	60.767	20.501	42.483	32.693
3	67.203	26.937	48.918	39.129
4	81.425	41.159	—	—

CELL CONTENTS —
FIT:DATA

ROW	ROW EFF	COL EFF
1	-21.5283	23.1798
2	-3.2179	-17.0867
3	3.2179	4.8949
4	17.4399	-4.8949

COL EFF			
23.1798	-17.0867	4.8949	-4.8949

TABLE MEDIAN 40.8056

Figure 7.9 Median polish for 5 cm Inclinometer Pegs - residual against fit.

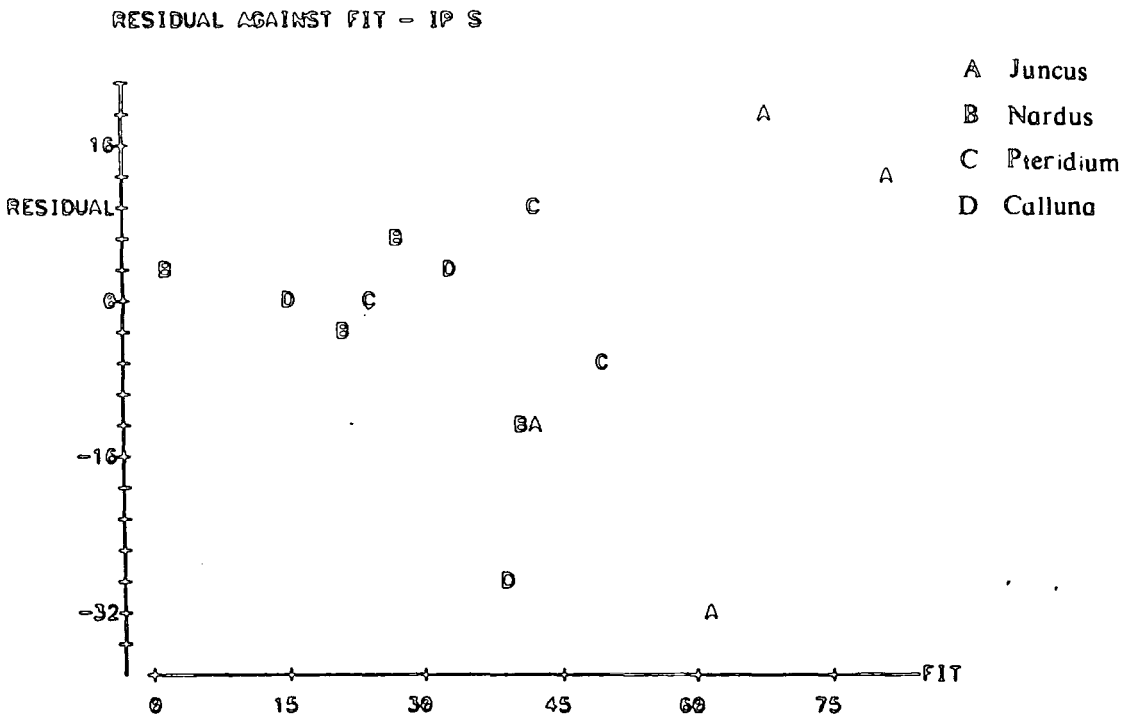

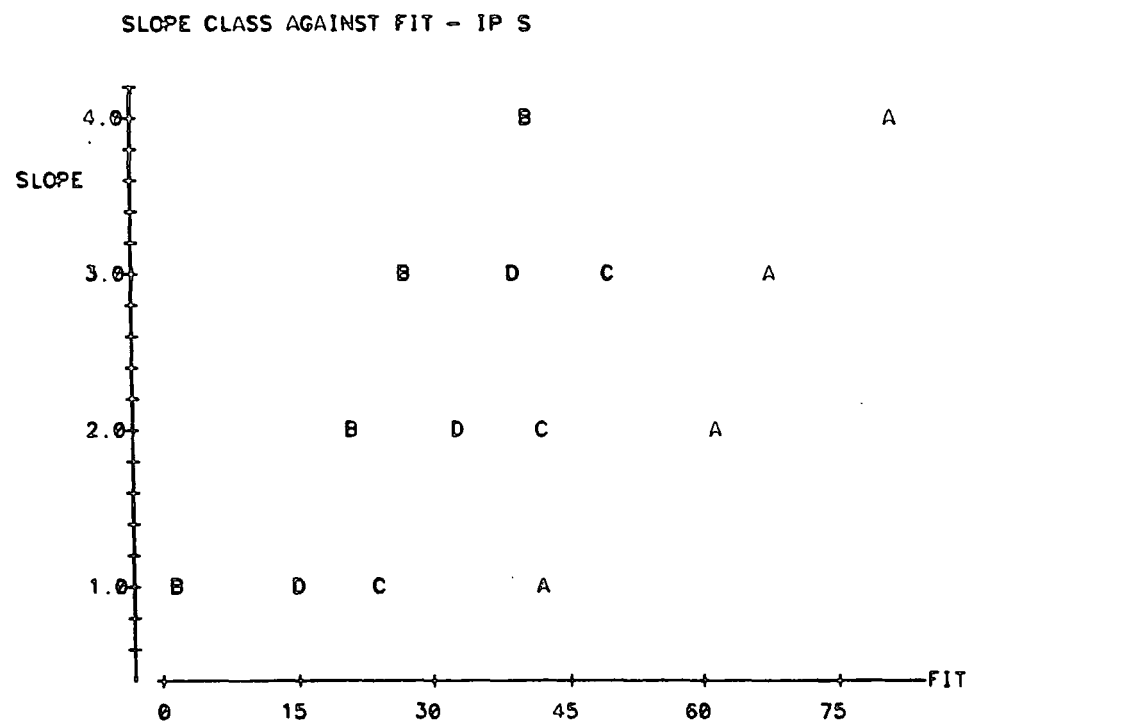

Figure 7.10 Median polish for 5 cm Inclinometer Pegs - slope class against fit.

Figure 7.11 Median polish for 5 cm Inclinometer Pegs - vegetation class and raw data against fit.

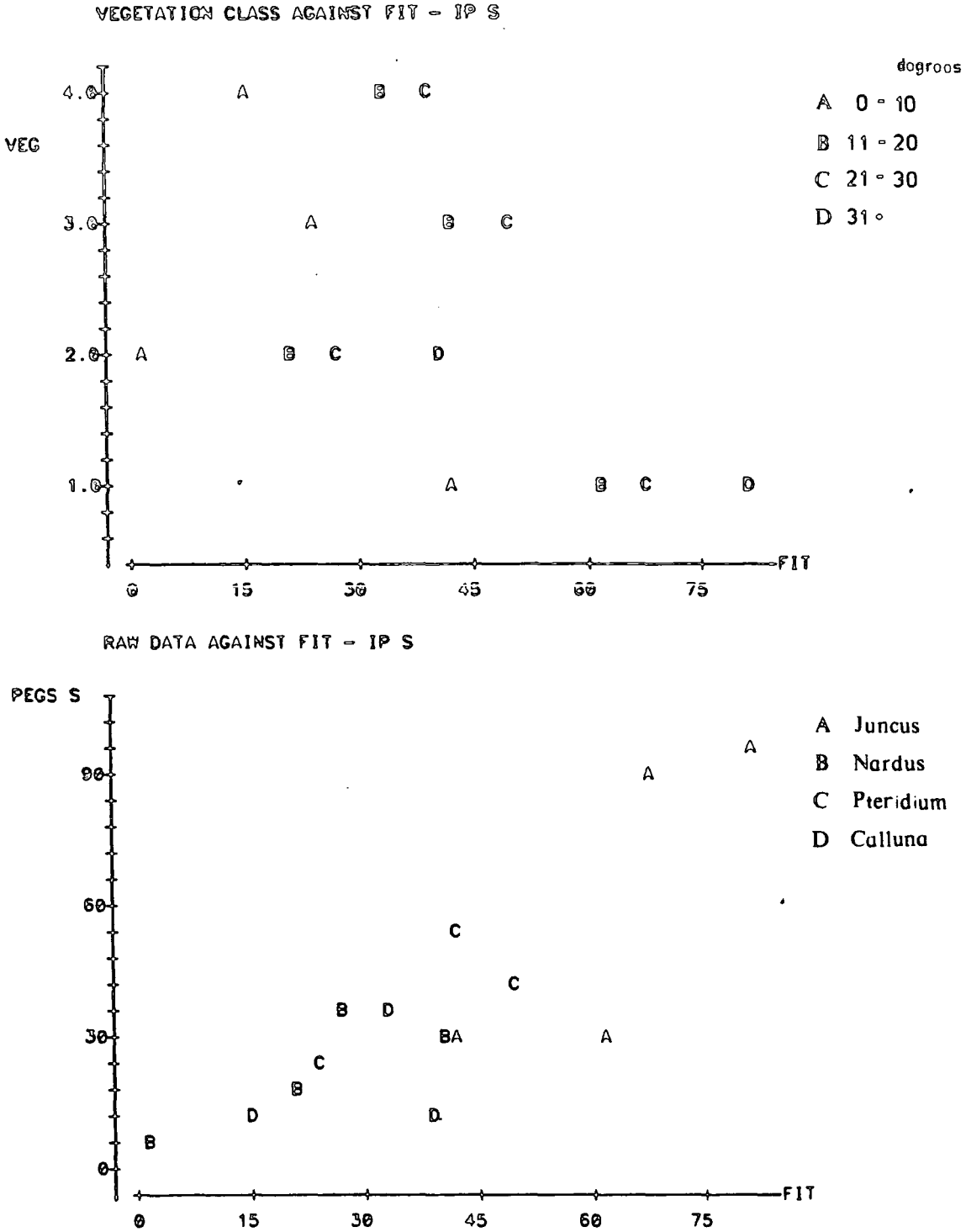

Median polish of IP data	
Typical value	Peg length
145.3 mm^2/yr	15 cm
104.9 mm^2/yr	10 cm
40.8 mm^2/yr	5 cm

Combining these results diagrammatically in figure 7.12 gives an indication of the relative contribution of each part of the depth profile. The results are purely illustrative since they summarize all vegetation and slope classes and because Inclinometer pegs always measure the integrated response of the soil to the depth of their insertion.

Anderson and Cox (1978) present a comparison of S.M.M. instruments in which the common scale is a linear measure standardized for a depth of 2.5 cm because this depth coincided with the maximum response of most instruments. The Anderson's Tube device however always records maximum movement at the surface as long as movement is downslope. The calculation of volumetric movement at each site for Anderson's Tubes suggested that a linear measurement was often misleading. Indeed, the correlation coefficient between the two measures was only 0.71, thereby explaining only 50% of the resultant variance. Therefore a separate median polish was included for both linear and volumetric measures in order to investigate the idea that the linear measure can be misleading.

$$\sum |S.M.M. - med_t| = 5.76$$

$$\sum |\epsilon| = 3.39$$

Table 7.15 shows the results for the linear measure of Anderson's Tube data. In this case the model explains 41.1% of the variance but again the *Juncus* and *Nardus* vegetation groups contain large residuals indicating

Figure 7.12 Combined movement - depth profile for all Inclinometer Peg data.

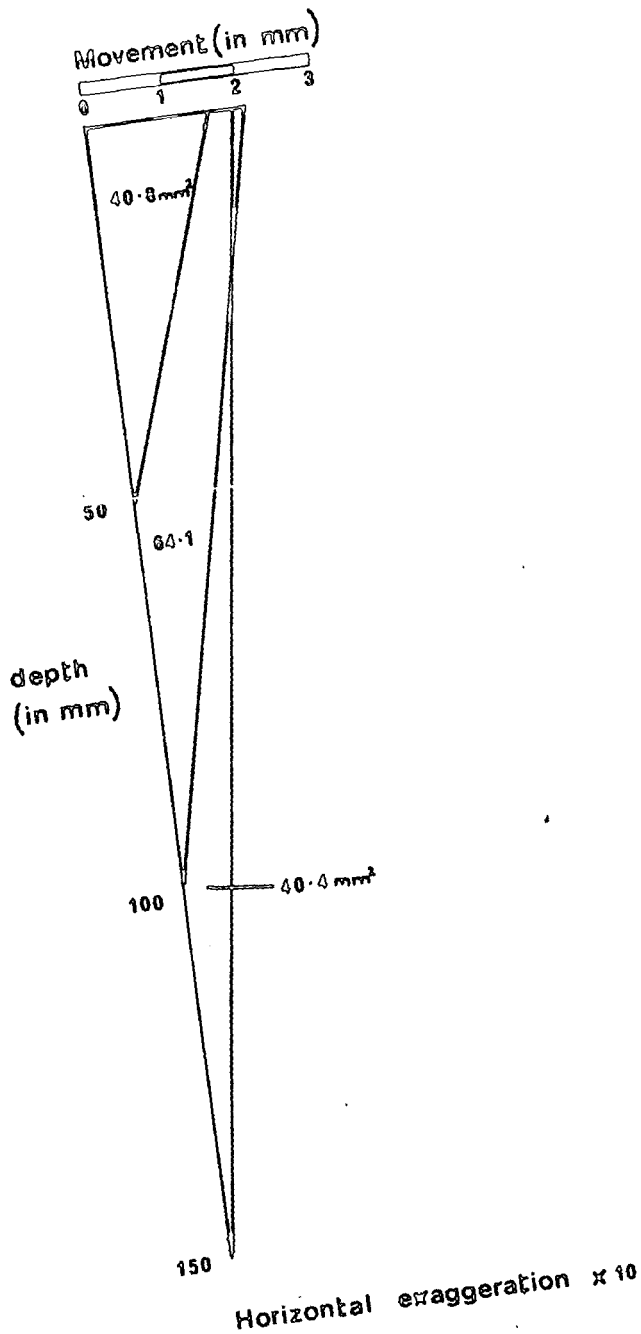

Table 7.15 Median-polish results AT linear.

ROWS: SLOPE COLUMNS: VEG

	1	2	3	4
1	0.5499	0.5137	0.3898	0.3988
2	1.0031	0.5560	0.9820	0.6738
3	0.1329	0.5137	1.3053	0.6950
4	2.4535	0.5318	—	—

CELL CONTENTS —
AT L:DATA

ROWS: SLOPE COLUMNS: VEG

	1	2	3	4
1	-0.04202	0.32481	-0.22303	0.02663
2	0.04202	-0.00208	0.00000	-0.06761
3	-0.78172	0.00208	0.36976	0.00000
4	0.75264	-0.76596	—	—

CELL CONTENTS —
RESIDUAL:DATA

ROWS: SLOPE COLUMNS: VEG

	1	2	3	4
1	0.5919	0.1888	0.6128	0.3722
2	0.9611	0.5580	0.9820	0.7414
3	0.9147	0.5116	0.9355	0.6950
4	1.7008	1.2977	—	—

CELL CONTENTS —
FIT:DATA

ROW	ROW EFF
1	-0.345964
2	0.023228
3	-0.023228
4	0.762933

COL EFF			
0.109861	-0.293229	0.130728	-0.109861

TABLE MEDIAN 0.828038

a poor fit for these groups. Again slope effects appear to be influenced by strange observations. In particular, slope class 3 for *Juncus* is clearly an anomalous value. It is also derived from a single observation because of instrument disturbance at other plots in this category. Figure 7.13 also illustrates the large residuals present in this data set. Plotting slope class against fitted data shows a confused pattern where results from the different vegetation classes overlap considerably, see figure 7.14. A plot of vegetation class against fitted data shows that higher movement rates are observed for slope class 2 than slope class 3 in all vegetation classes, see figure 7.15.

$$\sum |S.M.M. - med_t| = 916.26$$

$$\sum |\epsilon| = 597.66$$

The volumetric measure of S.M.M. for Anderson's Tubes, on the other hand, shows a much clearer relationship between slope class and movement rate, figure 7.16, despite the overall fit of the model being only 34.8%. Here again, the *Juncus* and *Nardus* classes contain anomalous values which result in extremely large residuals, table 7.16. The other vegetation groups, *Pteridium* and *Calluna*, display a clear linear trend between S.M.M. rate and slope class. The vegetation effect for these classes is about half the value of the slope effect. The pattern of movement both within and among vegetation groups corresponds well with the results presented for Indinometer Peg data. This agreement would appear to substantiate the decision to question the value of a linear measurements from Anderson's Tubes. The relatively poor fit of the linear model to the volumetric data is of some concern, however, and so the data are tested for non-additivity. Velleman and Hoaglin (1981) suggest plotting comparison values for the data against each residual. If the relationship, expressed as a resistant line, is not a horizontal line then

Figure 7.13 Median polish for Anderson's Tube data (linear) - residual against fit.

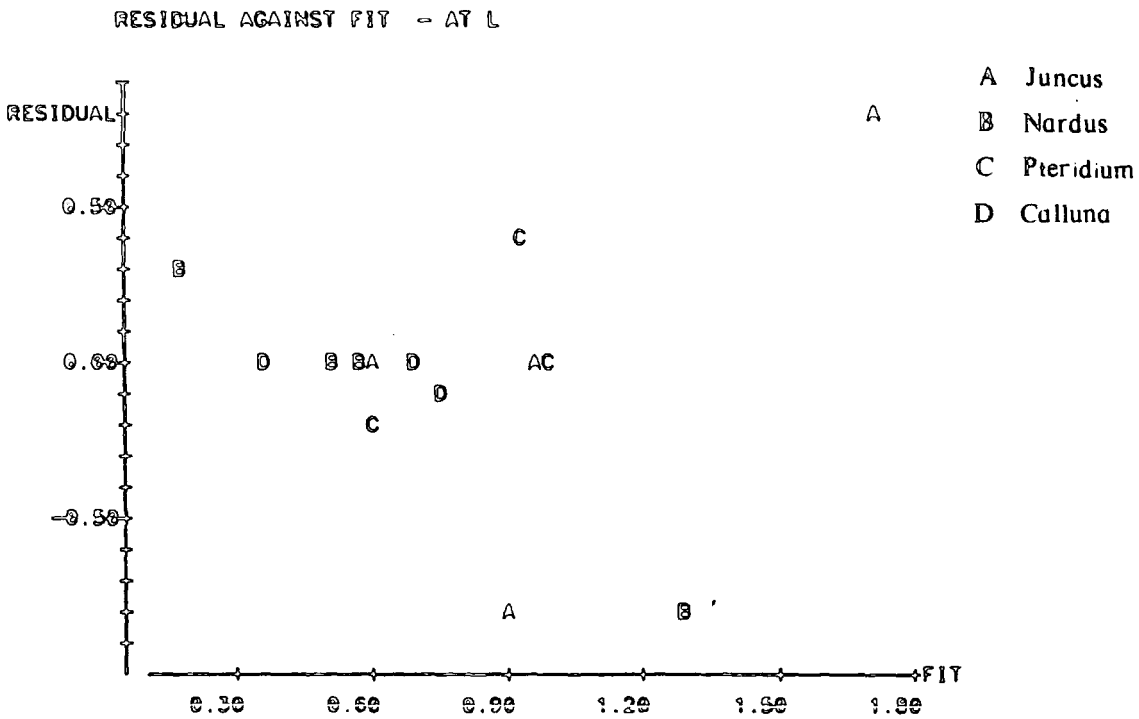

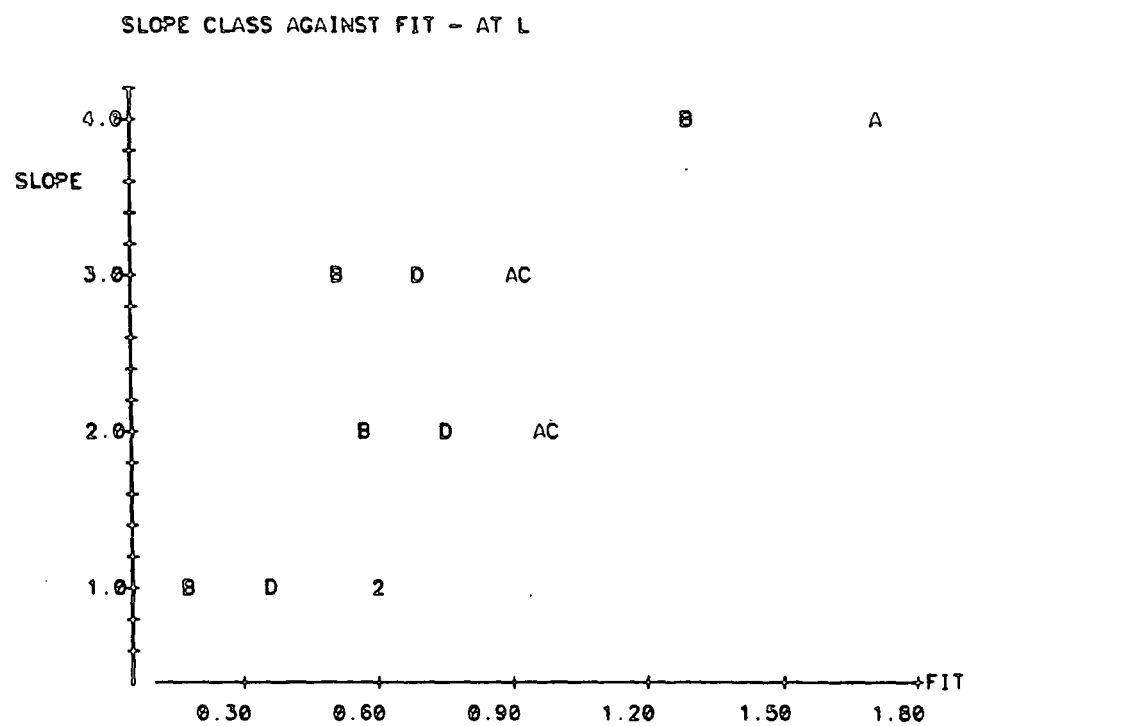

Figure 7.14 Median polish for Anderson's Tube data (linear) - slope class against fit.

Figure 7.15 Median polish for Anderson's Tube data (linear) - vegetation class and raw data against fit.

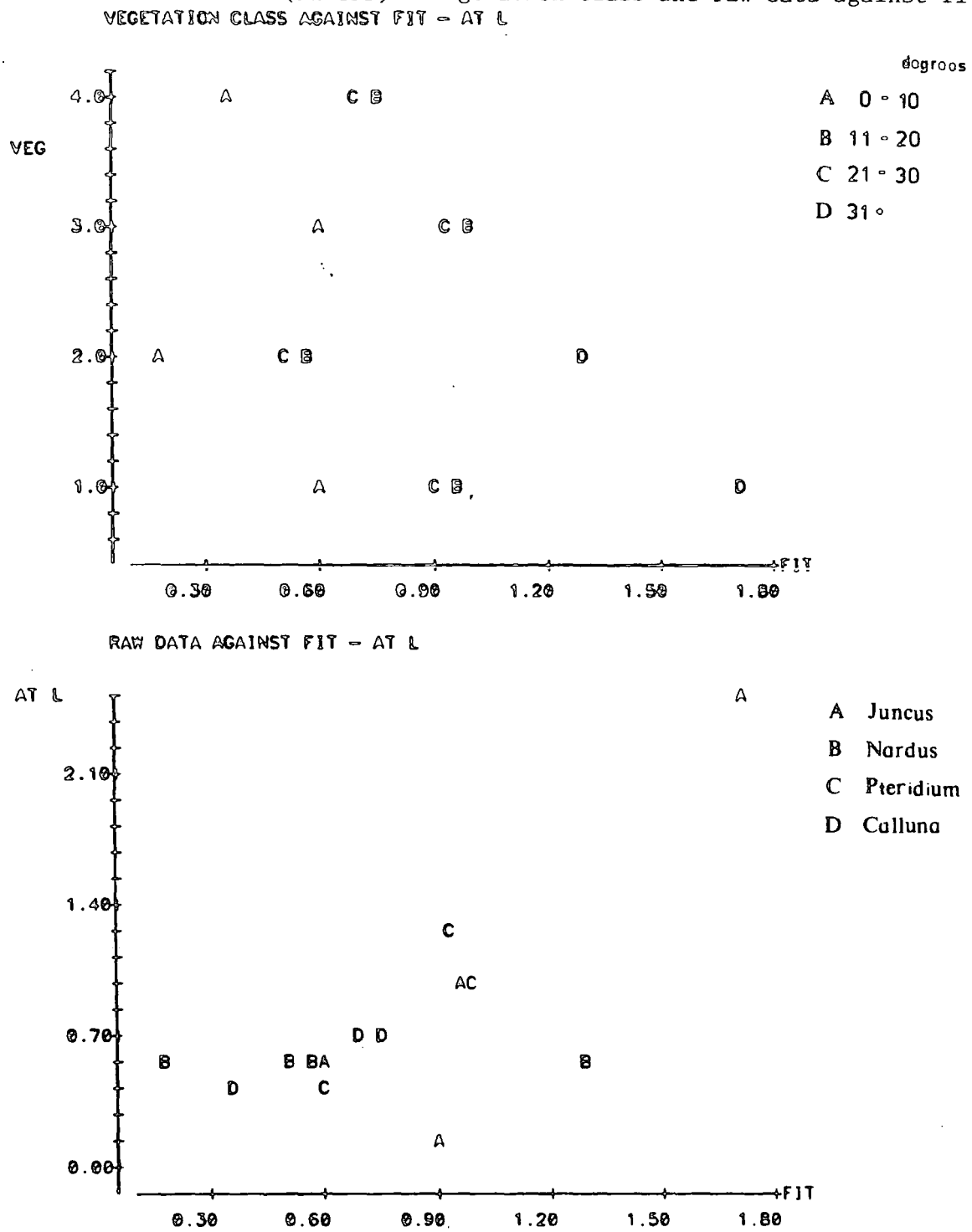

Figure 7.16 Median polish for Anderson's Tube data (volumetric) - residuals and slope class against fit.

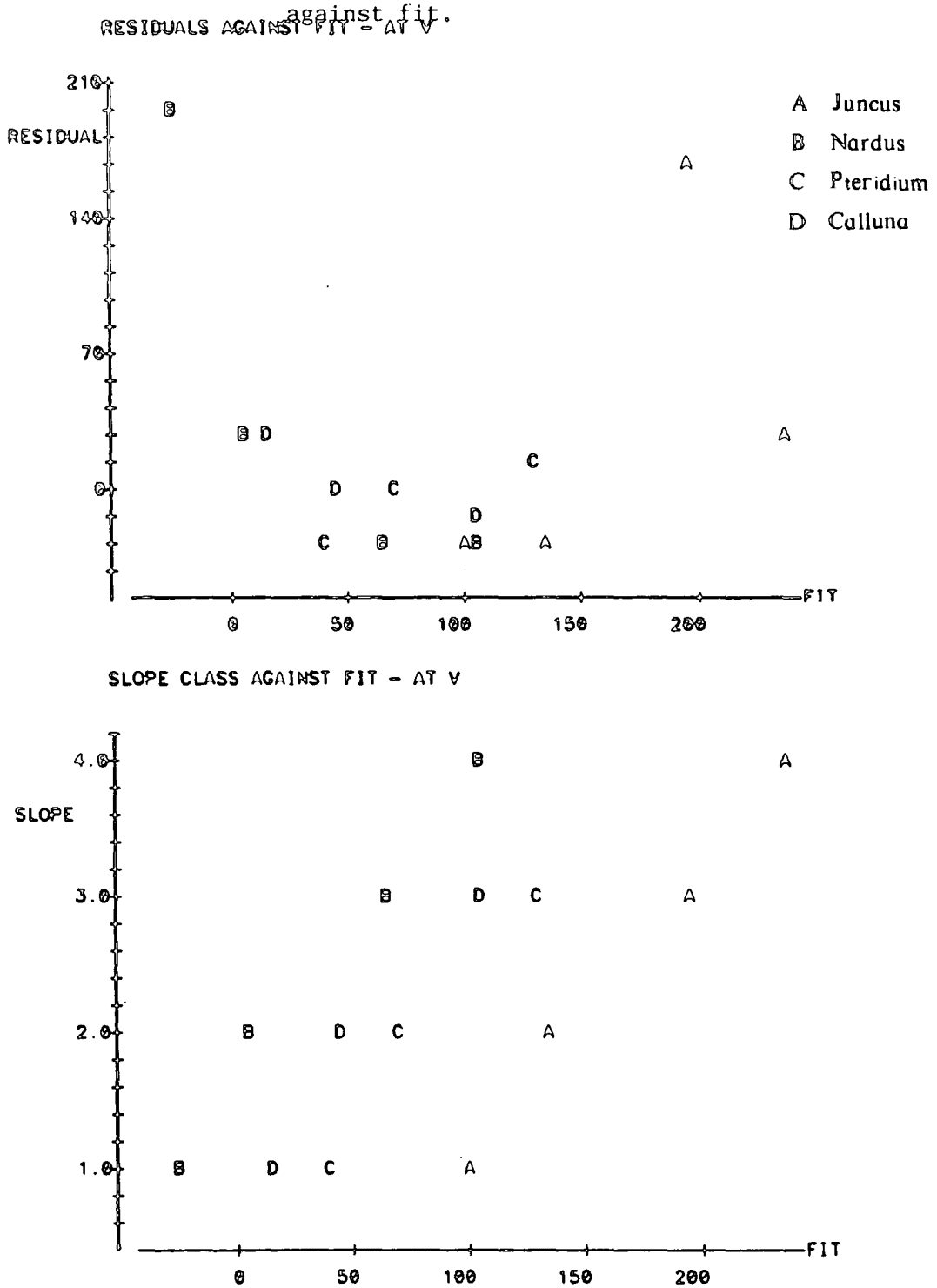

re-expression improve additivity. The comparison values data (i, j) are calculated from:

$$\frac{\alpha \cdot \beta}{\mu}$$

Slope effect = α

Vegetation effect = β

Typical value = μ

Equation 7 (4)

The slope of the line is calculated by fitting a straight line to the data which is resistant to outliers. The method used was MINITAB's implementation of a method which partitions the $x - y$ data into thirds and fits a line to the medians of these batches using an iterative algorithm to minimise the absolute magnitude of the residuals (Velleman and Hoaglin 1981). The volumetric Anderson's tube data gave a resistant line slope of 0.68 which suggested that a logarithmic transformation may improve additivity.

$$residual = -0.95 + 0.68 \cdot comparison$$

Equation 7 (5)

The median polish was re-calculated after transforming the annual Anderson's Tube data into natural logarithms, tables 7.17 and 7.18. This increased the percentage of total variation explained by the linear model from 34.8% to 36.7%. After transformation, a resistant line was again

Figure 7.17 Median polish for Anderson's Tube data (volumetric) - vegetation class and raw data against fit.

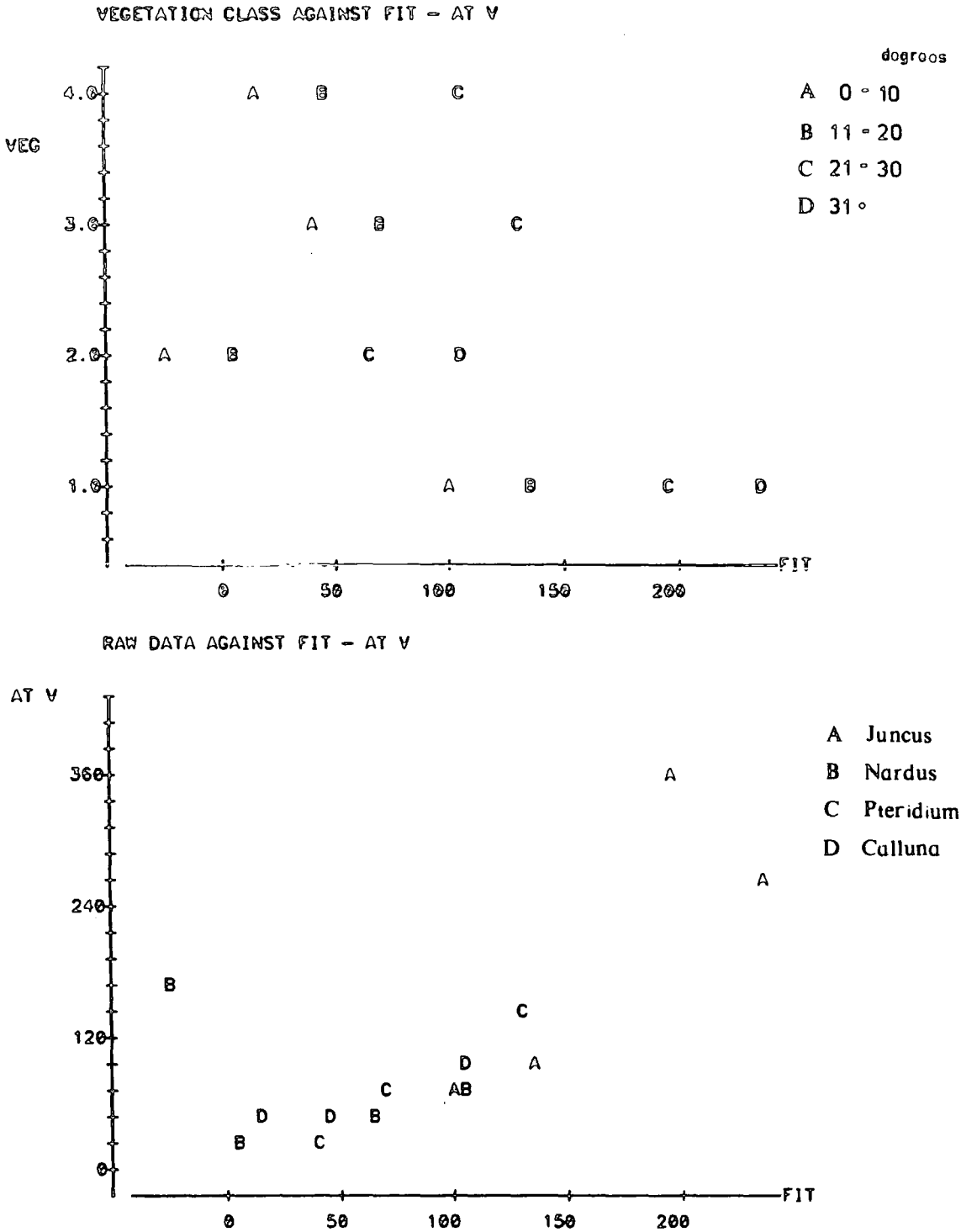

Table 7.16 Median-polish results for AT (volumetric)

ROWS: SLOPE COLUMNS: VEG

	1	2	3	4
1	75.54	167.91	15.48	37.46
2	107.29	29.16	71.95	45.98
3	365.60	44.56	148.93	88.33
4	259.30	79.51	—	—

CELL CONTENTS —
AT V:DATA

ROWS: SLOPE COLUMNS: VEG

	1	2	3	4
1	-26.160	193.377	-25.979	25.979
2	-26.898	22.130	0.000	0.000
3	171.749	-22.130	17.313	-17.313
4	26.160	-26.468	—	—

CELL CONTENTS —
RESIDUAL:DATA

ROWS: SLOPE COLUMNS: VEG

	1	2	3	4
1	101.70	-25.47	39.46	13.48
2	134.19	7.03	71.95	45.98
3	193.85	66.69	131.62	105.64
4	233.14	105.98	—	—

CELL CONTENTS —
FIT:DATA

ROW	ROW EFF
1	-62.3250
2	-29.8315
3	29.8315
4	69.1171

COL EFF			
75.2268	-51.9370	12.9895	-12.9895

TABLE MEDIAN 88.7965

Table 7.17 Median-polish results for AT (linear) log

```
ROWS: SLOPE     COLUMNS: VEG

          1        2        3        4

 1  -2.4043  -2.4651  -2.7572  -2.7181
 2  -1.7980  -2.4548  -1.8978  -2.2300
 3  -3.8167  -2.4651  -1.5647  -2.1628
 4  -0.9058  -2.4304      —        —

 CELL CONTENTS —
        AT LOG L:DATA


ROWS: SLOPE     COLUMNS: VEG

          1        2        3        4

 1 -0.03530  0.53003 -0.22371  0.00000
 2  0.03530  0.01264  0.00000 -0.04759
 3 -1.99837 -0.01264  0.41813  0.00463
 4  0.44639 -0.44408      —        —

 CELL CONTENTS —
        RESIDUAL:DATA


ROWS: SLOPE     COLUMNS: VEG

          1        2        3        4

 1  -2.3690  -3.0031  -2.5335  -2.7181
 2  -1.8333  -2.4674  -1.9978  -2.1824
 3  -1.8183  -2.4525  -1.9828  -2.1674
 4  -1.3522  -1.9863      —        —

 CELL CONTENTS —
             FIT:DATA

ROW     ROW EFF

   1  -0.543178
   2  -0.007487
   3   0.007487
   4   0.473625

COL EFF
  0.256800  -0.377333   0.092304  -0.092304

K1        -2.08262
```

Table 7.18 Median-polish results for AT (volumetric). log

ROWS: SLOPE COLUMNS: VEG

	1	2	3	4
1	2.5257	3.3245	0.9398	1.8244
2	2.8767	2.3591	3.4279	2.0292
3	4.1026	1.9980	3.1993	2.6821
4	3.7022	2.5696	—	—

CELL CONTENTS —
AT LOG V:DATA

ROWS: SLOPE COLUMNS: VEG

	1	2	3	4
1	-0.08658	1.60448	-1.35168	0.05012
2	-0.22092	0.15375	0.65109	-0.23041
3	0.58250	-0.62984	0.00000	0.00000
4	0.08658	-0.15375	—	—

CELL CONTENTS —
RESIDUAL:DATA

ROWS: SLOPE COLUMNS: VEG

	1	2	3	4
1	2.6123	1.7200	2.2915	1.7743
2	3.0976	2.2053	2.7768	2.2596
3	3.5201	2.6278	3.1993	2.6821
4	3.6156	2.7233	—	—

CELL CONTENTS —
FIT:DATA

ROW	ROW EFF
1	-0.696574
2	-0.211244
3	0.211245
4	0.306757

COL EFF
0.579403 -0.312863 0.258600 -0.258600

TABLE MEDIAN 2.72945

fitted between the residual and comparison value and the resultant slope was 0.06. This suggested that no further improvement in additivity will result from further re-expression. Of the Inclinometer Peg data sets, only the 10 cm peg showed any relationship between residual and comparison values.

Inclinometer pegs	
Peg	Resistant line slope
15 cm	-0.03
10 cm	0.37
5 cm	0.06

7.2.4 Summary of median polish results

(i) A two-way additive linear model based on medians summarises S.M.M. rates thought to be due to differences in slope angle and vegetation type. The model explains over half the variation in the Inclinometer Peg data but is less successfully applied to Anderson's tube volumetric data.

(ii) The variation in S.M.M. rate within each vegetation class appears to be consistent and is positively associated with slope angle.

(iii) The four vegetation classes show different rates of mass movement.

The *Nardus* class gives the lowest rates of movement and the least convincing relationship between movement and slope angle. *Juncus* has high residuals with all instruments which might suggest that it is more sensitive to other causal factors not considered or that it is most sensitive to the effects of random disturbance.

(iv) Typical rates of S.M.M. derived from a linear additive model for

each vegetation class and for each instrument, figure 7.16, show that sites in the *Juncus* class are most active followed by those in the *Pteridium*, *Calluna* and then *Nardus* classes.

(v) Highest movement rates are recorded by the 15 cm Inclinometer pegs for all but the *Juncus* class where the 10 cm pegs record consistently more displacement. This pattern may be due to a rapid decrease in moisture content with depth that is characteristic of *Juncus* vegetation plots. Anderson's tubes typically record less movement than 10 cm Inclinometer pegs but more than 5 cm pegs.

(vi) The slope and vegetation effects, derived from median polish, are of a similar magnitude for most instruments suggesting that vegetation type (and associated differences in soil and moisture status) are no less important than gradient in predicting S.M.M. rates.

7.3 Regression analysis

A number of researchers have applied regression models to predict S.M.M. rate from physical variables relating to soil consistency and slope morphology (Schumm 1966; Anderson 1977). In this section, previously suggested linear regression models are investigated for their ability to explain the observed S.M.M. variation among plots. Correlations among the physical variables for each plot are also investigated.

The use of a linear model, which describes the response of S.M.M. in terms of slope and soil variables by the use of a least-squares method, poses several severe problems.

(i) It must be assumed that the selected explanatory variables do indeed influence S.M.M.

(ii) It is usual for explanatory variables to be statistically independent of each other and have normal distributions.

The results of median polish analysis showed that the mass movement data contained many large positive residuals which were outlying values. These are likely to be very poorly predicted by regression analysis (Mosteller and Tukey 1977).

In view of these problems the following approach is adopted. First, the selection of suitable predicting variables is justified and the statistical structure of those data assessed. Second, the correlation and interdependance among the predicting variables is described. The likely relationship between S.M.M. and physical variables is investigated using simple scatter plots. Finally, the results from a formal linear regression analysis are presented.

7.3.1 Explanatory variables

Anderson (1977) described **soil creep** or S.M.M. as resulting from the interaction of pedological, hydrological and vegetational factors. Anderson and Cox (1984) use combinations of these factors in a regression analysis. They conclude, however, that a single predictor (winter moisture) best summarised the data. In addition, they note that sine of slope angle, saturation level, apparent cohesion, unconfined compression and penetrometer resistance gave weak correlations with $r^2 < 0.8$. The strongest correlations reported involved the moisture variable, plasticity index, and organic matter content.

The mechanical strength of the soil is a function of its granulometric composition, its effective stress state and compounding factors which may alter its apparent cohesion. Relevant variables are, therefore, particle size distribution, moisture content, slope angle and shear strength. In addition, soil index tests are usually a good guide to a soil's rheological

state for a given moisture content and loss on ignition test results are a reliable guide to its organic matter content. These overlap with the most influential variables recorded by Anderson (1977) and other researchers (Evans 1974; Williams 1970; Rashidian 1984). An additional categorical variable, root density per unit volume of sample, is also included in view of the observed importance of plant rootlets in modifying laboratory creep-shear test results.

Table 7.19 lists the variables selected for analysis and gives their summary statistics. Each variable was measured, either in the field, or in the laboratory from a bulk sample collected at the time of instrument installation. The laboratory techniques used to process soil samples are described in Chapter 3. Several variables contain missing data, denoted by N*, this may be due to the nature of the sample itself (say, organic material unsuitable for granulometric analysis) or disturbance of the instrument in the case of S.M.M. measurements.

Table 7.19 Summary statistics of soil variables.

HEATHERY BURN PHYSICAL VARIABLES

	N	N*	MEAN	MEDIAN	TRMEAN	STDEV	SEMEAN	MIN	MAX
SITE	69	0	469.0	502.0	465.6	271.8	32.7	101.0	908.0
LL	64	5	62.35	54.45	56.66	42.37	5.30	33.50	367.00
PL	63	6	46.09	39.13	41.28	35.02	4.41	22.20	293.00
PI	64	5	30.9	16.0	15.8	115.0	14.4	7.6	934.3
%MC	67	2	175.6	67.8	145.0	245.6	30.0	6.9	1143.3
%MC(100)	67	2	54.93	40.40	45.95	80.74	9.86	6.44	672.22
LOI	59	10	91.4	21.3	68.8	150.0	19.5	4.8	606.4
SLOPE	66	3	17.58	15.00	17.22	10.11	1.24	3.00	39.00
%CLAY	58	11	7.259	5.500	6.788	7.161	0.940	0.000	24.000
%SILT	58	11	40.69	42.50	40.37	16.57	2.18	13.00	84.00
%SAND	58	11	46.02	43.00	45.85	18.36	2.41	14.00	79.00
% GRAV	58	11	6.034	4.000	5.115	7.243	0.951	0.000	31.000
MEDIAN	58	11	122.9	70.0	112.6	115.1	15.1	8.0	430.0
ASPECT	64	5	18.00	14.50	17.45	11.33	1.42	5.00	43.00
PHI MEAN	63	6	3.762	3.830	3.736	1.543	0.194	1.250	6.790
PHI MED	63	6	3.927	3.830	3.914	1.329	0.167	1.450	6.960
PHI SKEW	63	6	-0.1127	-0.1510	-0.1183	0.2222	0.0280	-0.5060	0.5100
PHI KURT	63	6	3.0327	3.1400	3.0261	0.7128	0.0898	1.5300	4.5400
PHI SORT	63	6	1.0443	1.0100	1.0291	0.2006	0.0253	0.7300	2.0400

Figure 7.18 Box plots and histograms for soil variables.

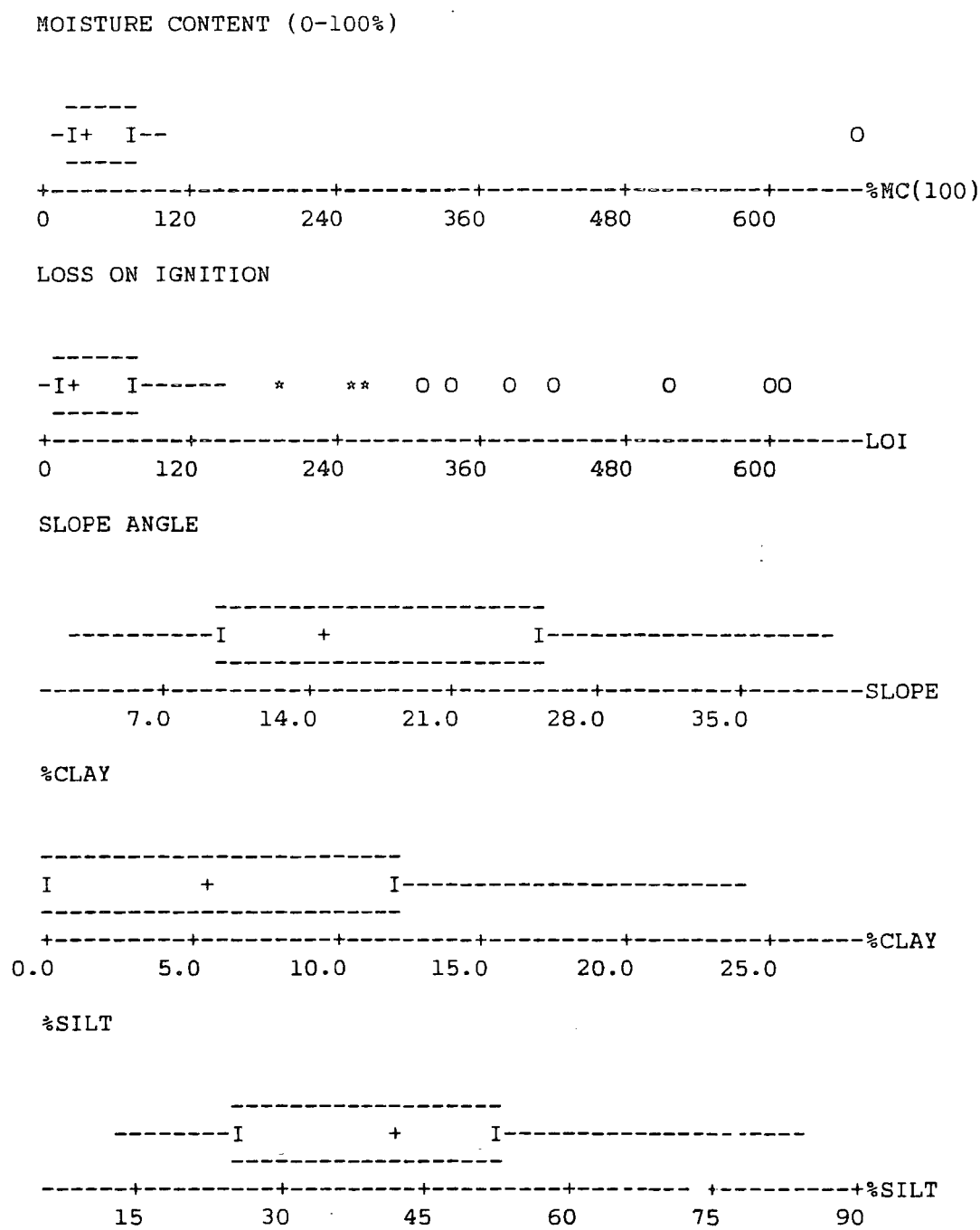

Figure 7.18 Box plots and histograms for soil variables.

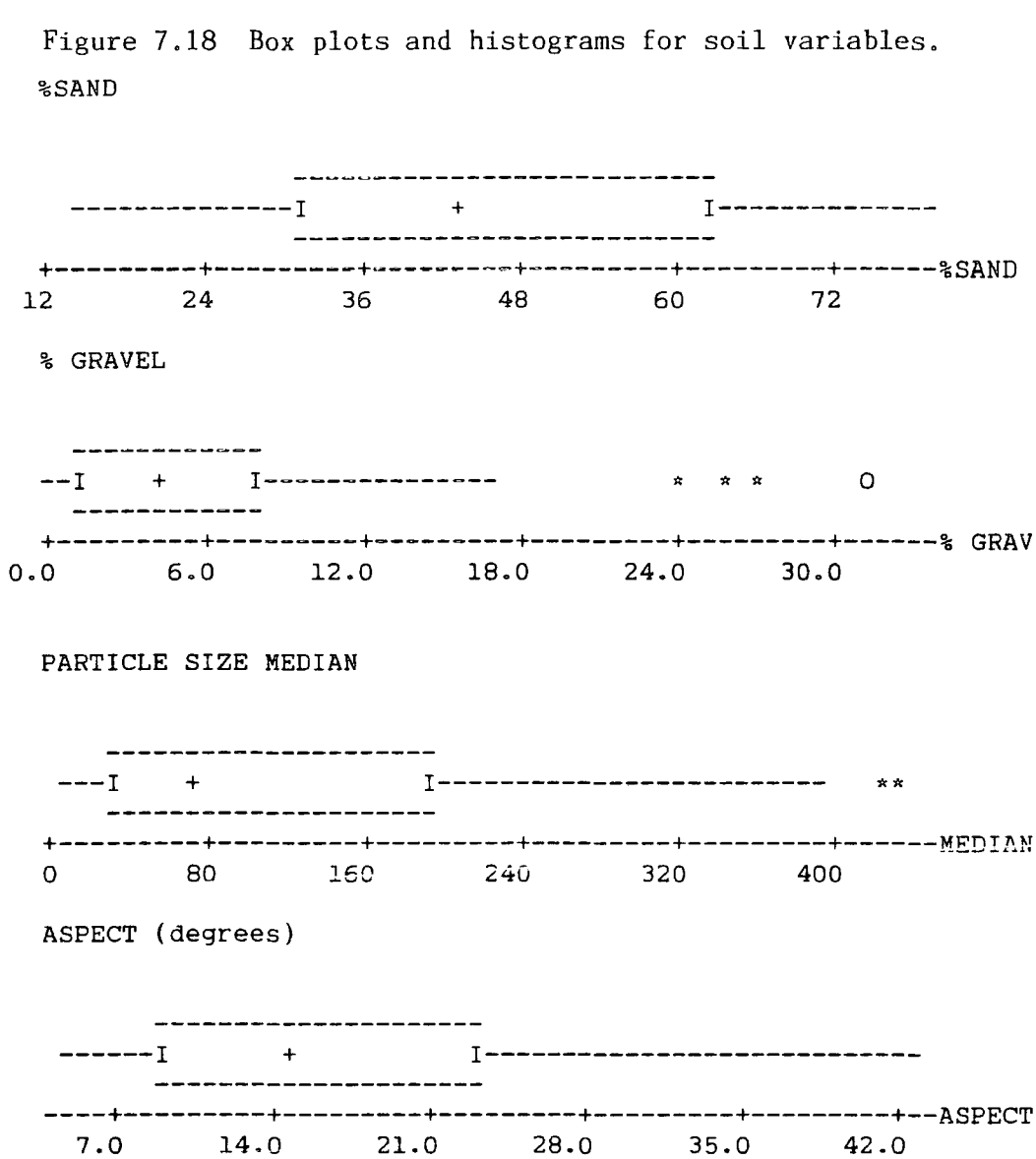

Figure 7.18 Box plots and histograms for soil variables.

Phi mean

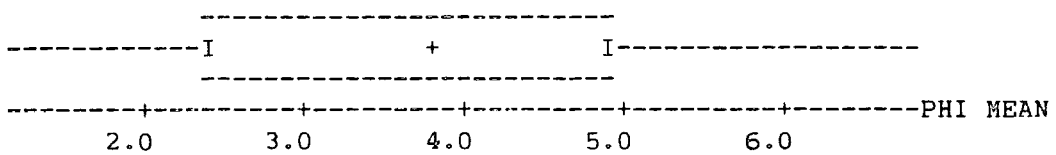

Phi median

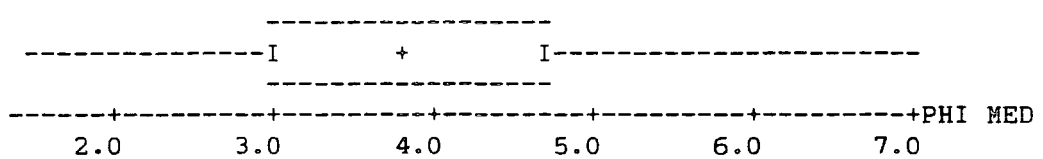

Phi skewness

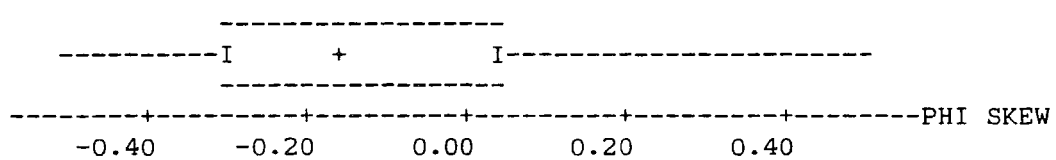

Phi kurtosis

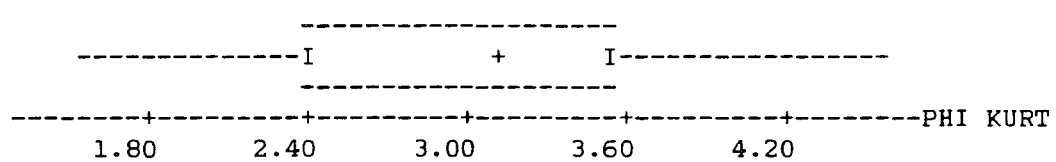

Phi sorting

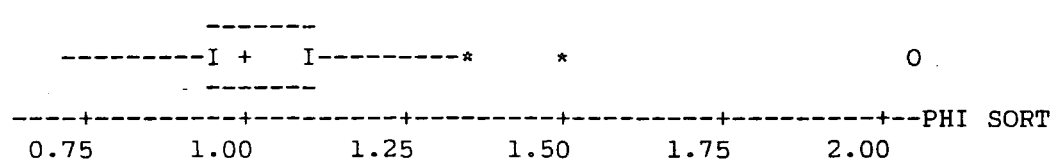

Figure 7.18 Box plots and histograms for soil variables.

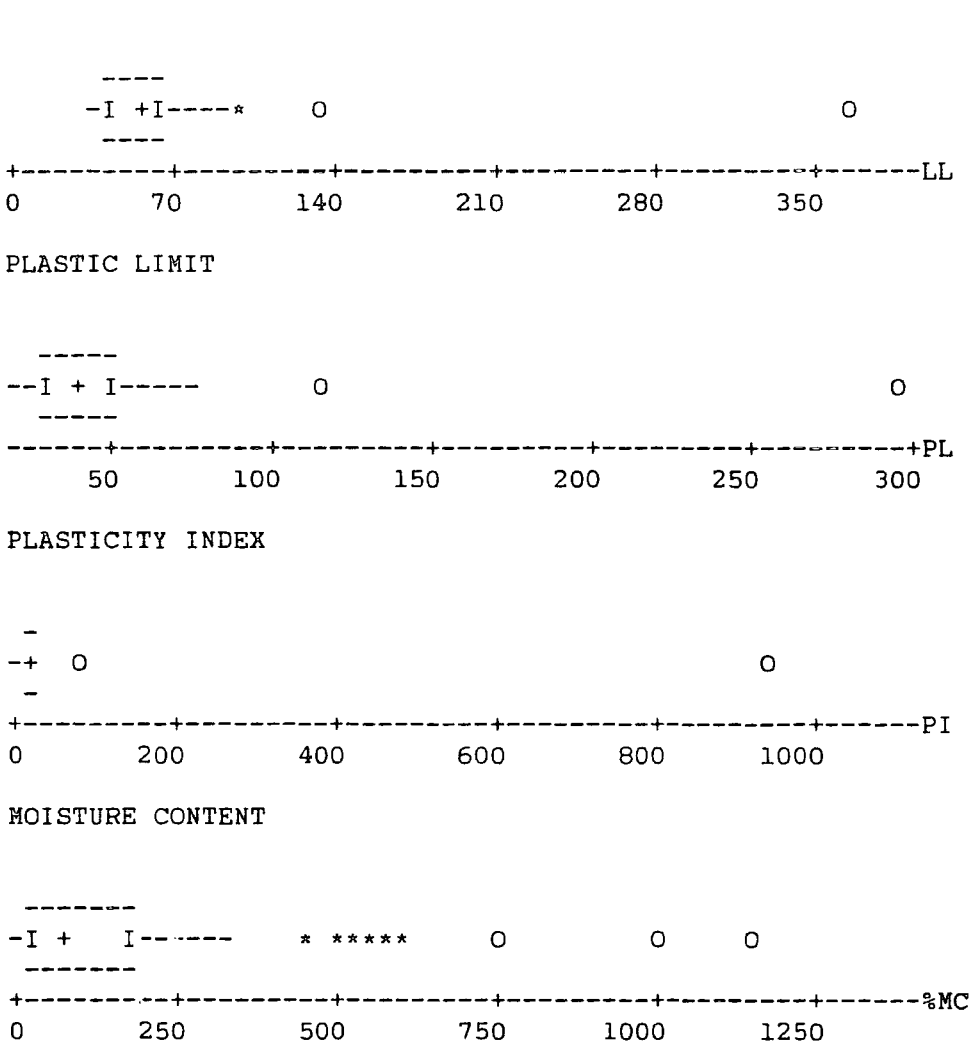

Figure 7.18 Box plots and histograms for soil variables.

```
Histogram of LL   N = 64   N* = 5

Midpoint   Count
      40      38  ****************************************
      80      24  *************************
     120       1  *
     160       0
     200       0
     240       0
     280       0
     320       0
     360       1  *


Histogram of PL   N = 63   N* = 6
Each * represents 2 obs.

Midpoint   Count
      40      57  ******************************
      80       4  **
     120       1  *
     160       0
     200       0
     240       0
     280       1  *
```

Figure 7.18 Box plots and histograms for soil variables.

Histogram of LOI N = 59 N* = 10

Midpoint	Count	
0	33	**********
50	11	***********
100	3	***
150	2	**
200	1	*
250	2	**
300	1	*
350	1	*
400	2	**
450	0	
500	1	*
550	0	
600	2	**

Histogram of SLOPE N = 66 N* = 3

Midpoint	Count	
5	10	**********
10	18	**********
15	9	*********
20	9	*********
25	8	********
30	4	****
35	6	******
40	2	**

Histogram of %CLAY N = 58 N* = 11

Midpoint	Count	
0	18	**********
2	4	****
4	2	**
6	7	*******
8	5	*****
10	3	***
12	7	*******
14	3	***
16	1	*
18	2	**
20	3	***
22	1	*
24	2	**

Figure 7.18 Box plots and histograms for soil variables.

```
Histogram of %SILT   N = 58   N* = 11

Midpoint   Count
      10       3  ***
      20       8  ********
      30      13  *************
      40       5  *****
      50      15  ***************
      60      10  **********
      70       3  ***
      80       1  *


Histogram of %SAND   N = 58   N* = 11

Midpoint   Count
      15       1  *
      20       5  *****
      25       5  *****
      30       7  *******
      35       2  **
      40       7  *******
      45       6  ******
      50       4  ****
      55       3  ***
      60       5  *****
      65       3  ***
      70       3  ***
      75       5  *****
      80       2  **


Histogram of % GRAV   N = 58   N* = 11

Midpoint   Count
       0      19  *******************
       4      19  *******************
       8      10  **********
      12       2  **
      16       4  ****
      20       0
      24       1  *
      28       2  **
      32       1  *
```

Figure 7.18 Box plots and histograms for soil variables.

```
Histogram of MEDIAN   N = 58   N* = 11

Midpoint   Count
       0      12  ************
      50      20  ********************
     100       1  *
     150       7  *******
     200       6  ******
     250       5  *****
     300       3  ***
     350       1  *
     400       1  *
     450       2  **


Histogram of ASPECT   N = 64   N* = 5

Midpoint   Count
       5      11  ***********
      10      18  ******************
      15       8  ********
      20       6  ******
      25       8  ********
      30       1  *
      35       5  *****
      40       6  ******
      45       1  *


Histogram of PHI MEAN   N = 63   N* = 6

Midpoint   Count
     1.5       4  ****
     2.0       8  ********
     2.5      10  **********
     3.0       6  ******
     3.5       3  ***
     4.0       5  *****
     4.5       7  *******
     5.0      10  **********
     5.5       3  ***
     6.0       2  **
     6.5       3  ***
     7.0       2  **
```

Figure 7.18 Box plots and histograms for soil variables.

Histogram of PHI MED N = 63 N* = 6

Midpoint	Count	
1.5	3	***
2.0	3	***
2.5	7	*******
3.0	7	*******
3.5	10	**********
4.0	10	**********
4.5	7	*******
5.0	3	***
5.5	4	****
6.0	7	*******
6.5	1	*
7.0	1	*

Histogram of PHI SKEW N = 63 N* = 6

Midpoint	Count	
-0.5	2	**
-0.4	7	*******
-0.3	11	**********
-0.2	12	**********
-0.1	4	****
0.0	12	**********
0.1	7	*******
0.2	5	*****
0.3	2	**
0.4	0	
0.5	1	*

Histogram of PHI KURT N = 63 N* = 6

Midpoint	Count	
1.6	2	**
2.0	6	******
2.4	11	**********
2.8	7	*******
3.2	17	**********
3.6	12	**********
4.0	4	****
4.4	4	****

Histogram of PHI SORT N = 63 N* = 6

Midpoint	Count	
0.7	2	**
0.8	5	*****
0.9	9	*********
1.0	19	**********
1.1	16	**********
1.2	5	*****
1.3	4	****
1.4	1	*
1.5	1	*
1.6	0	
1.7	0	
1.8	0	
1.9	0	
2.0	1	*

Figure 7.18 Box plots and histograms for soil variables.

```
Histogram of PI   N = 64   N* = 5
Each * represents 2 obs.

Midpoint   Count
       0      62  *********************************
     100       1  *
     200       0
     300       0
     400       0
     500       0
     600       0
     700       0
     800       0
     900       1  *


Histogram of %MC   N = 67   N* = 2

Midpoint   Count
       0      26  **************************
     100      21  *********************
     200       7  *******
     300       2  **
     400       0
     500       4  ****
     600       3  ***
     700       1  *
     800       1  *
     900       0
    1000       1  *
    1100       1  *


Histogram of %MC(100)   N = 67   N* = 2

Midpoint   Count
       0      17  *****************
      50      36  ************************************
     100      13  *************
     150       0
     200       0
     250       0
     300       0
     350       0
     400       0
     450       0
     500       0
     550       0
     600       0
     650       1  *
```

7.3.2 Structure of explanatory variables

Figure 7.18 shows boxplots for index tests, soil moisture, loss on ignition, slope angle and granulometric analyses. Each plot denotes the median (+), inner fences, outer fences, values between inner and outer fences (*), and outliers beyond the outer fence (0) in the notation of Tukey (1977). The solid box is equivalent to the interquartile range, with inner fences defined as -

lower quartile - (1.5 x interquartile range)

upper quartile + (1.5 x interquartile range)

and outer fences defined as -

lower quartile - (3 x interquartile range)

upper quartile + (3 x interquartile range).

Liquid limit and plastic limit data are positively skewed and both contain outlying values. Closer inspection of these outliers shows them to be associated with highly organic silt samples, for example, at site 5/2. These results are unusual because organic soil do not usually exhibit plastic behaviour. Such results will exert a high leverage if used in a regression or correlation calculation and because its relationship to the rest of the points is unclear it is omitted from further analysis. Percentage moisture content has been re-expressed as a percentage of wet weight and is thereby scaled between 0 and 100%. This helps to reduce the positive skewness, which results from saturated soils with low bulk densities. Loss on ignition data also exhibit strong positive skewness caused by highly organic samples. These data are logarithmically transformed to offset the effect of positive skewness.

The percentages of clay, silt, sand and gravel are clearly asymmetrically distributed; however, Krumbein (1934) suggested that sediments

have an approximately log-normal distribution. Therefore, the granulometric distributions of the samples are expressed as statistics derived from phi ($-log_e.d$) units. Phi mean and phi median indicate the general level of coarseness of the sediment and exhibit distributions similar to a Gaussian. Phi skewness, phi sorting and phi kurtosis are less well behaved but the deviations from normality can be interpreted in terms of the sedimentary or geotechnical nature of the soil. The scale of the phi sorting statistic is unbounded; this distribution does contain positive outliers which are extremely poorly sorted, glacially derived sediments. Figure 7.18 shows histograms of the transformed explanatory variables.

7.3.3 Correlation structure of predictive variables

Table 7.20 lists the Pearson-product moment correlation coefficients for the explanatory variables and S.M.M. variables. Outliers in the index test distribution have been omitted from the calculation.

Figure 7.19 summarizes the most important correlations which relate to predicting S.M.M. from Anderson's Tube data. Correlations involving S.M.M. are generally weak because of the large scatter and outliers present in that data. However, movement of Anderson's tubes is positively associated with high root density, positive skewness of the particle size distribution and slope angle. Other important correlations involve positive association among density of roots, loss on ignition and % moisture content. Slope angle is negatively associated with phi skewness and % silt, a result which might suggest that steep slopes tend toward threshold slopes with an increasingly coarse granular composition.

Preliminary plots of explanatory variables against the S.M.M. response variables indicate that outliers in the mass movement data considerably weaken linear correlations. The scatter of data in figure 7.20,

Table 7.20 Correlation matrix of instruments and soil variables.

	SITE	LL	PL	PI	%MC	%MC(100)	LOI	SLOPE
LL	0.037							
PL	0.022	0.996						
PI	-0.171	0.921	0.881					
%MC	-0.048	0.589	0.596	-0.002				
%MC(100)	-0.163	0.334	0.345	0.957	0.221			
LOI	-0.153	0.387	0.400	0.286	0.732	0.671		
SLOPE	0.110	-0.247	-0.265	-0.149	-0.156	-0.169	-0.364	
%CLAY	-0.070	0.044	-0.018	0.323	-0.108	-0.066	-0.035	-0.152
%SILT	0.092	0.311	0.225	0.452	0.158	0.288	0.320	-0.363
%SAND	-0.020	-0.215	-0.123	-0.424	0.007	-0.110	-0.157	0.243
% GRAV	-0.092	-0.211	-0.182	-0.275	-0.272	-0.317	-0.307	0.364
MEDIAN	0.002	-0.204	-0.114	-0.448	-0.115	-0.280	-0.236	0.355
ASPECT	0.089	-0.230	-0.254	-0.112	-0.196	-0.187	-0.360	0.968
PHI MEAN	0.075	0.300	0.218	0.434	0.058	0.174	0.236	-0.383
PHI MED	0.007	0.253	0.164	0.471	0.043	0.098	0.222	-0.331
PHI SKEW	0.293	0.304	0.236	0.361	-0.021	0.156	0.069	-0.252
PHI KURT	-0.002	-0.168	-0.211	0.111	-0.051	-0.040	-0.189	0.272
PHI SORT	0.027	0.048	0.047	0.015	0.080	0.060	-0.010	0.032
VEG GRP	-0.151	-0.100	-0.072	-0.172	-0.479	-0.317	-0.262	-0.256
SLOP GRP	0.141	-0.301	-0.316	-0.048	-0.189	-0.089	-0.381	0.953
ROOT GRP	0.430	0.292	0.290	0.195	0.516	0.342	0.335	0.146
IP 15	0.195	-0.047	-0.041	-0.054	-0.090	-0.055	-0.162	0.099
IP 10	0.112	-0.134	-0.141	0.132	-0.072	0.141	-0.344	0.413
IP 5	0.338	-0.159	-0.163	-0.005	0.102	0.074	-0.051	0.245
AT LIN	0.301	-0.269	-0.259	0.019	-0.006	0.003	-0.247	0.502
AT VOL	0.250	0.107	0.095	-0.045	0.163	-0.014	0.037	0.436

	%CLAY	%SILT	%SAND	% GRAV	MEDIAN	ASPECT	PHI MEAN	PHI MED
%SILT	0.283							
%SAND	-0.573	-0.866						
% GRAV	-0.185	-0.372	0.013					
MEDIAN	-0.485	-0.863	0.820	0.377				
ASPECT	-0.111	-0.387	0.257	0.348	0.346			
PHI MEAN	0.633	0.857	-0.859	-0.410	-0.911	-0.391		
PHI MED	0.765	0.791	-0.835	-0.450	-0.855	-0.329	0.923	
PHI SKEW	0.157	0.630	-0.582	-0.121	-0.560	-0.266	0.628	0.438
PHI KURT	0.485	-0.081	-0.307	0.486	-0.203	0.317	0.100	0.197
PHI SORT	-0.146	-0.116	0.232	-0.181	0.268	0.035	-0.261	-0.228
VEG GRP	-0.202	-0.173	0.195	0.102	0.252	-0.241	-0.138	-0.196
SLOP GRP	-0.129	-0.436	0.323	0.307	0.384	0.923	-0.435	-0.373
ROOT GRP	0.007	0.208	-0.141	-0.128	-0.107	0.108	0.187	0.113
IP 15	-0.156	0.047	0.004	0.036	-0.004	0.093	0.005	-0.068
IP 10	-0.032	-0.025	0.004	0.076	-0.032	-0.409	-0.013	-0.036
IP 5	-0.038	0.151	-0.118	-0.010	-0.062	0.248	0.036	0.048
AT LIN	0.008	-0.112	0.037	0.130	0.061	0.457	-0.015	-0.074
AT VOL	0.101	0.087	-0.112	-0.002	-0.163	0.366	0.160	0.074

	PHI SKEW	PHI KURT	PHI SORT	VEG GRP	SLOP GRP	ROOT GRP	IP 15	IP 10
PHI KURT	-0.063							
PHI SORT	-0.233	-0.325						
VEG GRP	-0.067	-0.383	0.135					
SLOP GRP	-0.331	0.286	0.073	-0.220				
ROOT GRP	0.277	0.041	0.078	-0.535	0.069			
IP 15	0.054	0.031	0.002	-0.035	0.091	0.250		
IP 10	0.147	0.042	-0.262	-0.299	0.328	0.315	0.221	
IP 5	-0.046	0.101	0.194	-0.200	0.263	0.440	0.295	0.236
AT LIN	0.031	0.146	-0.111	-0.286	0.430	0.500	0.348	0.552
AT VOL	0.141	0.185	-0.156	-0.395	0.366	0.522	0.112	0.437

IP 5	AT LIN
0.248	
0.037	0.785

Table 7.20 Correlation matrix of instruments and soil variables.

	SITE	LL	PL	PI	%MC	%MC(100)	LOI	SLOPE
LL	0.037							
PL	0.022	0.996						
PI	-0.171	0.921	0.881					
%MC	-0.048	0.589	0.596	-0.002				
%MC(100)	-0.163	0.334	0.345	0.957	0.221			
LOI	-0.153	0.387	0.400	0.286	0.732	0.671		
SLOPE	0.110	-0.247	-0.265	-0.149	-0.156	-0.169	-0.364	
%CLAY	-0.070	0.044	-0.018	0.323	-0.108	-0.066	-0.035	-0.152
%SILT	0.092	0.311	0.225	0.452	0.158	0.288	0.320	-0.363
%SAND	-0.020	-0.215	-0.123	-0.424	0.007	-0.110	-0.157	0.243
% GRAV	-0.092	-0.211	-0.182	-0.275	-0.272	-0.317	-0.307	0.364
MEDIAN	0.002	-0.204	-0.114	-0.448	-0.115	-0.280	-0.236	0.355
ASPECT	0.089	-0.230	-0.254	-0.112	-0.196	-0.187	-0.360	0.968
PHI MEAN	0.075	0.300	0.218	0.434	0.058	0.174	0.236	-0.383
PHI MED	0.007	0.253	0.164	0.471	0.043	0.098	0.222	-0.331
PHI SKEW	0.293	0.304	0.236	0.361	-0.021	0.156	0.069	-0.252
PHI KURT	-0.002	-0.168	-0.211	0.111	-0.051	-0.040	-0.189	0.272
PHI SORT	0.027	0.048	0.047	0.015	0.080	0.060	-0.010	0.032
VEG GRP	-0.151	-0.100	-0.072	-0.172	-0.479	-0.317	-0.262	-0.256
SLOP GRP	0.141	-0.301	-0.316	-0.048	-0.189	-0.089	-0.381	0.953
ROOT GRP	0.430	0.292	0.290	0.195	0.516	0.342	0.335	0.146
IP 15	0.195	-0.047	-0.041	-0.054	-0.090	-0.055	-0.162	0.099
IP 10	0.112	-0.134	-0.141	0.132	-0.072	0.141	-0.344	0.413
IP 5	0.338	-0.159	-0.163	-0.005	0.102	0.074	-0.051	0.245
AT LIN	0.301	-0.269	-0.259	0.019	-0.006	0.003	-0.247	0.502
AT VOL	0.250	0.107	0.095	-0.045	0.163	-0.014	0.037	0.436

	%CLAY	%SILT	%SAND	% GRAV	MEDIAN	ASPECT	PHI MEAN	PHI MED
%SILT	0.283							
%SAND	-0.573	-0.866						
% GRAV	-0.185	-0.372	0.013					
MEDIAN	-0.485	-0.863	0.820	0.377				
ASPECT	-0.111	-0.387	0.257	0.348	0.346			
PHI MEAN	0.633	0.857	-0.859	-0.410	-0.911	-0.391		
PHI MED	0.765	0.791	-0.835	-0.450	-0.855	-0.329	0.923	
PHI SKEW	0.157	0.630	-0.582	-0.121	-0.560	-0.266	0.628	0.438
PHI KURT	0.485	-0.081	-0.307	0.486	-0.203	0.317	0.100	0.197
PHI SORT	-0.146	-0.116	0.232	-0.181	0.268	0.035	-0.261	-0.228
VEG GRP	-0.202	-0.173	0.195	0.102	0.252	-0.241	-0.138	-0.196
SLOP GRP	-0.129	-0.436	0.323	0.307	0.384	0.923	-0.435	-0.373
ROOT GRP	0.007	0.208	-0.141	-0.128	-0.107	0.108	0.187	0.113
IP 15	-0.156	0.047	0.004	0.036	-0.004	0.093	0.005	-0.068
IP 10	-0.032	-0.025	0.004	0.076	0.032	0.409	-0.013	-0.036
IP 5	-0.038	0.151	-0.118	-0.010	-0.062	0.248	0.036	0.048
AT LIN	0.008	-0.112	0.037	0.130	0.061	0.457	-0.015	-0.074
AT VOL	0.101	0.087	-0.112	-0.002	-0.163	0.366	0.160	0.074

	PHI SKEW	PHI KURT	PHI SORT	VEG GRP	SLOP GRP	ROOT GRP	IP 15	IP 10
PHI KURT	-0.063							
PHI SORT	-0.233	-0.325						
VEG GRP	-0.067	-0.383	0.135					
SLOP GRP	-0.331	0.286	0.073	-0.220				
ROOT GRP	0.277	0.041	0.078	-0.535	0.069			
IP 15	0.054	0.031	0.002	-0.035	0.091	0.250		
IP 10	0.147	0.042	-0.262	-0.299	0.328	0.315	0.221	
IP 5	-0.046	0.101	0.194	-0.200	0.263	0.440	0.295	0.236
AT LIN	0.031	0.146	-0.111	-0.286	0.430	0.500	0.348	0.552
AT VOL	0.141	0.185	-0.156	-0.395	0.366	0.522	0.112	0.437

IP 5	AT LIN
0.248	
0.037	0.785

Figure 7.19 Correlation structure diagram showing the most important correlations which relate to predicting S.M.M. from Anderson's Tube data.

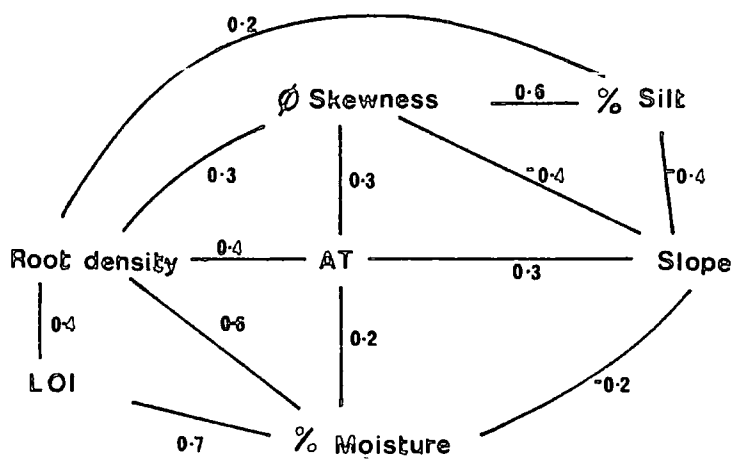

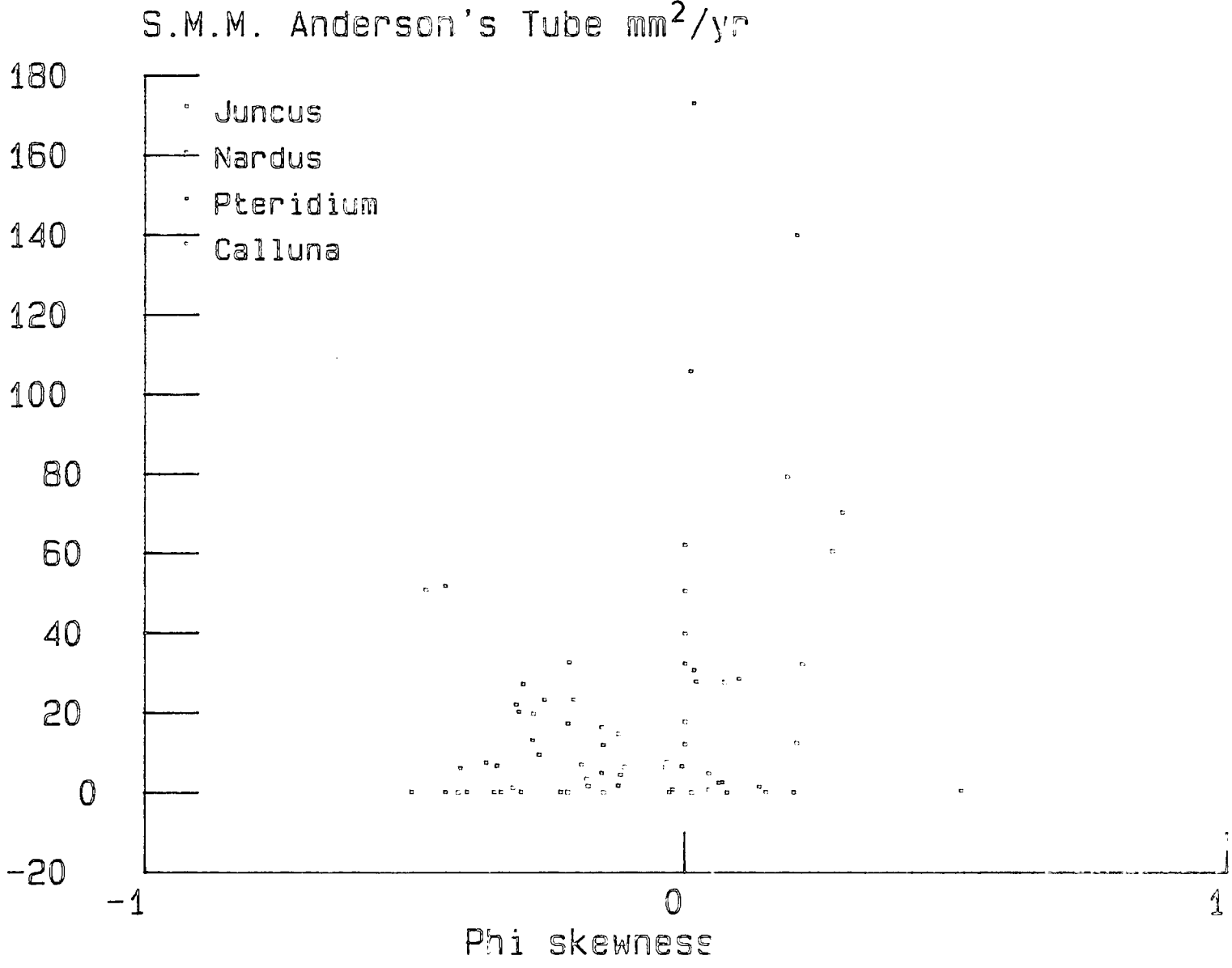
S.M.M. Anderson's Tube mm²/yr
180
160
140
120
100
80
60
40
20
0
-20
Juncus
Nardus
Pteridium
Calluna
-1
0
1
Phi skewness

Figure 7.20

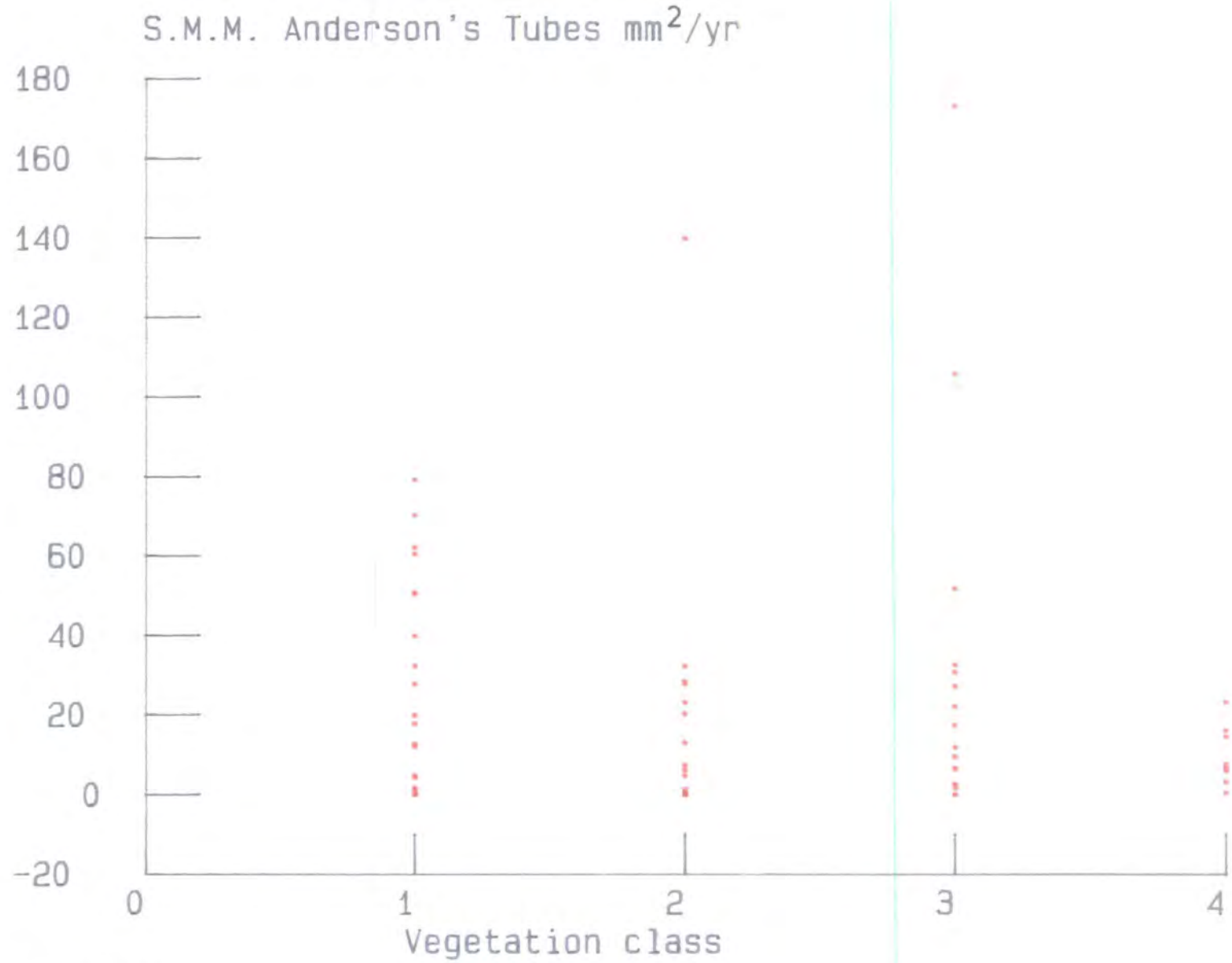
S.M.M. Anderson's Tubes mm2/yr
180
160
140
120
100
80
60
40
20
0
-20
0
1
2
3
4
Vegetation class

Figure 7.21

Anderson's tube data against phi skewness, contains several notable outliers, but the trend in the data suggests that mass movement rates increase as phi skewness increases (size distribution becomes finer). Figure 7.21 shows that the most extreme outliers in the Anderson's tube data are associated with the *Nardus* and *Pteridium* vegetation classes.

7.3.4 Regression results

Regressing slope against mass movement response variables in the first instance gives the following results.

$$IP_{15} = 178 + 1.96 \cdot Slope$$

$$r^2 = 0.01$$

$$IP_{10} = 13.6 + 7.78 \cdot Slope$$

$$r^2 = 0.17$$

$$IP_5 = 36 + 1.78 \cdot Slope$$

$$r^2 = 0.06$$

Figures 7.22, 7.23 and 7.24 show residuals plotted against the slope angle data for all three instruments. Each plot reveals an increase in the spread of the residuals as slope angle increases but no other systematic pattern emerges, other than a poor relationship. The IP_{10} data gives the best fit with 17% of the linear variation explained in the regression. Four large standardized residuals ($-2 < x \leq 2$) are evident:

Figure 7.22 Regression of 15 cm Inclinometer Peg data against slope angle.

REGRESSION OF IP 15 AGAINST SLOPE

The regression equation is
IP 15 = 178 + 1.96 SLOPE

56 cases used 13 cases contain missing values

Predictor	Coef	Stdev	t-ratio
Constant	177.75	55.25	3.22
SLOPE	1.963	2.696	0.73

s = 207.6 R-sq = 1.0% R-sq(adj) = 0.0%

Analysis of Variance

SOURCE	DF	SS	MS
Regression	1	22857	22857
Error	54	2327693	43105
Total	55	2350549	

Unusual Observations

Obs.	SLOPE	IP 15	Fit	Stdev.Fit	Residual	St.Resid
2	18.0	630.0	213.1	27.8	416.9	2.03R
56	34.0	1260.0	244.5	51.9	1015.5	5.05R
63	37.0	-483.8	250.4	58.9	-734.2	-3.69R

R denotes an obs. with a large st. resid.

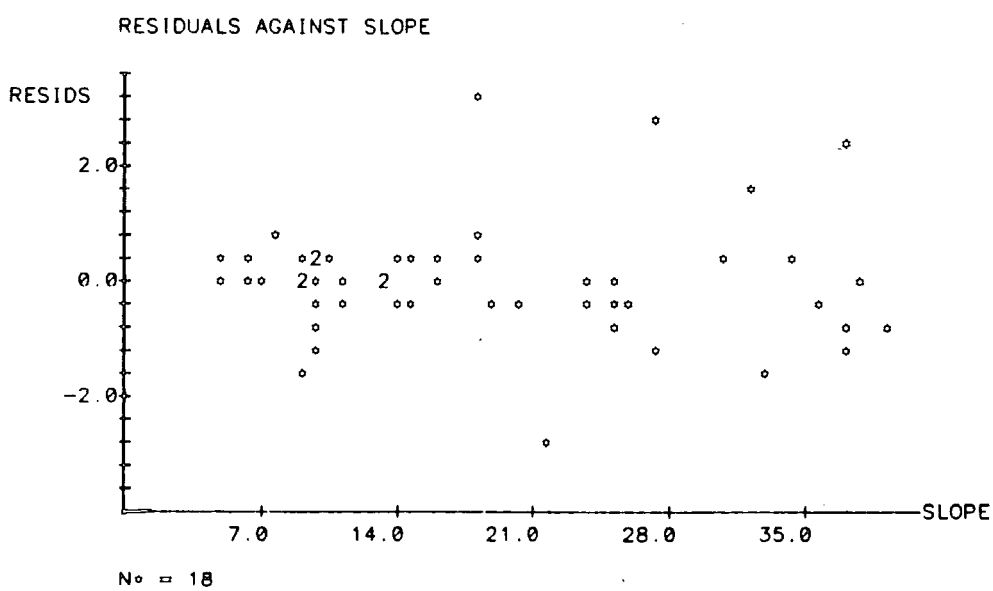

Figure 7.23 Regression of 10 cm Inclinometer Peg data against slope angle.

REGRESSION OF IP 10 AGAINST SLOPE

The regression equation is
IP 10 = 13.6 + 7.78 SLOPE

55 cases used 14 cases contain missing values

Predictor	Coef	Stdev	t-ratio
Constant	13.60	49.41	0.28
SLOPE	7.781	2.359	3 30

s = 177.0 R-sq = 17.0% R-sq(adj) = 15.5%

Analysis of Variance

SOURCE	DF	SS	MS
Regression	1	340692	340692
Error	53	1660267	31326
Total	54	2000958	

Unusual Observations

Obs.	SLOPE	IP 10	Fit	Stdev.Fit	Residual	St.Resid
2	18.0	690.0	153.7	23.9	536.3	3.06R
52	22.0	-300.0	184.8	25.4	-484.8	-2.77R
54	27.0	760.0	223.7	31.4	536.3	3.08R
59	37.0	710.0	301.5	50.1	408.5	2.41R

R denotes an obs. with a large st. resid.

RESIDUALS AGAINST SLOPE

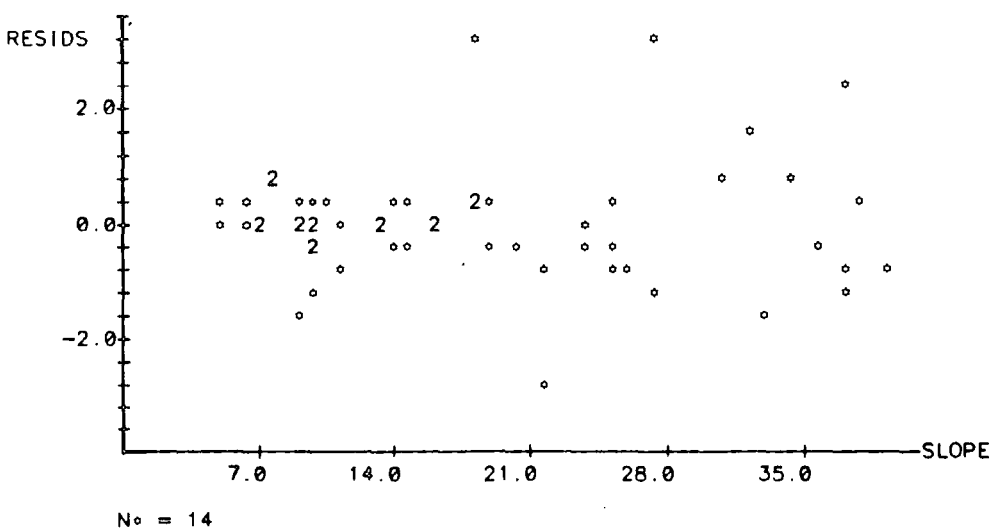

No = 14

Figure 7.24 Regression of 5 cm Inclinometer Peg data against slope angle.

REGRESSION OF IP 5 AGAINST SLOPE

The regression equation is
IP 5 = 36.0 + 1.78 SLOPE

61 cases used 8 cases contain missing values

Predictor	Coef	Stdev	t-ratio
Constant	36.01	18.05	1.99
SLOPE	1.7758	0.9168	1.94

s = 71.45 R-sq = 6.0% R-sq(adj) = 4.4%

Analysis of Variance

SOURCE	DF	SS	MS
Regression	1	19151	19151
Error	59	301159	5104
Total	60	320310	

Unusual Observations

Obs.	SLOPE	IP 5	Fit	Stdev.Fit	Residual	St.Resid
52	22.0	247.50	75.08	10.24	172.42	2.44R
55	38.0	346.20	103.49	21.34	242.71	3.56R
64	39.0	-93.80	105.26	22.17	-199.06	-2.93R
67	33.0	-53.80	94.61	17.31	-148.41	-2.14R

R denotes an obs. with a large st. resid.

RESIDUALS AGAINST SLOPE

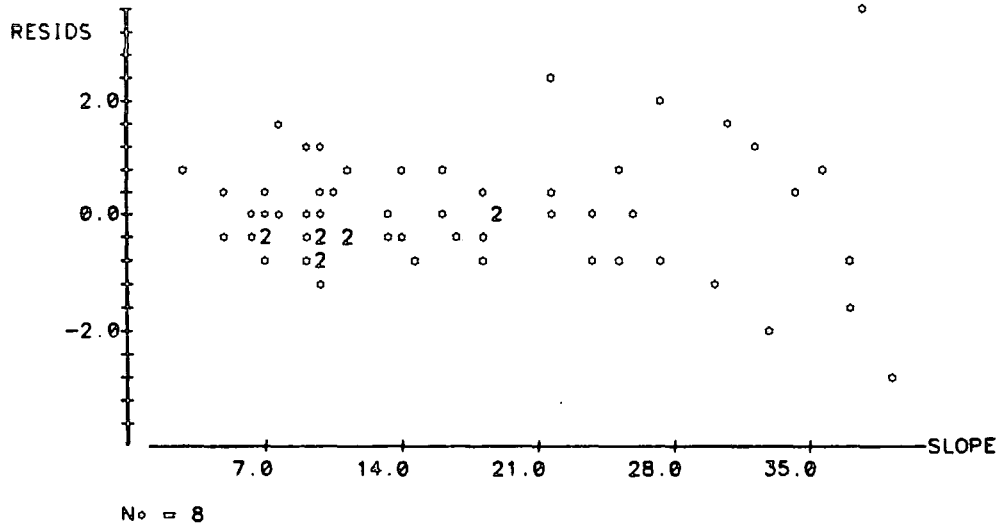

No = 8

Site 1/2	*Pteridium*	scarp face	18^o
Site 8/5	*Pteridium*	scarp face	22^o
Site 9/1	*Juncus*	toe of lobe	27^o
Site 9/6	*Juncus*	scarp behind lobe	37^o

These sites are associated with scarps and lobes which have a locally straight slope form but are part of more complex geomorphological feature. Tension cracks were observed at site 1/2 which seem to be associated with relatively rapid slope deformation.

Regressing slope against Anderson's tube data gave the following results.

$$ATvol = 130 + 0.763 \cdot Slope$$

$$r^2 = 0.05$$

$$ATlin = 0.07 + 0.0058 \cdot Slope$$

$$r^2 = 0.13$$

The plot of residuals against slope for AT linear data reveals two large positive residuals (site 1/2 and site 2/1) and an increase in the variability of S.M.M. data with increasing slope angle (figure 7.25). A similar plot for AT volumetric data shows a similar pattern but with three large positive residuals (site 1/2, site 6/6, site 8/4). All these sites are associated with scarp faces thought to be associated with the boundary between resistant sandstone outcrops and weaker shale and mudrock beds in the Yoredale cyclothem. When these outliers were removed the regression equations became:

$$ATvol = 54.9 + 0.785 \cdot Slope$$

$$r^2 = 0.19$$

Figure 7.25 Regression of Anderson's Tube data (linear) against slope angle.

REGRESSION OF AT LIN AGAINST SLOPE (OUTLIERS REMOVED)

The regression equation is
AT LIN = 0.0378 + 0.00631 SLOPE

47 cases used 22 cases contain missing values

Predictor	Coef	Stdev	t-ratio
Constant	0.03783	0.03387	1.12
SLOPE	0.006312	0.001620	3.90

s = 0.1183 R-sq, = 25.2% R-sq(adj) = 23.6%

Analysis of Variance

SOURCE	DF	SS	MS
Regression	1	0.21256	0.21256
Error	45	0.63001	0.01400
Total	46	0.84257	

Unusual Observations

Obs.	SLOPE	AT LIN	Fit	Stdev.Fit	Residual	St.Resid
10	13.0	0.3960	0.1199	0.0191	0.2761	2.36R
58	36.0	0.5340	0.2651	0.0339	0.2689	2.37R
59	37.0	0.5400	0.2714	0.0353	0.2686	2.38R

R denotes an obs. with a large st. resid.

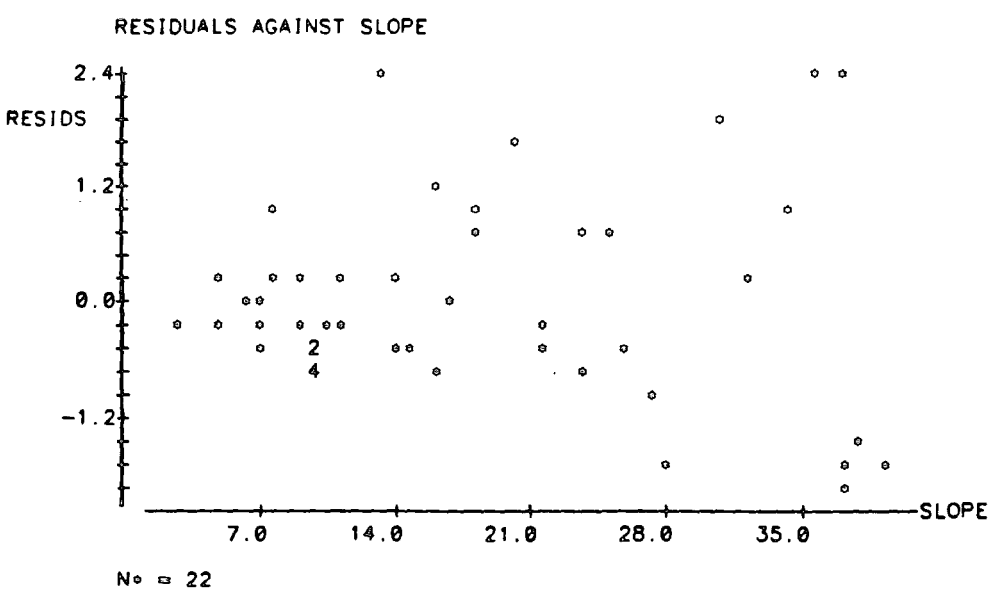

$$ATlin = 0.038 + 0.0063 \cdot Slope$$

$$r^2 = 0.25$$

Residual plots show no further detail; however, a scatter plot (figure 7.26) of AT volumetric movement against slope angle illustrates that the data are grouped according to their vegetation class. In particular, *Nardus* sites show less mass movement on steep slopes than the other groups and this seriously inhibits the performance of the regression model.

The plot of S.M.M. against slope angle gives the impression that S.M.M. does not depend on gradient. However, there is a strong relationship between the two, shown by median polish results, when the effect of vegetation is taken into account. A further problem with the S.M.M. data is its tendency towards large values (positive skewness). This results in the observed pattern of increasing levels of variance across residual plots. Figure 7.27 illustrates the extreme positive skewness in Anderson's tube volumetric data using a quantile - quantile plot (a normal distribution would plot as a straight line). One remedy for positive skewness is to re-express the data using logarithms. Figure 7.28 shows that the natural logarithms of the AT volumetric data correct for the effect of skewness.

Further regressions are calculated using the log transformed AT volumetric data.

$$\log_e ATvol = 14.7 + 0.0566 \cdot Slope$$

$$r^2 = 0.168$$

$$\log_e ATlin = -2.98 + 0.04 \cdot Slope$$

$$r^2 = 0.234$$

The goodness of fit is improved only slightly with the linear data and not at all in the case of the volumetric data. The transformation

Figure 7.26 Regression of Anderson's Tube data (volumetric) against slope angle.

RESRESSION OF AT VOL AGAINST SLOPE (OUTLIERS REMOVED)

The regression equation is
AT VOL = 5.49 + 0.785 SLOPE

48 cases used 21 cases contain missing values

Predictor	Coef	Stdev	t-ratio
Constant	5.488	4.934	1.11
SLOPE	0.7853	0.2391	3.28

s = 17.64 R-sq = 19.0% R-sq(adj) = 17.2%

Analysis of Variance

SOURCE	DF	SS	MS
Regression	1	3355.4	3355.4
Error	46	14310.6	311.1
Total	47	17666.1	

Unusual Observations

Obs.	SLOPE	AT VOL	Fit	Stdev.Fit	Residual	St.Resid
58	36.0	70.27	33.76	5.07	36.51	2.16R
59	37.0	79.30	34.54	5.28	44.76	2.66R

R denotes an obs. with a large st. resid.

RESIDUALS AGAINST SLOPE

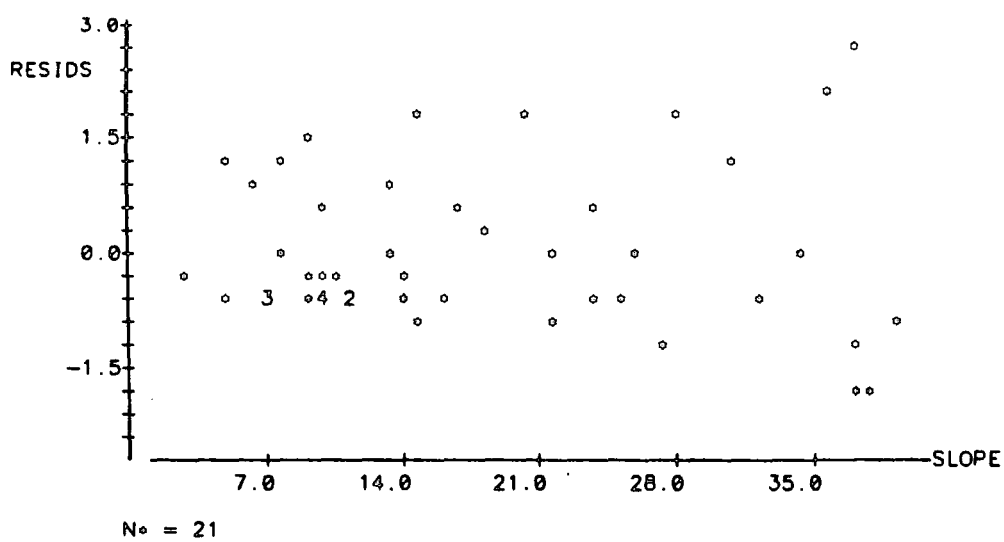

No = 21

Figure 7.27 Quantile - quantile plot of Anderson's Tube data (volumetric) against normal quantiles.

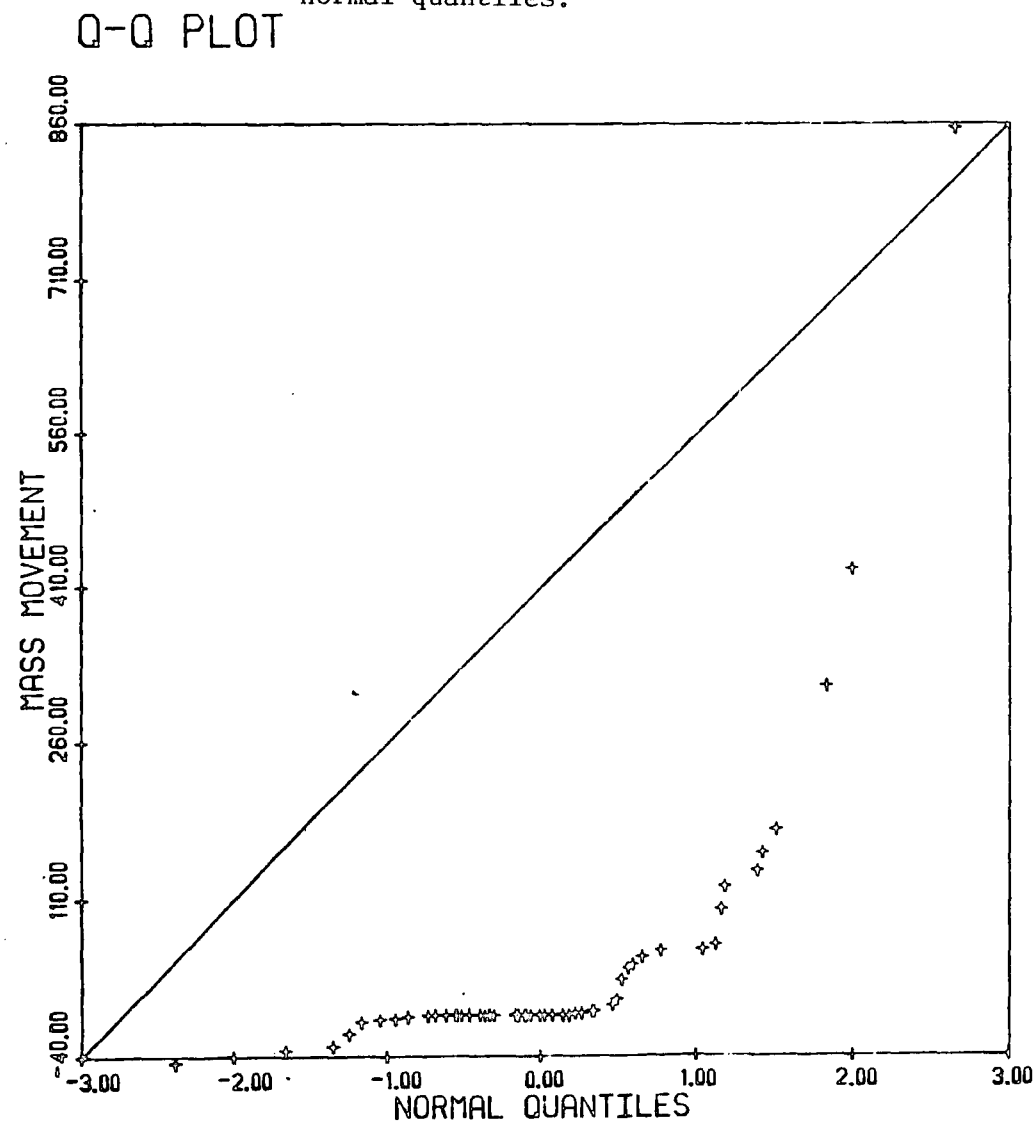

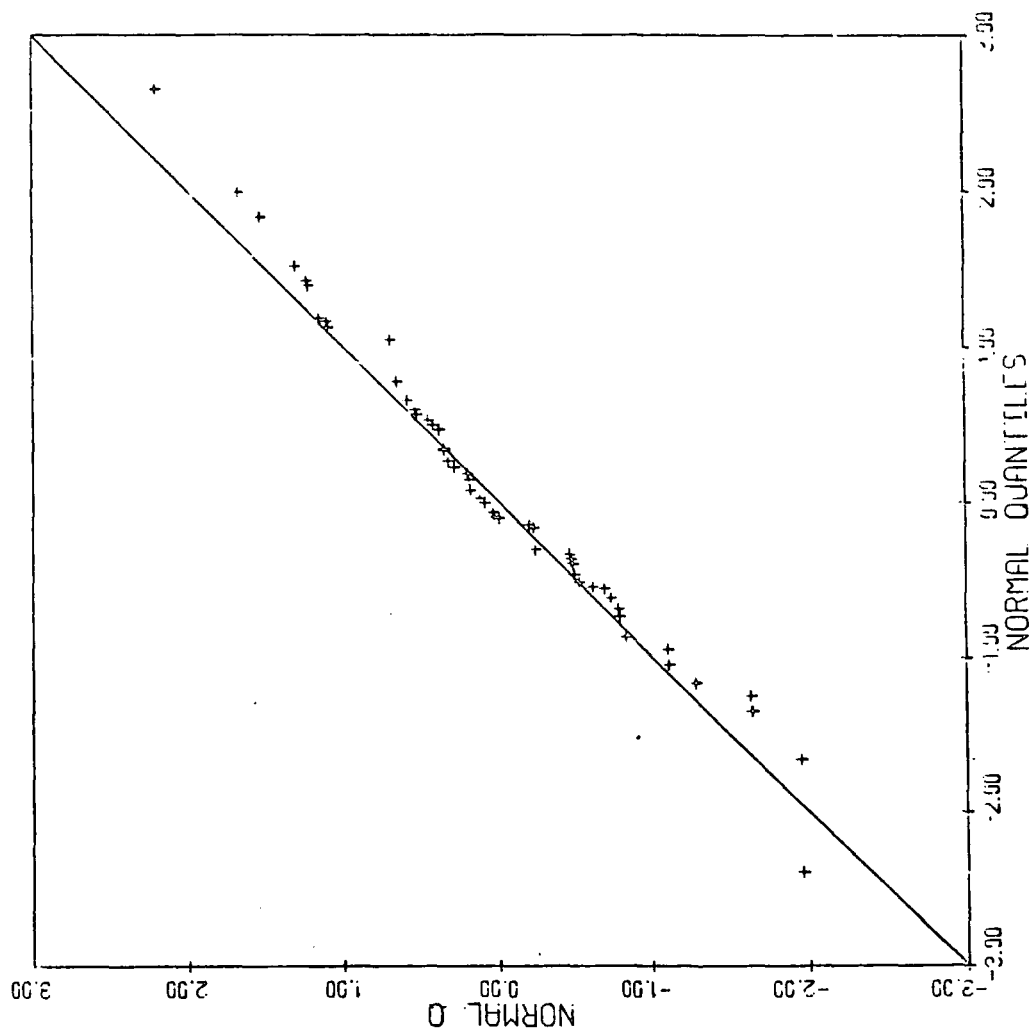

Figure 7.28 Normalized Anderson's Tube data (volumetric)against normal quantiles.

Figure 7.29 Regression of log transformed AT data (volumetric) against slope angle.

REGRESSION OF LOG AT VOL AGAINST SLOPE (OUTLIERS REMOVED)

The regression equation is
LOG AT V = 1.47 + 0.0566 SLOPE

51 cases used 18 cases contain missing values

Predictor	Coef	Stdev	t-ratio
Constant	1.4711	0.3679	4.00
SLOPE	0.05661	0.01798	3.15

s = 1.327 R-sq = 16.8% R-sq(adj) = 15.1%

Analysis of Variance

SOURCE	DF	SS	MS
Regression	1	17.444	17.444
Error	49	86.270	1.761
Total	50	103.714	

Unusual Observations

Obs.	SLOPE	LOG AT V	Fit	Stdev.Fit	Residual	St.Resid
2	18.0	5.154	2.490	0.186	2.664	2.03R
19	10.0	-0.761	2.037	0.231	-2.799	-2.14R
49	10.0	-0.842	2.037	0.231	-2.879	-2.20R

R denotes an obs. with a large st. resid.

RESIDUALS AGAINST SLOPE

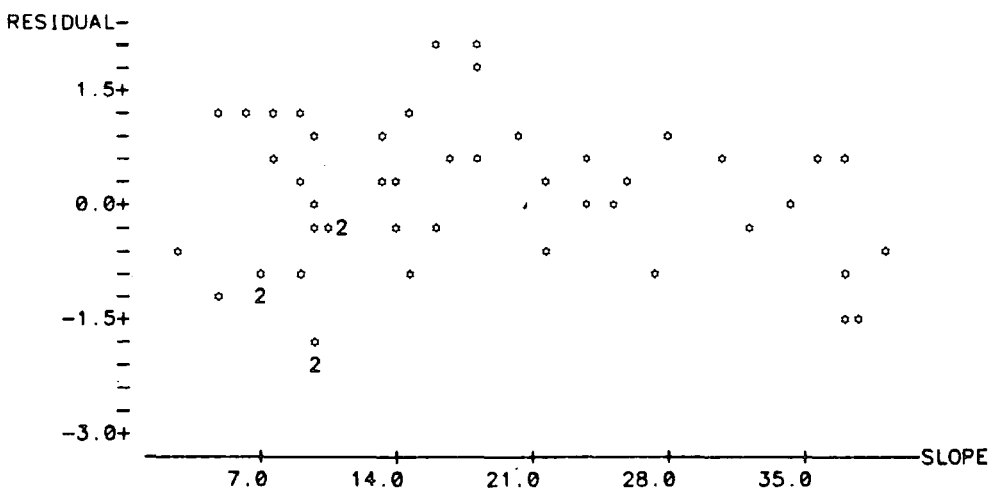

No = 18

does, however, correct for increasing variance with x in the residual plots, figure 7.29.

7.3.5 Summary of regression results

(i) The presence of outliers in both explanatory and response variables seriously affects the goodness of fit of a linear equation to the data using a least squares method.

(ii) Re-expressing the data to improve normality of frequency distributions does not significantly improve the model. The removal of obvious wild observations has a greater effect.

(iii) The underlying design configuration used to collect the data does not lend itself to regression analysis. In particular the different vegetation classes have a large influence.

(iv) Least squares fitting gives a poor relationship between S.M.M. and slope using all the data points, which corresponds with the results of Anderson and Cox (1984) and Rashidian (1984), see table 7.21.

Table 7.21

Correlation coefficient		
Author	AT (lin)	AT (vol)
Anderson and Cox (1984)	-0.44	-0.35
Rashidian (1984)	0.09	-
This study	0.50	0.44

7.4 Temporal patterns of movement

A knowledge of the behaviour of S.M.M. through time is essential for the process to be fully understood. A time series will represent the dynamic aspects of the process which must be understood in order to construct physical models and in order to extrapolate movement rates over longer time periods than the series itself. Temporal measurements also indicate the reliability of quantitative annual rates because it would make little sense to quote an annual rate if movement were in fact episodic without seasonal forcing. S.M.M. is often cited as a *continuous* process (Terzaghi 1960) and one which is *imperceptible*, except by measurements over long time periods (Sharpe 1938). More recently, geomorphologists have attempted to quantify how sediment is generated, transferred and modified during passage through a drainage basin and this requires knowledge of the relative ability of S.M.M. to transport sediment and its likely short and long term persistence (Dietrich *et al.* 1982). In the first instance it is important to establish the temporal patterns of S.M.M. with close sampling intervals in order to assess seasonal influences and short term persistence. Longer term persistence is important; Swanson and Fredrickson (1982) note that changes in vegetation cover, perhaps related to disturbance and recovery, have an important influence on slope processes in the long term. This is discussed further, in relation to a buried soil horizon, in Chapter 8, however, the question of selecting an appropriate timescale for measuring S.M.M. processes cannot be readily answered in the absence of long term data sets.

This section focuses on monthly measurements of Inclinometer Peg data for each sample plot. Inclinometer pegs are particularly sensitive to minor fluctuations and so are ideally suited to the analysis of seasonal

patterns. Anderson and Cox (1986) suggest that peg movement is related to a function of daily precipitation and Kirkby (1967) demonstrates that movement occurs through cycles of wetting and drying. Correlation and regression analyses show that S.M.M. cannot be readily predicted from soil variables which are measured from standard laboratory techniques. This may in part be due to the dynamic nature of variables which are important in controlling S.M.M. Therefore, shear strength has been measured for each plot at bi-monthly intervals in order to detect significant changes in soil strength which result from seasonal differences in effective stress conditions.

Anderson's tubes were also measured monthly at each plot; however, this instrument is less sensitive than the Inclinometer peg to small scale movement and so its time series show a pattern of smooth change which may be a function of the instrument rather than the underlying dynamics of the process. Figure 7.30 summarizes a typical movement pattern for Anderson's tubes. The advantages of Anderson's tubes are essentially their lack of sensitivity to minor change, and hence their robustness. Only 3 tubes were disturbed (by humans) during this research compared with 28 Inclinometer pegs and 35 Young's pits.

The series consists of between 13 and 18 consecutive monthly measurements for each peg. This corresponds to a time interval of 604 days; approximately 18 months from 10-11 August 1982 until 21-22 April 1984. Two full days were required, each month, to collect the data from each site. Monthly intervals were selected in order to minimise the possibility of disturbing the peg during the measurement process and to maximise the amount of seasonal variation that might be observed. Shear strength measurements were taken bi-monthly using the Geo-nor inspection vane so that ground disturbance could be minimised. A non-replacement random sampling scheme was used to locate shear strength measurement

Figure 7.30 A typical time series pattern for Anderson's Tube data. (line fitted using least squares method).

SITE 1/2

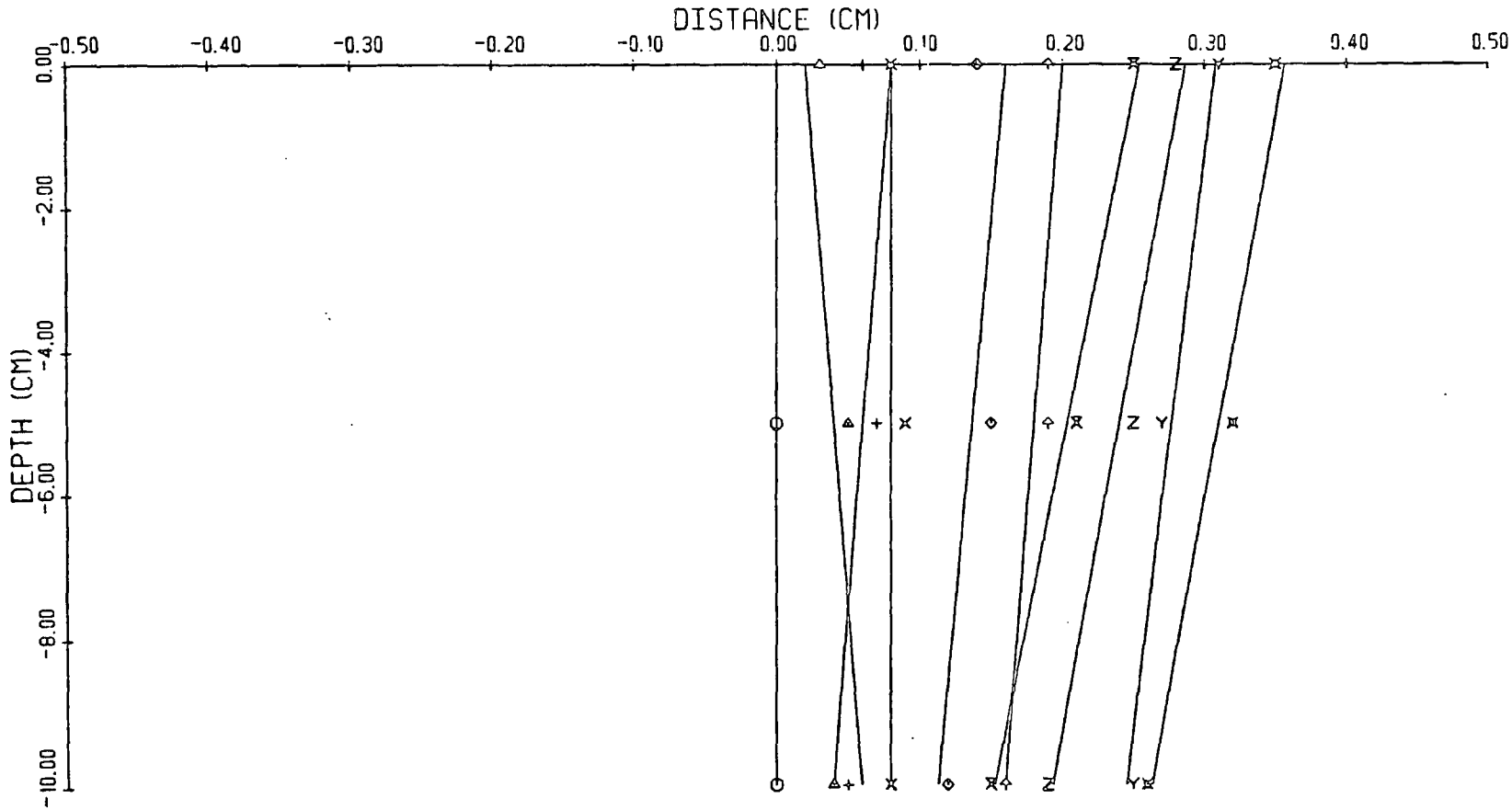

locations around the outer edge of the 1 m^2 plot area.

Changes in ground water table levels were recorded monthly, and monthly precipitation data acquired from a rain gauge in the neighbouring Waskerly catchment area, 1.5 km away.

Conventional statistical analysis of time series usually will involve quantitative assessment of trend, or systematic fluctuation in the response variable. This might be expressed as:-

data = trend + random variation

and would normally involve fitting a function such as a polynomial through the data. Statistical tests for trends in time series data are often based on the assumptions that the probability distribution function of the data is known, that the temporal spacing of the data is regular, that the length of the series is greater than about 30 observations and that any error component is randomly distributed. These assumptions are rather restrictive, because in this case little is known about the underlying nature of the process which generated the data. Therefore, an exploratory approach is adopted using methods of analysis which are distribution-free, where possible. Attention is focused on comparing trends from instruments within plots using cross-correlations, then examining the patterns exhibited by each vegetation class. Finally, the data are smoothed and residual variation is examined after the long term trend is removed.

7.4.1 Tests for randomness

The simplest time series analysis checks that the data do not result from random fluctuation. This does not imply that a non-random series exhibits either periodicity or an interesting trend, but it is an important first step in ruling out the possibility of a series being generated

completely by chance.

Two techniques are used (i) analysis of turning points (peaks and troughs in the series), used to test against systematic oscillation, and (ii) a difference sign test, used to test against linear trend.

In a random series the probability of finding a turning point in any given three values is 2/3; the middle value is either higher or lower than its adjacent values, because of the six possible orders only four are turning points. Therefore, the expected number of turning points in a random series is given by the probability -

$$E(p) = \sum_{i=1}^{n-2} E(x_i) = 2/3(n-2)$$

where, p = probability of each element x in the series n.

$$p = \sum_{i=1}^{n-2} x_i$$

and variance of p is given by-

$$E(p^2) - (E(p))^2 = \frac{16n - 29}{90}$$

Equation 7 (6)

Table 7.22 lists the results of counting the turning points in the Inclinometer peg data. These show that, at some sites, the null hypothesis of a randomly generated series cannot be confidently rejected. Turning point analysis is useful for testing against an oscillatory series but it performs poorly if used as a test against linear trend. This is because a series may exhibit an apparent random fluctuation about a mild linear trend and so would show the same set of turning points as if the trend were absent. Therefore, the difference sign test is used to test against linear trend. This method involves counting the number of positive first differences in a series where it increases. For a random series, the number of points of increase, c, equals-

$$E(c) = E\left(\sum_{i=1}^{n-1} x_i\right) = 1/2(n-1)$$

Table 7.22

COUNT DATA FOR TURNING POINTS IN INCLINOMETER PEG TIME SERIES SHOWING OBSERVED AND EXPECTED COUNTS

	J	P	P	C	P	J	J	N	N
0-15	8	6	11	9	8	7	8	7	8
0-10	4	9	9	10	9	5	8	10	10
0-5	10	3	10	8	6	6	7	8	9
E	10	10	10	10.67	10.67	10.67	10.67	10	10.67

	P	J	C	P	P	N	J	P	C
0-15	4	5	8	11	6	6	6	6	5
0-10	8	6	4	5	8	6	7	9	7
0-5	7	7	9	8	4	4	7	7	4
E	10.67	10.67	10.67	10.67	10.67	10	10.67	10.67	10.67

	C	J	J	N	P	P	C	J	J
0-15	9	10	7	6	9	3	4	6	8
0-10	4	4	7	4	1	7	0	7	9
0-5	8	5	8	5	9	7	2	9	10
E	10.67	10.67	9.33	10	10.67	10.67	5.33	10.67	10.67

	J	J	N	N	N	J	P	C	J
0-15	10	7	6	10	7	11	5	8	6
0-10	6	4	4	6	8	8	9	10	11
0-5	5	3	5	7	7	5	4	6	8
E	8.67	10	6.67	10.67	10.67	10.67	10.67	10.67	10.67

/...cont

	J	P	P	P	P	P	P	N	N
0-15	8	4	8	9	4	13	10	8	11
0-10	7	11	7	10	6	8	8	4	8
0-5	7	7	7	10	7	5	7	5	8
E	10.67	10.67	10.67	10.67	10.67	10.67	10.67	8	10.67

	C	C	N	N	J	N	P	C	J
0-15	11	8	6	9	5	7	11	9	6
0-10	10	8	5	8	-	8	6	7	8
0-5	10	10	3	10	10	6	10	9	6
E	10.67	10.67	8.67	10.67	10	10	10	10.67	10

	J	J	J	J	J	N	N	N	N
0-15	10	7	3	7	6	7	5	11	8
0-10	5	6	2	6	6	8	7	11	9
0-5	8	7	3	3	10	9	6	9	9
E	10	10	5.33	10	10	10	10	10.67	10.67

	N	N	N	N	N	N
0-15	11	10	9	11	7	7
0-10	7	8	7	9	8	7
0-5	7	5	7	6	8	11
E	10.67	10	10	10	10	10

Table 7.23

COUNTS OF FIRST DIFFERENCES IN 15 cm INCLINOMETER PEG TIME SERIES

O	4	4	6	5	5	4	5	4	4	3
E	8	8	8	8.5	8.5	8.5	8.5	8	8.5	8.5
$\frac{(O-E)^2}{E}$	2	2	0.5	1.44	1.44	2.38	1.44	2	2.38	3.56
O	3	5	5	3	4	4	4	3	5	5
E	8.5	8.5	8.5	8.5	8	8.5	8.5	8.5	8.5	8.5
$\frac{(O-E)^2}{E}$	3.58	1.44	1.44	3.56	2	2.38	2.38	3.56	1.44	1.44
O	4	3	5	2	2	3	4	5	4	3
E	7.5	8	8.5	8.5	4.5	8.5	8.5	7	8	5.5
$\frac{(O-E)^2}{E}$	1.63	3.12	1.44	4.97	1.39	3.56	2.38	0.57	2	1.14
O	5	4	6	3	5	4	4	3	4	5
E	8.5	8.5	8.5	8.5	8.5	8.5	8.5	8.5	8.5	8.5
$\frac{(O-E)^2}{E}$	1.44	2.38	0.74	3.56	1.44	2.38	2.38	3.56	2.38	1.44
O	2	7	5	5	5	6	5	4	5	4
E	8.5	8.5	8.5	6.5	8.5	8.5	8.5	7	8.5	8
$\frac{(O-E)^2}{E}$	4.97	0.26	1.44	0.35	1.44	0.74	1.44	1.29	1.44	2
O	4	6	5	3	6	4	2	4	3	4
E	8	8	8.5	8	8	8	4.5	8	8	8
$\frac{(O-E)^2}{E}$	2	0.5	1.44	3.12	0.5	2	1.39	2	3.12	2
O	3	6	4	6	5	5	5	4	4	
E	8	8.5	8.5	8.5	8	8	8	8	8	
$\frac{(O-E)^2}{E}$	3.12	0.74	2.38	0.74	1.12	1.12	1.12	2	2	

Figure 7.31 Time series plot for Calluna vegetation (site 2/7)

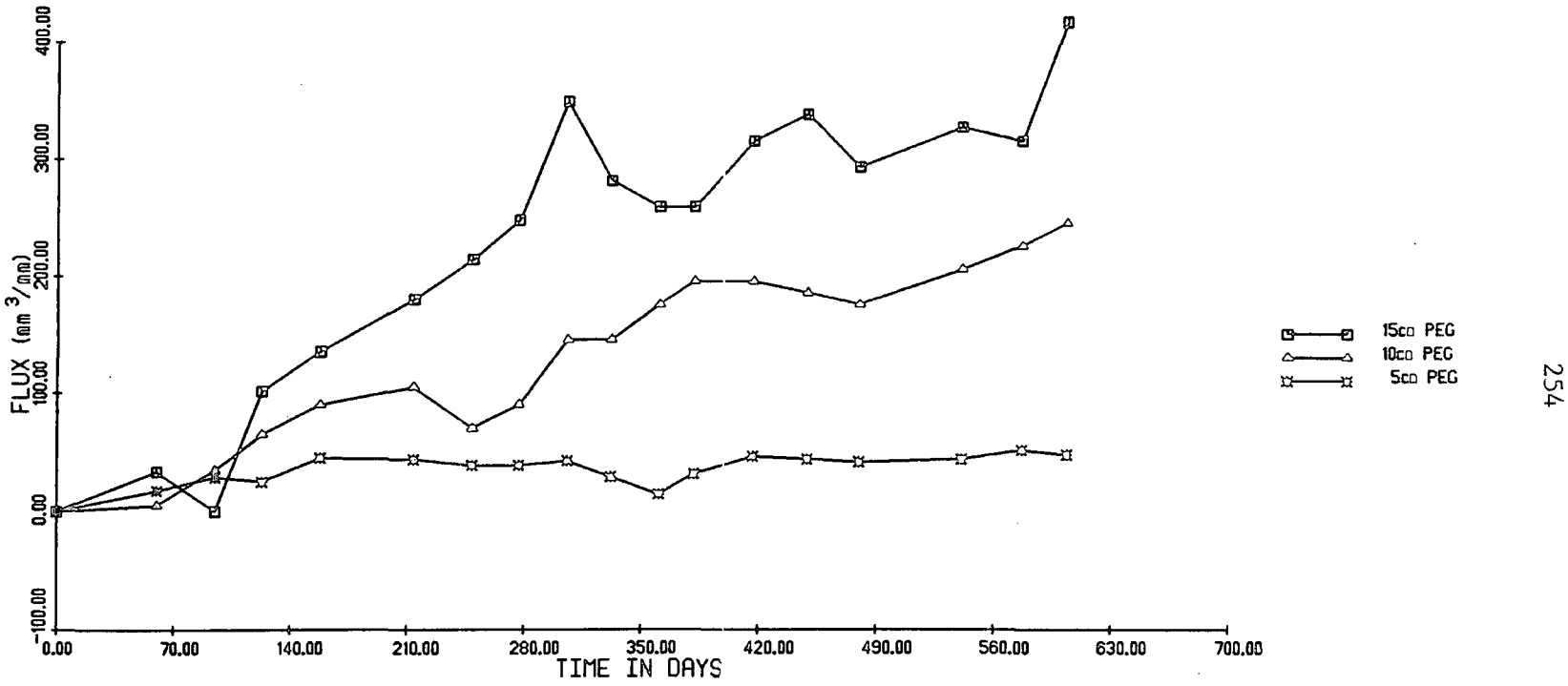

Figure 7.32 Time series plot for Nardus vegetation.

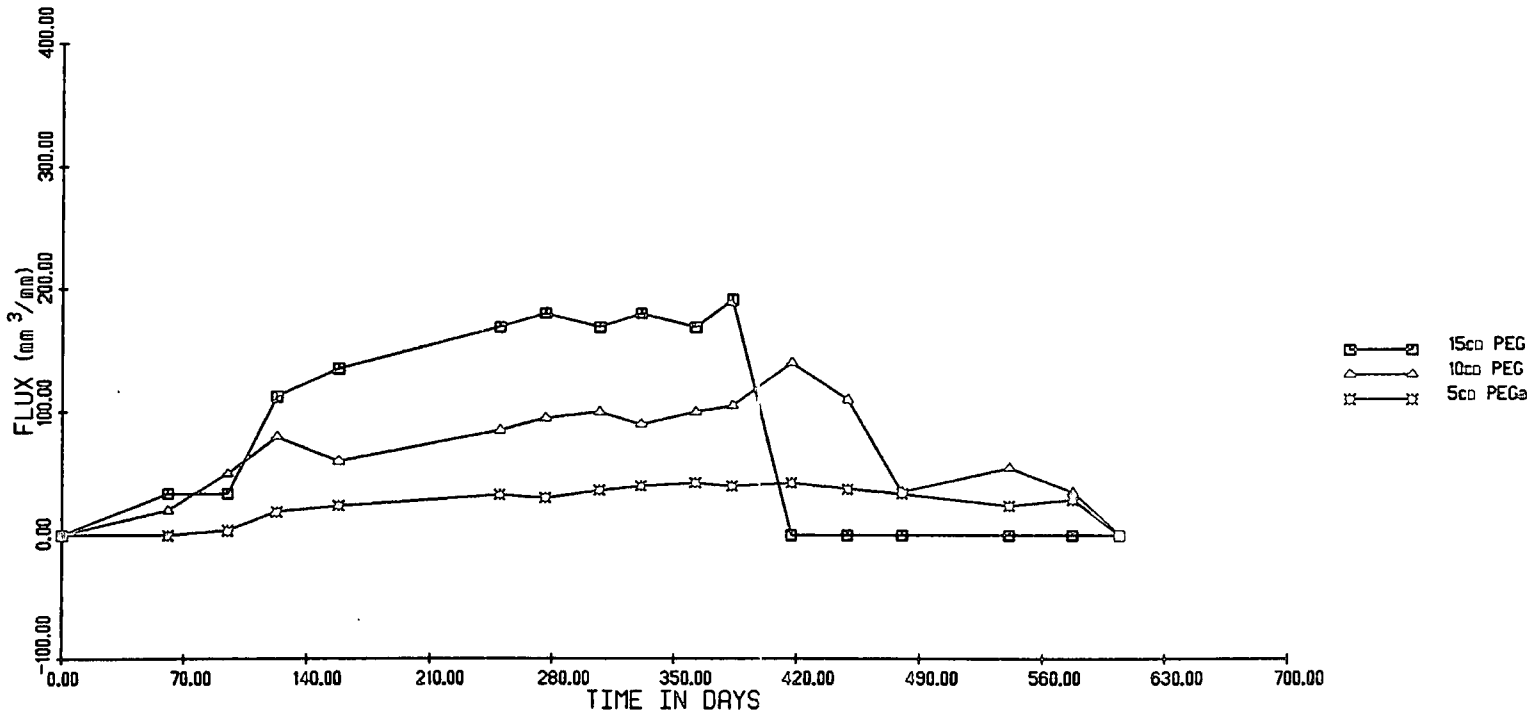

Figure 7.33 Time series plot for Pteridium vegetation.

SITE 7/2

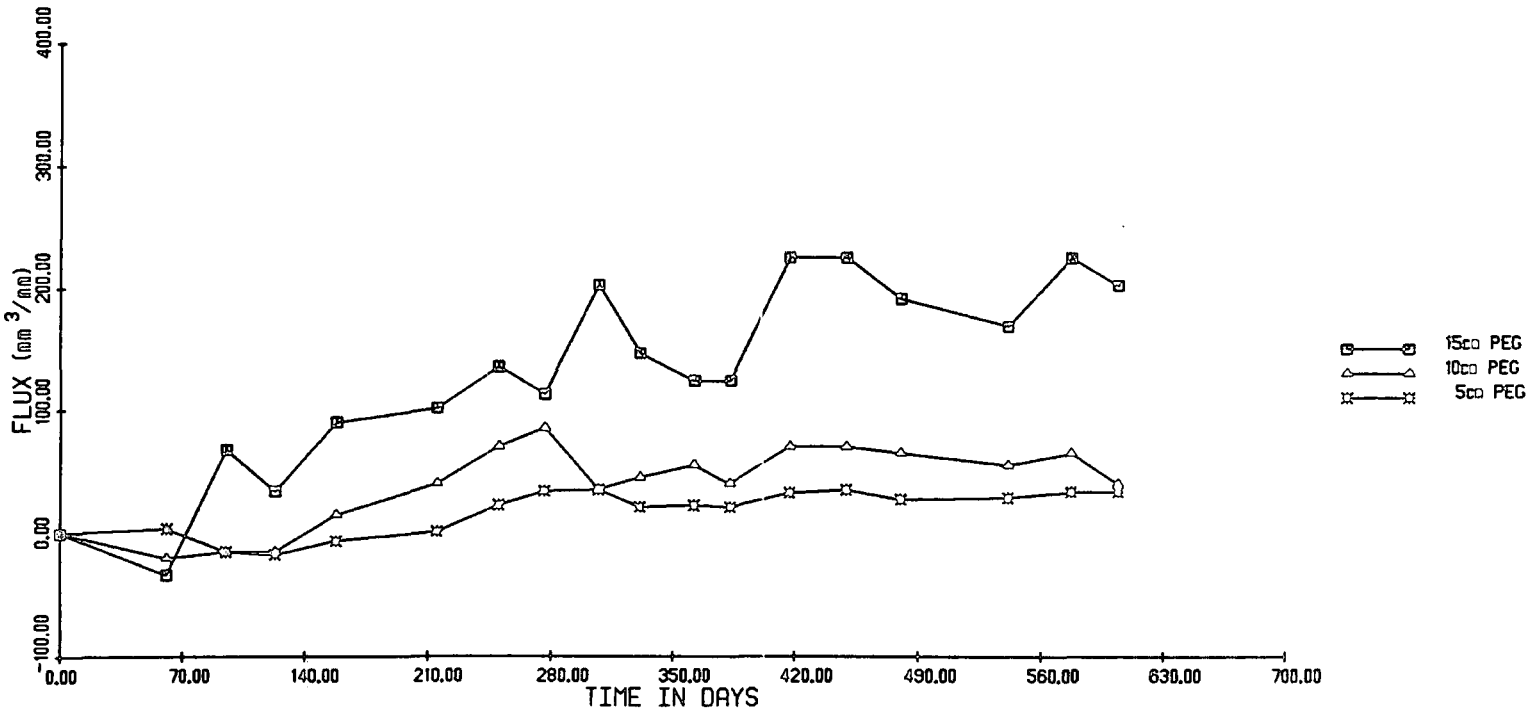

Figure 7.34 Time series plot for Juncus vegetation.

SITE 5/2

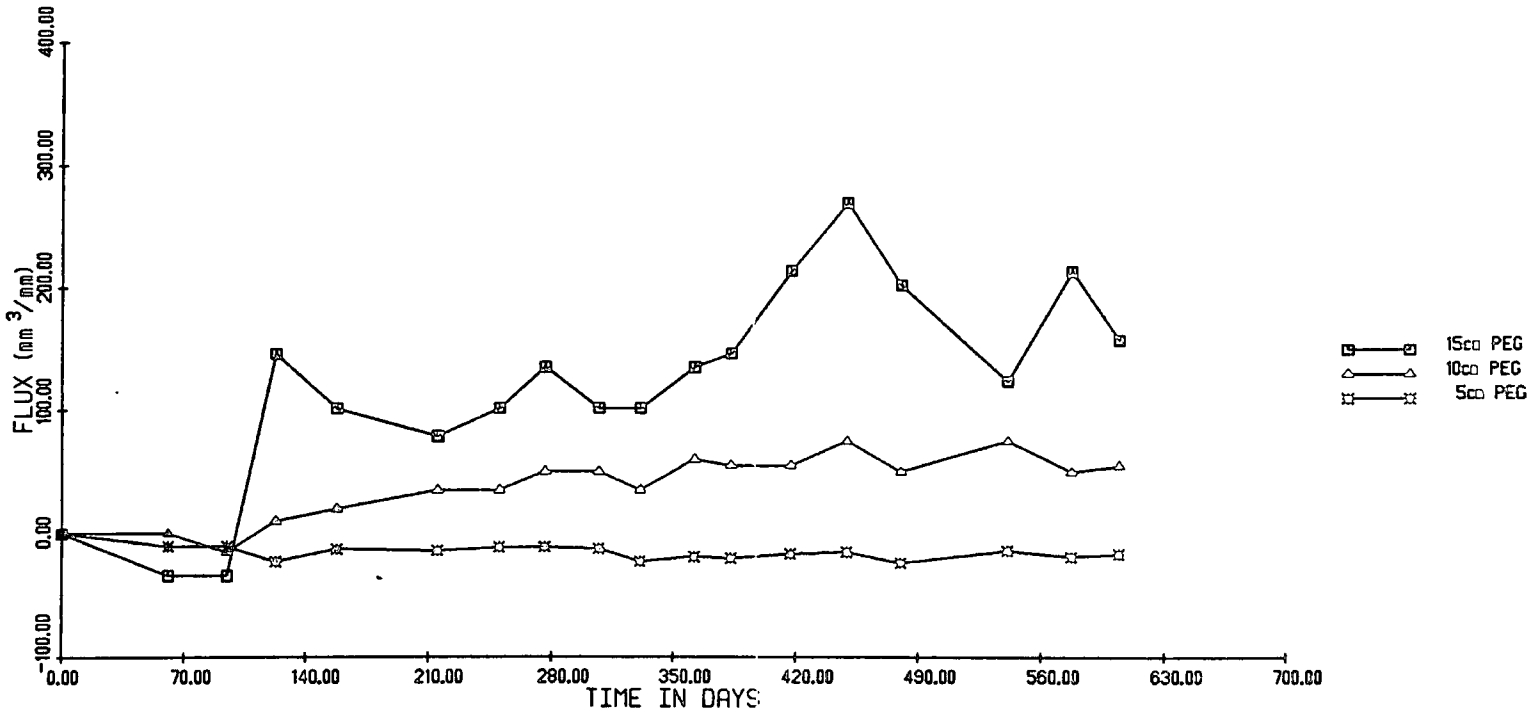

variance (c) is given by-

$$c = 1/12(n + 1)$$

Equation 7 (7)

Table 7.23 shows results of the difference sign test applied to 15 cm Inclinometer peg series. In this case none of the observed counts in the series match any of the counts expected from a random series. The rather poor performance of the turning point analysis for some of the sites indicates that oscillations in the series over short time intervals are typical. Anderson and Cox (1986) also present details of series containing large oscillations over short time intervals.

Graphs of all the Inclinometer peg series are presented in appendix C; however, figures 7.31 - 7.34 show typical series for sites of the four vegetation classes. Each of these series contain fluctuations which are large compared with the overall trend in the data. Cross-correlation analysis is used to check that the fluctuations in the three pegs at each site correspond temporally.

7.4.2 Correlations between instruments

Cross-correlation analysis between pairs of time series for different instruments gives a good indication of the confidence that can be placed in the shape of the series for each plot. A weak correlation would indicate that trends or fluctuations from neighbouring instruments do not correspond and may be due to random error. Conversely, a strong correlation lends support to the belief that fluctuations are a real and important part of the pattern.

Table 7.24 lists cross-correlations derived from fitting a correlation coefficient to pairs of instruments in turn. The calculations

		COEFFICIENT OF DETERMINATION			CROSS CORRELATION COEFFICIENT		
		15 cm	10 cm	5 cm	15/10	15/5	10/5
1/1	J	.569	.881	.899	.662	.783	.944
1/2	Pt	.900	.660	.885	.859	.911	.836
1/3	Pt	.816	.892	.420	.89	.49	.77
1/4	C	.676	.610	.558	.94	.79	.80
1/5	Pt	.663	.756	.902	.95	.91	.95
2/1	J	.351	.317	.081	.97	.80	.80
2/2	J	.417	.826	.521	.66	.30	.81
2/3	N	.794	.805	.835	.86	.94	.86
2/4	N	.479	.034	.082	.23	.08	-.10
2/5	Pt	.804	.617	.023	.78	.33	.23
2/6	J	.394	.933	.796	.62	.71	.87
2/7	C	.840	.920	.660	.92	.67	.62
3/1	Pt	.694	.574	.766	.859	.733	.594
3/2	Pt	.658	.134	.677	.682	.771	.636
3/3	N	.370	.067	.001	.608	.470	.749
3/4	J	.232	.438	.545	.714	.710	.811
3/5	Pt	.736	.446	.735	.710	.832	.719
3/6	C	.387	.504	.442	.754	.711	.912
3/7	C	.748	.637	.008	.885	.153	.206
4/1	J	.874	-	-	-	-	-
4/2	J	.085	.097	.432	-.237	.321	.653
4/3	N	.576	.127	.057	.605	.559	.279
4/4	Pt	.555	-	.823	-	.855	-
4/5	Pt	.803	.791	.688	.918	.874	.835
4/6	C	-	.762	.619	-	-	.739
5/1	J	.648	.873	.535	.921	.718	.715
5/2	J	.597	.739	.312	.802	-.618	-.591
5/3	J	.550	.742	.898	.637	.791	.926
5/4	J	.855	.837	.923	.822	.949	.882
5/5	N	-	.597	.003	-	-	.268
5/6	N	.075	.637	.492	.560	.513	.634
5/7	N	.336	.825	.765	.648	.638	.848
5/8	J	.478	.363	.601	-.077	.767	-.186
5/9	Pt	.720	.604	.830	.846	.764	.756
5/10	C	.776	.793	.666	.816	.746	.592

Table 7.24

Coefficient of determination values for a linear model fitted to IP time series and cross-correlation coefficients for 15 cm, 10 cm and 5 cm pegs.

Table 7.24 Coefficient of determination values for a linear model fitted to IP time series and cross-correlation coefficients for 15 cm, 10 cm and 5 cm pegs.

		COEFFICIENT OF DETERMINATION			CROSS CORRELATION COEFFICIENT		
		15 cm	10 cm	5 cm	15/10	15/5	10/5
6/1	J	.478	.276	.914	.570	.669	.602
6/2	J	.718	.931	.102	.818	-.181	.322
6/3	Pt	.952	.014	.763	-.158	.869	-.104
6/4	Pt	.708	.456	.902	-.515	.775	-.664
6/5	Pt	.454	.804	.527	.832	.770	.826
6/6	Pt	.710	.550	.001	-	-	-
7/1	Pt	.258	.677	.592	.596	.816	.824
7/2	Pt	.775	.519	.649	-	-	.845
7/3	N	.001	.036	.086	.492	.715	.840
7/4	N	.023	.130	.249	.555	.635	.632
7/5	C	.762	.595	.769	.836	.864	.860
7/6	C	.481	.827	.002	.796	.681	.210
8/1	N	.047	.044	.893	.136	.208	-.065
8/2	N	.002	.097	.359	.246	.514	.605
8/3	J	.266	.001	.522	-.550	.335	.118
8/4	N	.561	.460	.468	.638	.438	.574
8/5	Pt	.656	.303	.536	-.364	.606	-.149
8/6	C	.706	.902	.573	.864	.697	.742
9/1	J	.702	.501	.673	.636	.748	.972
9/2	J	.803	.959	.771	.931	.857	.904
9/3	J	.658	.914	.851	.895	.783	.915
9/4	-	-	-	-	-	-	-
9/5	J	.130	.132	.923	.623	.377	.245
9/6	J	.025	.914	.157	-.260	-.350	-.376
9/7	N	.608	.052	.711	.473	.870	.240
9/8	N	.865	.843	.931	.941	.967	.923
10/1	N	.619	.652	.325	.502	.388	.690
10/2	N	.291	.746	.133	-.521	.105	-.219
10/3	N	.414	.689	.154	.639	.247	-.069
10/4	N	.653	.297	.405	.778	.598	.598
10/5	N	.756	.023	.089	.466	-.273	-.156
10/6	N	.736	.078	.077	.402	-.094	0.686
10/7	N	.611	.571	.901	.893	.831	.811
10/8	N	.666	.026	.144	.544	.593	.875

were performed using the MIDAS statistical package (Fox and Guire 1976). Table 7.25 summarises this data by listing the number of sites where the cross-correlation coefficients do not exceed 0.5 for at least two of the three instruments in the plot. Only six out of sixty nine sites give coefficients less than 0.5. Rather more sites give coefficients less than 0.8 but these sites are dominantly associated with the *Nardus* vegetation class. Sixty five percent of all the *Nardus* sites show poor agreement within plots compared with 37.5% for *Juncus* sites, 28.5% for *Calluna* sites and only 23% for *Pteridium* sites. Correlograms showed improved correlations at a few sites with a lag of 1 or 2, but this is not considered important since neighbouring instruments should respond in sympathy to forcing phenomena at monthly timescales. A more important consideration is the length of the different pegs. In theory, the 15 cm and the 5 cm pegs should show the poorest agreement because they may be responding to influences occurring at different depths. Scrutiny of table 7.26 shows that this does not appear to be the case. This suggests that all lengths of pegs are influenced by the same forces.

The strength of agreement between neighbouring instruments will be lessened because of instrument disturbance at some sites and because of local differences in soil and vegetation properties with each plot. Figure 7.35 shows clear evidence of instrument disturbance which appears as a single anomalous increase. This may be due to human or sheep disturbance of the peg which protrudes above the ground by 5 cm.

It is interesting that when the cross correlation data are segmented by vegetation class, *Nardus* grassland yields the least consistent results. A visual inspection of the trends for some *Nardus* sites confirms that often these series show no regular trend but that there is some evidence of agreement among the instruments in the plot, see figures 7.36 to 7.38. On the other hand, a few *Nardus* sites show both strong correlations

Table 7.25

Count data for sites where the cross correlations of Inclinometer peg time series do not exceed 0.5 and 0.8 within each plot

	r 0.5	r 0.8	n	% 0.5	% 0.8
Juncus	2	6	16	12.5	37.5
Nardus	4	13	20	20.0	65
Pteridium	0	3	13	0	23
Calluna	0	2	7	0	28.5

Table 7.26

Count data for sites with r^2 values of less than 0.5 when a linear trend has been fitted to the series

	0.15	0.10	0.05	Total	n	%
Juncus	10	7	5	22	58	38
Nardus	10	13	16	39	65	60
Pteridium	2	5	3	10	50	20
Calluna	2	0	4	6	25	24
Total	24	25	28	77		
n	65	66	67		198	
%	37	38	42	39		

Figure 7.35 Time series plot for Juncus vegetation.

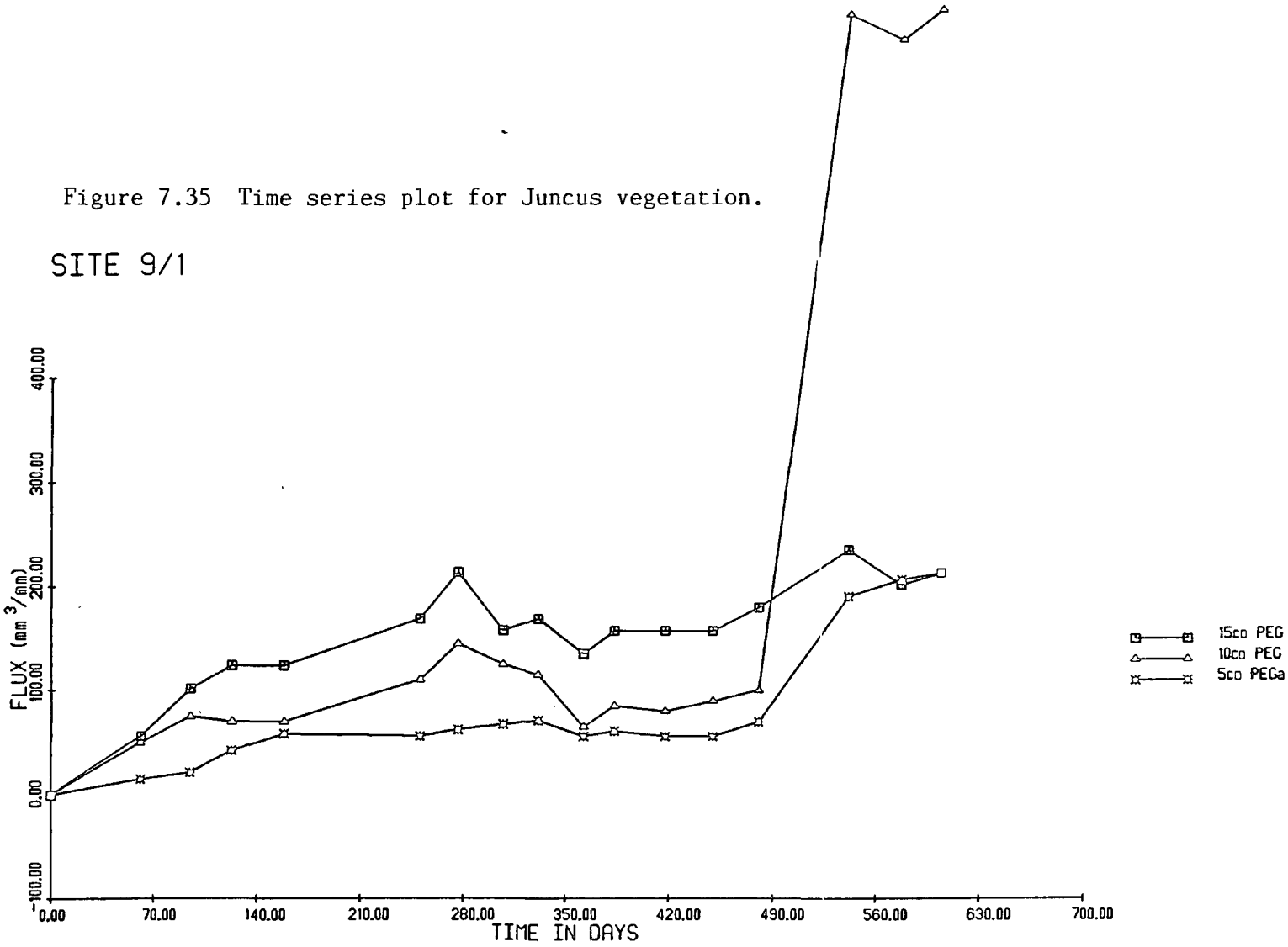

Figure 7.36 Time series plot for Nardus vegetation.

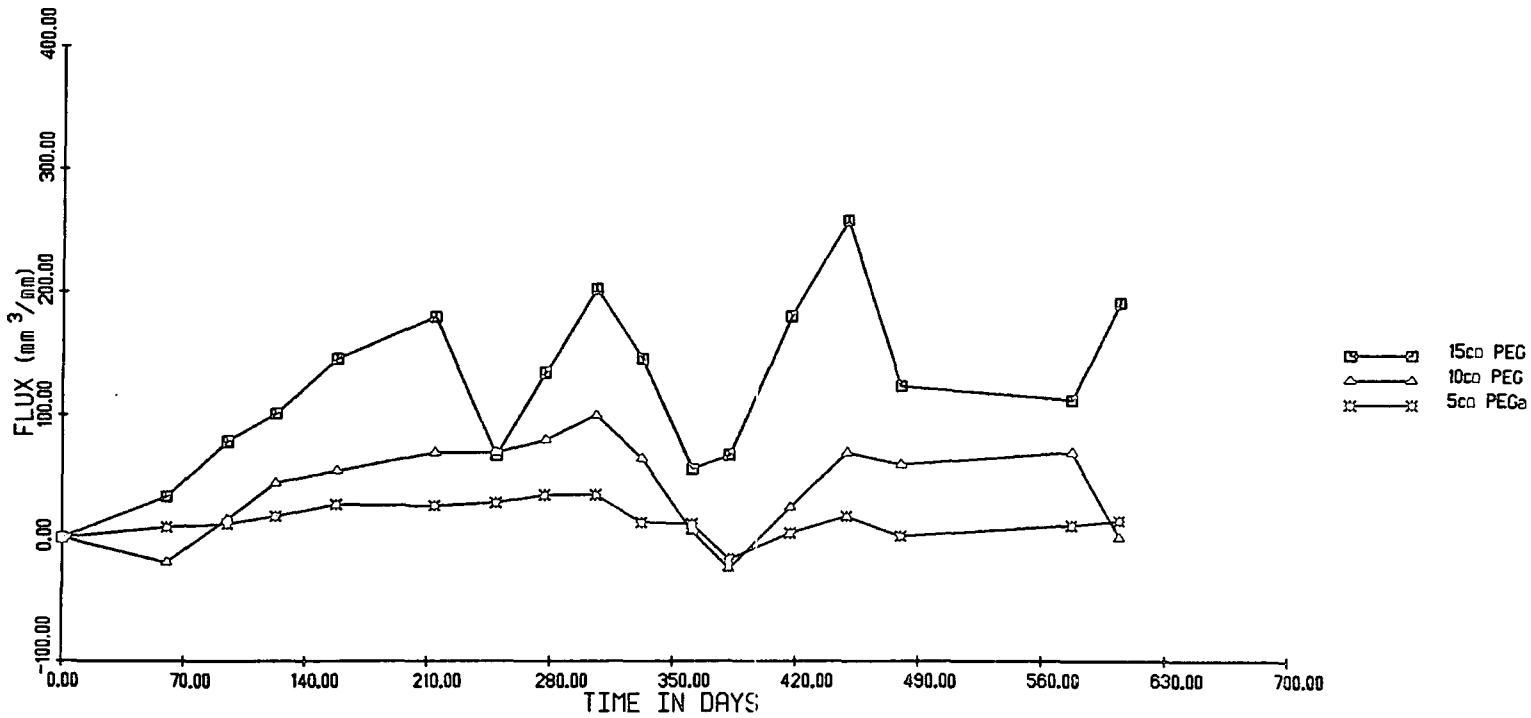

Figure 7.37 Time series plot for Nardus vegetation

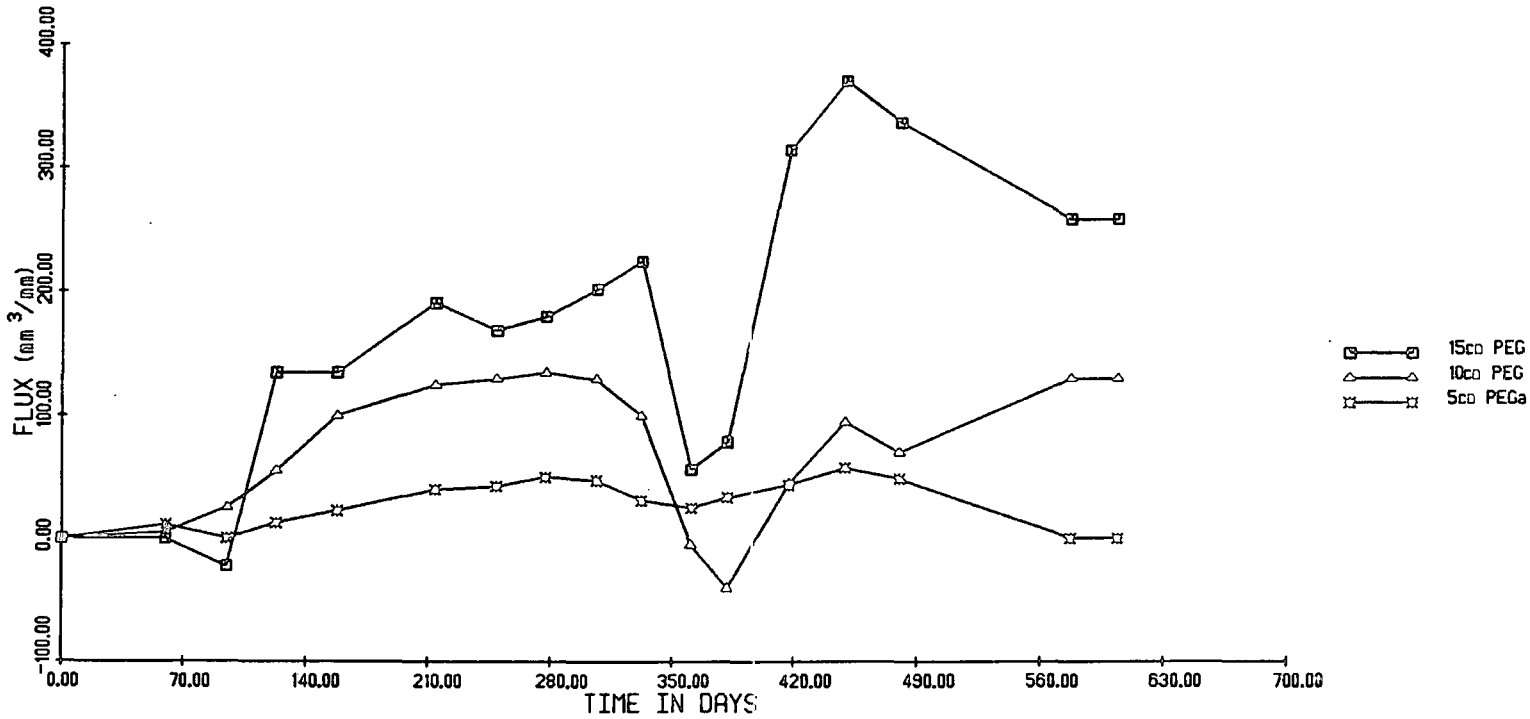

Figure 7.38 Time series plot for Nardus vegetation.

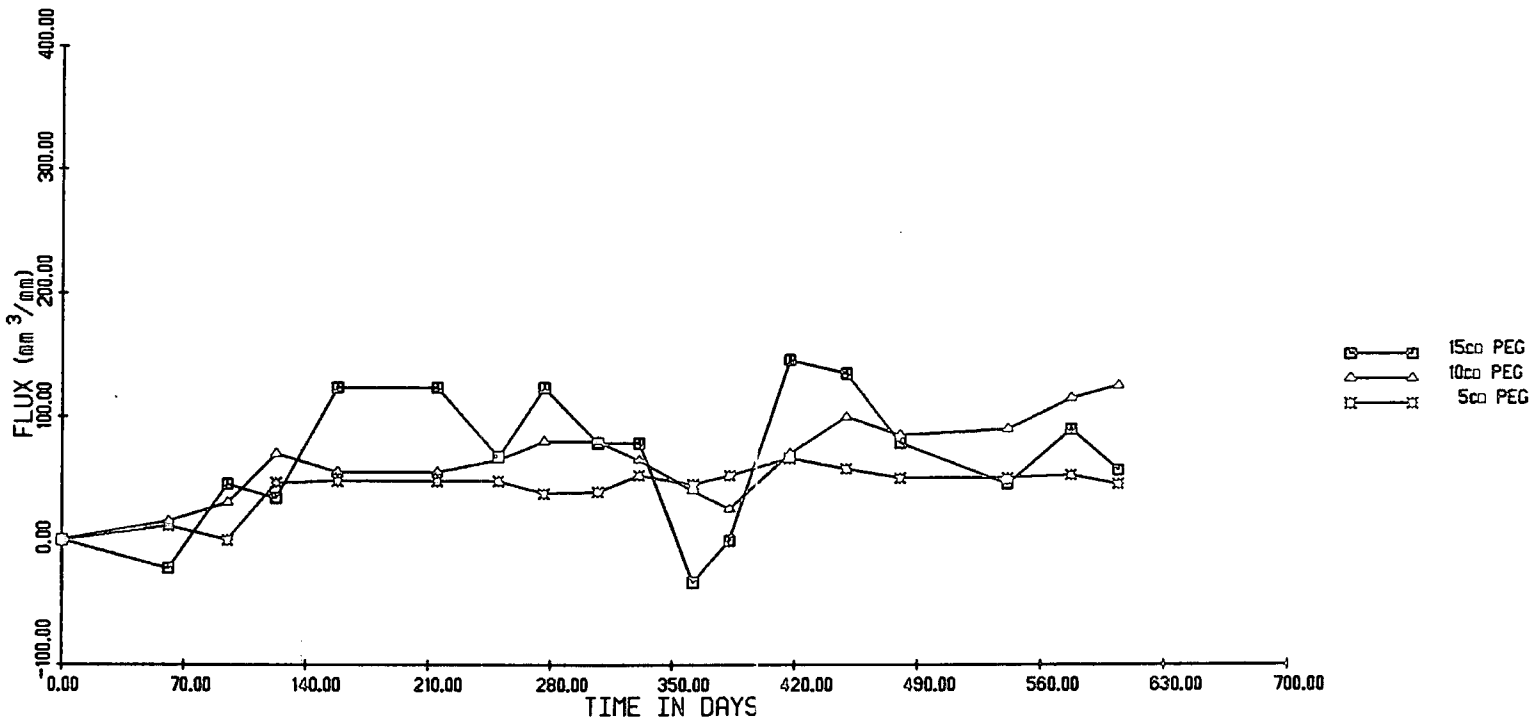

Figure 7.39 Time series plot for Nardus vegetation.

SITE 2/3

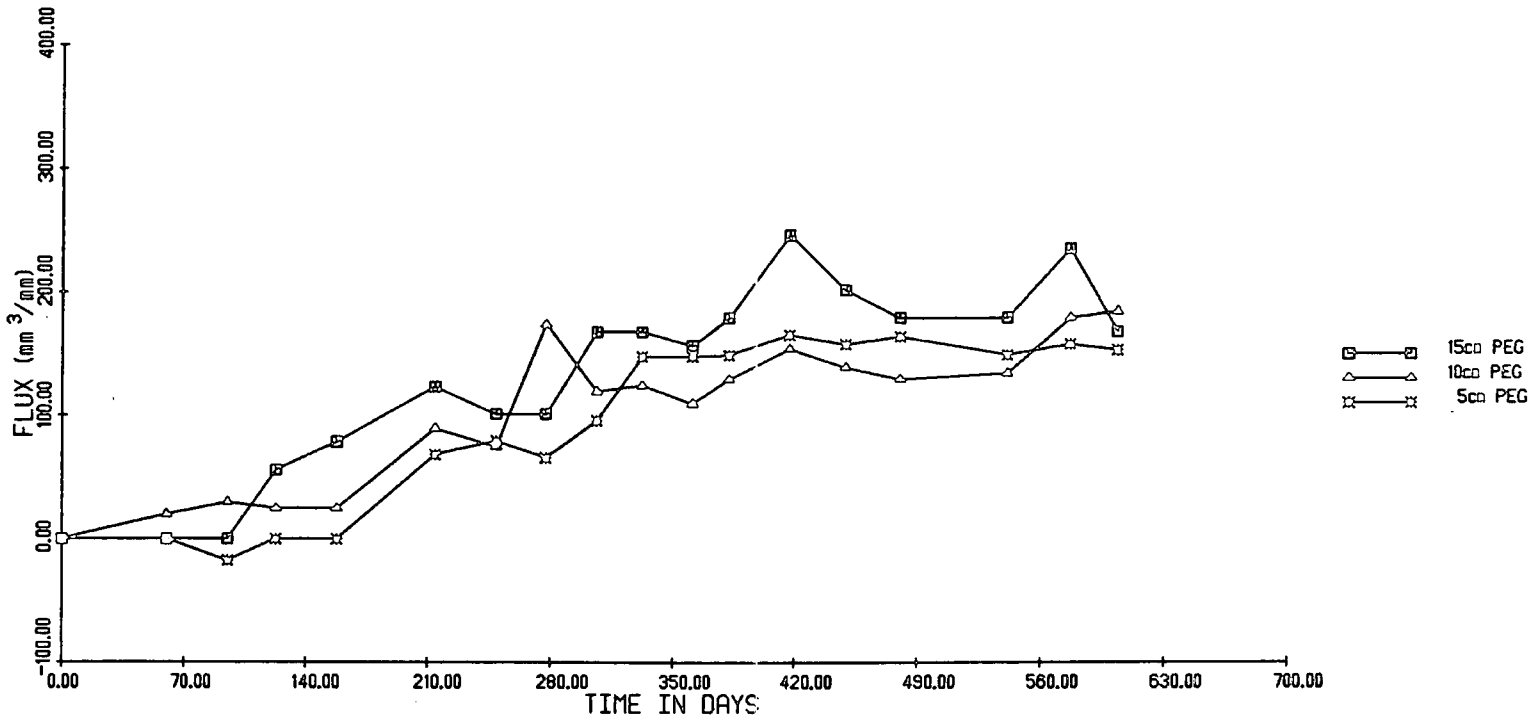

Figure 7.40 Time series plot for Juncus vegetation.

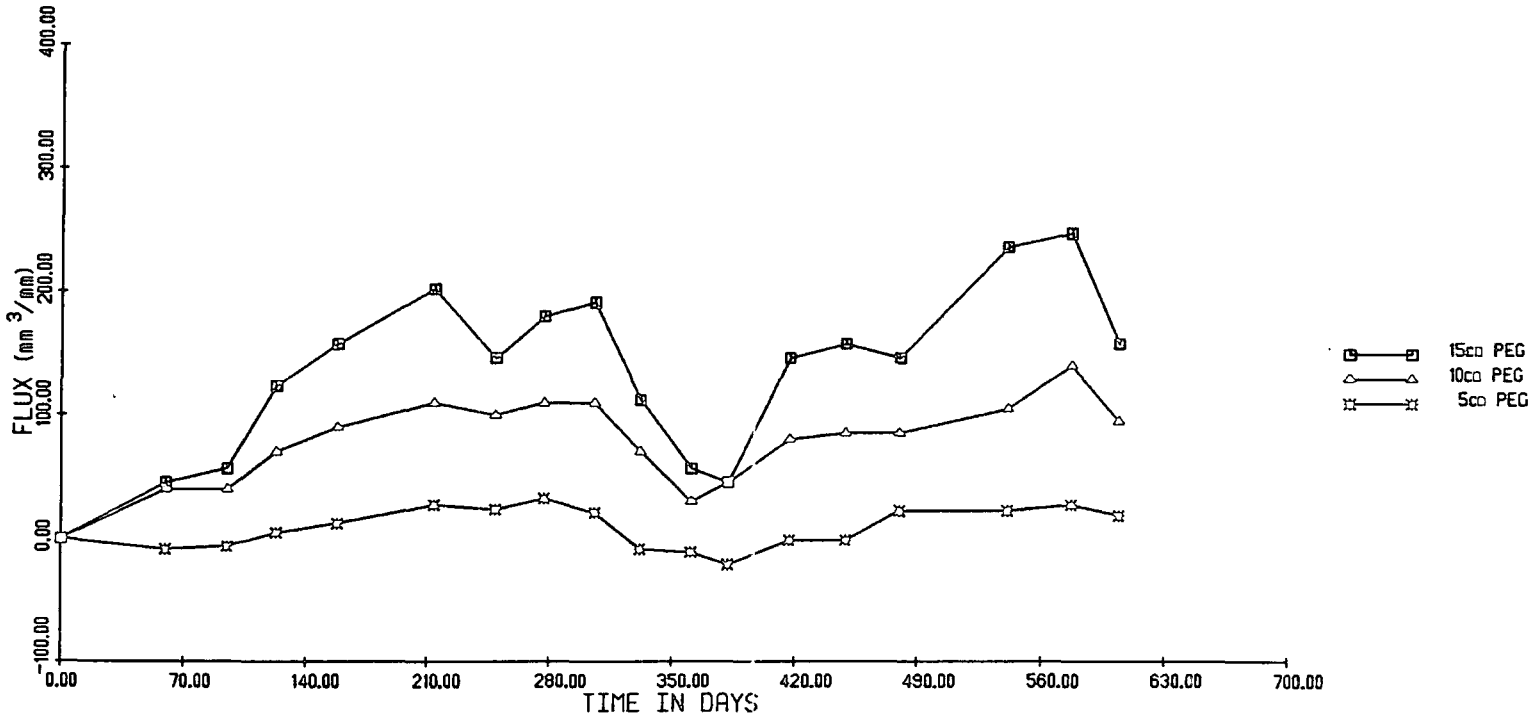

among instruments and exhibit a strong linear trend, for example, site 2/3 (figure 7.39).

A visual inspection of time series plots often reveals the reason for poor agreement between instruments. For example, the plot of site 4/3 shown in figure 7.37 shows a close agreement among the instruments with one or two small deviations which are sufficient to lower the coefficient between the 10 cm and the 5 cm pegs to 0.28. Note that a pronounced seasonal tendency is apparent. Figure 7.40 shows that site 2/1 has a similar annual trend. The majority of sites show no such seasonal influence; rather, a weak linear trend is evident. In order to test this assertion quantitatively, a linear function is fitted to the data using a least-squares method.

7.4.3 Fitting a linear model

A linear model assesses the hypothesis that S.M.M. responds as a function of time, thus:

$$S.M.M. = a \cdot time + b$$

where a and b are empirical coefficients.

The success of the model is given by r^2; the goodness of fit statistic from a least squares fit. Table 7.24 lists the r^2 values derived from a linear fit to all the Inclinometer peg time series. The results range from almost no variance explained by the linear model, to almost all the variance explained. There are also notable differences in the success of the model when applied to different instruments within the same plot, for example, see figures 7.41 to 7.43. At site 2/4 the 5 cm and 10 cm pegs (r^2 values 0.08 + 0.03) show no discernible trend but the 15 cm peg ($r^2 = 0.48$) shows a clear trend of downslope movement with large oscillations about the trend. The same pattern is evident at sites 2/5 and 4/1 where the

Figure 7.41 Time series plot for Nardus vegetation.

SITE 2/4

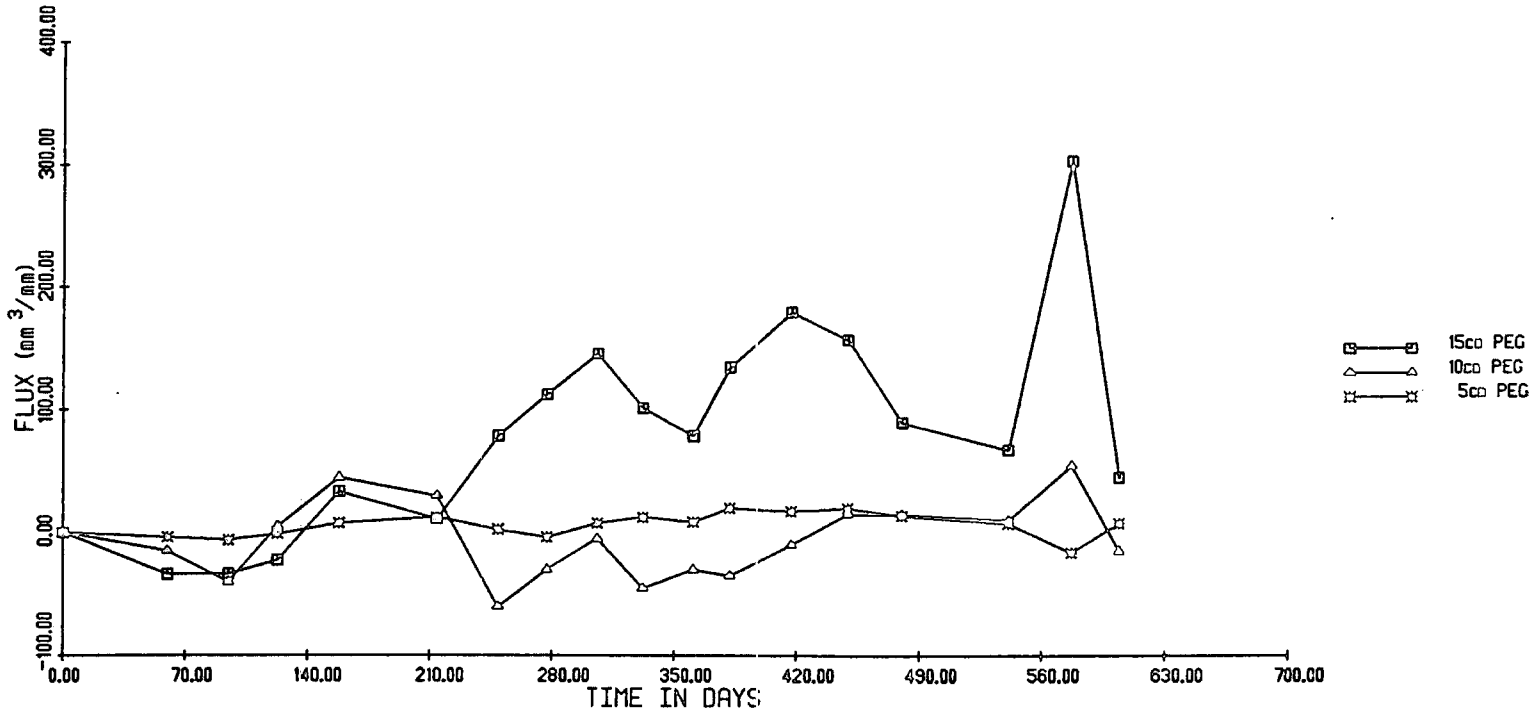

Figure 7.42 Time series plot for Pteridium vegetation.

SITE 2/5

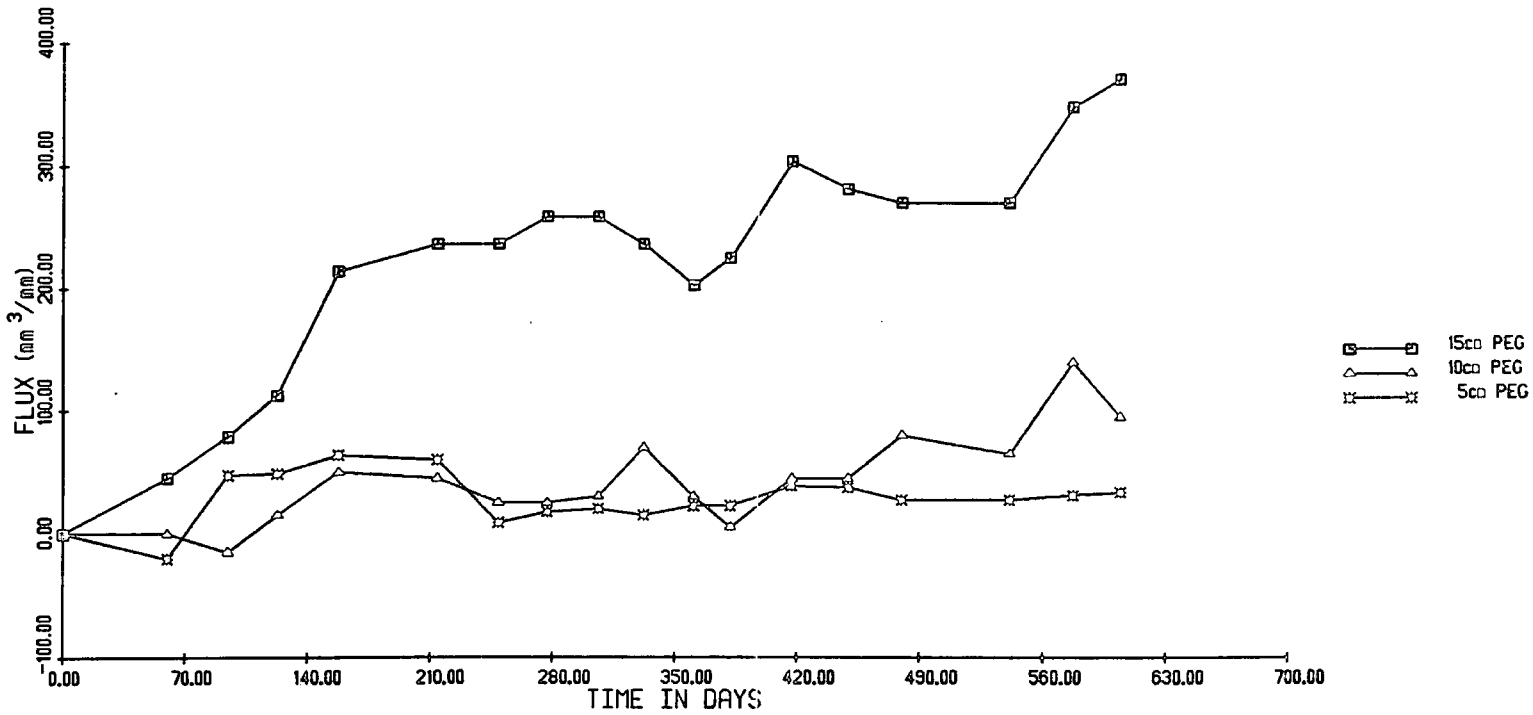

Figure 7.43 Time series plot for Juncus vegetation.

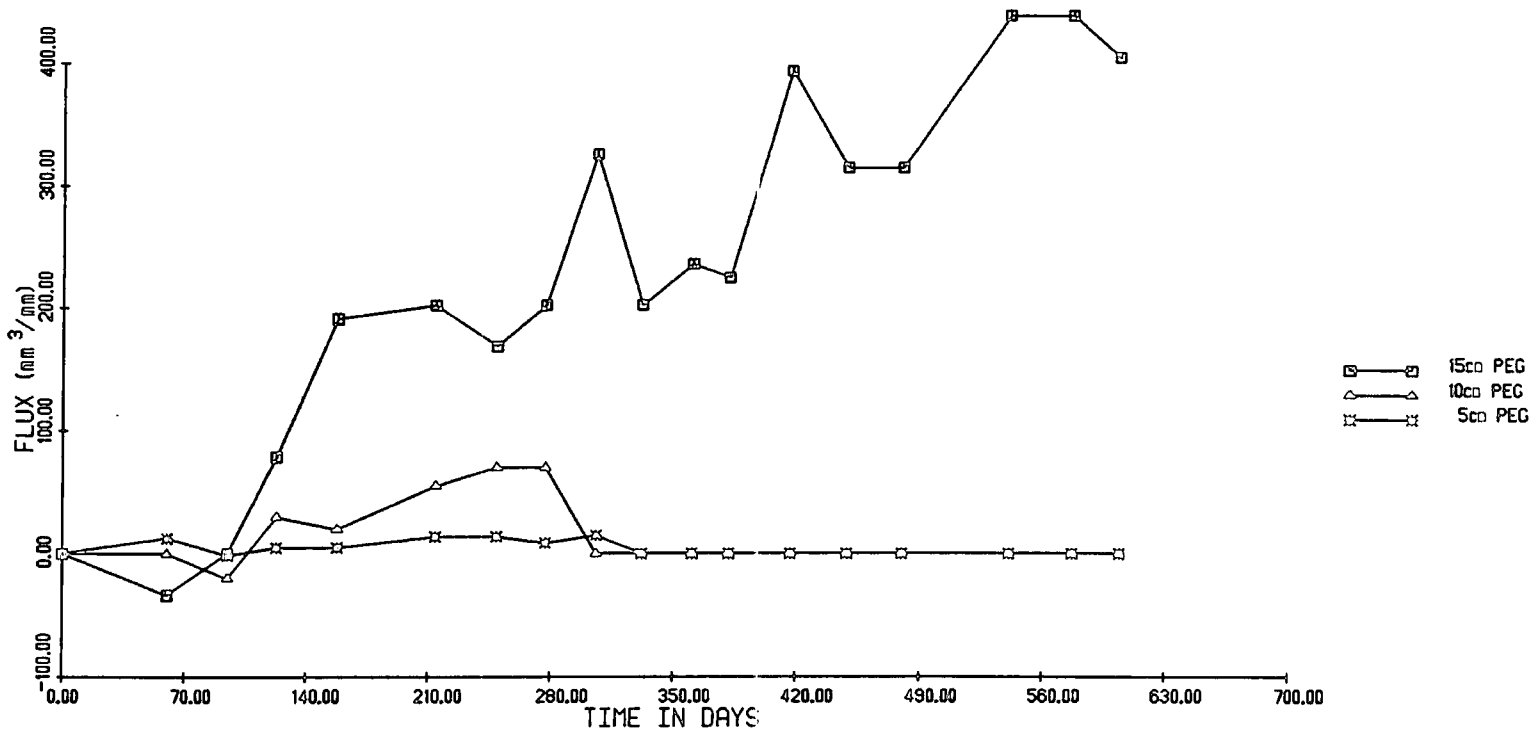

Figure 7.44 Time series plot for Pteridium vegetation.

SITE 3/2

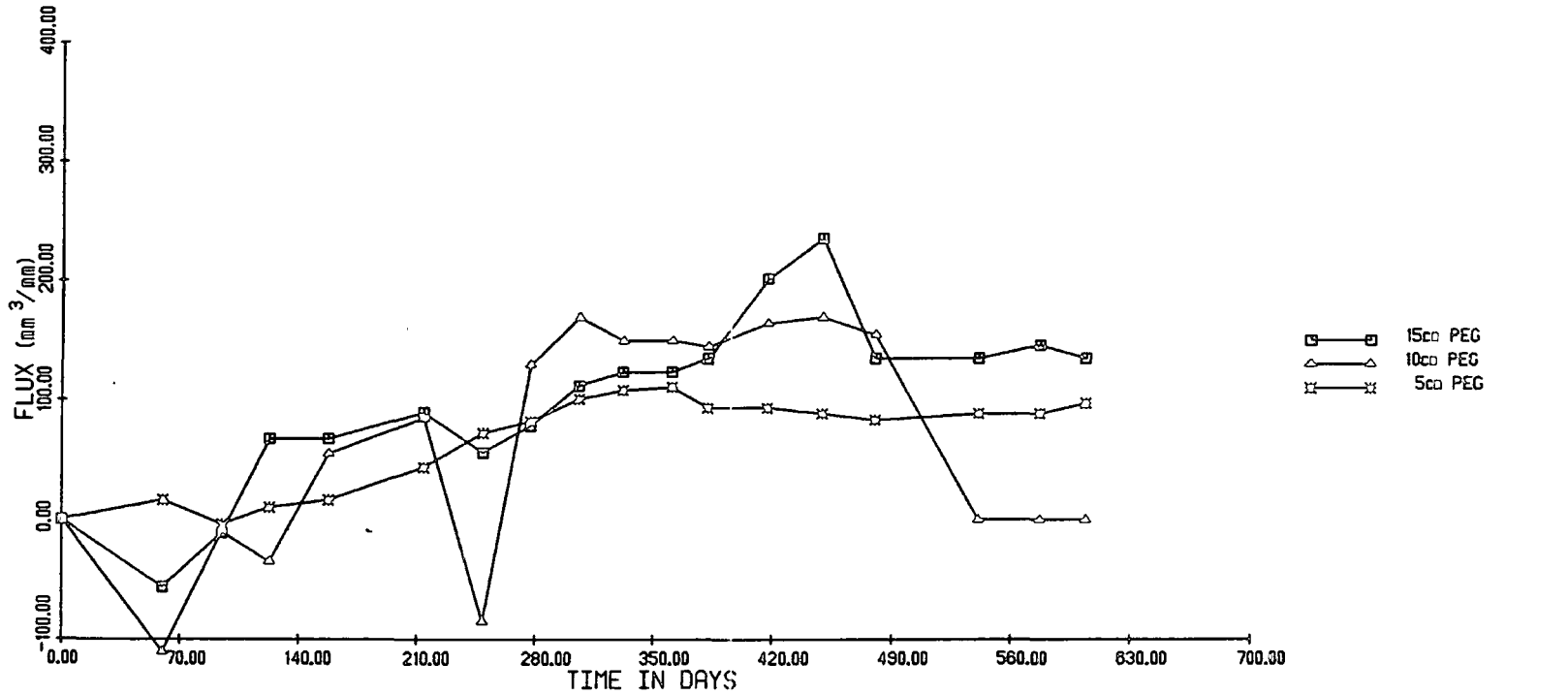

linear trend in the 15 cm peg is strong (r^2 values 0.80 + 0.87). The r^2 statistic can be misleading, however, since the goodness of fit of a least squares linear equation is severely affected by outliers. The pattern at site 3/2, figure 7.44, shows that all three pegs display similar temporal trends but the 10 cm peg contains some large oscillations, which reduce the variance explained by a linear trend to 13.4% compared with 66% and 68% for the other pegs. Possible explanations for this response are:-

(i) that the process is non-linear in nature;

(ii) that the series comprise both a general linear trend and a seasonal non-linear component.

(iii) that deviations from linearity are random fluctuations.

(iv) that differences in response are due to local site differences; in particular, vegetation effects or changes in soil properties.

Table 7.27 lists the linear equations for all instruments. The magnitude of the trend, given by coefficient a, is stronger on average for the 15 cm pegs than for the 10 cm pegs, and many of the 5 cm pegs show a negligible trend. A decrease in the magnitude of coefficient a, is expected because of differences in peg length but this should not decline to near zero even in the presence of a very weak trend. Table 7.28, a subsample of table 7.27, illustrates the apparent absence of a linear trend in the 5 cm peg series of sites 7/2 and 7/5, whereas a weak trend for 5 cm pegs at sites 5/2 and 9/8 can still be explained by a linear model. The table also shows that a linear model can be applied successfully to series from all vegetation classes but a closer inspection of the data, table 7.27, suggests that vegetation class is important in determining the overall success of the model. For example, the proportion of sites in which the variance explained by the model does not exceed 50% is similar for all three instruments but quite different proportions exist when the data are divided into vegetation classes. *Nardus* vegetation has 60% of its sites

Table 7.27a

LINEAR EQUATIONS FOR 15 cm INCLINOMETER PEG TIME SERIES

Site	Veg	y = a.SLOPE + b		r^2	std error
1/1	J	0.39	25.01	0.57	61.59
1/2	Pt	0.98	- 8.99	0.90	59.38
1/3	Pt			0.82	80.00
1/4	C	0.32	30.79	0.68	40.22
1/5	Pt	0.34	36.17	0.66	44.98
2/1	J	0.23	62.68	0.35	57.67
2/2	J	0.20	32.45	0.42	44.55
2/3	N	0.38	10.44	0.79	36.54
2/4	N	0.32	- 22.43	0.48	64.06
2/5	Pt	0.49	64.42	0.80	45.60
2/6	J	0.22	30.34	0.39	51.93
2/7	C				
3/1	Pt	0.34	27.09	0.69	41.50
3/2	Pt	0.32	- 2.56	0.66	43.56
3/3	N	0.24	49.18	0.37	58.71
3/4	J	0.16	47.52	0.23	54.22
3/5	Pt	0.46	43.71	0.74	51.11
3/6	C	0.28	66.22	0.39	66.19
3/7	C	0.32	- 30.60	0.75	34.41
4/1	J	0.77	- 11.61	0.87	54.18
4/2	J	0.12	55.06	0.09	69.84
4/3	N	0.51	16.74	0.58	80.40
4/4	Pt	0.25	14.24	0.55	41.48
4/5	Pt	0.44	5.58	0.80	33.26
4/6	C				
5/1	J	0.50	- 16.73	0.65	68.51
5/2	J	0.35	10.04	0.60	53.80
5/3	J	0.34	- 41.96	0.55	46.86
5/4	J	0.84	- 73.95	0.85	53.28
5/5	N				
5/6	N	0.08	39.09	0.08	54.19
5/7	N	0.20	36.84	0.34	51.33
5/8	J	0.32	- 17.12	0.48	63.18
5/9	Pt	0.44	- 42.22	0.72	51.26
5/10	C	0.39	6.06	0.78	39.44
6/1	J	0.32	53.04	0.48	62.30
6/2	J	1.39	- 156.50	0.72	162.38
6/3	Pt	1.03	- 24.62	0.95	43.45
6/4	Pt	0.42	6.48	0.71	51.14
6/5	Pt	0.35	- 0.06	0.45	73.55
6/6	Pt	0.43	- 45.54	0.71	51.15
7/1	Pt	0.22	18.47	0.26	68.45
7/2	Pt	0.37	11.52	0.78	38.01
7/3	N	-0.015	76.53	0.00	74.17
7/4	N	-0.03	- 9.98	0.02	41.33
7/5	C	0.59	18.44	0.76	61.24
7/6	C	0.35	25.01	0.48	67.22
8/1	N	0.11	68.73	0.05	89.21
8/2	N	-0.02	15.31	0.002	78.49
8/3	J	0.36	120.89	0.27	112.27
8/4	N	0.27	- 43.64	0.56	44.71
8/5	Pt	0.42	- 79.31	0.66	56.54
8/6	C	0.45	- 24.04	0.71	54.37

/...cont

Table 7.27a

LINEAR EQUATIONS FOR 15 cm INCLINOMETER PEG TIME SERIES

Site	Veg	y = a.SLOPE + b		r^2	std error
9/1	J	0.27	65.15	0.70	33.17
9/2	J	0.51	55.41	0.80	48.28
9/3	J	1.99	- 224.25	0.66	273.55
9/4	J				
9/5	J	0.26	84.47	0.13	128.46
9/6	J	-0.12	47.25	0.02	145.80
9/7	N	0.43	- 24.12	0.61	66.34
9/8	N	0.49	19.47	0.86	27.04
10/1	N	0.48	- 9.99	0.62	69.77
10/2	N	-0.63	129.91	0.29	183.63
10/3	N	0.25	- 2.76	0.41	56.04
10/4	N	0.34	- 12.06	0.65	47.43
10/5	N	0.39	- 28.58	0.76	42.56
10/6	N	0.37	- 34.96	0.74	42.44
10/7	N	0.51	54.61	0.61	77.83
10/8	N	0.39	48.97	0.67	53.33

Table 7.27b
LINEAR EQUATIONS FOR 10 cm INCLINOMETER PEG TIME SERIES

SITE	VEG	Y = a.SLOPE + b	r^2	STD ERROR
1/1	J	y = 0.13 - 1.20	0.90	8.18
1/2	Pt	y = 1.42 + 51.94	0.66	185.85
1/3	Pt	y = +	0.89	61.13
1/4	C	y = 0.17 - 0.25	0.61	24.58
1/5	Pt	y = 0.28 + 36.84	0.76	29.80
2/1	J	y = 0.11 + 43.71	0.32	30.04
2/2	J	y = 0.28 - 9.06	0.83	23.64
2/3	N	y = 0.30 + 9.74	0.80	27.27
2/4	N	y = 0.03 - 16.09	0.03	31.73
2/5	Pt	y = 0.17 - 10.38	0.62	24.47
2/6	J	y = 0.43 - 23.30	0.93	21.52
2/7	C	y = 0.40 + 4.87	0.93	21.11
3/1	Pt	y = 0.15 - 24.07	0.57	23.92
3/2	Pt	y = 0.19 + 3.42	0.13	90.51
3/3	N	y = 0.05 + 23.08	0.07	37.96
3/4	J	y = 0.09 + 39.50	0.44	21.00
3/5	Pt	y = 0.15 - 22.49	0.45	31.76
3/6	C	y = 0.17 + 2.24	0.50	31.83
3/7	C	y = 0.20 + 20.37	0.64	28.72
4/1	J			
4/2	J	y = 0.07 - 43.45	0.10	40.34
4/3	N	y = 0.12 + 37.49	0.13	55.92
4/4	Pt			
4/5	Pt	y = 0.25 - 15.40	0.79	19.45
4/6	C	y = 0.26 + 28.96	0.76	26.66
5/1	J	y = 0.75 - 7.61	0.87	53.27
5/2	J	y = 0.12 - 0.64	0.74	13.69
5/3	J	y = 0.26 + 31.70	0.74	23.99
5/4	J	y = 1.06 + 30.12	0.84	71.70
5/5	N	y = 0.18 + 32.42	0.60	27.76
5/6	N	y = 0.15 + 18.28	0.64	20.88
5/7	N	y = 0.14 - 3.86	0.82	11.96
5/8	J	y = -0.29 + 26.28	0.36	72.02
5/9	Pt	y = 0.16 + 12.99	0.60	24.83
5/10	C	y = 0.25 + 30.95	0.79	23.83
6/1	J	y = 0.23 + 154.90	0.28	69.55
6/2	J	y = 0.75 + 3.80	0.93	37.81
6/3	Pt	y = -0.02 - 17.08	0.01	37.49
6/4	Pt	y = -0.31 + 89.15	0.46	62.71
6/5	Pt	y = 0.23 - 1.30	0.80	21.29
6/6	Pt	y = 0.28 + 42.66	0.55	47.10
7/1	Pt	y = 0.12 + 14.34	0.68	15.70
7/2	Pt	y = 0.13 - 2.02	0.52	23.48
7/3	N	y = -0.08 + 84.66	0.04	76.99
7/4	N	y = 0.06 + 49.77	0.13	28.18
7/5	C	y = 0.13 + 0.15	0.59	19.73
7/6	C	y = 0.40 - 23.04	0.83	34.41

/...cont

Table 7.27b

SITE	VEG	y = a.SLOPE + b	r^2	STD ERROR
8/1	N	y = -0.0 + 78.95	0.04	58.48
8/2	N	y = -0.10 + 98.04	0.10	54.43
8/3	J	y = -0.01 - 39.22	0.0007	66.43
8/4	N	y = 0.18 + 47.74	0.46	35.70
8/5	Pt	y = -0.72 + 225.15	0.30	204.55
8/6	C	y = 0.39 - 13.71	0.52	6.29
9/1		y = 1.01 + 119.59	0.50	191.88
9/2		y = 0.63 + 17.79	0.96	25.17
9/3		y = 0.75 - 53.33	0.91	43.50
9/4				
9/5		y = 0.25 - 42.57	0.13	123.05
9/6		y = 1.43 - 55.17	0.91	83.54
9/7		y = 0.01 - 10.96	0.05	11.49
9/8		y = 0.24 + 19.20	0.84	14.61
10/1		y = 0.17 + 19.95	0.65	23.46
10/2		y = 0.36 - 23.44	0.75	39.14
10/3		y = 0,33 + 61.26	0.69	41.18
10/4		y = 0.08 + 5.88	0.29	23.55
10/5		y = 0.03 + 17.27	0.02	40.81
10/6		y = 0.06 - 36.18	0.08	41.75
10/7		y = 0.27 + 15.99	0.57	45.11
10/8		y = 0.05 + 65.06	0.03	55.57

Table 7.27c

LINEAR EQUATIONS FOR 5 cm INCLINOMETER PEG TIME SERIES

Site	Veg	y = a.SLOPE + b		r^2	std error
1/1	J	0.76 -	94.42	0.88	50.95
1/2	Pt	0.14	8.44	0.88	9.08
1/3	Pt			0.42	141.94
1/4	C	0.39	0.59	0.56	6.31
1/5	Pt	0.19	6.98	0.90	11.73
2/1	J	0.01	4.33	0.20	0.52
2/2	J	0.08 -	7.04	0.52	13.78
2/3	N	0.35 -	16.81	0.83	29.41
2/4	N	0.01	1.03	0.08	9.66
2/5	Pt	0.02	22.56	0.02	21.02
2/6	J	0.10 -	2.16	0.80	9.53
2/7	C	0.05	19.29	0.44	10.58
3/1	Pt	0.06	1.05	0.77	6.47
3/2	Pt	0.18	9.01	0.68	23.62
3/3	N	-0.003	14.23	0.00	14.06
3/4	J	0.06	10.35	0.54	10.00
3/5	Pt	0.05 -	7.55	0.73	5.17
3/6	C	0.07	15.43	0.44	15.50
3/7	C	0.002	0.93	0.01	4.57
4/1	J				
4/2	J	0.05	3.84	0.43	10.87
4/3	N	0.03	19.29	0.06	20.22
4/4	Pt	0.05 -	2.45	0.82	4.31
4/5	Pt	0.08	4.88	0.69	7.88
4/6	C	0.08	13.24	0.62	12.08
5/1	J	0.24	118.75	0.53	41.71
5/2	J	-0.02 -	9.37	0.31	4.93
5/3	J	0.16 -	2.87	0.90	8.25
5/4	J	0.40 -	44.53	0.92	17.89
5/5	N	-0.003	12.53	0.00	9.05
5/6	N	0.07	18.88	0.49	13.71
5/7	N	0.12	23.99	0.77	12.84
5/8	J	0.21	17.38	0.60	31.67
5/9	Pt	0.18	17.29	0.83	14.98
5/10	C	0.13 -	7.33	0.67	17.77
6/1	J	0.23	7.48	0.91	13.29
6/2	J	0.08	18.14	0.10	46.16
6/3	Pt	0.17	19.32	0.76	18.08
6/4	Pt	0.16 -	5.00	0.90	9.68
6/5	Pt	0.12	13.82	0.53	22.02
6/6	Pt	0.001	7.61	0.00	8.12
7/1	Pt	0.11	21.14	0.59	17.36
7/2	Pt	0.08 -	7.73	0.65	11.01
7/3	N	-0.01	10.15	0.09	8.79
7/4	N	0.02 -	0.51	0.25	6.29
7/5	C	0.06 -	0.04	0.77	6.47
7/6	C	0.002	2.72	0.00	8.87
8/1	N	0.18	4.29	0.89	11.34
8/2	N	-0.08	29.66	0.36	20.53
8/3	J	0.13	5.56	0.52	23.57
8/4	N	0.17	3.19	0.47	34.26
8/5	Pt	0.29	107.17	0.54	50.45
8/6	C				

Table 7.27c

LINEAR EQUATIONS FOR 5 cm INCLINOMETER PEG TIME SERIES

Site	Veg	y = a.SLOPE + b	r^2	std error
9/1		0.28 - 13.71	0.67	37.78
9/2		0.51 90.96	0.77	53.05
9/3		0.27 - 21.71	0.85	21.19
9/4				
9/5		0.28 - 1.65	0.92	15.69
9/6		-0.03 1.37	0.16	14.86
9/7		0.05 5.11	0.71	5.63
9/8		0.12 - 1.40	0.93	4.53
10/1		0.11 15.23	0.32	28.78
10/2		-0.03 14.65	0.13	14.99
10/3		-0.12 54.10	0.15	50.34
10/4		0.04 13.82	0.40	9.66
10/5		-0.02 14.38	0.09	12.15
10/6		-0.02 - 20.35	0.08	16.83
10/7		0.14 - 5.75	0.90	9.01
10/8		0.04 21.79	0.14	20.87

Table 7.28

LINEAR EQUATIONS

SITE	VEG	PEG	Y = a.SLOPE + b	r^2	STD ERROR
5/2	J	15 cm	0.84 - 73.95	0.85	53.28
		10 cm	0.26 + 31.70	0.74	23.99
		5 cm	0.16 - 2.87	0.90	8.25
7/2	pt	15 cm	0.37 + 11.52	0.78	38.01
		10 cm	0.13 - 2.02	0.52	23.48
		5 cm	0.08 - 7.73	0.65	11.01
7/5	C	15 cm	0.59 + 18.44	0.76	61.24
		10 cm	0.13 + 0.15	0.59	19.73
		5 cm	0.06 - 0.04	0.77	6.47
9/8	N	15 cm	0.49 + 19.47	0.86	27.04
		10 cm	0.24 + 19.20	0.84	14.61
		5 cm	0.12 - 1.40	0.93	4.53

with r^2 values less than 0.5, *Juncus* shows 38% of sites poorly explained while *Pteridium* and *Calluna* only give 20% and 24% respectively of sites poorly explained by the linear model. Stem and leaf plots allow the pattern to be analysed in more detail, see figure 7.45. Low r^2 values of 15 cm peg data are mainly associated with *Nardus* and *Juncus* vegetation classes. *Juncus* , gives an even spread of r^2 values indicating that the model performs poorly for 15 cm pegs. The other classes show distinct clustering of sites around r^2 values of 0.6 and 0.7 but all have negatively skewed distributions with the *Nardus* class having the lowest r^2 values.

The 10 cm and 5 cm pegs show a consistent pattern for the *Pteridium* and *Calluna* classes; however, *Juncus* and *Nardus* behave differently. The r^2 values improve as peg length decreases until only 5 sites give values less than 0.5 in the 5 cm peg data. On the other hand, the r^2 values decrease sharply with peg length for the *Nardus* class. Here only 6 sites have r^2 values greater than 0.5 in the 5cm peg data.

These results suggest that the dense root mat associated with *Nardus* grassland species influences the movement patterns. The depth to which S.M.M. is recorded does not seem to alter the temporal behaviour of the *Juncus*, *Pteridium* or *Calluna* sites but graphs of the data do reveal exceptions. For example, site 2/1 (figure 7.40), site 4/4 (figure 7.46) and site 7/6 (figure 7.47) have strong, apparently seasonal, patterns in *Juncus*, *Pteridium* and *Calluna* classes respectively.

The procedure of summarising the time series data *globally* with a linear model is not ideal. The technique averages seasonal components so that plotting residuals against the fitted line may give misleading results in the presence of outliers. A better approach for summarising non-linear time series is to divide the data into a *smooth* trend component, and a second *rough* component which indicates short term fluctuations from the trend (Tukey 1977). Tukey demonstrates the value of smoothing

Figure 7.45 Stem-and-leaf plots of r^2 values of linear equations fitted to Inclinometer Peg time series data.

IP_{15} r^2 VALUES		JUNCUS	NARDUS	PTERIDIUM	CALLUNA
0·0	8 8 0 2 5 0 2	2 8	0 0 2 5 8		
0·1	3	3			
0·2	3 0 7 9	3 7	9	0	
0·3	5 9 7 9 4	5	4 7	9	9
0·4	2 8 8 8 5 8 1	2 8 8	1 8	5	8
0·5	7 8 6 5 6	7 5	6 8	6	
0·6	8 6 9 6 5 0 6 6 1 2 5 1 7	0 5 6	1 1 2 5 7	6 6 6 9	8
0·7	9 4 5 2 8 2 1 1 8 6 1 0 6 4	0 2	4 6 9	1 1 2 4 8	1 5 6 8
0·8	2 0 7 0 6 0 6	0 6 7	6	0 0 2	
0·9	0 5			0	

IP_{10} r^2 VALUES					
0·0	3 7 1 4 4 0 5 2 8 3	0 3	2 3 4 4 5 7 8	1	
0·1	3 0 3 3 0 3	0 3	0 3 3	3	
0·2	8		8		
0·3	2 6 0 0 0	0 0 2 6		0	
0·4	4 5 6 6	4	6	5 6	
0·5	7 0 5 2 0 7	0	7	2 5 7	0
0·6	6 1 2 4 0 4 8 0 5 9		0 4 5 9	2 6 8	0 1 4
0·7	6 9 6 4 4 9 5 3 4	4 4	5	6 9	6 9
0·8	8 9 3 0 7 4 2 0	4 7 8	0 2 3 4	0 9	3
0·9	3 3 3 0 6 1 1	1 1 3 3 6			0 3

IP_5 r^2 VALUES					
0·0	8 8 2 0 1 6 0 0 9 0 9 8	8	0 0 6 8 8 9 9	0 2	0 1
0·1	0 6 3 5 4	0 6	3 4 5		
0·2	5		5		
0·3	1 6 2	1	2 6		
0·4	2 4 4 3 9 7 0	3	0 7 9	2	4 4
0·5	6 2 4 4 3 9 2 4 7	2 2 4 4		3 4 9	6 7
0·6	8 9 2 0 7 5 7	0 7		5 8 9	2 7
0·7	7 4 6 6 7 7 1	7		4 6 7	7
0·8	9 4 0 2 3 9 5	0 5		2 3 9	
0·9	0 0 0 2 1 0 2 3 0	0 0 1 2 2		0 0	

Figure 7.46 Time series plot for Pteridium vegetation.

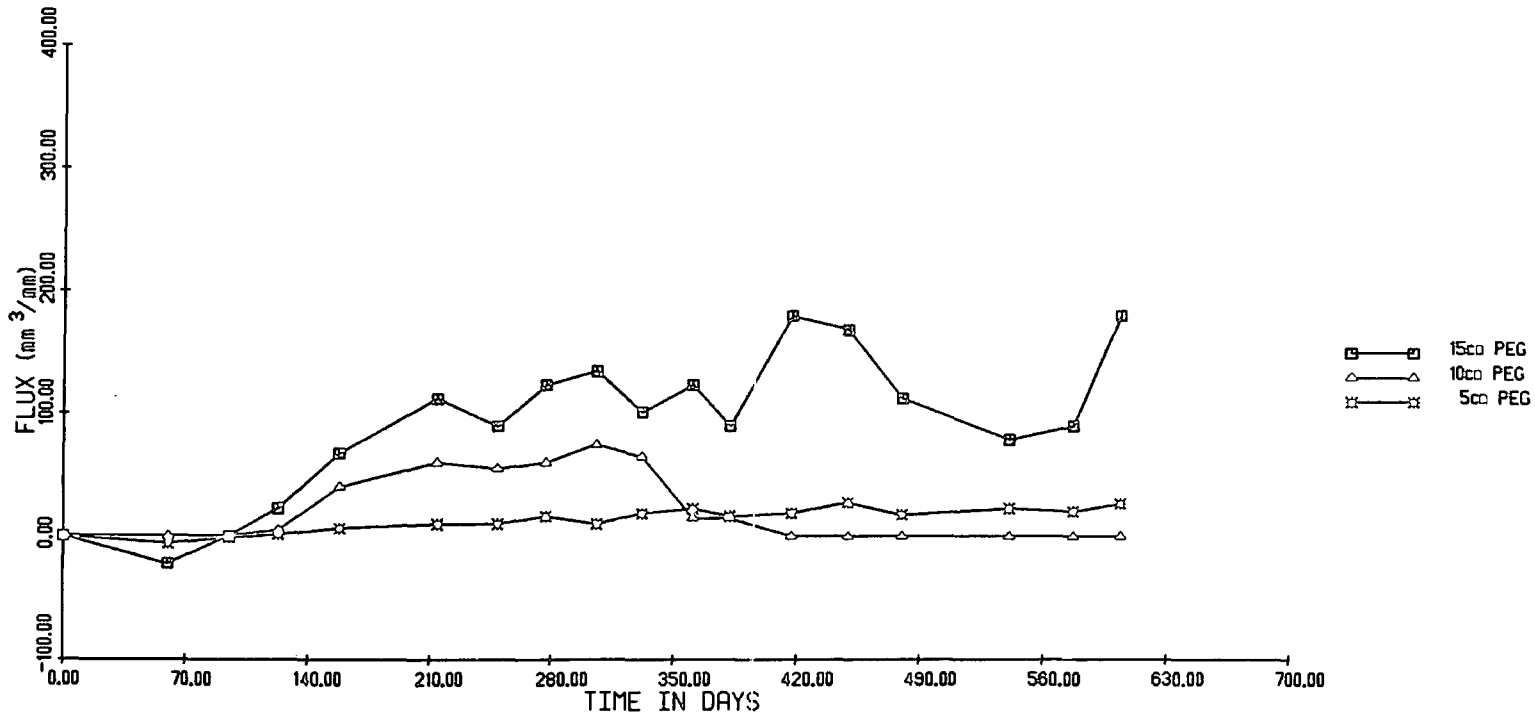

Figure 7.47 Time series plot for Calluna vegetation.

SITE 7/6

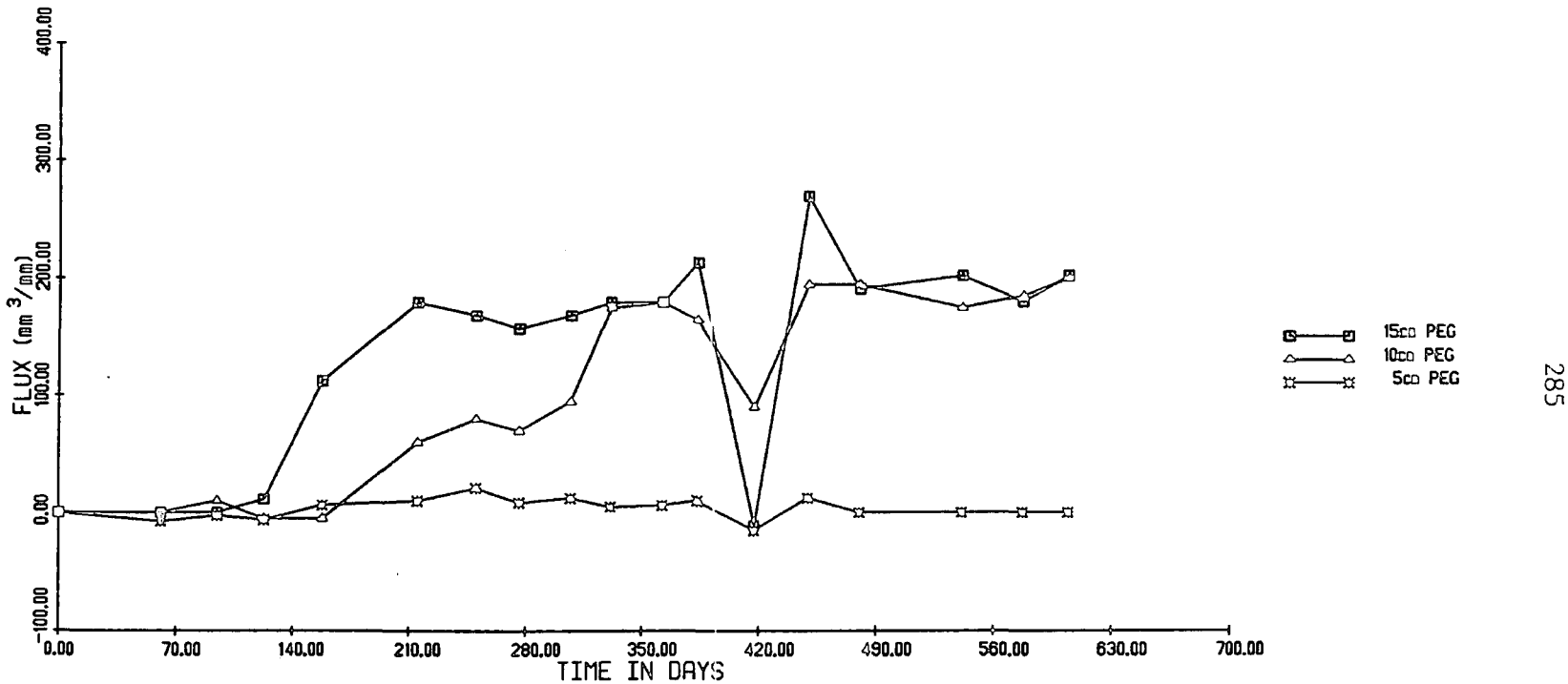

data series using running medians instead of the more usual method of running means because the median is resistant to an isolated outlier in a series.

7.4.4 Smoothing by resistant methods

Non-linear smoothing of time series data using running medians provides a method whereby a curve can be fitted to the data which summarises the large scale trend without being adversely affected by isolated spikes. Residuals from the fitted smooth curve are termed the *rough* component by Tukey (1977). Analysis of the rough component provides an important method of assessing the ability of the smooth curve to summarise all the important temporal patterns in the data. Velleman and Hoaglin (1981), in a review of smoothing algorithms, suggest an approach whereby a series is smoothed progressively; at each step the previously smoothed sequence is resmoothed until the process yields no further changes. Typical smoothing sequences are running medians of 3, 4 and 5. Running medians of 3 are only resistant to one spike; however, this is preferred to longer sequences in this case because of limited length of the series and because resmoothing provided an adequate method for removing the most obvious spikes in the data.

A computer program was written, based on the algorithms of Velleman and Hoaglin (1981) and Tukey (1977), to process the Inclinometer peg S.M.M. data using the technique of progressive smoothing. A listing of the FORTRAN code used in this operation is given in appendix A. The program began by smoothing each series by running medians of 3, resmoothing by running medians of 3 then finally smoothing with a running weighted average (0.25, 0.5, 0.25). The rough component is generated by subtracting the smooth curve from the original data since the

model has the form:

data = smooth + rough.

This method was found, by experiment, to summarise the series in a way that allows the smooth component to be compared with temporal changes in precipitation and shear strength. The rough component can then be analysed for any residual trend or pattern.

For many sites, the effect of smoothing is to reinforce the impression of a linear pattern of movement. Site 3/7, for example (figure 7.48) displays a smooth linear trend for 15 cm and 10 cm Inclinometer pegs while the effect on the 5 cm peg has been to remove all variation leaving an apparently stationary instrument. Site 1/3 (Pt) also displays a strong linear trend in the raw data but the smoothed curve reveals evidence for seasonal non-linearity in the 15 cm peg and 5 cm peg data (figure 7.49). Table 7.29 lists the cross-correlation coefficients from fitting a linear model to the raw, smoothed and residual data for site 1/3. This confirms that only the 10 cm peg data retain a strong linear trend when smoothed. The table also shows the cross-correlations among precipitation amount, shear strength and each of the instruments. The 15 cm peg series in its raw and smoothed forms correlate strongly with variation in shear strength through time; the strongest correlation being - 0.77 with the smoothed series. The 10 cm peg smoothed data gives a weaker correlation of -0.67 and the 5 cm peg gives a very poor correlation of -0.33. Correlations with precipitation are weak for the 10 cm and 5 cm pegs but the 15 cm peg shows moderate agreement (-0.68 with raw data). Most of the information which contributes to this correlation is contained in the residual or rough component of the time series as this yields a coefficient of -0.66. A plot of the rough component is shown in figure 7.50 and the cross-correlations are shown in table 7.29. The rough component of the series was tested for randomness since it might be supposed that the

Figure 7.48 Non-linear smoothing of site 3/7 (Calluna).

SITE 3/7

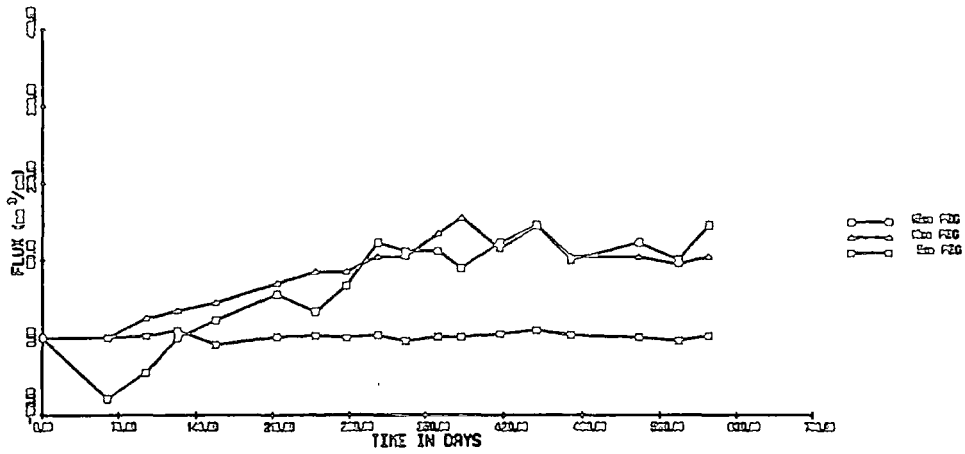

SITE 3/7 SMOOTHED S3R

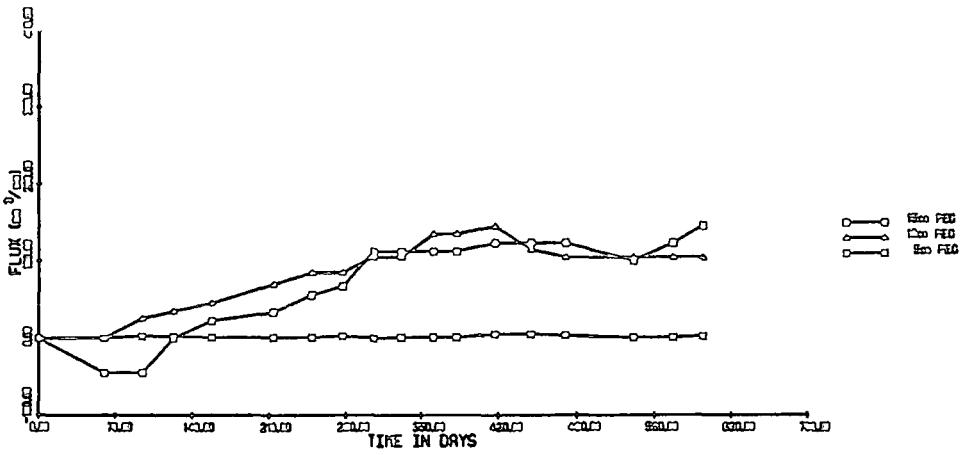

SITE 3/7 SMOOTHED S3R+HANN

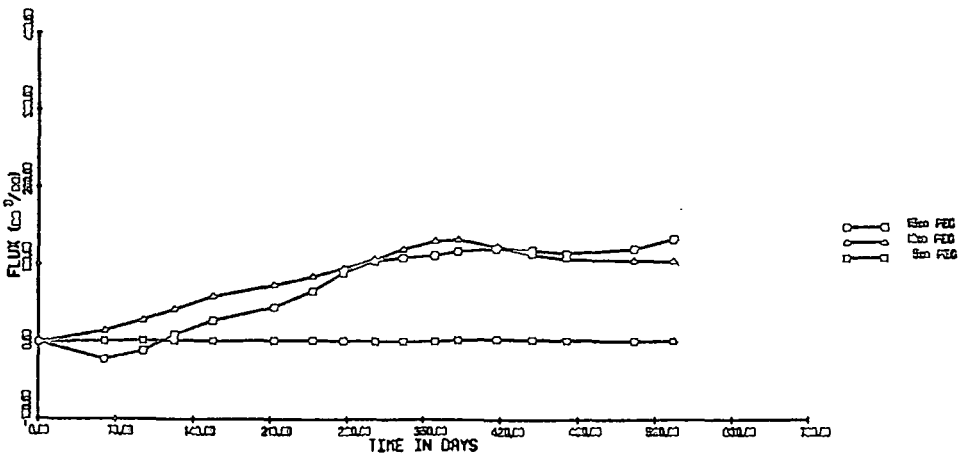

Figure 7.49 Non-linear smoothing of site 1/3 (Pteridium).

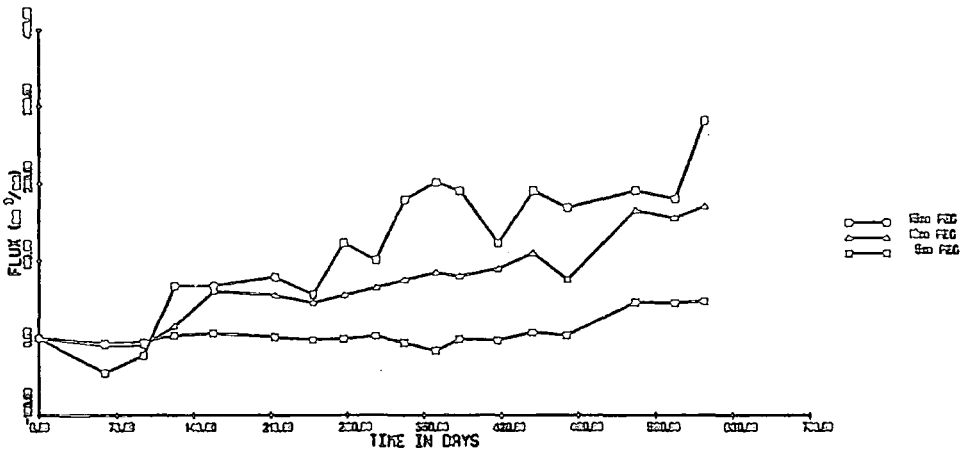

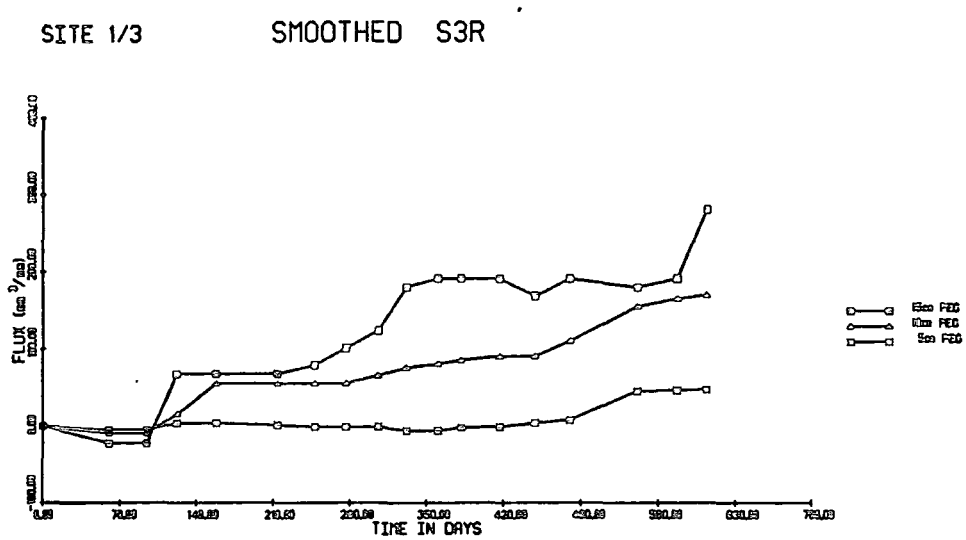

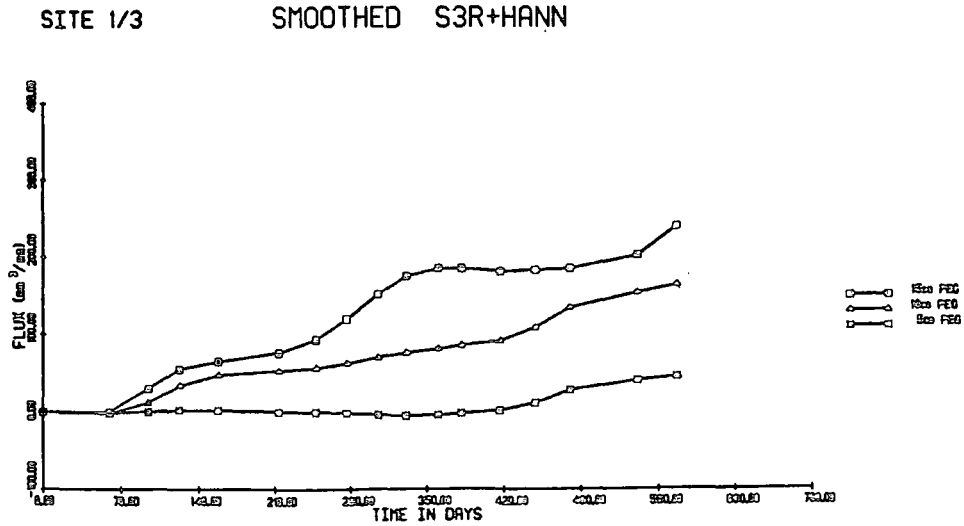

Figure 7.50 Residual component of time series from site 1/3.

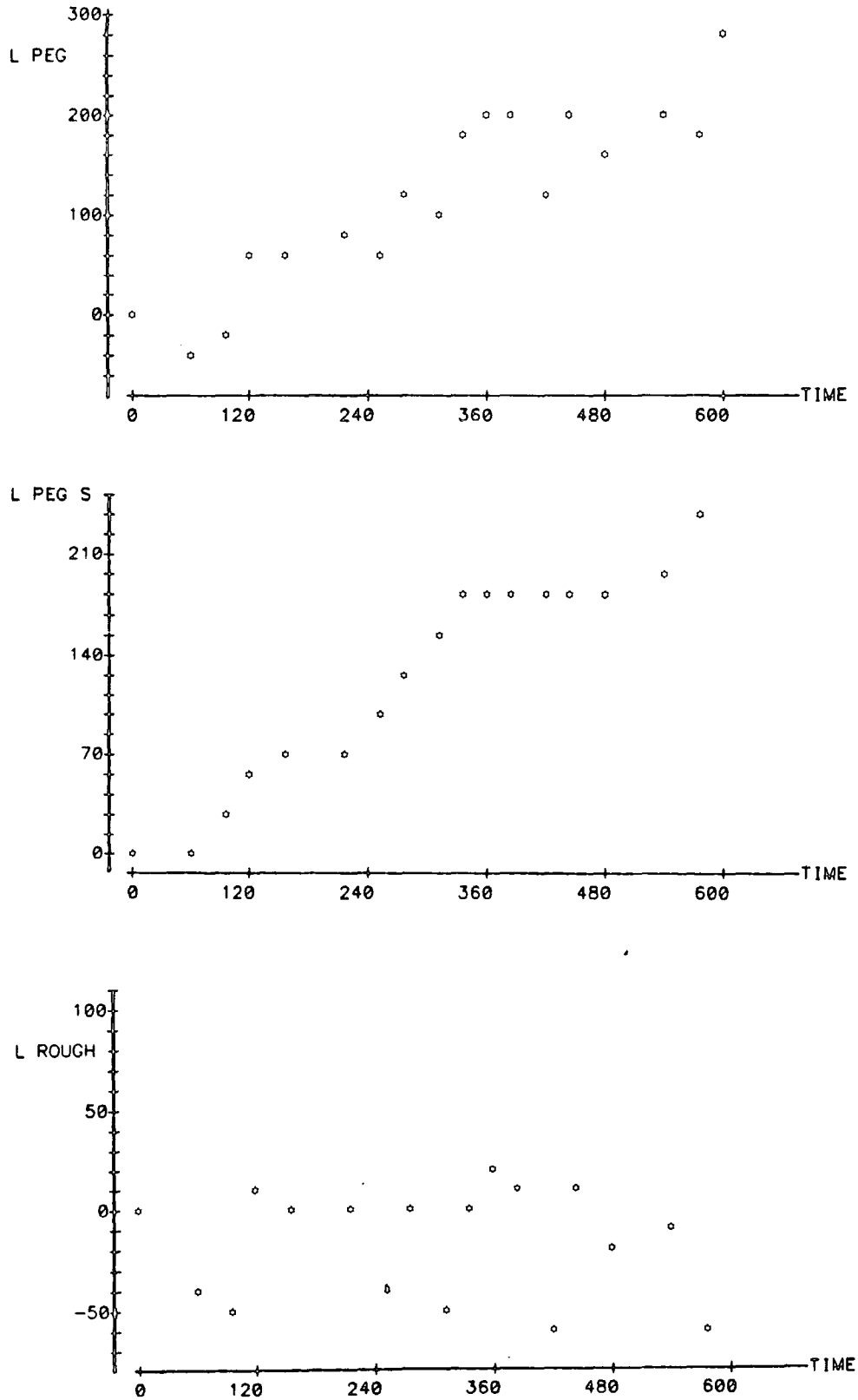

Figure 7.50 Residual component of time series from site 1/3.

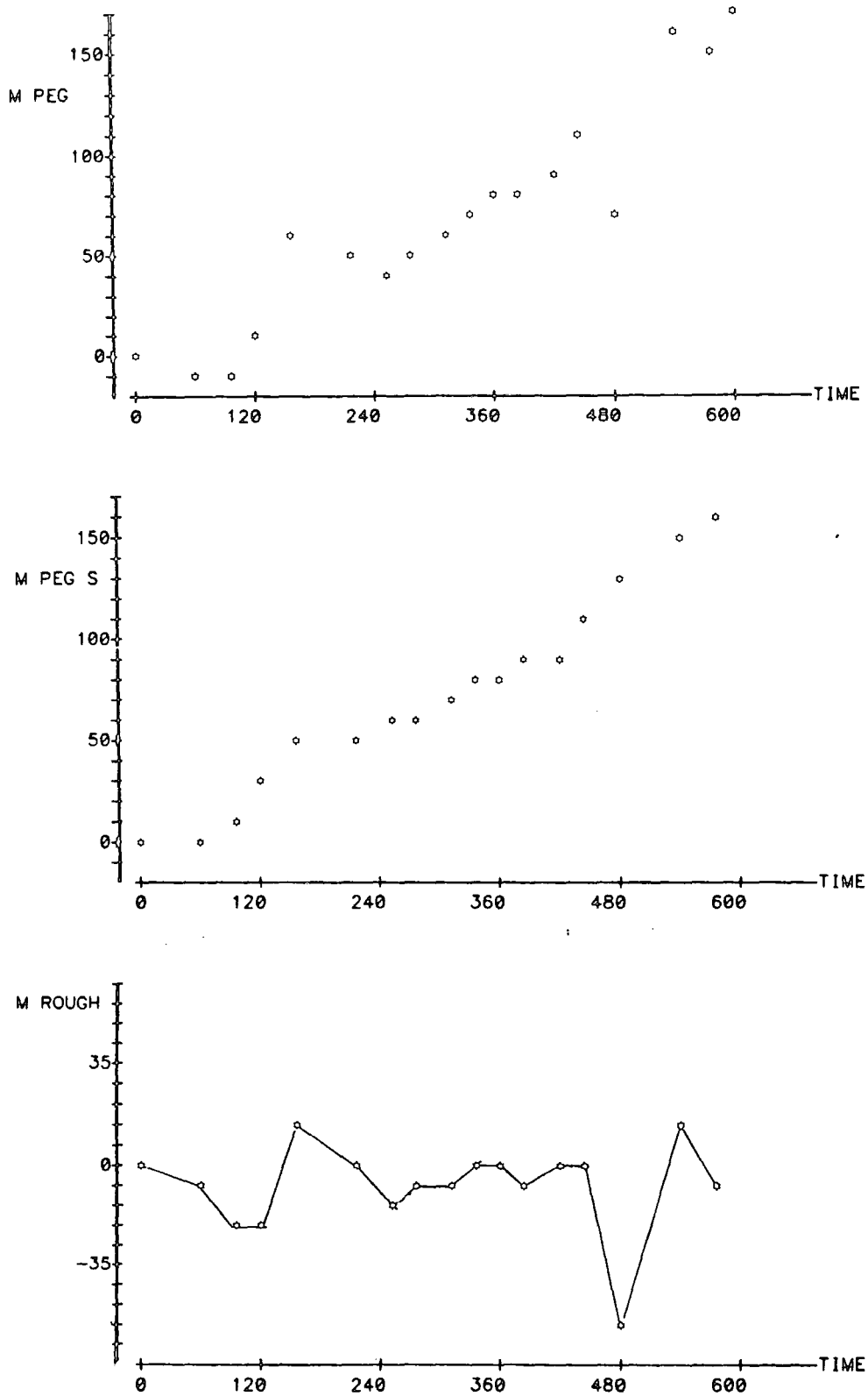

Figure 7.50 Residual component of time series from site 1/3.

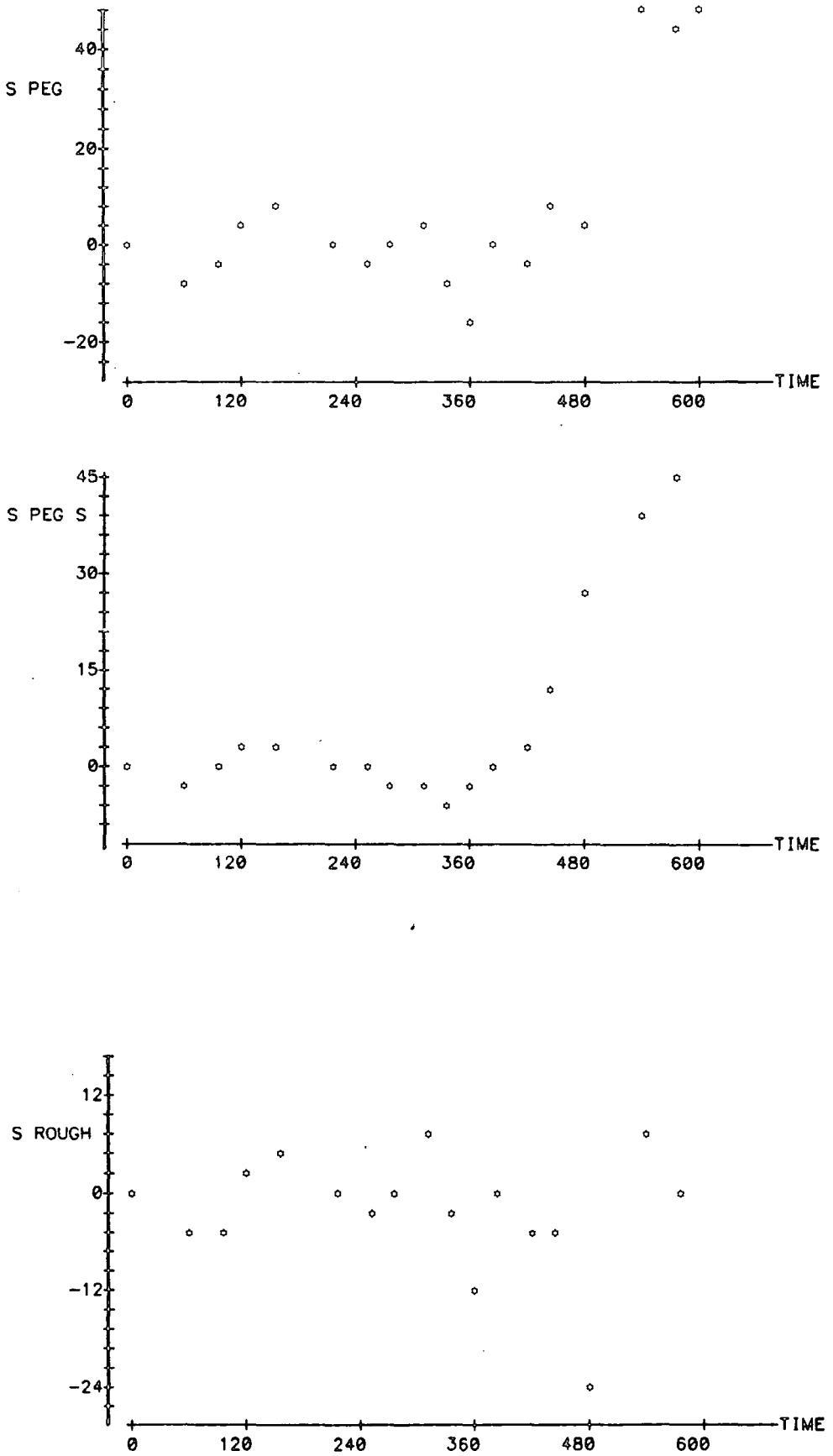

Table 7.29 Cross-correlation functions for raw, smooth and residual time-series data for sample 1/3.

	precip	shear_st	IP-15	IP-10	IP-5	SM-15	SM-10	SM-5
shear_st	0.380							
IP-15	-0.681	-0.747						
IP-10	-0.576	-0.504	0.880					
IP-5	-0.407	-0.325	0.605	0.840				
SM-15	-0.532	-0.771	0.909	0.826	0.472			
SM-10	-0.511	-0.672	0.836	0.922	0.756	0.894		
SM-5	-0.363	-0.328	0.548	0.823	0.973	0.496	0.793	
ROUGH-15	-0.660	-0.441	0.776	0.645	0.589	0.443	0.445	0.429
ROUGH-10	-0.505	-0.115	0.693	0.827	0.721	0.490	0.545	0.630
ROUGH-5	-0.416	-0.240	0.599	0.681	0.825	0.298	0.485	0.673

	ROUGH-15	ROUGH-10
ROUGH-10	0.751	
ROUGH-5	0.837	0.771

smooth component could account for systematic trend,the rough component being added random variation. As discussed previously, turning points are used to test against randomness in an oscillatory series and the number of positive first differences is used as a test against linear trend. The results for site 1/3 are given in table 7.30 and show that the rough component is not significantly different from a random series but the different sign test suggests a weak trend in the residual data. Inspection of figure 7.50 reveals that most of the largest residuals for each instrument are associated with erratic movement during the winter months. This might be due to the effect of frost action in the soil or lying snow disturbing the protruding pegs. Severe disturbance is not evident, however, because the magnitude of the residuals is similar for all three inclinometer pegs.

Site 2/7 (C) shows a strong linear trend in the 15 cm and 10 cm peg series, see figure 7.51. Progressive non-linear smoothing, however, enhances a weak pattern of seasonal fluctuation superimposed upon a strong downslope movement trend. The 5 cm peg shows no trend whatsoever when smoothed. Table 7.31 lists cross-correlation coefficients for precipitation, shear strength and S.M.M. time series and shows that a linear model gives a poorer fit with the smoothed series than with the raw data. At this site the residual variation in the series is strongly correlated with shear strength variation. This indicates that deviation from a linear downslope pattern is primarily associated with temporal variations in soil strength but other factors contribute to the trend seen in the smooth components of the 15 cm and 10 cm pegs. Precipitation amount is moderately correlated with the raw and residual 15 cm and 10 cm peg data which also suggests that the fluctuations in the raw data have a physical cause and are not due to random variation alone.

Site 2/1 (J), unlike the previous examples, is dominated by a seasonal

Table 7.30 Tests for randomness.

Site 1/3			
	15cm	10cm	5cm
TP_O	11	9	9
TP_E	10.67	10.67	10.67
$Diff_O$	6	5	5
$Diff_E$	8.5	8.5	8.5

Table 7.32 Tests for randomness.

Site 2/1			
	15cm	10cm	5cm
TP_O	8	9	12
TP_E	10.67	10.67	10.67
$Diff_O$	4	5	6
$Diff_E$	8.5	8.5	8.5

Figure 7.51 Non-linear smoothing of site 2/7 (Calluna).

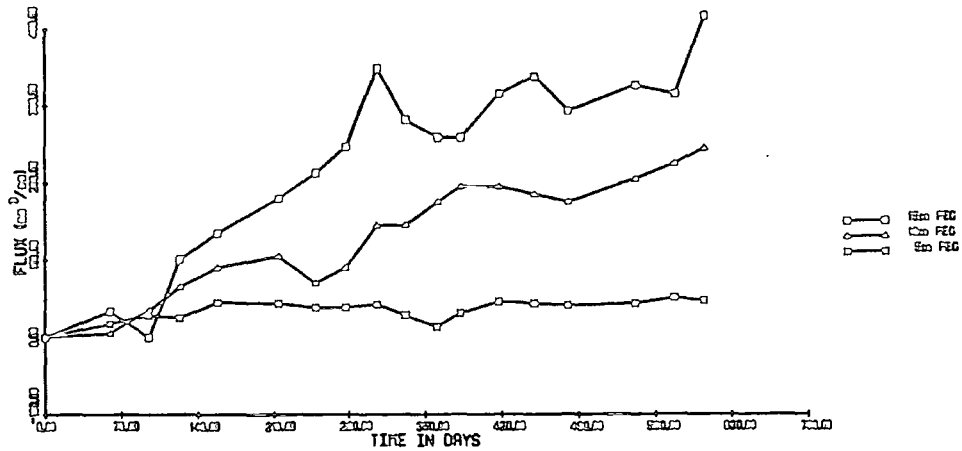

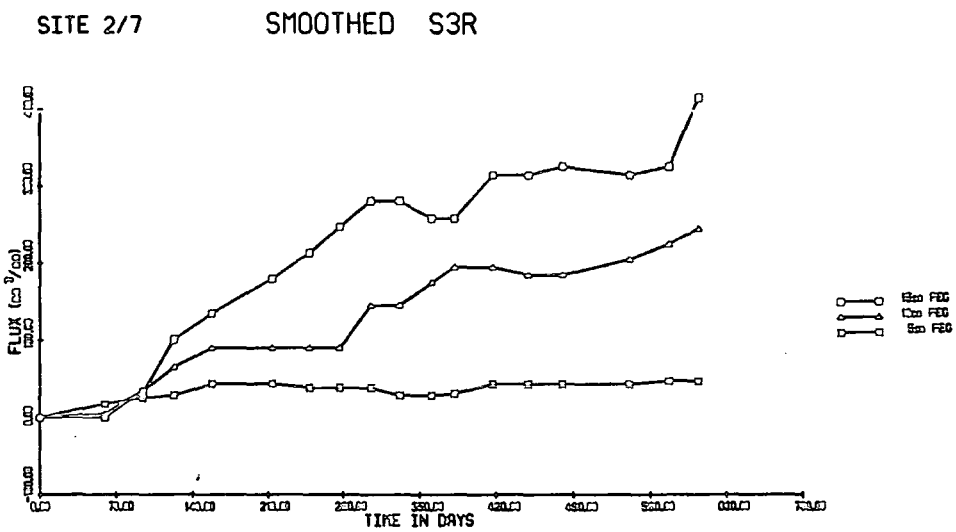

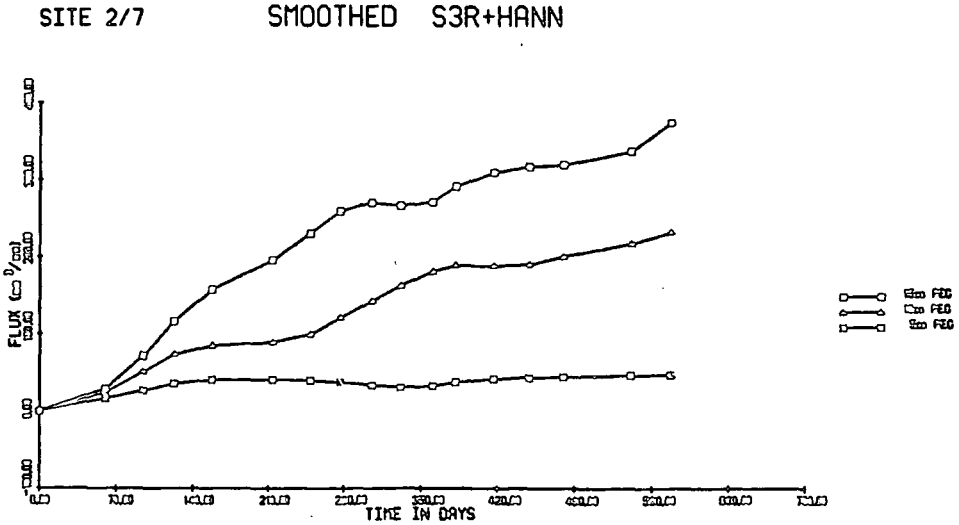

Table 7.31 Cross-correlation functions for raw, smooth and residual time-series data for sample 2/1.

	precip	shear_st	IP-15	IP-10	IP-5	SM-15	SM-10	SM-5
shear_st	0.142							
IP-15	-0.152	-0.520						
IP-10	-0.136	-0.570	0.953					
IP-5	0.150	-0.297	0.861	0.915				
SM-15	0.103	-0.572	0.865	0.775	0.692			
SM-10	0.212	-0.660	0.823	0.826	0.753	0.922		
SM-5	0.057	-0.306	0.882	0.871	0.906	0.838	0.845	
ROUGH-15	-0.396	-0.280	0.812	0.831	0.760	0.409	0.424	0.629
ROUGH-10	-0.503	-0.165	0.626	0.706	0.649	0.191	0.183	0.456
ROUGH-5	0.220	-0.221	0.647	0.761	0.883	0.378	0.485	0.601

	ROUGH-15	ROUGH-10
ROUGH-10	0.916	
ROUGH-5	0.736	0.718

rather than a linear trend. Figure 7.52 shows the effect of progressive smoothing of this series where the outcome is a smooth annual fluctuation with a weak downslope component in the 10 cm and 15 cm pegs. The seasonal trend in the 10 cm and 15 cm pegs correlates moderately with shear strength variations, -0.57 and -0.66 respectively. In this case the residual component does not appear to be associated with variations in either shear strength or precipitation amount. Correlograms illustrate that the correlations are weak and the response is not lagged.

Plots of the residual variation show a fluctuating pattern with a period of between 2 and 4 months; however, there is little evidence of seasonal or systematic variation in these series. Table 7.32 indicates that the residuals are not significantly different from a random series.

The three sites discussed above illustrate the spectrum of behaviour observed in the time series data for Inclinometer pegs. At the extremes, plots either display a strong linear downslope trend with residual variation, associated with seasonal changes in soil strength, or they display a strong seasonal pattern of movement with a weak downslope component; the seasonal component at these sites seems to be associated with variations in soil strength. The majority of sites contain some seasonal component but *Juncus* and *Nardus* dominated sites show the strongest seasonal influence.

This suggests that the temporal variability of soil strength is extremely important for predicting movement at these sites; indeed, the highest residuals from median polish and regression analysis were associated with *Juncus* and *Nardus* sites. *Pteridium* and *Calluna* dominated plots show less seasonal influence in their time series plots and so S.M.M. at these sites can be predicted more accurately from measurements of soil properties taken at any point in time.

Non-linear smoothing techniques provide a powerful tool for

Figure 7.52 Non-linear smoothing for site 2/1 (Juncus).

SITE 2/1

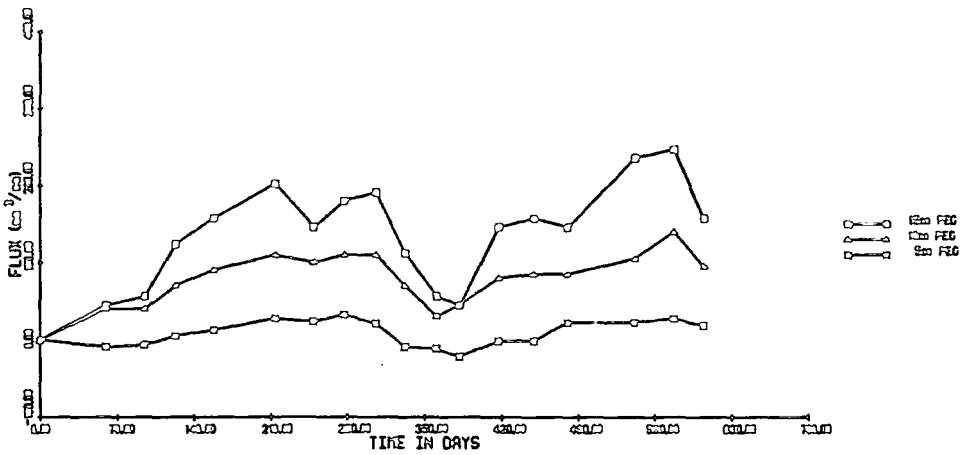

SITE 2/1 SMOOTHED S3R

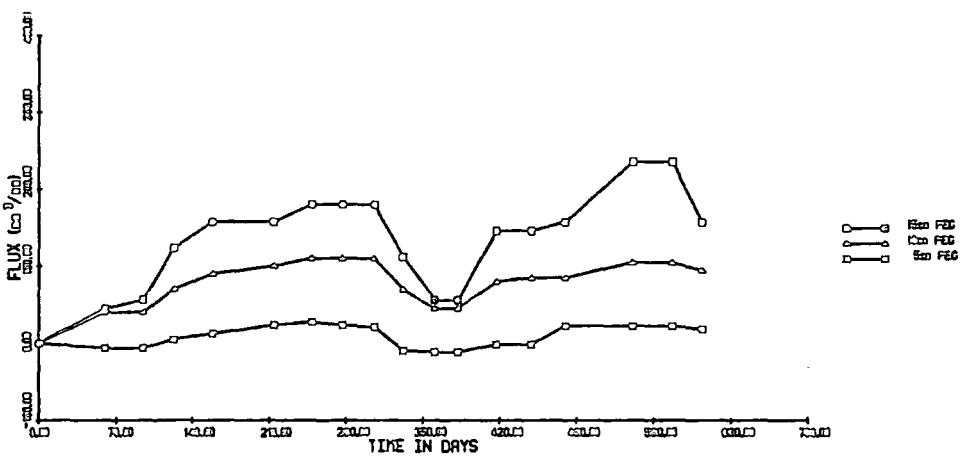

SITE 2/1 SMOOTHED S3R+HANN

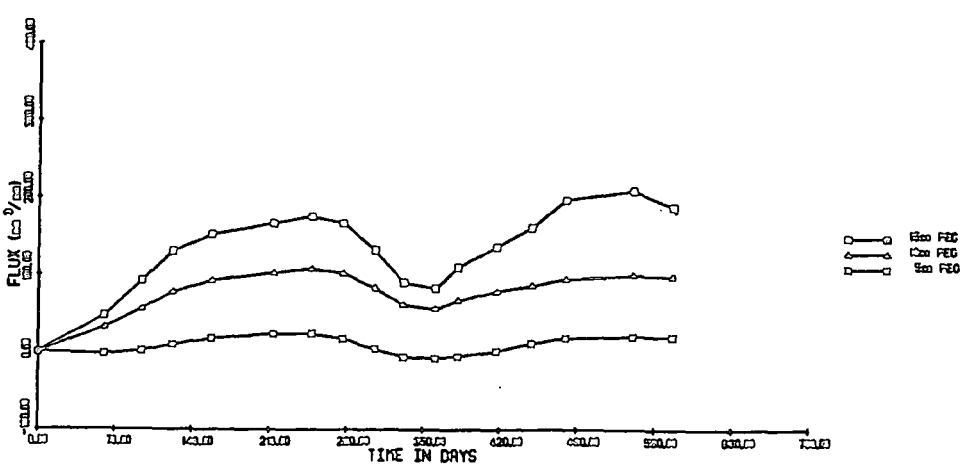

analysing S.M.M. time series because of the importance of seasonal variation in soil and vegetation properties at each site. For example, it might have been expected that spring growth of bracken rhizomes may accentuate movement or disturbance of *Pteridium* plots. There is some evidence for such a pattern at site 1/3 from the 15 cm peg for example. Figure 7.49 shows that the movement at this site occurs during the growth phase of *Pteridium* in the spring and summer.

Analysis of the rough or residual component of each series allows quantitative comparison of fluctuations in the series with either random or physical variation in soil properties. The technique holds considerable promise for future measurement programmes which could examine the temporal variation in soil properties and behaviour in more detail.

7.5 Summary of statistical analyses

The design of the field experiment imposed a sampling scheme which reflects the maximum possible variability in slope angle and vegetation type within a small catchment area. The results, therefore, reflect that variability and do not typify a catchment area that is dominated by *Calluna* and relatively gentle gradient.

Measurements were obtained from instruments which could record S.M.M. accurately and consistently at each site thereby allowing quantitative comparison of relative movement rates among sites.

A temporal component was added to the experiment by recording Inclinometer pegs and Anderson's tubes at monthly intervals in order to establish the nature of seasonal fluctuations in movement rate.

The analysis of the experimental data is based on several assumptions. First, it is assumed that the data set will contain many unreliable data points. Second, the techniques adopted serve to explore patterns

and trends in the data rather than to test specific hypotheses.

In particular, the statistics used do not rely heavily on the assumption of aussian distribution of the data and where possible, techniques are robust to outlying or wild observations.

The first stage of analysis was to model S.M.M. as the additive effect of gradient and vegetation cover at each site. When considered separately, neither the slope angle or the vegetation groupings could provide statistically significant differences using one-way analysis of variance. This was partly due to bias in the group means introduced by a few wild observations. However, a two-way additive model based on medians, rather than means, was capable of explaining about 50% of the observed variation for each instrument. The technique of median polish illustrates that within each vegetation class, slope angle and S.M.M. are positively related. The *Nardus* grassland class shows the most unpredictable movement patterns; it exhibits low rates on gentle and steep slopes alike.

Surprisingly, annual S.M.M. rates are not strongly correlated with measured soil variables, although weak correlations were found with phi skewness, shear strength, density of roots and with slope angle. In addition correlations with soil plasticity and % clay content were very weak.

A linear trend was found to summarise the temporal pattern of Inclinometer peg data at a large number of sites. In particular, sites dominated by *Pteridium* and *Calluna* vegetation exhibited linear downslope trends. At other sites, where *Juncus* and *Nardus* were the dominant vegetation types, non-linear trends were most evident and these were strongly correlated with temporal variations in soil shear strength. *Nardus* sites showed the least downslope movement and showed the strongest seasonal fluctuations. At several sites the 5cm Inclinometer pegs showed no discernible downslope movement. This may be due to the effect of dense

fibrous root networks binding the soil and producing an elastic response to expansion and contraction forces.

Cross correlation analysis of instrument series within plots and analysis of residual variation from non-linear smoothed curves suggests that deviations from linearity or a smooth trend do not represent random variation. Linear models appear to have limited success in explaining variation in the S.M.M. data; however, when sites are grouped according to vegetation cover then the association with slope gradient and soil shear strength becomes evident. The temporal patterns of S.M.M. are also strongly associated with vegetation cover type.

Chapter 8

Conspectus

Contents

8.1 Spatial distribution of S.M.M.

Field observations of S.M.M. rates in the Heathery Burn catchment area taken from Inclinometer pegs and from Anderson's tubes show that vegetation strongly influences the mechanical behaviour of the soil. This is in part explained by the ecological setting of each site, whereby the distribution of soil type and moisture content is controlled by the underlying geology and by the distribution of saturated soils. These are predominantly located in hillslope hollows and areas adjacent to the stream channel.

Figure 8.1 shows the distribution of the major vegetation classes in the catchment area, and figure 8.2 shows the spatial distribution of the measurement plots. There is a notable clustering of the plots because the experimental design attempts to sample a broad range of slope angles: steep angled slopes are notably clustered around the lower incised part of the catchment and around the breaks of slope associated with *Pteridium* vegetation. The sample sites are also located on the path of hillslope profiles. Analysis of the experimental data in chapter 7 revealed an association between the sites with the largest movement rates and particular landforms such as lobes and scarp features behind lobes. Figure 8.3 shows the spatial distribution of S.M.M. volumetric rates taken from Anderson's tubes in a simplified form. The pattern of movement confirms the association between vegetation type and S.M.M. rate described in chapter 7. In addition, however, high rates are also associated with distinct lobate features which may be single units of slowly deforming soil. There is evidence of past landslide activity at several locations within the catchment area and some of the tubes showed reversed tilting which is difficult to attribute to S.M.M. but which may be due to rotational deformation of

Figure 8.1 Spatial distribution of major vegetation classes.

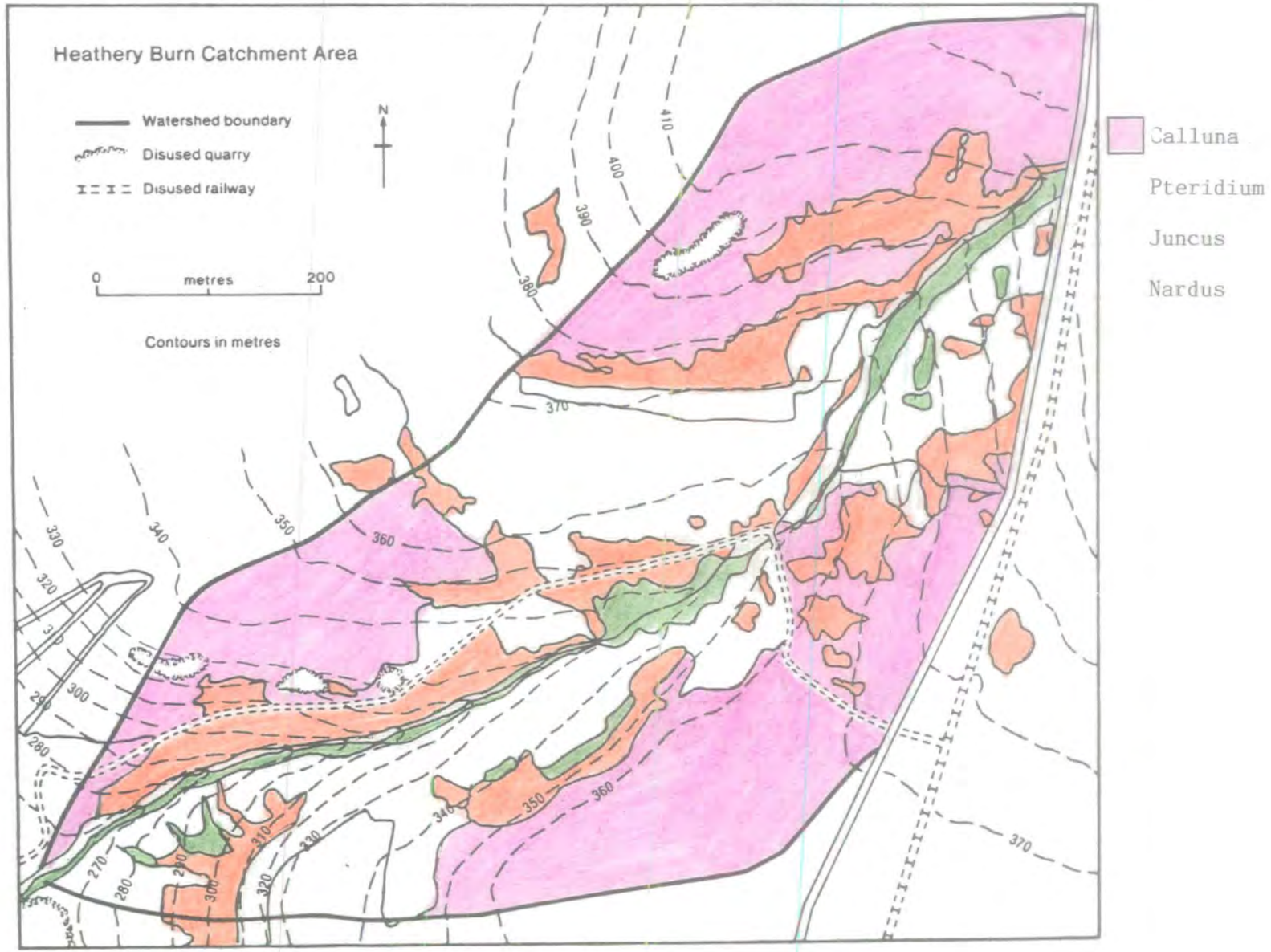

Figure 8.2 Location of instrument plots showing vegetation classes.

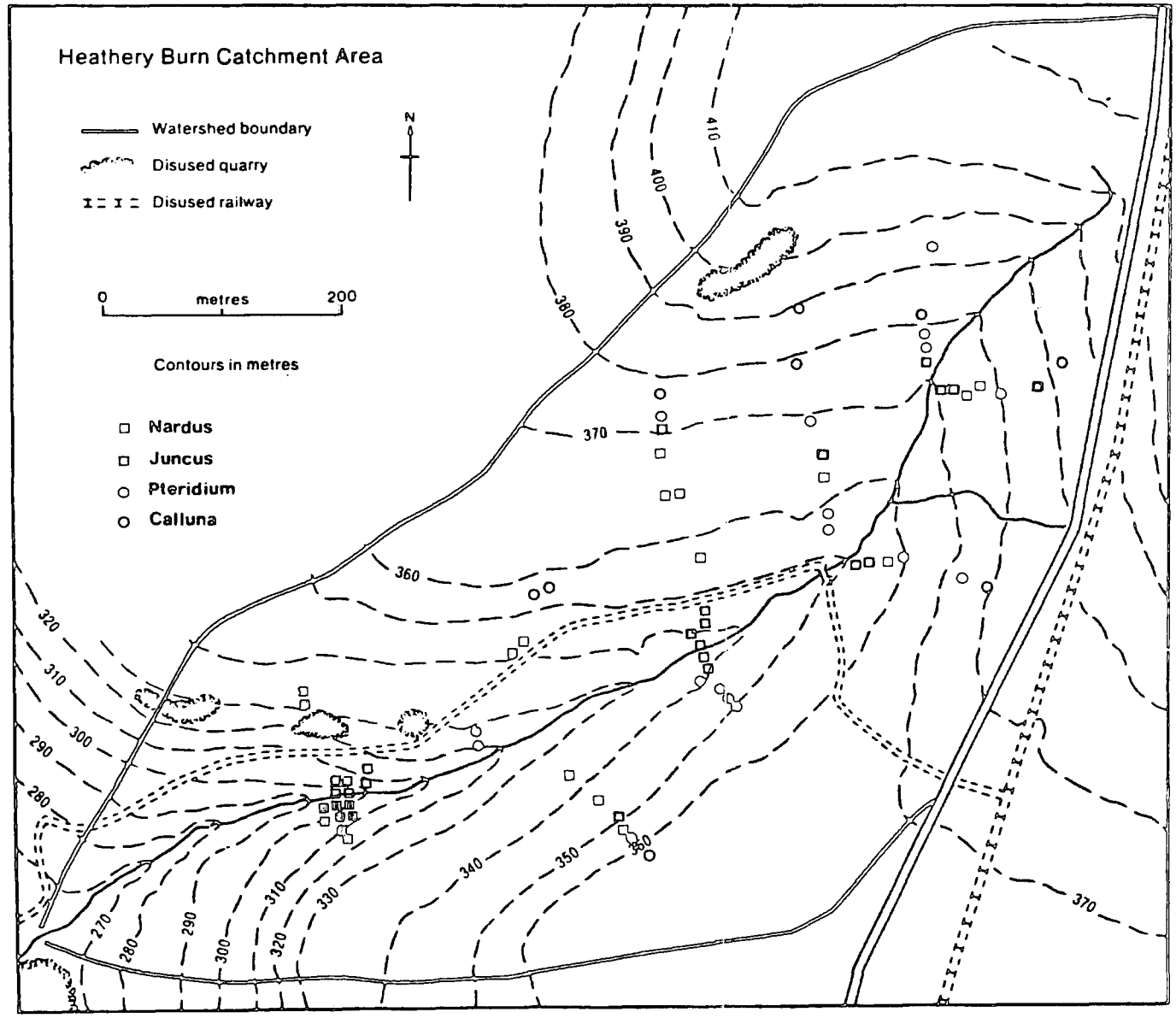

Figure 8.3 Spatial distribution of S.M.M. rate measured from Anderson's Tubes.

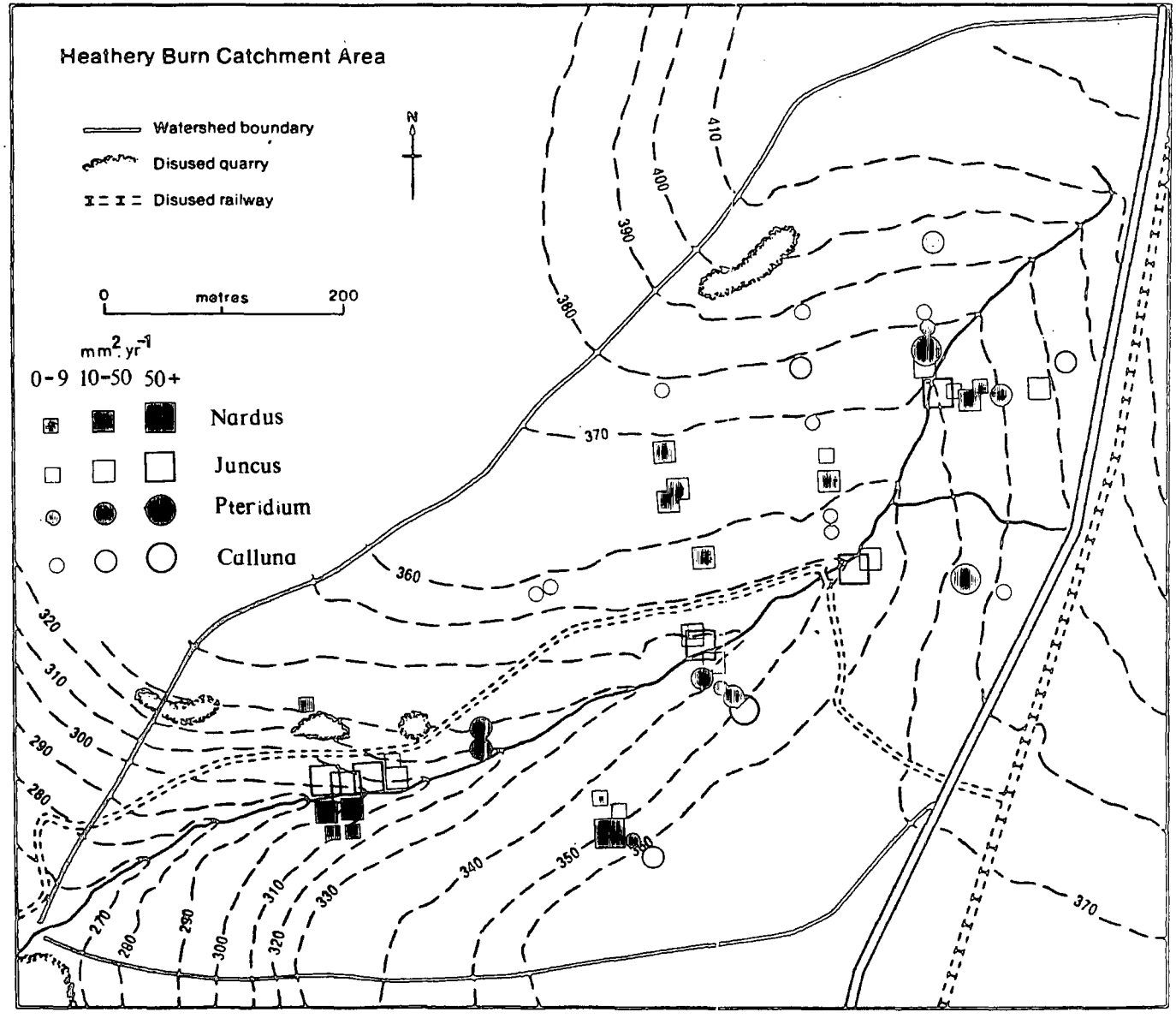

the soil mass at depth. These sites are missing from figure 8.3.

The pattern of movement shown in figure 8.3 does not represent a simple cascade of sediment transported downslope at a rate determined by a function of gradient. The field experiment described in Chapter 7 incorporates slope gradient as an important explanatory variable, however, the experiment may not account for the adjustment of slopes to a position of relative stability, either to its angle of repose or, by the anchoring of soil by vegetation. Consider an imaginary stepped slope profile in which sediment is distributed evenly over the slope and the only transporting process is S.M.M. (see figure 8.4). The profile might develop initially with high rates of movement associated with steep slopes, all other factors being equal, but through time the supply of transportable sediment will wane and so downslope gradients will gradually lessen as sediment accumulates in hollows and swales. In the latter case movement rates become dependent upon the rate of removal of sediment from the base of the profile, but a realistic analog would also incorporate natural weathering products and hydrological complexities. Although appearing simple, this model of slope evolution does highlight a number of interesting slope responses.

(i) Soil consistency will change progressively downslope - probably with its size distribution becoming skewed towards the size range most susceptible to S.M.M.

(ii) Where bluffs persist as landforms they retain high rates of S.M.M. which are only limited by the supply of transportable sediment.

(iii) As hollows fill and gradients decrease, local moisture and slope factors become more important than slope angle in controlling rates of S.M.M.

(iv) The rate of S.M.M. averaged over the profile will decrease unless sediment removed at the base of the slope maintains gradients sufficiently

Figure 8.4 Development of a hypothetical slope profile

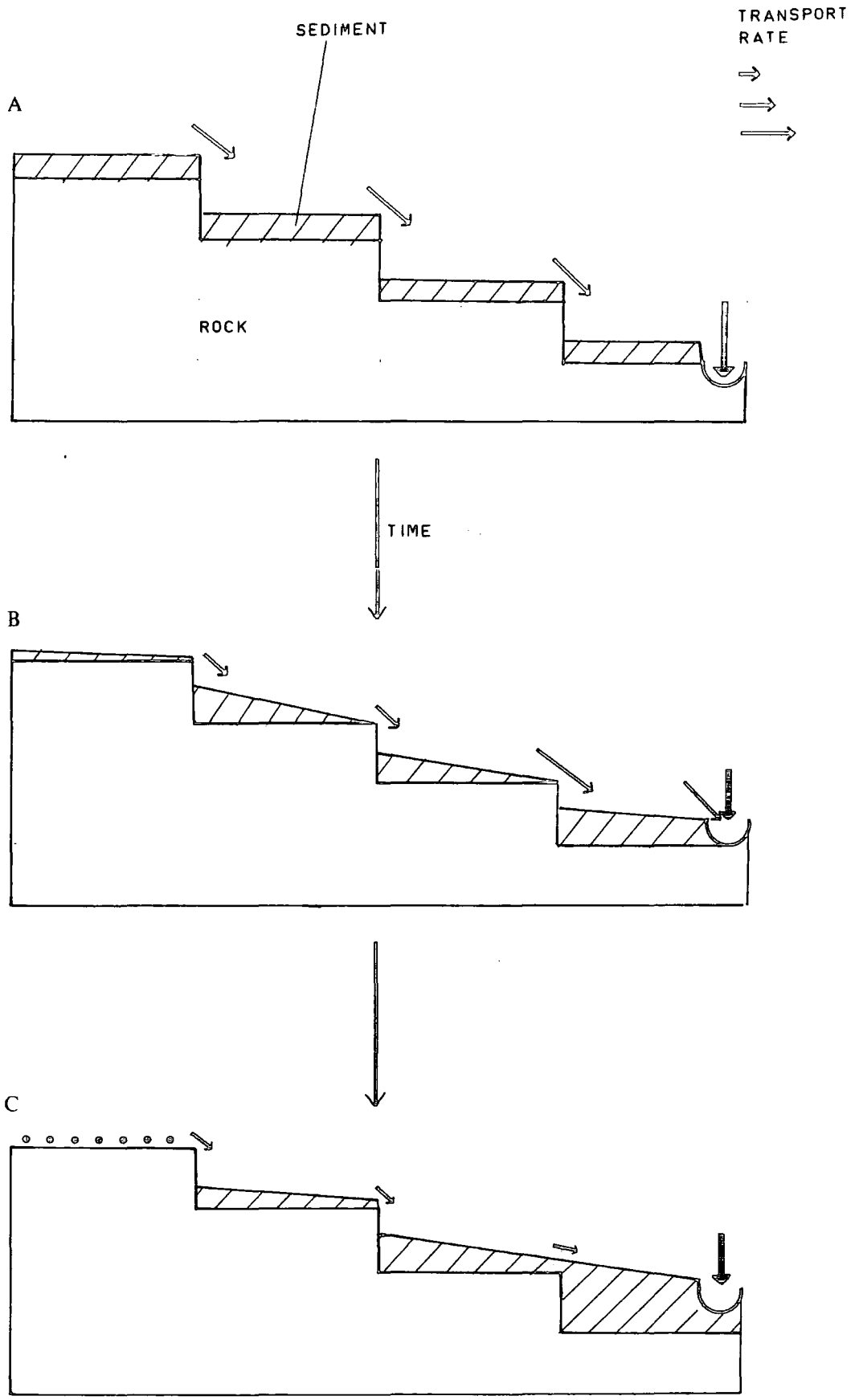

steep to prevent sediment accumulation.

If hillslope profiles in the Heathery Burn catchment area have developed in this way then the bi-factorial experiment described in Chapter 7 will not account for the following geomorphological factors because it assumed slope angle and vegetation cover to be additive effects.

(i) Low rates of movement may be observed on steep slopes because the angle of repose has adjusted to course granular sediments.

(ii) Very low rates of movement may occur on gentle slopes because the supply of susceptible sediment has become exhausted.

(iii) Very high rates may occur on gentle slopes where stream incision removes basal material thus causing instability.

Fluvial processes are difficult to quantify because they vary in magnitude, intensity and persistence in both space and time. Predicting the activity of S.M.M. through time is as important as understanding its spatial distribution because its effectiveness as a denudational agent can only be considered in the long term.

Figure 8.5 summarises the time series observed for an eighteen month measurement period for all vegetation and slope angle classes using 15cm Inclinometer pegs. The results of the time series analysis in chapter 7 showed that many of the sites displayed linear trends but that vegetation type strongly influenced this pattern. Fitting non-linear trends gave some evidence that short term variation in factors such as soil moisture and field shear strength could be important in understanding the details of the series. Frequency distributions for six selected time periods in figure 8.5 show a steady increase in mass movement through time. However the distributions show positive skewness increasing with time showing a large spread of movement rates. The majority of sites show a consistent pattern which suggests that a median annual rate of movement is a meaningful result. Future research might consider temporal variation

Figure 8.5

Frequency distributions of 15cm inclinometer pegs for six selected time intervals

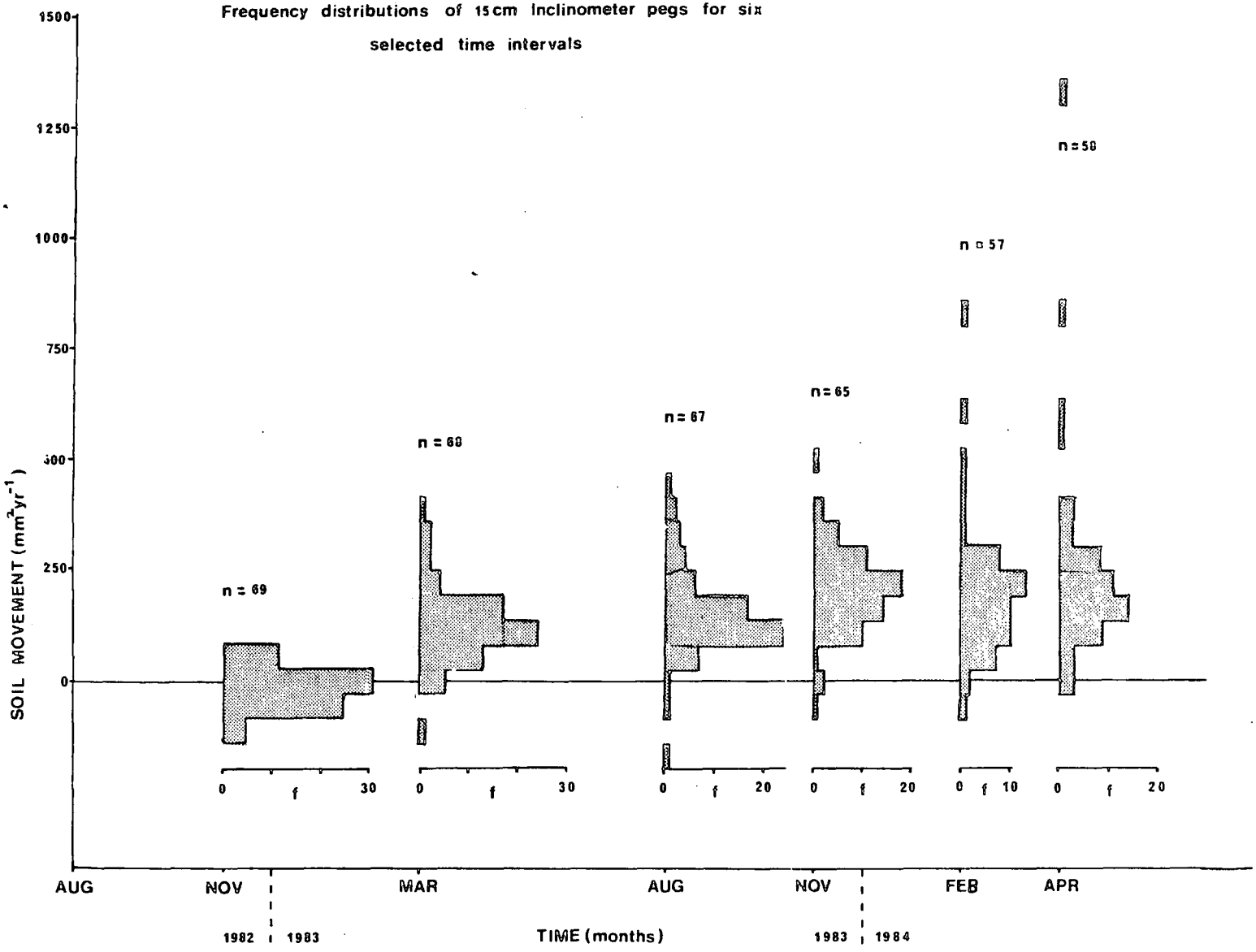

in S.M.M. in more detail since the results obtained in this thesis suggest that Inclinometer pegs give accurate and consistent measurements. In addition, non-linear smoothing of the series provides a useful technique for examining the influence of soil and other physical variables on S.M.M.

A major limitation of instruments which measure relative S.M.M. is their inability to detect accurate changes in movement with depth. Instruments that do allow estimation of the displacement-depth profile, such as those developed by Young(1960), Rudberg(1962), Finlayson(1976) and Rashidian(1986), are particularly valuable since the data can then be tested against theoretical models. Figure 8.6 shows four theoretical models of mass movement. These are based upon the assumption of uniform bulk density throughout the profile: apparent viscosity increases as a function of depth due to the weight of overburden. Profile A, an exponential decay curve, describes a process which decreases in effectiveness from the air-soil interface representing disturbance events such as wetting and drying or freezing and thawing. Profile B, a modified exponential decay curve, describes a process where effective shear stress represents an important control over movement (Carson and Kirkby 1972). Profiles C and D represent viscous flows with differing boundary conditions. Profile C, although identical in form to profile B, is derived from a viscous flow law (Allen 1982). Profile D represents a case where an abrupt change in material imposes a sharp lower boundary to the flow giving a region of shear flow and an upper region of plug flow (Allen 1982). Friction at the air-soil boundary is assumed negligible; however, this might not hold true were a snow or ice cover present.

It is clear from figure 8.6 that in the absence of distinct shear planes or complex boundary conditions, the mechanisms of particulate shearing and viscous flowing cannot be separated using predicted displacement-depth profiles. However, data were collected from Young's

FIGURE 8.6 Four theoretically predicted soil movement - depth curves and four empirically derived curves from Young's pits.

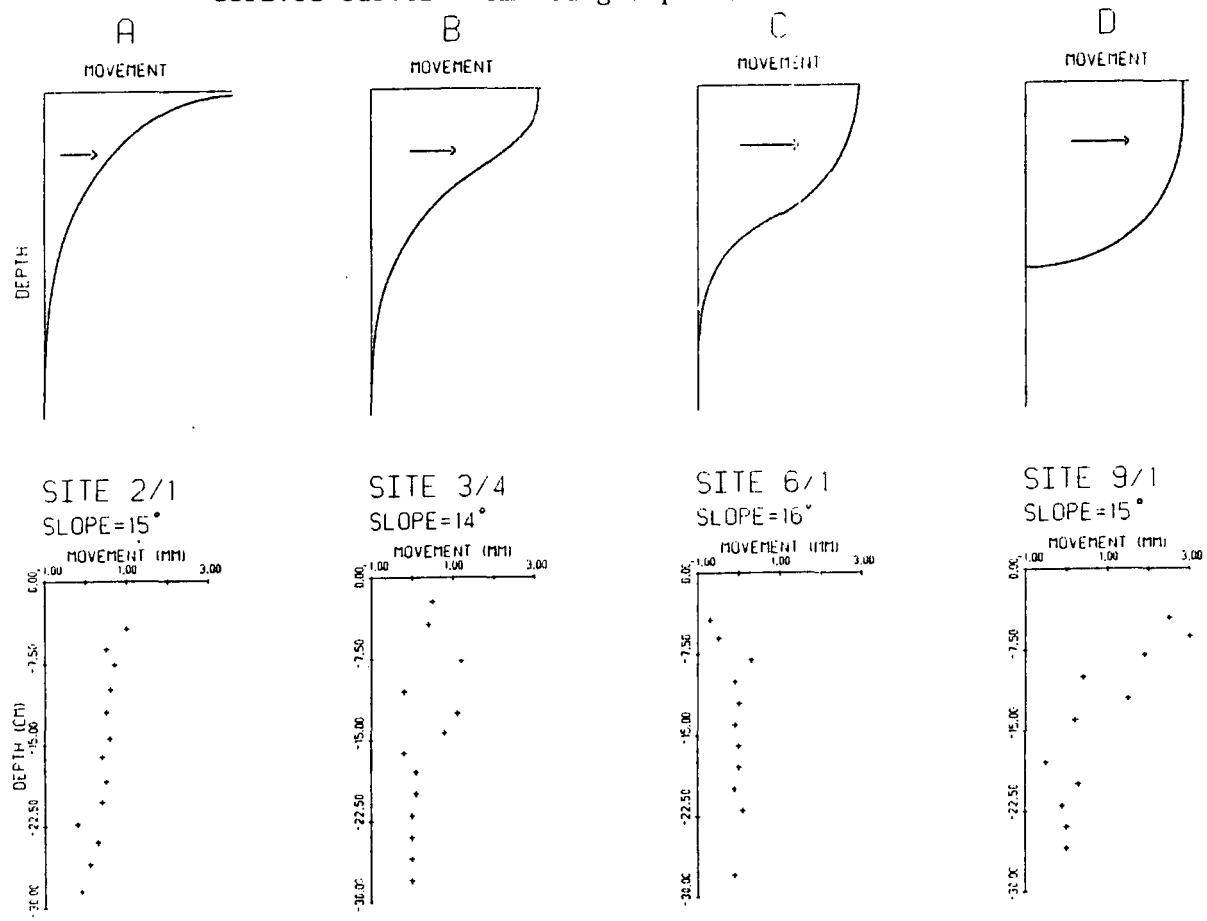

pits (Young 1960) in order to examine the nature of depth profile in the catchment area. Considerable problems were encountered when recovering the positions of the buried rods accurately. Each rod was inserted into the soil pit by passing it through a perspex plate which had each hole correctly positioned. The measurement procedure involved excavation of the rods and this seemed to be very imprecise. Four of the profiles for which most of the small welding rods were recovered are shown in figure 8.6. The sites presented are all taken from the *Juncus* vegetation class and from the third slope class. Therefore, they might be expected to show similar profiles as well as uniformity of soil properties. The pits were left undisturbed for two years before re-excavation.

The recorded profiles show no consistent agreement with any of the theoretical curves, but they indicate mean volumetric rates of 200-300 mm^2/yr with most of the movement confined to the upper 20cm of the soil profile. Maximum movement occurs between 5 and 10 cm below the surface before declining sharply with depth. Near surface movement appears erratic, perhaps indicating instrument unreliability in this zone. This would lead to serious inaccuracies in soil displacement estimation if the end points were used in the calculation of volumetric movement.

Movement mechanisms cannot be identified by comparing theoretical and empirical displacement-depth curves at this site because more variance exists within the observed profiles than occurs among the theoretical profiles.

Figure 8.7 summarises the empirical observations of S.M.M. in the Heathery Burn catchment area. The data represent median volumetric movement from Inclinometer pegs and from Anderson's tubes. These instruments were selected to give a relative measurement of S.M.M. and so these rates cannot be taken to represent the total mass movement rates within the catchment. The diagram clearly indicates that Inclinometer

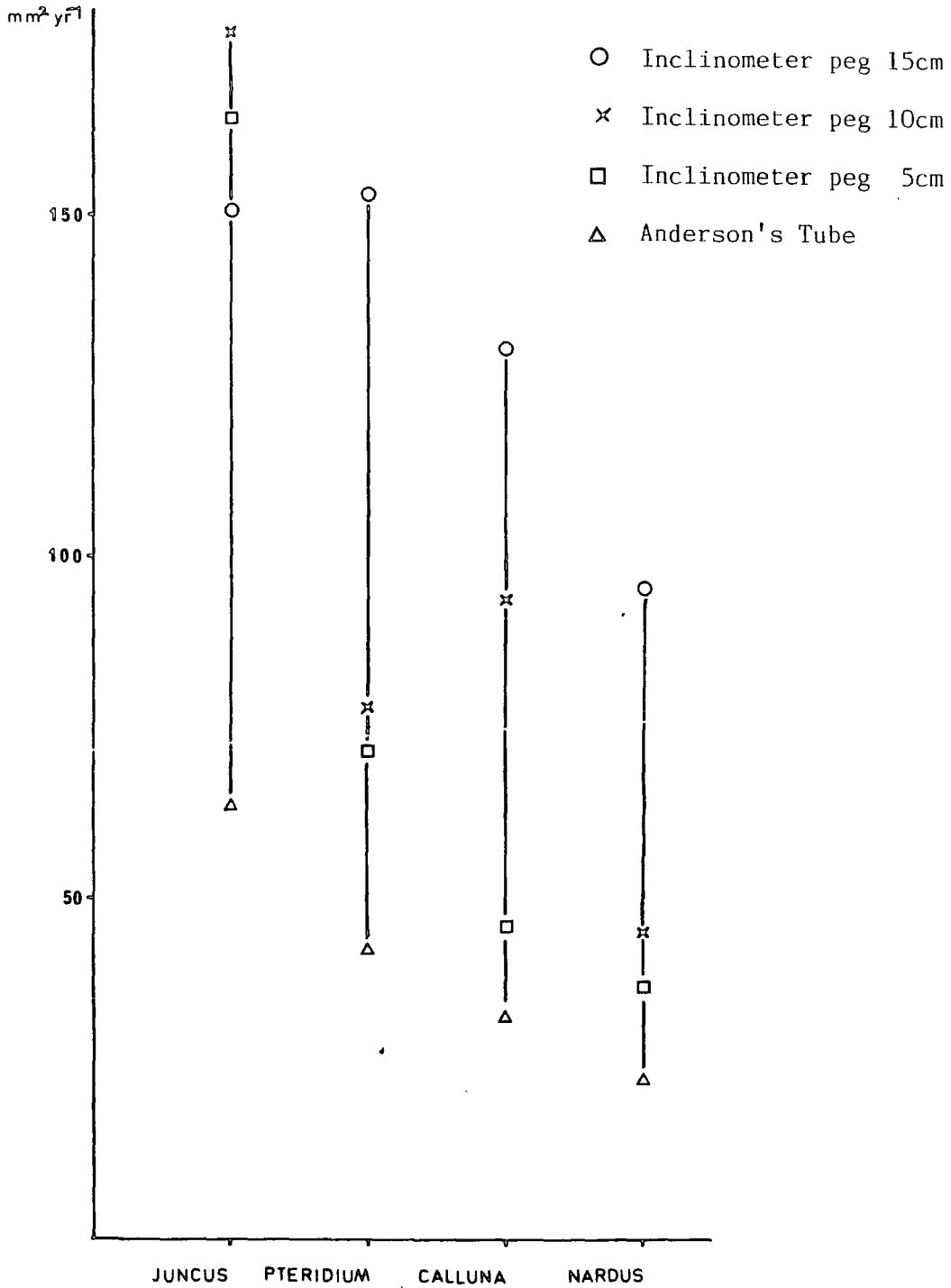

Figure 8.7

ANNUAL S.M.M. RATE FOR FOUR INSTRUMENTS AND FOUR VEGETATION CLASSES (MEDIAN RATE FOR ALL SAMPLES).

pegs give larger readings than the tubes. The tubes are inserted to a depth of 30cm and so this suggests that the upper 15cm of the soil are most important for S.M.M. activity. Figure 8.7 also summarises the importance of vegetation cover as a control over S.M.M.

The following two sections describe stratigraphic and sedimentological techniques which give supplementary evidence for S.M.M. activity in the field and methods for assessing its activity experimentally.

8.2 Relative dating of slope deposits

Interpretation of slope deposits is often hindered by inadequate methods for assessing their age. Deposits in the Heathery Burn catchment area have been shown to have accumulated in hollows at the base of the slopes. These may have been deposited there by ice of Devensian age; however, the stratigraphy will have been modified by downslope transportation of material since deglaciation.

At one site in the upper part of the catchment area an eroded stream bank revealed two distinct organic layers intercalated with dark brown silty clay sediment. These organic layers and the surrounding sediments were sampled for included pollen which could give an indication of the relative age of burial since the vegetation history of the Northern Pennines has been documented in detail by previous researchers (Raistrick and Blackburn 1932; Godwin 1975; Turner and Hodgson 1979, 1981). Several processes may account for the burial of these organic layers:

(i) Organic soil buried by solifluction deposits.

(ii) Organic soil buried by accumulated wash and creep deposits

(iii) The material may be a complex and include deposits of various ages. For example, bogburst events are known to deposit a mixed peat sequence over a wide area.

(iv) The organic material may represent channel deposits relict from previous lateral migration.

(v) The material which buries the organic layers may have been derived from local disturbance caused by road or railway construction some 100m upslope.

Investigation of the pollen content in both the organic and inorganic units in the sedimentary sequence should give an indication of the environment at the time the soil was buried and the likely mode of deposition of the inorganic material. For example, soliflucted material should not contain a high proportion of pollen since vegetation would have been sparse during the late-glacial. On the other hand, pollen could be incorporated into mineral soil by biotic mixing and by through-flow if the relative rate of material deposition were slow.

The stratigraphy of the site consists of a basal material of dark brown clay silt; a black, well humified peat; a dark brown silty clay; a black, moderately humified peat; a thin coarse gravel deposit; a dark brown silty clay with some included sand lenses. Above 1m the material was a silt clay sand. The section was cut back 30cm before being sampled in a monolith tin.

All samples were prepared by standard procedures including pretreatment with NaOH and boiling in HF to remove silica then strained with Saphronin and mounted in silica gel. The slides were not fixed in order that grains could be rotated under the cover slip as an aid to identification.

Lycopodium spores were introduced as an exotic type of known concentration, to be used as a reference with which to compare the frequencies of other taxa. This is termed absolute pollen analysis.

Figure 8.8 is a diagram of pollen concentration for the buried soil horizon and adjacent deposits. The bars on the diagram represent the

Figure 8.8 Pollen concentration diagram for buried soil horizon and associated deposits.

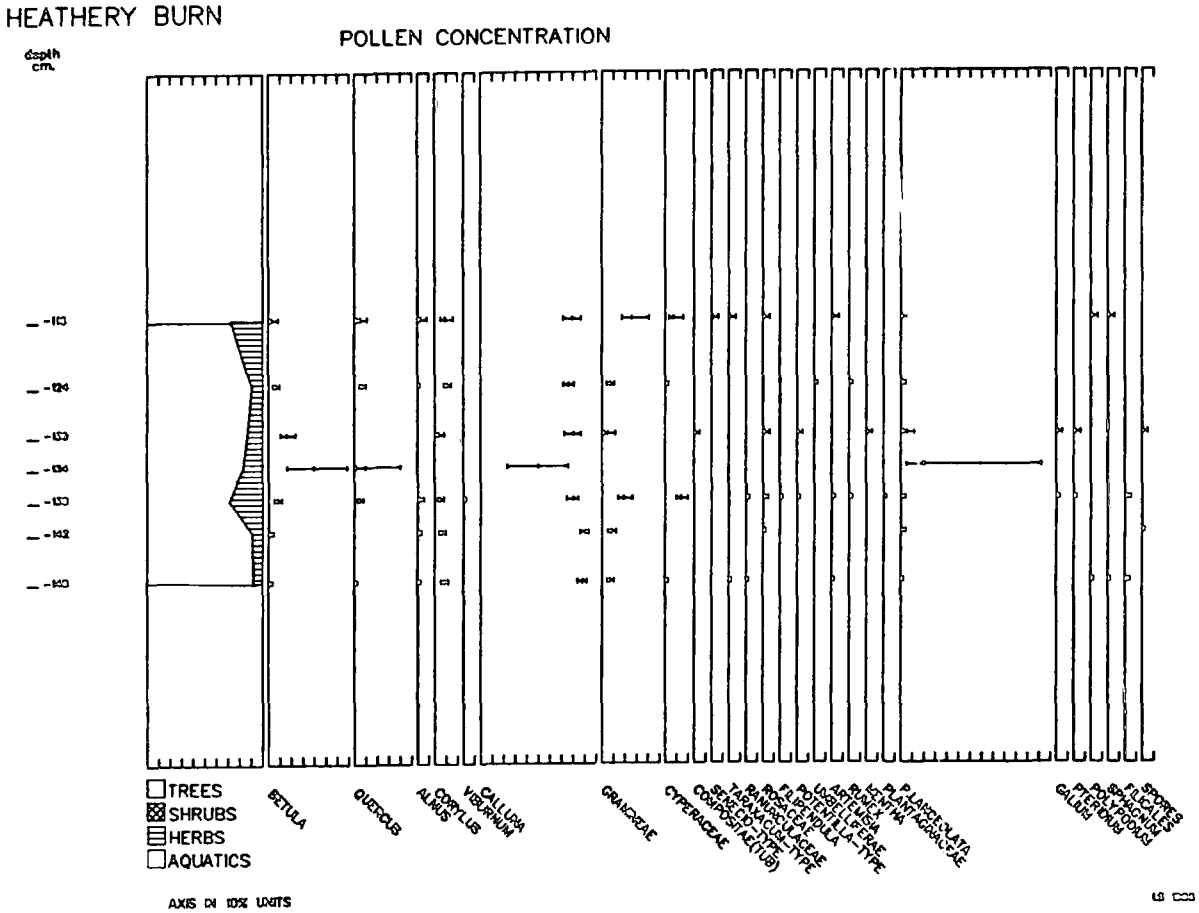

Figure 8.9 Valley transect across hillslope profiles 1 and 2 showing the relative depth of slope hollow infill.

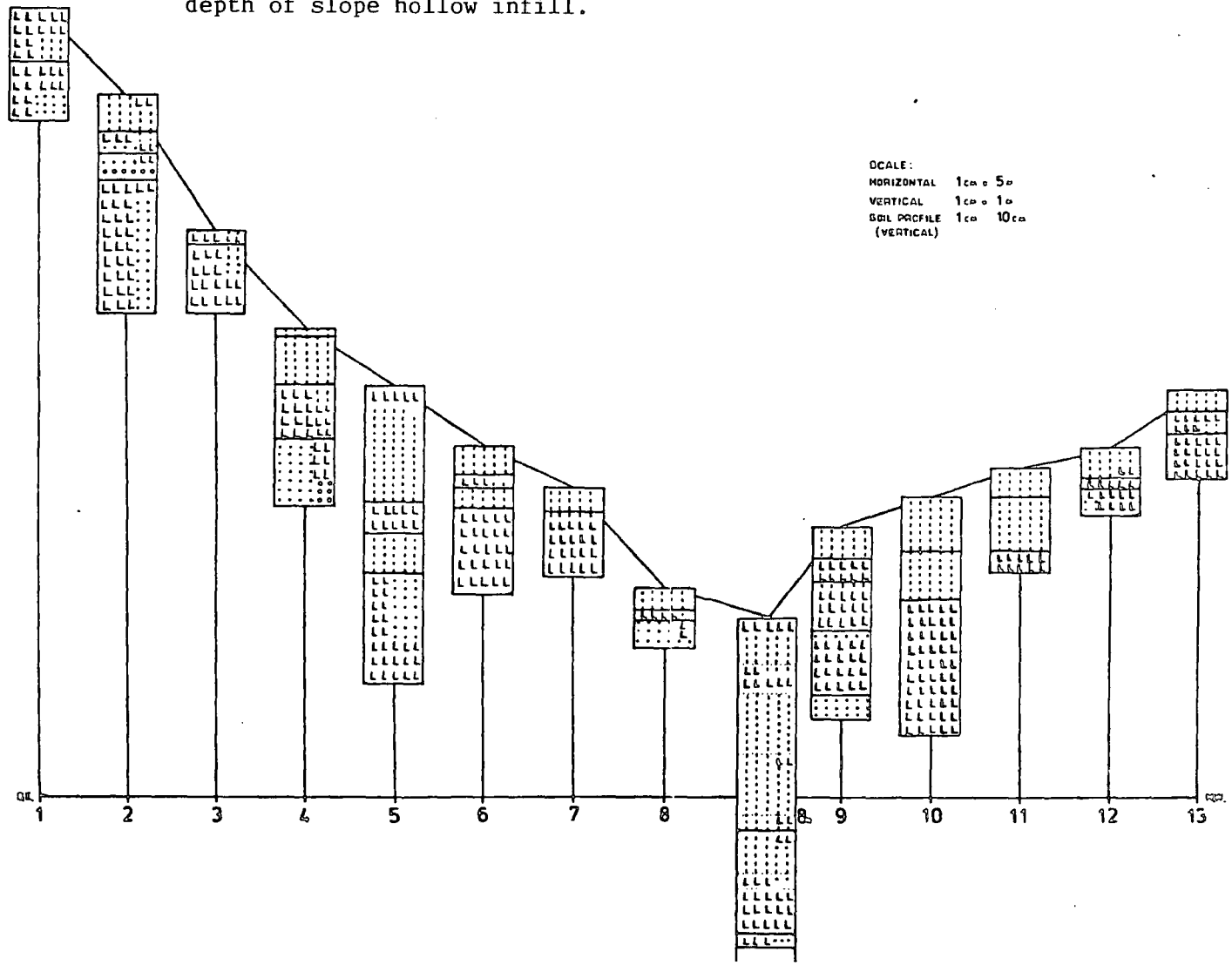

mean pollen count and one standard error either side of the mean. The diagram has several notable features:

(i) Generally low levels of pollen at all levels.

(ii) The dominant taxon is *Calluna vulgaris* which is associated with open moorland environments such as is present today.

(iii) Pollen concentrations appear remarkably consistent throughout all the levels counted, within both organic and inorganic horizons.

(iv) Tree pollen is virtually absent from all levels except the buried organic horizon. Of tree species counted, birch, oak and elm do not grow in the locality of Heathery Burn today but they are found in pollen rain.

These results are most easily interpreted as a soil buried in recent times because of the abundance of *Calluna* pollen. In addition, the diagram does not show levels which correspond with late or mid-Flandrian levels in diagrams produced by Turner(1979,1981). The abundance of shrub pollen, combined with the lack of tree pollen, indicates that the soil must have been buried as the land has been extensively cleared of trees since iron-age times. No further detail can be derived without radio-carbon dating.

A valley transect across the catchment area following the lines of hillslope profiles 1 and 2 revealed the presence of hollows filled with fine-grained sediments (see figure 8.9). This shows that slope form has been considerably modified by fluvial processes since the late-Devensian and that infilling has occurred to a depth of several metres, particularly at the base of the slopes. Thin soils occur (see bore-holes 3, 7, 8, 12 and 13) where resistant sandstone benches outcrop and these are often associated with steep well-drained slopes. It is clear from figure 8.9 that steep gradients, associated with hollows and bluffs in the original landsurface, have been reduced through time as sediment has accumulated in hollows and at the base of the slope. Fine material in particular, has accumulated

at the base of these hollows. Fluvial processes have modified the form of the catchment and the grain size of the surface material: both of these factors affect S.M.M. rates.

8.3 Experimentation

Theoretical predictions of the movement of spheroidal particles in a viscous medium were discussed in chapter 5 because they may provide a method of distinguishing among movement mechanisms. Techniques derived for other applications investigate the degree to which the primary (or original) fabric of the deposit is altered by subsequent deformation. Fabric shape has been investigated by Mills(1983) in the context of S.M.M. using field observations. In this study it was decided to investigate the micro-fabric of soils while subjected to slow rates of direct shearing in the laboratory. The resultant fabic shape was not compared quantitatively with the original but visual comparison reveals interesting features which suggest that the techniques of micro-fabric analysis may be of value in further research. For example, figures 8.10 and 8.11 show scanning electron micrographs of a sandy-silt sample taken from site 2/1. The sample was taken directly from the field, from a depth of 30cm and its orientation carefully noted. A method of critical point drying was used to extract the moisture from the sample so that the structure of the fabric would not be disturbed by shrinkage during drying. Each sample was splutter coated with 10 Å of gold to avoid a build up of charge on the sample surface. The rough nature of soil samples makes it difficult to produce an even gold coating, which causes striping and focusing problems in the final images. Figure 8.11 shows this effect with 40μm images.

Figure 8.10 shows the fabric shape for the sample (site 2/1) imaged before a strain-controlled direct shear test as described in Chapter 6.

Figure 8.10 Scanning electron micrographs of soil sample 2/1 showing fine sand and silt particles embedded in an illite clay matrix.

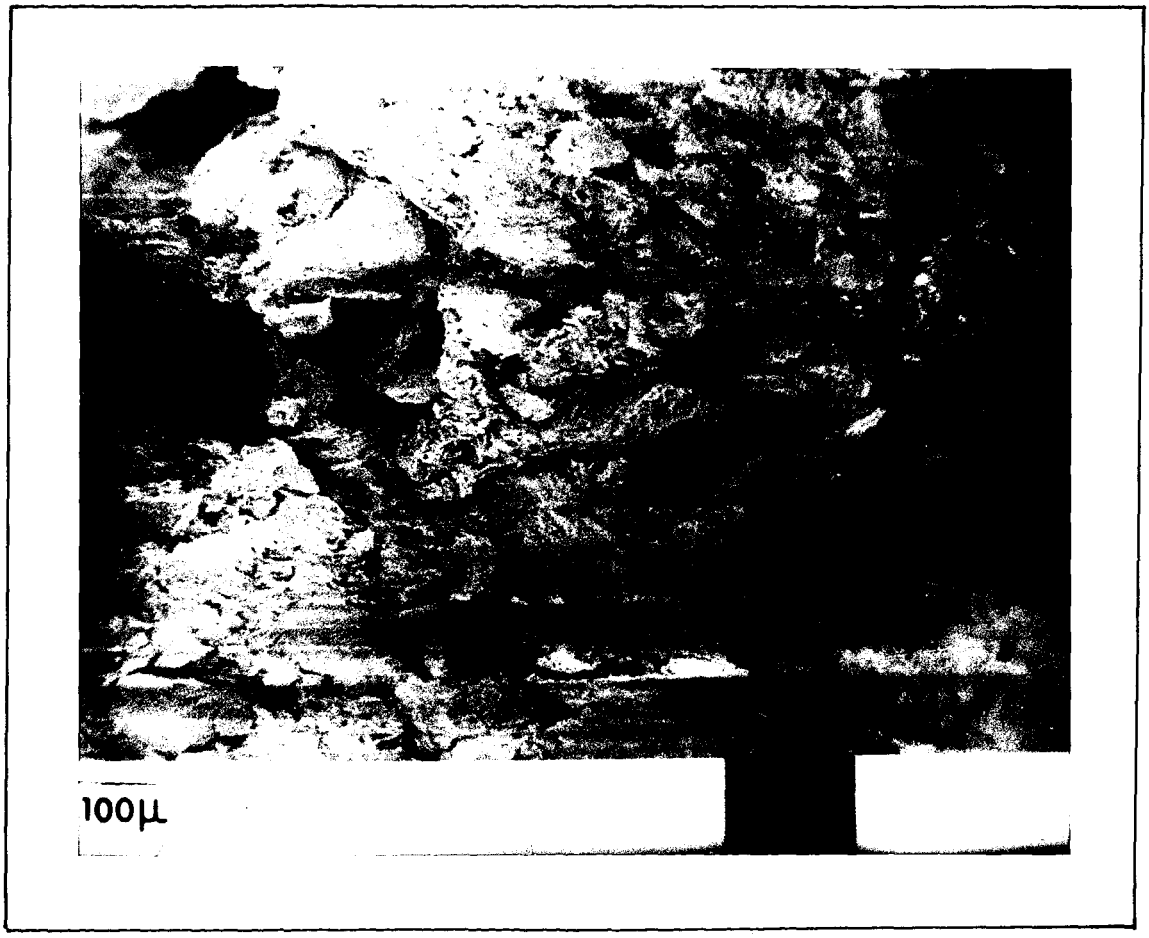

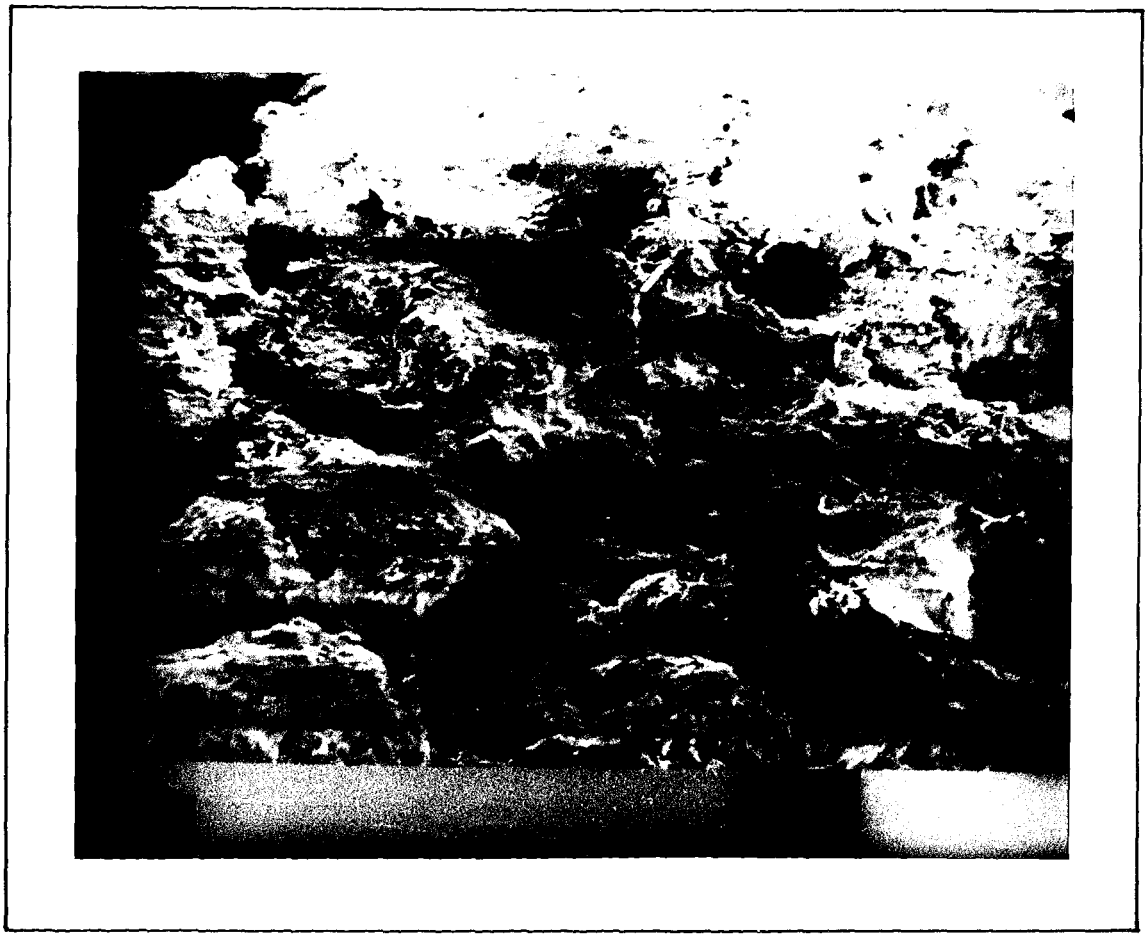

Figure 8.11 Scanning electron micrographs of soil sample 2/1 imaged following a strain-controlled creep-shear test showing dilation and disruption of the primary fabric.

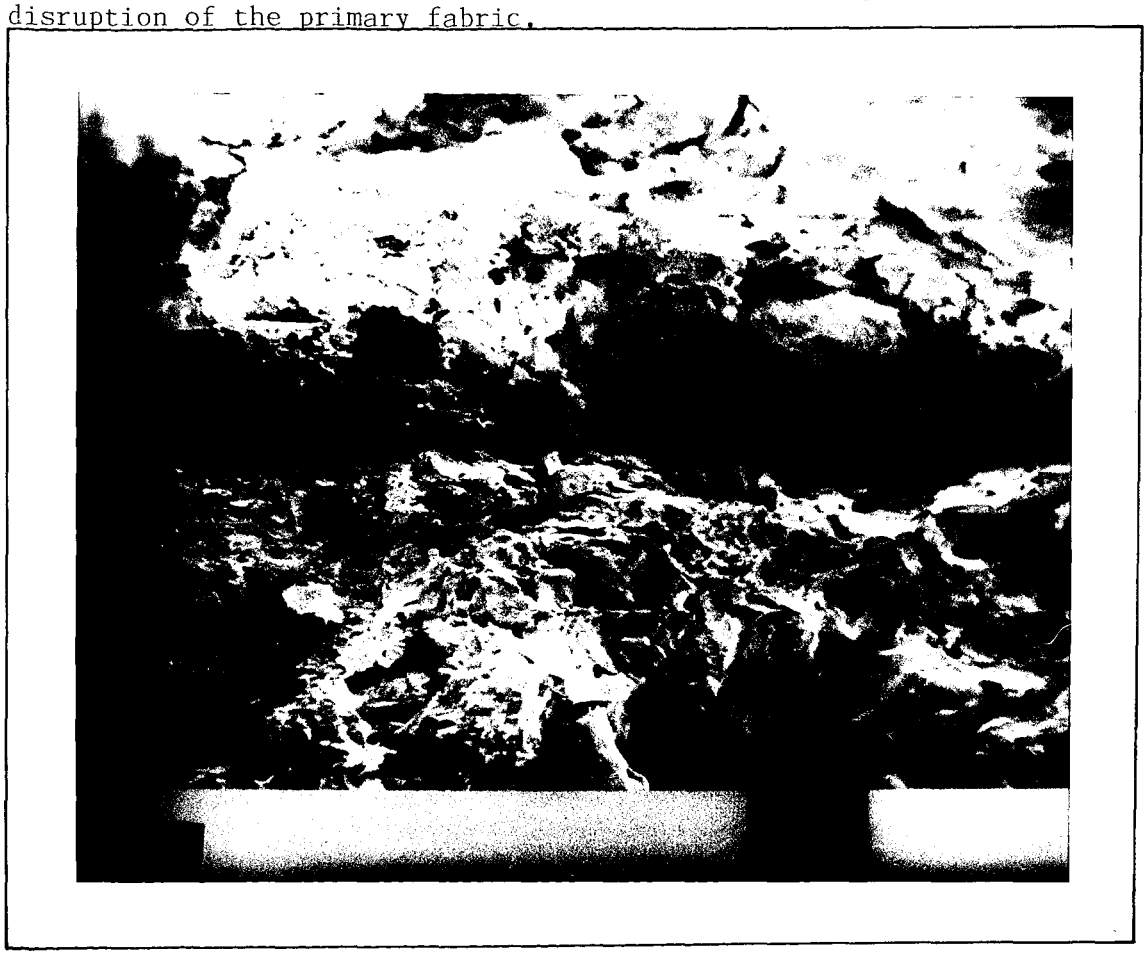

The fabric consists of small sand grains embedded in a matrix of silt and clay particles. The clay coating on the sand particles can be seen on the 40μm image as a wavy structure. The same sample was later imaged close to the shear plane after the test; this corresponds with figure 6.11. After shearing the sample shows evidence of considerable dilation and readjustment of the fabric. In particular, the close-knit clay material has been disrupted and resembles a series of plates with variable orientations. The upper image of figure 8.11 shows an area where there is a large amount of pore space and few inter-connecting silt or clay platelets; this may represent a shear plane. However, the lower image is typical of the region around the shear plane showing cha otic orientation.

Experimental work in the laboratory should be directed towards identifying the typical micro-fabric response to physical processes likely to cause S.M.M. It is particularly important to investigate the behaviour of samples under stress conditions that would normally be found in the field. Engineering work on soil samples rarely considers the effect of long-term application of low deviatoric stresses; however, such processes are of considerable importance in geomorphology.

8.4 Conclusions

This thesis has the following conclusions:

(i) The terminology of mass movement processes is confusing and inconsistent: the term S.M.M. is a helpful descriptive term that does not imply that the mechanism causing movement is known.

(ii) Laboratory simulation experiments of a shearing process using samples taken directly from the field show that soil fabric and plant rootlets play an important role in modifying soil strength by up to 50%.

(iii) Strain-controlled direct shear testing provides a useful threshold at which the soil exhibits time-dependent yielding (yield stress). This can be compared with the stress state of field samples in order to analyse their susceptibility to S.M.M. in the field.

(iv) In the field, a two-way additive linear model summarises S.M.M. rates thought to be influenced by slope angle and vegetation cover differences in the catchment area. The model is based on median measurements from Anderson's tubes and Inclinometer pegs taken from $1m^2$ sample plots. This explains between 35% and 50% of the variation in the data.

(v) Vegetation cover strongly influences the correlation between slope angle and S.M.M. This relationship is much clearer than in previous studies where analysis was not stratified by land-use or vegetation cover.

(vi) Correlations between S.M.M. rate and soil consistency variables are surprisingly weak. However, this might be explained in part by temporal changes in soil consistency within the catchment area. For example, measurements of soil shear strength at each sample site show considerable variation throughout the time period of this research.

(vii) Analysis of the temporal patterns of S.M.M. using Inclinometer peg data showed that the time-series of many sites could be explained by a linear model. On the other hand, sites which showed non-linear behaviour (investigated using smoothing techniques) showed that temporal variations in soil moisture and shear strength clearly affected S.M.M.

The above results provide an insight into a much mis-understood geomorphological process. If landscape development is to be understood fully then the mechanics of mass movement must be investigated in more detail. In addition, with the increasing exploitation of the landscape

by man, a clearer indication of the influence of variables, such as land-use and land-cover, on slope processes is imperative. It is hoped that this research will stimulate closer investigation of the fundamental slope processes and thereby lead to a clearer understanding of their mechanisms and operation within the landscape.

REFERENCES

ABRAHAM, P. S. (1877): Stone Rivers, Nature, 15: 431.

ABRAHAMS, A. D., A. J. PARSONS and P. J. HIRSH (1985): Hillslope gradient - particle size relations: evidence for the formation of debris slopes by hydraulic processes in the Mojave Desert.
Journal of Geology , 93: 347-357.

ALLEN, J. R. (1982): Sedimentary structures - their character and physical basis, Vol I. Elsevier Scientific Publishing Company, Amsterdam.

ALLEN, J. R. (1982): Sedimentary structures - their character and physical basis. Vol II Elsevier Scientific Publishing Company, Amsterdam.

ANDERSLAND and DOUGLAS (1970): Soil deformation rates and activation energies. **Geotechnique**, 20: 1-16.

ANDERSON, D. G. and K. H. STOKOE (1978): Shear modulus, a time dependent soil property in dynamic geotechnical testing (Wheeler S. B. ed) American Soc. for testing and materials, Spec. Tech. Pub., Phil, Pennsylvania, 654: 66-89.

ANDERSON, E. W. (1971): The nature, classification and formation of terracettes on certain hillslopes in Western Britain. Unpub. MA Thesis, University of Manchester.

ANDERSON, E. W. (1977): Soil creep. An assessment of certain controlling factors with special reference to Upper Weardale, England. Unpub. Ph.D Thesis, University of Durham.

ANDERSON, E. W. and N. J. COX (1978): A comparison of instruments for measuring soil creep. **Catena**, 5: 81-93.

ANDERSON, E. W. and N. J. COX (1984): The relationship between soil creep rate and certain controlling variables in a catchment in upper Weardale, northern England. In Burt, T. P. and Walling, D. E. (Eds.) Catchment experiments in fluvial geomorphology. Geo Books, Norwich.

ANDERSON, E. W. and N. J. COX (1986): An asssessment of soil movement time series from Brandon, County Durham , U.K. Z. Geomorph. N.F. Suppl. Band, 58:145-154.

ANDERSON, E. W. and B. FINLAYSON (1975): Instruments for measuring soil creep. BGRG Tech.Bull., 16.

ANDERSSON, J. G. (1906): Solifluction: a component of subaerial denudation. Journal of Geology, 14: 91-112.

ARCHER, J. R. (1975): Soil consistency. In Soil physical conditions and crop production. Tech. Bull. Soil Survey of England and Wales, 29: 289-297, M.A.F.F., London

ATKINSON, K. (1968): An investigation of the pedology of Upper Weardale, Co. Durham. Unpublished Ph.D. thesis, University of Durham.

AUZET, A. V. (1982): La mesure du creep : mise au point bibliographique. Recherches Geographiques a Strasbourg 19-21: 211-218.

AUZET, A. V. (1985): La Reptation: Mesure in site en relation avec les conditions hydriques et thermiques du sol (site forestier dans les Vosges granitiques). These de Doctorate de l'Universite Louis Pasteur, Strasbourg 1.

AVERY, B. W. (1980): Soil classification for England and Wales (higher categories), Technical Monograph No. 14, Soil Survey, Harpenden, England.

BAGNOLD, R. A. (1956): The flow of cohesionless grains in fluid. Phil. Trans. Roy. Soc. Lond. A, 249:235-297.

BAGNOLD, R. A. (1966): An approach to sediment transport from general physics. U.S. Geol. Surv. Prof. Paper, 5: 223-241.

BARDEN, L., A.O. MADEDOR and G.R. SIDES (1969): Volume change characteristics of unsaturated clay. J. Soil Mech. Ground Divn., Proc. Am. Soc. Civ. Eng. 95 SM 1:33-53

BARR, D. J. and D. N. SWANSTON (1970): Measurement of creep in a shallow slide prone till soil. Amer.J.Sci. , 269(5): 467-478.

BENEDICT, J. B. (1976): Frost creep and gelifluction features: a review. Quaternary Research, 6: 55-76.

BISHOP, A. W. (1966): The strength of soils as engineering materials. Geotechnique, 16: 2: 91-128.

BJERRUM, L. (1968): Progressive failure in slopes of overconsolidated plastic clay and shales. **J. Soil Mech. Ground Divn.**, Am. Soc. Civ. Eng. 93 SM5: 1-49.

BLACK, R. F. and T. D. HAMILTON (1972): Mass-movement studies near Madison ,Wisconsin. In Morisawa (Ed) Quantitative Geomorphology: Some aspects and application. PODC Second annual geomorphology symposium series. Binghamton State University, New York. 121-179.

BOULTON, G. S. (1967):The development of a complex supraglacial moraine at the margin of Sorbreen N.Y. Friesland, Vestspitzbergen. **J. Glaciol.**, 6: 717-735.

BOUGHTON, W. C. (1967): Plots for evaluating the catchment characteristics affecting soil loss, 1: design of experiments. **N. Z. J. Hydrology**, 6: 113-119.

BRITISH STANDARD 1377. (1975): Methods of testing soils for civil engineering purposes, British Standards Institution, London.

BRUCKL, E. and A. E. SCHEIDEGGER (1973): Application of the theory of plasticity to slow mud flows. **Geotechnique**, 23: 101-107.

BRUNNER, F.K.,E. GERBER and A.E. SCHEIDEGGER (1975): On the mechanism of surficial creep in hilly regions.
Rivista Italiana di Geofisca, 2(1): 53-57.

BURGESS, I. C. and D. W. HOLLIDAY (1979): Geology of the country around Brough under Stainmore. Geological survey of G.B., HMSO, London.

BURROUGHS, E. R. and B. R. THOMAS (1977): Declining root strength in Douglas - fir after felling as a factor in slope stability. U.S.D.A. Forest Service. Research paper INT 190. P1-28.

CAINE, T. N. (1965): Movement of low angle scree slopes in the Lake District, Northern England. Revue de Geomorphologie Dynamique, 15: 171-177.

CAINE, T. N. (1971): A conceptual model for alpine slope process study. Arctic and Alpine Research, 3: 319-329.

CAINE, T. N. (1976): A uniform measure of subaerial erosion. Geol. Soc. Am. Bull., 87:137-140.

CAMPANELLA, R. G. and J.K. MITCHELL (1968): The application of rate process theory to the creep behaviour of sensitive clay soils. Geotechnique, 18: 202-232.

CAMPBELL, D. J. (1976): Plastic limit determination using a drop-cone penet meter. J. Soil Sci., 27, 295-300.

CAMPBELL, D. J., J. V. STAFFORD and P. S. BLACKWELL (1980): The plastic limit, as determined by the drop-cone test, in relation to the mechanical behaviour of soil. J. Soil Sci., 31: 11-24.

CARSON, M. A. (1967): The magnitude of variability in samples of certain geomorphic characteristics drawn from valley side slopes.
Journal of Geology, 75: 93-100.

CARSON, M. A. (1969): Models of hillslope development under mass failure. Geographical Analysis, 1: 76-100.

CARSON, M. A. and M. J. KIRKBY (1972): Hillslope form and process. Cambridge University Press, London.

CARTER, C. S. and R. J. CHORLEY (1961): Early slope development in an expanding stream system. Geological Magazine , 98: 117-129.

CASAGRANDE, A. (1932): Research on the Atterberg limits of soil. Public Roads, 13: 121-136.

CASAGRANDE, A. (1936): Characteristics of cohesionless soils affecting the stability of slopes and earth fills. J. Boston Soc. Civil Eng., 23: 13-32.

CASAGRANDE, A. (1948): Classification and Identification of soils. Trans. A.S.C.E., 113: 901.

CHAMBERS, J. M., W. S. CLEVELAND, B. KLEINER, and P. TUKEY (1983): Graphical methods for data analysis. Duxbury Press, Boston.

CHANDLER, R. J. (1972): Periglacial mudslides in Vestspitzbergen and their bearing on the origin of fossil solifluction shears in low-angled clay slopes. Q. J. Eng. Geol., 5: 223-241.

CHANDLER, R. J. (1977): The application of soil mechanics methods to the study of slopes. In Applied Geomorphology, J. R. Hails p 157-182, Elsevier, Oxford.

CHANDLER, R. J. (1982): Two early contributions to the study of slopes. Geotechnique, 32: 553-554.

CHANDLER, R. J. and M. J. POOK (1971): Creep movements in low gradient slopes since the late glacial. Nature, 229: 399-400.

CHORLEY, R. J. (1964): Geomorphological evaluation of factors controlling shearing resistance of surface soils in sandstone. J. Geophysical Res., 69: 1507-1516.

CHORLEY, R. J., A. J. DUNN and R. P. BECKINSALE (1964): The history of the study of landforms. Methuen, London.

CHOWDHURY, R. N. (1978): Slope analysis: Developments in geotechnical engineering vol 22. Elsevier, Amst, Oxford, New York.

CHURCH, M. (1981): On experimental method in geomorphology. Paper presented to the I.G.U. Commission on field experiments in geomorphology, U.K. meeting, August 1981, Exeter.

CLAPPERTON, C. M. (1966): The influence of topography on the superimposition of glacial meltwater streams. Brit. Geomorph. Res. Group Occ. paper 3, 13-18.

CLARKE, J. V. (1976): The origin and development of terracettes. Unpub. Ph.D thesis, University of Salford.

CLEVELAND, W. S. (1979): Robust locally weighted regression and smoothing scatterplots. J. Amer. Stat. Ass., 74: 829-836.

COBBOLD, P. R. (1976): Fold shapes as functions of progressive strain. Royal Soc. Phil. Trans. A 283: 129-188.

COLLINS, K. and A. McGOWN (1974): Form and function of microfabric features in a variety of natural soils. Geotechnique, 24(2): 223-254.

CORTE, A. E. (1963): Particle sorting by repeated freezing and thawing. Science ,142: 499-501.

COX, N. J. (1978): Hillslope profile analysis, Area, 10: 131-133.

COX, N. J. (1979): Models and methods in hillslope profile morphometry. Unpub. Ph.D. Thesis. Univ. of Durham.

COX, N. J. (1981): Hillslope profile determination and analysis. In A. Goudie (ed) Geomorphological Techniques. Allen and Unwin, London.

CRUSE, R. M. (1977): Effect of soil shear strength on soil detachment due to raindrop impact. Soil Sci. Soc. Am. J., 41: 777-781.

CULLING, W. E. H. (1963): Soil creep and the development of hillside slopes. Journal of Geology, 71: 127-161.

CULLING, W. E. H. (1965): Theory of erosion on soil covered slopes. Journal of Geology ,73 :230-254.

CULLING, W. E. H. (1981): New methods of measurement of slow particulate transport processes on hillside slopes. In Erosion and sediment transport measurement, 267-274. Proc Florence symp., IAHS Publn 133.

CULLING, W. E. H. (1983a): Slow particulate flow in condensed media as an escape mechanism: mean translation distance. In Rainfall simulation, runoff and erosion, J de Ploey (ed.): 161-190 Catena suppl. 4. Cremlingen: Catena Verlag.

CULLING, W. E. H. (1983b): Rate process theory of geomorphic soil creep. In Rainfall simulation, runoff and erosion, J. de Ploey (ed.): 191-214. Catena suppl .4. Cremlingen: Catena Verlag.

DAKESSIAN, S. (1981): Strength characteristics of root re-inforced soils. Unpub. Ph.D. Thesis. University of California, Berkeley.

DALRYMPLE, J. B. and C. Y. JIM (1984): Experimental study of soil microfabrics induced by isotropic stresses of wetting and drying. **Geoderma**, 34: 43-68.

DAVIS, W. M. (1892): The convex profile of badland divides. **Science**, 20: 245.

DAVISON, C. (1888): Note on the measurement of scree material. **Q. J. Geol. Soc. Lond.**, 44: 232-238

DAVISON, C. (1889): On the creeping of the soil cap through frost action. Geological Magazine 6: 255-261.

DAVIDSON, D. A. (1983): Problems in the determination of plastic and liquid limits of remoulded soils using a drop-cone penetrometer. Earth Surface Processes and Landforms, 8, 171-175.

DEMARS, K. R. and R. D. CHARLES (1982): Soil volume changes induced by temperature cycling. Can. Geotech. J., 19: 188-194.

DEMEK, J. (1967): Shift of rock fragments. Revue de Geomorphologie Dynamique, 17(4): 177-178.

DIETRICH, W. E. and T. DUNNE (1978): Sediment budget for a small catchment in mountainous terrains. Z. Geomorph.,Suppl. band, 29: 191-206.

DIETRICH, W. E., C. J. WILSON and S. L. RENEAU (1986): Hollows, colluvium, and landslides in soil-mantled landscapes. In ABRAHAMS, A. D., Hillslope Processes. Allen and Unwin, Boston.

DONOGHUE, D. N. M. (1986): Review and analysis of slow mass movement mechanisms with reference to a Weardale catchment, N. England. Z. Geomorph. N. F., Suppl. Band, 60: 41-54.

DUNCAN, J. M. and S. G. WRIGHT (1980): The accuracy of equilibrium methods of slope stability analysis. Engineering Geology, 16: 5-17.

DUNHAM, K. C. (1948): Geology of the north Pennine ore field; vol 1, Tyne to Stainmore. Mem. Geol. Surv. Gt. Br. H.M.S.O. London.

DUVAL, P. (1981): Creep and fabrics and polycrystalline ice under shear and compression. Journal of Glaciology, 27(95): 129-140.

DWERRYHOUSE, A. R. (1902): Glaciation of Teeside, Weardale and the Tyne Valley and their tributary Valleys. Q. J. Geol. Soc., 58: 572-608.

DYKE, L. D. (1979): Mechanisms of downhill creep in expansive soils. Unpub. Ph.D. Thesis, Texas A and M University.

DYLIK, J. (1967): Solifluxion, congelifluxion and related slope processes. Geografiska Annaler A. 49A(2-4): 167-177.

EMMETT, W. W. and L. B. LEOPOLD (1967): Slopes, processes, rates and amounts. Revue de Geomorphologie Dynamique, 17(4): 157-158.

EVANS, I. (1980): An integrated system of terrain analysis and slope mapping Z.Geomorph.,Suppl. Band, 36: 274-295.

EVANS, R. (1967): Inclinometers or T bars. Revue de Geomorphologie Dynamique, 17(4): 176-177.

EVANS, R. (1974): A study of selected erosion processes acting in slopes in a small drainage basin. Unpub. Ph.D. Thesis, University of Sheffield.

EYLES, R. J. and R. HO (1970): Rates of seasonal creep of a silty clay soil. Q. J. Eng. Geol., 8: 1-29.

EYLES, R. J. and R. HO (1970): Soil creep on a humid tropical slope. J. Tropical Geography, 31: 40-42.

FALCONER, A. (1970): An investigation of the surficial deposits of County Durham. Unpub. Ph.D Thesis. University of Durham.

FELIX, B. (1980): Le fluage des sols argileux. Etoide bibliographique. Rapp. Rech. Lab. Central, Ponts et Chaussees. Paris, 93:1-231.

FELTHAM, P. (1968): A stochastic model of creep. Phys. Stat. Sol., 30: 135-140.

FELTHAM, P. (1979): The inter-relationship: earth sciences - material sciences. Mechanisms of deformation and fracture. Pergamon, London.

FINLAYSON, B. L. (1976): Measurements of Geomorphic Processes in a Small Drainage Basin. Unpub. Ph.D. Thesis. University of Bristol.

FINLAYSON, B. L. (1981): Field measurements of soil creep. Earth Surface Processes and Landforms, 6: 35-48.

FINLAYSON, B. L. (1977): Runoff Contributing areas and Erosion School of Geography, Univ. of Oxford Research Paper 18. Mansfield Road, Oxford.

FINLAYSON, B. L. (1985): Soil creep: a formidable fossil of misconception. In Richards, K. S. Arnett, R. R. and Ellis, S. (eds) (1985). Geomorphology and soils. Allen and Unwin, London.

FINLAYSON, B. L. and H. A. OSMASTON (1977): An instrument system for measuring soil movements. B.G.R.G. Tech. Bull. 19

FLAVELL, W. S. (1986): Field investigation of soil movement: A different approach. Z. Geomorph. Suppl. Band, 60: 83-91.

FLEMING, R. W. (1972): Soil creep in the vicinity of Stanford University. Unpub. Ph.D. Thesis, Stanford University, U.S.A.

FLEMING, R. W. (1973): Instrument for measuring seasonal soil creep. Bull. Ass. Eng. Geol., 10(2): 83-93.

FLEMING, R. W. and A. M. JOHNSON (1975): Rates of seasonal creep in a silty clay soil. Q. J. Eng. Geol., 10: 83-93.

FOX, D. J. and K. E. GUIRE (1976): Documentation for M.I.D.A.S. Statis. Res. Lab. Univ. of Michigan.

FURRER, G. (1972): Measurement of movement in solifluction layers. Z. Geomorph., Suppl.Band, 13: 87-101.

GAY, N. C. (1966): Orientation of mineral lineation along lines of flow direction in rocks. **Tectonophysics**, 3: 559-562.

GAY, N. C. (1968): The motion of rigid particles embedded in a viscous fluid during pure shear deformation of the fluid. **Tectonophysics**, 5: 81-88.

GEIKIE, J. (1877): The movement of the soil cap. Nature 15: 397-398.

GERLACH T. (1967): On the placement of stakes for measuring downhill creep. Revue de Geomorphologie Dynamique, 17(4): 167-168.

GEONOR. (1966): Working instructions for Inspection Vane Borer. Geonor, Oslo.

GILBERT, G. K. (1909): Convexity of Hillslopes. Journal of Geology,17: 344-350.

GILLOT, J. E. (1968): Clay in engineering geology. Elsevier, London.

GILLOT, J. E. (1970): Fabric of Leda clay investigated by optical, electron and X-ray diffraction methods. Eng. Geol., 4: 133-153.

GODWIN, H. (1940): Pollen analysis and forest history of England and Wales. New Phytologist, 39: 370-400.

GOLDSTEIN, M. and G. TER-STEPANIAN. (1957): The long term strength of clays and deep creep of soils. Fourth Int. Conf. Soil Mech. and Fdn. Eng. Proc. 2: 311-314.

GRIM, R. E. (1953): Clay mineralogy. McGraw – Hill, New York, London, Toronto.

HAEFELI, R. (1965): Creep and progressive failure in snow , soil, rock and ice. Sixth Int. Conf. Soil Mech. End. Eng. Proc. Vol 3: 134-148.

HALLET, B. (1979): Subglacial regolation waterfilm. J. Glaciol.,23: 321 -333.

HARDY, F. (1923): The physical significance of the shrinkage co-efficient of clays and soils. J. Agricultural Sci., 13: 243-264.

HARRIS, C. (1977): Engineering properties of soils. Q. J. Eng Geol, 10: 27-43.

HARRIS, C. (1981): Periglacial mass-wasting: a review of research. B.G.R.G. Research Monograph 4, Geobooks, Norwich.

HARRIS, S. A. (1972): Preliminary observation on downhill movements of soil during the Fall of the Chinook belt of Alberta. In YATSU and FALCONER (Eds) Research methods in Pleistocene Geomorphology 275-285.

HARRIS, S. A. (1973): Studies of soil creep. W. Alberta 1970-72. Arctic and Alpine Research, 59(2A): 171 -180.

HARRISON, J. L. and H. H. MURRAY (1959): Clays and clay minerals. Proceedings of the 6th National Conference. London.

HERZOG, P. and A. HOFER: (1981): Uniaxial creep tests on a morainic material. Engineering Geology, 18: 79-87.

HEWLETT, J. D. and A. R. HIBBERT (1963): Moisture and energy conditions within a sloping soil mass during drainage. J. Geophysical Res, 68: 1081-7.

HIGGINS, C. (1982): Grazing-step terracettes and their significance. Z. Geomorph., 26(4): 459-472.

HILLEL, D. (1980): Fundamentals of Soil Physics. Academic Press, London.

HOAGLIN, D. C., MOSTELLER, F. and J. W. TUKEY (1983): Understanding robust and exploratory data analysis. Wiley, New York.

HOLDEN, J. T., R. H. JONES, and S. J. M. DUDEK. (1981): Heat and mass flow associated with a freezing front. Eng.Geol, 18: 153-164.

HOLLINGSWORTH, R. and G. S. KOVACS. (1981): Soil slumps and debris flows: prediction and protection. Bull. Ass. Eng. Geol., 18(1): 17-28.

HOWSE, R. (1864): On the glaciation of the counties of Durham and Northumberland. Trans. N. of Eng. Min. Eng., 13: 169-185.

HUTCHINSON, J. N. (1968): Mass Movement. In Fairbridge R. W. The encyclopedia of geomorphology N. Y. Reinhold. 688-696

HUTCHINSON, J. N. and D. BRUNSDEN (1975): Mudflows: a review and classification.

Q. J. Eng. Geol., 7: 1-5.

ICHIM I. (1978): Recherches experimentales effectuees dan le terrain.

Z. Geomorph., Suppl. Band, 29: 93-103.

IVERNOVA, M. I. (1964): Stationary studies of the recent denudation processes on the slopes of the River Tchan. Z. Geomorph., Suppl. Band, 5: 207-212.

IVERSON, R. M. (1983): A model for creeping flow in landslides.Bull. Ass. Eng. Geol., 20(4), 455-459.

IVERSON, R. M. (1984): Unsteady, non-uniform landslide motion: theory and measurement. Unpub. Ph.D. Thesis, Stanford University, U.S.A.

IVERSON, R. M. (1985): A constitutive equation for mass-movement behaviour. Journal of Geology, 93: 143-160.

IVERSON, R. M. (1986): Dynamics of slow landslides: a theory for time-dependent behavior. In Hillslope Processes, Editor A. D. Abrahams.

JAHN, A. (1979): On Holocene and present day morphogenetic processes in the Tatra Mountains. Studia Geomorph.Carpatho Balcanica, 13; 111-129.

JAHN, A. and M. CIELINSKA (1974): The rate of soil movement in the Sudenty Mountains. Abhand. Akad. Wissenschaft, Gottingen. Math-Phys. K1. 3 No 29.

JEFFERY, G. B. (1922): The motion of ellipsoidal particles immersed in a viscous fluid. Proc. Roy. Soc. Lond. A, 102: 161-179.

JOHNSON, A. I. (1962): Methods of measuring soil moisture in the field. USGS Water Supply Paper 1619: 22pp.

JOHNSON, A. M. (1970): Physical Processes in Geology, Freeman, San Francisco

JOHNSON, G. A. L. (1967): Basement control of Carboniferous sedimentation in northern England. Proc. Yorks. Geol. Soc., 36: 175-194.

JOHNSON, R. H. (1980): Hillslope stability and landslide hazard. A case study from Longendale, Near Derbyshire, England. Proc. Geol. Assoc. Lond., 91(4): 315-325.

KALLSTENIUS, T. and W. BERGAU (1961): In situ determination of horizontal ground movements. Proc 5 Int. Conf. Soil. Mech. Fndn. Eng., Paris 1: 481-485.

KENDALL, P. F. (1902): A System of Glacier-Lakes in the Cleveland Hills. Q. J. Geol. Soc. Lond., 58: 471-571.

KERR, W. C. (1881): On the action of frost in the arrangement of superficial earthy material. Amer. J. Sci., 21: 345-358.

KIRKBY, M. J. (1963): A study of the rates of erosion and mass movements on slopes, with special reference to Galloway. Unpub. Ph.D. Thesis. Univ. of Cambridge.

KIRKBY, M. J. (1967): Measurement and theory of soil creep. Journal of Geology, 75: 359-378.

KIRKBY, M. J. (1971): Hillslope process-response models based on the continuity equation. Inst. Brit. Geog. Spec. Pub., 3: 15-30.

KITTREDGE, J. Jr. (1939): The annual accumulation and creep of litter and other surface materials in the Chaparal of the San Gabriel mountains, California. J. of Agricultural Research., 58 (7): 537-541.

KOJAN, E. (1967): Mechanics and rates of natural soil creep. In Proceedings 5th Annual Eng. Geol. and Soils Eng. Symposium. Pocatello, Idaho.:233-253.

KOJAN, E. (1968): Mechanics and rates of natural soil creep. Proc .Conf. Int. Ass. Eng. Geol., Prague,: 122-154.

KOMAMURA, F. and R. J. HUANG (1974): New rheological model for soil behaviour. J. Soil Mech. Fdn. Eng., ASCE Proc. Vol 100: 807-824.

KONRAD, J. M. and N. MORGENSTERN (1980): A mechanistic theory of ice lens formation in fine grain soils. Can. Geotech J., 17: 473-486.

KRINITZSKY, F. L. (1970): Radiography in the earth sciences. Cambridge Univ. Press.

LAKATOS, I. (1978): The methodolgy of scientific research programmes. Cambridge Univ. Press, London.

LAMBE, T. N. and R. V. WHITMAN (1979): Soil mechanics, SI version, Wiley, New York.

LEHRE, A. K. (1982): Sediment budget of a small coast range drainage basin in north-central California. In F. J. Swanson, R. J. Janda, T. Dunne, and D. N. Swanston (Eds). Sediment Budgets and Routing in Forested Drainage Basins. U.S. Dept. of Agric. Forest Service. General Technical Report. PNW-141: 67-77.

LEOPOLD, L. B. (1970): Review of studies of hillslopes - USA. Z. Geomorph., Suppl. Band, 9: 57-66.

LEOPOLD, L. B. and W. W. EMMETT (1972): Some rates of geomorphological processes. Geographia Polonica, 23: 27-35.

LEOPOLD, L. B., W. W. EMMETT and R. H. MYRICK (1966): Channel and hillslope processes in a semi arid area, New Mexico. U.S.G.S. Prof. paper, 352-G. 193-253.

LEOPOLD, L.B., M.G. WOLMAN and J.P. MILLER (1964): Fluvial processes in geomorphology. Freeman, San Francisco.

LEWIS, L. A. (1974): Slow movement of earth under tropical rain forest conditions. Geology, 2: 9-10.

LEWIS, L. A. (1976): Soil movement in the tropics - a general model. Z. Geomorph Suppl. band, 25: 132-144.

LOHNES, R. A. and R. L. HANDY (1968): Rheological approach to soil creep. Geol. Soc. Am. Spec. Paper, 115: 132-133.

MACKAY, J. Ross, (1981): Active layer slope movement in a continuous permafrost environment, Garry Island, Northwest Territories, Canada. Can. J. Earth Sci., 18: 1666-1680.

MACKAY, J. Ross, (1984): The frost heave of stones in the active layer above permafrost with downward and upward freezing. Arctic and Alpine Research, 16(4): 439-446.

MANLEY, R. St J., A. P. ARLOV and S. G. MASON. (1955): Rotations, orientations and collisions of suspended particles in velocity gradients. Nature, 175: 682-683.

McCUMBER, M. C. and R. A. PIELKE (1981): Simulation of the effects of surface fluxes of heat and moisture in a mesoscale numerical model. J. of Geophysical Research, 86(C10): 9929-9938.

MALING, D. H. (1955): The geomorphology of the Wear Valley. Unpub. Ph.D. Thesis. Univ. of Durham.

MARCH$\widehat{\ }$AND, D. E. (1971): Rates and modes of denudation, White Mountains, Eastern California. Amer. J. Sci., 270: 109-135.

MEDAWAR, P. and J. MEDAWAR (1985): Aristotle to Zoos, Oxford University Press, Oxford.

MICHAUD, J. (1950): Emploi de marques dan l'etude des mouvements du sol. Revue Geomorphologie Dynamique, 1: 180-193.

MILLER, E. E. (1975): Physics of swelling and cracking soils, J. Colloid Interface Sci., 52: 434-443.

MILLS, H. H. (1983): Clast fabric strength in hillslope colluvium as a function of slope angle. Geografiska Annaler, 65 A: 255-262.

MITCHELL, J. K. (1976): Fundamentals of soil behaviour, Wiley, New York.

MITCHELL, J. K., R. G. CAMPANELLA and A. SINGH (1968): Soil creep as a rate process. J. Soil Mech. Fdn. Eng. ASCE Proc.: 236-243.

MITCHELL, R. J. and W. J. EDEN: (1972): Measured movements of clay slopes in the Ottawa area. Can. J. Earth Sci., 9(8):1001-1013.

MORGENSTERN, N. R. (1981): Stress-strain-time behaviour of ice permeated silty clay soils. Geotechnique ,31(3): 305-365.

MOSELEY, H. (1869): On the descent of a solid body on an inclined plane when subjected to alteration of temperature. Lond., Edin., Dublin Phil. Mag., 38: 99-118.

MOSLEY, P. (1981): Slopes and slope processes. Progress in Physical Geography 5(1): 115-121.

MOSTELLER, F. and J. W. TUKEY (1977): Data analysis and regression: a second course in statistics. Addison-Wesley Publishing Company.

NELSON, J. D. and E. G. THOMPSON (1977): A theory of creep failure in over consolidated clay. J. Geotech. Eng. Fdn. Div., ASCE VOL. 103 GT11: 1281-1294.

NEMCOK, A., J. PASEK and J.RYBAR (1972): Classification and landslides and other mass movements. Rock Mechanics, 4: 71-78.

NIEWENUIS, J. D. and D. KLEINDORST (1971): The measurement of small displacements in a Dutch hillslope. Engineering Geology, 5: 271-289.

NIXON, J. F. (1982): Field frost heave predictions using the segregation potential concept. Can. Geotech. J., 19: 526-529.

NYE, J. F. (1973): Water at the bed of a glacier. IASH, 95: 189-194.

ODA, M. (1977): Co-ordination number and its relation to shear strength in granular material. Soil Fdn., 17: 29-42.

OWENS, I. F. (1969): Causes and rates of soil creep in the Chilton Valley, Lars, N.Z. Arctic and Alpine Research, 1, 31: 213-220.

PARIZEK, E. J. and J. F. WOODRUFF (1956): Apparent absence of soil creep in the East Georgia Piedmont. Bull. Geol. Soc. Am., 67: 1111-1116.

PARIZEK, E. J. and J. F. WOODRUFF (1965): Soil creep: a note on terminology. Journal of Geology 73: 172-175.

PAUL, C. L. and J. DeVRIES (1979): Prediction of soil strength from hydrological and mechanical properties. Can. J. Soil Sci., 59: 301-312.

PEARCE, A. J. and J. E. ELSON (1973): Postglacial rates of denudation by soil movement, free face retreat and fluvial erosion, Quebec. Can. J. Earth Sci., 10(1): 91-101.

PEEL, R. F. (1949): A study of two Northumbrian spillways. Trans. Inst. Brit. Geog., 15: 73-89.

PEEL, R. F. (1956): The profiles of glacial drainage channels. Geogr. J., 122: 483-487.

PHIPPS, R. L. (1974): The soil creep - curved tree fallacy. J. Res. U.S. Geol. Survey, 2(3): 371-377.

PITTY, A. (1966): Some problems in the location and determination of slope profiles. Z. Geomorph., 10: 454-461.

POMEROY, C. D. (editor) (1978): Creep of engineering materials: A Journal of Strain Analysis Monograph. Mech. Eng. Pub. Ltd, London.

PREVOST, J. H. (1980): Mechanics of continuous porous media. Int. J. Eng. Sci., 18: 787-800.

PRICE, L. W. and C. S. ALEXANDER (1971): Methods of measuring mass wasting:review and critique. Proc. Ass. Amer. Geog., 3: 135-139.

PUSCH, R. (1967): A technique for investigation of clay microstructure. J. Microscopie, 6: 963-986.

PUSCH, R. (1979): A physical clay creep model and its mathematical analogy. Proc. 3rd Int. Conf. Numerical Methods. Geomech, Aachen 1: 485-491.

PUSCH, R. and P. FELTHAM (1980): A stochastic model of the creep of soils. Geotechnique, 30(4): 497-506.

QUANSAH, C. (1981): The effect of soil type, slope, rain intensity and their interaction on splash detachment and transport. J. Soil Sci., 32: 215-224.

RAISTRICK, A. and K. B. BLACKBURN (1931): The late glacial and post glacial periods in the N. Pennines (W. Yorks. and Durham). Proc. Univ. Durham Phil. Soc, 8: 351-358

RAPP, A. (1960): Recent developments of mountain slopes in Karkevagge and surroundings, N. Scandinavia. Geografiska Annaler, 42A: 73-200.

RASHIDIAN, K. H. (1984): Soil creep, a process study in Killhope basin, Upper Weardale, N. Pennines, England. Unpub. Ph.D. Thesis, University of Durham.

RASHIDIAN, K. H. (1986): A new technique for field measurement of soil creep displacement profiles. Z. Geomorph. N. F. Suppl. Band, 60: 93-103.

RASTRICK, A. (1931): Glaciation of Northumberland and Durham. Proc. Geol. Ass. 42: 281-291.

RICHARDS, K. (1982): Rivers: Form and process in alluvial channels. Methuen, London.

ROBERTS, B. K., J. TURNER and P. F. WARD (1973): Recent forest history and landuse in Weardale, Northern England. In H. J. B. Birks and R. G. West(Eds), Quaternary Plant Ecology. Blackwells, Oxford : 207-221.

ROGERS, N. W. and M. J. SELBY (1980): Mechanism of shallow translational landsliding during summer rainstorms, N. Island, N. Z. Geografiska Annaler , 62A: 11-21.

ROYAL SOCIETY (1977): Symposium on creep of Eng. materials and of the earth. Eds Kelly, Cook, Greenwood. Roy Soc Lond, London.

RUDBERG, S. (1964): Slow mass movements, processes and slope development, Lapland. Z. Geomorph, Suppl. Band 5, : 192-203.

RUDBERG, S. (1967): On the use of painted rocks aligned along a contour and the preferred orientation of stones. Revue de Geomorphologie Dynamique, 17(4): 161, 178-179.

RUXTON, B. P. (1958): Weathering and subsurface erosion in granite piedmont angle, Balos, Sudan. Geological Magazine, 95: 353.

RYAN, T. A., B. L. JOINER, and B. F. RYAN (1981): MINITAB Reference Manual, University Park, Pennsylvania, Minitab Project, The Pennsylvania State University.

SAITO, M. (1965): Forecasting the time of occurrence of slope failure. Proc. 6th Int.Conf.Soil Mech. Fdn. Eng. Mcntreal, 2: 537-541.

SAITO, M. and H. UEZAWA (1961): Failure of soil due to creep. 5th Int. Conf. Soil Mech. Fdn. Eng. Proc. Vol. 1: 315-318.

SAUNDERS, I. and A. YOUNG (1983): Rates of surface processes on slopes, slope retreat and denudation. **Earth Surface Processes and Landforms**, 8: 473-501.

SAVAGE, W. Z. and A. F. CHLEBORAD (1982): A model for creeping flow in landslides. **Bull. Ass. Eng. Geol.**, 19: 333-338.

SCHEIDEGGER, A. E. (1970): Theoretical Geomorphology. Berlin, Springer-Verlag.

SCHEIDEGGER, A. E. (1984): A review of recent work on mass movements on slopes and on rock falls. **Earth-Science Reviews**, 21: 225-249.

SCHEPERS, J. L. (1978): Le creep sur les talus de l'autoroute 'E5'. **Bull. Soc. Geogr. Liege**, 13: 22-28.

SCHUMM, S. A. (1964): Seasonal variations in erosion rates and processes on hillslopes in W. Colorado. **Z. Geomorph.**, Suppl. Band 5: 215-235.

SCHUMM, S. A. (1966): Rates of surficial rock creep on hillslopes in Western Colorado. **Science**, 155: 560-562

SELBY, M. J. (1966): Methods for measuring soil creep. **N.Z. J. Hydrology**, 5: 54-63.

SELBY, M. J. (1968): Cones for measuring soil creep. **N.Z. J. Hydrology**, 7(2): 136-137.

SELBY, M. J. (1982): Hillslope materials and processes. Oxford University Press. Oxford.

SHARPE, C. F. S. (1938): Landslides and related phenomena. Columbia University Press, New York.

SHARPE, C. F. S. and E. F. DOSCH (1942): Relation of soil creep to earth flow in the Appalachian Plateaus. J. Geomorph., 5(4): 312-324.

SHERWOOD, P. T. and D. M. RYLEY (1970): An investigation of a cone-penetrometer method for the determination of the liquid limit. Geotechnique, 20: 203-208.

SINGH, A. and J. K. MITCHELL (1968): General stress strain time function for soil. J. Soil Mech. Fdn. Eng., ASCE Proc., 94: 21-46.

SISSONS (1960): Some aspects of glacial drainage channels in Britain Pt II Scottish Geogr. Mag. 77: 15-36

SKEMPTON, A. W. (1953): Soil mechanics in relation to geology. Proc. Yorks. Geol. Soc., 29: 33-62.

SKEMPTON, A. W. and J. N. HUTCHISON (1969): Stability in natural slopes and embankment foundations, state of the art report, 7th Int. Conf. Soil Mech. Fdn. Eng., Mexico, 291-335.

SLAYMAKER, H. O. (1965): The instrumentation of small catchments to determine patterns of sub-aerial erosion. In Rates of erosion and weathering in British Isles. Inst. Brit. Geog., Geomorphological Symposium. Bristol: 23-26.

SLAYMAKER, H. O. (1972) Patterns of present sub-aerial erosion in landforms in Mid Wales. Trans. Inst. Brit. Geog., 55: 67-68.

SMITH, J. (1956): Some moving soils in Spitzbergen. J. Soil Sci., 7: 10-21.

SMITH, S. (1923): Memoirs of the Geological Survey: Special reports on the mineral resourses of Gt. Britain. Vol XXV Lead and Zinc ores of Northumberland and Alston Moor.

STATHAM, I. (1977): Earth Surface Sediment Transport. Clarendon Press, Oxford.

STEARN, A. N. (1935): Structure and creep. Journal of Geology, 43(3): 323-7.

SUGDEN, K. C. (1973): Investigation of a method for measuring soil creep. Unpub. B.Sc. Project A21 Dept A Physics Univ. of Bristol.

SWANSON, F. J., R. L.FREDRIKSEN and F. M. McCORISON (1982): Material transfer in a Western Oregon forested watershed. In: EDMONDS, R. L.(ed) Analysis of coniferous forest ecosystems in the Western U.S.A., Hutchinson Ross, Stroudsburg.

SWANSON, F. J. and D. N. SWANSTON (1977): Complex mass-movement terrains in the western Cascade Range, Oregon. U.S. Dept. of Agric. Forest Service Research Paper PNW-188, Portland, Oregon.

SWANSTON, D. N. (1981): Creep and earth flow from undisturbed and management impacted slopes in the Coast and Cascade ranges of the Pacific. N.W. USA. Erosion and sediment transport in Pacific rim Steeplands IAHS Publ No132 Christchurch 1981.

TABER, S. (1930): The mechanics of frost heaving. **Journal of Geology**, 38: 303-317.

TABOR, D. (1979): Gases, liquids and solids. Cambridge University Press, London.

TAMBURI, A. J. (1974): Creep of single rocks on bedrock. **Bull. Geol. Soc. Am.**, 85: 351-356.

TANAKA. M. (1976): Rate of erosion in the Tanzawa Mountains, Central Japan. Geografiska Annaler., 58A: 155-163.

TAVENAS, F. and S. LEROUEIL (1981): Creep and failure of slopes in clays. Can.Geotech.J., 18(1): 106-120.

TAYLOR, G. I. (1922): The motion of a sphere in a rotating liquid. Proc. R. Soc. Lond. Series A, 102: 180-189.

TER-STEPANIAN, G. (1963): On the long term stability of slopes. Norwegian Technical Inst., 52, 1-14.

TERZAGHI, K. (1931): On the static rigidity of plastic clays. J. Rheology, 2: 253-262.

TERZAGHI, K. (1950): Mechanics of landslides. Application of geology to engineering practice, Geol, Soc Amer, Berkeley. Volume, Harvard Soil Mechanics Series, 83-123.

TERZAGHI, K. (1953): Some miscellaneous notes on creep. Proc. 3rd Int. Conf. on Soil Mech. and Fdn. Eng. Vol. 3: 205-206.

TICE, A. R., D. M. ANDERSON and A. BANIN. (1976): The prediction of unfrozen water contents in frozen soils from liquid limits. US Army Corps of Engineers Cold Regions Research and Engineering Lab Hanover New York. Report 76-8.

TING, J. M. (1983): On the nature of the minimum creep rate. Can. Geotech. J. , 20: 176-182.

THOMSON, C. W. (1877): The movement of the soil cap. Nature, 15: 359-360.

THOMPSON, B. (1896-7): The junction beds of the Upper Lias and Inferior Oolite in Northamptonshire. J. Northampt. Nat. Hist. Soc. 9.

THORNES, J. B. (1979): Processes and interrelationships, rates and changes. In Embleton, C. and J. B. Thornes. Process in Geomorphology. Edward Arnold, London.

TROEH, F. R. (1975): A method for measuring soil creep. Soil Sci. Soc. Amer., 39: 707-709.

TROTTER, F. M. (1929): The Tertiary uplift and resultant drainage of the Alston block and adjacent areas. Proc. Yorks. Geol., 21: 161-180.

TUKEY, J. W. (1977): Exploratory Data Analysis. Addison-Wesley, Reading, MA.

TURNER, J. (1979): The Environment of north-east England during Roman times as shown by Pollen Analysis. J. Archaeological Sci., 6(3): 285-290.

TURNER, J. and J. HODGSON (1979): Studies in the vegetational history of the Northern Pennines. I. Variations in the composition of the early Flandrian forests. J. Ecology, 67: 629-646.

TURNER, J. and J. HODGSON (1981): Studies in the vegetational history of the Northern Pennines. II. An atypical pollen diagram from Pow Hill, Co. Durham. J. Ecology, 69: 171-188.

VAID, Y. P. and R. G. CAMPANELLA (1977): Time dependent behaviour of undisturbed clay. J. Geotech. Eng. Div., ASCE Proc. Vol. 103: 693-710.

VALLEJO, L. E. (1979): An explanation for mudflows. Geotechnique, 29(3): 351-354.

VAN ASCH, Th. W. J. (1984): Creep processes in landslides. **Earth Surface Processes and Landforms.**, 9: 573-583.

VAN STEIGN, H. (1977): The development of a laboratory set up to measure creep induced by freeze thaw cycles. **Earth Surface Processes and Landforms** , 2: 247-250.

VARNES, D. J. (1958): Landslide types and processes. In landslides and engineerng practices. Ed E. B. Eckel Highways Research Bureau. Spec. report 29 :20-47.

VARNES, D. J. (1975): Slope movements in the Western United States. In Mass Wasting, Geobooks, Norwich: 1-17.

VAUGHAN, R. R. and C. W. KWAN (1984): Weathering, structure and in situ stress in residual soils.Geotechnique, 34: 43-59.

VELLEMAN, P. F. and D. C. HOAGLIN (1981): Applications, Basics,and Computing of Exploratory Data Analysis. Duxbury Press, Boston, MA.

VIALOV, S. S. and A. M. SKIBITSKY (1961): Problems of the rheology of soils. Proc 5th Int. Conf. Soil Mech. and Found.Eng. 1: 387-391.

VINCENT, P. J. (1969): The glacial history and deposits of a selected part of the Alston Block. Unpubl. Ph.D. Thesis, University of Durham.

WADDINGTON, C. H. (1977): Tools for thought. Paladin, St. Albans.

WALDRON, L. J., S. DAKESSIAN and J. A. NEMSON (1983): Shear resistance enhancement of 1.22 metre diameter soil cross sections by pine and alfalfa roots. **Soil Sci. Soc. Am. J.**, 47: 9-14.

WARD, W. H. (1953): Soil movement and weather. Proc. 3rd Int. Congress Soil Mech. Fdn. Eng. 1(4): 477-482.

WASHBURN, A. L. (1967): Instrumental observations of mass wasting in the Mesters district, Northeast Greenland. **Meddelelser an Gronland** 166.

WEERTMAN, J. (1973): Creep of ice. In E. Whalley, S. J. Jones and L. W. Gold Physics and Chemistry of Ice. Royal Soc. of Canada, Ottawa, Canada. : 320-337.

WHITE, S. E. (1949): Processes of erosion on steep slopes of Aoahu, Hawaii. **Am. J. Sci.**, 247(3): 168-86.

WILLIAMS, M. A. J. (1972): The influence of slope soil and plant cover on runoff and erosion in the upper Shoalhaven area 1966 - 1968. J. Soil Conservation Service of New South Wales, 28(1): 51-62.

WILLIAMS, M. A. J. (1973): The efficacy of creep and slopewash in tropical and temperate Australia. Austr. Geogr. Stud., 11: 62-78.

WILLIAMS, M. A. J. (1974): Surface rock-creep on sandstone slopes in N. Territory, Australia. Austr. Geogr., 12: 339-347.

WILLIAMS, P. J. (1957): The direct recording of solifluction movements. Am. J. of Sc., vol. 255 : 707-715.

WILLIAMS, P. J. (1962): Quantitative investigations of soil movement. Biuletyn Peryglacjalmy, 11: 353-363.

WILLIAMS, P. J. (1970): Processes of slope formation: recent quantitative studies in Canada. Z. Geomorph. Suppl. Band, 9: 67-70.

WILLIAMS, P. J. (1970): Quantitative investigations of soil movement. Bull. Periglac., 11: 353-363.

WILLIAMS, W. H. (1978): A sampler on sampling, Wiley, New York.

WILSON, J. W. (1952): Vegetation patterns associated with soil movement in Jan Mayen Island. J. Ecology, 40: 249-284.

WILSON, S. D. (1970): Observational data on ground movements related to slope instability. J. Soil Mech. Fdn. Eng. Am. Soc. Civ. Eng. Proc., Vol. 96: 1521-1544 illus.

WILSON, W. (1952): Vegetation patterns associated with soil movements on Jan Mayen Island. J. Ecology, 40(2).

WOJCHIECHOWSKI, J. and H. KLIMOWICZ (1970): Geodetical observations of slope creep as a source of information on the rheological properties of natural soils. Proc. Semin. Soil Mech. Fdn. Eng. 2nd Lodz., 757-773.

WOLMAN, M. G. and J. P. MILLER (1960): Magnitude and frequency of forces in geomorphic processes. Journal of Geology, 68: 54-74.

WOOD, D. M. and C. P. WROTH (1978): The use of the cone penetrometer to determine the plastic limit of soils. Ground Engineering, 11: 37.

YAGASHITA, K. and R. C. MORRIS (1979): Microfabrics of a recumbent fold in cross-bedded sandstones.Geol Mag, 116: 105-116.

YALIN, M. S. (1977): Mechanics of sediment transport. Oxford, Pergamon.

YEN, B. C. (1969): Stability of slopes undergoing creep deformation. J. Soil Mech. Fdn. Eng. ASCE Proc. Vol 96, SM2: 609-630.

YOUNG, A. (1958): Some consideration of slope form and development. Unpub.Ph.D Thesis. University of Sheffield.

YOUNG, A. (1960): Soil movement by denudational processes in slopes. Nature, 188: 120-122.

YOUNG, A. (1963): Soil movement on slopes. Nature, 200: 129-130.

YOUNG, A. (1969): Present rate of land erosion. Nature, 224: 851-852.

YOUNG, A. (1972): Slopes. Edinburgh. Oliver and Boyd.

YOUNG, A. (1974): Slope profile survey. BGRG Tech. Bull. 11.

YOUNG, A. (1974): The rate of slope retreat. Inst. Brit. Geog. Special Publication 7: 65-78.

YOUNG, A. (1978): A twelve year record of soil movement on a slope. Z. Geomorph., Suppl. Band, 29: 104-110.

APPENDIX A

COMPUTER PROGRAMS

The following programs were written in FORTRAN 77 using IBM s FORTRANVS compiler on Durhams Michigan Terminal System. Graphics were developed using the PLOTSYS subroutine library and output was generated on a QMS800 laserprinter.

IPLOT - Non-linear smoothing and plotting of time-series data

ATPLOT - Calculates movement rates from Anderson's tube data using a least-squares method and plots the results.

QQPLOT - Produces quantile - quantile plots from a generated Gaussian and an empirical distribution.

```
C-------------------------------------------------C
C                                                 C
C          PLOTS INCLINOMETER PEG DATA TIME SERIES C
C          D.N.M.DONOGHUE DURHAM 19/8/83.         C
C                                                 C
C          UPDATE 25/4/88                         C
C                                                 C
C          UNIT 1 = DATA FILE                     C
C          UNIT 2 = OUTPUT FILE                   C
C          UNIT 9 = PLOT FILE                     C
C-------------------------------------------------C
      DIMENSION X(100),YL(100),YM(100),YS(100)
      DIMENSION TL(100),TM(100),TS(100)
      REAL DX1(2)/12.5,13.0/
      REAL DY1(2)/4.5,4.5/
      REAL DY2(2)/4.3,4.3/
      REAL DY3(2)/4.1,4.1/
      CHARACTER*10 TITLE
      CHARACTER*1 CHAR
      INTEGER NPLOTS,M,SMOOTH
      PRINT *,'ENTER NO OF PLOTS: '
      READ(5,'(I2)')NPLOTS
      PRINT *,'ENTER NO OF DATA POINTS: '
      READ(5,'(I2)')M
      PRINT *,'SMOOTH ?(Y/N): '
      READ(5,'(A)') CHAR
      IF(CHAR.NE.'Y') THEN
         SMOOTH=1
      ELSE
          SMOOTH=5
      ENDIF
      DO 1 K=1,NPLOTS
  100 FORMAT(24H  DAYS  LONG  MED  SHORT/(1X,F4.0,1X,3F6.1))
  200 FORMAT('INCLINOMETER PEG TIME SERIES DATA')
  400 FORMAT('RAW DATA')
  500 FORMAT('S3R SMOOTH')
  600 FORMAT('S3R+HANN')
  700 FORMAT('S3R+HANN+HANN3')
  800 FORMAT(6X,3F6.1)
      WRITE(2,200)
      CALL REED(TITLE,X,YL,YM,YS,18,TL,TM,TS)
      WRITE(2,'(A10)')TITLE
      DO 2 I=1,SMOOTH
C
      IF(I.EQ.2)CALL SSR(YL,M,.TRUE.)
      IF(I.EQ.2)CALL SSR(YM,M,.TRUE.)
      IF(I.EQ.2)CALL SSR(YS,M,.TRUE.)
C
      IF(I.EQ.3) CALL HANN(YL,YM,YS,M)
C     IF(I.EQ.5) CALL S3R(YL,YM,YS,M)

      IF(I.EQ.4) CALL RMEAN3(YL,YM,YS,M)
C
      IF(I.EQ.1) WRITE(2,400)
      IF(I.EQ.2) WRITE(2,500)
      IF(I.EQ.3) WRITE(2,600)
      IF(I.EQ.4) WRITE(2,700)
C     CALL PENCHG('BLAC')
C
      WRITE(2,100)(X(J),YL(J),YM(J),YS(J),J=1,M)
```

```
      CALL PLTSIZ(.8)
      CALL PLTOFS(0.,70.,-100.,100.,2.,2.)
      CALL PAXIS(2.,2.,'TIME IN DAYS',-12,10.0,0.0,0.0,70.0,1.0)
      CALL PAXIS(2.,2.,'FLUX (mm /mm)',13,5.0,90.0,-100.,100.0,1.0)
      CALL PSYM(1.65,4.75,.1,'3',90.,1,0)
      CALL PLINE(X(1),YL(1),M,1,1,0,1.0)
      CALL PLINE(DX1(1),DY1(1),2,1,1,0,0)
      CALL PLINE(X(1),YM(1),M,1,1,2,1.0)
      CALL PLINE(DX1,DY2,2,1,1,2,0)
      CALL PLINE(X(1),YS(1),M,1,1,11,1.0)
      CALL PLINE(DX1(1),DY3(1),2,1,1,11,0)
      CALL PALPHA('ROMAN.3',0)
      CALL PSYM(2.,8.,0.2,TITLE,0.0,10)
C     CALL PSYM(5.,8.,0.2,'INCLINOMETER PEGS V TIME',0.,24,0)
      IF(I.EQ.2) CALL PSYM(5.,8.0,0.25,'SMOOTHED  S3R',0.,13,0)
      IF(I.EQ.3) CALL PSYM(5.,8.0,0.25,'SMOOTHED  S3R+HANN',0.,18,0)
      IF(I.EQ.4) CALL PSYM(5.,8.0,0.25,'SMOOTHED  S3R+HANN',0.,18,0)
      CALL PALPHA('STANDARD ',0)
      CALL PSYM(13.3,4.5,0.1,'15cm PEG',0.,8,0)
      CALL PSYM(13.3,4.3,0.1,'10cm PEG',0.,8,0)
      CALL PSYM(13.3,4.1,0.1,' 5cm PEG',0.,8,0)
C     CALL PGRID(1.,1.,15.,8.,1,1)
      CALL PLTEND
    2 CONTINUE
    1 CONTINUE
      STOP
      END


C-------------------------------------------------C
C     SUBPROGRAMS                                 C
C-------------------------------------------------C
      SUBROUTINE REED(TITLE,A,B,C,D,N,TL,TM,TS)
      DIMENSION A(N),B(N),C(N),D(N)
      REAL TL,TM,TS
      CHARACTER*10 TITLE
      READ(1,10)TITLE
   10 FORMAT(1X,A10)
      READ(1,20,END=9)(A(J),J=1,N)
   20 FORMAT(18F3.0)
    9 READ(1,30,END=91)(B(J),J=1,N)
   91 READ(1,30,END=92 )(C(J),J=1,N)
   92 READ(1,30,END=93 )(D(J),J=1,N)
   93 CONTINUE
   30 FORMAT(18F5.1)
      DO 1 K=1,N
      B(K)=(B(K)*112.5)
      C(K)=(C(K)*50.0)
      D(K)=(D(K)*12.5)
    1 CONTINUE
      DO 2 I=2,N
      TL=TL+(B(I)-B(I-1))
      TM=TM+(C(I)-C(I-1))
      TS=TS+(D(I)-D(I-1))
    2 CONTINUE
      RETURN
      END
C
      SUBROUTINE SSR(A,N,CHANGE)
      INTEGER N
```

```
      REAL A(N)
      LOGICAL CHANGE
      REAL A1,A2,A3
      INTEGER NM1
      A2=A(1)
      A3=A(2)
      NM1=N-1
      DO 1 J=2,NM1
      A1=A2
      A2=A3
      A3=A(J+1)
      CALL MED(A1,A2,A3,A(J),CHANGE)
    1 CONTINUE
      RETURN
      END
      SUBROUTINE MED(X1,X2,X3,XM,CHANGE)
      REAL X1,X2,X3,XM
      LOGICAL CHANGE
      REAL A1,A2,A3
      A1=X1
      A2=X2
      A3=X3
C
      XM=A2
      IF((A2-A1)*(A3-A2).GE.0.0) GOTO 999
      CHANGE= .TRUE.
      XM=A1
      IF((A3-A1)*(A3-A2).GT.0.0) GOTO 999
      XM=A3
  999 RETURN
      END
      SUBROUTINE S3R(A,B,C,N)
      DIMENSION A(N),B(N),C(N)
      N1=N-1
      DO 1 J=2,N1
      IF(A(J-1).GT.A(J)) CALL SORT(A(J-1),A(J))
      IF(A(J-1).GT.A(J+1)) CALL SORT(A(J-1),A(J+1))
      IF(A(J).GT.A(J+1)) CALL SORT(A(J),A(J+1))
C
      IF(B(J-1).GT.B(J)) CALL SORT(B(J-1),B(J))
      IF(B(J-1).GT.B(J+1)) CALL SORT(B(J-1),B(J+1))
      IF(B(J).GT.B(J+1)) CALL SORT(B(J),B(J+1))
C
      IF(C(J-1).GT.C(J)) CALL SORT(C(J-1),C(J))
      IF(C(J-1).GT.C(J+1)) CALL SORT(C(J-1),C(J+1))
      IF(C(J).GT.C(J+1)) CALL SORT(C(J),C(J+1))
    1 CONTINUE
      RETURN
      END
C
      SUBROUTINE HANN(A,B,C,N)
      DIMENSION A(N),B(N),C(N)
      N1=N-1
      DO 1 J=2,N1
      A(J)=(A(J)+A(J+1))/2
      B(J)=(B(J)+B(J+1))/2
      C(J)=(C(J)+C(J+1))/2
    1 CONTINUE
      RETURN
      END
C
```

```
      SUBROUTINE RMEAN3(A,B,C,N)
      DIMENSION A(N),B(N),C(N)
      DO 1 J=2,N
      A(J)=(A(J-1)+A(J)+A(J+1))/3
      B(J)=(B(J-1)+B(J)+B(J+1))/3
      C(J)=(C(J-1)+C(J)+C(J+1))/3
    1 CONTINUE
      RETURN
      END
C
      SUBROUTINE SORT(A,B)
      C=A
      A=B
      B=C
      RETURN
      END
```

```
C-----------------------------------------------------------------------C
C                                                                       C
C      PROGRAM PLOTS ANDERSON TUBE DATA AS TIME SERIES                  C
C                                                                       C
C      N.B. PLOTS ARE BEST FIT LINES FROM RAW DATA                      C
C                                                                       C
C      D.N.M.DONOGHUE DURHAM 19/8/83.                                   C
C                                                                       C
C-----------------------------------------------------------------------C
      DIMENSION A(50),A1(50),B(3),X(2),Y(2),P(50),Z(50),Q(50)
  100 FORMAT(F7.2,F6.2)
  101 FORMAT(F7.2,F6.2)
   50 FORMAT('    B',3X,'   A')
  102 FORMAT('GRADIENT'F10.2,'INTERCEPT'F10.2)
  103 FORMAT(F7.2,3F6.2)
  104 FORMAT('MEAN DEPTH OF MOVEMENT'F10.2)
  105 FORMAT('SUM OF INTERCEPTS'F10.2)
  106 FORMAT('N       'I2)
  107 FORMAT('VOLUMETRIC FLUX='F10.2)
      N=0
      TCPT=0
      DO 1 I=1,20
      IF(I.GE.1.0) GOTO 77
      Z(I)=0.0
   77 CONTINUE
      WRITE(6,50)
      DO 2 J=1,3
      READ(5,100,END=99)A1(J),B(J)
      A(J)=-A1(J)
      IF (I.NE.1) GOTO 8
      P(J)=A(J)
      A(J)=A(J)-A(J)
      WRITE(6,101)B(J),A(J)
      GOTO 2
    8 Q(J)=A(J)-P(J)
      WRITE(6,101)B(J),Q(J)
    2 CONTINUE
      SUMXY=0
      SUMXY=0
      SUMX=0
      SUMY=0
      XSQR=0
      OX=0.0
      OY=0.0
      AREA=0.0
C-----------------------------------------------------------------------C
C                                                                       C
C                  REGRESSION CALCULATIONS                              C
C                                                                       C
C-----------------------------------------------------------------------C
      DO 3 J=1,3
      A(J)=A(J)-P(J)
      IF (I.EQ.1) GOTO 33
      SUMXY = SUMXY + A(J)*B(J)
      SUMX =SUMX +A(J)
      SUMY = SUMY + B(J)
      XSQR = XSQR + A(J)*A(J)
    3 CONTINUE
      AA = (SUMXY - SUMX * SUMY /3.0)/(XSQR-SUMX*SUMX/3.0)
      IF(AA.NE.0.0)GOTO 44
```

```
      BB=0.0
      GO TO 55
   44 BB=(SUMY-AA*SUMX)/3.0
      IF(BB.GE.0.0)GO TO 22
   55 TCPT=TCPT+BB
      N=N+1
   22 CONTINUE
C END OF CALCS
C
C WRITE OUTPUT
C
   20 FORMAT('    X1,Y1'8X,'X2,Y2')
      WRITE(6,102)AA,BB
C
C PLOTTING COORDS
C
   33 Y(1)=B(1)
      Y(2)=B(3)
      IF(AA.NE.0.0) GOTO 9
      X(1)=A(1)
      X(2)=A(3)
      GOTO 7
    9 IF(I.NE.1) GOTO 6
      X(1)=0.0
      X(2)=0.0
      GOTO 7
    6 CONTINUE
      X(1)=((Y(1)-BB)/AA)
      X(2)=((Y(2)-BB)/AA)
    7 CONTINUE
      WRITE(6,20)
      WRITE(6,103)X(1),Y(1),X(2),Y(2)
C-------------------------------------------------------------------------------
C          AREACALCULATION
C-------------------------------------------------------------------------------
      OX=A(1)
      OY=-BB
      WRITE(6,200)OX
      WRITE(6,300)OY
  200 FORMAT('OX    ',F10.2)
  300 FORMAT('OY    ',F10.2)
      AREA=0.5*(OX*OY)
      WRITE(6,107)AREA
      Z(I)=Z(I)+AREA
      WRITE(6,108)Z(I)
  108 FORMAT('CHANGE IN FLUX= ',F10.2)
      IF (I.NE.1) GOTO 5
C-------------------------------------------------------------------------------C
C                                                                               C
C                  PLOTTING ROUTINE                                             C
C                                                                               C
C-------------------------------------------------------------------------------C
      CALL PLTOFS(-0.5,0.1,-10.0,2.0,1.0,1.0)
      CALL PAXIS(1.0,1.0,'DEPTH (CM)',10,5.0,90.0,-10.0,2.0,1.0)
      CALL PAXIS(1.0,6.0,'DISTANCE (CM)',13,10.,0.0,-0.5,0.1,1.0)
      CALL PALPHA('ROMAN.3',0)
      CALL PSYM(1.,7.,0.2,'SITE 1/2',0.0,8)
      CALL PALPHA('STANDARD ',0)
    5 CONTINUE
      CALL PLINE(A(1),B(1),3,1,-1,I,1.0)
```

```
      CALL PLINE(X(1),Y(1),2,1,0,0,1.0)
    1 CONTINUE
   99 CONTINUE
      WRITE(6,105)TCPT
      C=TCPT/N
      WRITE(6,106)N
      WRITE(6,104)C
      CALL PLTEND
      STOP
      END
```

```
C-----------------------------------------------------------------------C
C     Q-Q PLOTTING                                                      C
C                                                                       C
C     DATA1= GENERATED GAUSSIAN DISTRIBUTION *READ FROM CHANNEL 1*      C
C                                                                       C
C     DATA2= EMPIRICAL DISTRIBUTION          *READ FROM CHANNEL 2*      C
C     N1 = 100                                                          C
C     N2 = 56                                                           C
C     D.N.M.DONOGHUE   DURHAM 21/3/84                                   C
C                                                                       C
C-----------------------------------------------------------------------C

      DIMENSION DATA1(100),DATA2(100),QDAT2(100)
      INTEGER N1,N2
      PRINT *,'ENTER NO OF GAUSSIAN DATA POINTS'
      READ(*,'(BN,I4)N1
      PRINT *,'ENTER NO OF EMPIRICAL DATA POINTS'
      READ(*,'(BN,I4)N2
      CALL REED(DATA1,N1)
      CALL RED(DATA2,N2)
      CALL QSRT(DATA1,N1)
      CALL QSRT(DATA2,N2)
C
C
      CALL NQUANT(DATA1,QDAT2,N1,N2)
      DO 1 I=1,N2
       WRITE(6,100)DATA2(I),QDAT2(I)
  100  FORMAT(2F8.2)
    1 CONTINUE
      CALL QQPLT(DATA2,QDAT2,N2)
      STOP
      END

      SUBROUTINE REED(X,N1)
      INTEGER N1
      REAL X(N1)
  100 FORMAT(F6.2)
      DO 1 I=1,N1
         READ(1,100,END=99)X(I)
    1 CONTINUE
   99 CONTINUE
      RETURN
      END
      SUBROUTINE RED(X,N2)
      INTEGER N2
      REAL X(N2)
  100 FORMAT(F7.2)
      DO 1 I=1,N2
         READ(2,100,END=99)X(I)
    1 CONTINUE
   99 CONTINUE
      RETURN
      END
      SUBROUTINE QSRT(Y,N)
C ROUTINE FOR QUICK SORT ONLY
C USE ONLY SMALL DATA SETS <100 ELEMENTS!!!
      INTEGER N
      REAL Y(N)
      INTEGER I,J,J1,GAP,NMG
      REAL TEMP
```

```
          GAP=N

   20 GAP=GAP/2
      NMG=N-GAP
      DO 40 J1=1,NMG
          I=J1+GAP
C
C     DO J=J1,1,-GAP
          J=J1
   30 IF(Y(J).LE.Y(I)) GOTO 40
C
      TEMP=Y(I)
      Y(I)=Y(J)
      Y(J)=TEMP
C
      I=J
      J=J-GAP
      IF(J.GE.1) GOTO 30
   40 CONTINUE
      IF(GAP.GT.1) GOTO 20
      RETURN
      END
      SUBROUTINE NQUANT(X,X1,N1,N2)
      INTEGER N1,N2
      REAL X(N1),X1(N2)
      REAL Q
      DO 1 J=1,N2
           Q=((N1/N2)*(J 0.5))+0.5
           Q=INT(Q+SIGN(0.5,Q))
           X1(J)=X(Q)
  100 FORMAT(F6.2)
      WRITE(6,100)X1(J)
    1 CONTINUE
      RETURN
      END
      SUBROUTINE QQPLT(X,Y,N)
      INTEGER N
      REAL X(N),Y(N)
      CALL SCALE(X,N,XMIN,XF)
      CALL SCALE(Y,N,YMIN,YF)
      CALL PLTOFS(YMIN,YF,XMIN,XF,1.,1.)
      CALL PAXIS(1.,1.,'NORMAL QUANTILES',-16,6.0,0.,YMIN,YF,1.0)
      CALL PAXIS(1.,1.,'SOIL DEPTH',10,6.0,90.,YMIN,YF,1.0)
      CALL PLINE(Y(1),X(1),N,1,-1,3,1.0)
      CALL PENUPS(YMIN,XMIN)
      CALL PENDN(7.0,7.0)
      CALL PENUP(1.0,7.0)
      CALL PENDN(7.0,7.0)
      CALL PENDN(7.0,1.0)
      CALL PSYM(1.,7.5,0.2,'Q-Q PLOT  N=',0.0,12)
      CALL PSYM(3.,7.5,0.2,'69',0.0,2)
      CALL PLTEND
      RETURN
      END
      SUBROUTINE SCALE(X,N,NMIN,NF)
      INTEGER N
      REAL X(N),NMIN,NMAX,NF
      CALL QSRT(X,N)
      NMIN=X(1)
      NMAX=X(N)
      NF=(NMAX-NMIN)/6
      RETURN
      END
```

APPENDIX B

Cumulative particle size distribution curves for all samples.

Graphical measures were calculated from the following percentiles-

MEAN - (75 + 50 + 25) / 3

MEDIAN - 50

SKEWNESS - ((84 - 50) / (84 - 16)) - ((50 - 10) / (90 - 10))

SORTING - (90 + 80 + 70 - 30 - 20 - 10) / 5.3

KURTOSIS - (90 - 10) / (1.9 (75 - 25))

PARTICLE SIZE DISTRIBUTION

LOCATION No..... BORE HOLE No..... SAMPLE No. 1/2 PRETREATMENT DETAILS H_2O_2

DATE OF TEST..... DESCRIPTION..... LOSS ON PRETREATMENT.....%

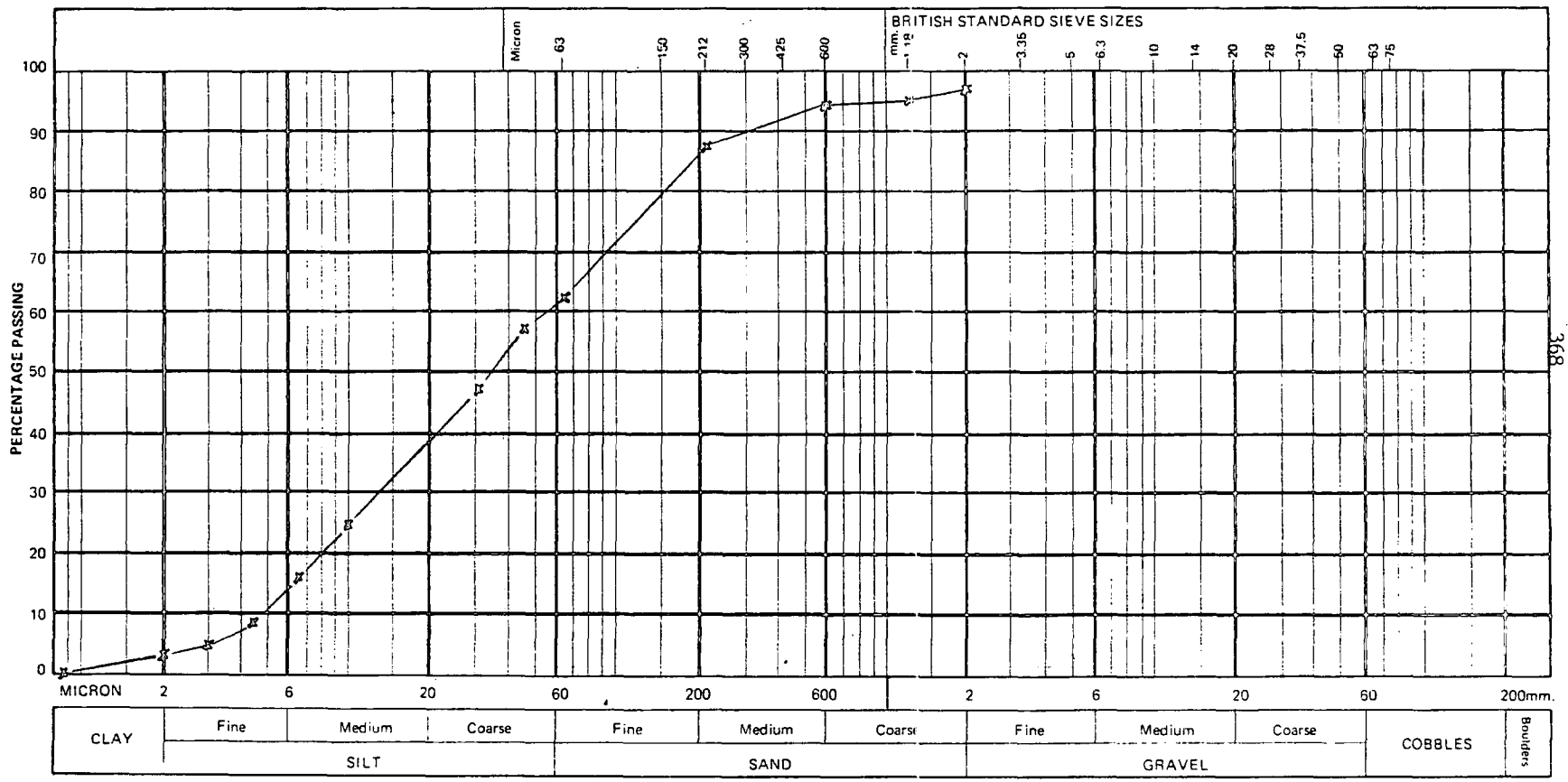

PARTICLE SIZE DISTRIBUTION

Form No. K4

LOCATION No..... BORE HOLE No..... SAMPLE No. 1|3 PRETREATMENT DETAILS H_2O_2

DATE OF TEST..... DESCRIPTION..... LOSS ON PRETREATMENT.....%

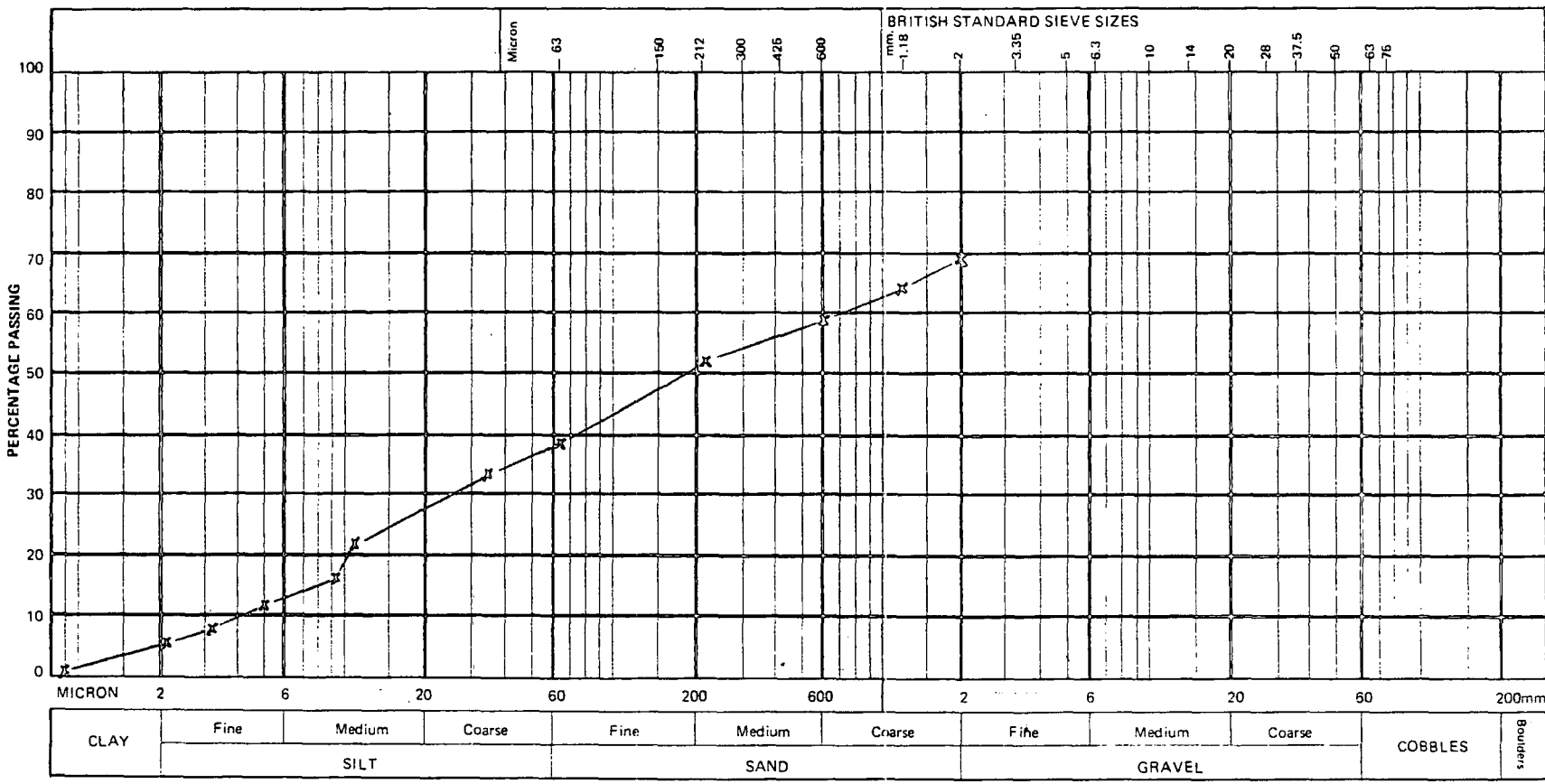

369

Signed.....

PARTICLE SIZE DISTRIBUTION

Form No. K4

LOCATION No..... BORE HOLE No..... SAMPLE No. 1/4 PRETREATMENT DETAILS H_2O_2

DATE OF TEST..... DESCRIPTION..... LOSS ON PRETREATMENT.....%

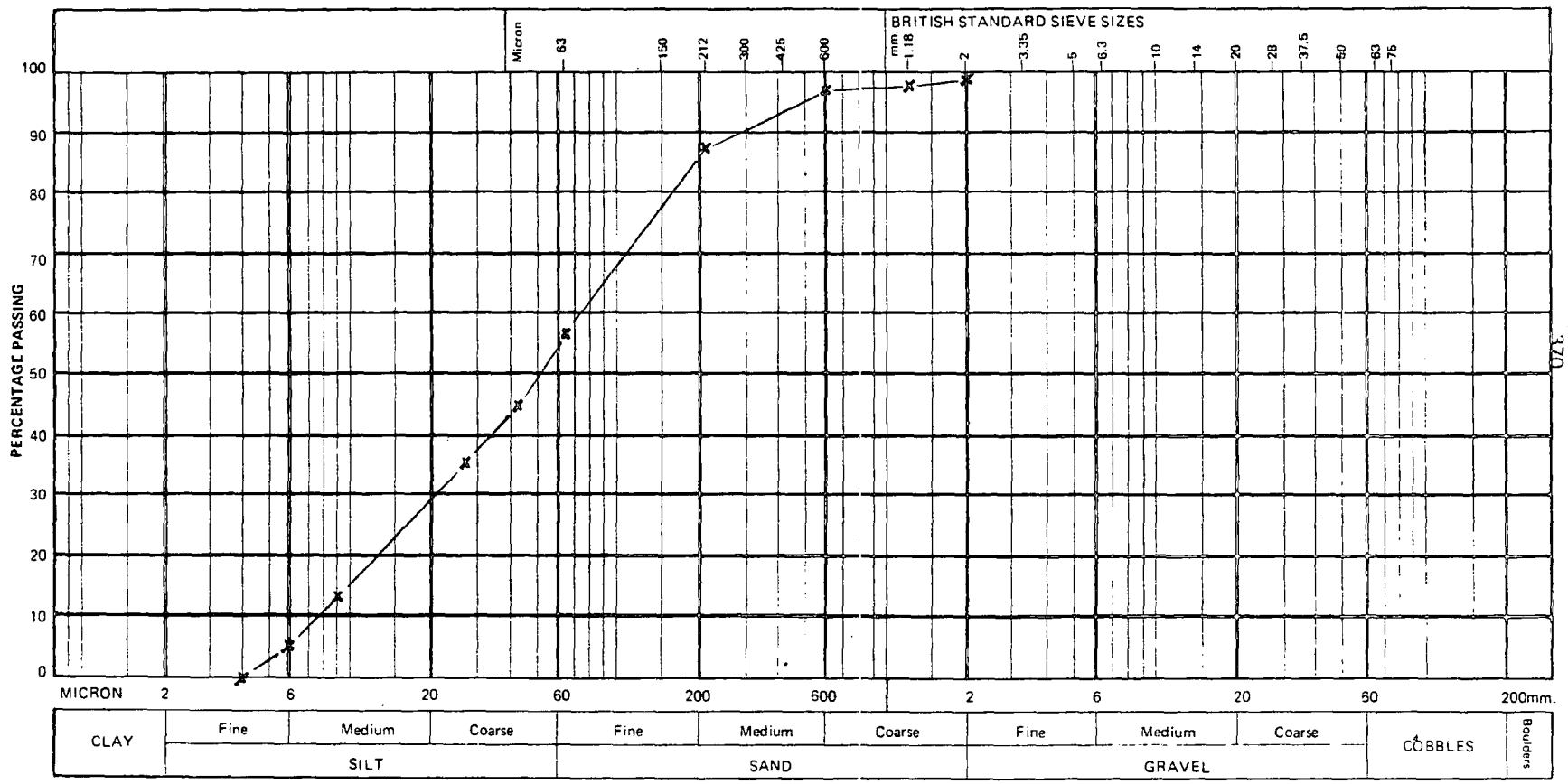

Signed.....

PARTICLE SIZE DISTRIBUTION

Form No. K4

LOCATION No..... BORE HOLE No..... SAMPLE No. 1/5 PRETREATMENT DETAILS H_2O_2

DATE OF TEST..... DESCRIPTION..... LOSS ON PRETREATMENT.....%

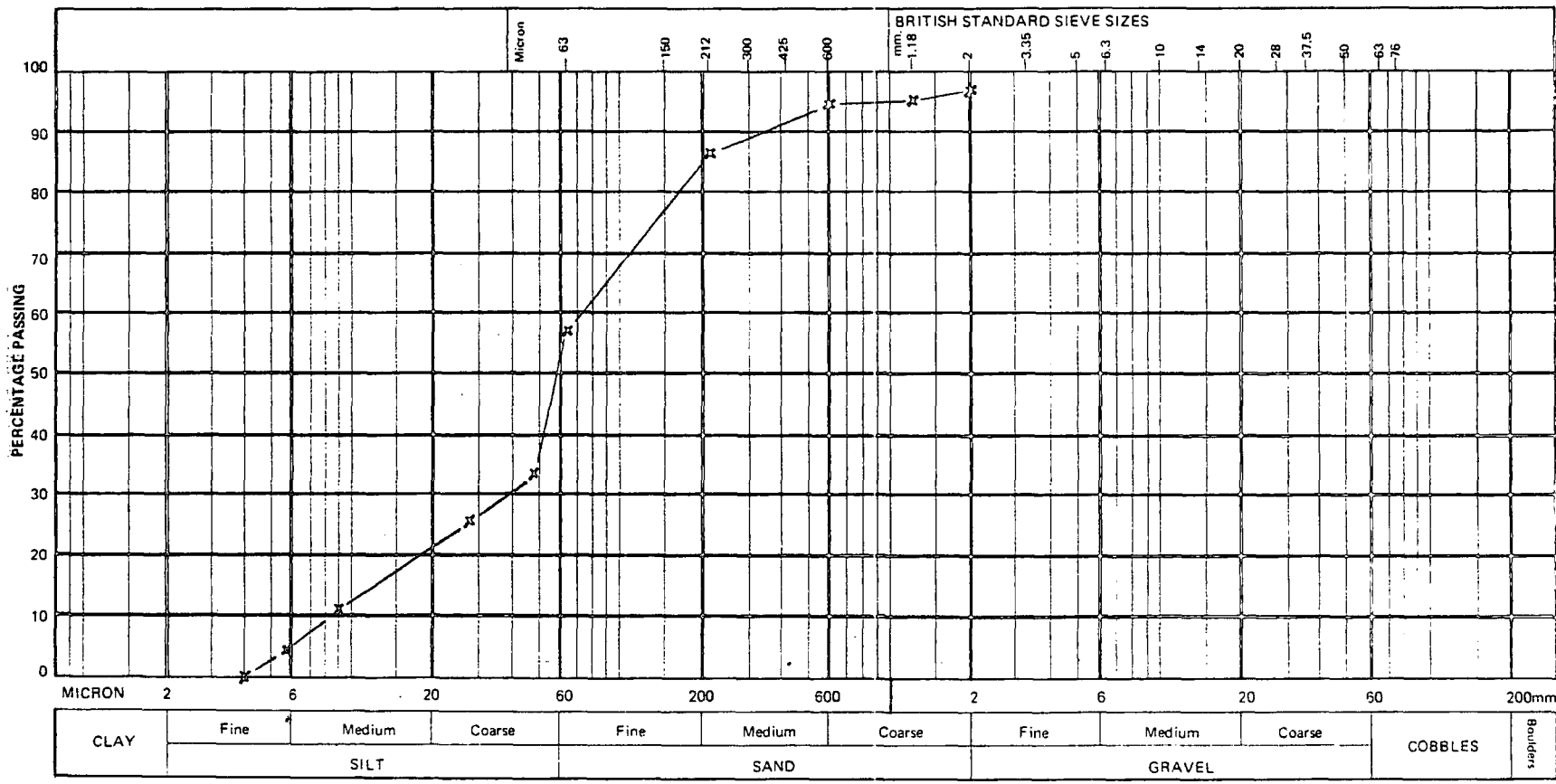

Signed.....

PARTICLE SIZE DISTRIBUTION

Form No. K4

LOCATION No..... BORE HOLE No..... SAMPLE No. 2-11 PRETREATMENT DETAILS H2O2

DATE OF TEST..... DESCRIPTION..... LOSS ON PRETREATMENT.....%

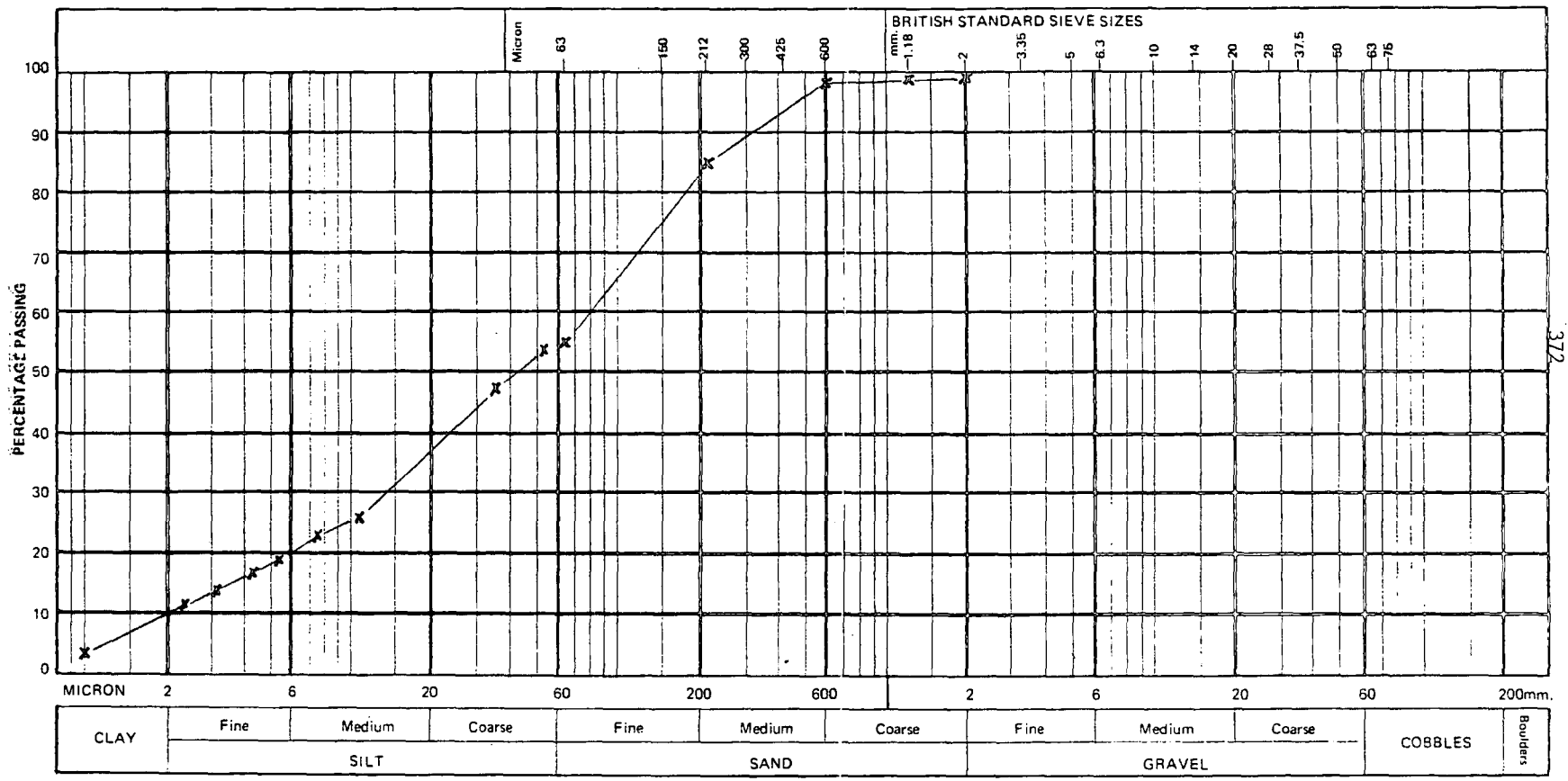

372

Signed.....

Form No. K4

PARTICLE SIZE DISTRIBUTION

LOCATION No..... BORE HOLE No..... SAMPLE No. 2 | 2

PRETREATMENT DETAILS H_2O_2

DATE OF TEST..... DESCRIPTION..... LOSS ON PRETREATMENT.....%

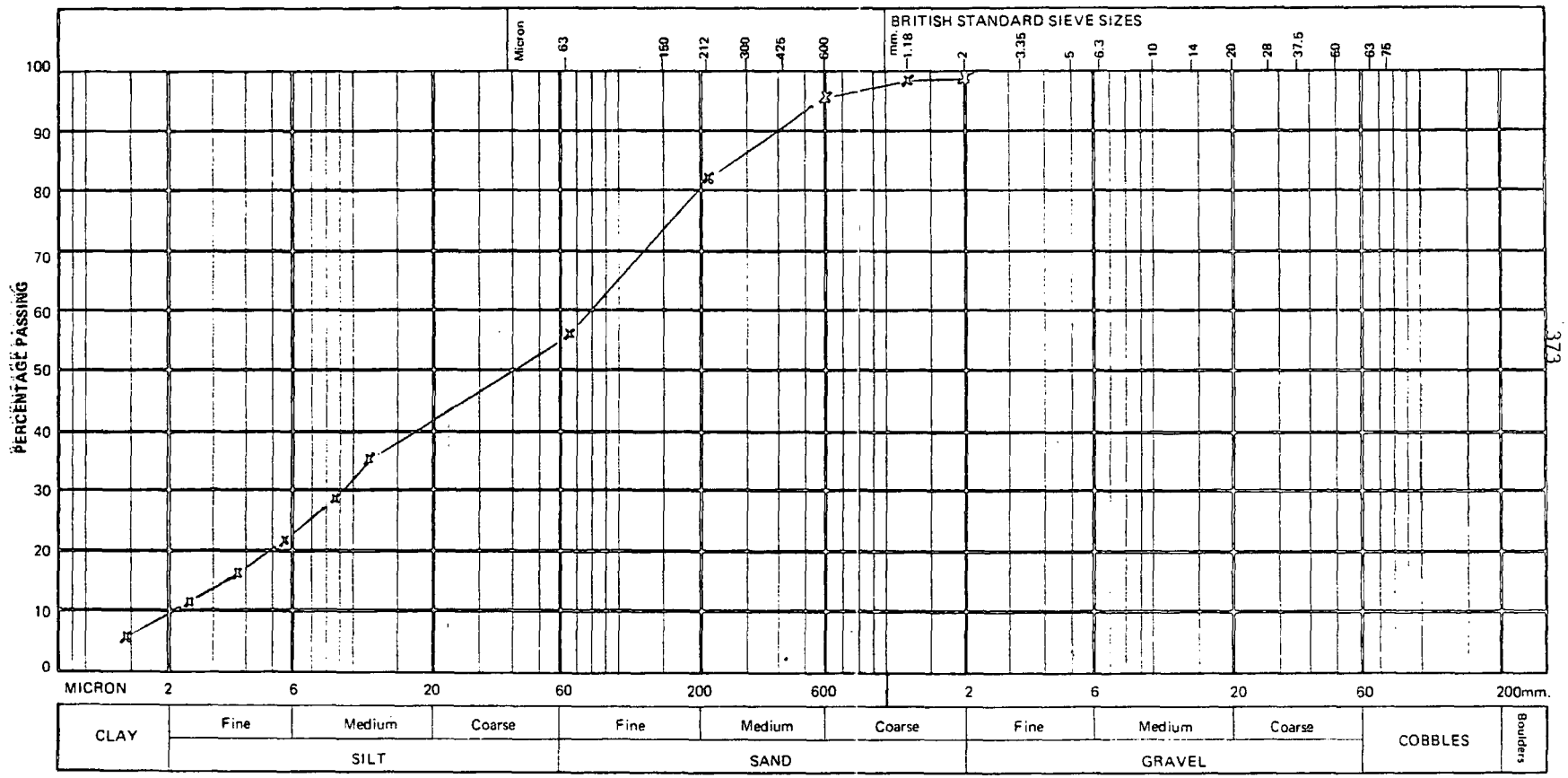

373

Signed.....

Form No. K4

PARTICLE SIZE DISTRIBUTION

LOCATION No..... BORE HOLE No..... SAMPLE No. 2/4 PRETREATMENT DETAILS H_2O_2

DATE OF TEST..... DESCRIPTION..... LOSS ON PRETREATMENT.....%

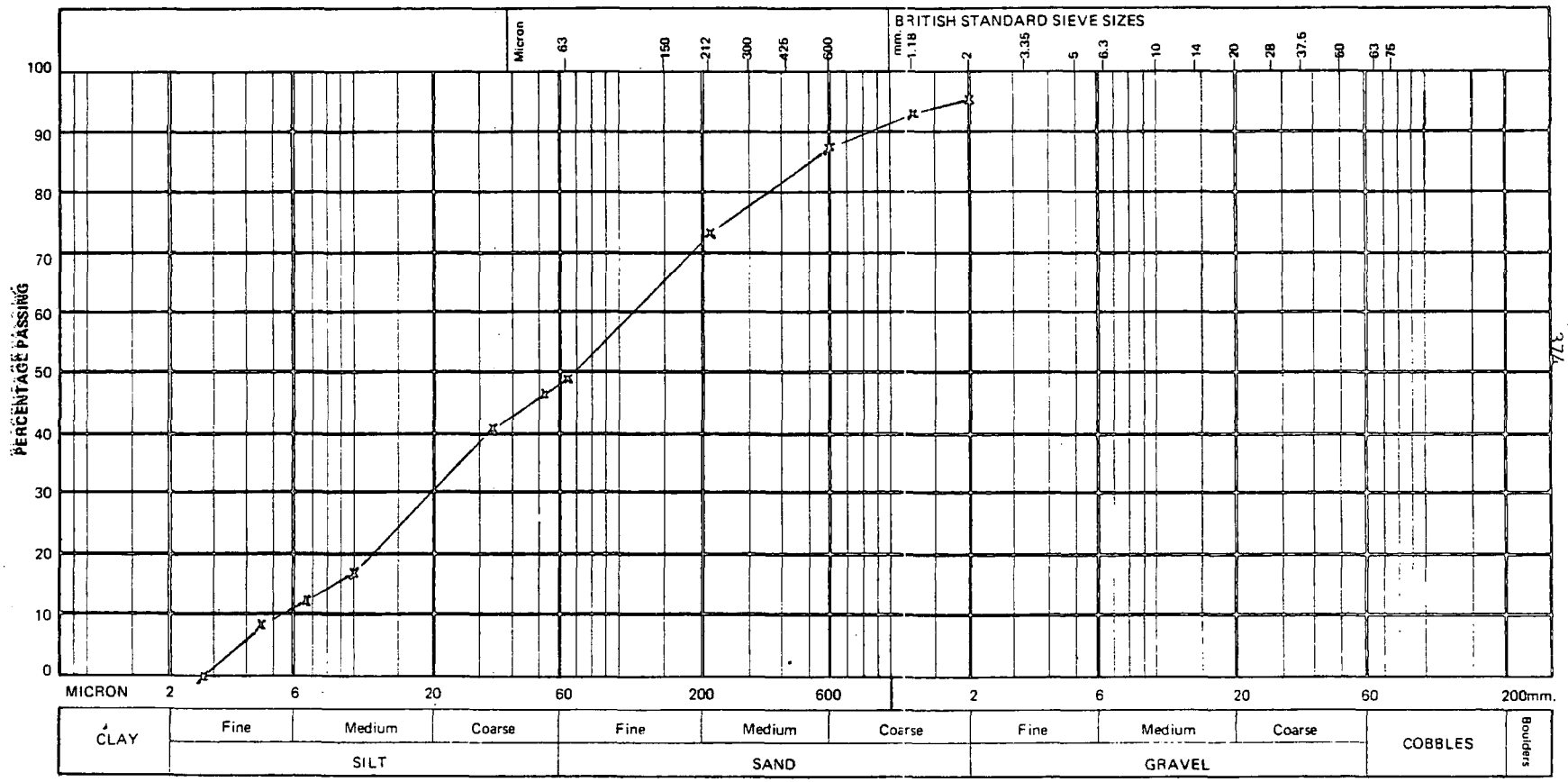

Signed.....

Form No. K4

PARTICLE SIZE DISTRIBUTION

LOCATION No..... BORE HOLE No..... SAMPLE No. 2/5 PRETREATMENT DETAILS H_2O_2 (20 vol)

DATE OF TEST..... DESCRIPTION..... LOSS ON PRETREATMENT.....%

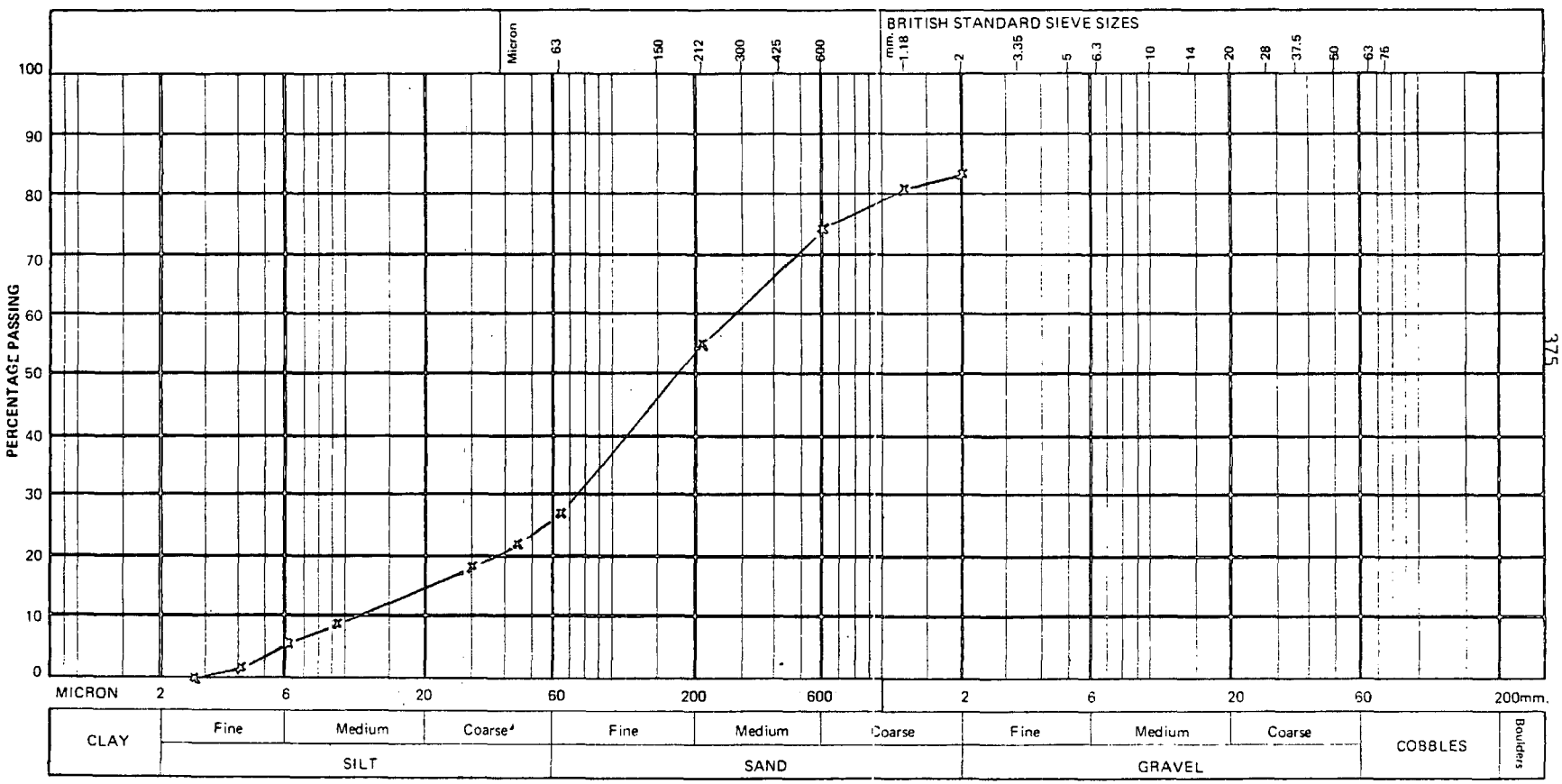

375

Signed.....

Form No. K4

PARTICLE SIZE DISTRIBUTION

LOCATION No..... BORE HOLE No..... SAMPLE No. 2/6 PRETREATMENT DETAILS H_2O_2 (20 vol)

DATE OF TEST..... DESCRIPTION..... LOSS ON PRETREATMENT.....%

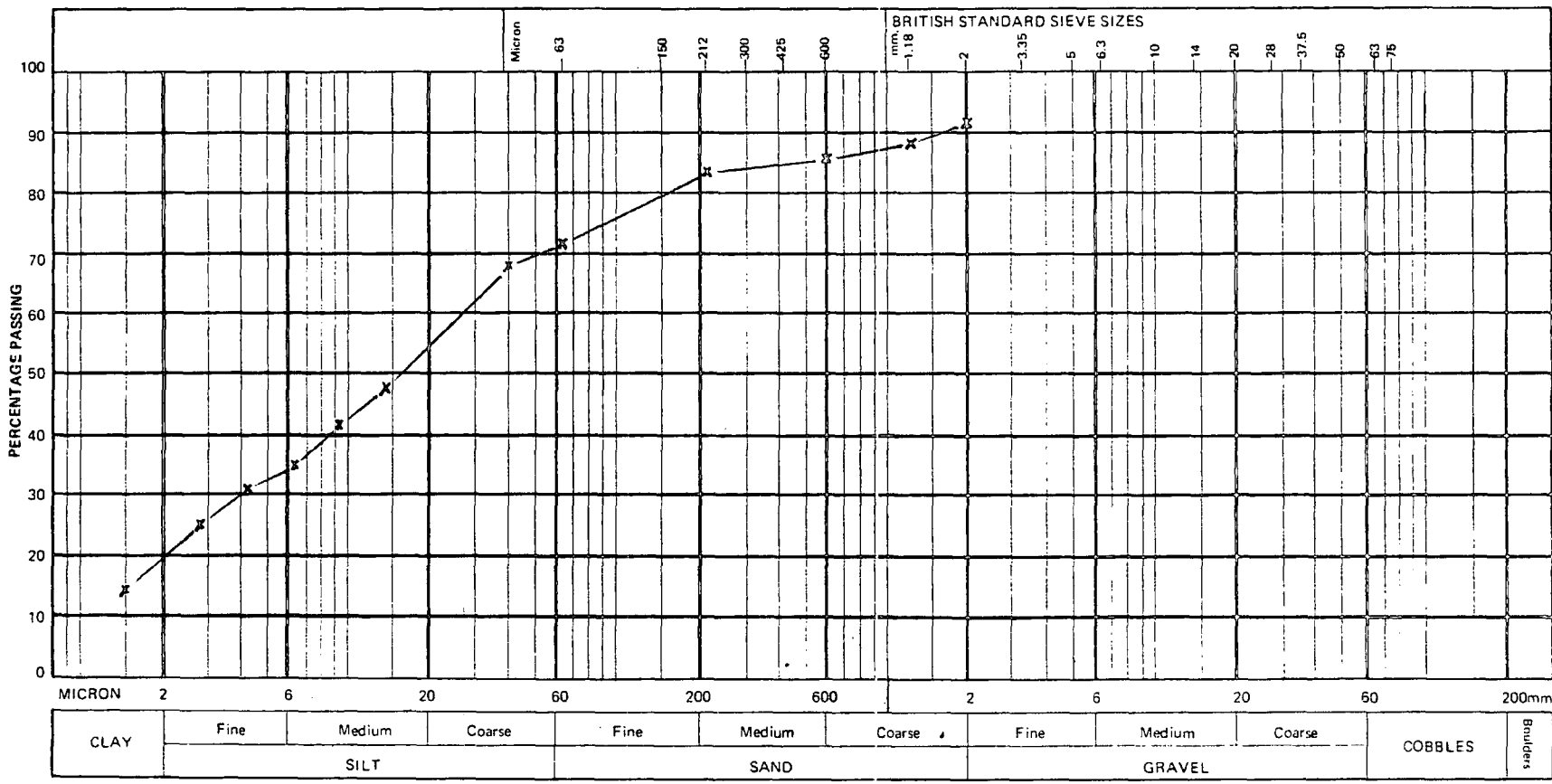

376

Signed.....

PARTICLE SIZE DISTRIBUTION

Form No. K4

LOCATION No..... BORE HOLE No..... SAMPLE No. 2/7 PRETREATMENT DETAILS H_2O_2

DATE OF TEST..... DESCRIPTION..... LOSS ON PRETREATMENT.....%

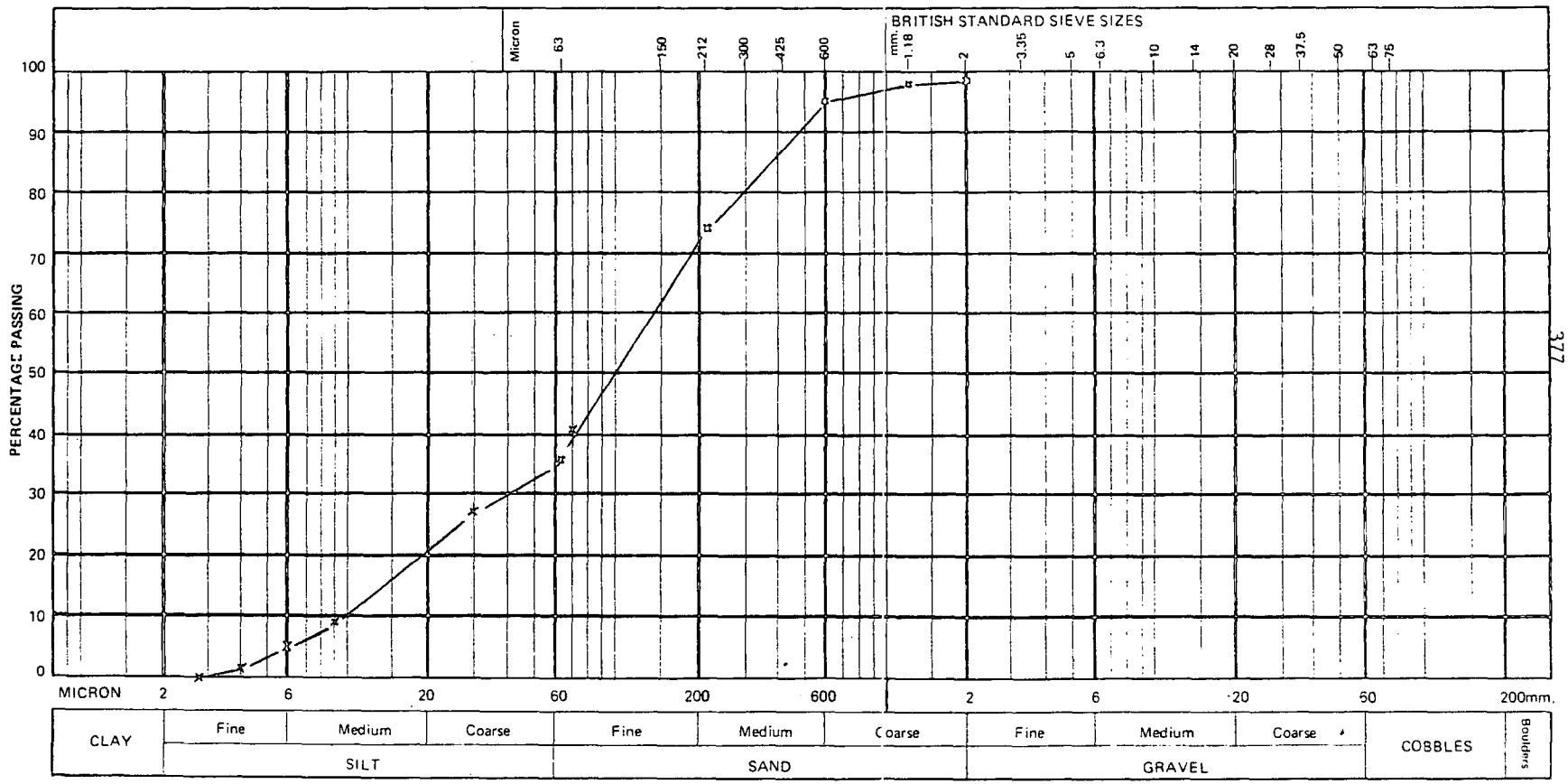

377

Signed.....

PARTICLE SIZE DISTRIBUTION

Form No. K4

LOCATION No..... BORE HOLE No..... SAMPLE No. 3/1 PRETREATMENT DETAILS H_2O_2

DATE OF TEST..... DESCRIPTION..... LOSS ON PRETREATMENT.....%

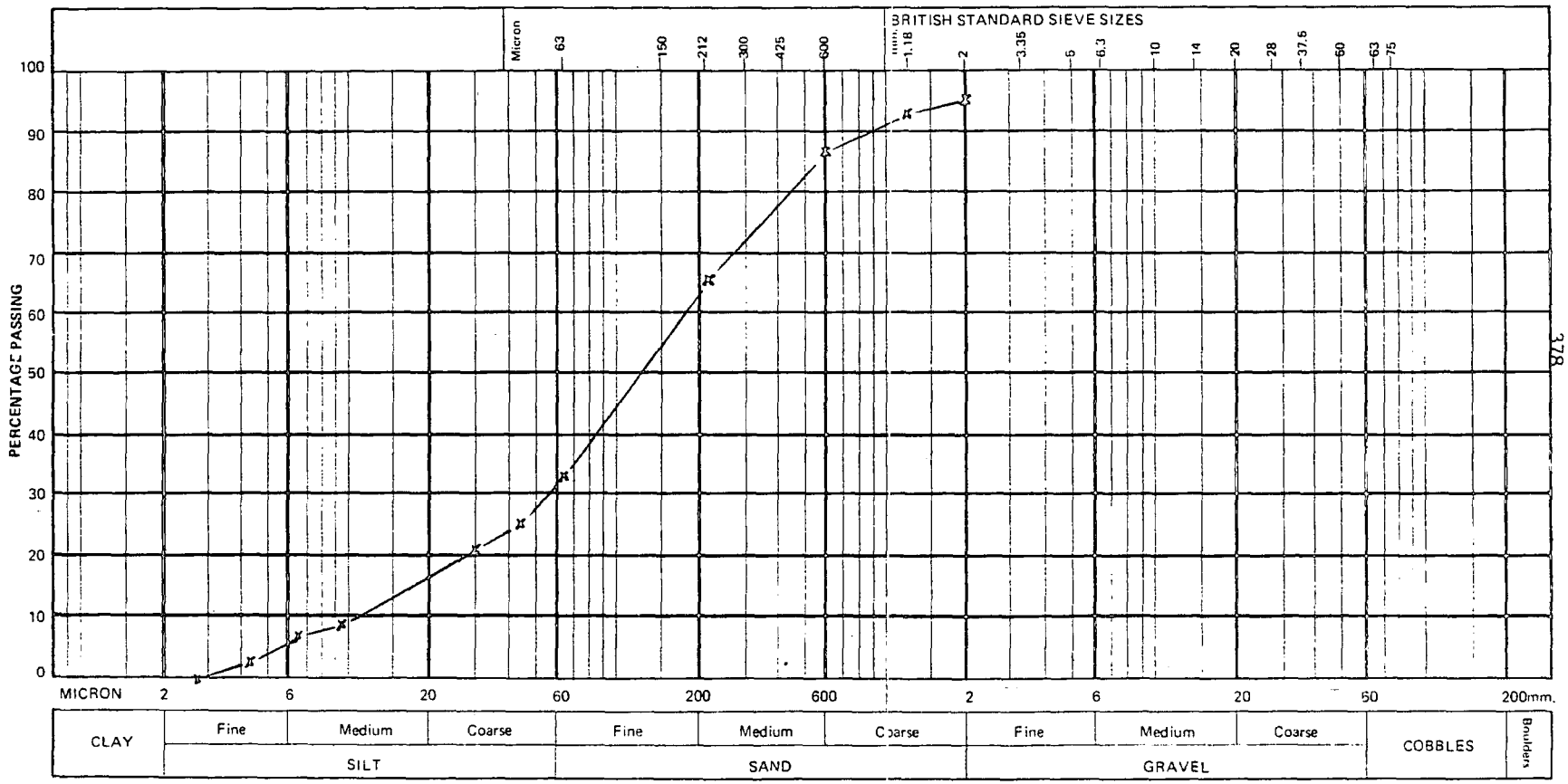

378

Signed.....

PARTICLE SIZE DISTRIBUTION

Form No. K4

LOCATION No..... BORE HOLE No..... SAMPLE No. 3/2..... PRETREATMENT DETAILS H_2O_2.....

DATE OF TEST..... DESCRIPTION..... LOSS ON PRETREATMENT.....%

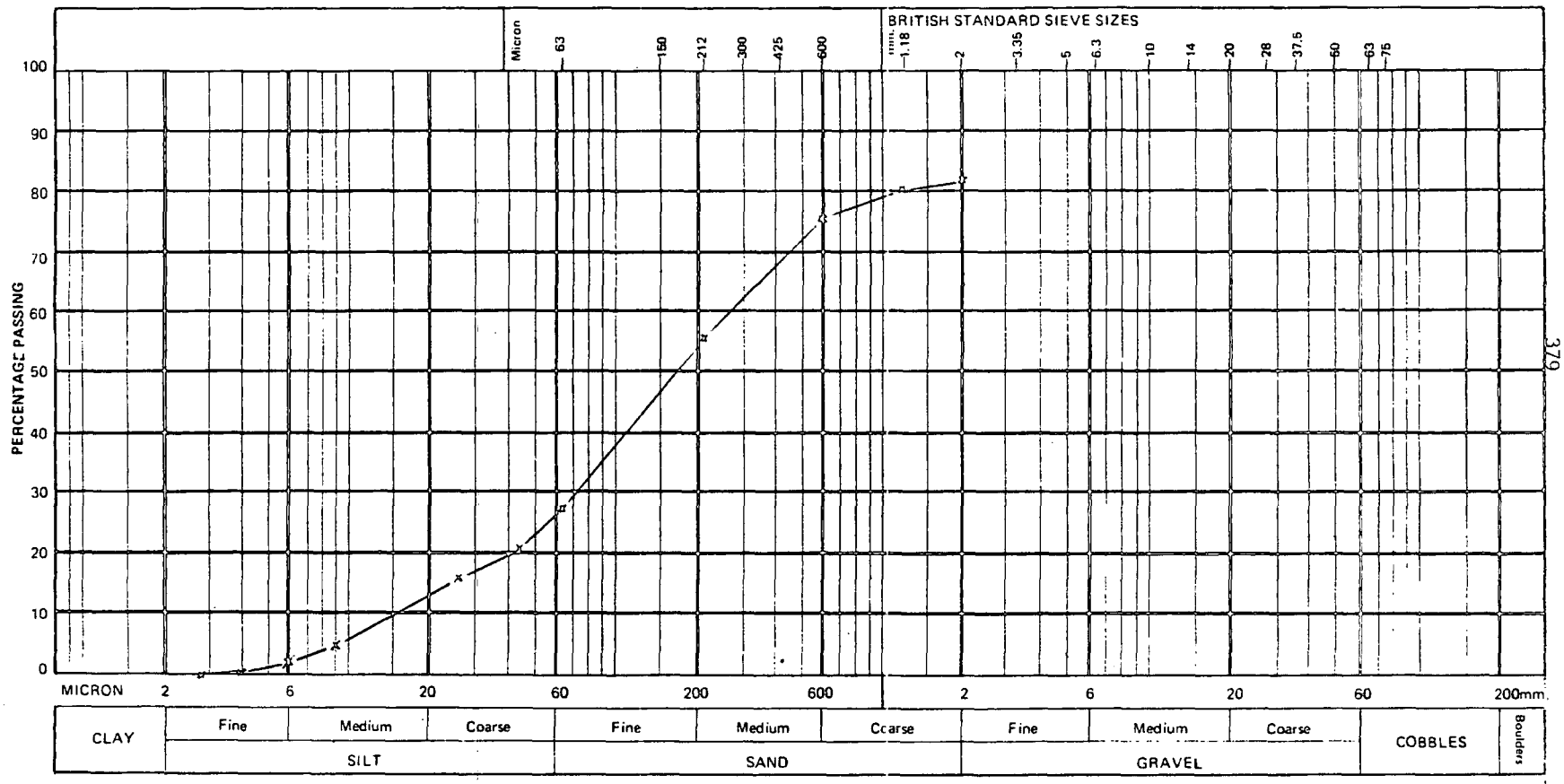

379

Signed.....

PARTICLE SIZE DISTRIBUTION

Form No. K4

LOCATION No..... BORE HOLE No..... SAMPLE No. 3/3 PRETREATMENT DETAILS H_2O_2

DATE OF TEST..... DESCRIPTION..... LOSS ON PRETREATMENT.....%

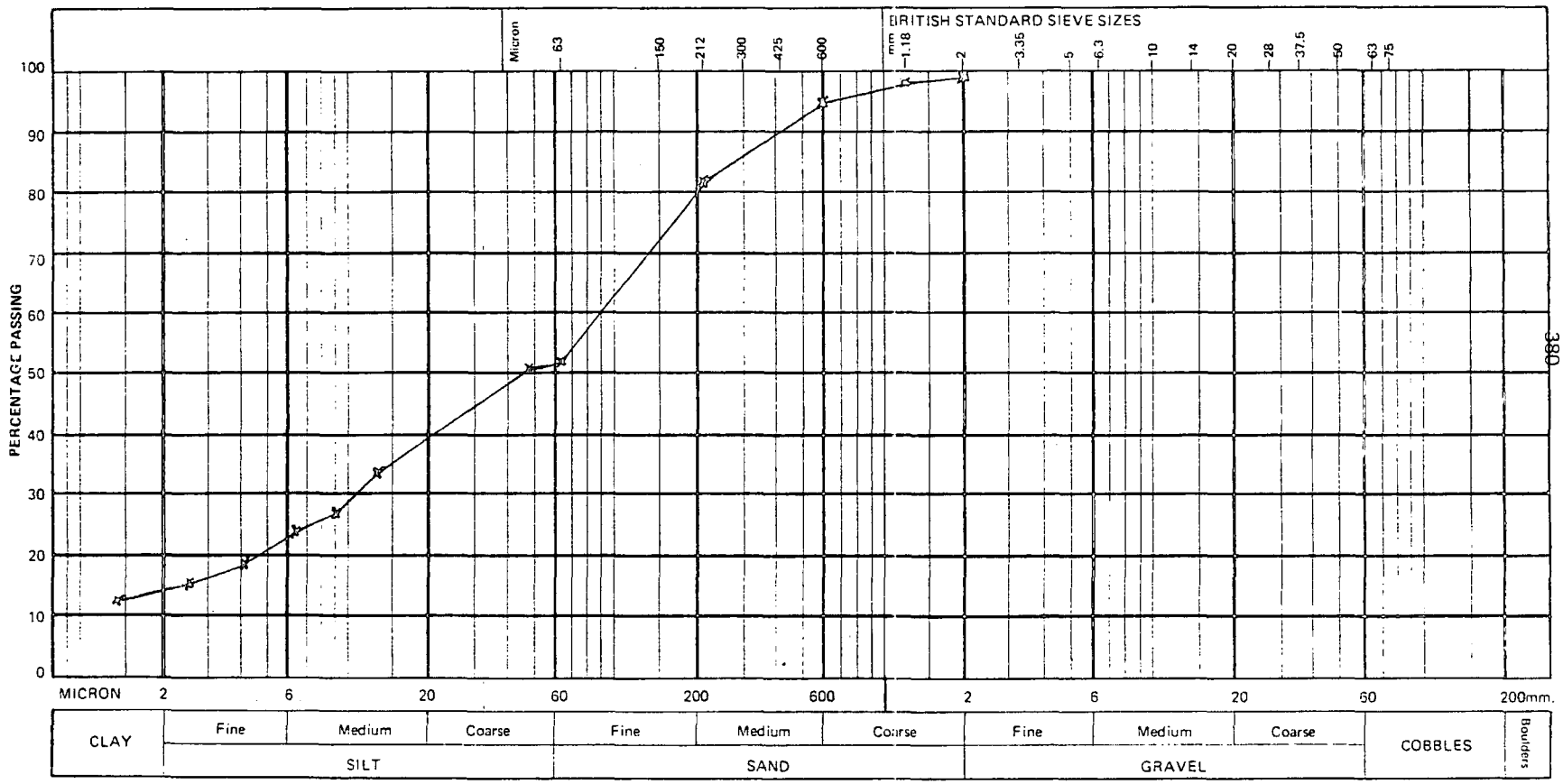

380

Signed.....

Form No. K4

PARTICLE SIZE DISTRIBUTION

LOCATION No..... BORE HOLE No..... SAMPLE No. 3/4 PRETREATMENT DETAILS H_2O_2

DATE OF TEST..... DESCRIPTION..... LOSS ON PRETREATMENT.....%

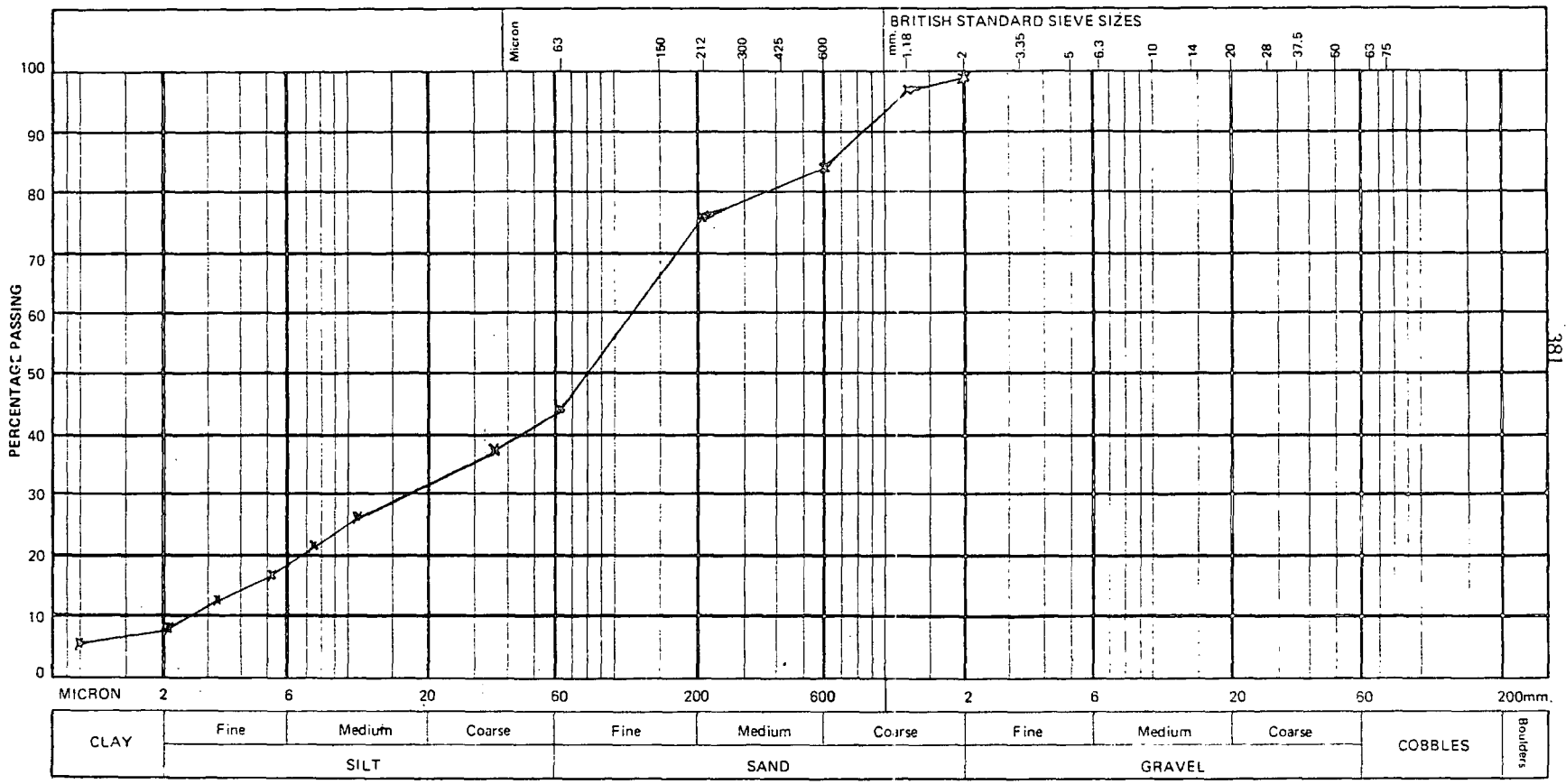

Signed.....

Form No. K4

PARTICLE SIZE DISTRIBUTION

LOCATION No. ..... BORE HOLE No. ..... SAMPLE No. 3/5 PRETREATMENT DETAILS H_2O_2

DATE OF TEST. ..... DESCRIPTION. ..... LOSS ON PRETREATMENT. .....%

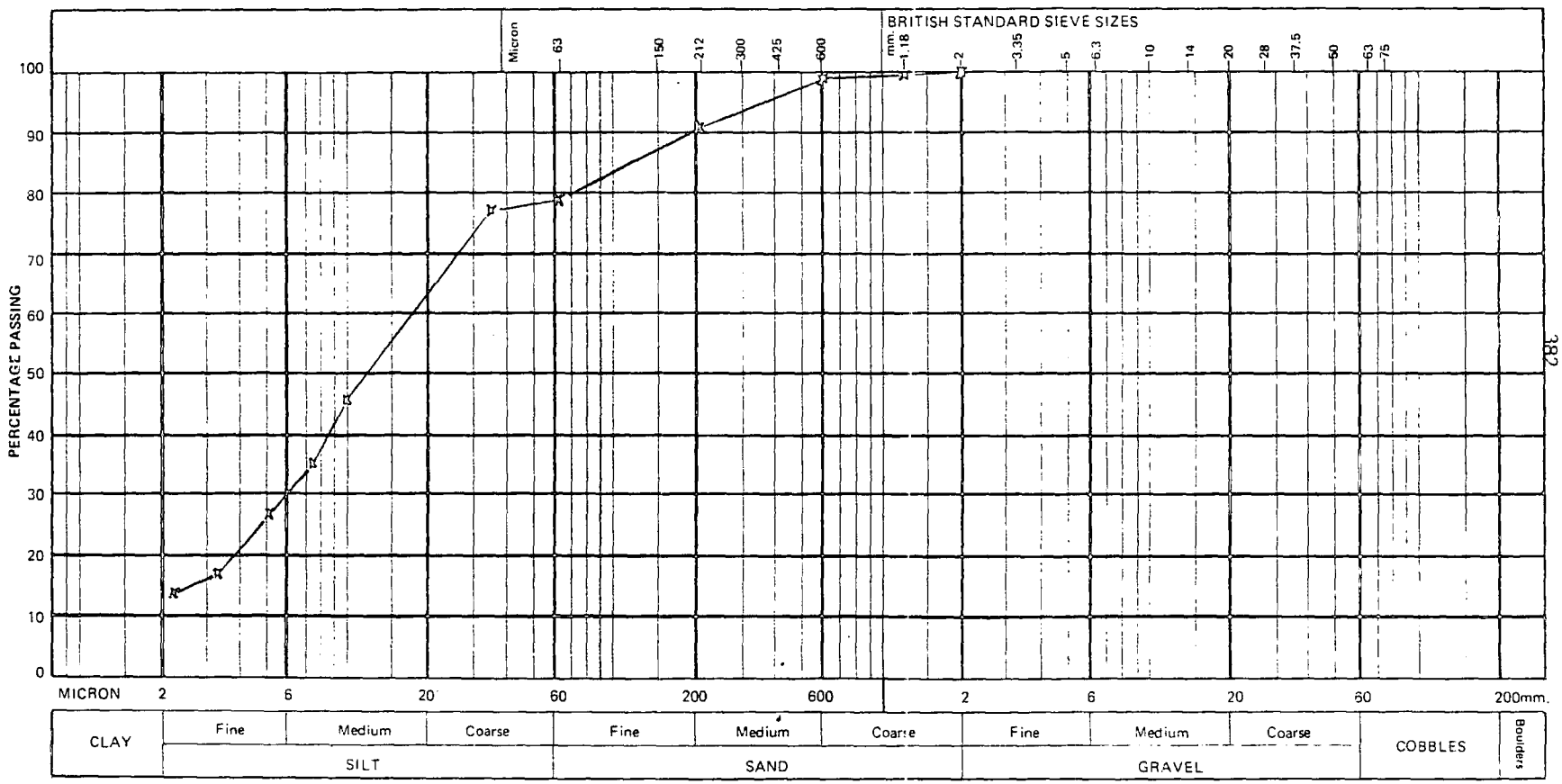

382

Signed. .....

PARTICLE SIZE DISTRIBUTION

Form No. K4

LOCATION No..... BORE HOLE No..... SAMPLE No. 3/6 PRETREATMENT DETAILS H_2O_2

DATE OF TEST..... DESCRIPTION..... LOSS ON PRETREATMENT.....%

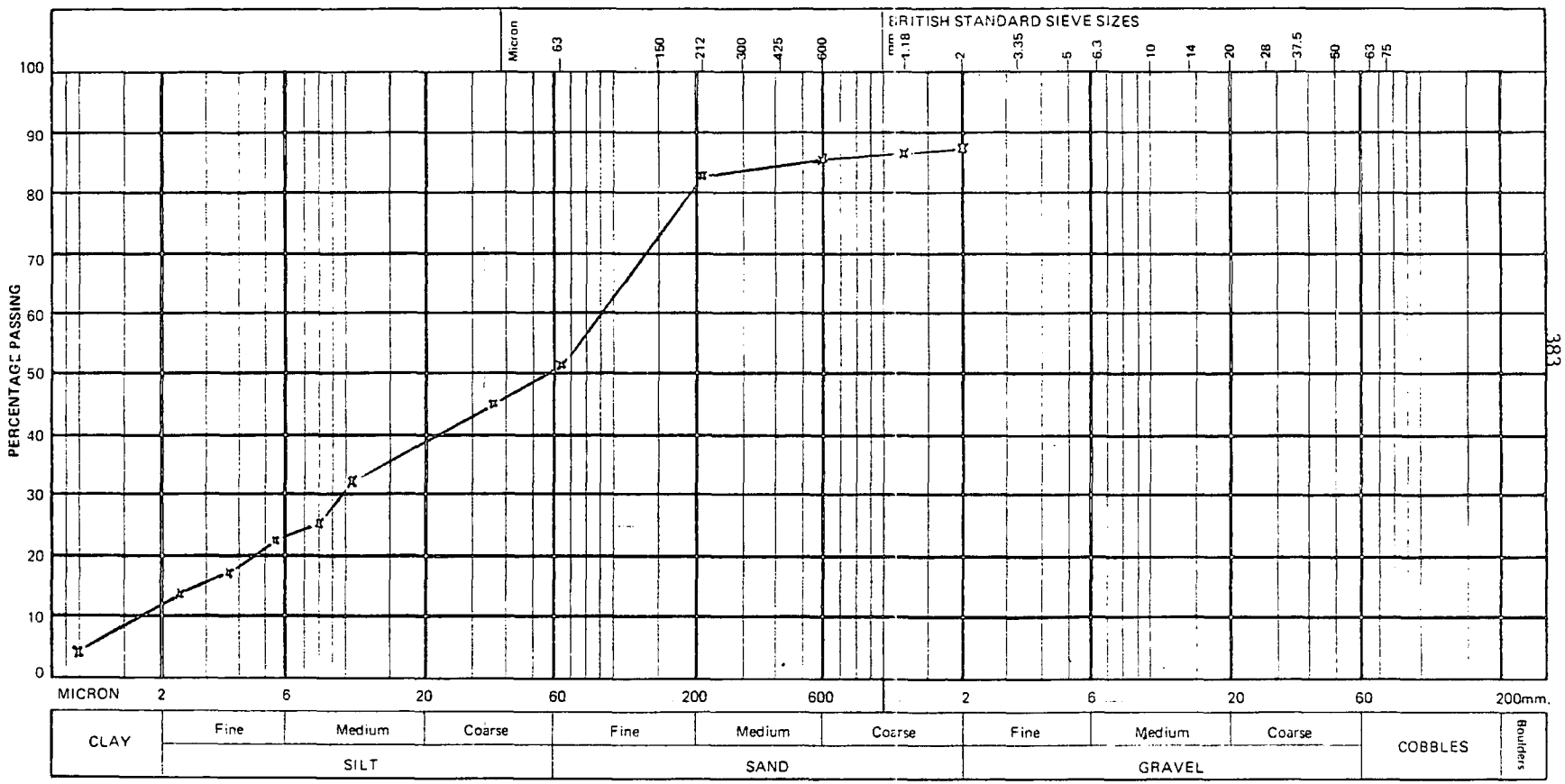

383

Signed.....

PARTICLE SIZE DISTRIBUTION

Form No. K4

LOCATION No..... BORE HOLE No..... SAMPLE No. 3/7 PRETREATMENT DETAILS H_2O_2

DATE OF TEST..... DESCRIPTION..... LOSS ON PRETREATMENT.....%

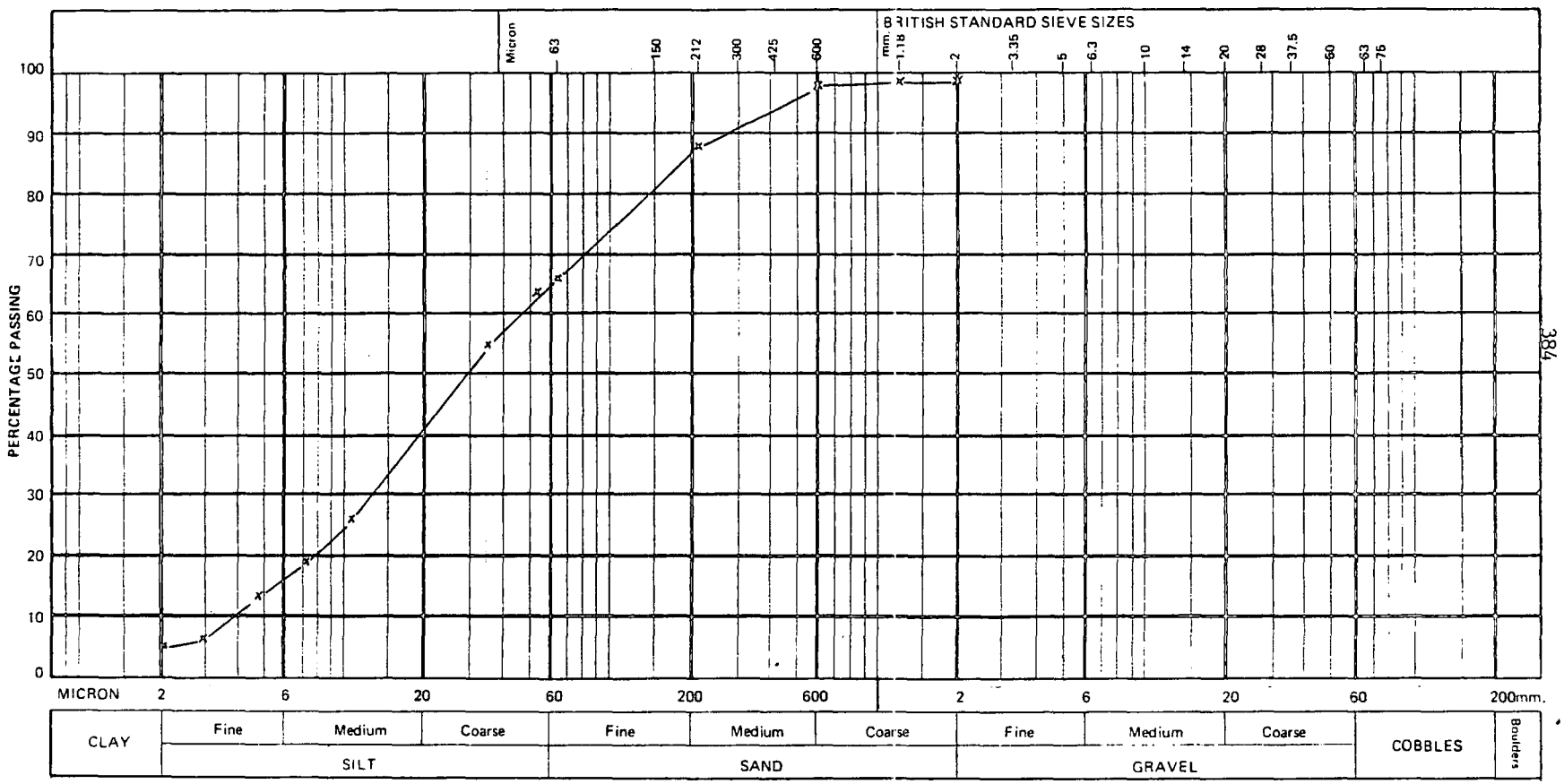

384

Signed.....

ELE

PARTICLE SIZE DISTRIBUTION

Form No. K4

LOCATION No..... BORE HOLE No..... SAMPLE No. 4/2. PRETREATMENT DETAILS H_2O_2

DATE OF TEST..... DESCRIPTION..... LOSS ON PRETREATMENT.....%

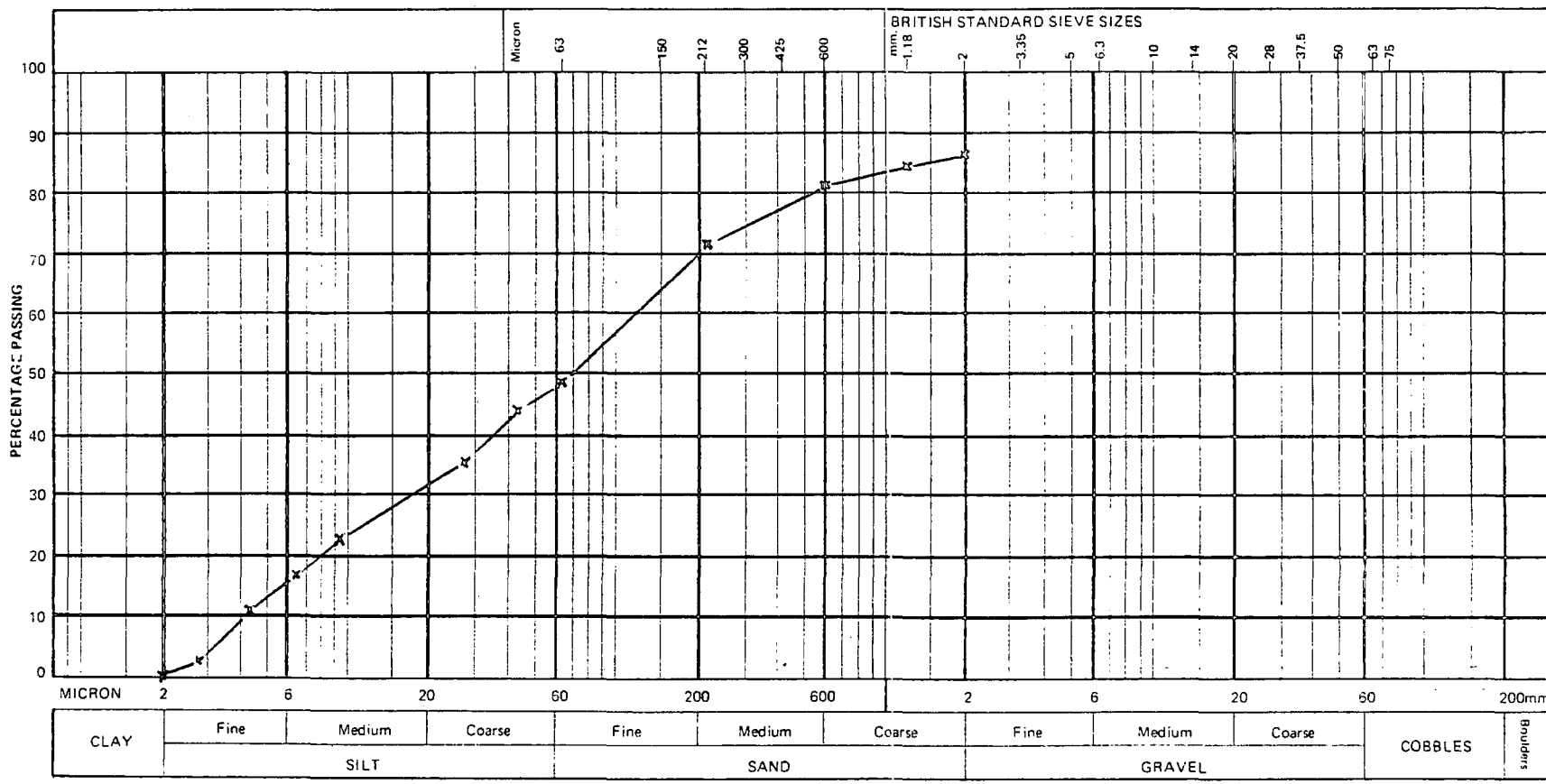

Signed.....

PARTICLE SIZE DISTRIBUTION

Form No. K4

LOCATION No..... BORE HOLE No..... SAMPLE No. 4/3 PRETREATMENT DETAILS.....

DATE OF TEST..... DESCRIPTION..... LOSS ON PRETREATMENT.....%

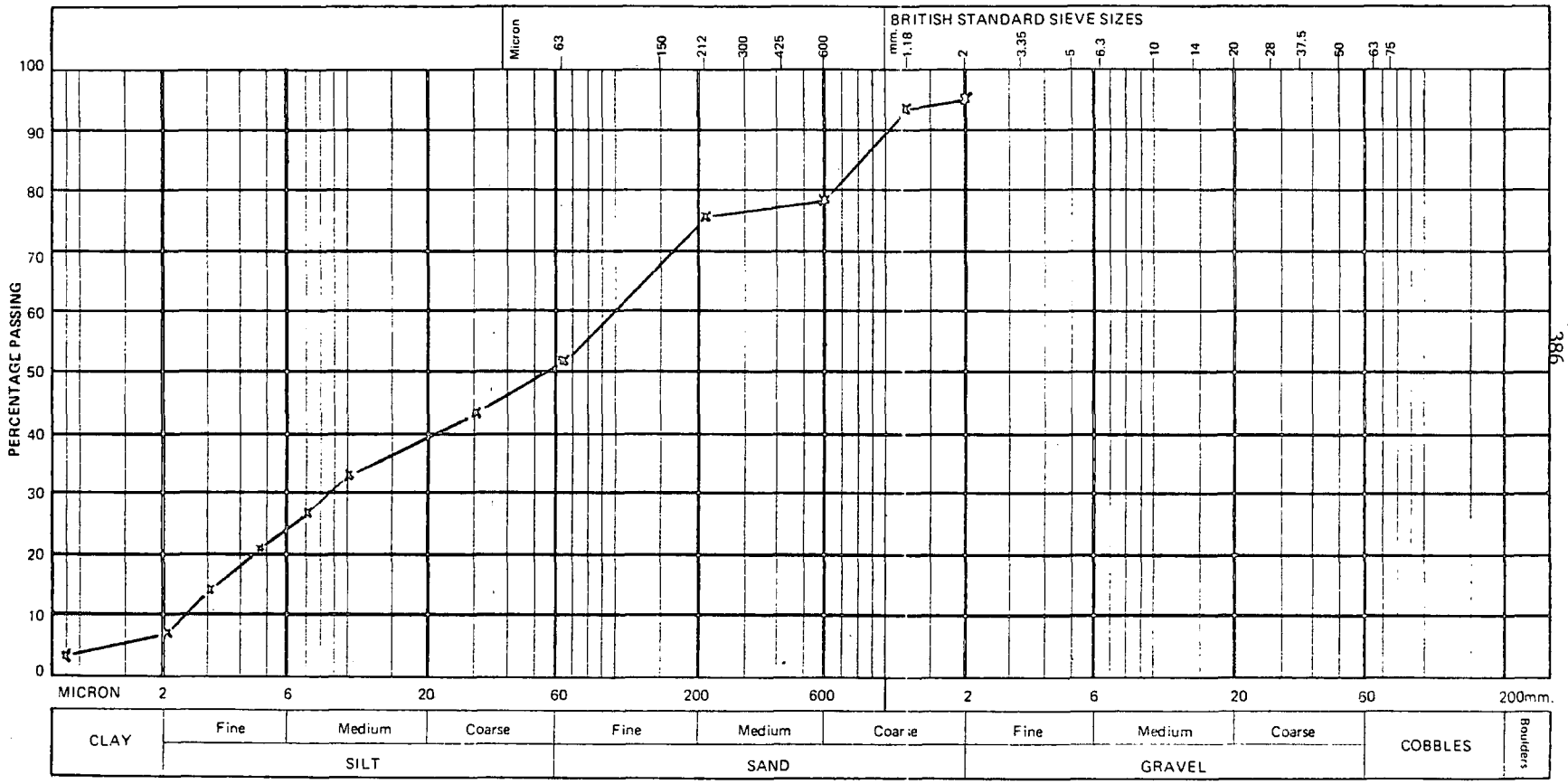

386

Signed.....

Form No. K4

PARTICLE SIZE DISTRIBUTION

LOCATION No..... BORE HOLE No..... SAMPLE No. 4/4 PRETREATMENT DETAILS H_2O_2

DATE OF TEST..... DESCRIPTION..... LOSS ON PRETREATMENT.....%

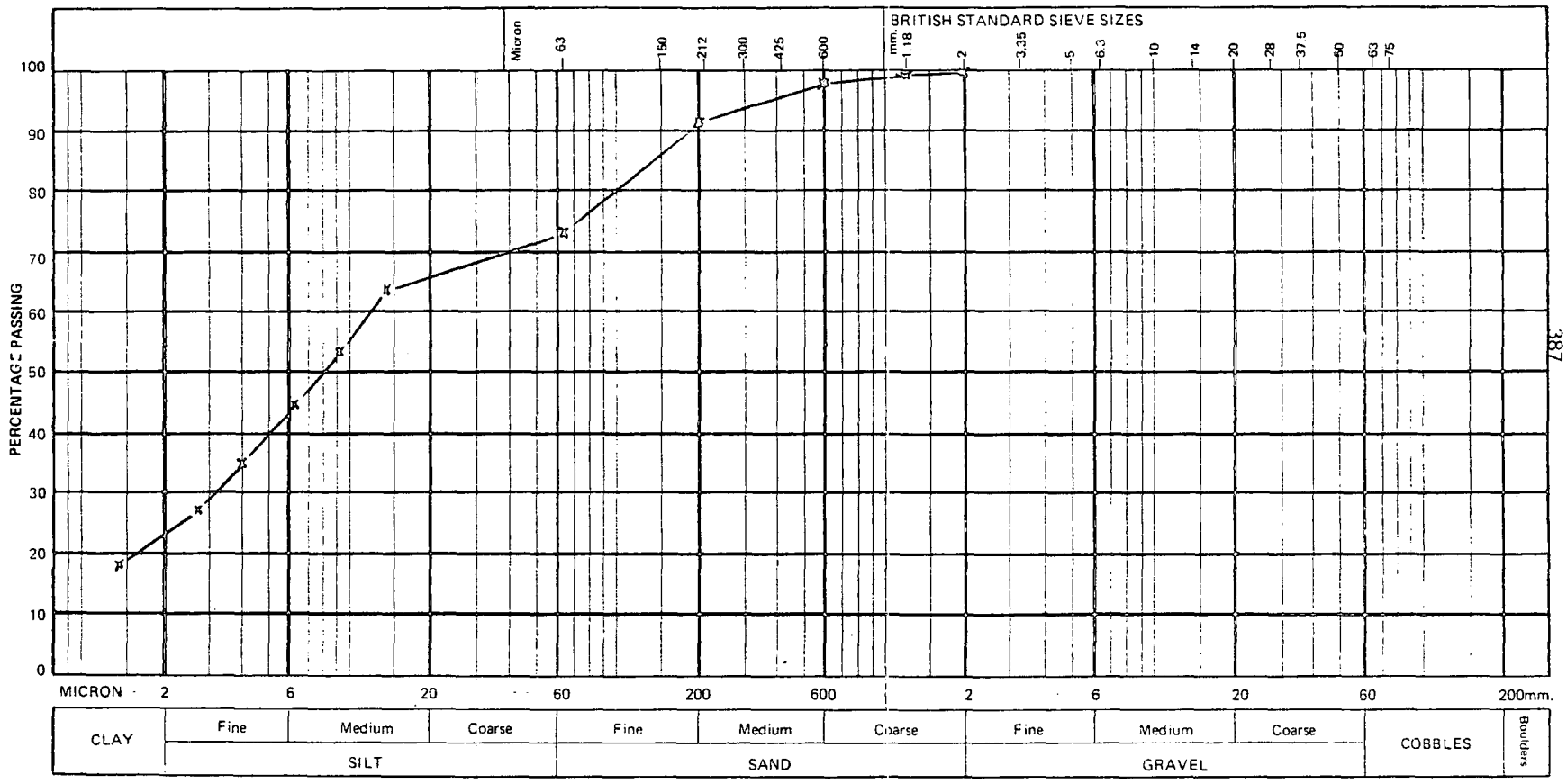

Signed.....

PARTICLE SIZE DISTRIBUTION

Form No. K4

LOCATION No..... BORE HOLE No..... SAMPLE No. 4/5 PRETREATMENT DETAILS H_2O_2

DATE OF TEST..... DESCRIPTION..... LOSS ON PRETREATMENT.....%

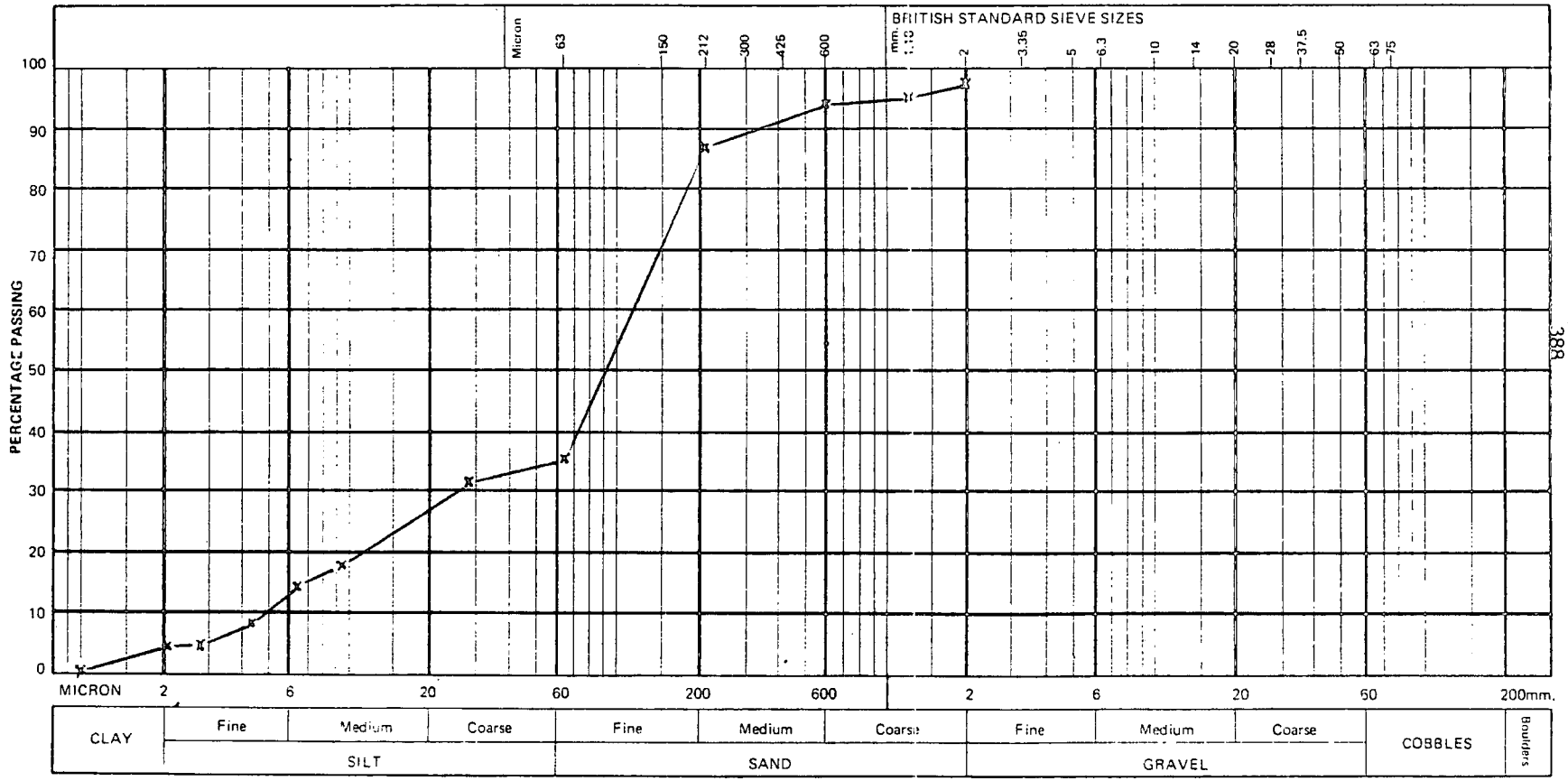

388

Signed.....

PARTICLE SIZE DISTRIBUTION

Form No. K4

LOCATION No. ..... BORE HOLE No. ..... SAMPLE No. 4/6 PRETREATMENT DETAILS H_2O_2

DATE OF TEST ..... DESCRIPTION ..... LOSS ON PRETREATMENT ..... %

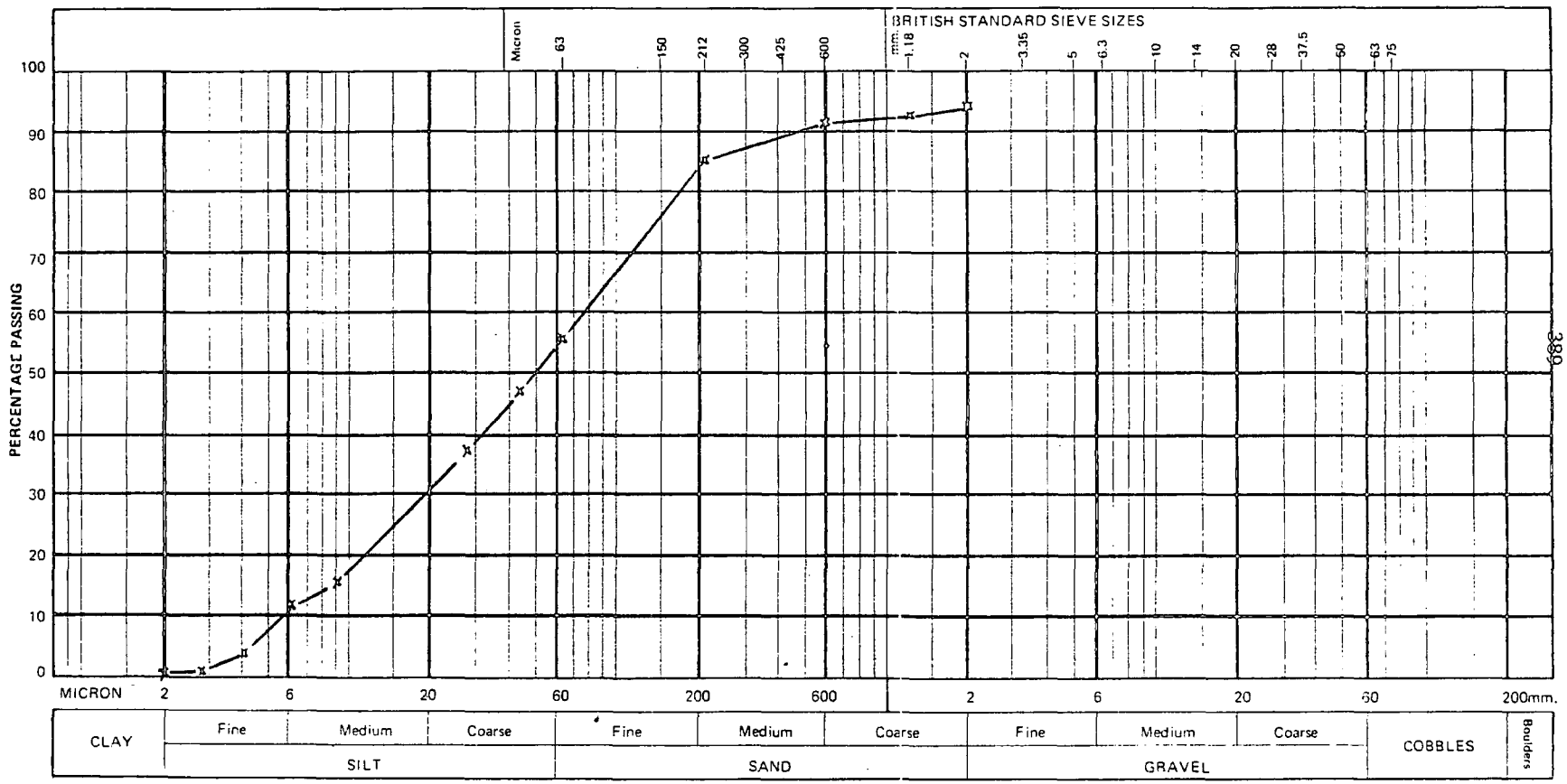

Signed .....

PARTICLE SIZE DISTRIBUTION

Form No. K4

LOCATION No..... BORE HOLE No..... SAMPLE No. 5/1 PRETREATMENT DETAILS H_2O_2

DATE OF TEST..... DESCRIPTION..... LOSS ON PRETREATMENT.....%

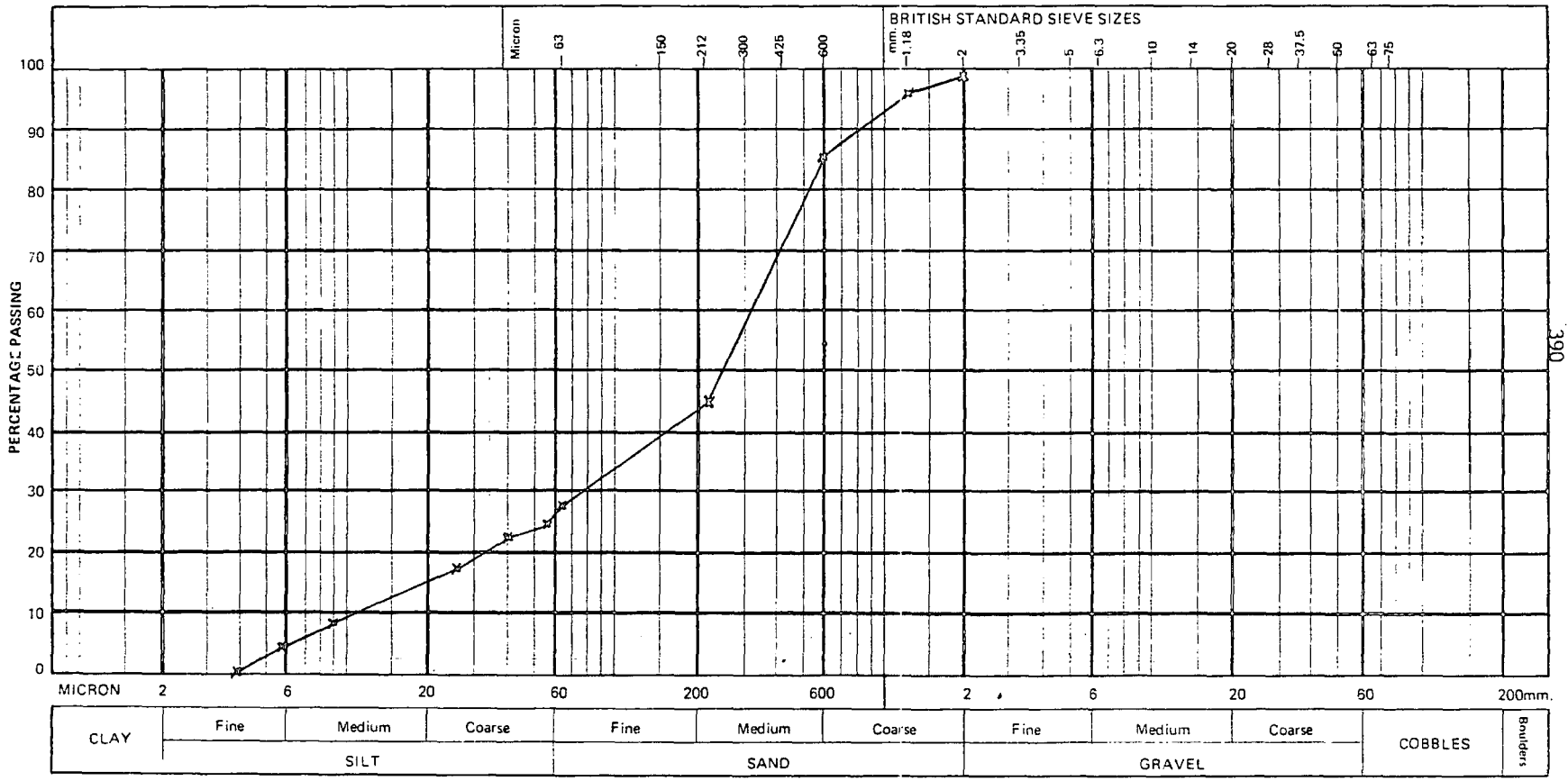

390

Signed.....

Form No. K4

PARTICLE SIZE DISTRIBUTION

LOCATION No..... BORE HOLE No..... SAMPLE No. 5/3 PRETREATMENT DETAILS H_2O_2

DATE OF TEST..... DESCRIPTION..... LOSS ON PRETREATMENT.....%

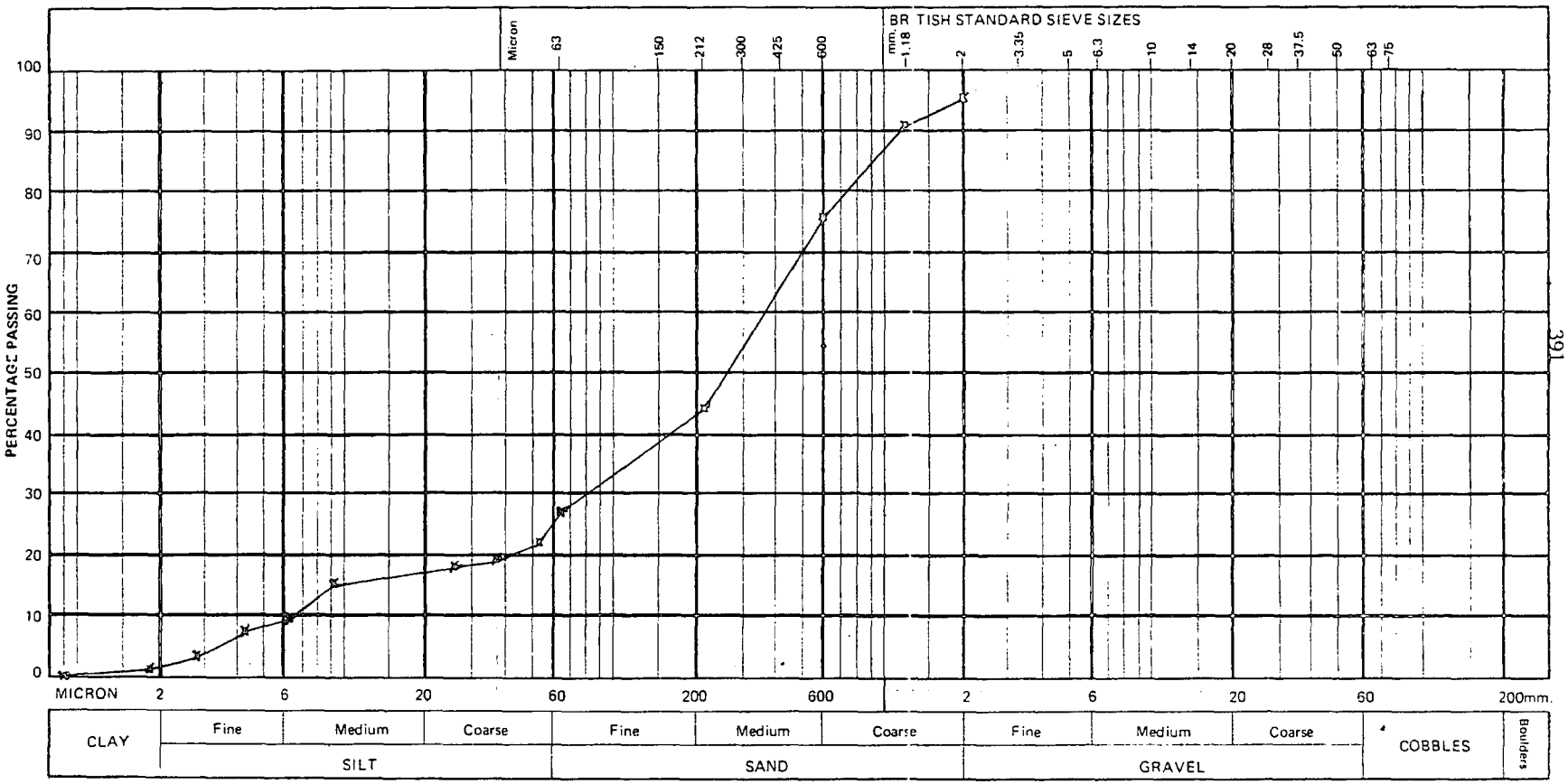

Signed.....

PARTICLE SIZE DISTRIBUTION

Form No. K4

LOCATION No..... BORE HOLE No..... SAMPLE No. 5/4 PRETREATMENT DETAILS H_2O_2

DATE OF TEST..... DESCRIPTION..... LOSS ON PRETREATMENT.....%

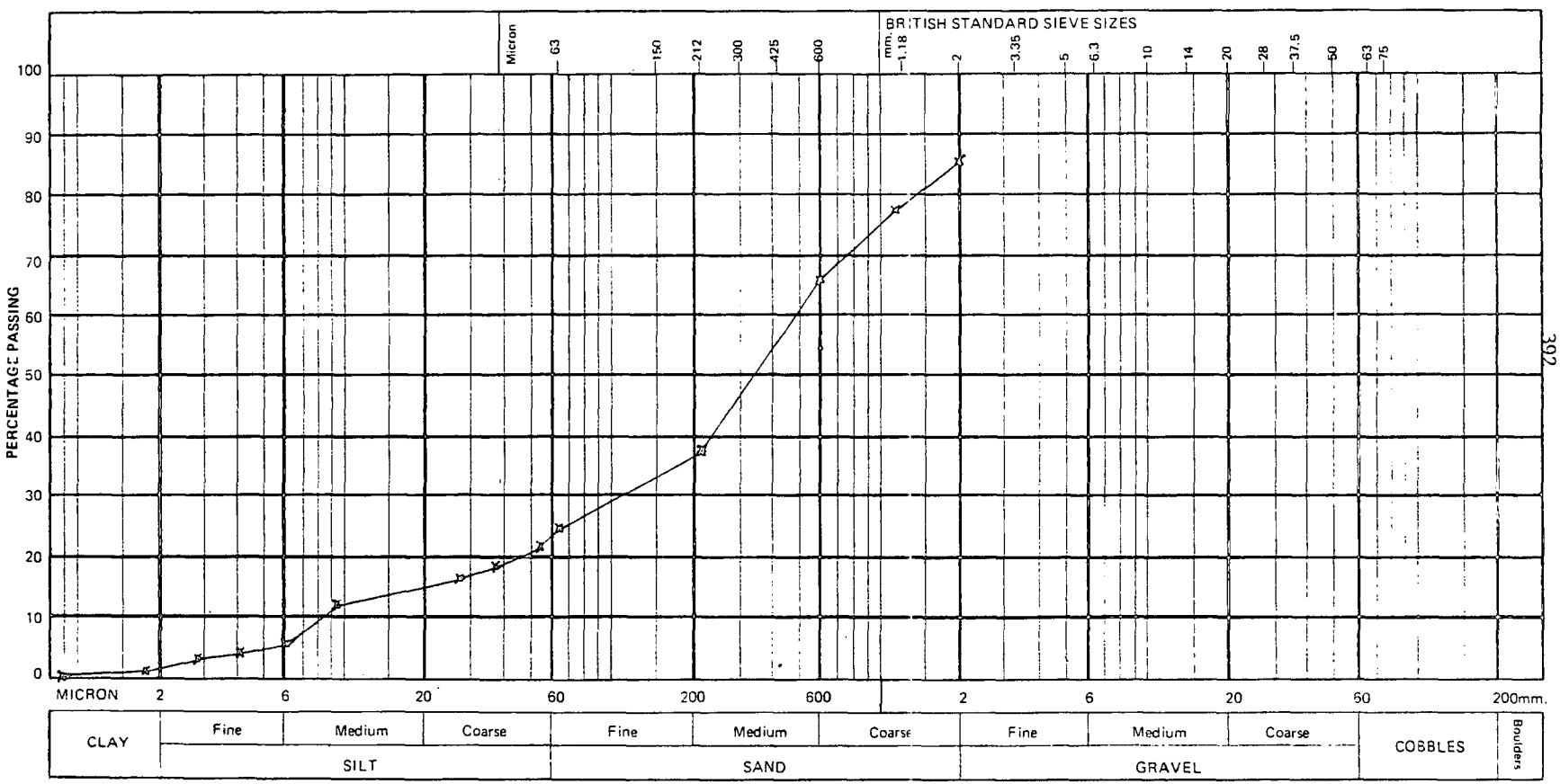

392

Signed.....

ELE

PARTICLE SIZE DISTRIBUTION

Form No. K4

LOCATION No..... BORE HOLE No..... SAMPLE No. 5/5 PRETREATMENT DETAILS H_2O_2

DATE OF TEST..... DESCRIPTION..... LOSS ON PRETREATMENT.....%

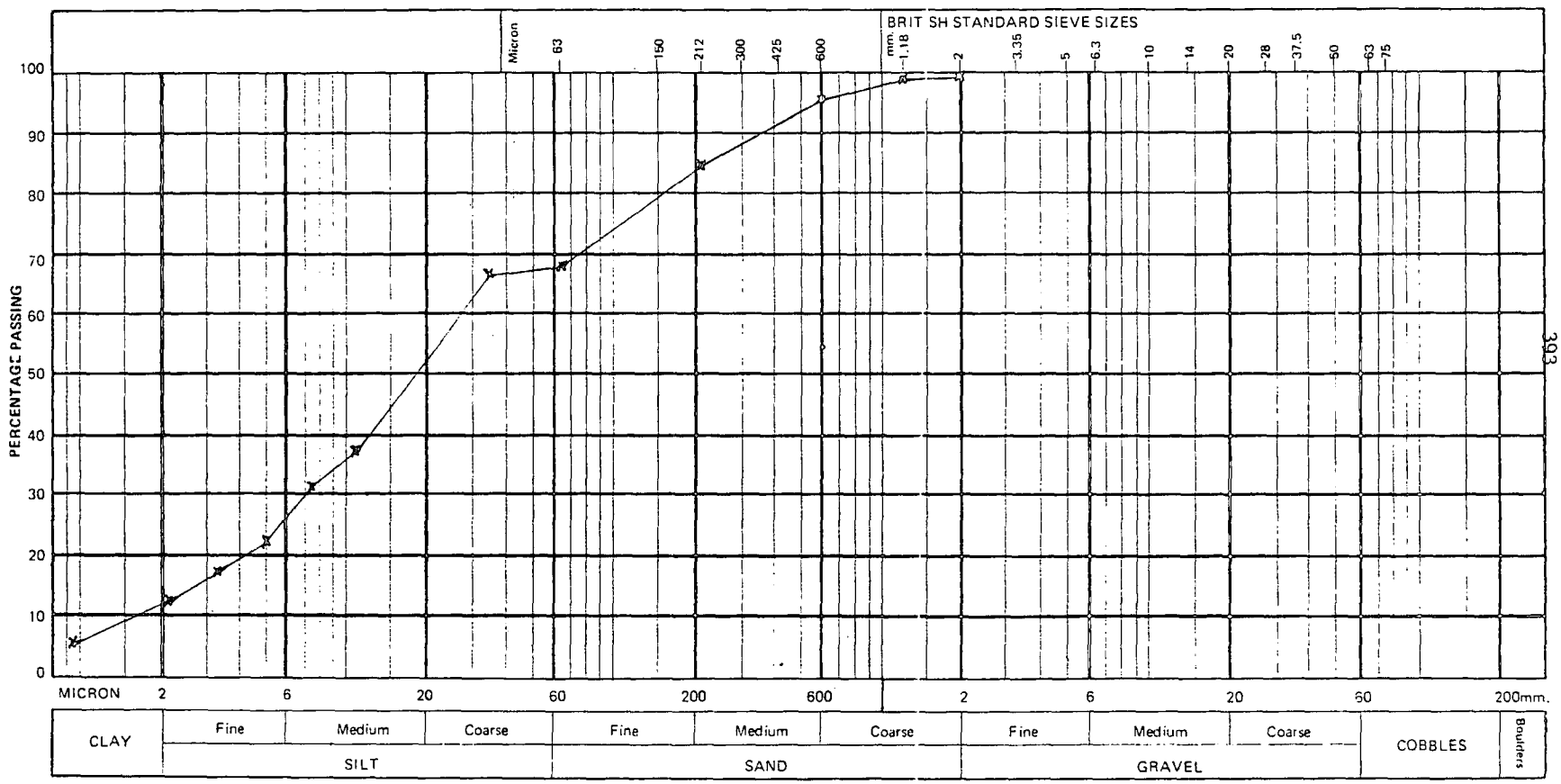

393

Signed.....

PARTICLE SIZE DISTRIBUTION

Form No. K4

LOCATION No..... BORE HOLE No..... SAMPLE No. 5/6 PRETREATMENT DETAILS H_2O_2

DATE OF TEST..... DESCRIPTION..... LOSS ON PRETREATMENT.....%

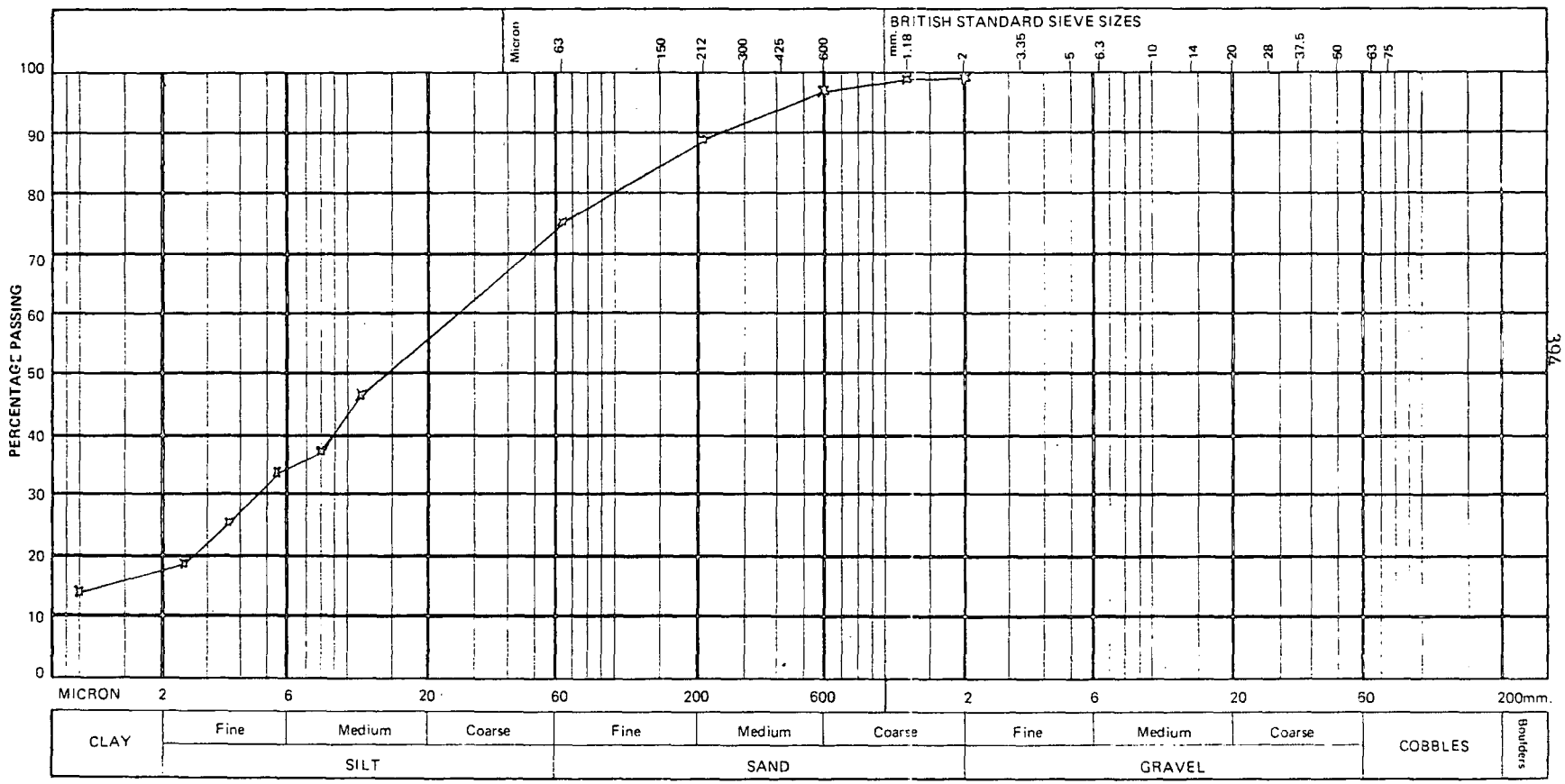

Signed.....

Form No. K4

PARTICLE SIZE DISTRIBUTION

LOCATION No..... BORE HOLE No..... SAMPLE No. 5|7 PRETREATMENT DETAILS H_2O_2

DATE OF TEST..... DESCRIPTION..... LOSS ON PRETREATMENT.....%

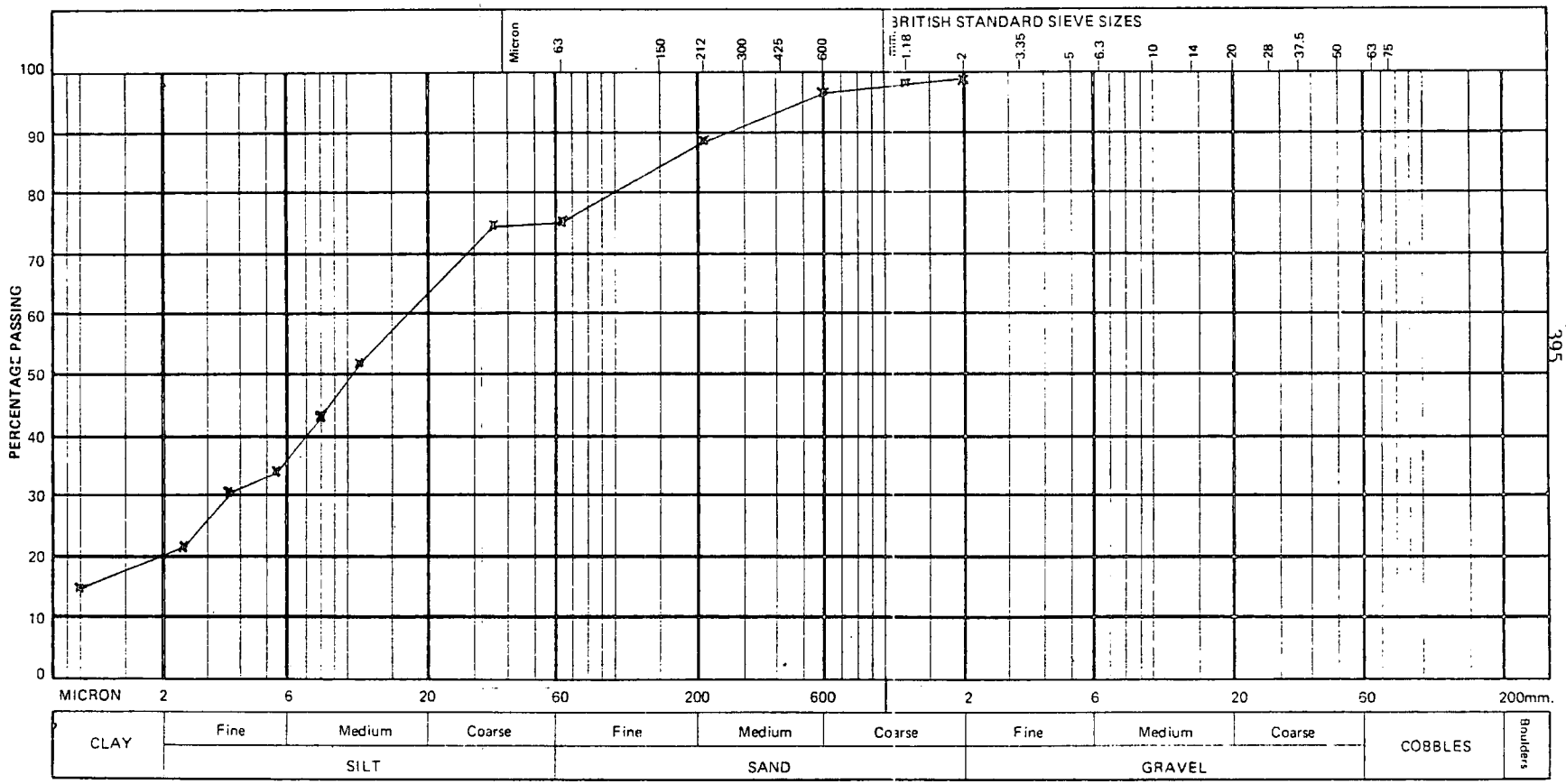

Signed.....

Form No. K4

PARTICLE SIZE DISTRIBUTION

LOCATION No..... BORE HOLE No..... SAMPLE No. 5/8 PRETREATMENT DETAILS H_2O_2

DATE OF TEST..... DESCRIPTION..... LOSS ON PRETREATMENT.....%

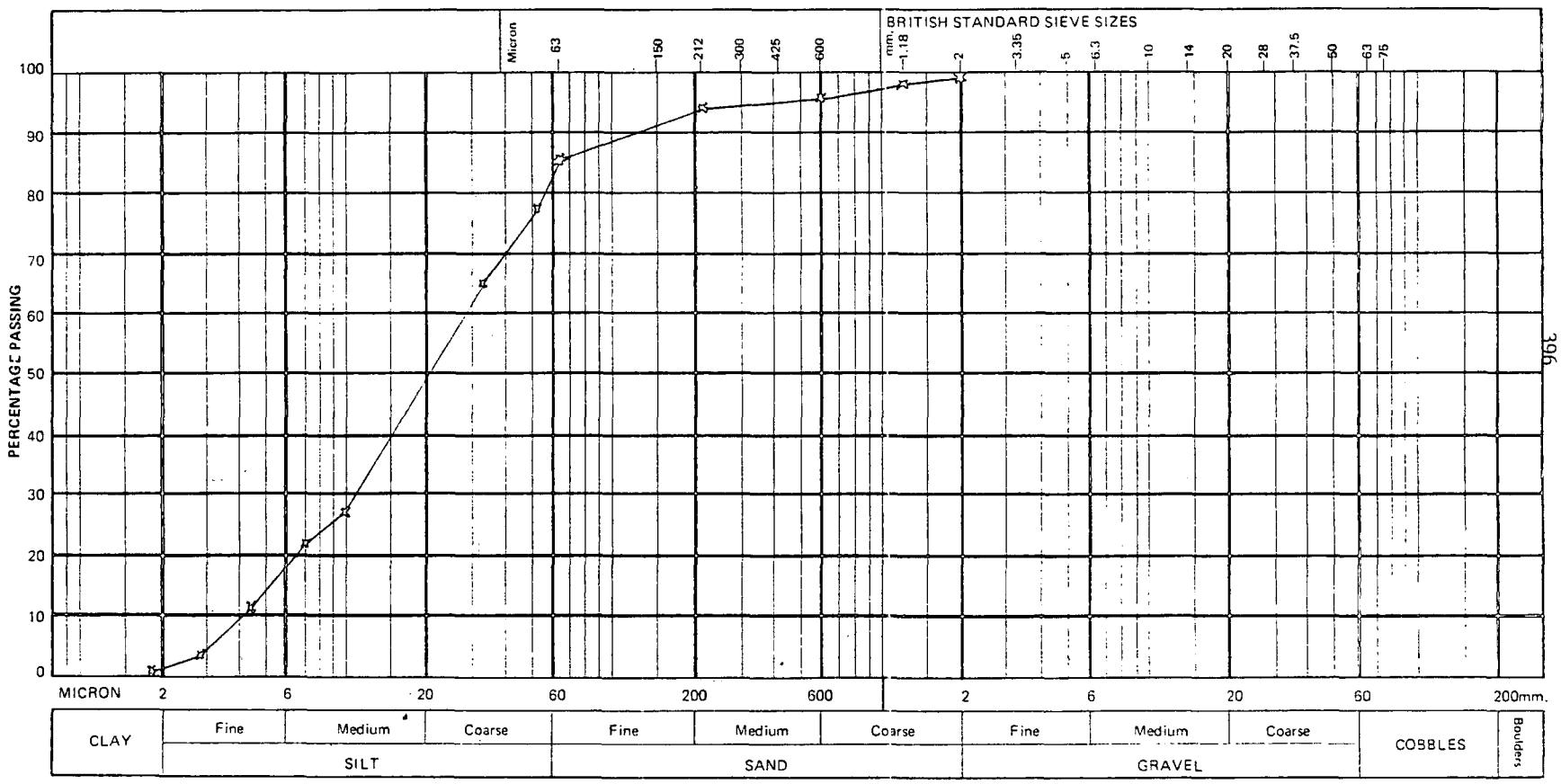

Signed.....

Form No. K4

PARTICLE SIZE DISTRIBUTION

LOCATION No..... BORE HOLE No..... SAMPLE No. 5/9 PRETREATMENT DETAILS H_2O_2

DATE OF TEST..... DESCRIPTION..... LOSS ON PRETREATMENT.....%

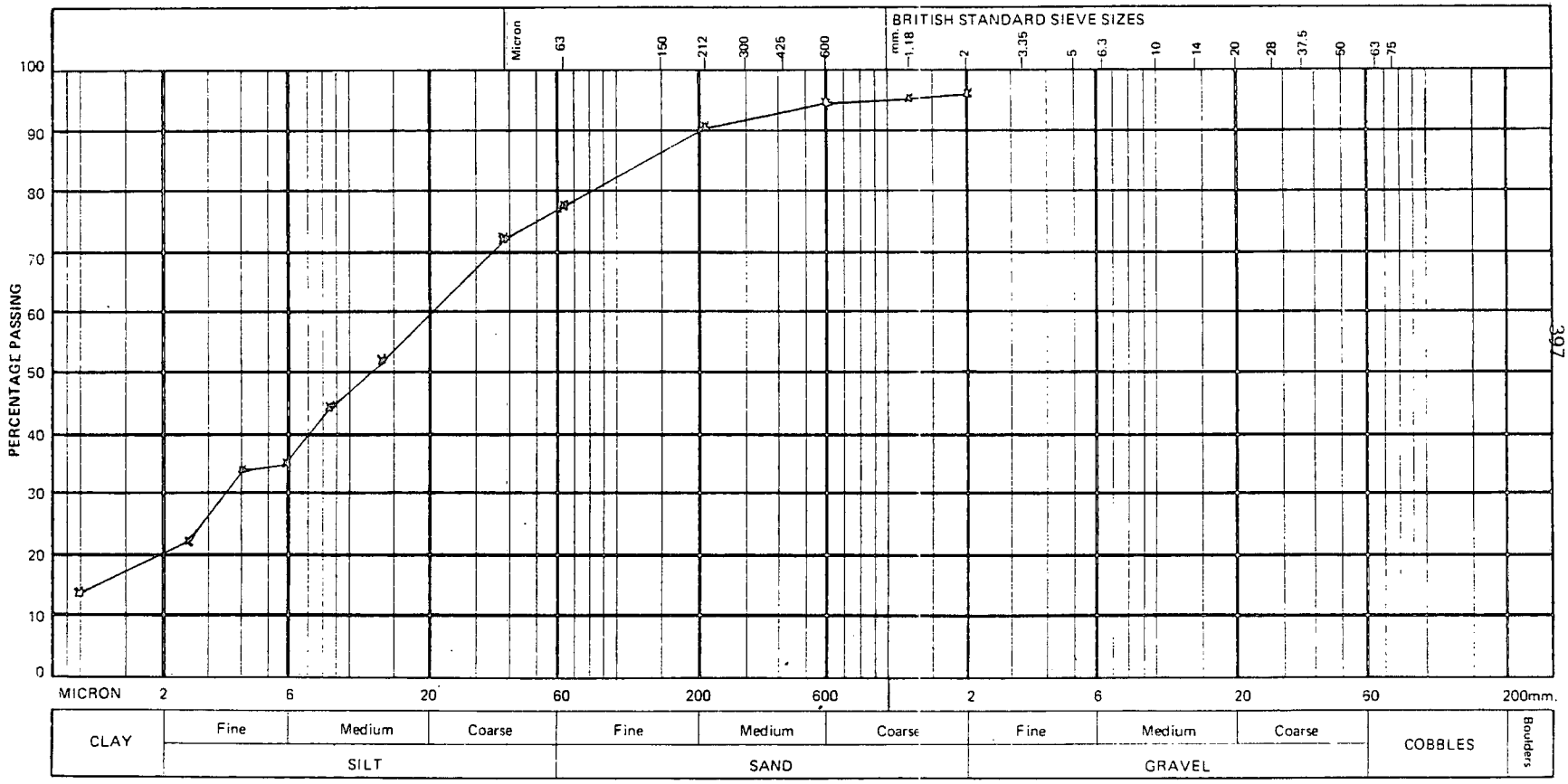

Signed.....

Form No. K4

PARTICLE SIZE DISTRIBUTION

LOCATION No..... BORE HOLE No..... SAMPLE No. 5/10 PRETREATMENT DETAILS H_2O_2

DATE OF TEST..... DESCRIPTION..... LOSS ON PRETREATMENT.....%

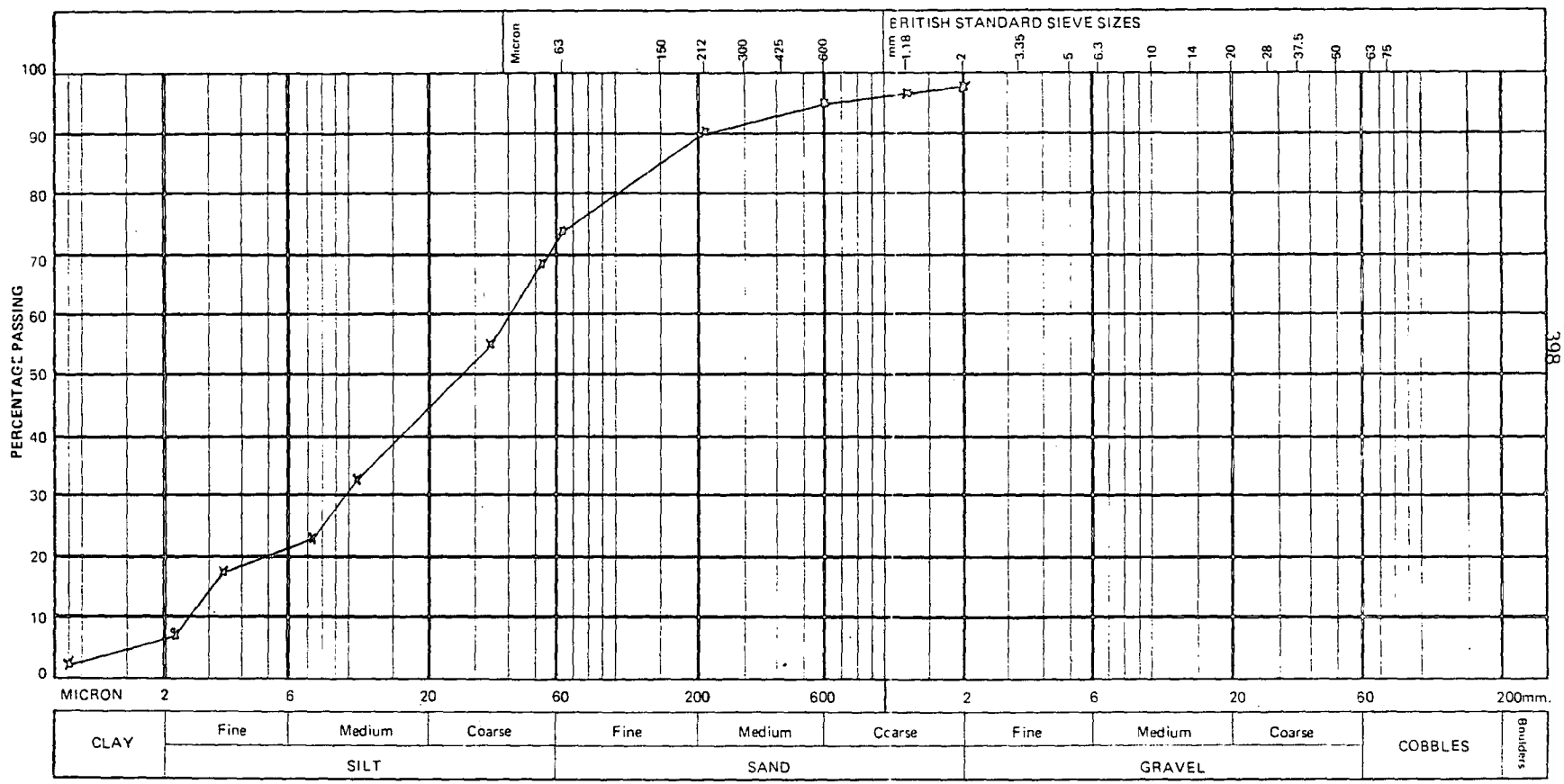

Signed.....

PARTICLE SIZE DISTRIBUTION

Form No. K4

LOCATION No..... BORE HOLE No..... SAMPLE No. 6/1 PRETREATMENT DETAILS H_2O_2

DATE OF TEST..... DESCRIPTION..... LOSS ON PRETREATMENT.....%

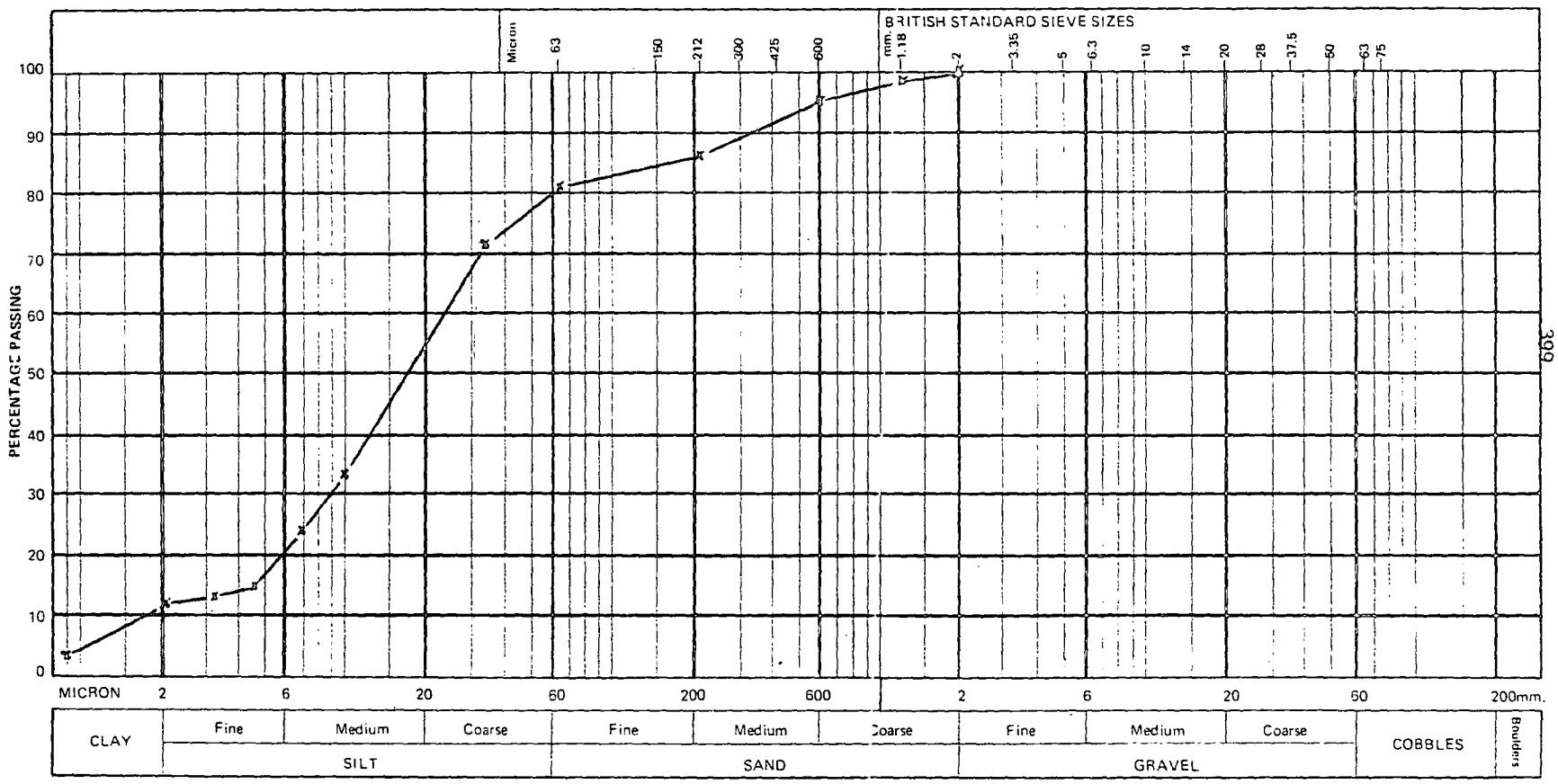

Signed.....

PARTICLE SIZE DISTRIBUTION

Form No. K4

LOCATION No..... BORE HOLE No..... SAMPLE No. 6/3 PRETREATMENT DETAILS H_2O_2

DATE OF TEST..... DESCRIPTION..... LOSS ON PRETREATMENT.....%

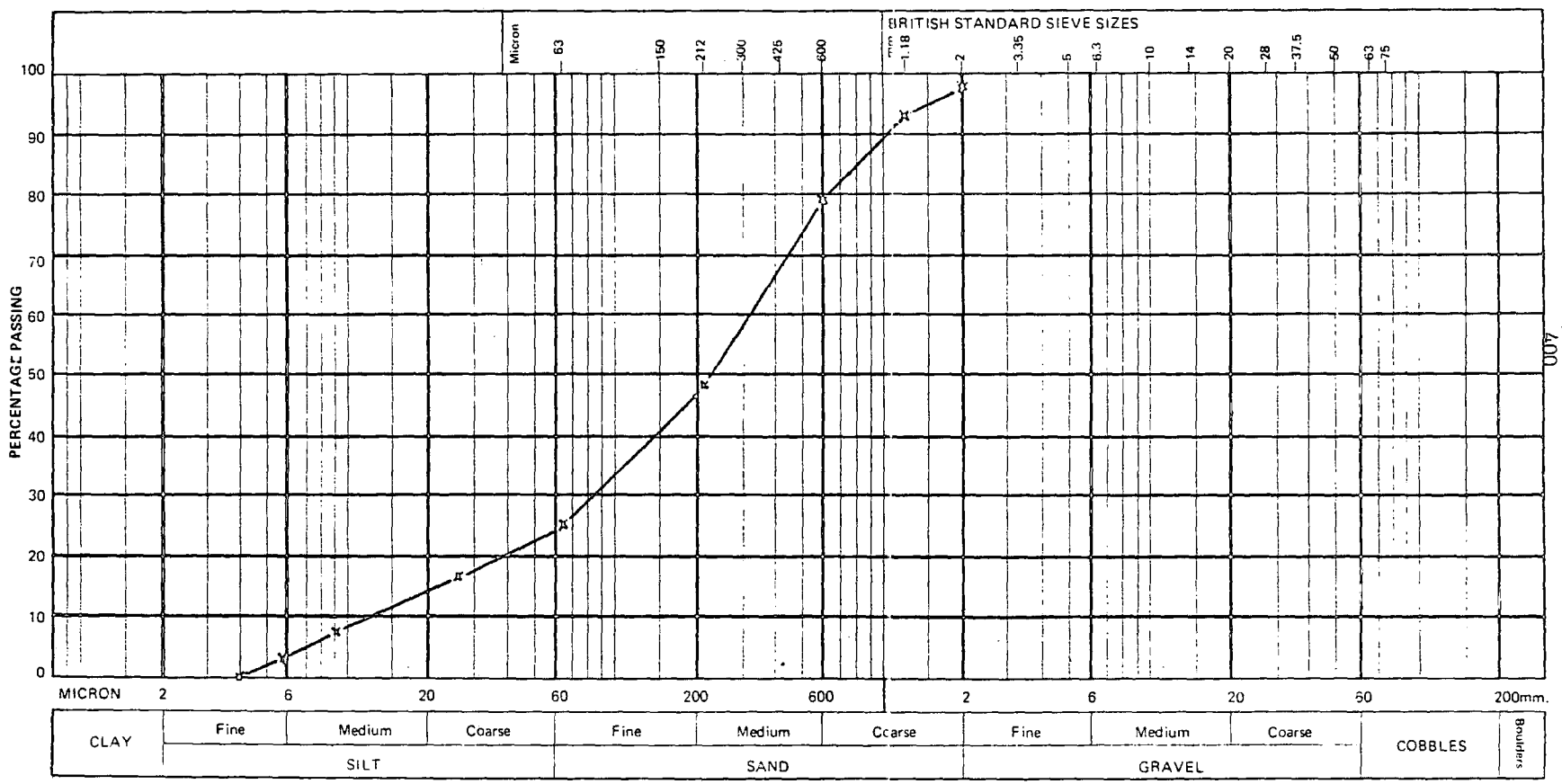

Signed.....

Form No. K4

PARTICLE SIZE DISTRIBUTION

LOCATION No. ..... BORE HOLE No. ..... SAMPLE No. 6/4 PRETREATMENT DETAILS H_2O_2

DATE OF TEST ..... DESCRIPTION ..... LOSS ON PRETREATMENT .....%

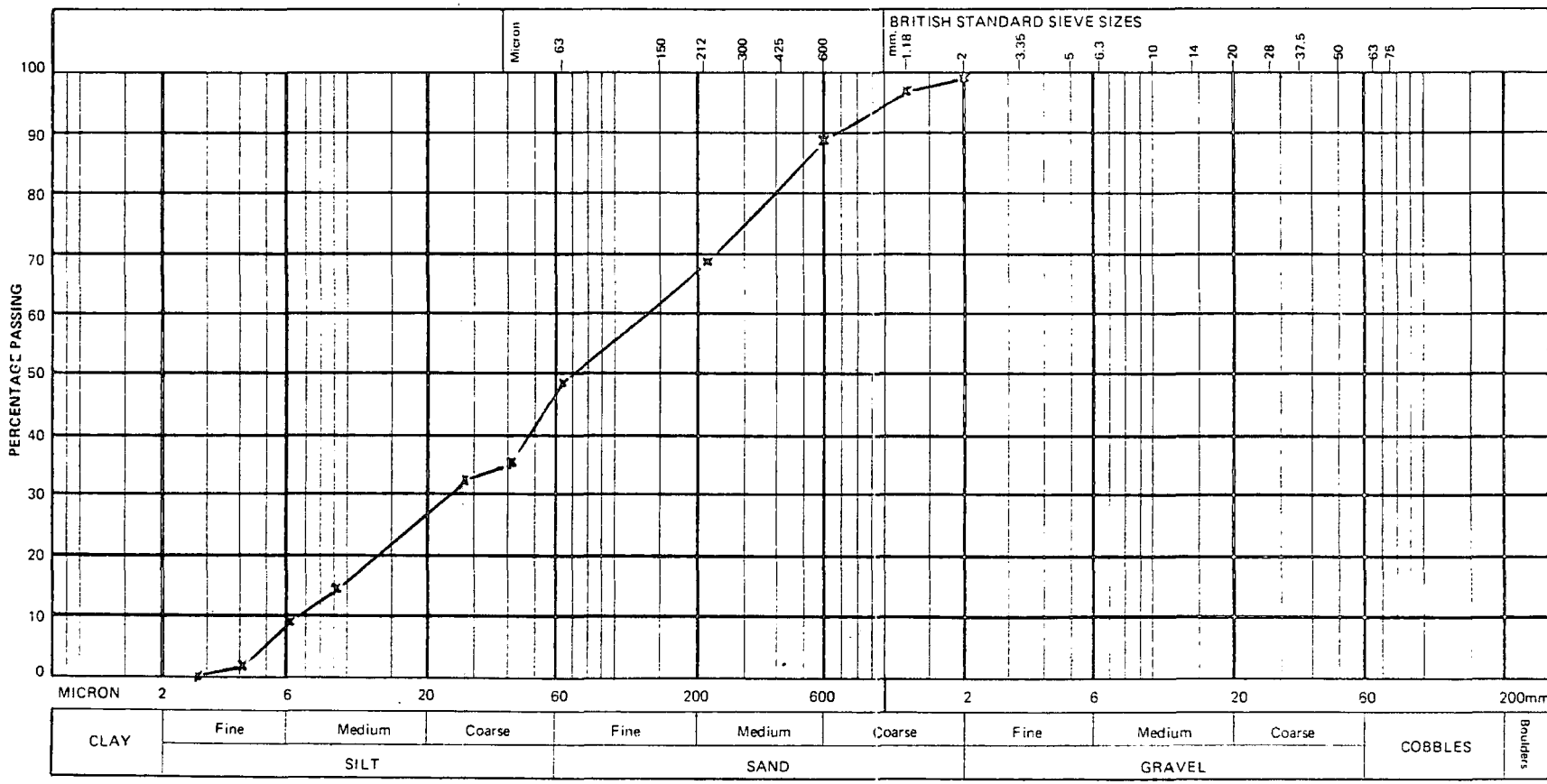

Signed .....

Form No. K4

PARTICLE SIZE DISTRIBUTION

LOCATION No..... BORE HOLE No..... SAMPLE No. 6/5 PRETREATMENT DETAILS H_2O_2

DATE OF TEST..... DESCRIPTION..... LOSS ON PRETREATMENT.....%

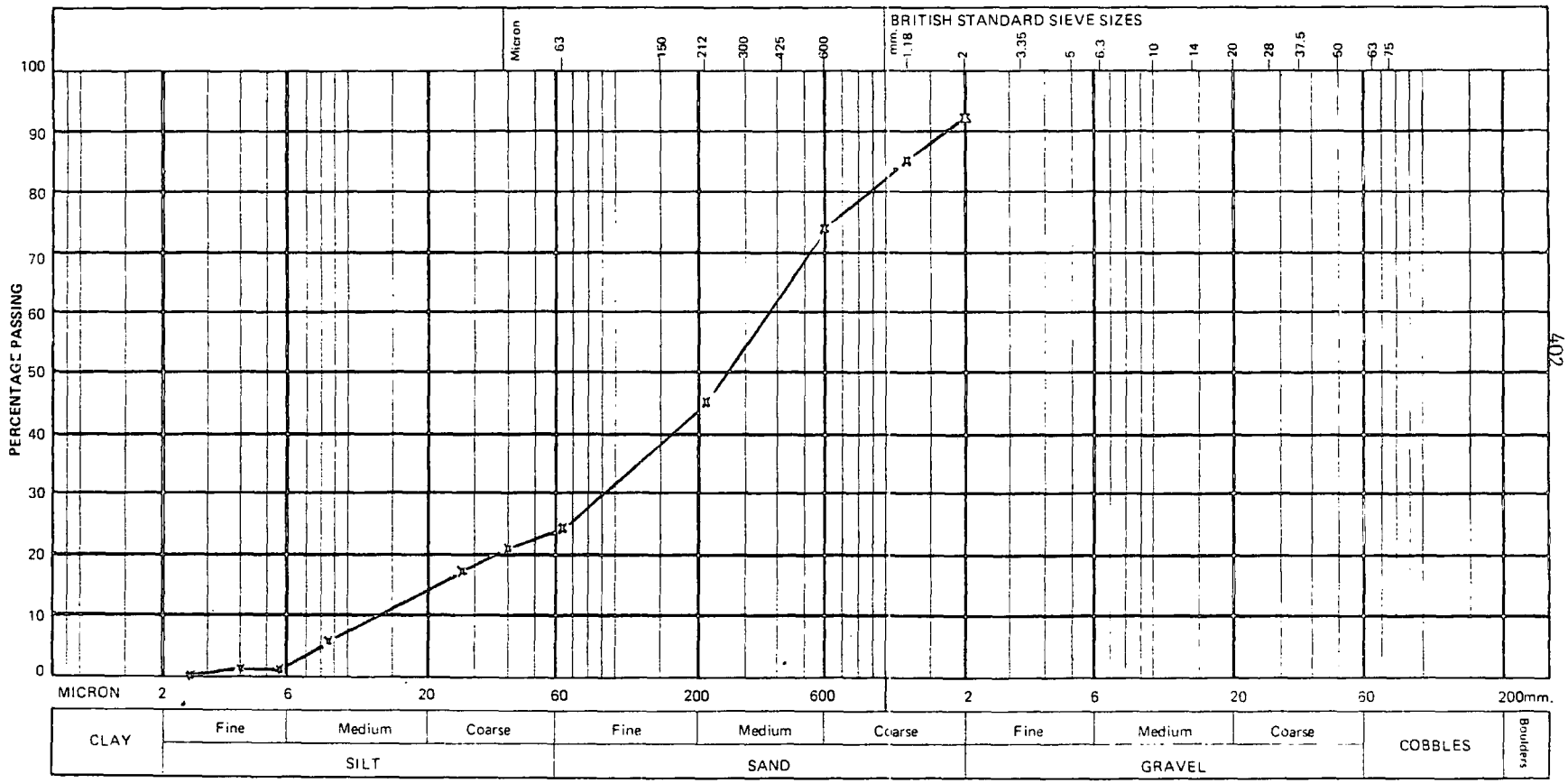

402

Signed.....

Form No. K4

PARTICLE SIZE DISTRIBUTION

LOCATION No..... BORE HOLE No..... SAMPLE No. 6/6 PRETREATMENT DETAILS H_2O_2

DATE OF TEST..... DESCRIPTION..... LOSS ON PRETREATMENT.....%

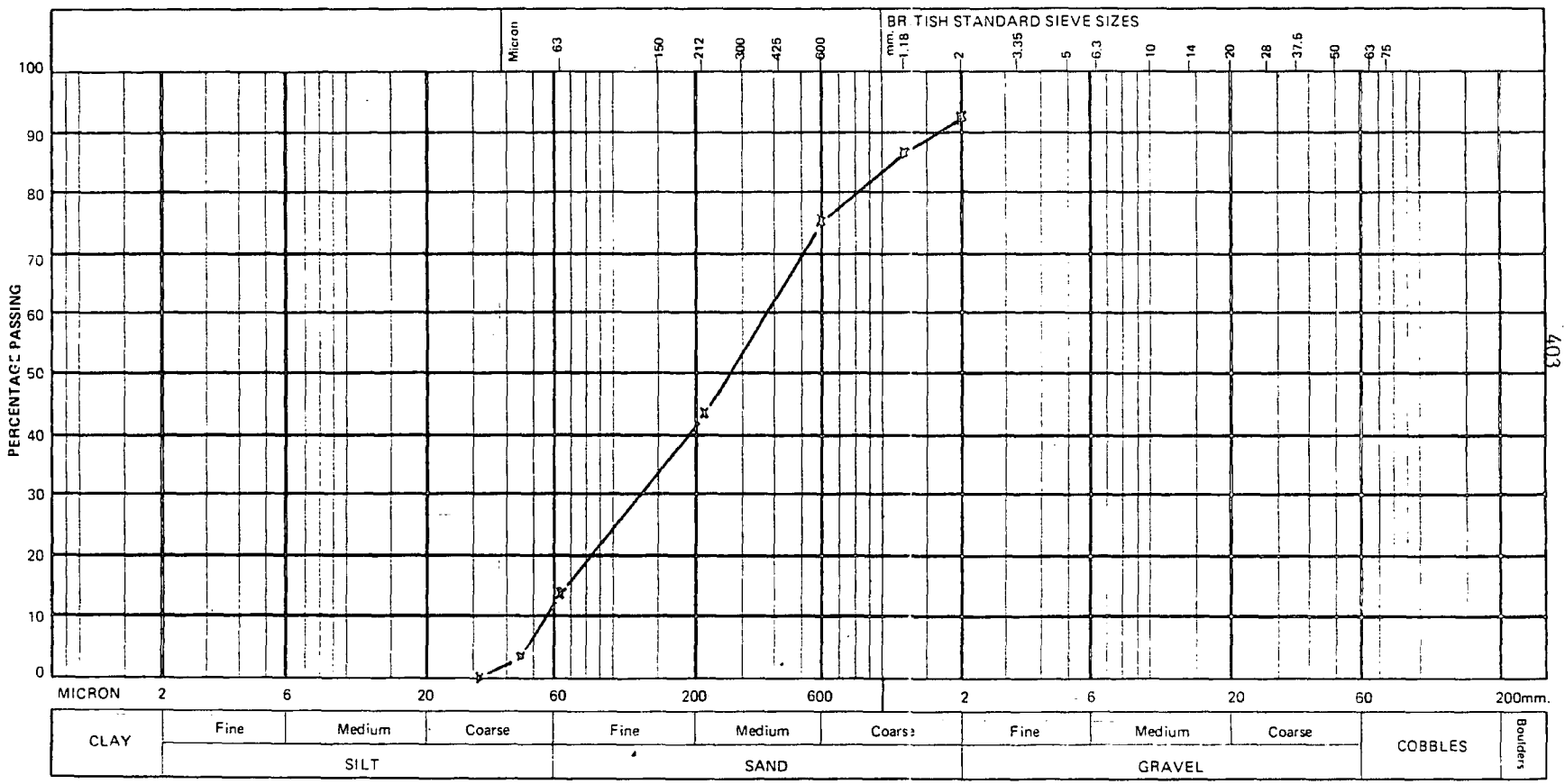

403

Signed.....

Form No. K4

PARTICLE SIZE DISTRIBUTION

LOCATION No..... BORE HOLE No..... SAMPLE No. 7/1 PRETREATMENT DETAILS H_2O_2

DATE OF TEST..... DESCRIPTION..... LOSS ON PRETREATMENT.....%

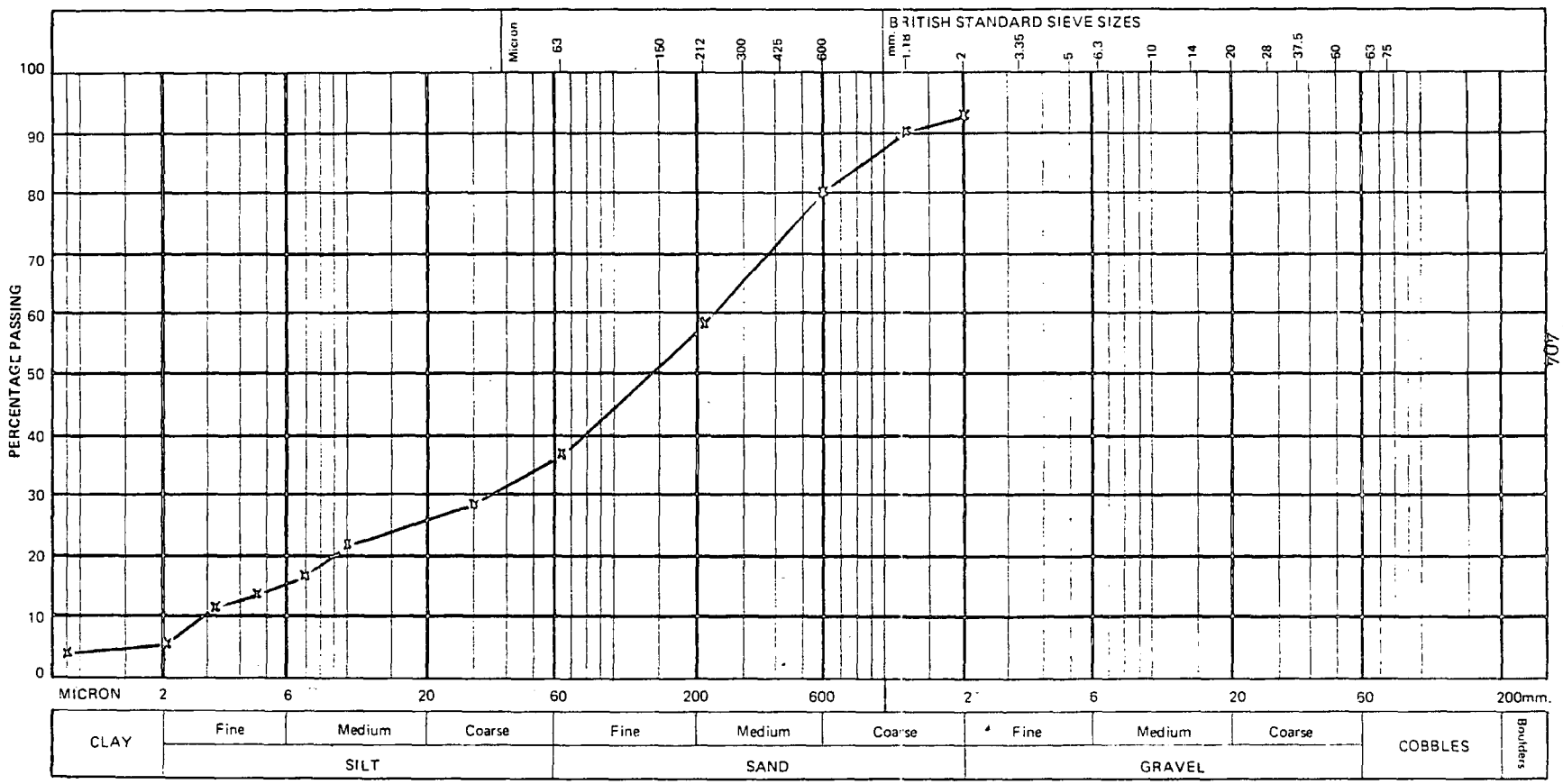

Signed.....

ELE

PARTICLE SIZE DISTRIBUTION

Form No. K4

LOCATION No..... BORE HOLE No..... SAMPLE No. 7/2 PRETREATMENT DETAILS H_2O_2

DATE OF TEST..... DESCRIPTION..... LOSS ON PRETREATMENT.....%

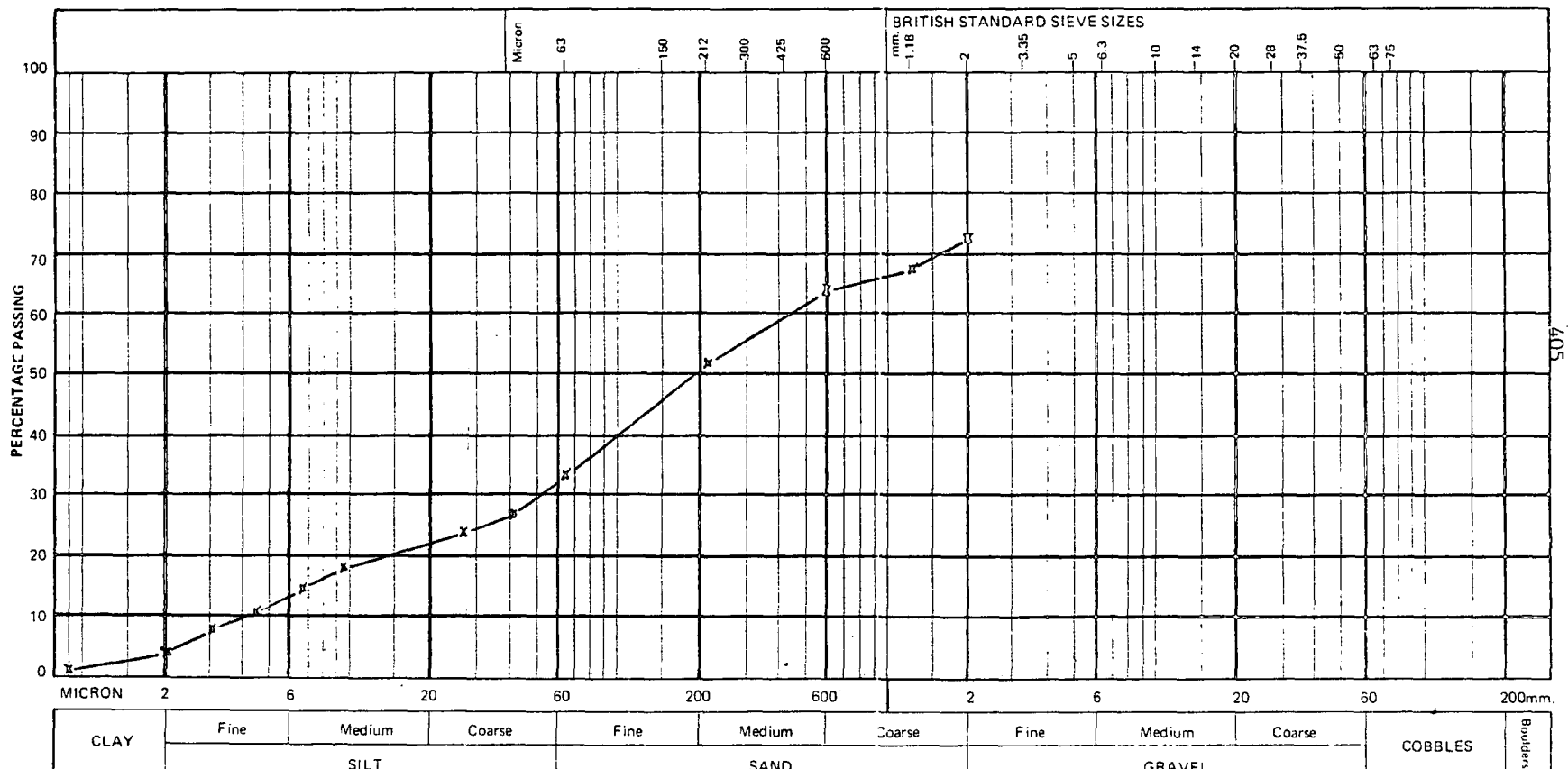

Signed.....

ELE

PARTICLE SIZE DISTRIBUTION

Form No. K4

LOCATION No..... BORE HOLE No..... SAMPLE No. 7/3 PRETREATMENT DETAILS H_2O_2

DATE OF TEST..... DESCRIPTION..... LOSS ON PRETREATMENT.....%

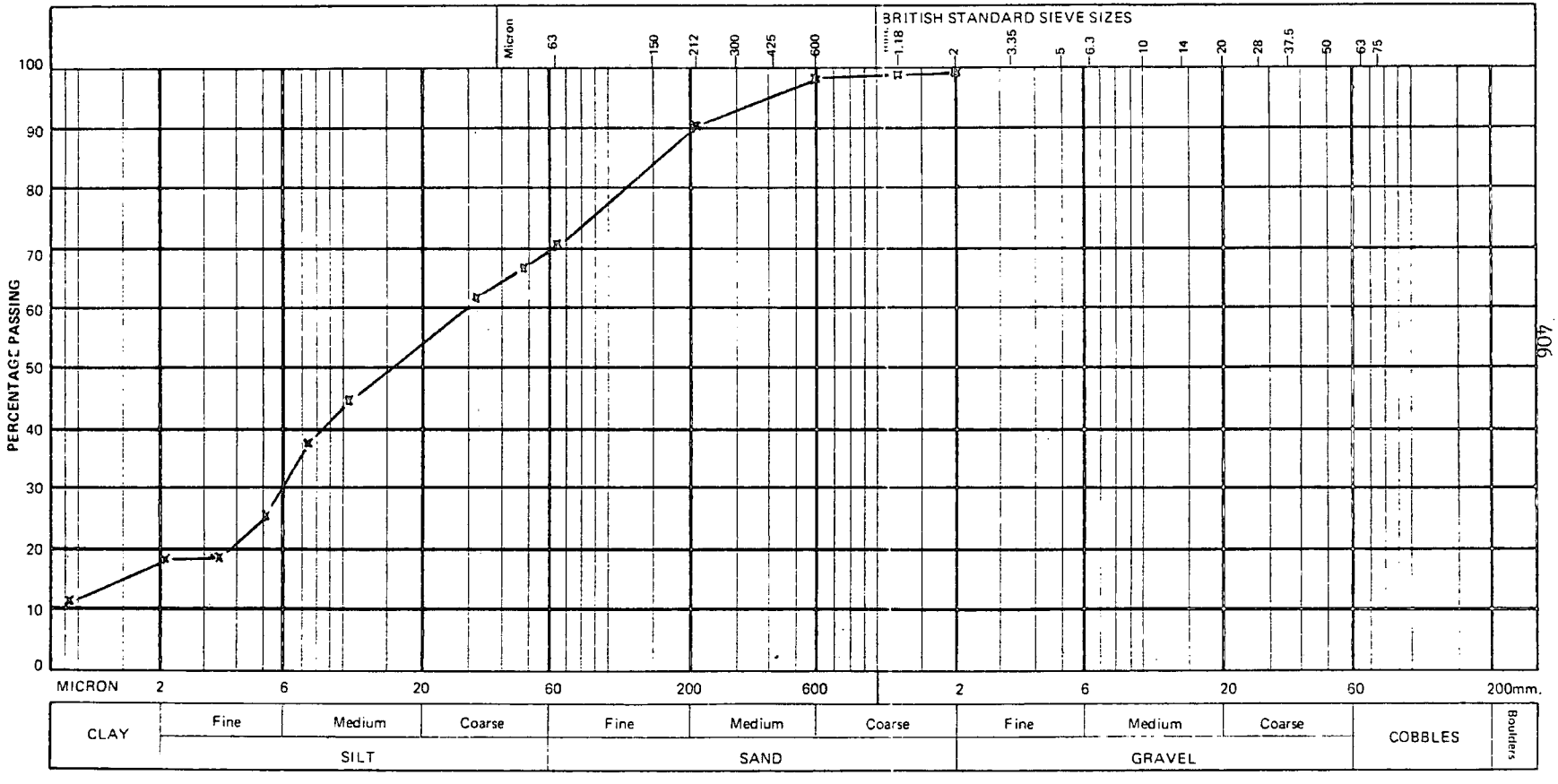

406

Signed.....

ELE

PARTICLE SIZE DISTRIBUTION

Form No. K4

LOCATION No..... BORE HOLE No..... SAMPLE No. 7/4 PRETREATMENT DETAILS H_2O_2

DATE OF TEST..... DESCRIPTION..... LOSS ON PRETREATMENT.....%

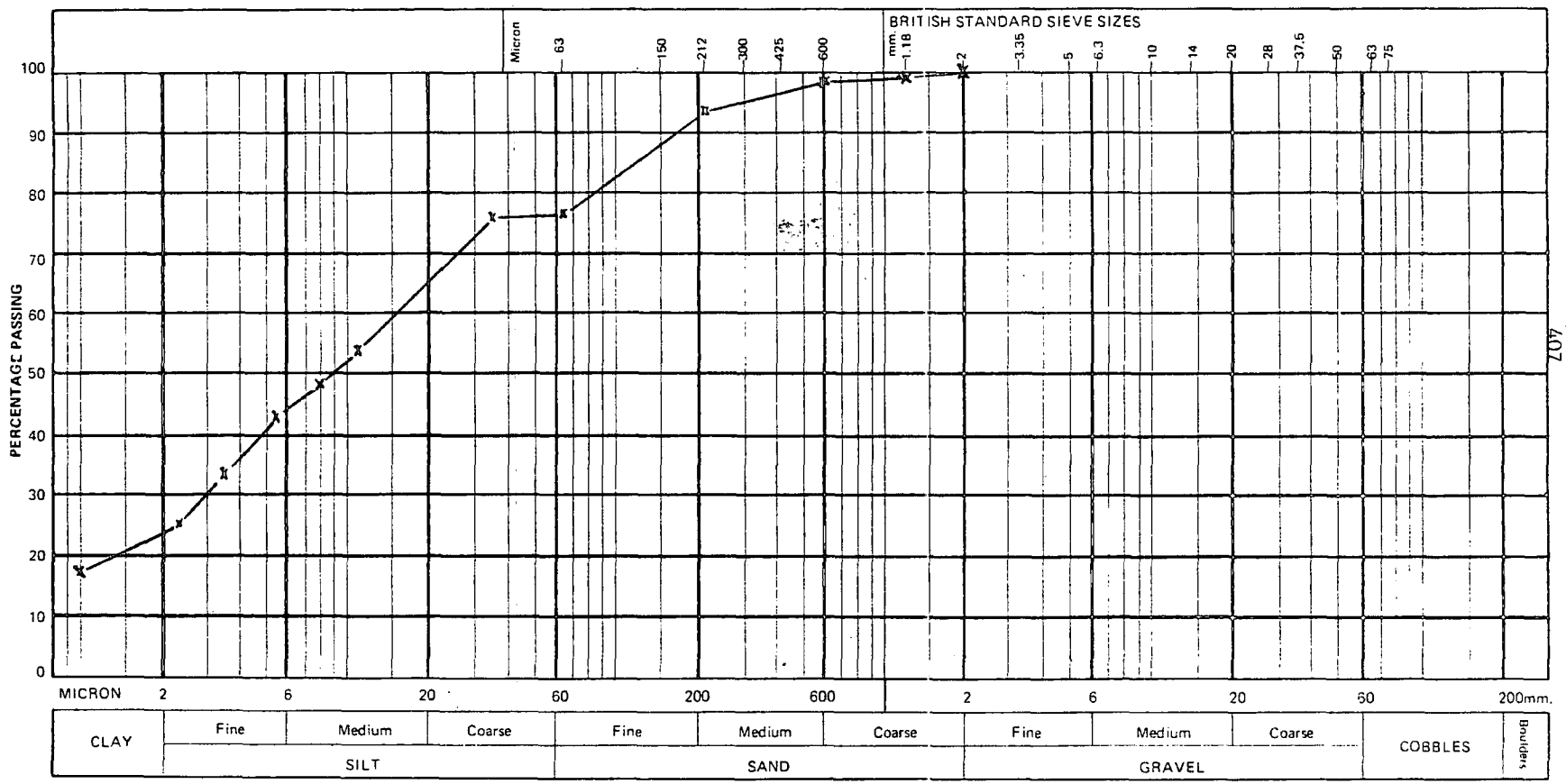

407

Signed.....

Form No. K4

PARTICLE SIZE DISTRIBUTION

LOCATION No..... BORE HOLE No..... SAMPLE No. 7/5 PRETREATMENT DETAILS $1\frac{1}{2}O_2$

DATE OF TEST..... DESCRIPTION..... LOSS ON PRETREATMENT.....%

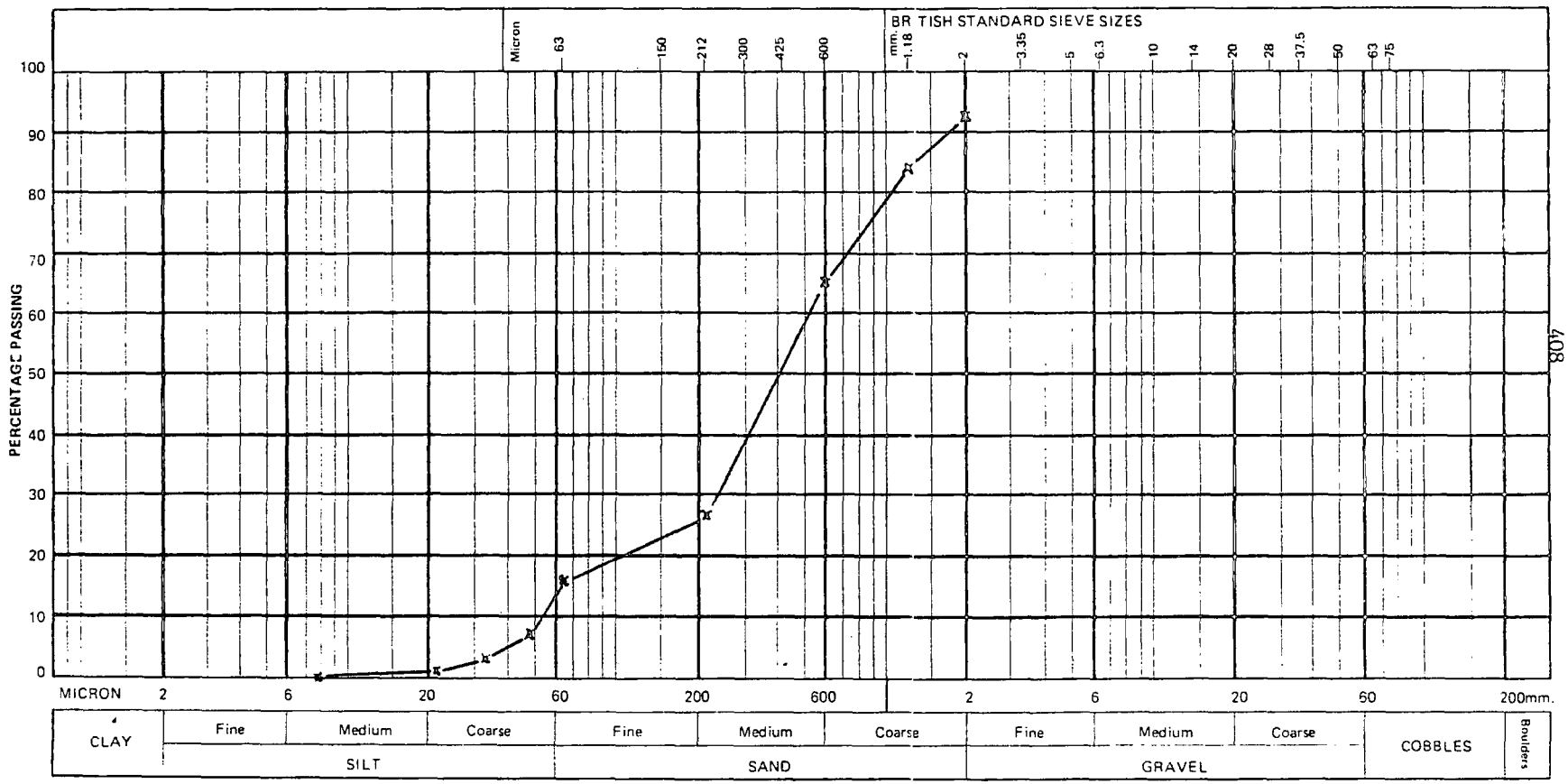

408

Signed.....

Form No. K4

PARTICLE SIZE DISTRIBUTION

LOCATION No. ..... BORE HOLE No. ..... SAMPLE No. 7/6 PRETREATMENT DETAILS H_2O_2

DATE OF TEST ..... DESCRIPTION ..... LOSS ON PRETREATMENT .....%

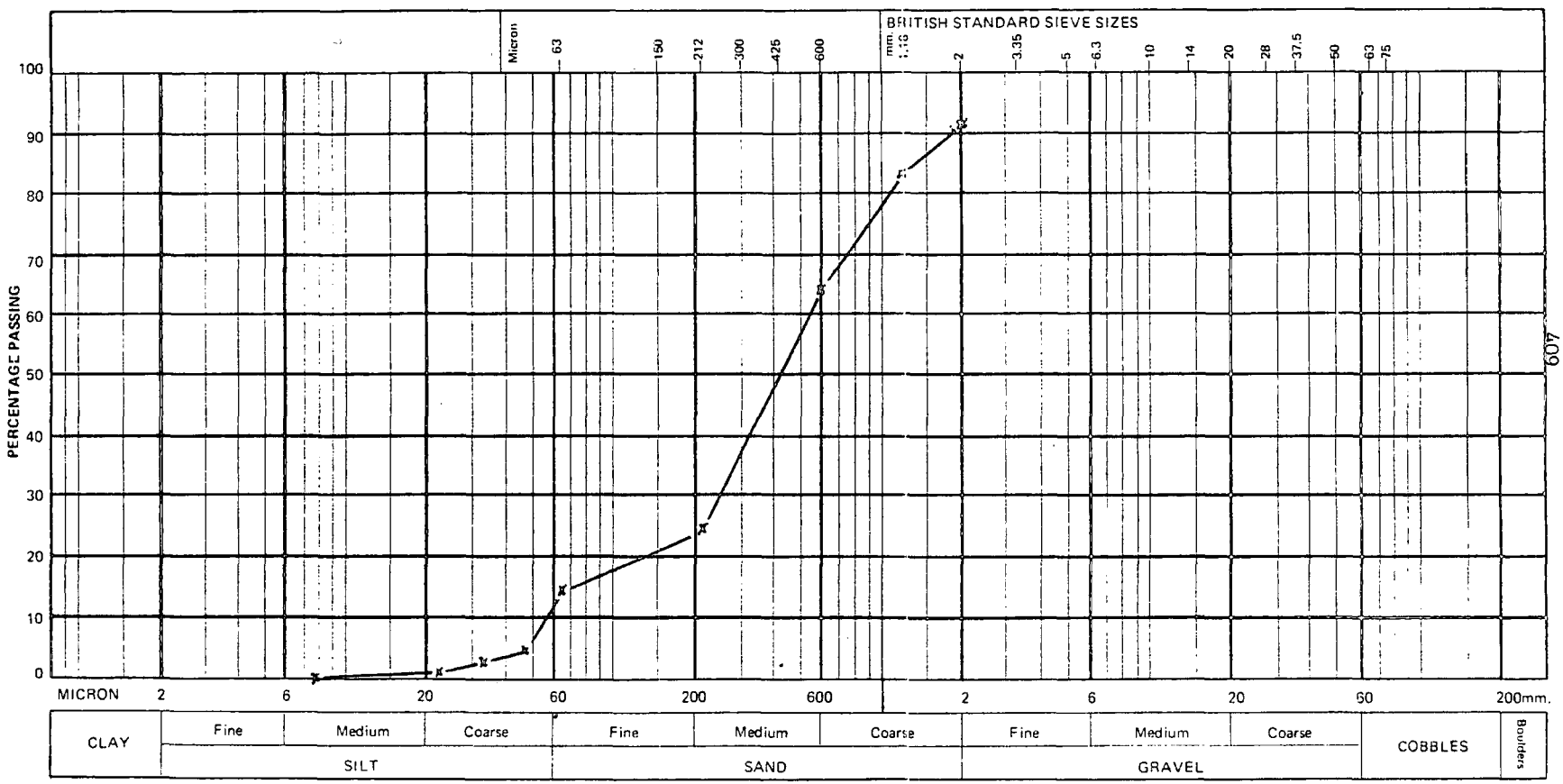

Signed .....

Form No. K4

PARTICLE SIZE DISTRIBUTION

LOCATION No..... BORE HOLE No..... SAMPLE No. 8/1 PRETREATMENT DETAILS H_2O_2

DATE OF TEST..... DESCRIPTION..... LOSS ON PRETREATMENT.....%

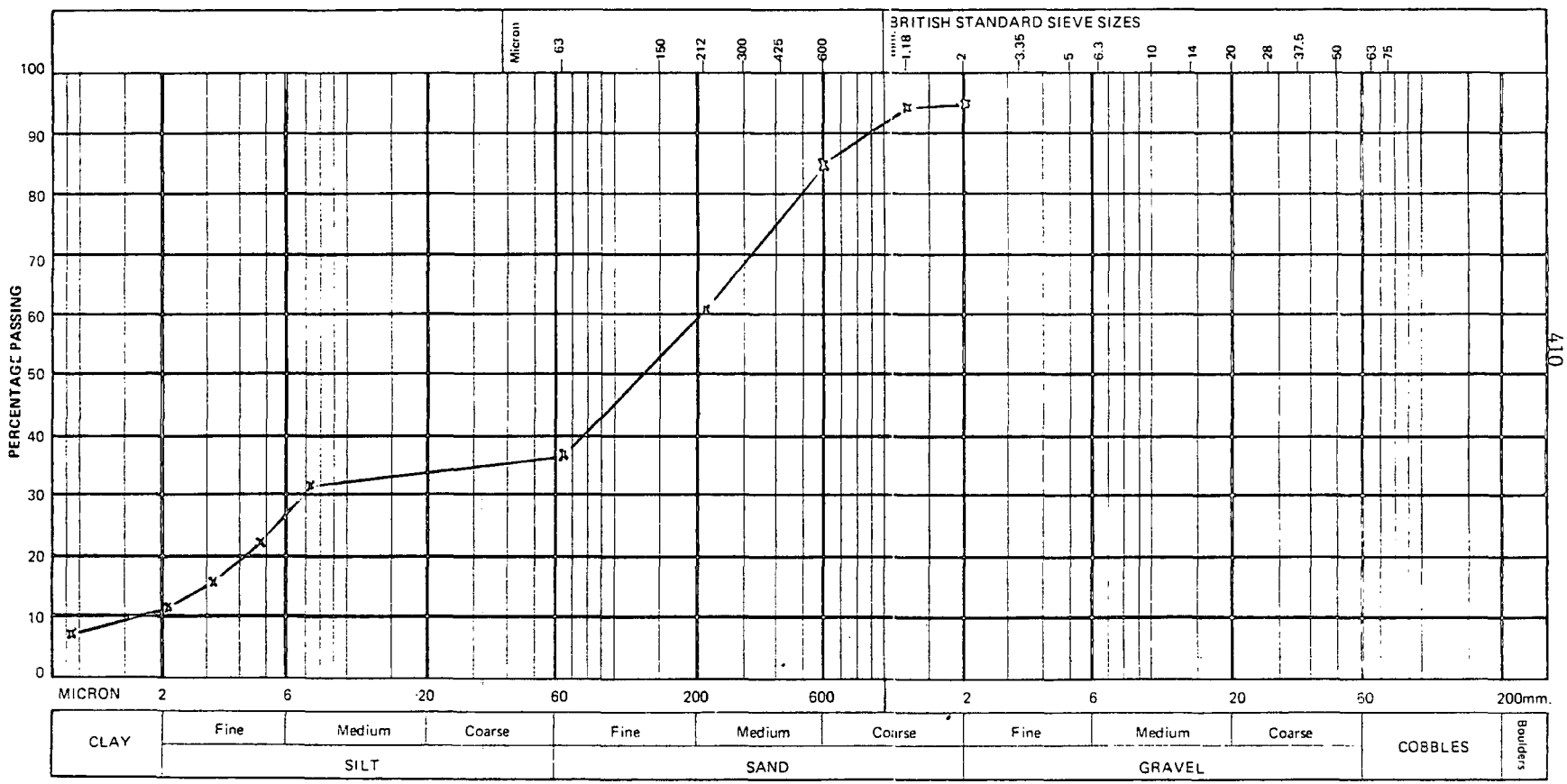

410

Signed.....

Form No. K4

PARTICLE SIZE DISTRIBUTION

LOCATION No..... BORE HOLE No..... SAMPLE No. 8/2 PRETREATMENT DETAILS H_2O_2

DATE OF TEST..... DESCRIPTION..... LOSS ON PRETREATMENT..... %

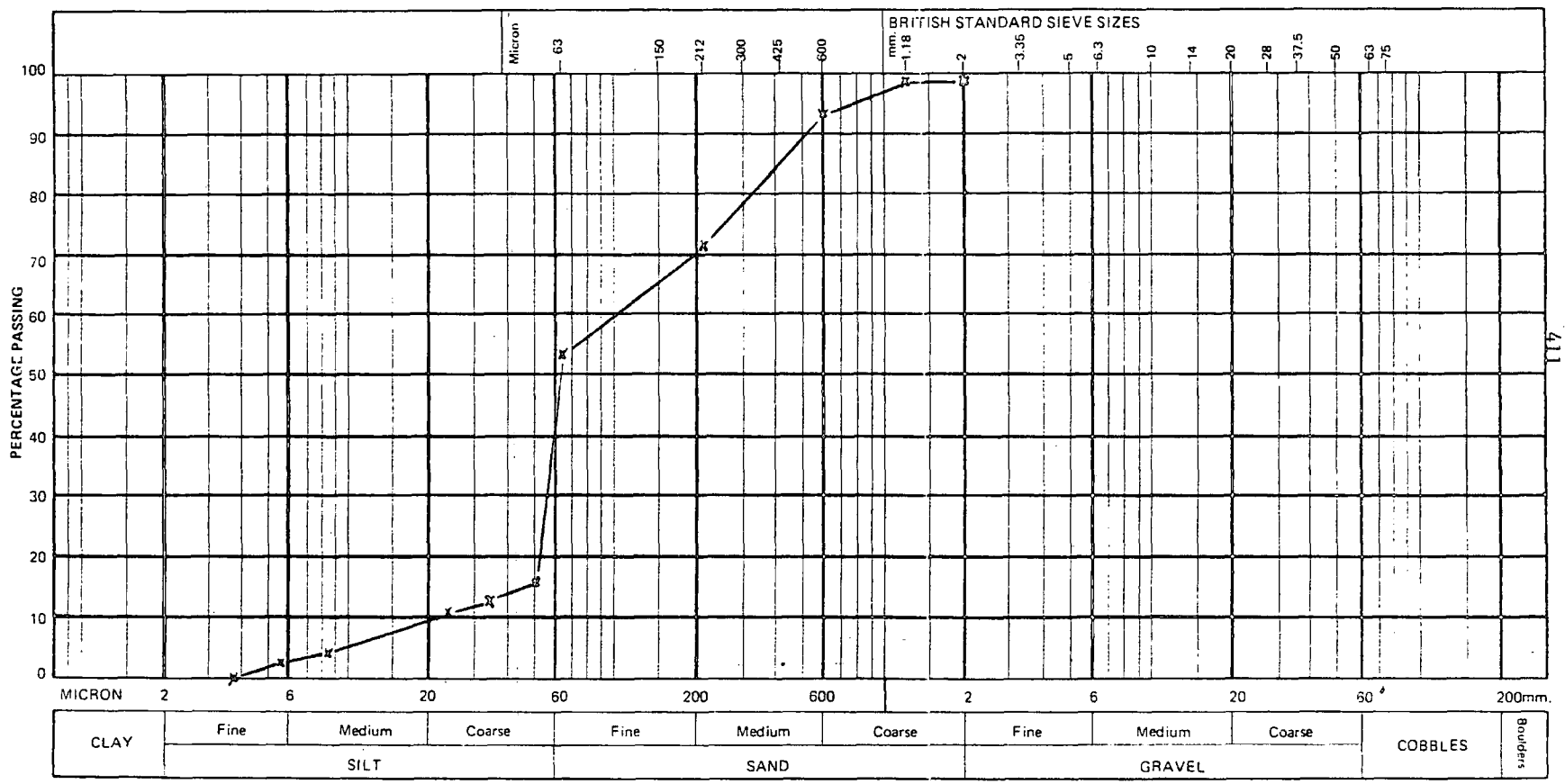

411

Signed.....

PARTICLE SIZE DISTRIBUTION

Form No. K4

LOCATION No..... BORE HOLE No..... SAMPLE No. 8/3 PRETREATMENT DETAILS H_2O_2

DATE OF TEST..... DESCRIPTION..... LOSS ON PRETREATMENT.....%

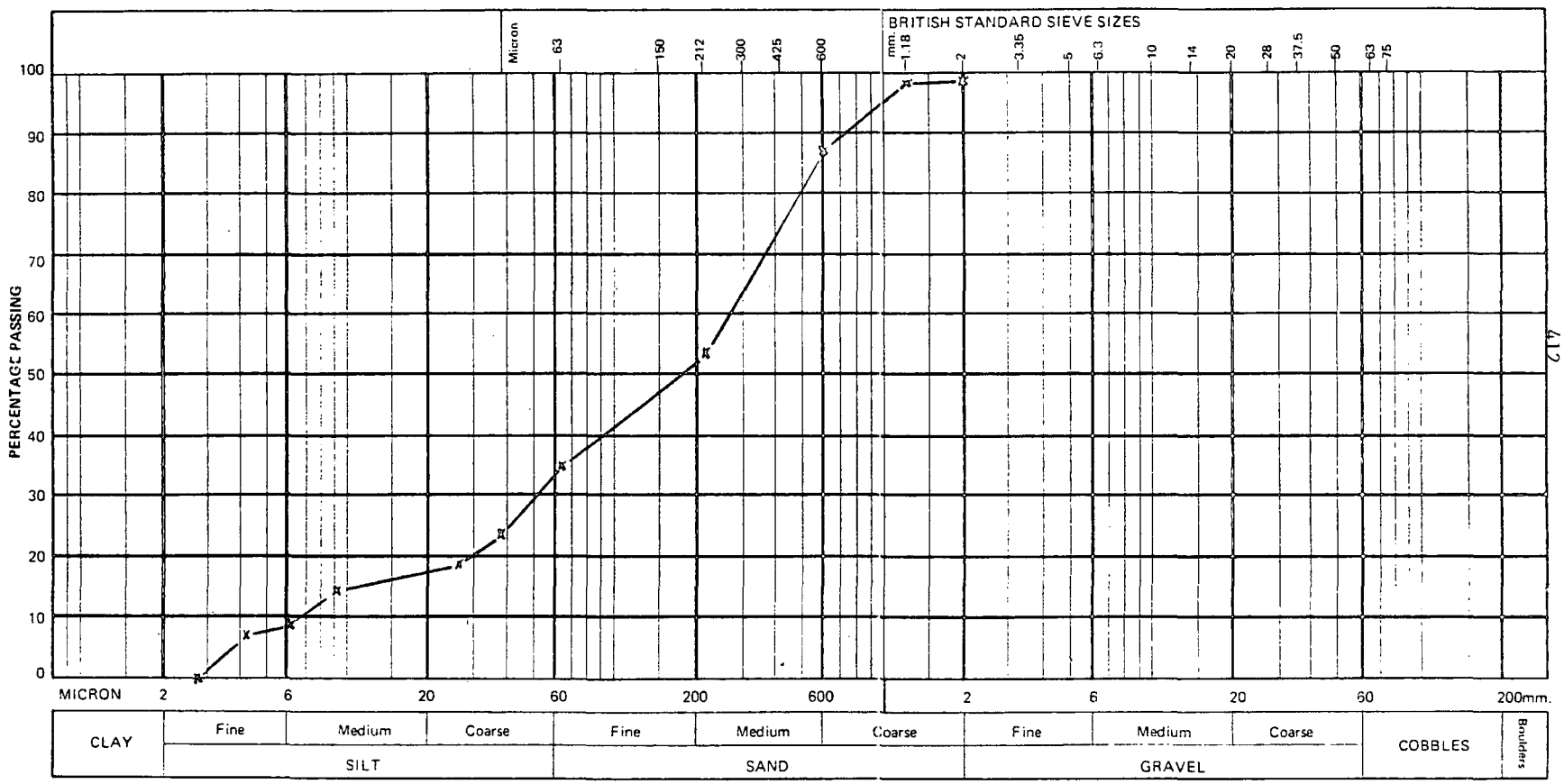

Signed.....

PARTICLE SIZE DISTRIBUTION

Form No. K4

LOCATION No..... BORE HOLE No..... SAMPLE No. 8/4 PRETREATMENT DETAILS H_2O_2

DATE OF TEST..... DESCRIPTION..... LOSS ON PRETREATMENT.....%

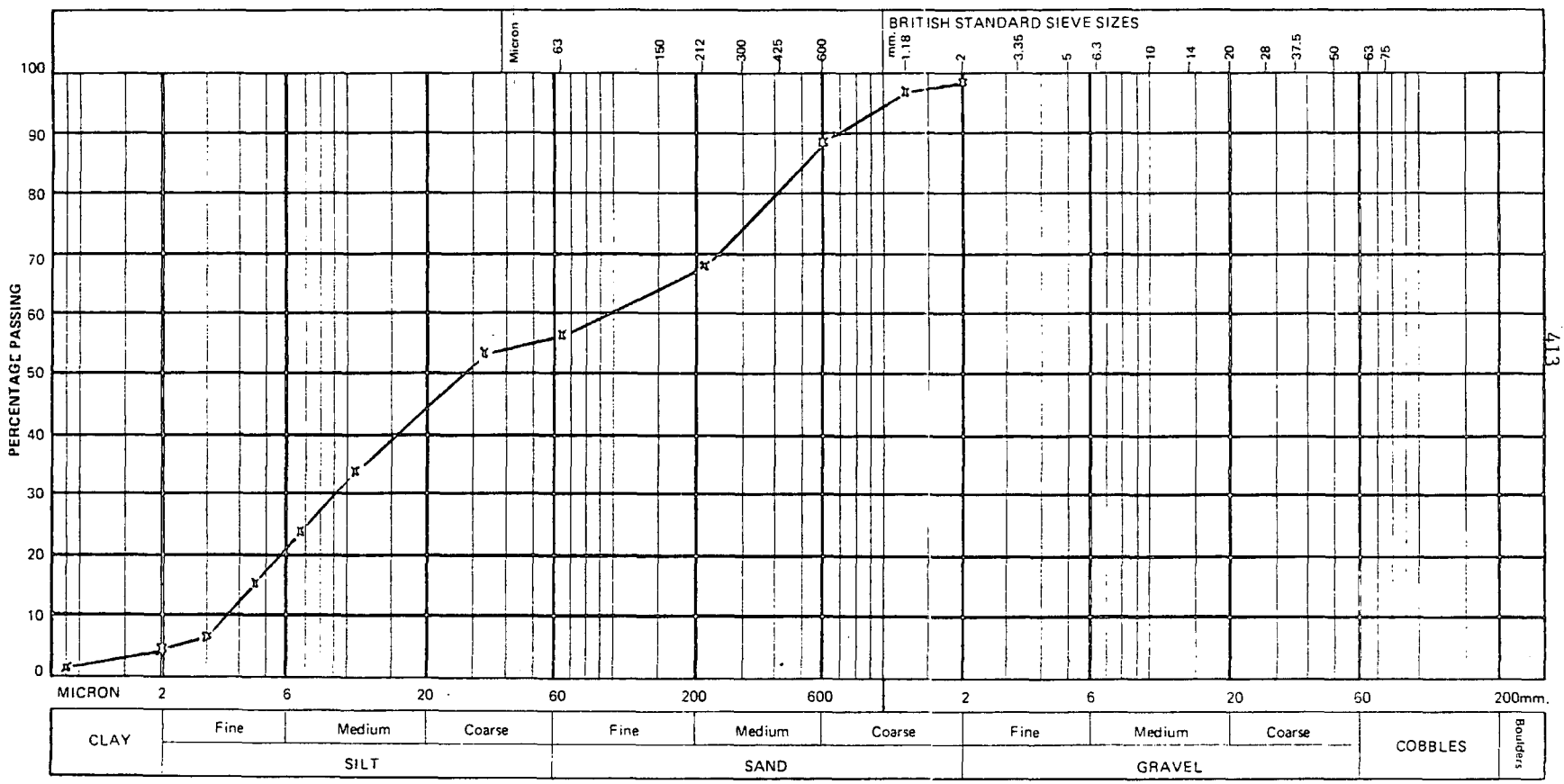

413

Signed.....

PARTICLE SIZE DISTRIBUTION

Form No. K4

LOCATION No..... BORE HOLE No..... SAMPLE No. 8/5 PRETREATMENT DETAILS H_2O_2

DATE OF TEST..... DESCRIPTION..... LOSS ON PRETREATMENT.....%

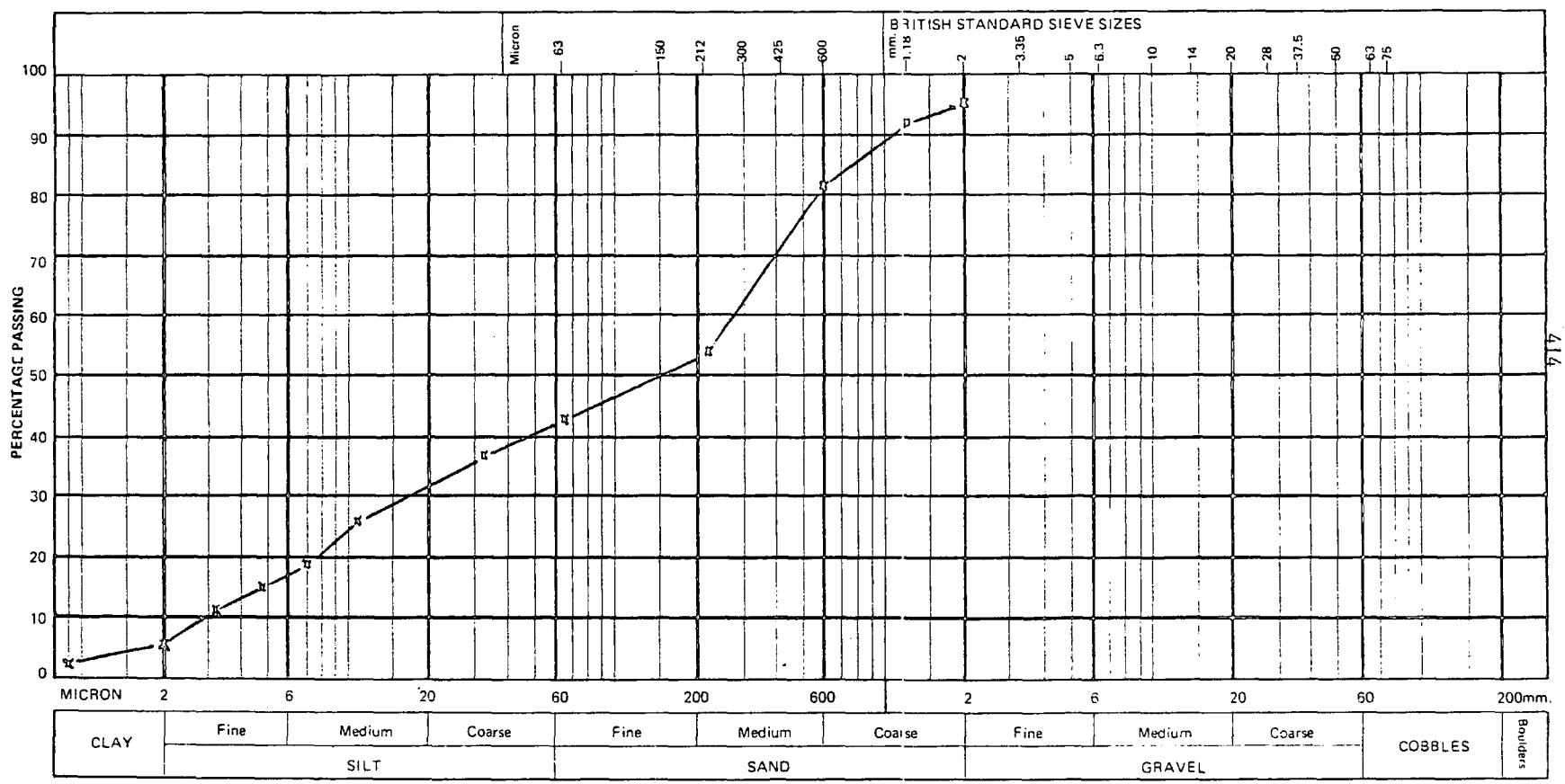

414

Signed.....

Form No. K4

PARTICLE SIZE DISTRIBUTION

LOCATION No..... BORE HOLE No..... SAMPLE No. 8/6 PRETREATMENT DETAILS H_2O_2

DATE OF TEST..... DESCRIPTION..... LOSS ON PRETREATMENT.....%

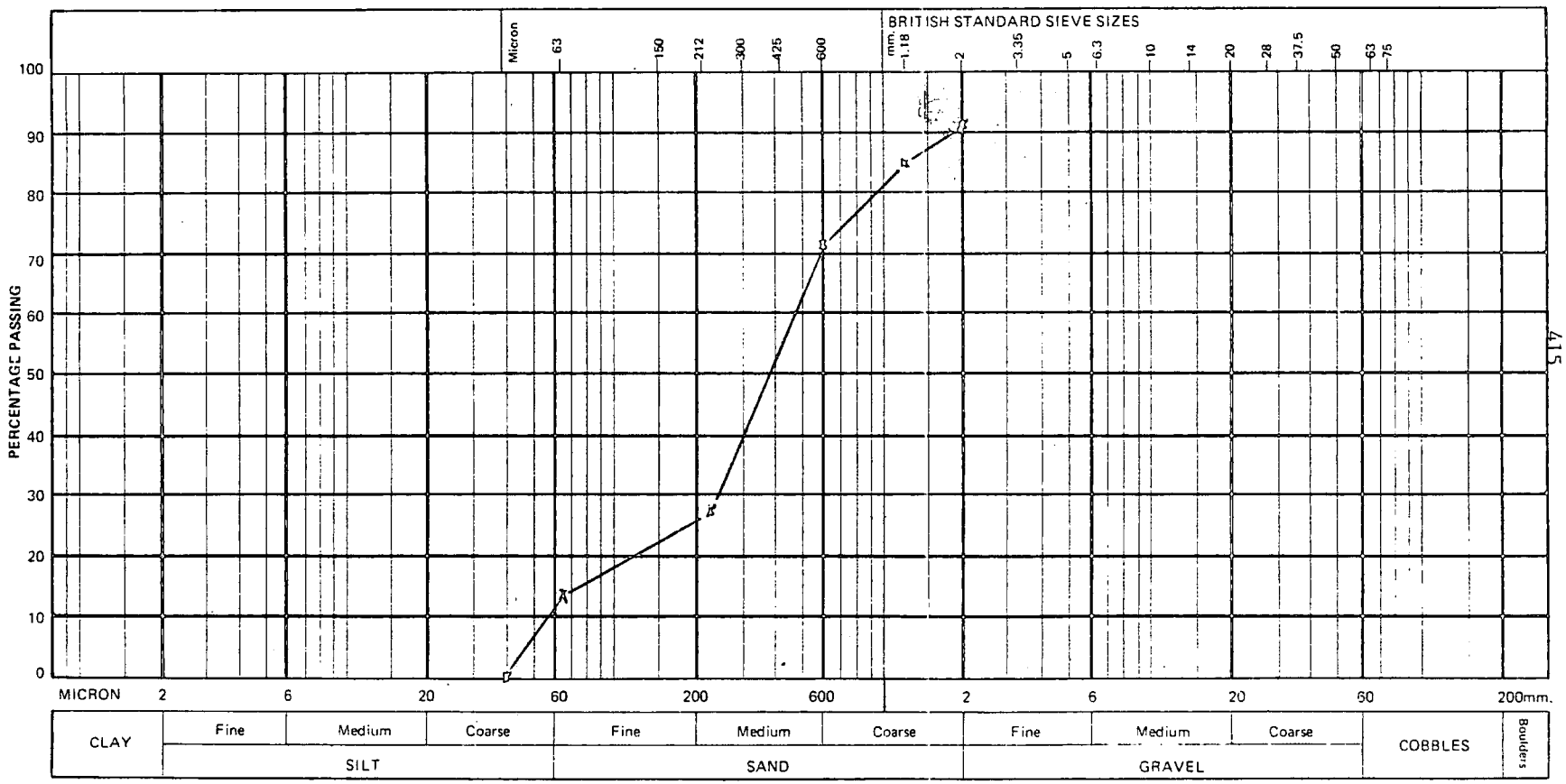

415

Signed.....

PARTICLE SIZE DISTRIBUTION

Form No. K4

LOCATION No..... BORE HOLE No..... SAMPLE No. 9/1 PRETREATMENT DETAILS H_2O_2.....

DATE OF TEST..... DESCRIPTION..... LOSS ON PRETREATMENT.....%

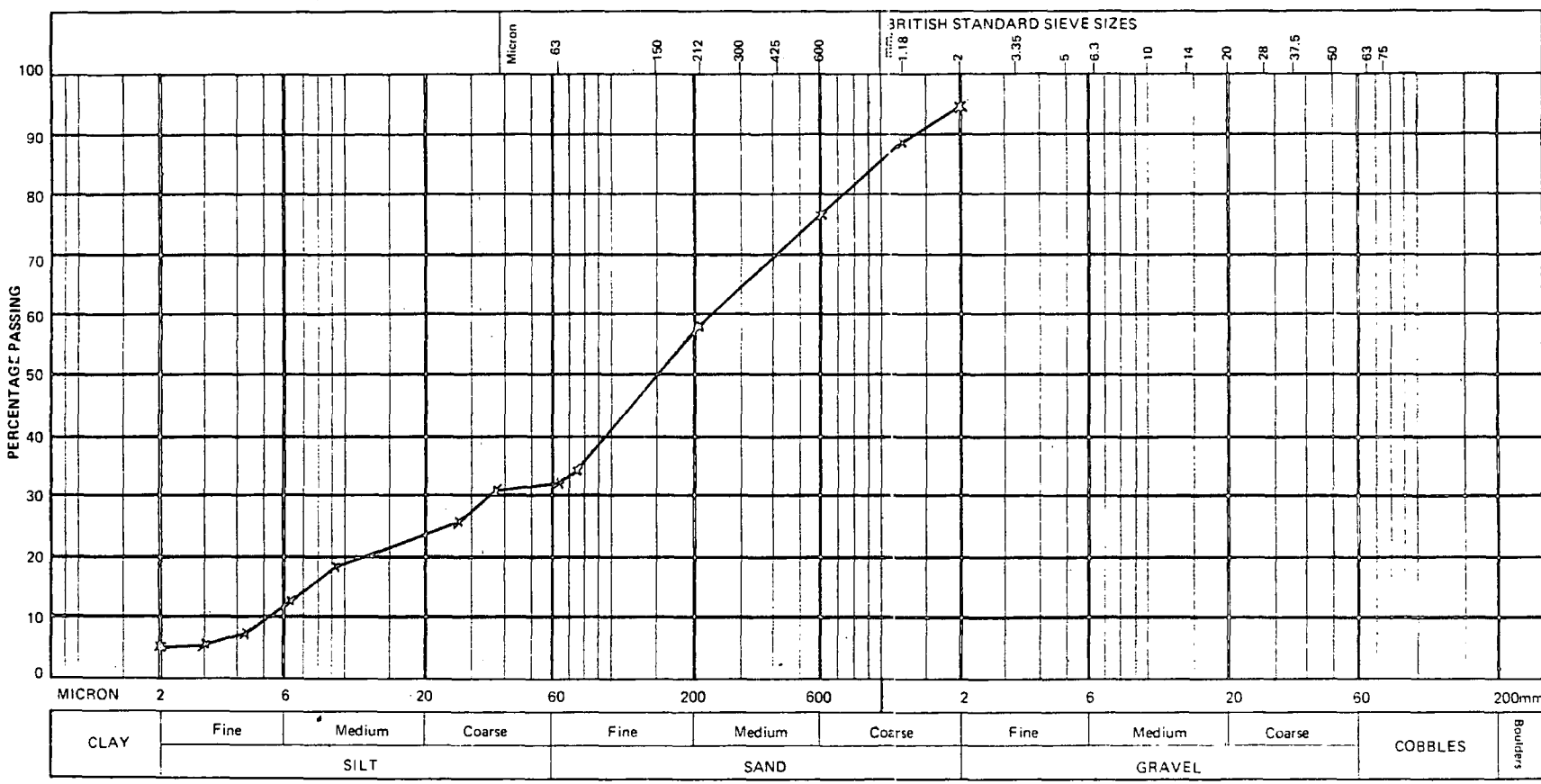

Signed.....

Form No. K4

PARTICLE SIZE DISTRIBUTION

LOCATION No..... BORE HOLE No..... SAMPLE No. 9/2 PRETREATMENT DETAILS H_2O_2

DATE OF TEST..... DESCRIPTION..... LOSS ON PRETREATMENT.....%

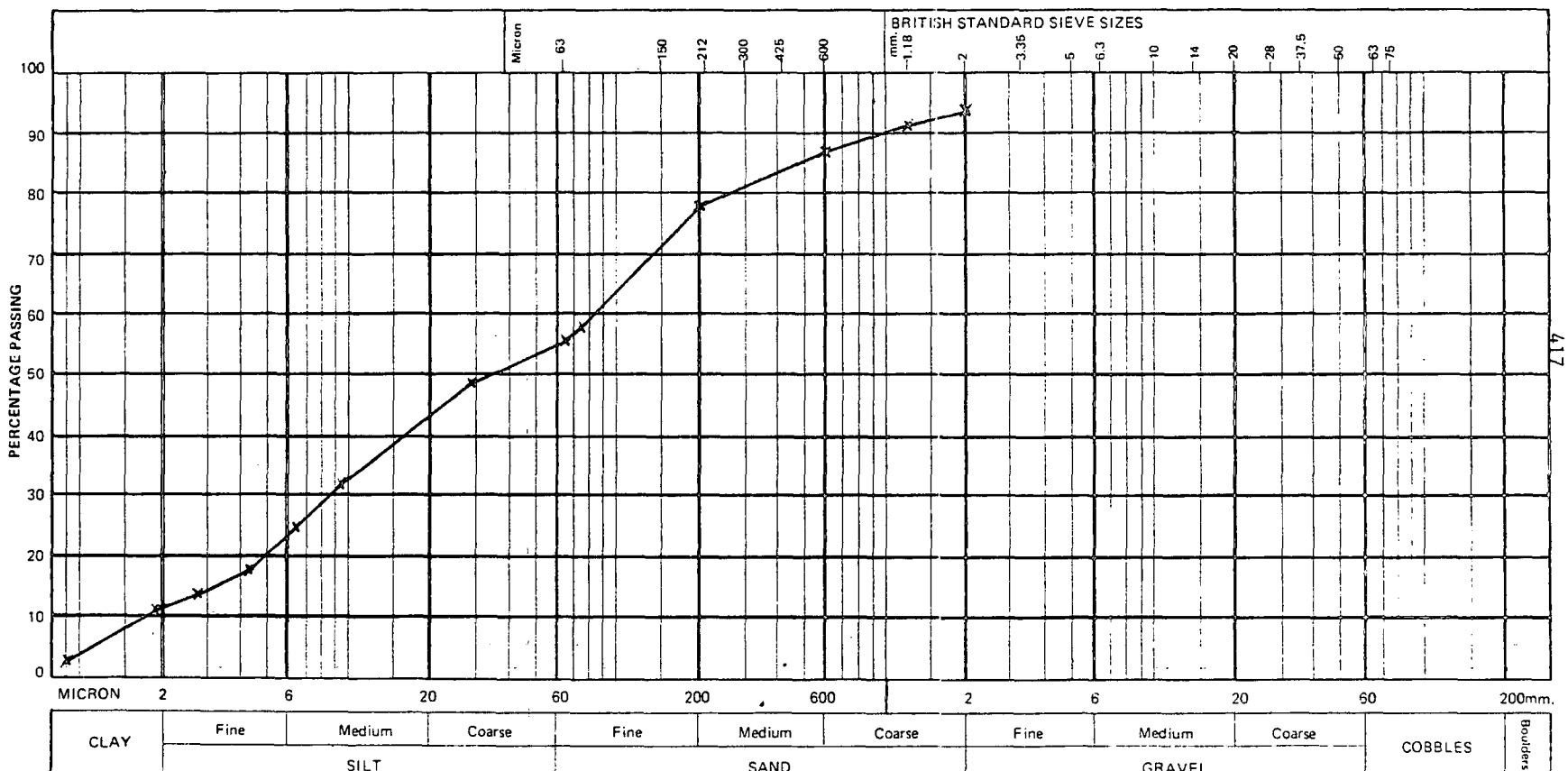

417

Signed.....

Form No. K4

PARTICLE SIZE DISTRIBUTION

LOCATION No..... BORE HOLE No..... SAMPLE No. 9/3 PRETREATMENT DETAILS H_2O_2

DATE OF TEST..... DESCRIPTION..... LOSS ON PRETREATMENT.....%

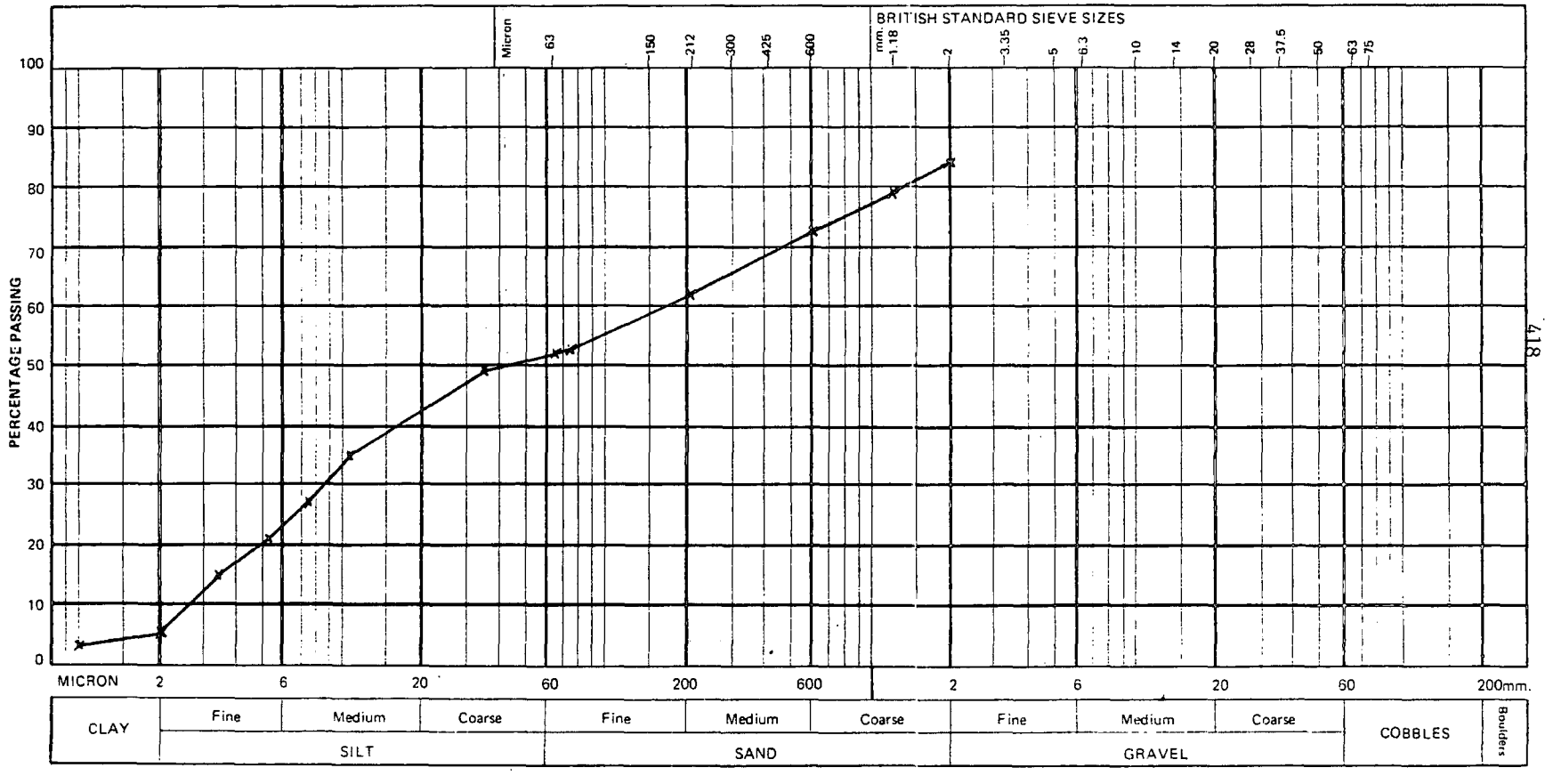

418

Signed.....

PARTICLE SIZE DISTRIBUTION

Form No. K4

LOCATION No..... BORE HOLE No..... SAMPLE No. 9/4 PRETREATMENT DETAILS H_2O_2

DATE OF TEST..... DESCRIPTION..... LOSS ON PRETREATMENT.....%

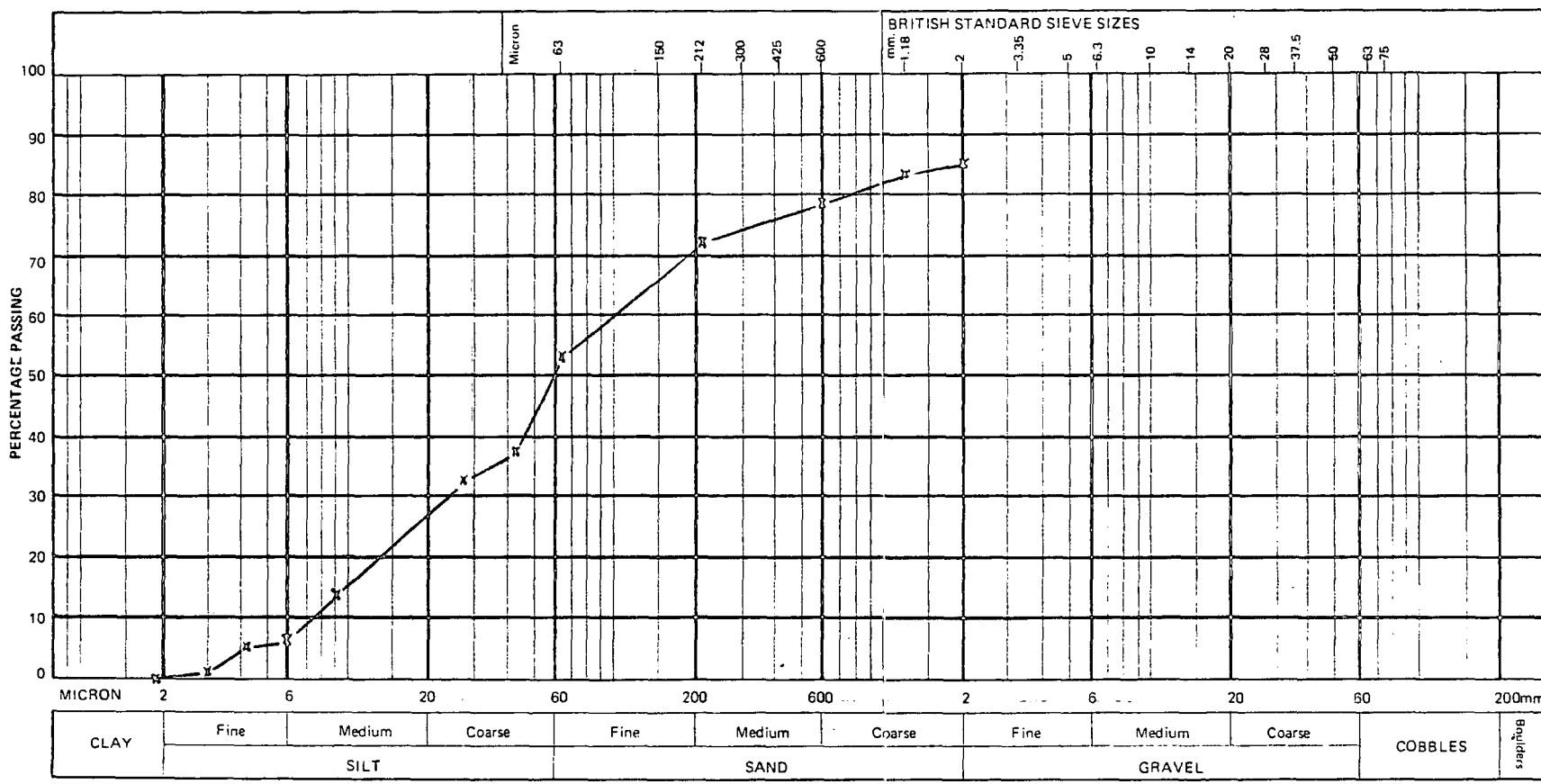

A19

Signed.....

Form No. K4

PARTICLE SIZE DISTRIBUTION

LOCATION No..... BORE HOLE No..... SAMPLE No. 9/5 PRETREATMENT DETAILS H_2O_2

DATE OF TEST..... DESCRIPTION..... LOSS ON PRETREATMENT.....%

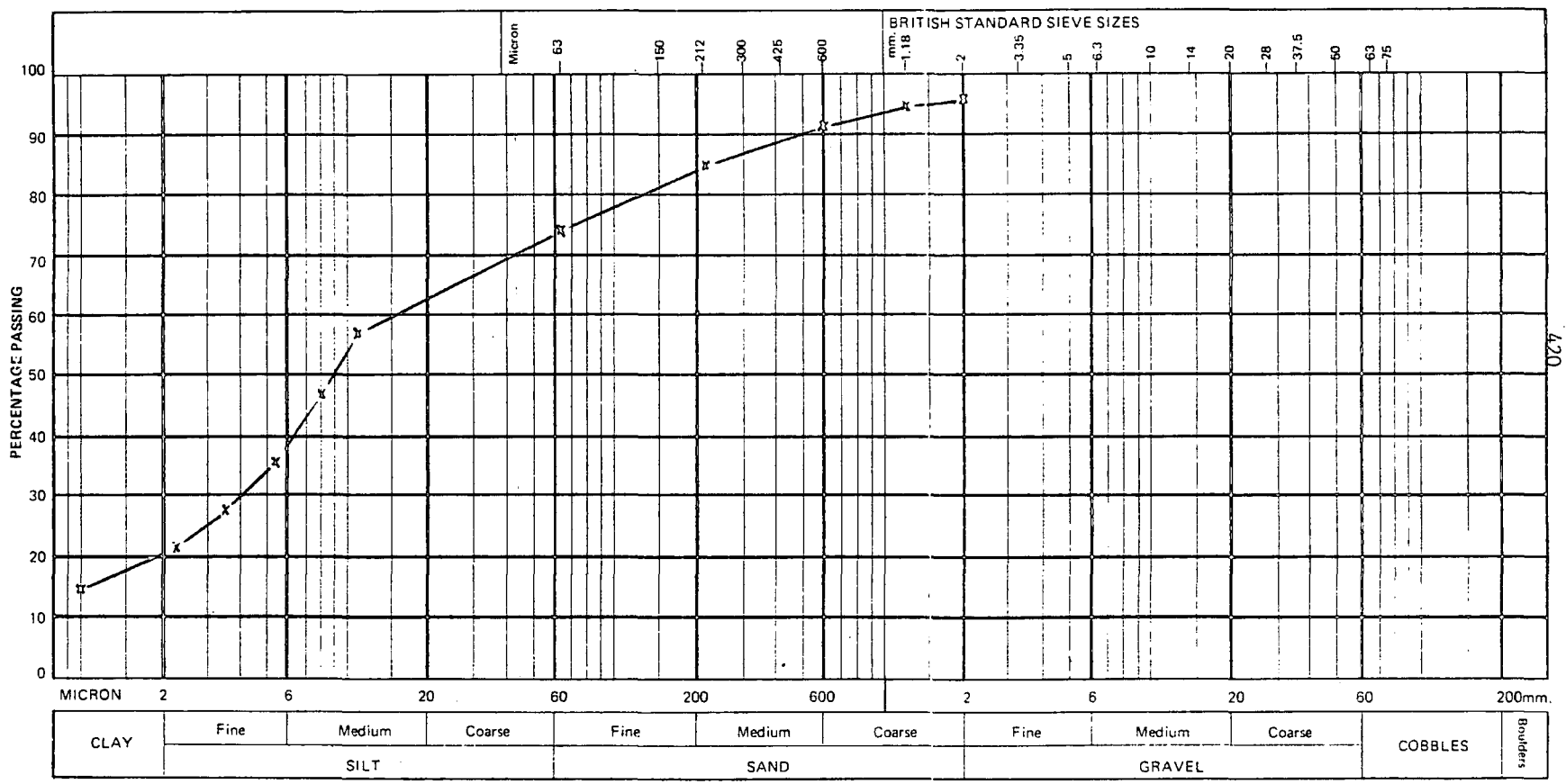

420

Signed.....

Form No. K4

PARTICLE SIZE DISTRIBUTION

LOCATION No..... BORE HOLE No..... SAMPLE No. 9/6 PRETREATMENT DETAILS H_2O_2

DATE OF TEST..... DESCRIPTION..... LOSS ON PRETREATMENT.....%

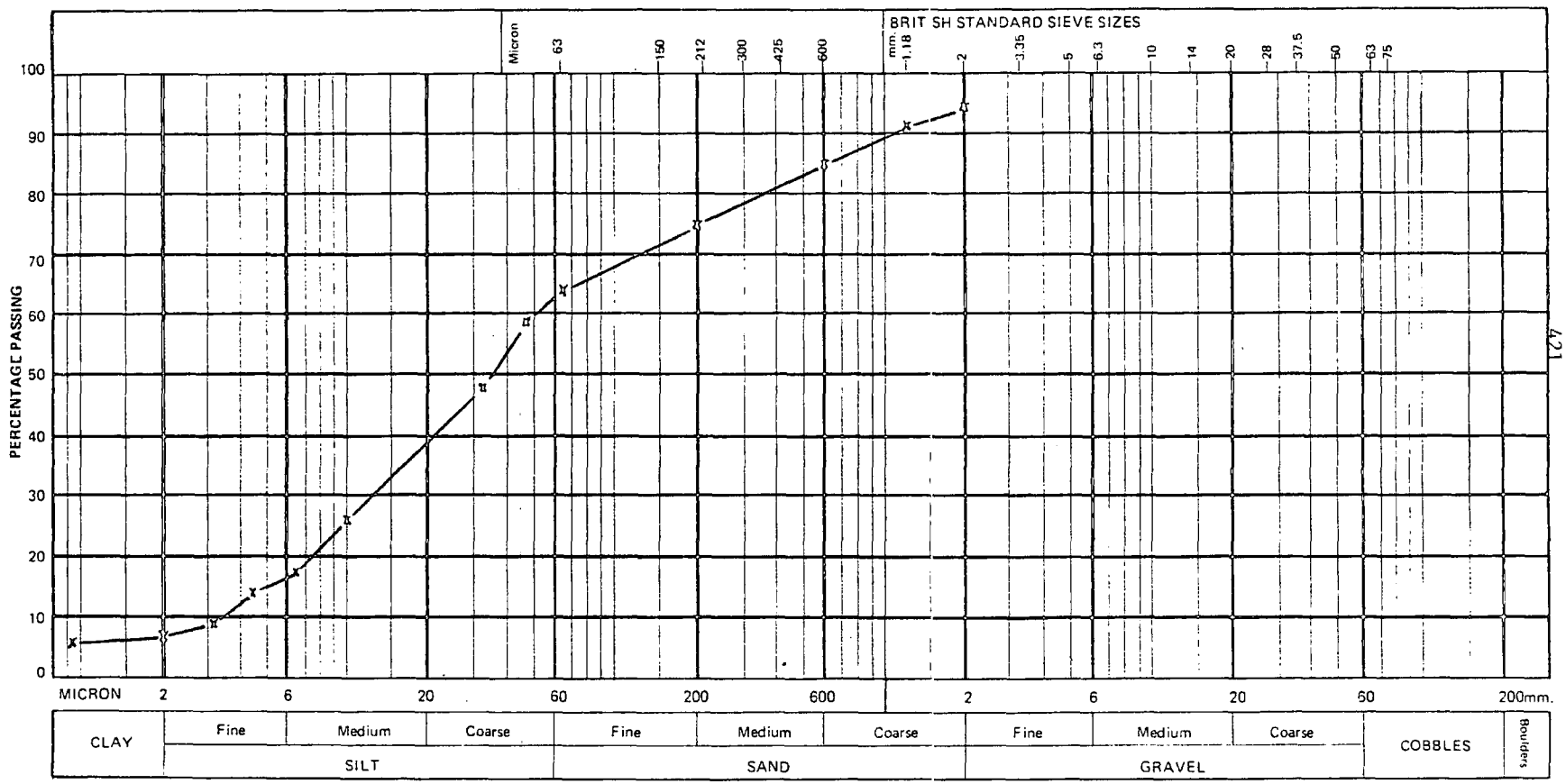

Signed.....

PARTICLE SIZE DISTRIBUTION

Form No. K4

LOCATION No..... BORE HOLE No..... SAMPLE No. 9/7 PRETREATMENT DETAILS H_2O_2

DATE OF TEST..... DESCRIPTION..... LOSS ON PRETREATMENT.....%

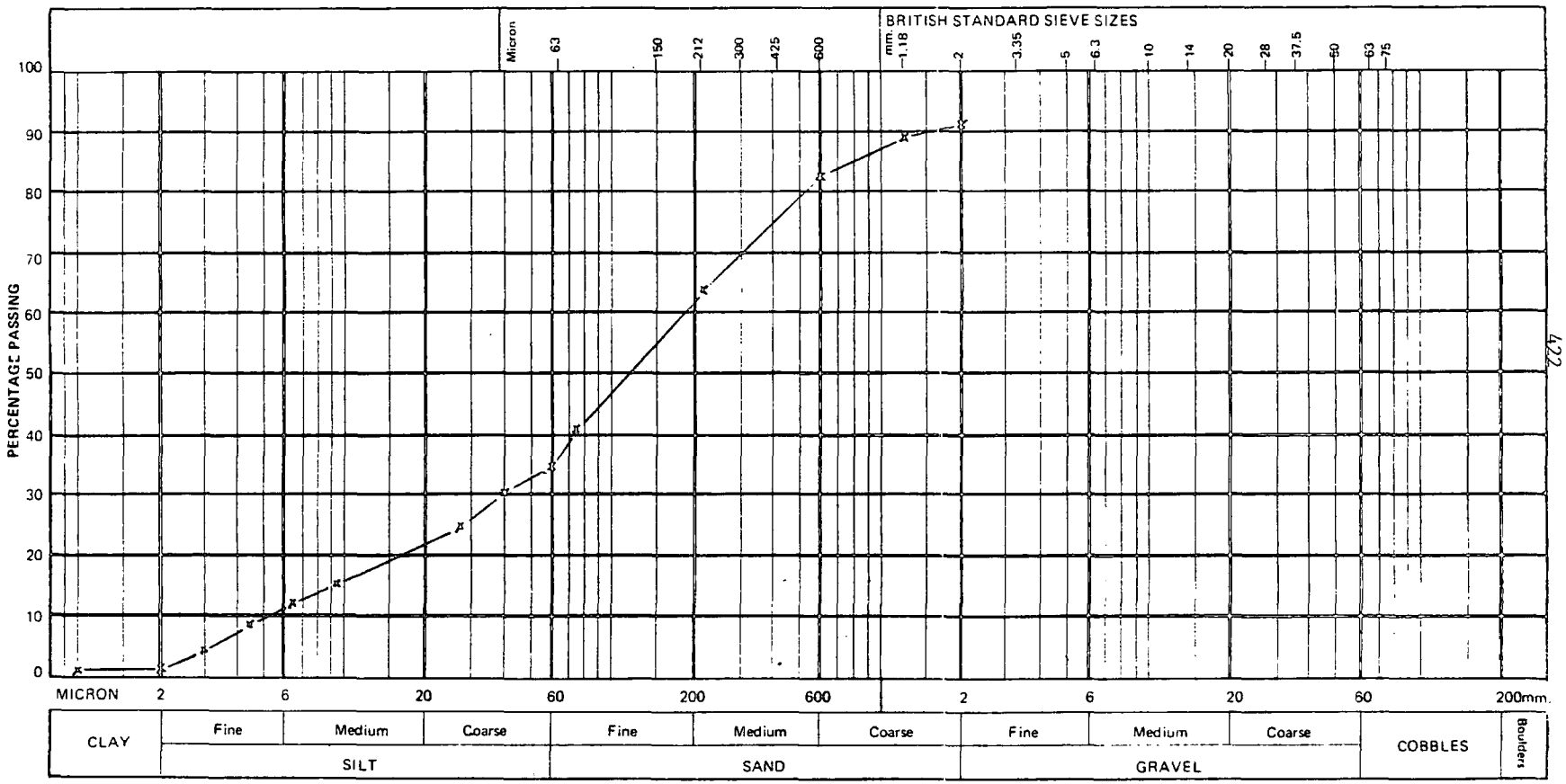

422

Signed.....

Form No. K4

PARTICLE SIZE DISTRIBUTION

LOCATION No..... BORE HOLE No..... SAMPLE No. 9/8 PRETREATMENT DETAILS H_2O_2

DATE OF TEST..... DESCRIPTION..... LOSS ON PRETREATMENT.....%

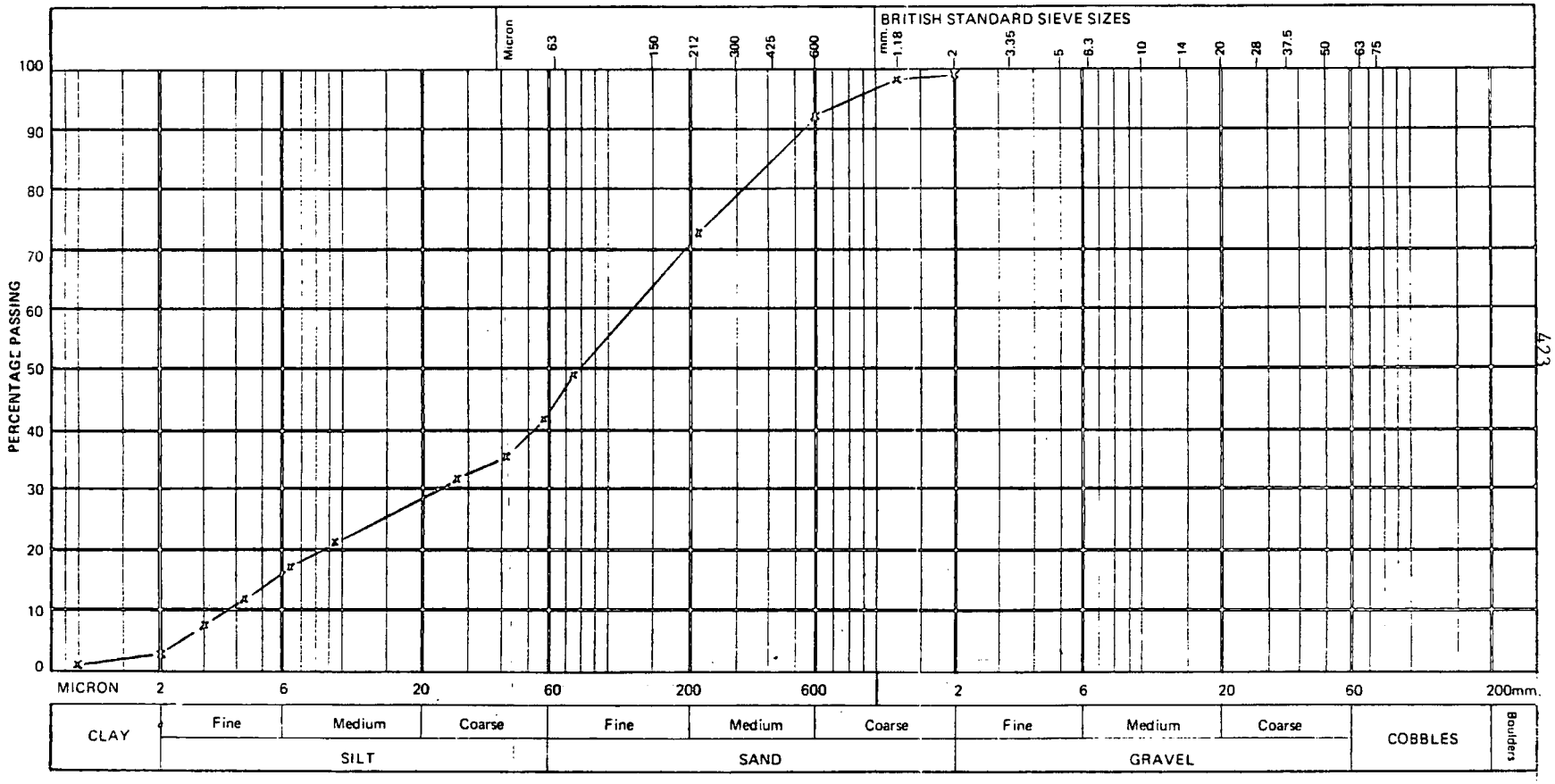

Signed.....

PARTICLE SIZE DISTRIBUTION

Form No. K4

LOCATION No..... BORE HOLE No..... SAMPLE No. 10/1

DATE OF TEST..... DESCRIPTION..... 10/2

PRETREATMENT DETAILS H_2O_2

LOSS ON PRETREATMENT.....%

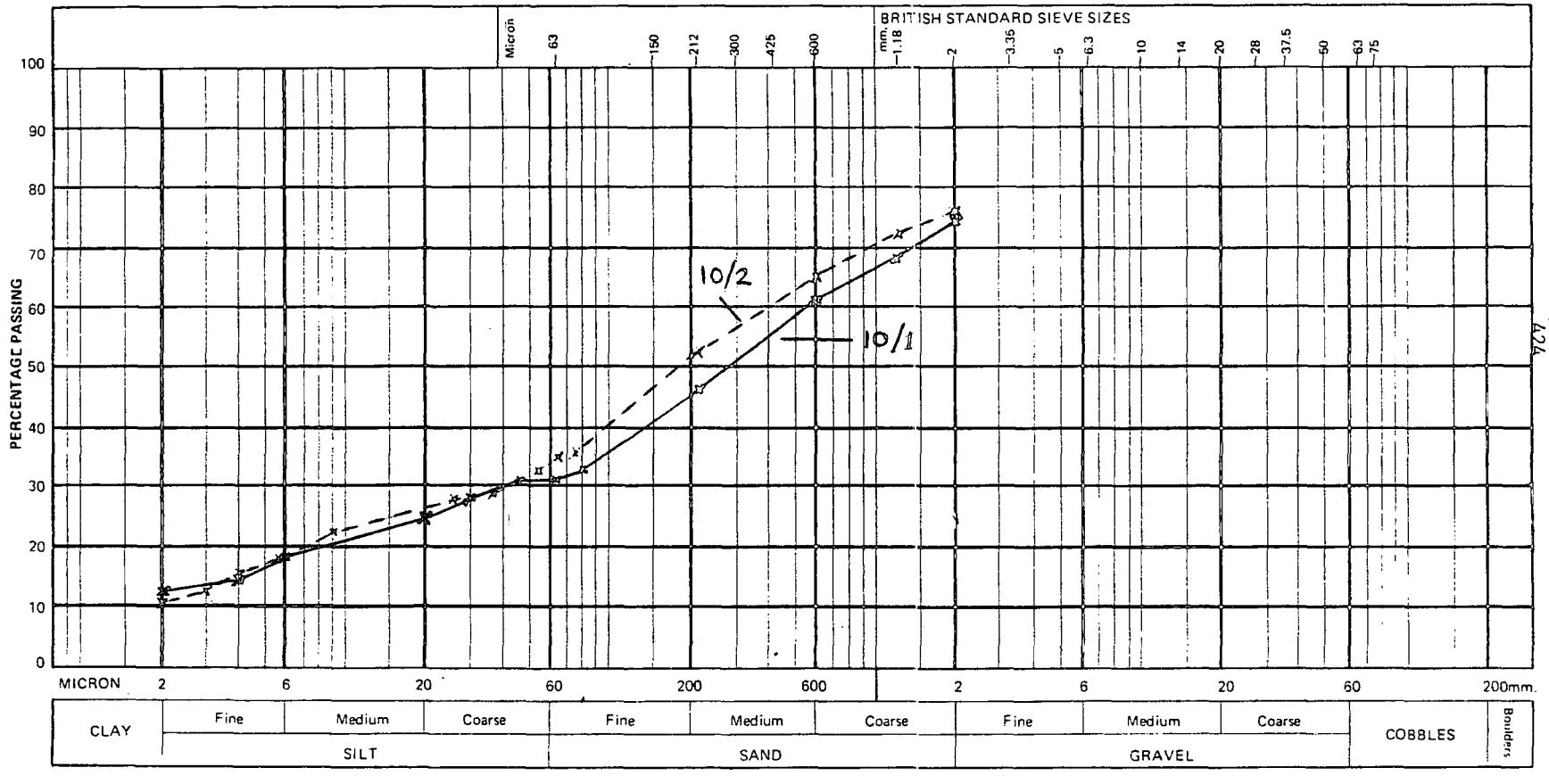

424

Signed.....

Form No. K4

PARTICLE SIZE DISTRIBUTION

LOCATION No..... BORE HOLE No..... SAMPLE No. 10/3 PRETREATMENT DETAILS H_2O_2

DATE OF TEST..... DESCRIPTION..... LOSS ON PRETREATMENT.....%

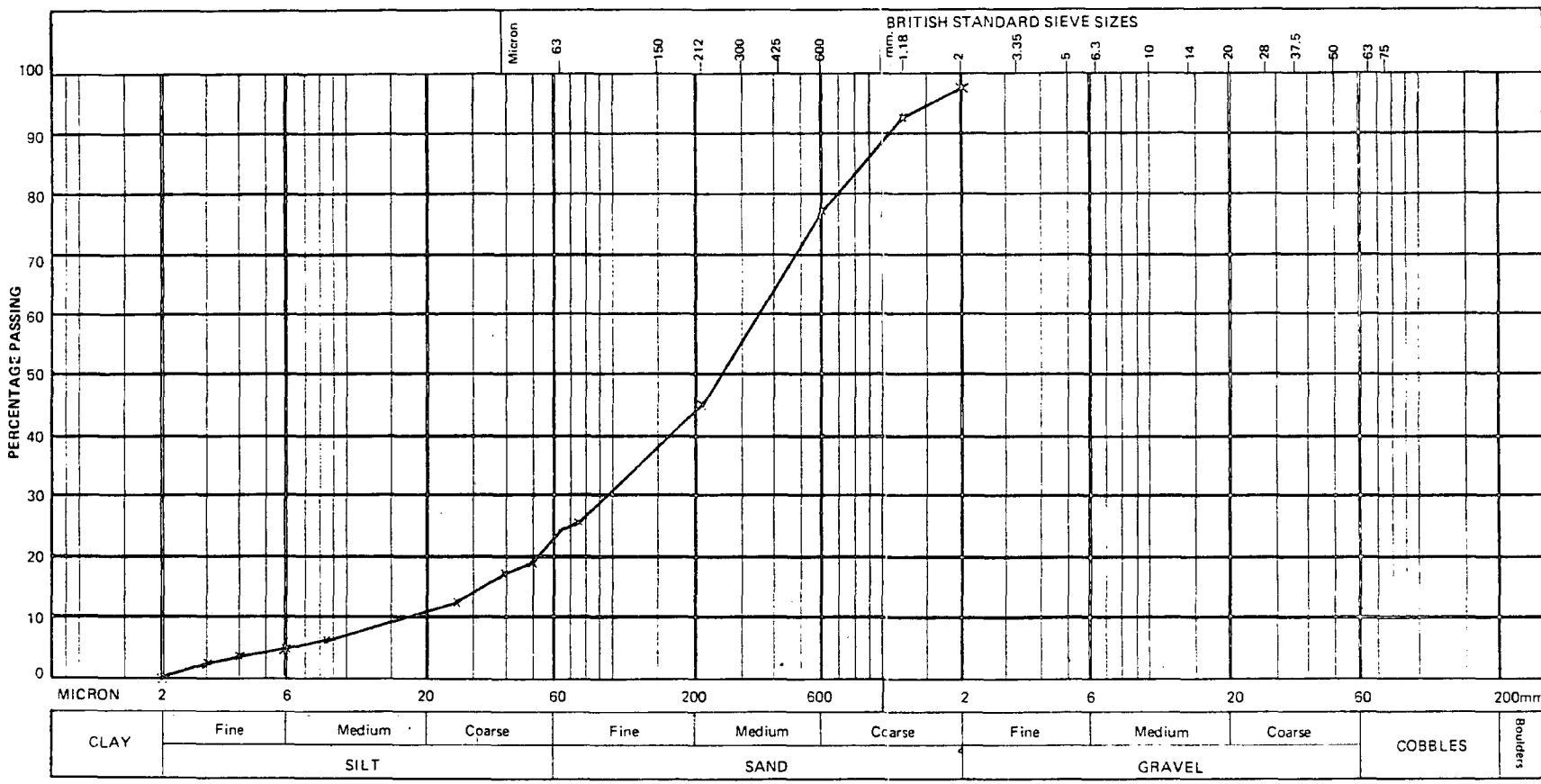

425

Signed.....

PARTICLE SIZE DISTRIBUTION

Form No. K4

LOCATION No..... BORE HOLE No..... SAMPLE No. 10/4 PRETREATMENT DETAILS H_2O_2

DATE OF TEST..... DESCRIPTION..... LOSS ON PRETREATMENT.....%

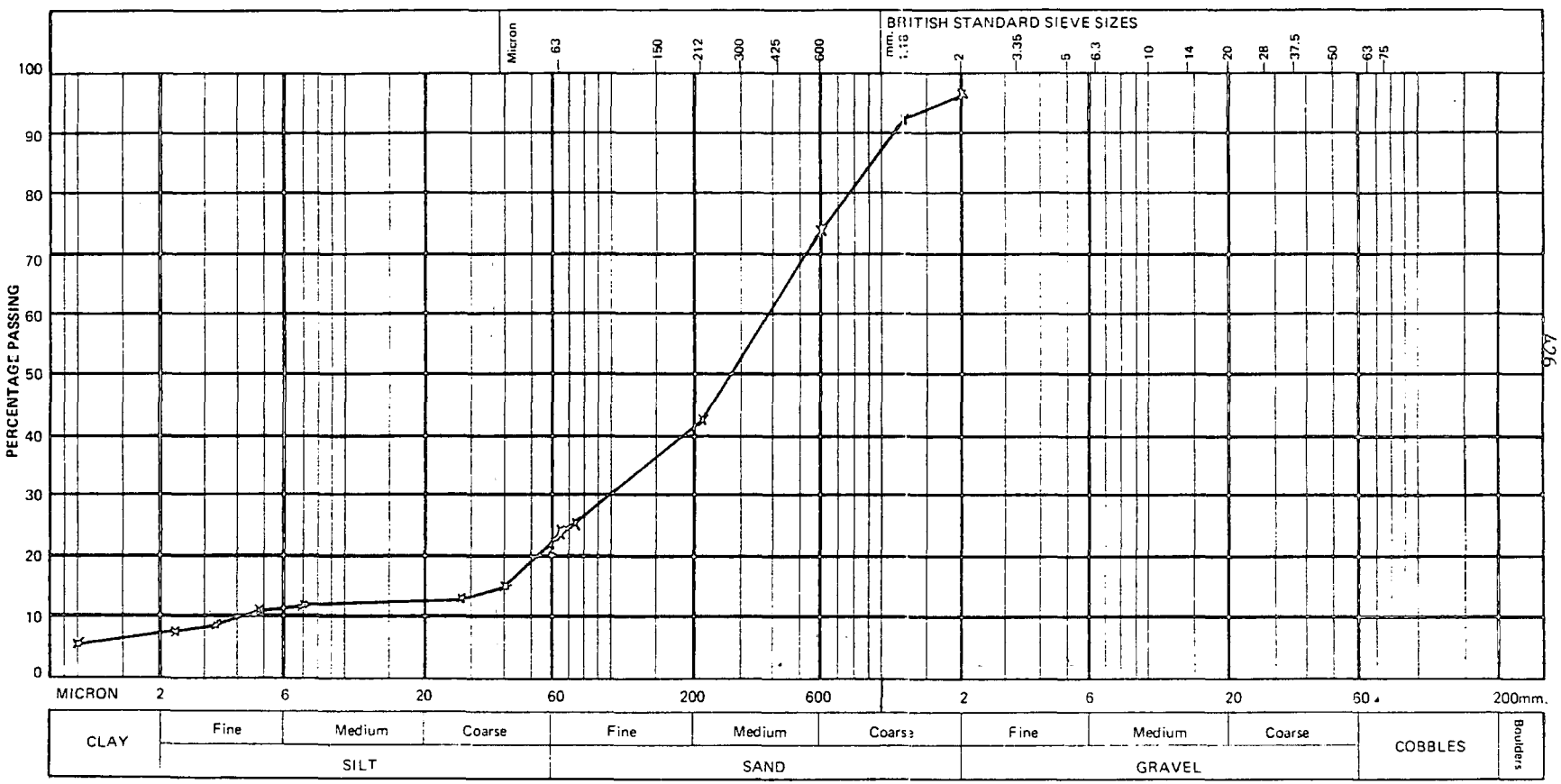

Signed.....

Form No. K4

PARTICLE SIZE DISTRIBUTION

LOCATION No..... BORE HOLE No..... SAMPLE No. 10/5 PRETREATMENT DETAILS H_2O_2

DATE OF TEST..... DESCRIPTION..... LOSS ON PRETREATMENT.....%

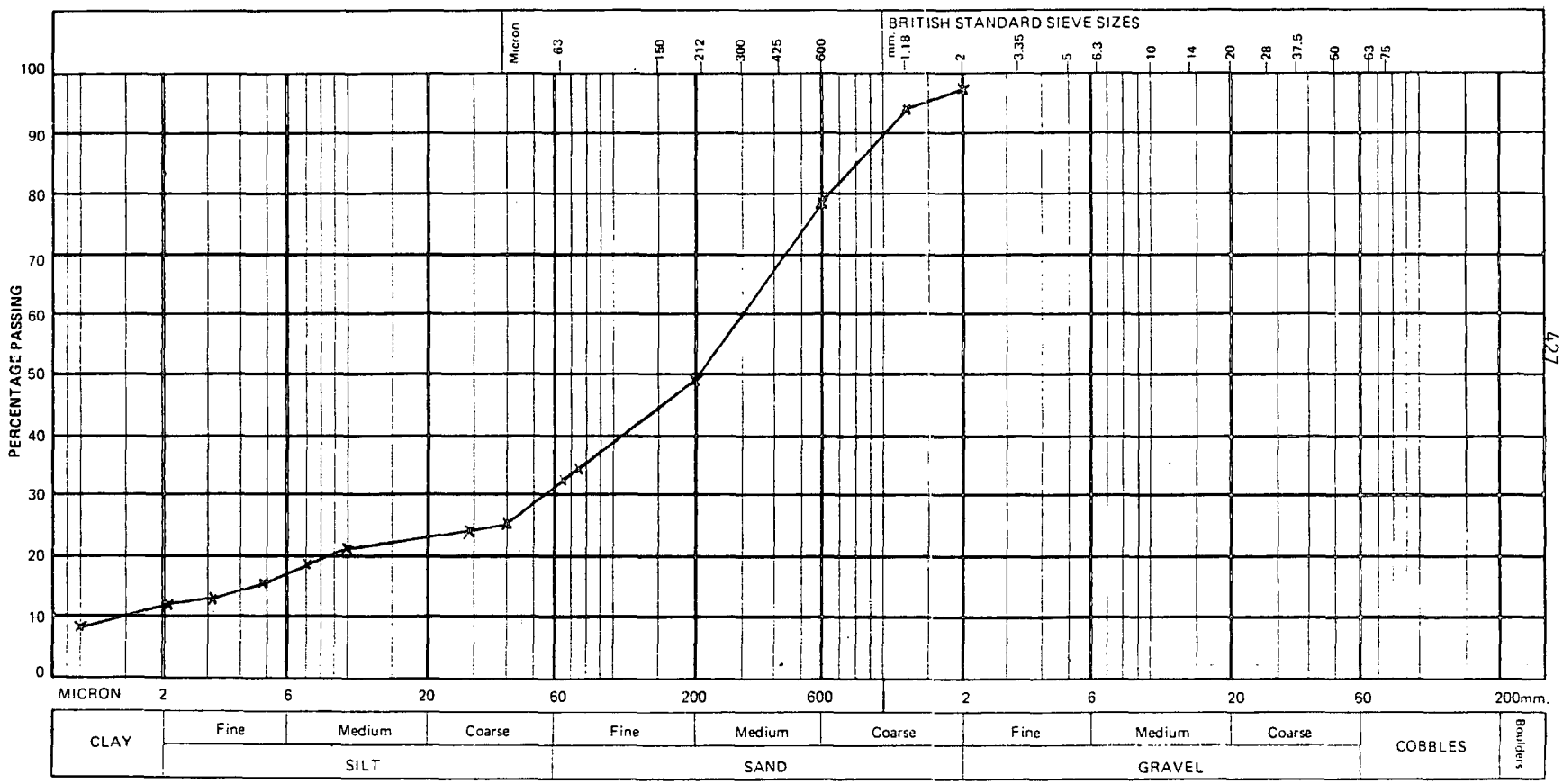

427

Signed.....

PARTICLE SIZE DISTRIBUTION

Form No. K4

LOCATION No..... BORE HOLE No..... SAMPLE No. 10/6 PRETREATMENT DETAILS H_2O_2

DATE OF TEST..... DESCRIPTION..... LOSS ON PRETREATMENT.....%

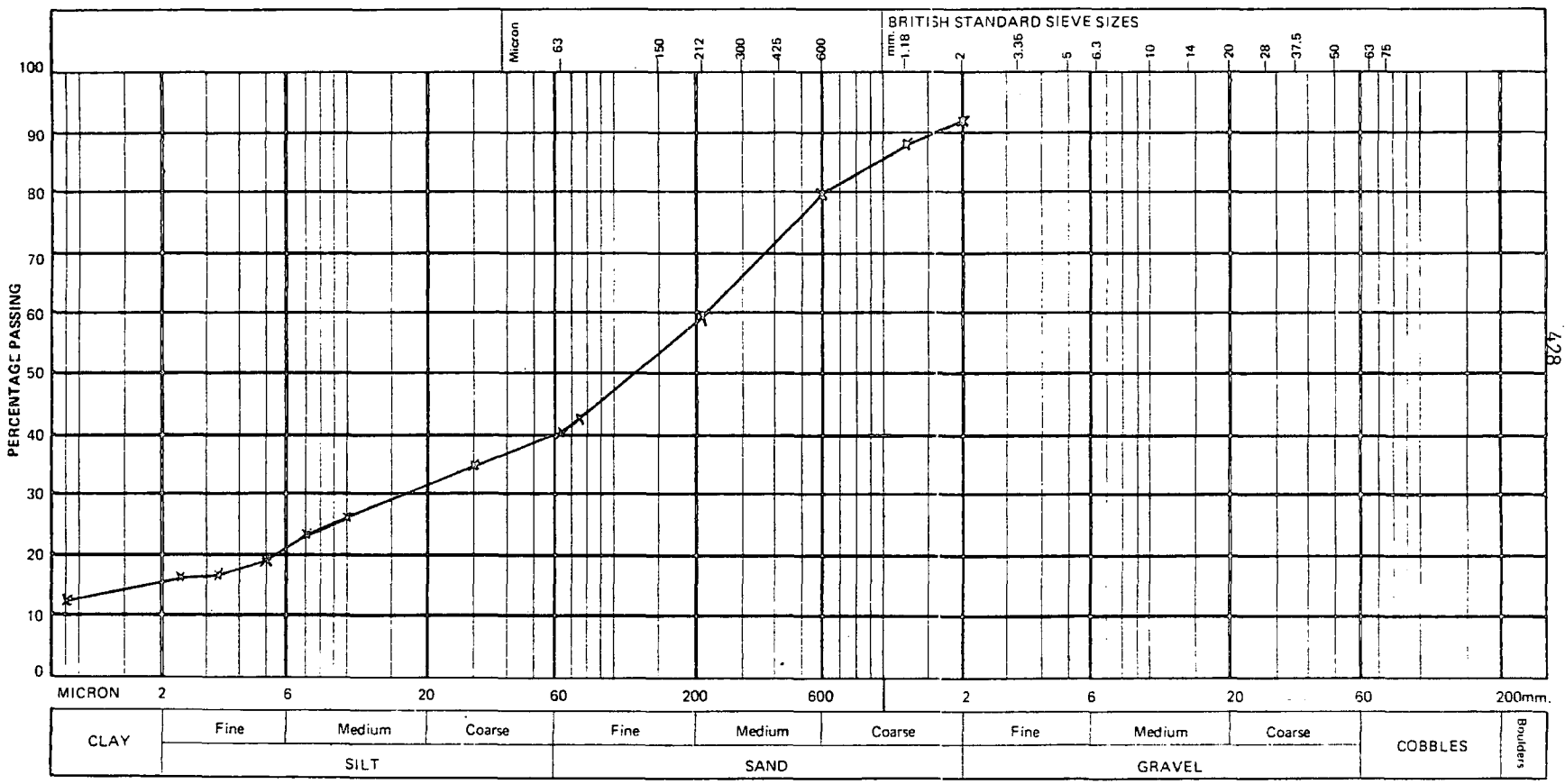

428

Signed.....

PARTICLE SIZE DISTRIBUTION

Form No. K4

LOCATION No..... BORE HOLE No..... SAMPLE No. 1017 PRETREATMENT DETAILS H_2O_2

DATE OF TEST..... DESCRIPTION..... LOSS ON PRETREATMENT.....%

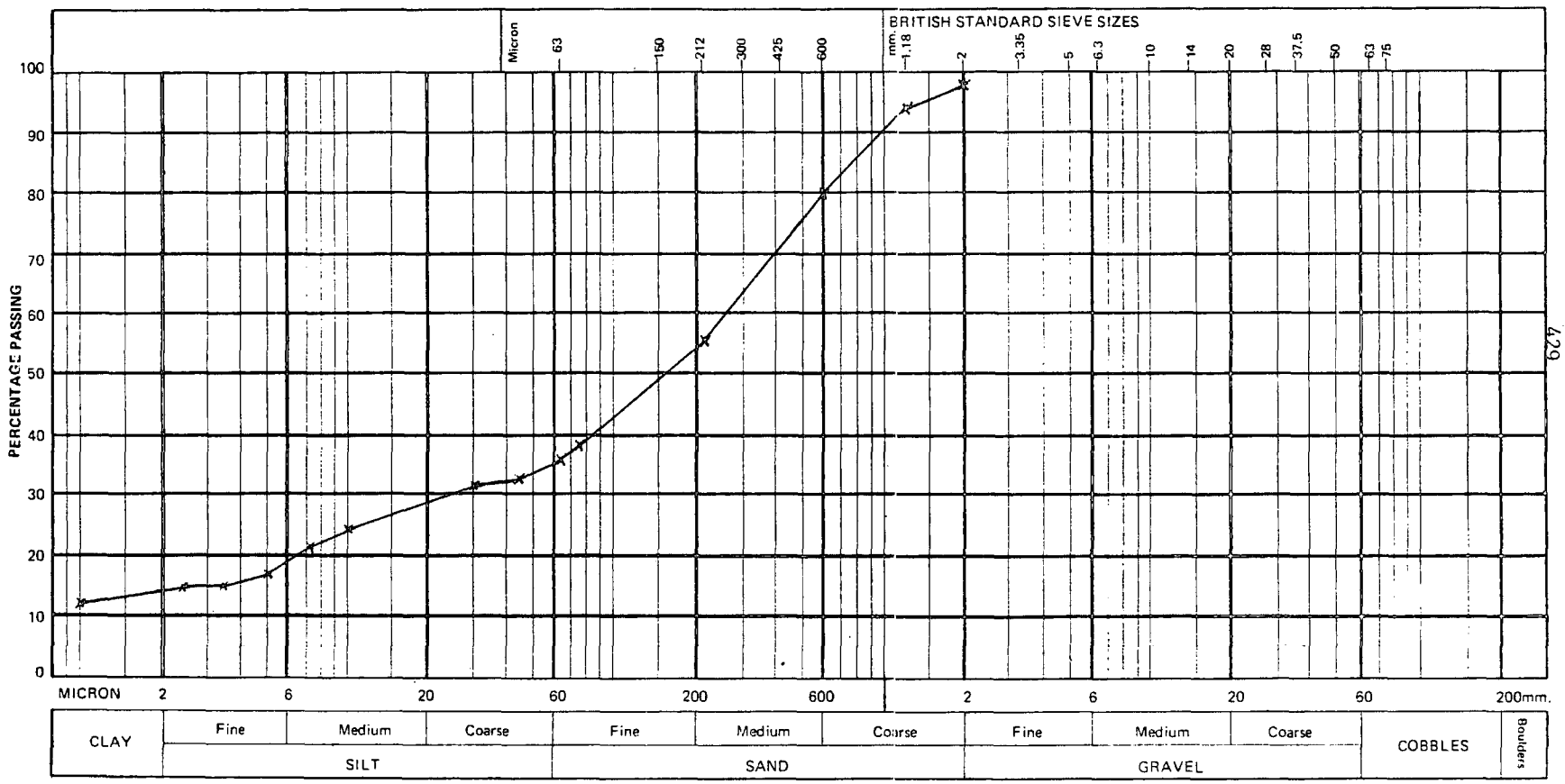

429

Signed.....

PARTICLE SIZE DISTRIBUTION

Form No. K4

LOCATION No..... BORE HOLE No..... SAMPLE No. 10/8 PRETREATMENT DETAILS H_2O_2

DATE OF TEST..... DESCRIPTION..... LOSS ON PRETREATMENT.....%

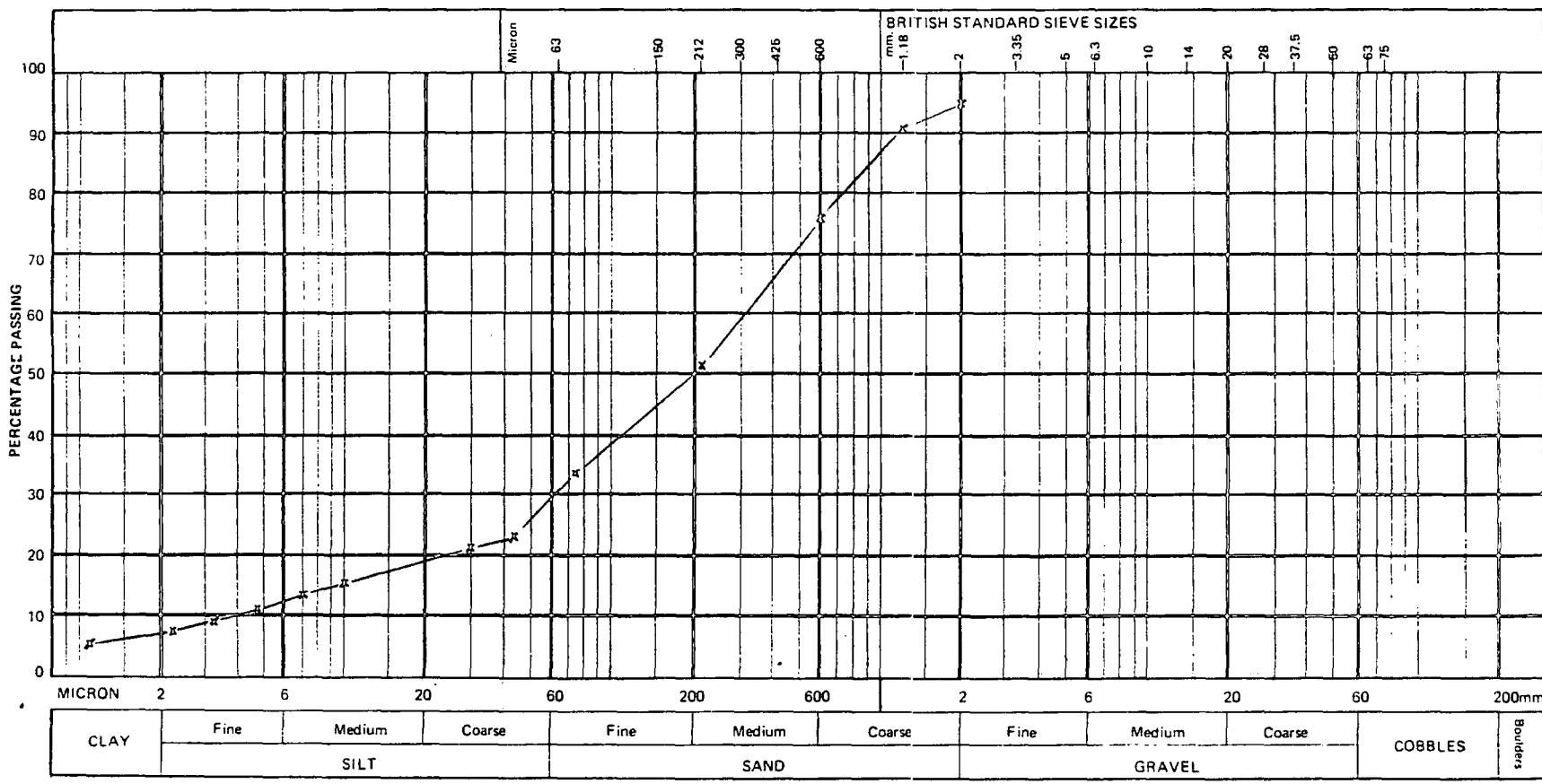

4.30

Signed.....

APPENDIX C

Engineering drawing of strain-controlled direct-shear apparatus described in Chapter six.

This shear-box equipment was designed by the author and constructed by Mr. A. Swan of the Engineering Geology Department. The measurement apparatus, linear motion transducers and chart recorders were kindly loaned by the Engineering Geology Department. The construction of the shear-box was financed by the Department of Geography.

STRAIN-CONTROLLED DIRECT SHEAR APPARATUS.

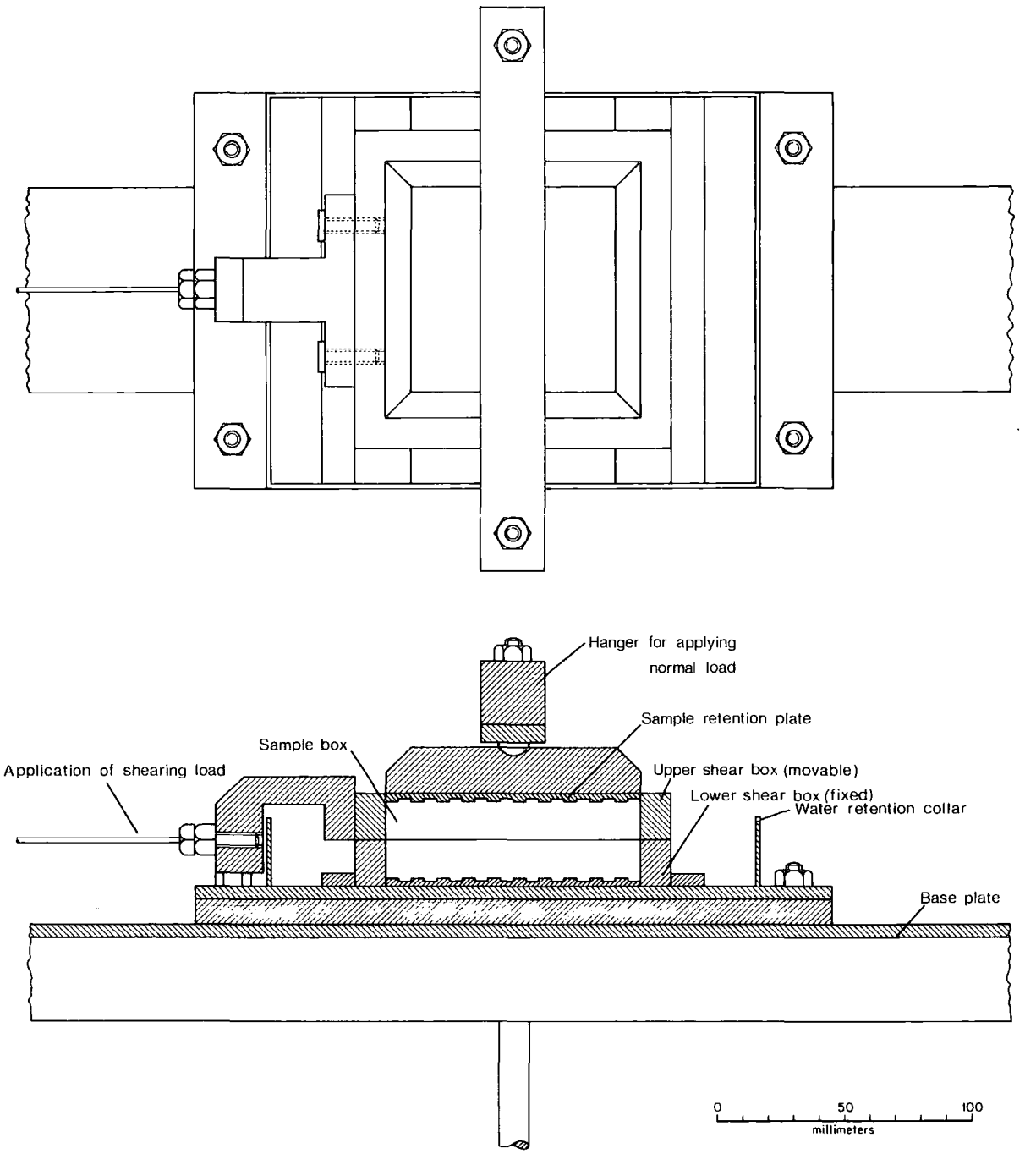

APPENDIX D

The appendix contain tables and graphs of the raw data collected during the eighteen month measurement period. The time series curves presented are the remainder of the sites which were not shown in Chapter Seven. The curves were produced using the IPLOT progam described and listed in appendix A.

Raw data for Anderson's Tubes - total movement for 604 days.

	Depth mm	Surface movement cm	Volumetric flux mm^2	Goodness of fit r^2	Direction of movement degrees	
1/1	- 13.70	0.177	12.113	0.997	22	
1/2	-479.5	0.722	173.088	0.996	32	
1/3	-169.5	0.112	9.455	0.957	11	
1/4	-188.5	0.066	6.199	0.889	45	*
1/5	-325.0	0.073	11.907	0.976	51	*
2/1	-144.6	0.699	50.551	0.910	58	*
2/2	-319.2	0.028	4.416	0.923	27	
2/3	-329.2	0.196	32.345	0.089	48	*
2/4	- 61.9	0.021	0.650	0.955	0	
2/5	-155.4	0.396	30.812	0.999	34	
2/6	245.9	0.102	12.500	0.871	27	
2/7	195.9	0.237	23.236	0.991	0	
3/1	66.1	0.053	1.760	0.882	14	
3/2	137.0	0.036	2.449	0.998	27	
3/3	790.4	0.059	23.204	0.942	31	
3/4	103.3	0.031	1.601	-	56	*
3/5	70.4	0.076	2.675	1.000	23	
3/6	154.8	0.209	16.197	0.991	43	*
3/7	28.4	0.033	0.467	0.977	45	*
4/1	267.2	0.465	62.124	-	12	
4/2	357.3	0.155	27.661	0.923	78	*
4/3				no tilt	24	
4/4				reverse tilt	27	
4/5	296.6	0.350	51.905	1.000	4	
4/6	239.1	0.064	7.608	0.939	22	
5/1	229.4	0.444	50.892	0.998	7	
5/2	355.5	0.224	39.816	-	27	
5/3				reverse tilt	18	
5/4	143.9	0.276	19.845	0.976	23	
5/5	636.5	0.090	28.552	0.993	14	
5/6	653.8	0.085	27.786	-	45	*
5/7	653.4	0.041	13.450	0.999	76	*
5/8				reverse tilt	0	
5/9				no tilt	48	*
5/10	145.4	0.088	6.427	0.987	68	*
6/1				reverse tilt	29	
6/2	107.7	0.330	17.755	0.999	19	
6/3	273.2	0.162	22.125	0.997	11	
6/4	457.1	0.028	6.501	0.964	45	*
6/5	242.2	0.270	32.708	0.995	6	
6/6	840.0	0.252	105.840	-	28	
7/1	391.7	0.139	27.166	0.960	20	
7/2	122.7	0.281	17.255	0.982	34	
7/3				reverse tilt	14	
7/4				reverse tilt	47	*
7/5	97.6	0.141	6.900	0.966	90	*
7/6	80.7	0.082	3.289	0.999	30	

contd.

	Depth mm	Surface movement cm	Volumetric flux mm^2	Goodness of fit r^2	Direction of movement degrees	
8/1				no tilt	26	
8/2	41.9	0.021	0.431	0.855	45	*
8/3	28.9	0.070	1.154	0.959	84	*
8/4	500+	0.280	139.921+	0.999	0	
8/5	120.2	0.111	6.653	0.836	63	*
8/6	127.6	0.115	14.616	0.847	31	
9/1				reverse tilt	27	
9/2	77.2	0.126	4.852	0.989	21	
9/3	175.3	0.368	32.291	0.999	2	
9/4	550.0	0.022	60.500	0.750	3	
9/5	263.1	0.534	70.270	0.999	34	
9/6	293.5	0.540	79.304	0.994	20	
9/7	77.0	0.125	4.825	0.996	37	
9/8				reverse tilt	51	*
10/1	194.9	0.063	6.161	0.832	68	*
10/2	296.0	0.088	13.060	0.839	27	
10/3	450.0	0.090	20.250	1.000	7	
10/4	86.7	0.085	3.685	-	56	*
10/5				reverse tilt	0	

Raw data for Inclinometer Pegs - total movement for 604 days.

	15 cm	10 cm	5 cm	VEG	SLOPE	ROOTS
1/1	135	355.0	67.5	J	2	5
1/2	630	690.0	85.0	P	2	2
3	281.25	170.0	47.5	P	1	2
4	146.25	65.0	23.75	H	1	1
5	191.25	165.0	115.0	P	2	1
2/1	157.5	95.0	18.75	J	2	5
2	112.5	140.0	56.25	J	2	2
3	168.75	185.75	153.75	N	1	5
4	45	-15.0	7.5	N	1	1
5	371.25	95.0	33.75	P	2	3
6	157.5	245.0	47.5	J	1	5
7	416.25	245.0	47.5	H	2	2
3/1	202.5	45.0	40.0	P	1	2
2	135	-	97.5	P	1	1
3	191.25	-	13.75	N	2	2
4	123.75	80.0	23.75	J	1	4
5	292.5	80.0	26.25	P	1	1
6	135	135.0	70.0	H	2	1
7	146.25	105.0	2.5	H	1	3
4/1	405	-	-	J	1	5
2	-	-	33.75	J	2	2
3	258.75	130	-	N	3	2
4	180	-	26.25	P	1	1
5	-	85.0	-	P	3	2
6	-	170	75.0	H	2	1
5/1	180	375.0	216.25	J	4	5
2	157.5	55	-16.25	J	1	5
3	-	-	68.75	J	3	5
4	-	570.0	168.75	J	4	5
5	-	130.0	7.5	N	1	3
6	56.25	125.0	45.0	N	1	3
7	112.5	70.0	78.75	N	1	2
8	202.51	-200.0	131.25	J	1	5
9	270	115.0	128.75	P	2	3
10	202.51	165.0	86.25	H	1	

contd.

	15 cm	10 cm	5 cm	Veg	Slope	Roots
6/1	303.75	270.0	145.0	J	1	3
6/2	866.25	385.0	-	J	1	2
6/3	573.75	15.0	97.5	P	3	3
6/4	236.25	-130.0	90.0	P	3	2
6/5	225.00	115.0	67.5	P	3	3
6/6	157.50	230.0	15.0	P	3	2
7/1	78.75	85.0	68.75	P	3	3
7/2	202.50	40.0	33.75	P	3	3
7/3	-	-	-7.5	N	2	1
7/4	0.00	55.0	7.5	N	2	1
7/5	360.00	60.0	27.5	H	4	2
7/6	202.50	200.0	-	H	4	2
8/1	-	-	111.25	N	2	2
8/2	11.25	-	-21.25	N	2	2
8/3	247.50	-	88.75	J	1	1
8/4	112.50	155.0	115.0	N	2	2
8/5	281.25	-300.0	247.5	P	3	3
8/6	247.50	210.0	16.25	H	4	3
9/1	213.7	760.0	213.8	J	1	3
9/2	315.0	365.0	346.2	J	1	4
9/3	1260.0	390.0	131.3	J	1	4
9/4	-	-	-	J	1	3
9/5	281.3	230.0	146.2	J	1	4
9/6	-22.5	710.0	0.0	J	1	4
9/7	202.5	-10.0	31.3	N	2	2
9/8	-	35.0	28.8	N	2	2
10/1	191.2	100.0	46.2	N	2	4
10/2	-483.8	170.0	-	N	2	4
10/3	101.2	215.0	-93.8	N	2	4
10/4	135.0	30.0	36.2	N	2	3
10/5	180.0	-	2.5	N	2	4
10/6	168.8	-30.0	-53.8	N	2	4
10/7	337.5	210.0	80.0	N	2	3
10/8	258.8	100.0	57.5	N	2	3

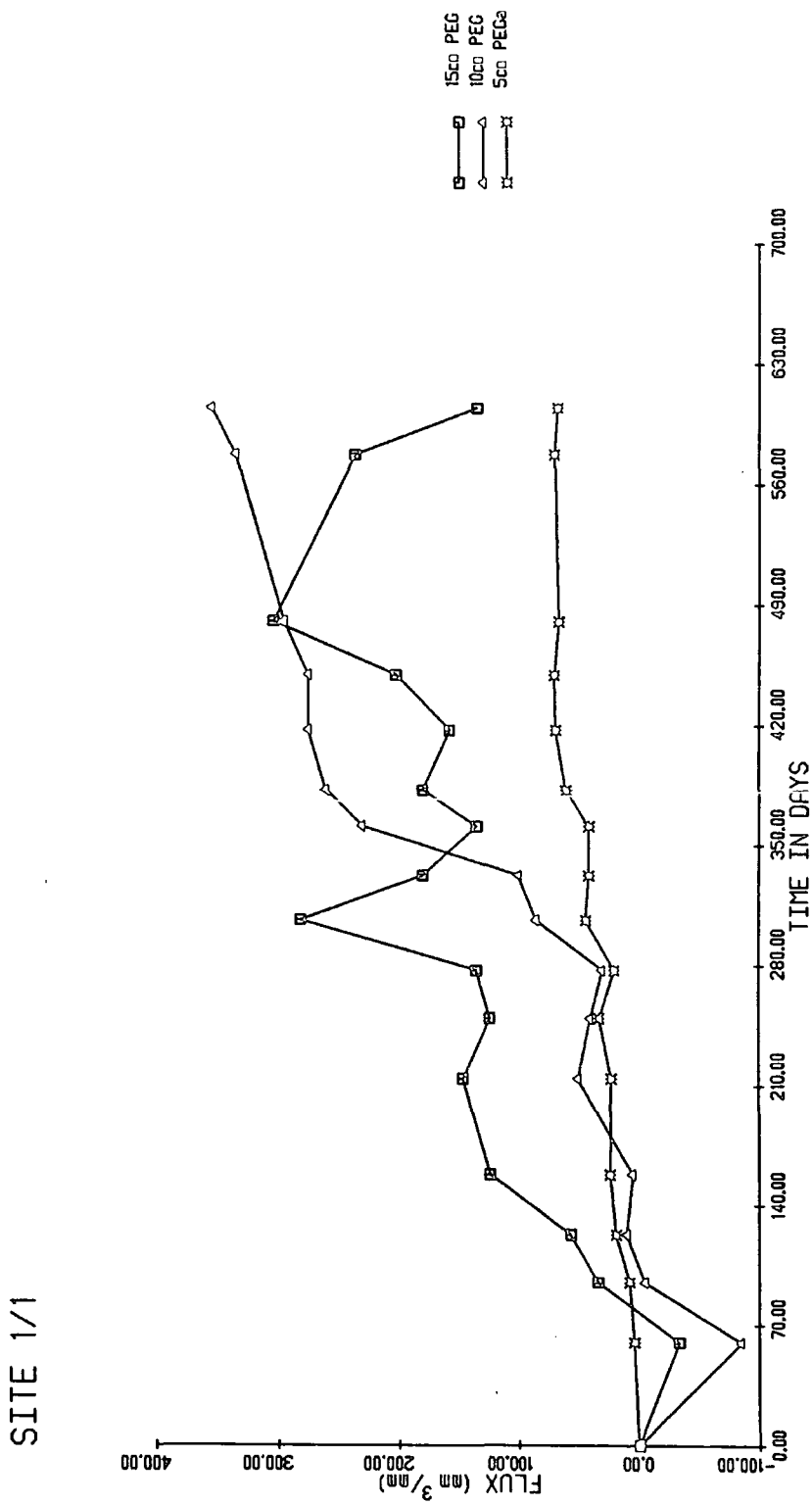
SITE 1/1
15cc PEG
10cc PEG
5cc PEGa
FLUX (mm 3/mm)
-100.00
0.00
100.00
200.00
300.00
400.00
0.00
70.00
140.00
210.00
280.00
350.00
420.00
490.00
560.00
630.00
700.00
TIME IN DAYS

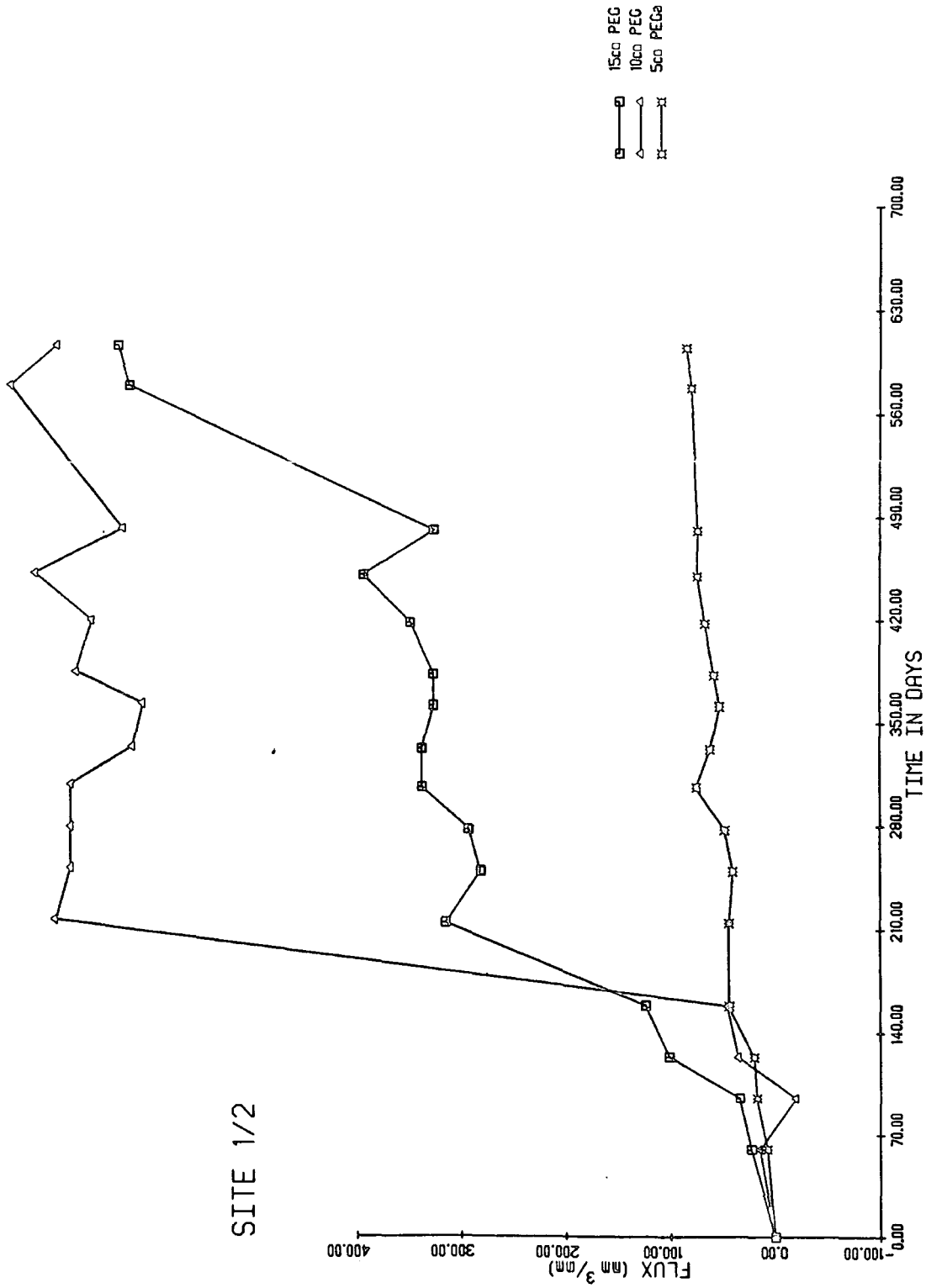
SITE 1/2
15cm PEG
10cm PEG
5cm PEGa
FLUX (mm 3/mm)
TIME IN DAYS
-100.00
0.00
100.00
200.00
300.00
400.00
0.00
70.00
140.00
210.00
280.00
350.00
420.00
490.00
560.00
630.00
700.00

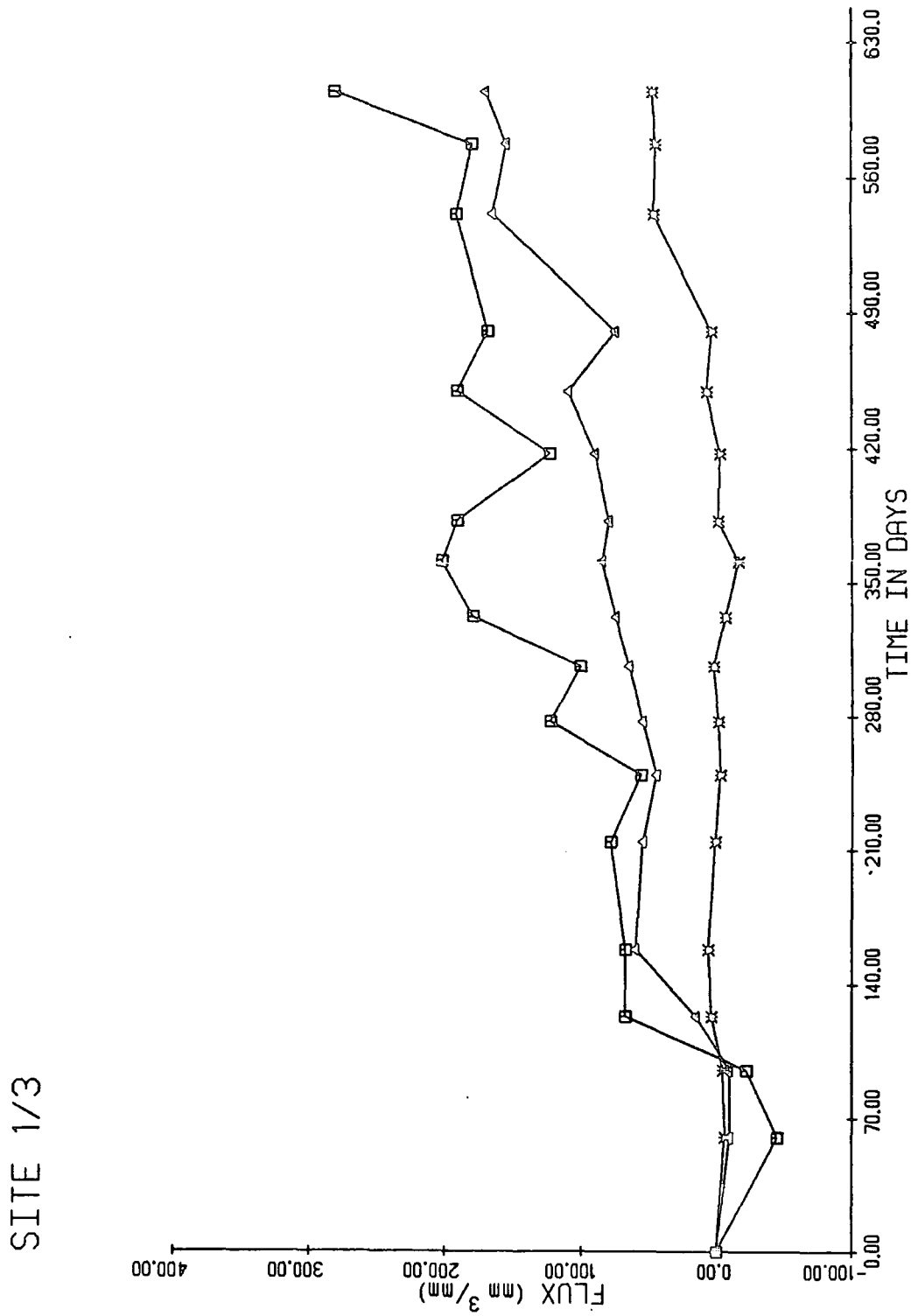
SITE 1/3
FLUX (mm 3/mm)
400.00
300.00
200.00
100.00
0.00
-100.00
0.00
70.00
140.00
210.00
280.00
350.00
420.00
490.00
560.00
630.0
TIME IN DAYS

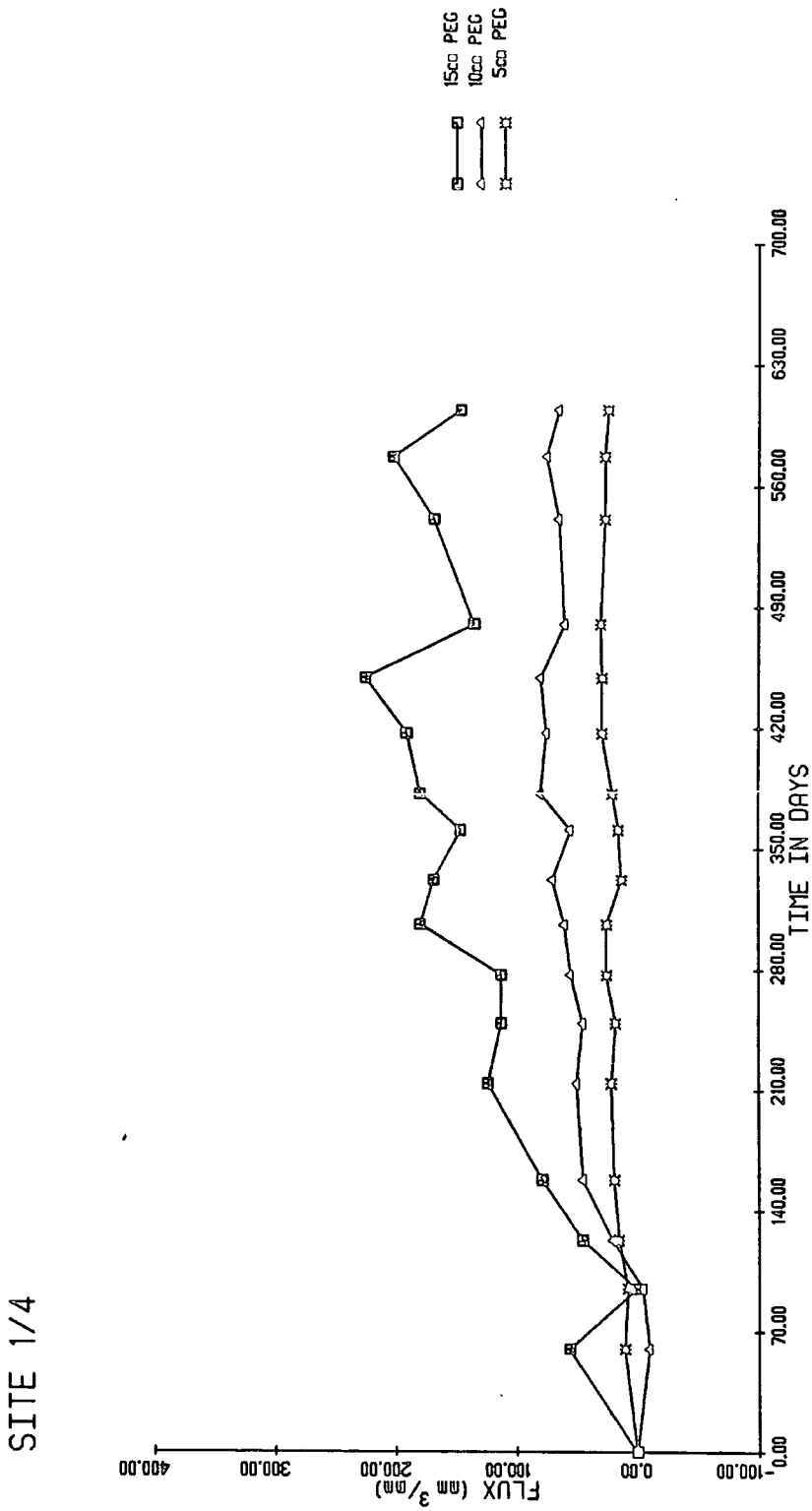
SITE 1/4
15cc PEG
10cc PEG
5cc PEG
FLUX (mm 3/mm)
400.00
300.00
200.00
100.00
0.00
-100.00
0.00
70.00
140.00
210.00
280.00
350.00
420.00
490.00
560.00
630.00
700.00
TIME IN DAYS

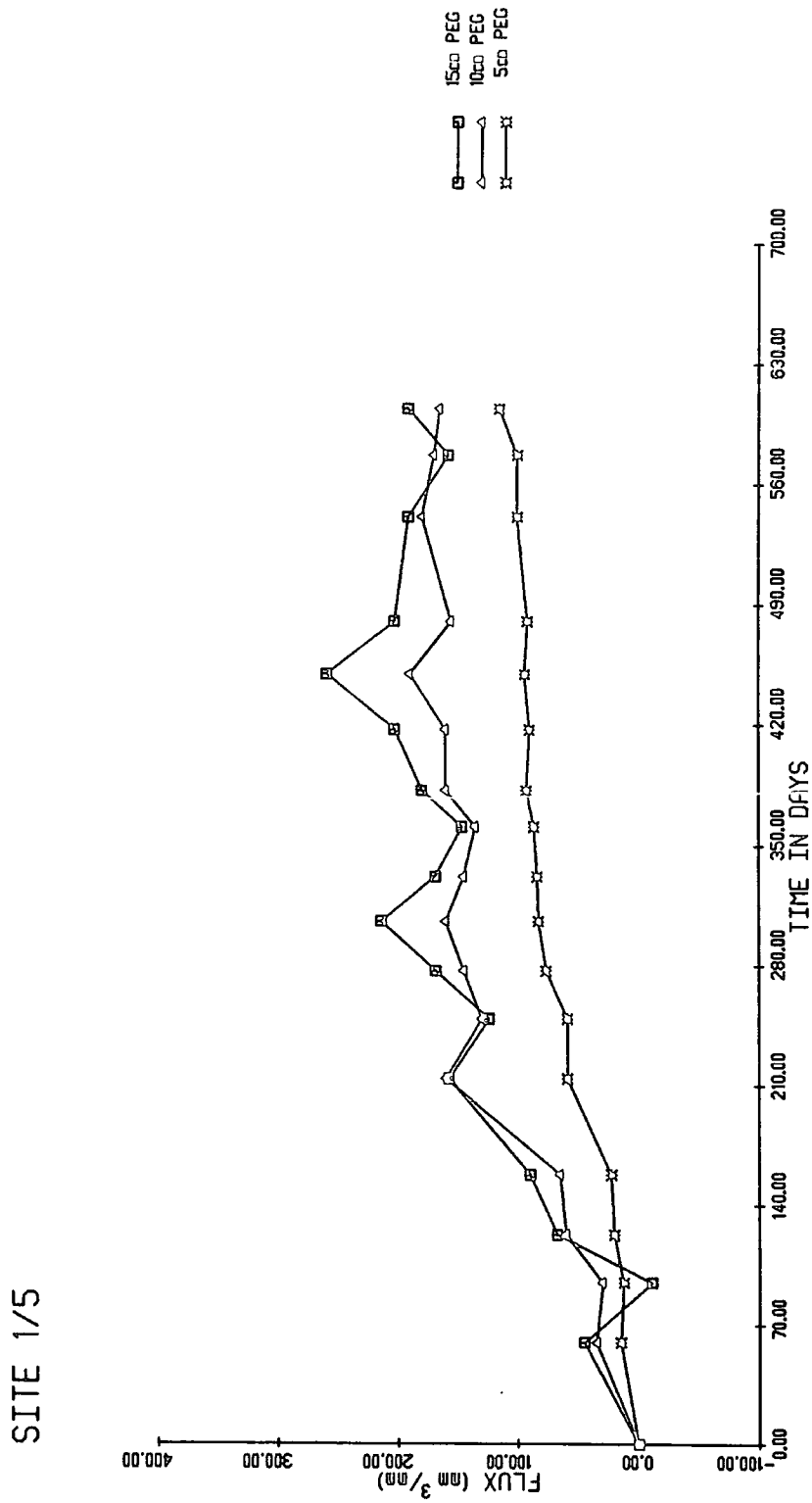
SITE 1/5
15cm PEG
10cm PEG
5cm PEG
FLUX (gm 3/gm)
400.00
300.00
200.00
100.00
0.00
-100.00
0.00
70.00
140.00
210.00
280.00
350.00
420.00
490.00
560.00
630.00
700.00
TIME IN DAYS

SITE 2/2

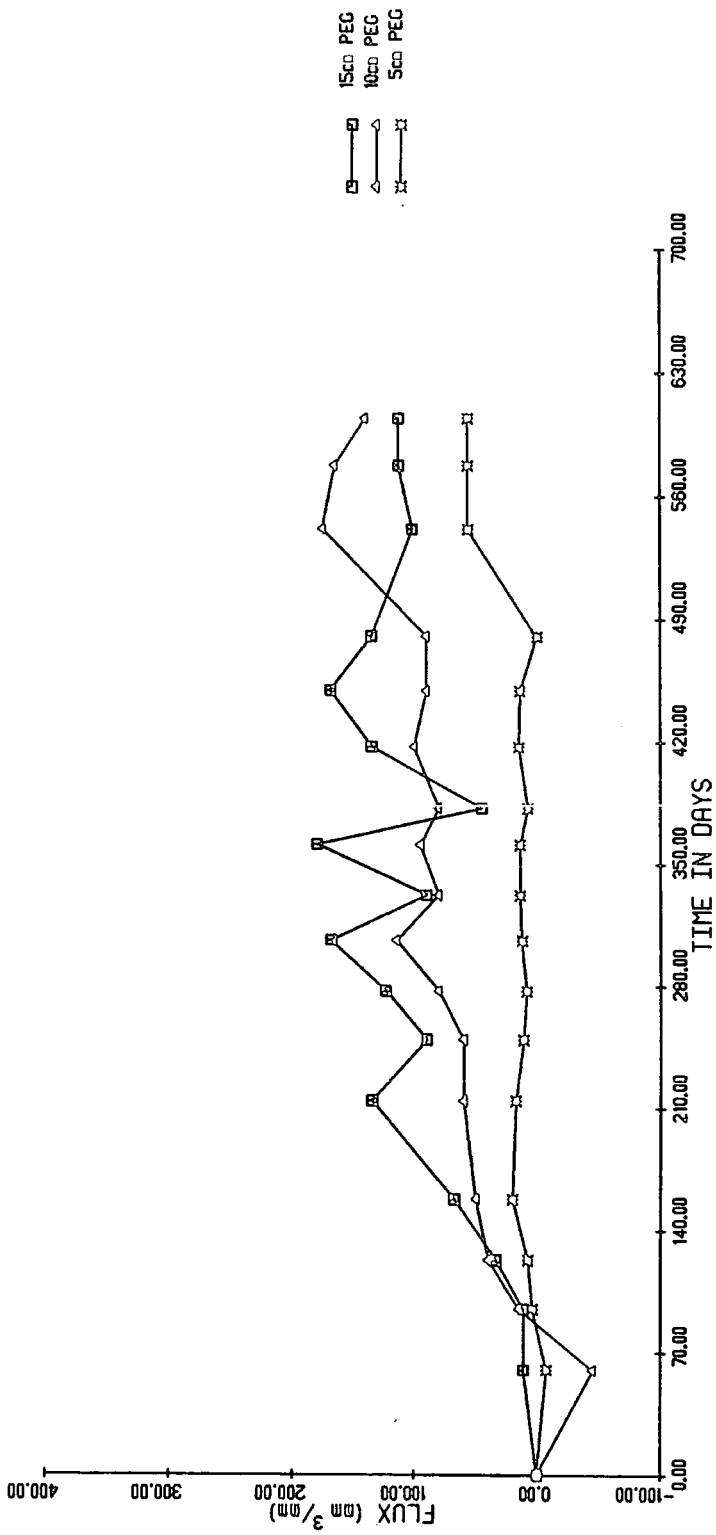
15□ PEG
10□ PEG
5□ PEG
FLUX (m 3/m)
400.00
300.00
200.00
100.00
0.00
-100.00
0.00
70.00
140.00
210.00
280.00
350.00
420.00
490.00
560.00
630.00
700.00
TIME IN DAYS

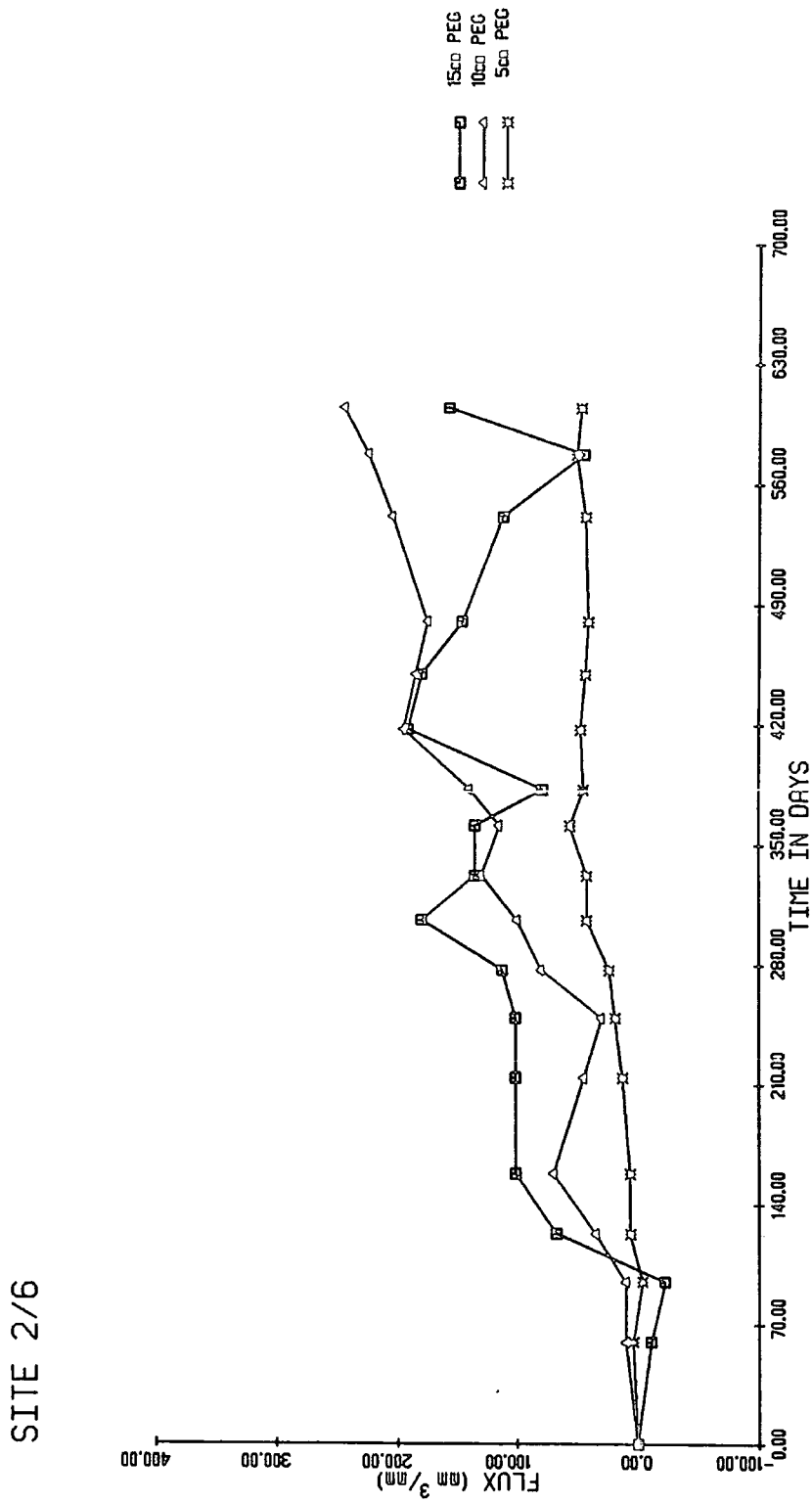
SITE 2/6
15cm PEG
10cm PEG
5cm PEG
FLUX (mm 3/mm)
400.00
300.00
200.00
100.00
0.00
-100.00
0.00
70.00
140.00
210.00
280.00
350.00
420.00
490.00
560.00
630.00
700.00
TIME IN DAYS

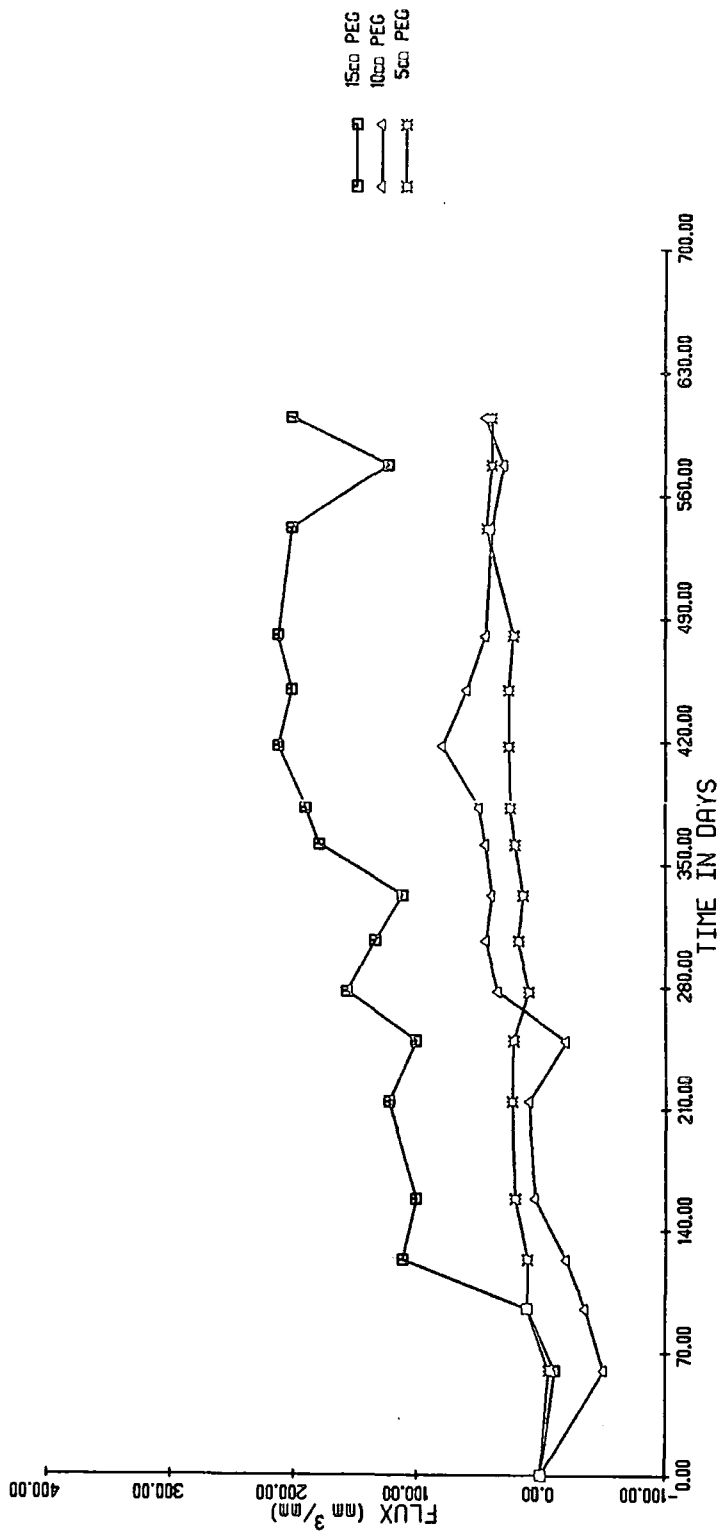
SITE 3/1
15cm PEG
10cm PEG
5cm PEG
FLUX (mm 3/mm)
400.00
300.00
200.00
100.00
0.00
-100.00
0.00
70.00
140.00
210.00
280.00
350.00
420.00
490.00
560.00
630.00
700.00
TIME IN DAYS

SITE 3/4

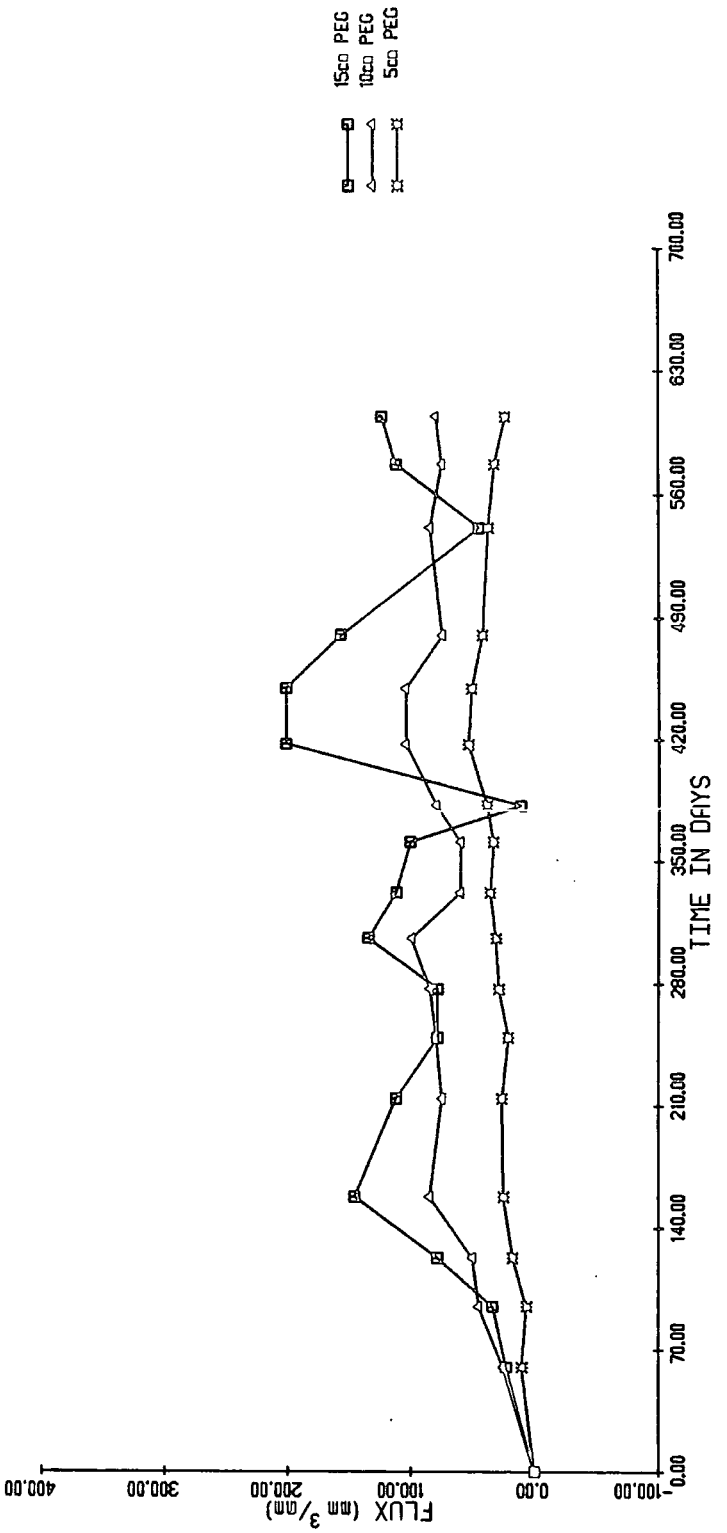
15cm PEG
10cm PEG
5cm PEG
FLUX (mm 3/mm)
400.00
300.00
200.00
100.00
0.00
-100.00
0.00
70.00
140.00
210.00
280.00
350.00
420.00
490.00
560.00
630.00
700.00
TIME IN DAYS

SITE 3/5

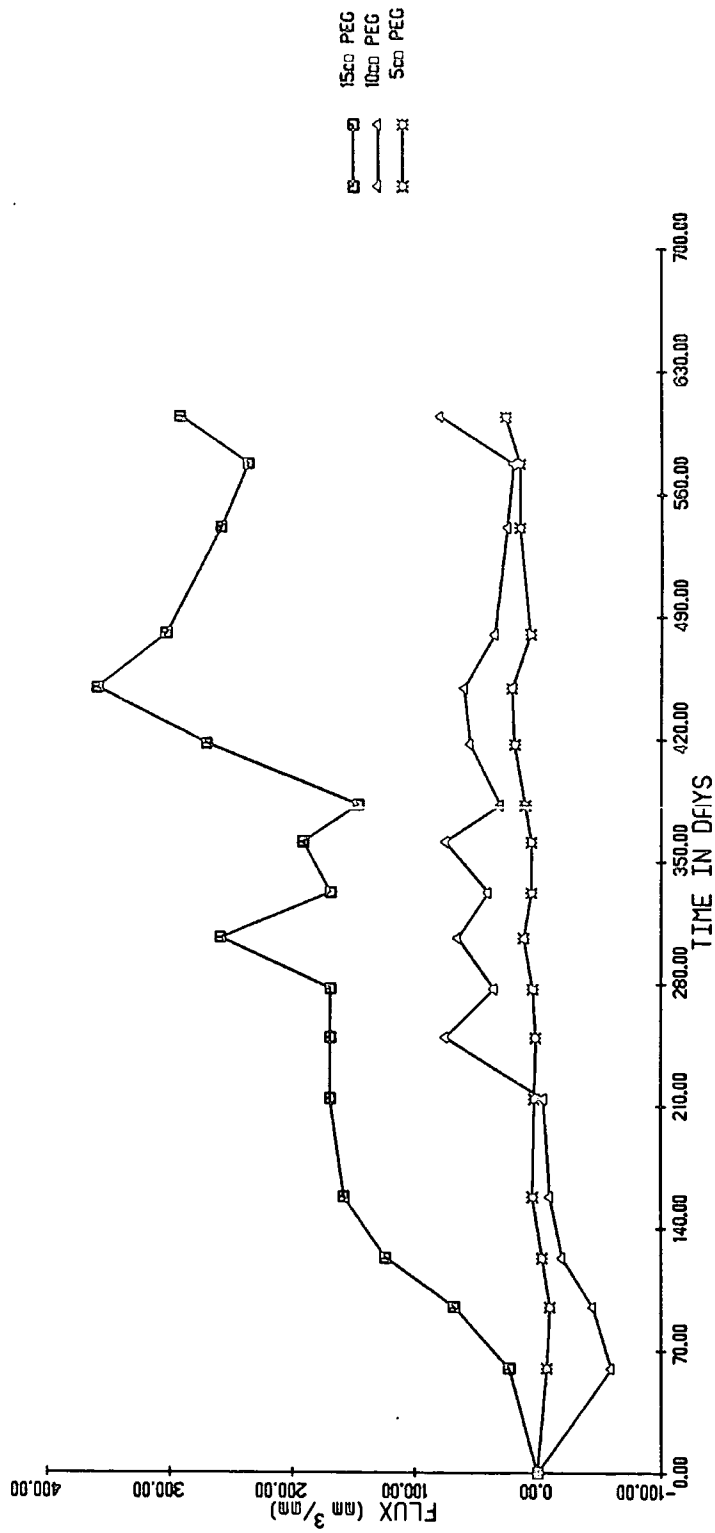
15c□ PEG
10c□ PEG
5c□ PEG
FLUX (mm 3/mm)
400.00
300.00
200.00
100.00
0.00
-100.00
0.00
70.00
140.00
210.00
280.00
350.00
420.00
490.00
560.00
630.00
700.00
TIME IN DAYS

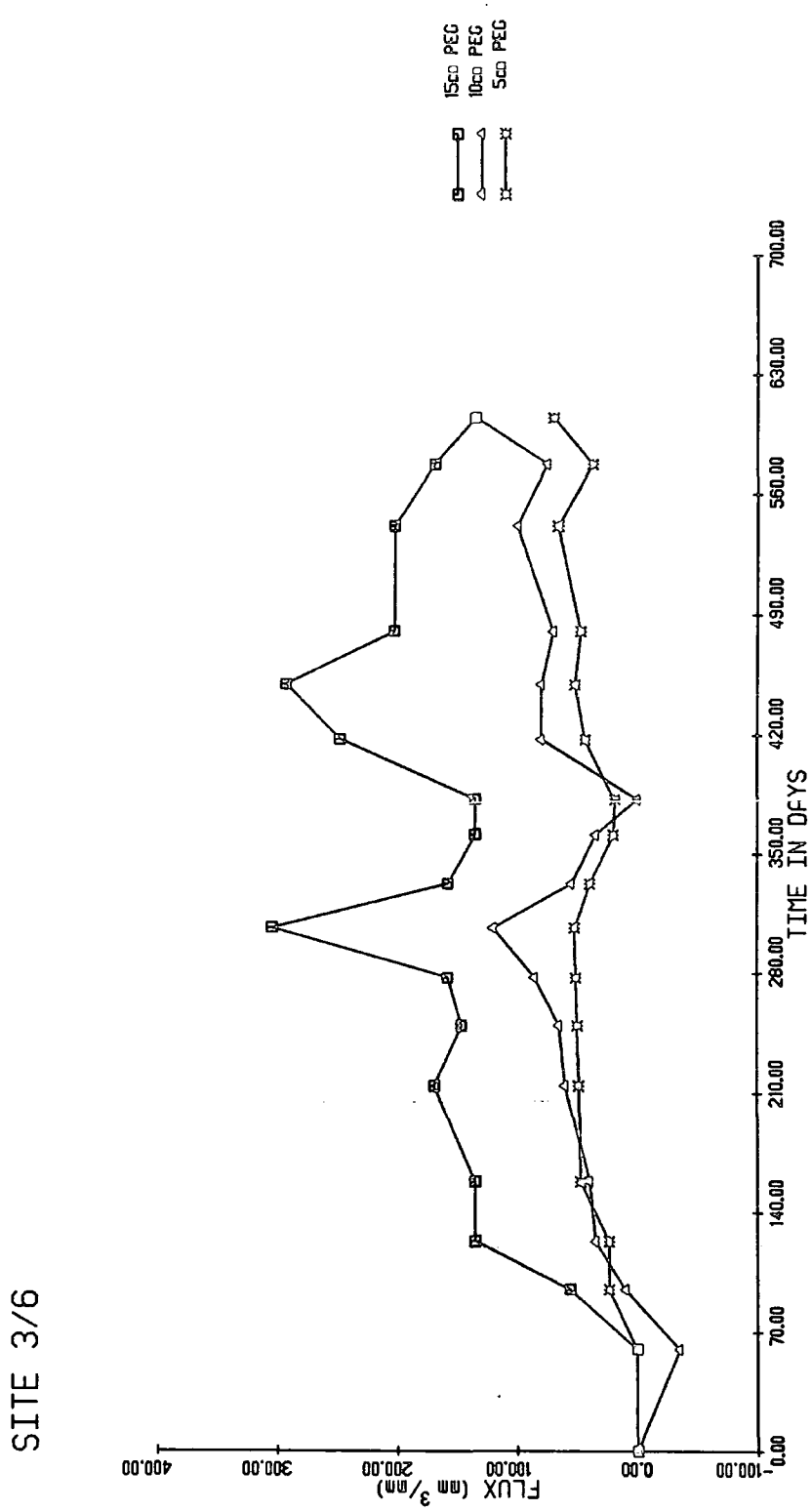
SITE 3/6
15□ PEG
10□ PEG
5□ PEG
FLUX (mm 3/mm)
400.00
300.00
200.00
100.00
0.00
-100.00
0.00
70.00
140.00
210.00
280.00
350.00
420.00
490.00
560.00
630.00
700.00
TIME IN DAYS

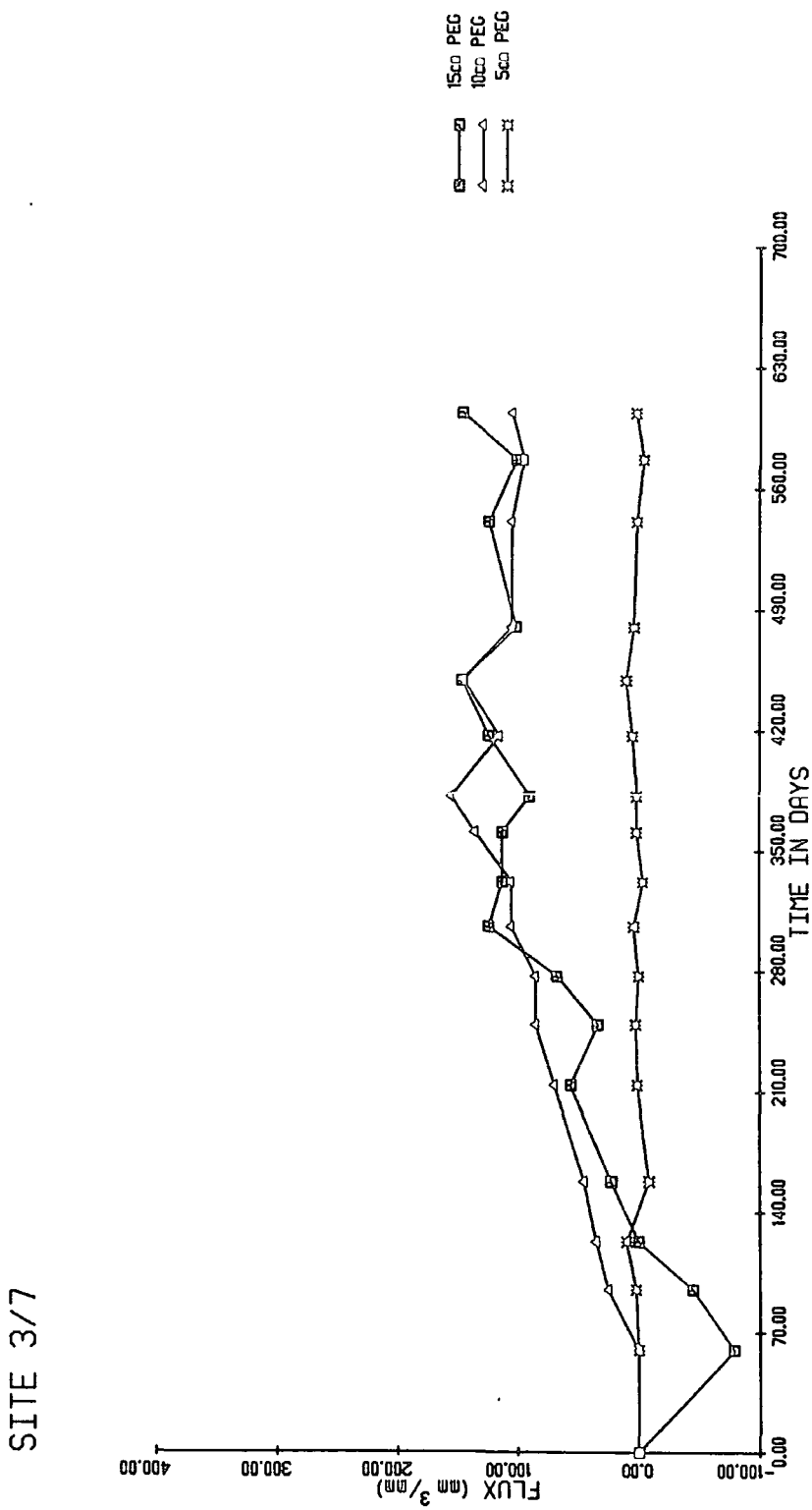
SITE 3/7
15cm PEG
10cm PEG
5cm PEG
FLUX (mm 3/mm)
400.00
300.00
200.00
100.00
0.00
-100.00
0.00
70.00
140.00
210.00
280.00
350.00
420.00
490.00
560.00
630.00
700.00
TIME IN DAYS

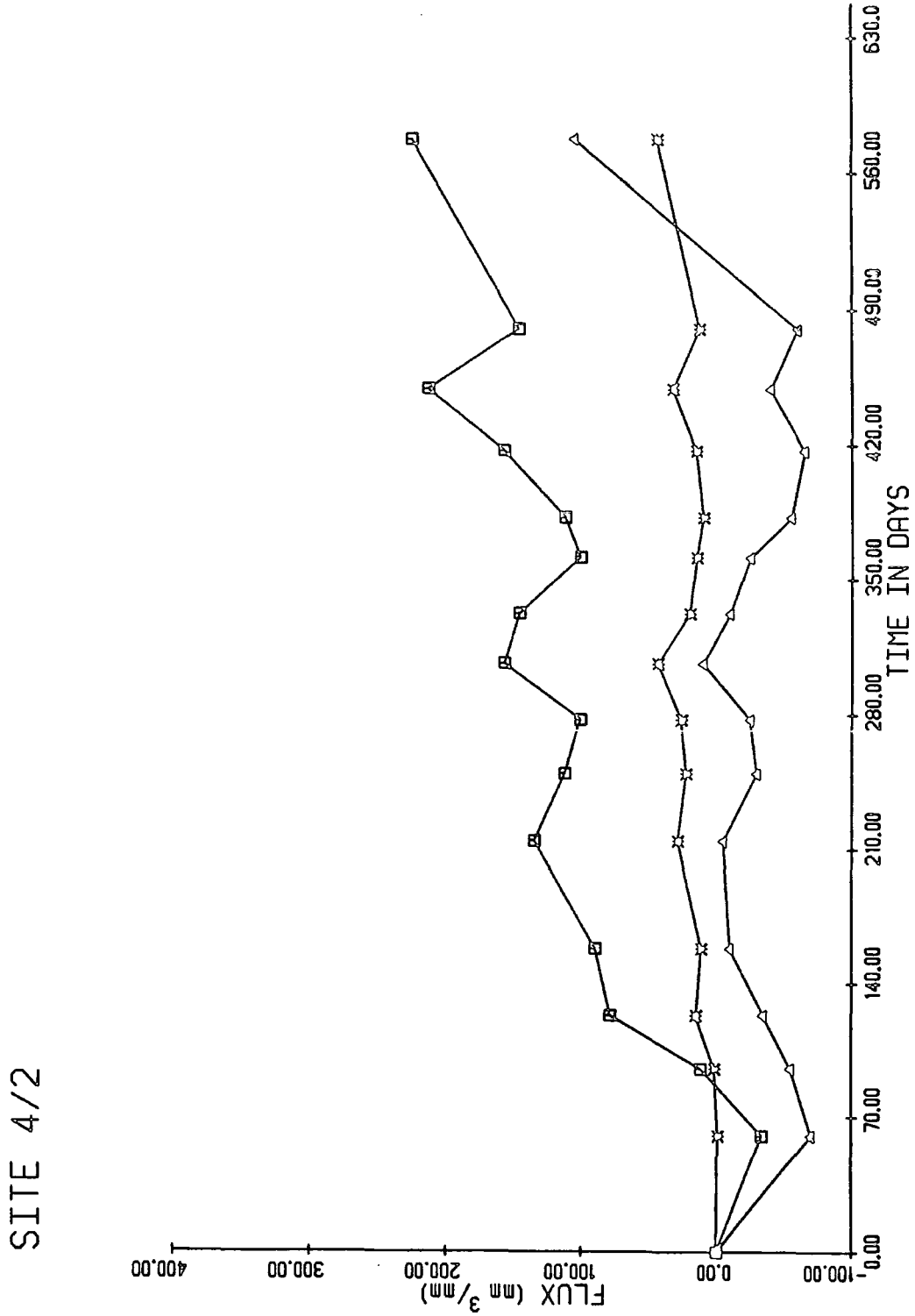
SITE 4/2
FLUX (mm 3/mm)
400.00
300.00
200.00
100.00
0.00
-100.00
0.00
70.00
140.00
210.00
280.00
350.00
420.00
490.00
560.00
630.0
TIME IN DAYS

SITE 4/5

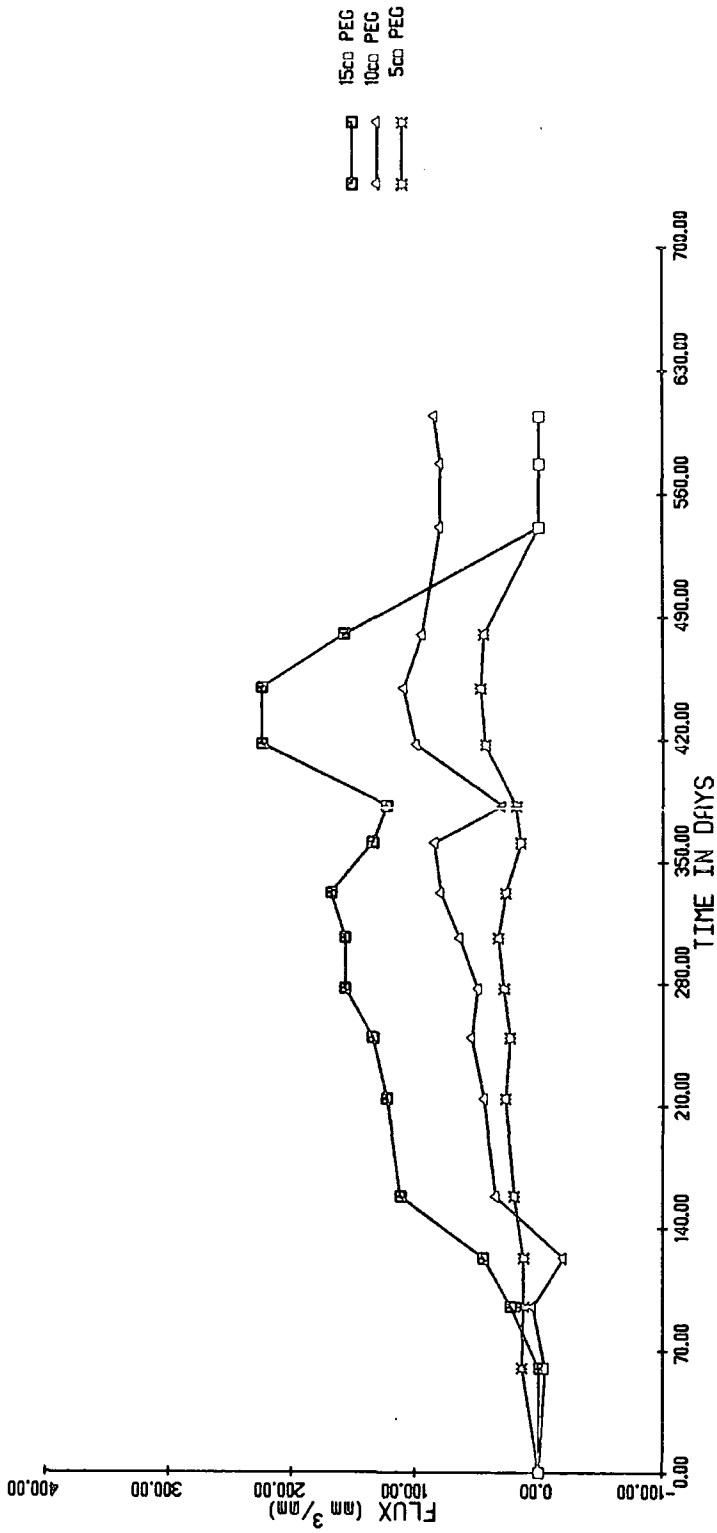
15cm PEG
10cm PEG
5cm PEG
FLUX (mm 3/mm)
-100.00
0.00
100.00
200.00
300.00
400.00
0.00
70.00
140.00
210.00
280.00
350.00
420.00
490.00
560.00
630.00
700.00
TIME IN DAYS

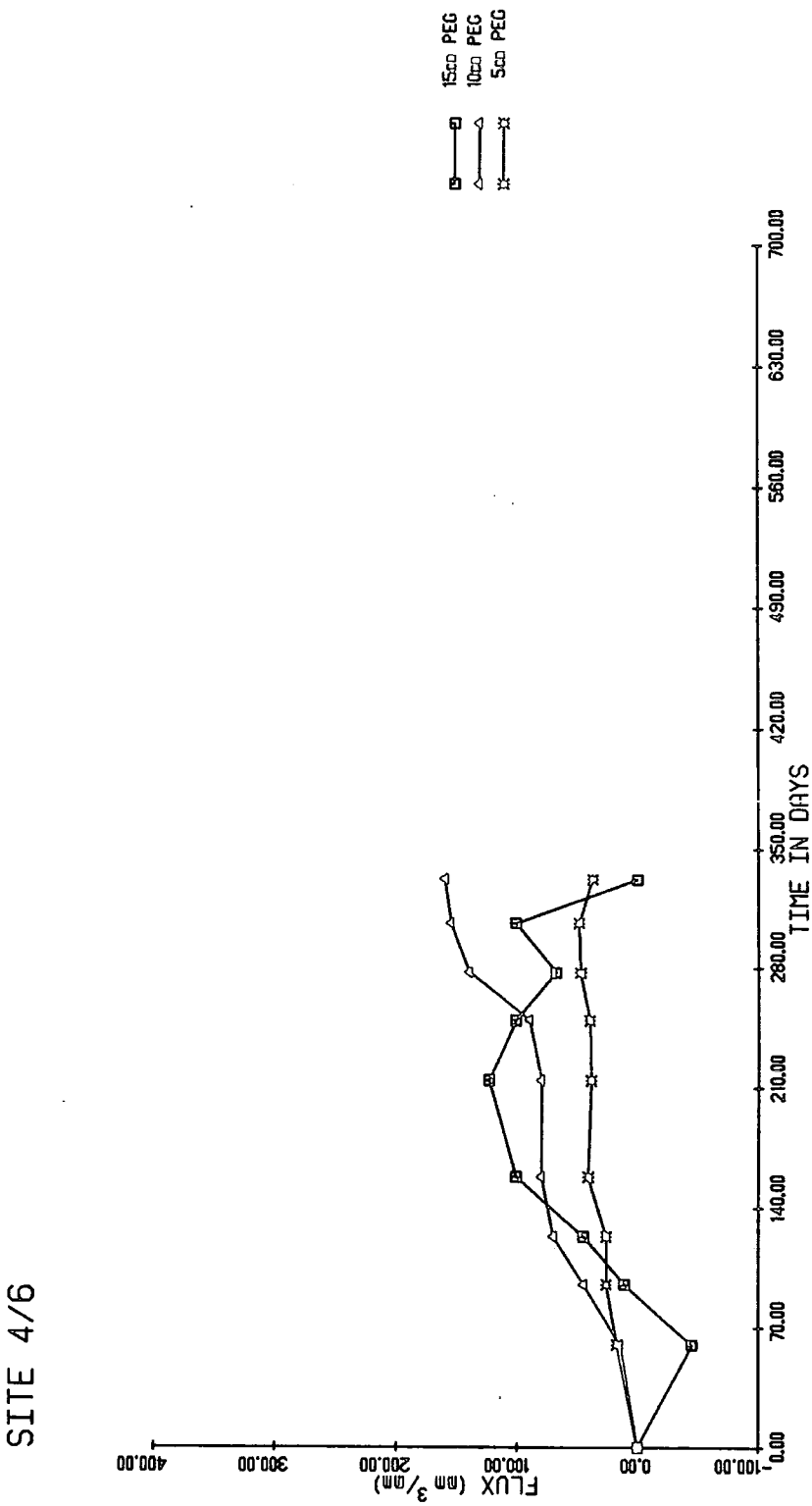
SITE 4/6
15□□ PEG
10□□ PEG
5□□ PEG
FLUX (mm 3/mm)
-100.00
0.00
100.00
200.00
300.00
400.00
0.00
70.00
140.00
210.00
280.00
350.00
420.00
490.00
560.00
630.00
700.00
TIME IN DAYS

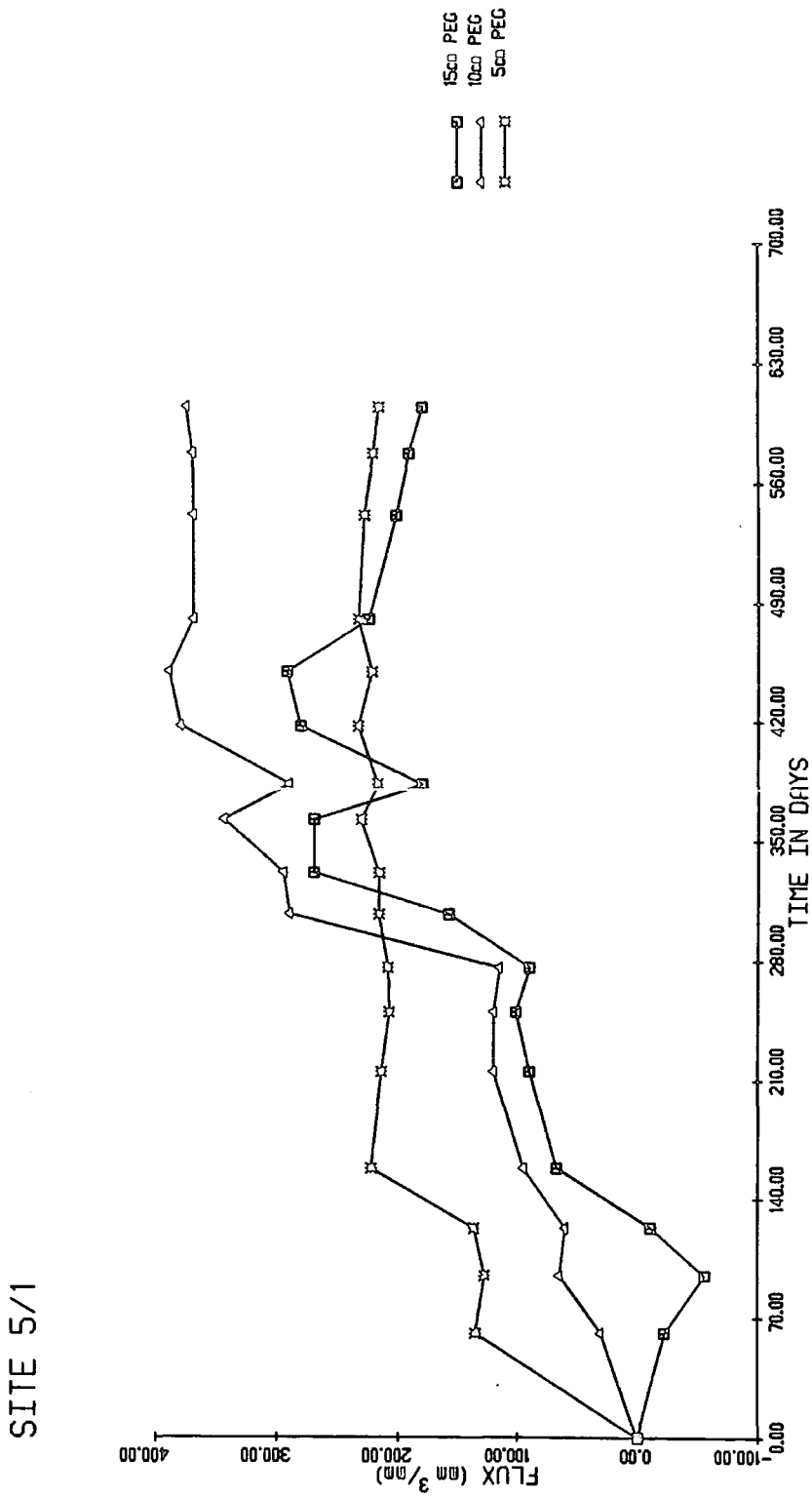
SITE 5/1
15□□ PEG
10□□ PEG
5□□ PEG
FLUX (mm 3/mm)
400.00
300.00
200.00
100.00
0.00
-100.00
0.00
70.00
140.00
210.00
280.00
350.00
420.00
490.00
560.00
630.00
700.00
TIME IN DAYS

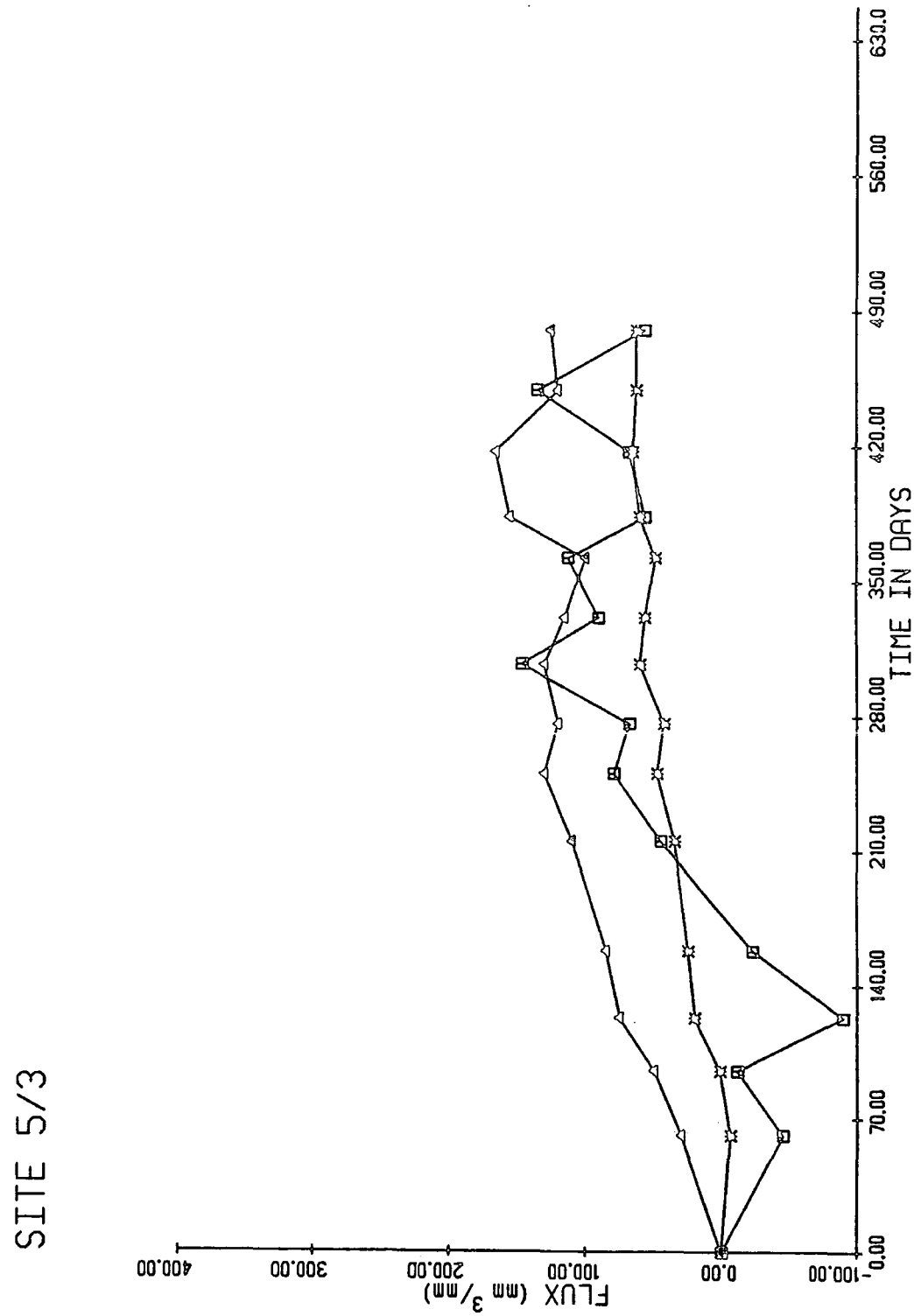
SITE 5/3
FLUX (mm 3/mm)
-100.00
0.00
100.00
200.00
300.00
400.00
0.00
70.00
140.00
210.00
280.00
350.00
420.00
490.00
560.00
630.0
TIME IN DAYS

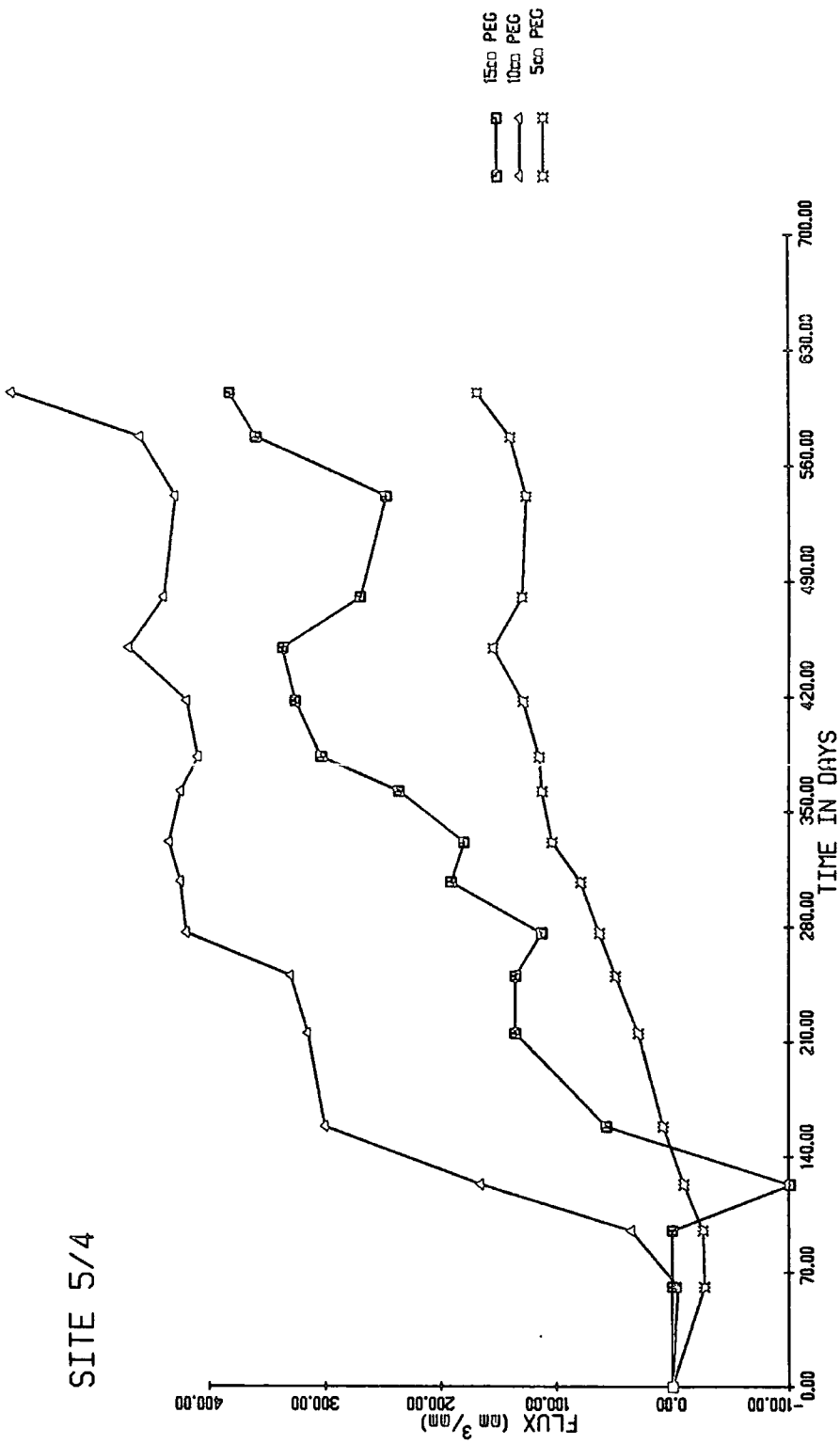
SITE 5/4
15cm PEG
10cm PEG
5cm PEG
FLUX (cm 3/cm)
400.00
300.00
200.00
100.00
0.00
-100.00
0.00
70.00
140.00
210.00
280.00
350.00
420.00
490.00
560.00
630.00
700.00
TIME IN DAYS

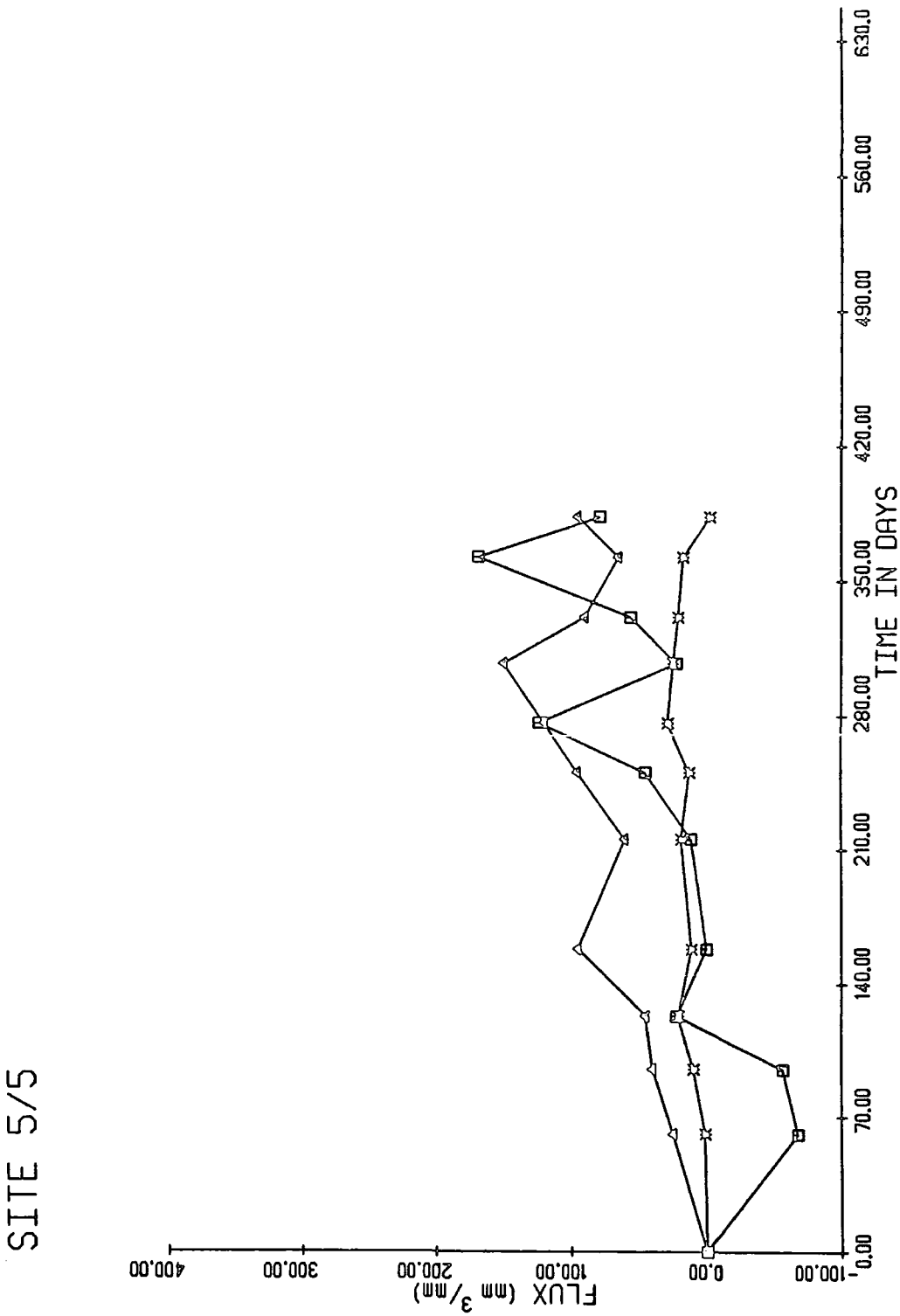
SITE 5/5
FLUX (mm 3/mm)
-100.00
0.00
100.00
200.00
300.00
400.00
0.00
70.00
140.00
210.00
280.00
350.00
420.00
490.00
560.00
630.0
TIME IN DAYS

SITE 5/7

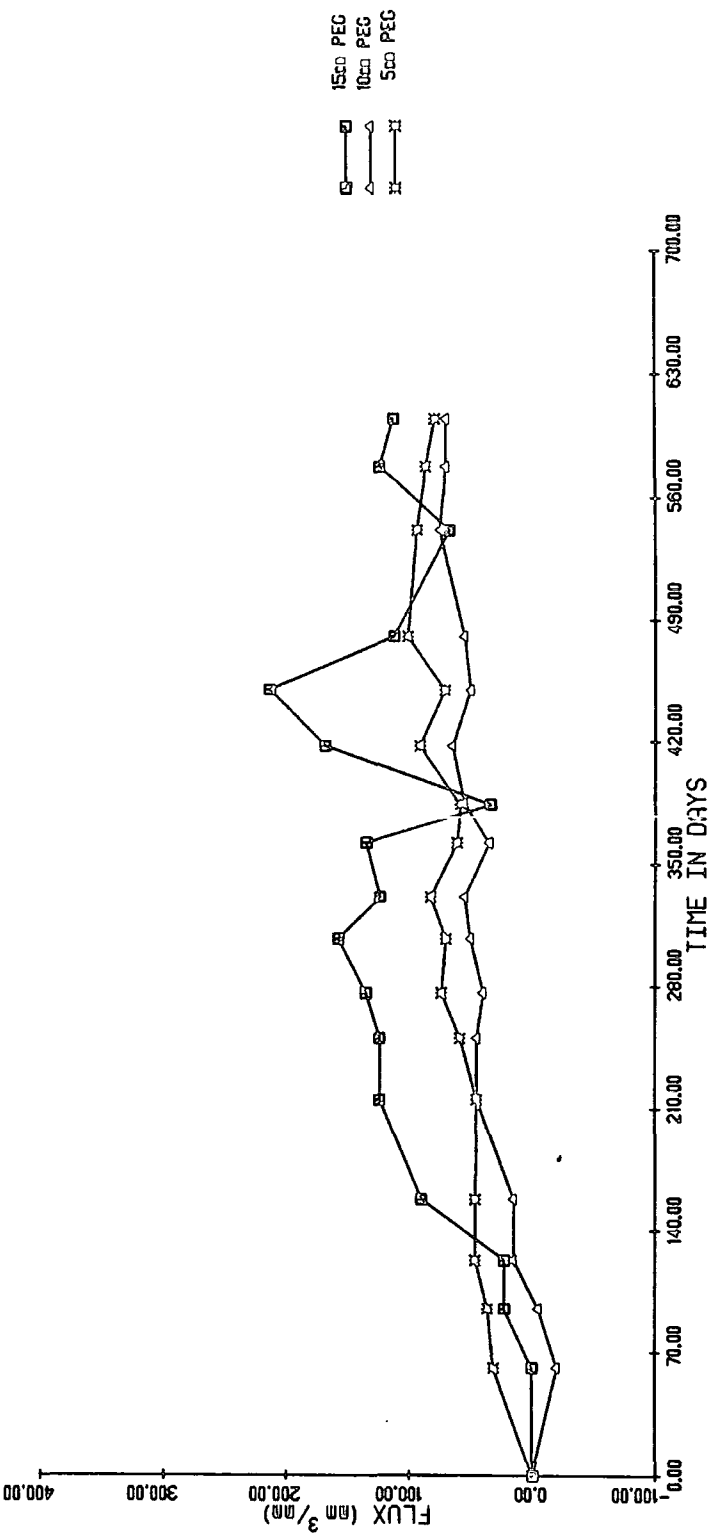
15cm PEG
10cm PEG
5cm PEG
FLUX (mm 3/mm)
-100.00
0.00
100.00
200.00
300.00
400.00
0.00
70.00
140.00
210.00
280.00
350.00
420.00
490.00
560.00
630.00
700.00
TIME IN DAYS

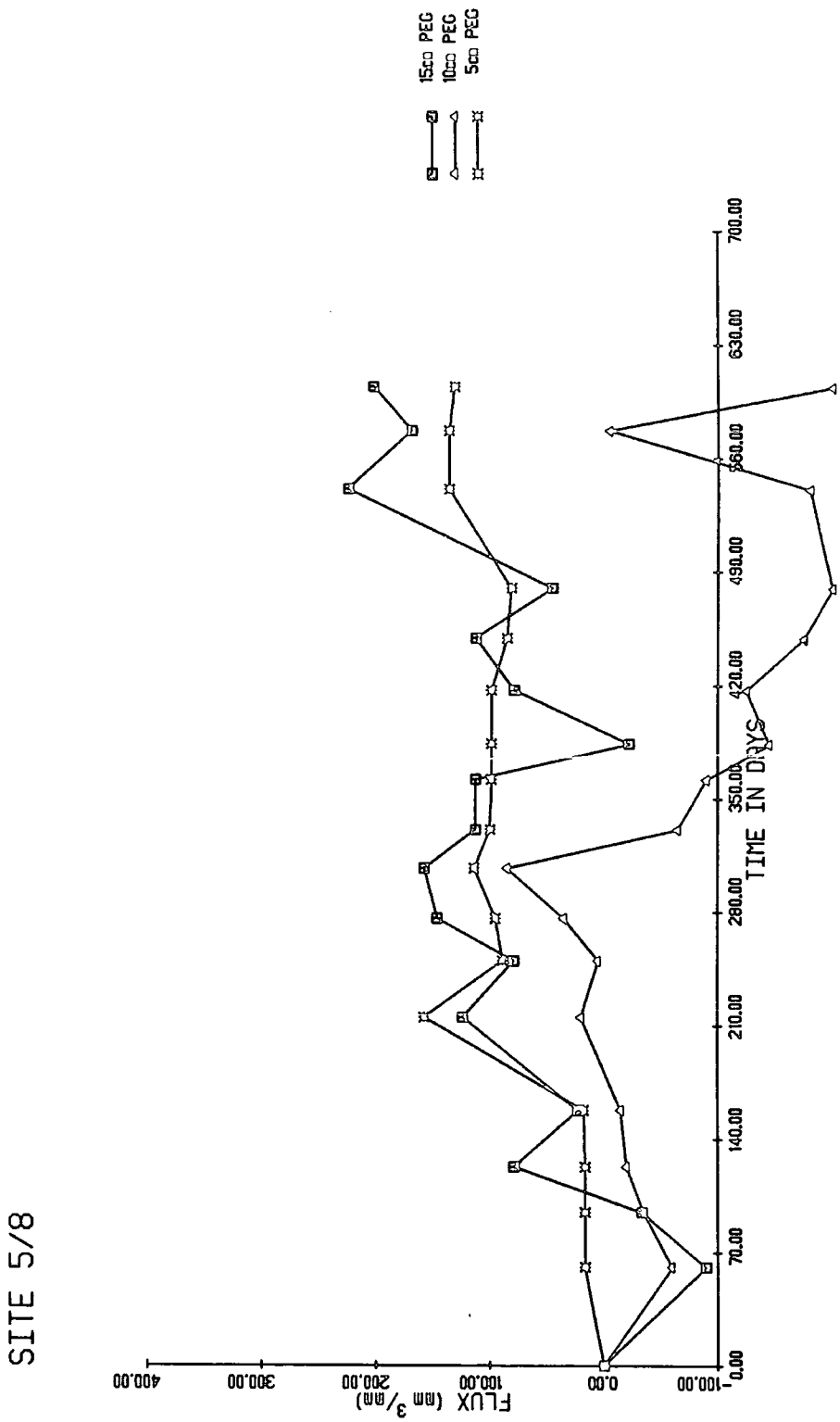
SITE 5/8
15cm PEG
10cm PEG
5cm PEG
FLUX (mm 3/mm)
400.00
300.00
200.00
100.00
0.00
-100.00
0.00
70.00
140.00
210.00
280.00
350.00
420.00
490.00
560.00
630.00
700.00
TIME IN DAYS

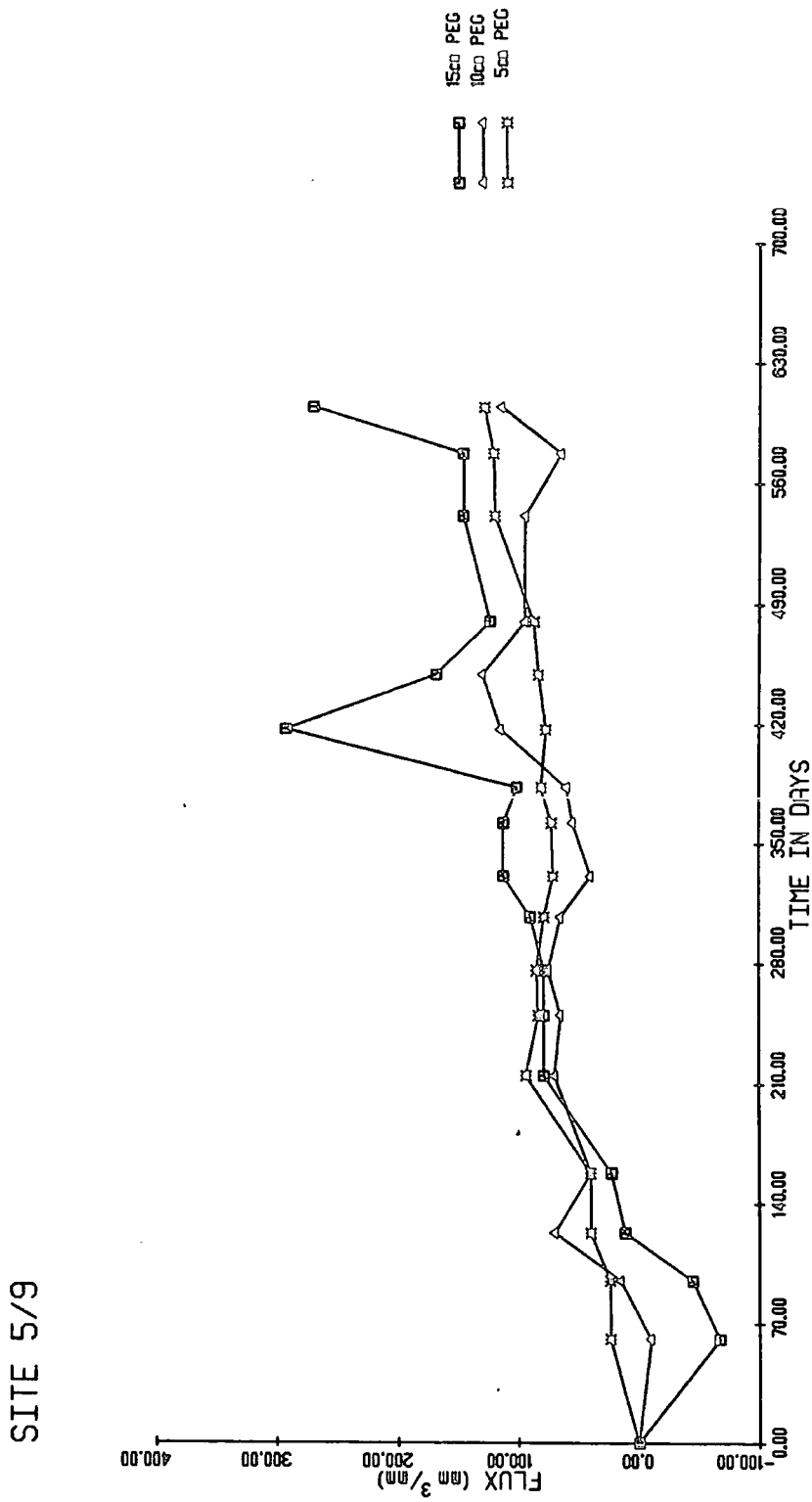
SITE 5/9
15cm PEG
10cm PEG
5cm PEG
FLUX (mm 3/mm)
-100.00
0.00
100.00
200.00
300.00
400.00
0.00
70.00
140.00
210.00
280.00
350.00
420.00
490.00
560.00
630.00
700.00
TIME IN DAYS

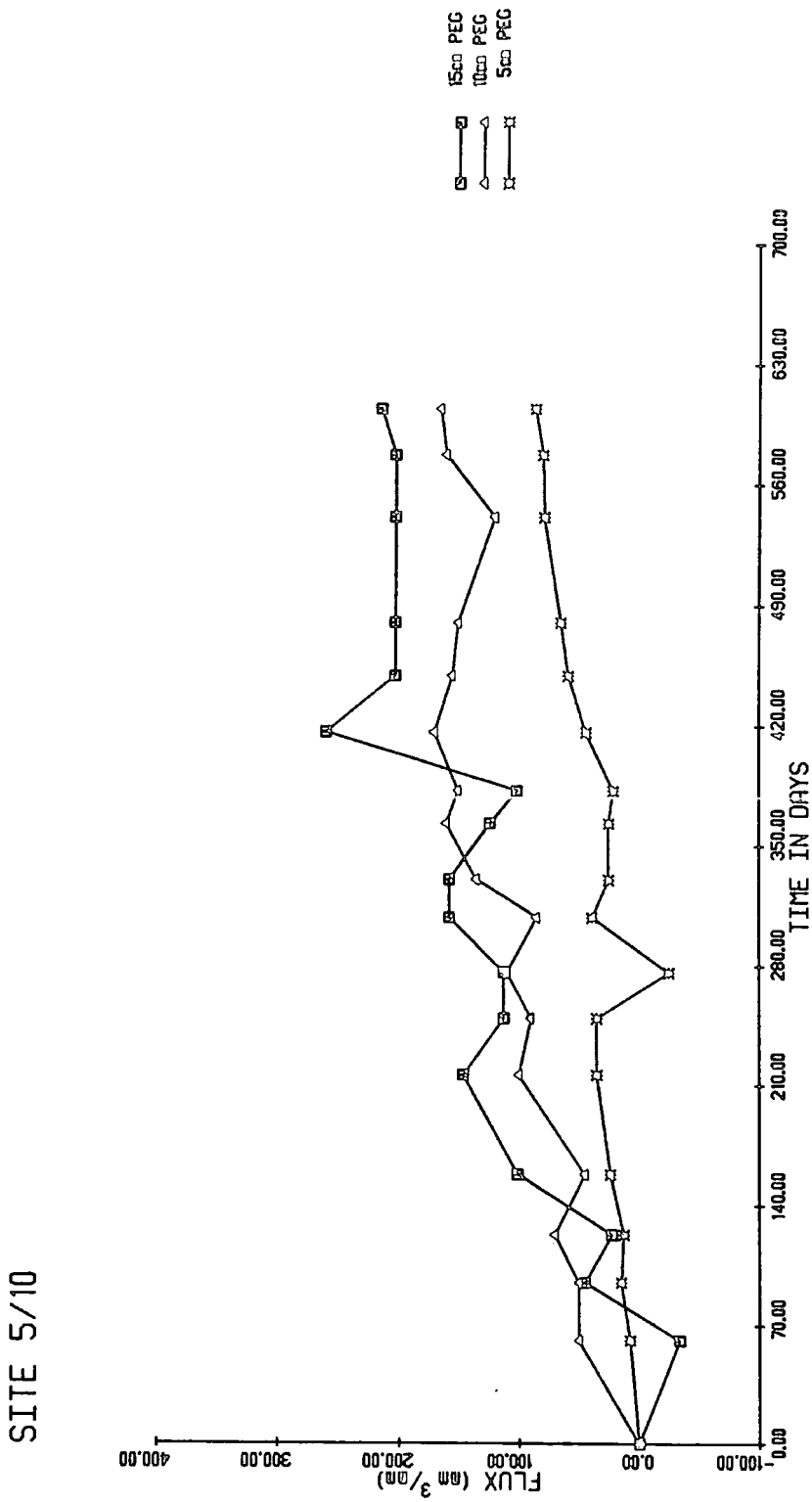
SITE 5/10
15□□ PEG
10□□ PEG
5□□ PEG
FLUX (mm 3/mm)
400.00
300.00
200.00
100.00
0.00
-100.00
0.00
70.00
140.00
210.00
280.00
350.00
420.00
490.00
560.00
630.00
700.00
TIME IN DAYS

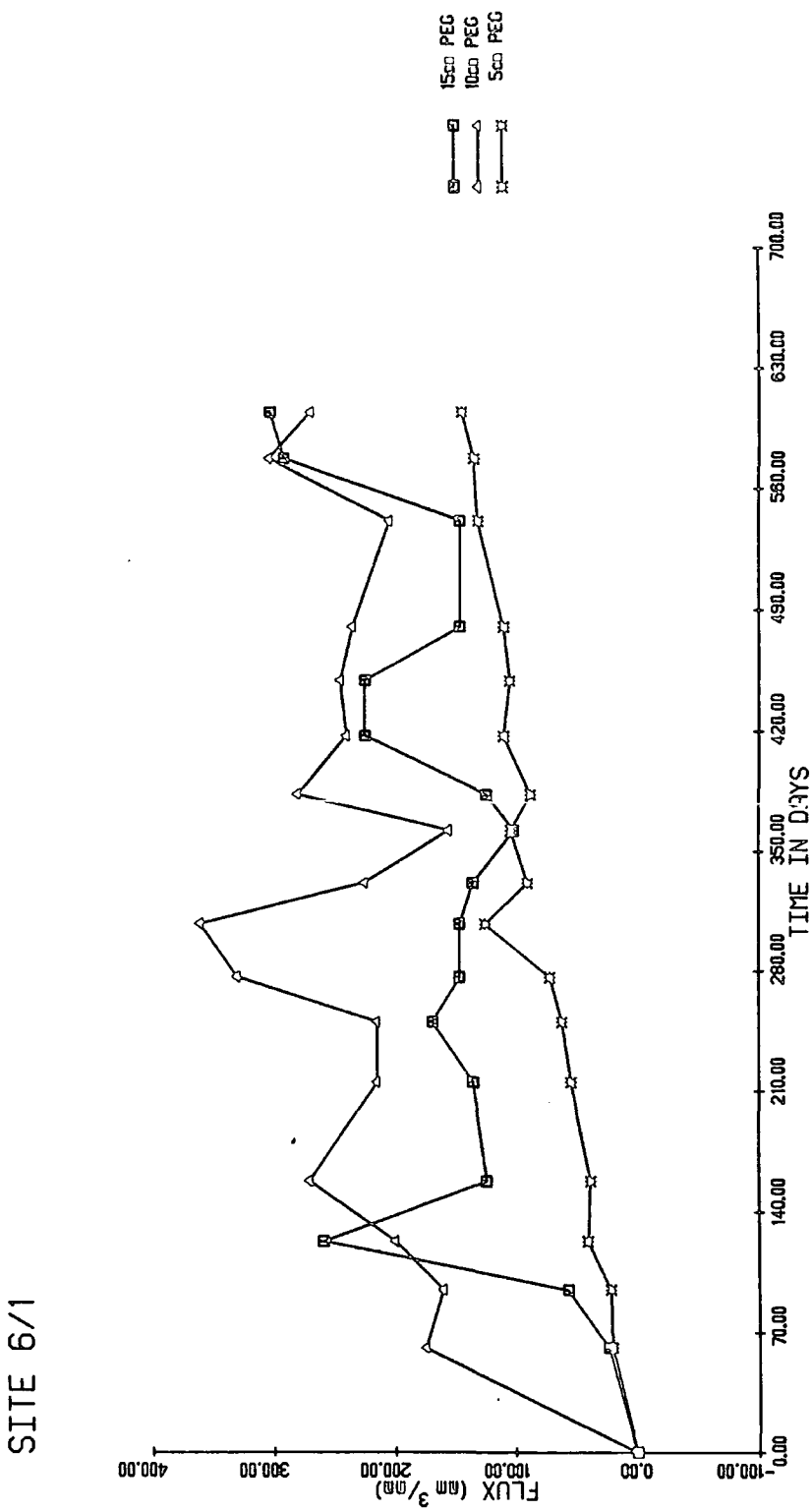
SITE 6/1
15cm PEG
10cm PEG
5cm PEG
FLUX (mm 3/mm)
400.00
300.00
200.00
100.00
0.00
-100.00
0.00
70.00
140.00
210.00
280.00
350.00
420.00
490.00
560.00
630.00
700.00
TIME IN DAYS

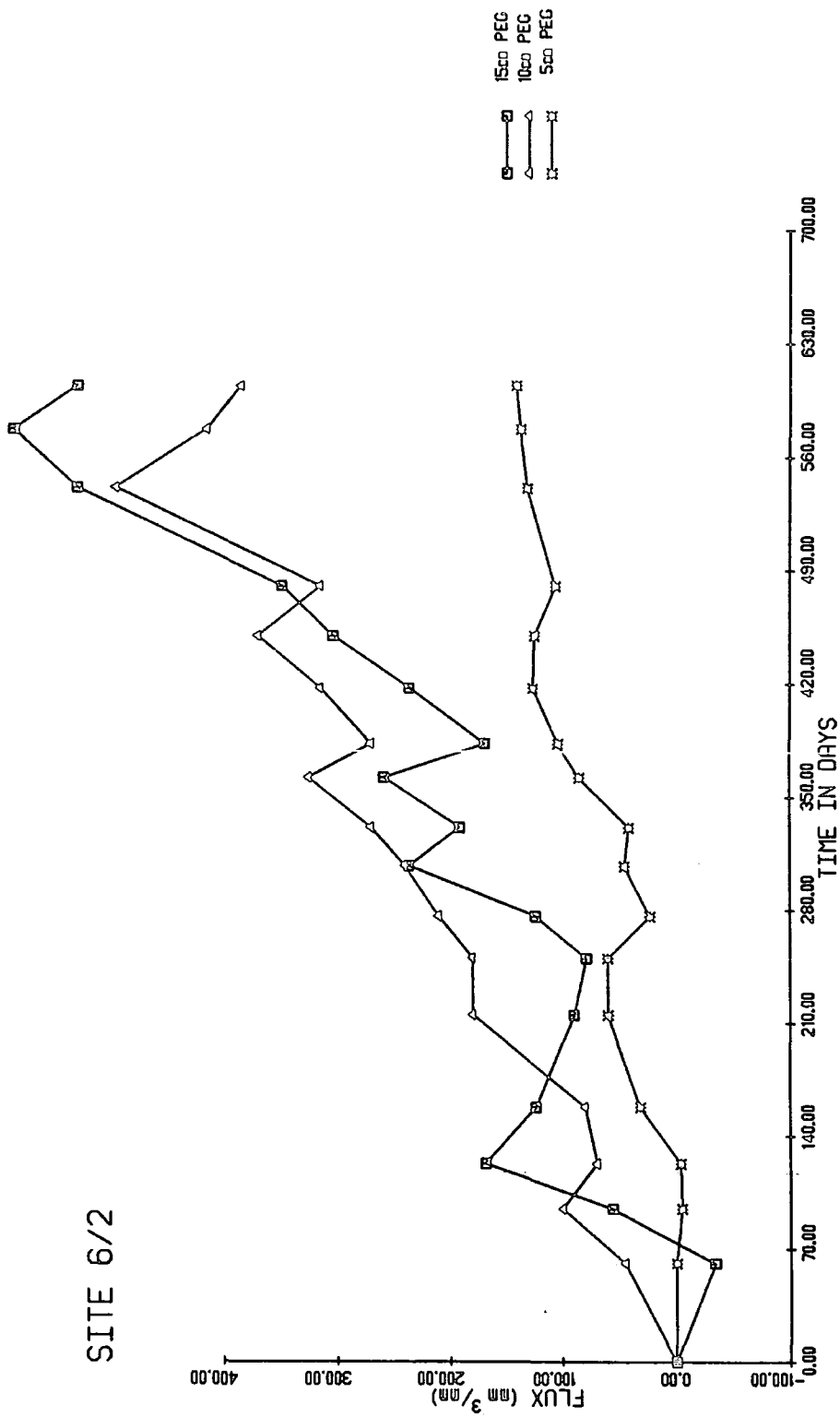
SITE 6/2
15cm PEG
10cm PEG
5cm PEG
FLUX (mm 3/mm)
-100.00
0.00
100.00
200.00
300.00
400.00
TIME IN DAYS
0.00
70.00
140.00
210.00
280.00
350.00
420.00
490.00
560.00
630.00
700.00

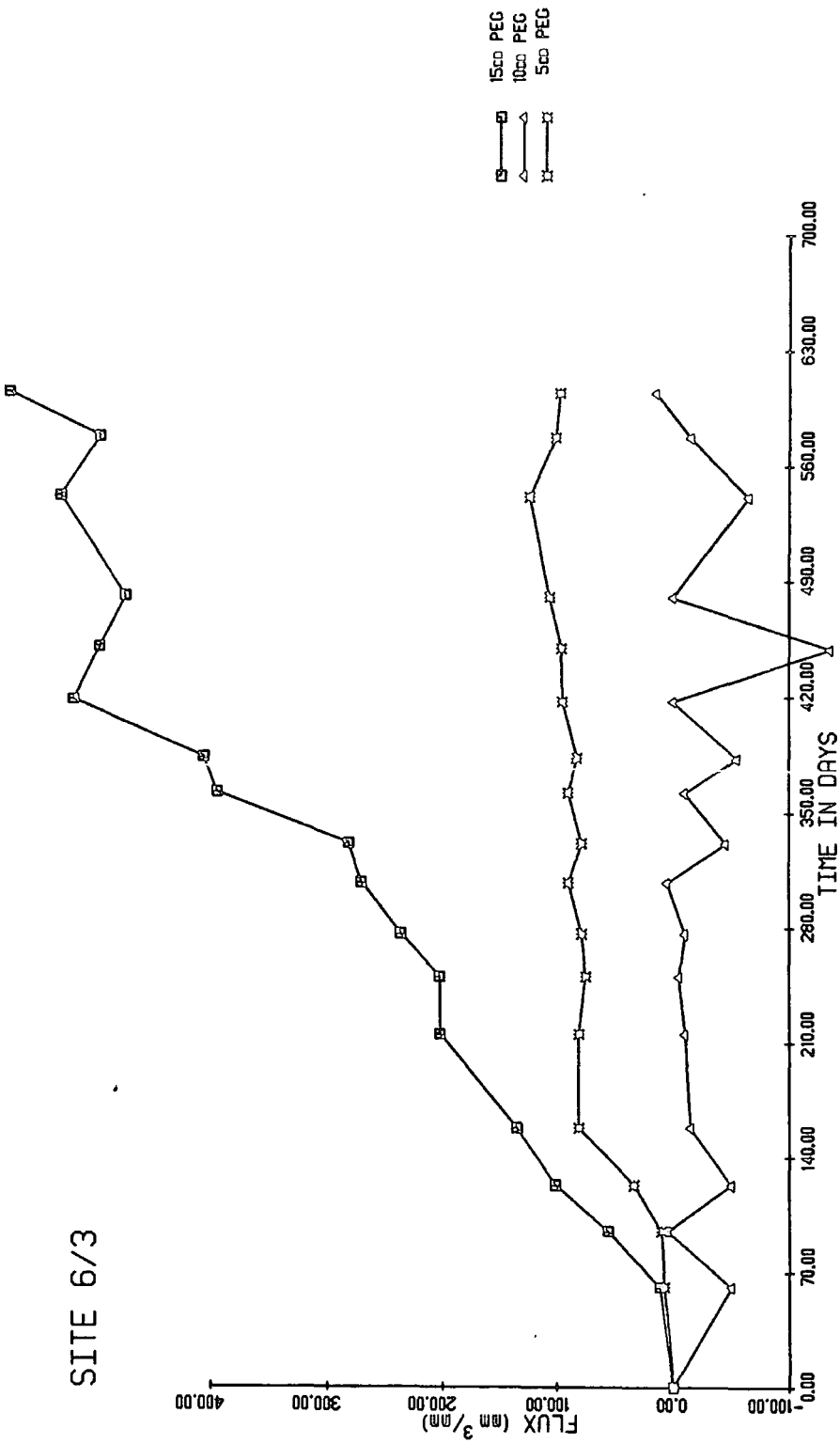
SITE 6/3
15cm PEG
10cm PEG
5cm PEG
FLUX (mm 3/mm)
-100.00
0.00
100.00
200.00
300.00
400.00
0.00
70.00
140.00
210.00
280.00
350.00
420.00
490.00
560.00
630.00
700.00
TIME IN DAYS

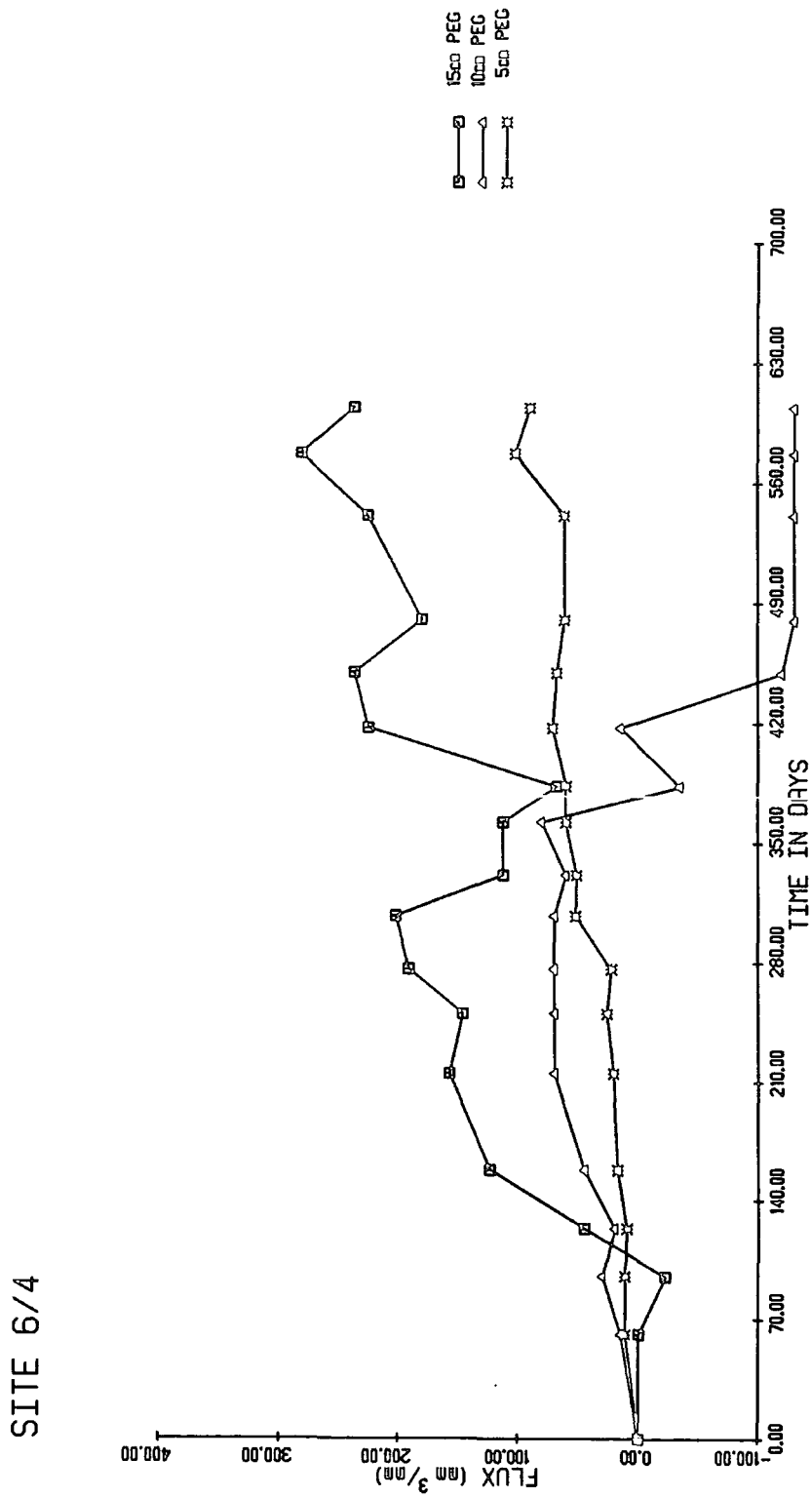
SITE 6/4
15cm PEG
10cm PEG
5cm PEG
FLUX (mm 3/mm)
400.00
300.00
200.00
100.00
0.00
-100.00
0.00
70.00
140.00
210.00
280.00
350.00
420.00
490.00
560.00
630.00
700.00
TIME IN DAYS

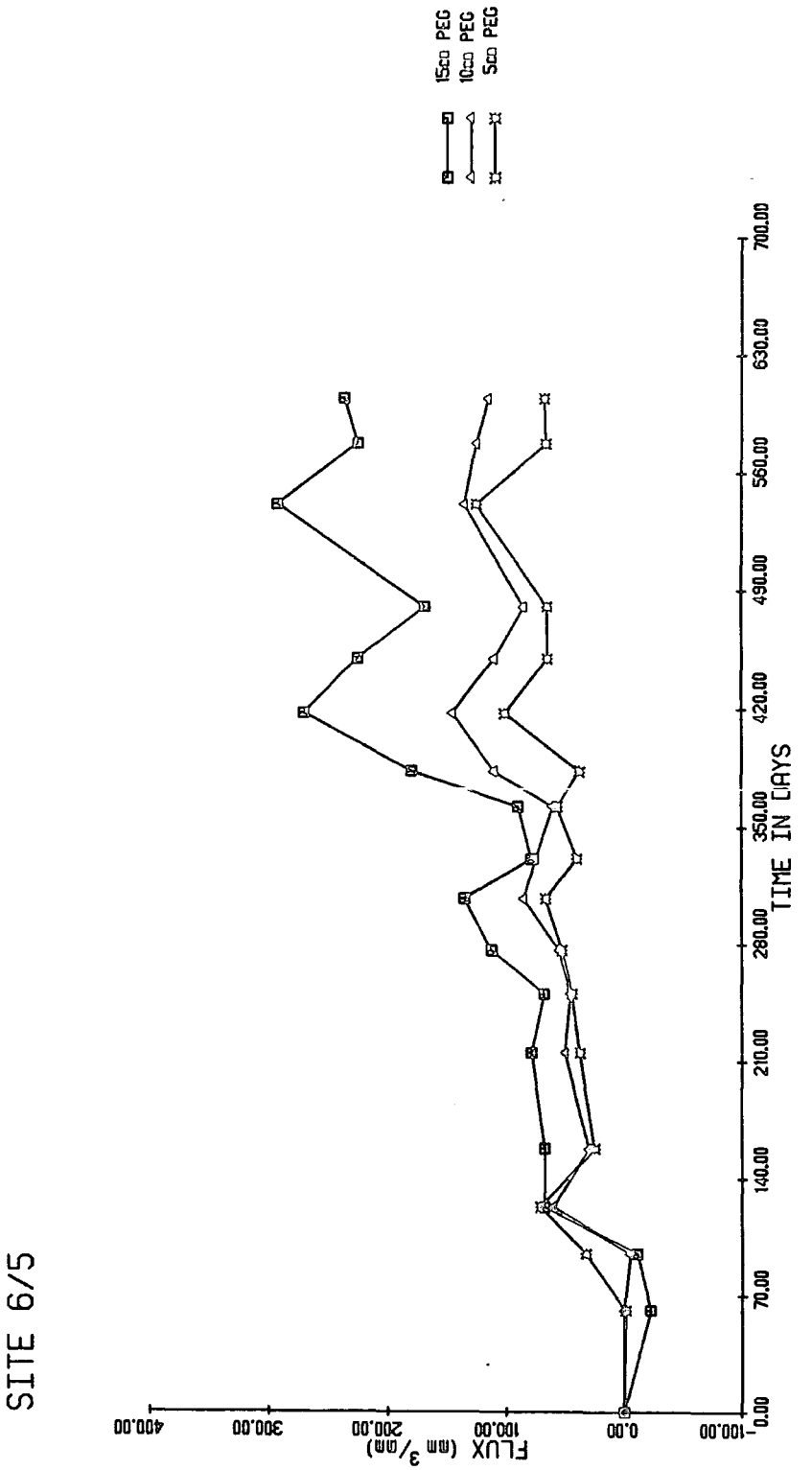
SITE 6/5
15□□ PEG
10□□ PEG
5□□ PEG
FLUX (mm 3/mm)
-100.00
0.00
100.00
200.00
300.00
400.00
0.00
70.00
140.00
210.00
280.00
350.00
420.00
490.00
560.00
630.00
700.00
TIME IN DAYS

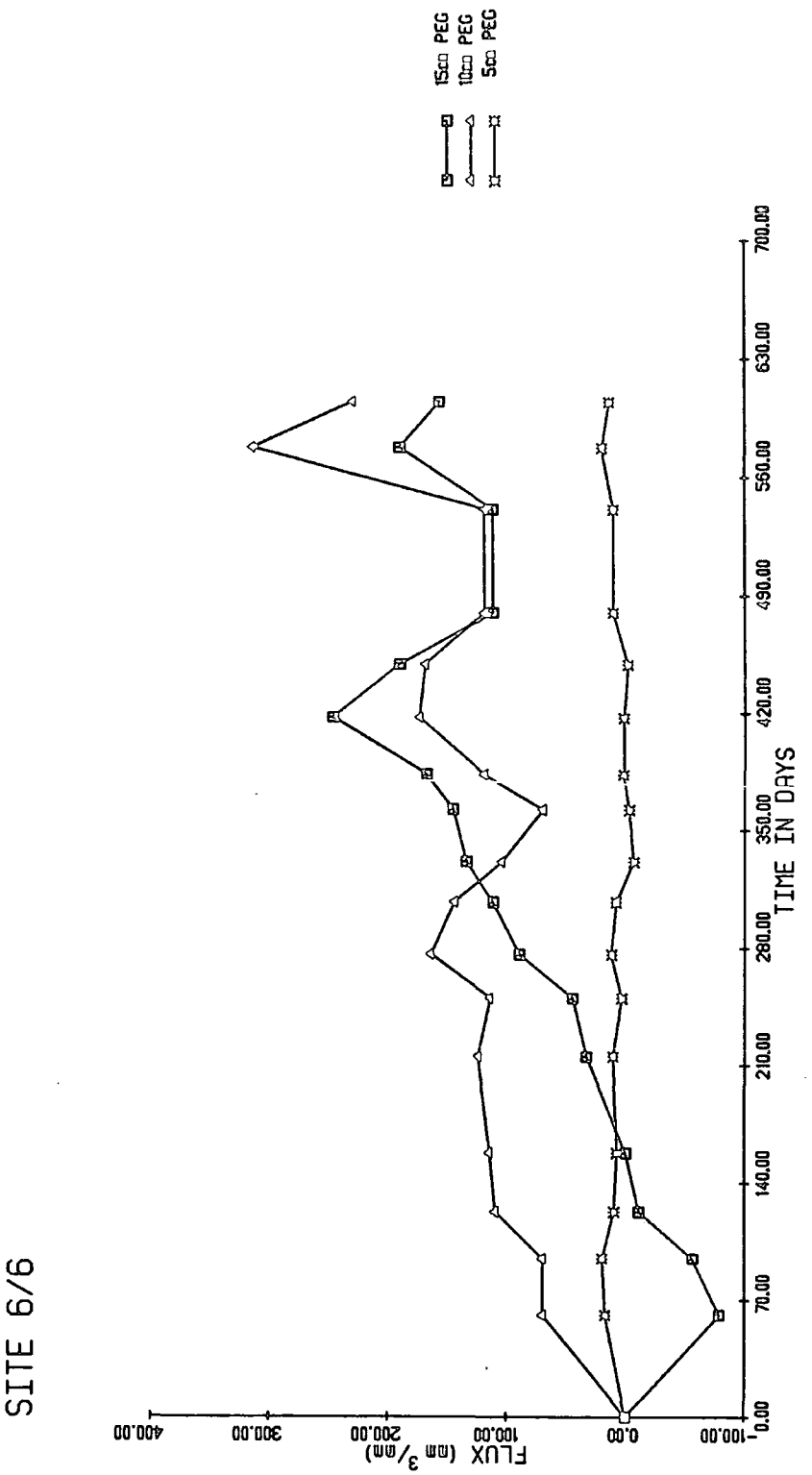
SITE 6/6
15□□ PEG
10□□ PEG
5□□ PEG
FLUX (mm 3/mm)
400.00
300.00
200.00
100.00
0.00
-100.00
0.00
70.00
140.00
210.00
280.00
350.00
420.00
490.00
560.00
630.00
700.00
TIME IN DAYS

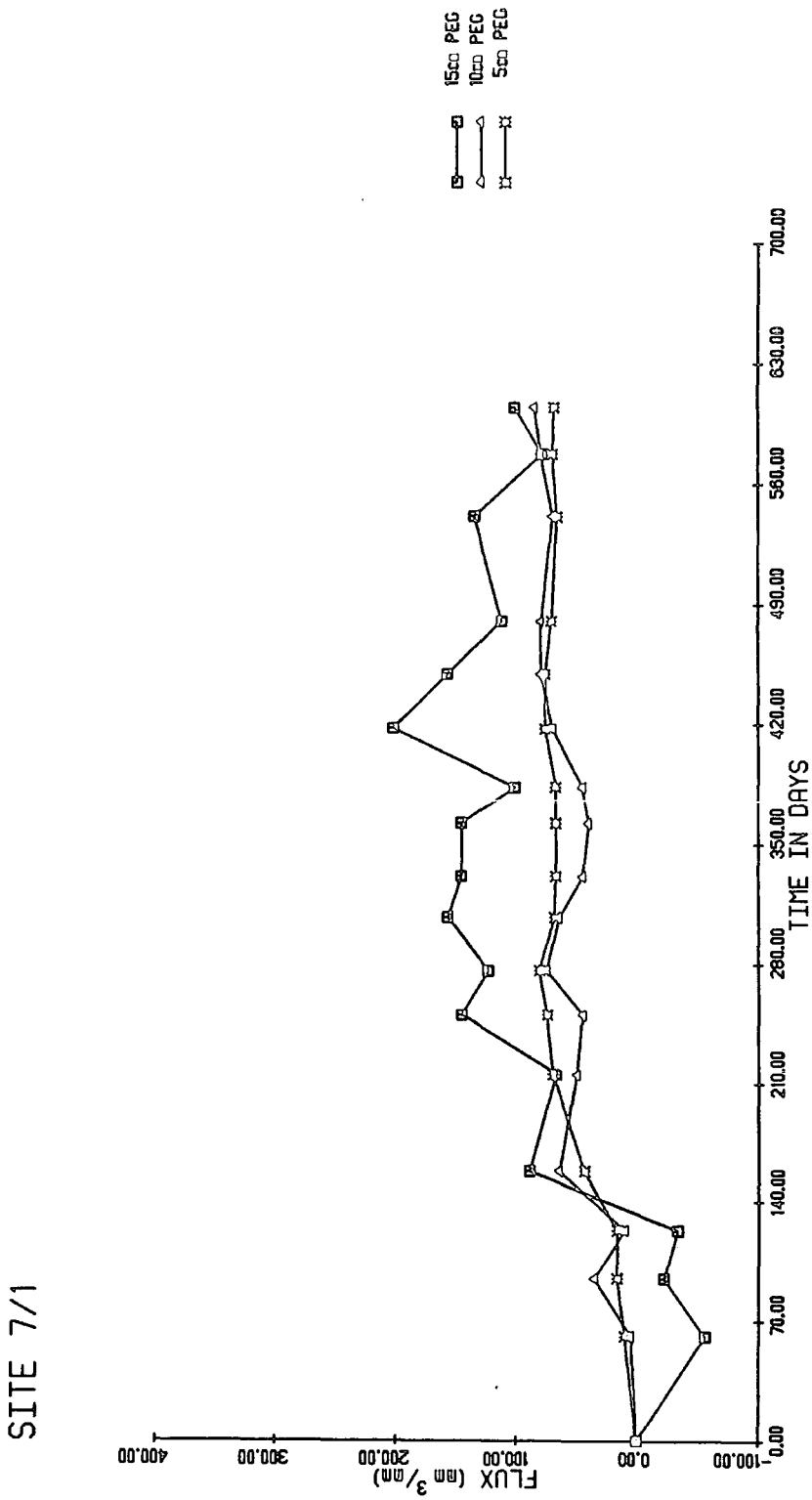
SITE 7/1
15□□ PEG
10□□ PEG
5□□ PEG
FLUX (m 3/m)
400.00
300.00
200.00
100.00
0.00
-100.00
0.00
70.00
140.00
210.00
280.00
350.00
420.00
490.00
560.00
630.00
700.00
TIME IN DAYS

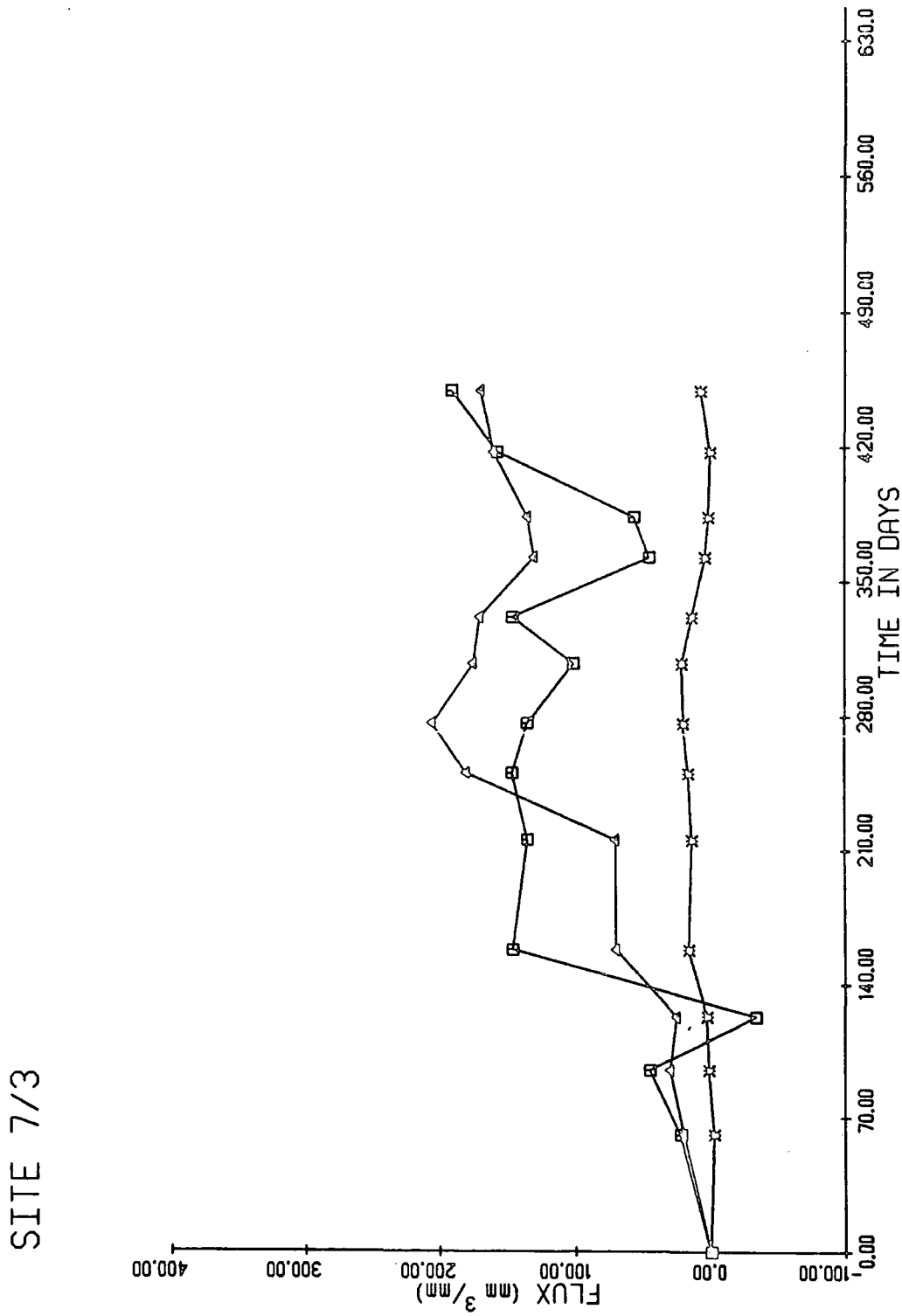
SITE 7/3
FLUX (mm 3/mm)
-100.00
0.00
100.00
200.00
300.00
400.00
0.00
70.00
140.00
210.00
280.00
350.00
420.00
490.00
560.00
630.0
TIME IN DAYS

SITE 7/4

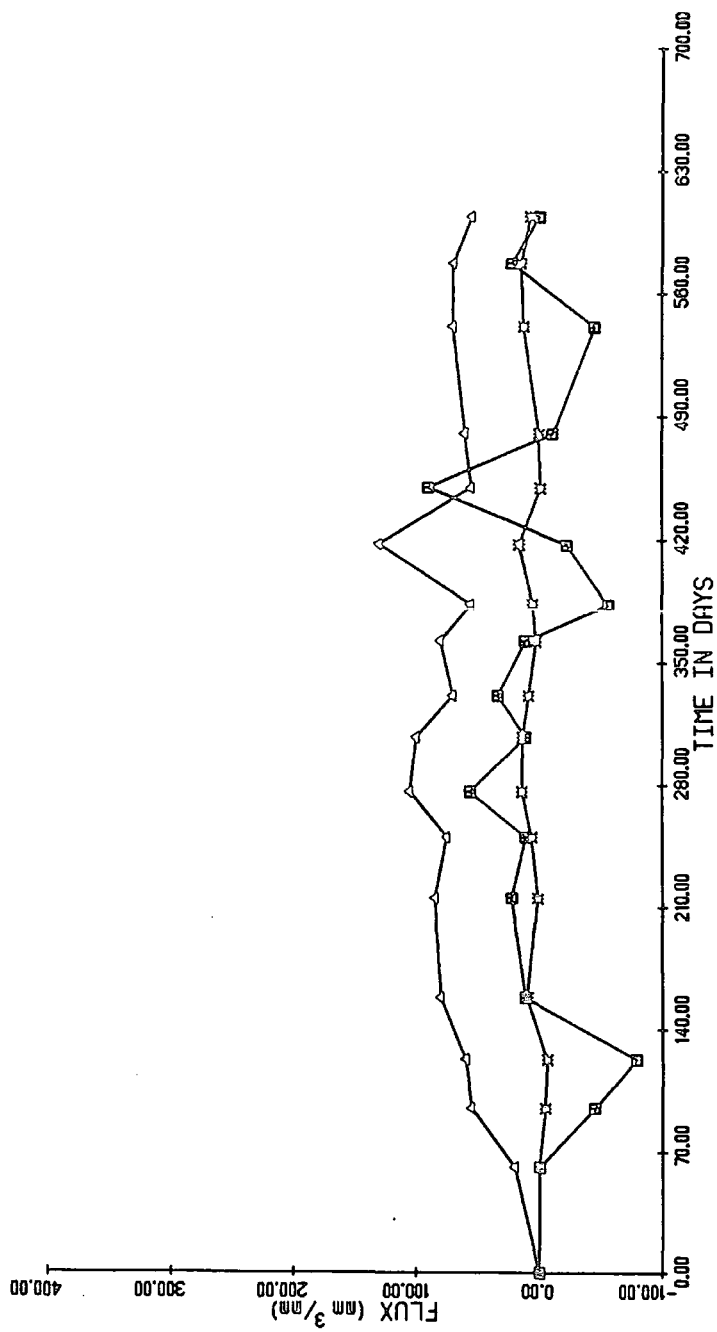
15cm PEG
10cm PEG
5cm PEG
FLUX (mm 3/mm)
-100.00
0.00
100.00
200.00
300.00
400.00
0.00
70.00
140.00
210.00
280.00
350.00
420.00
490.00
560.00
630.00
700.00
TIME IN DAYS

SITE 7/5

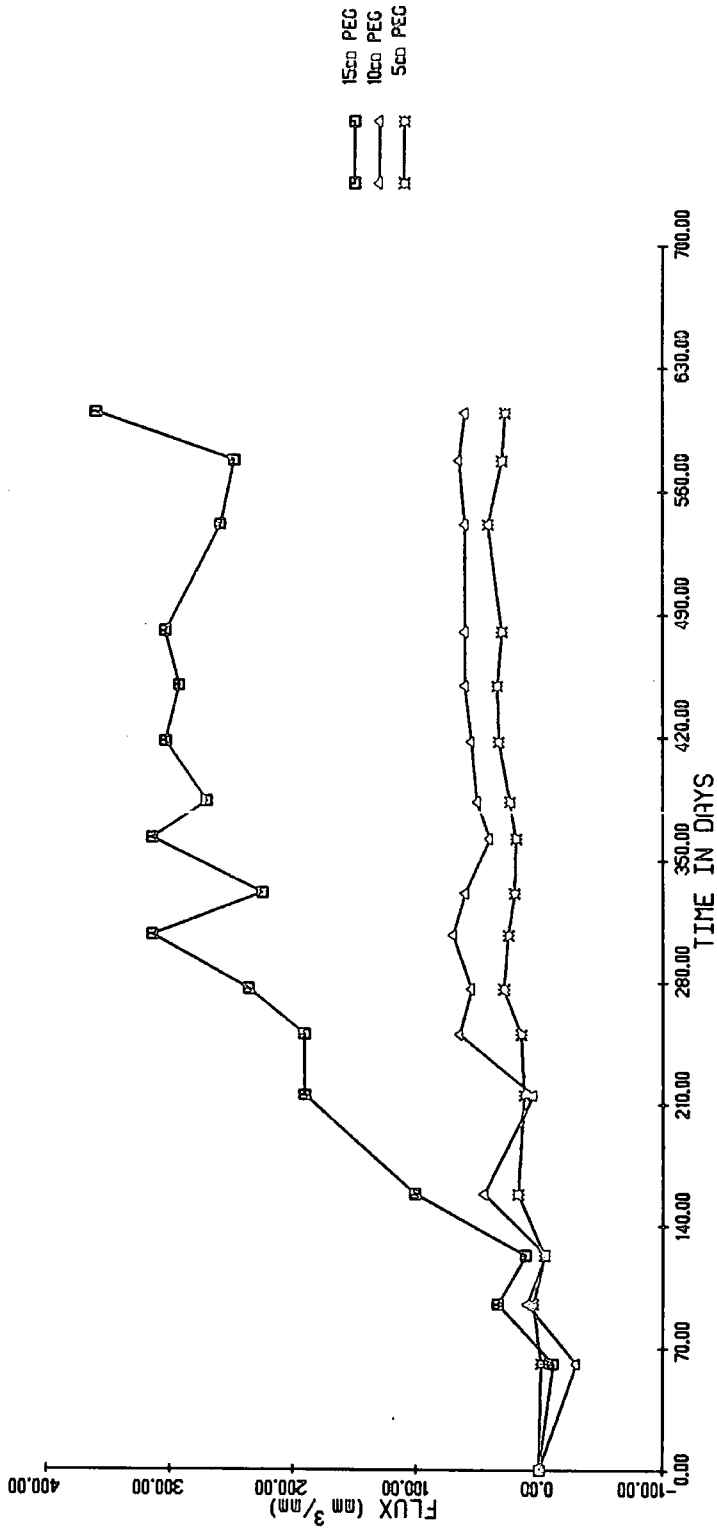
15□□ PEG
10□□ PEG
5□□ PEG
FLUX (mm 3/mm)
400.00
300.00
200.00
100.00
0.00
-100.00
0.00
70.00
140.00
210.00
280.00
350.00
420.00
490.00
560.00
630.00
700.00
TIME IN DAYS

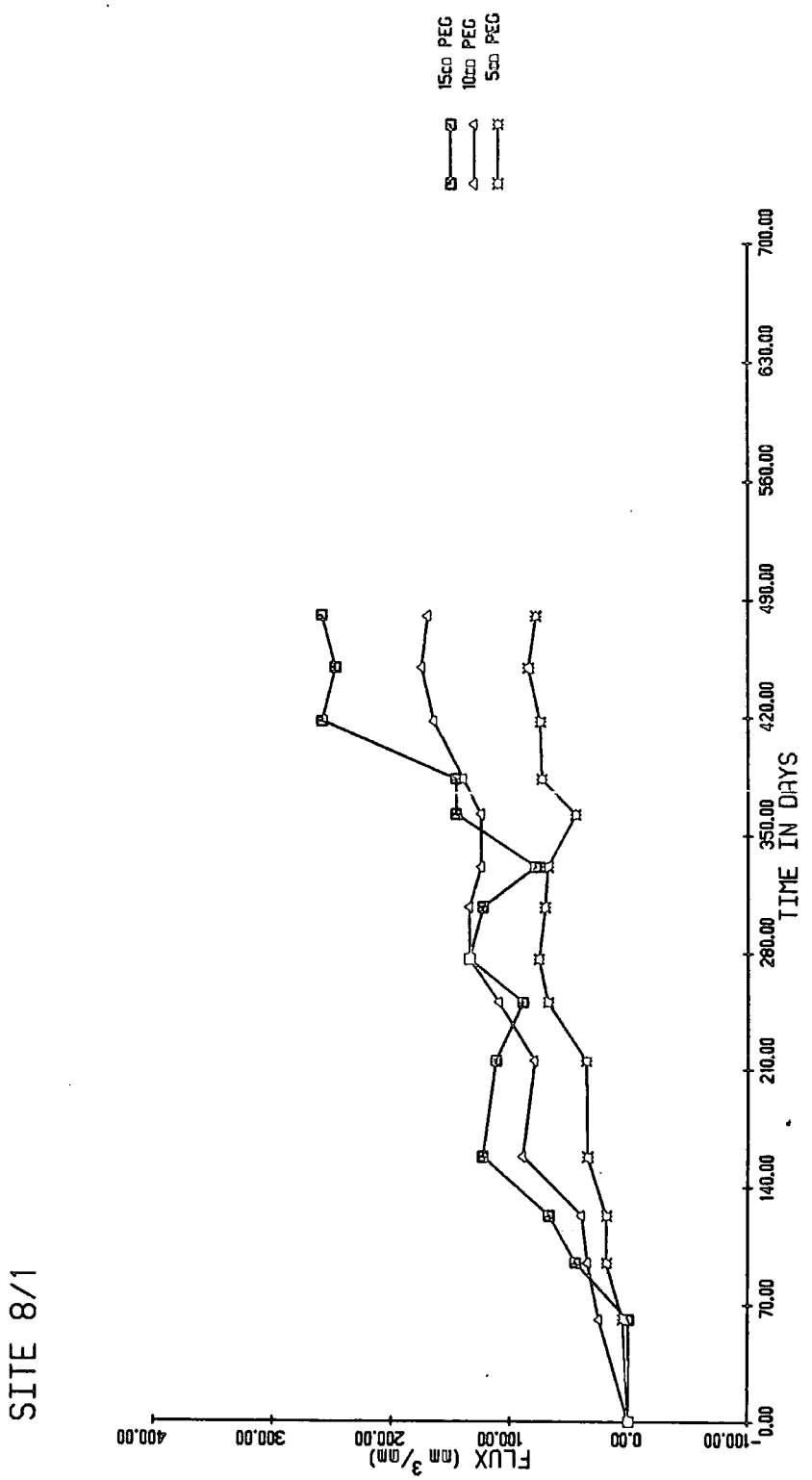
SITE 8/1
15cm PEG
10cm PEG
5cm PEG
FLUX (mm 3/mm)
400.00
300.00
200.00
100.00
0.00
-100.00
0.00
70.00
140.00
210.00
280.00
350.00
420.00
490.00
560.00
630.00
700.00
TIME IN DAYS

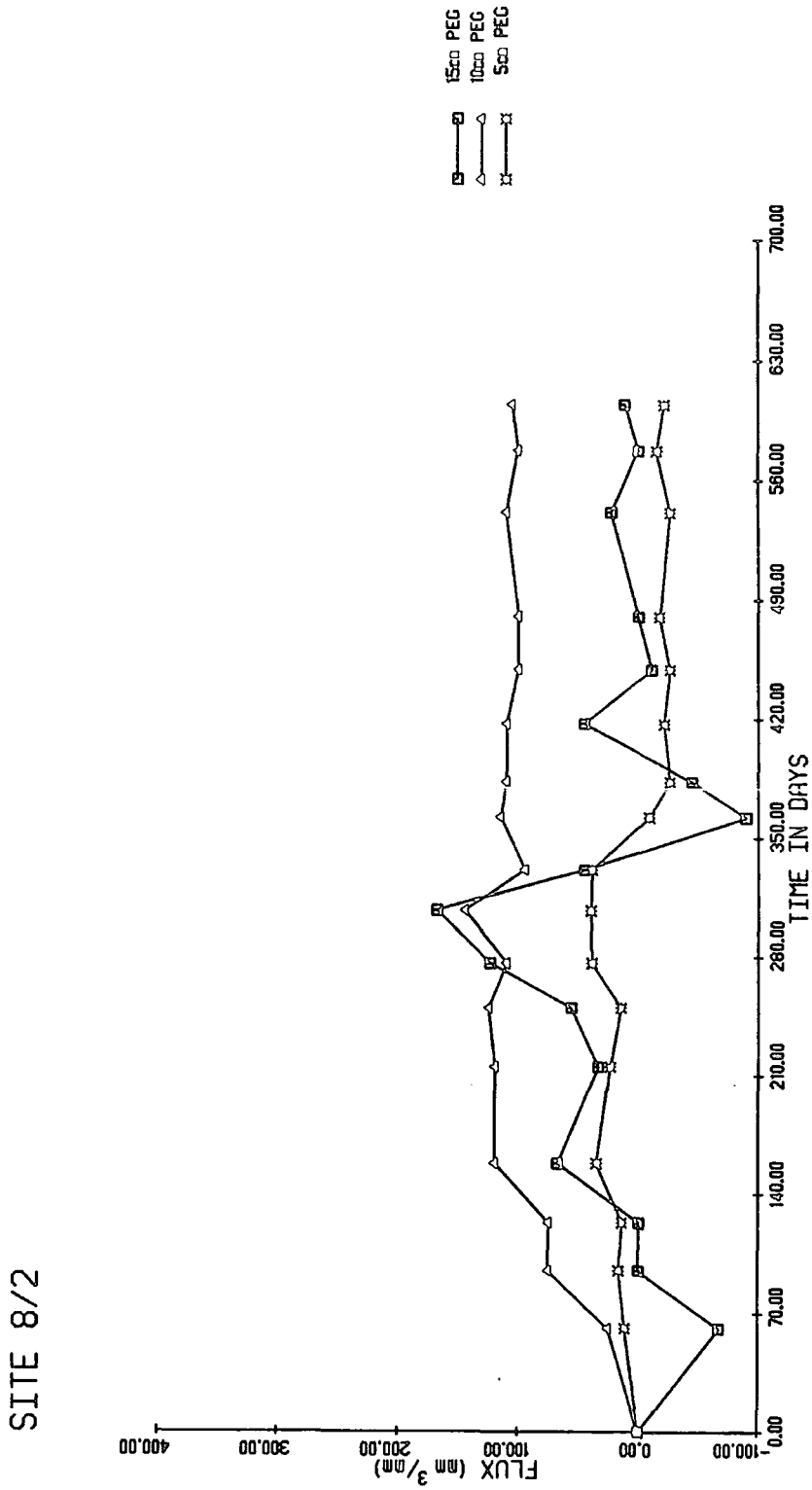
SITE 8/2
15□ PEG
10□ PEG
5□ PEG
FLUX (mm 3/mm)
400.00
300.00
200.00
100.00
0.00
-100.00
0.00
70.00
140.00
210.00
280.00
350.00
420.00
490.00
560.00
630.00
700.00
TIME IN DAYS

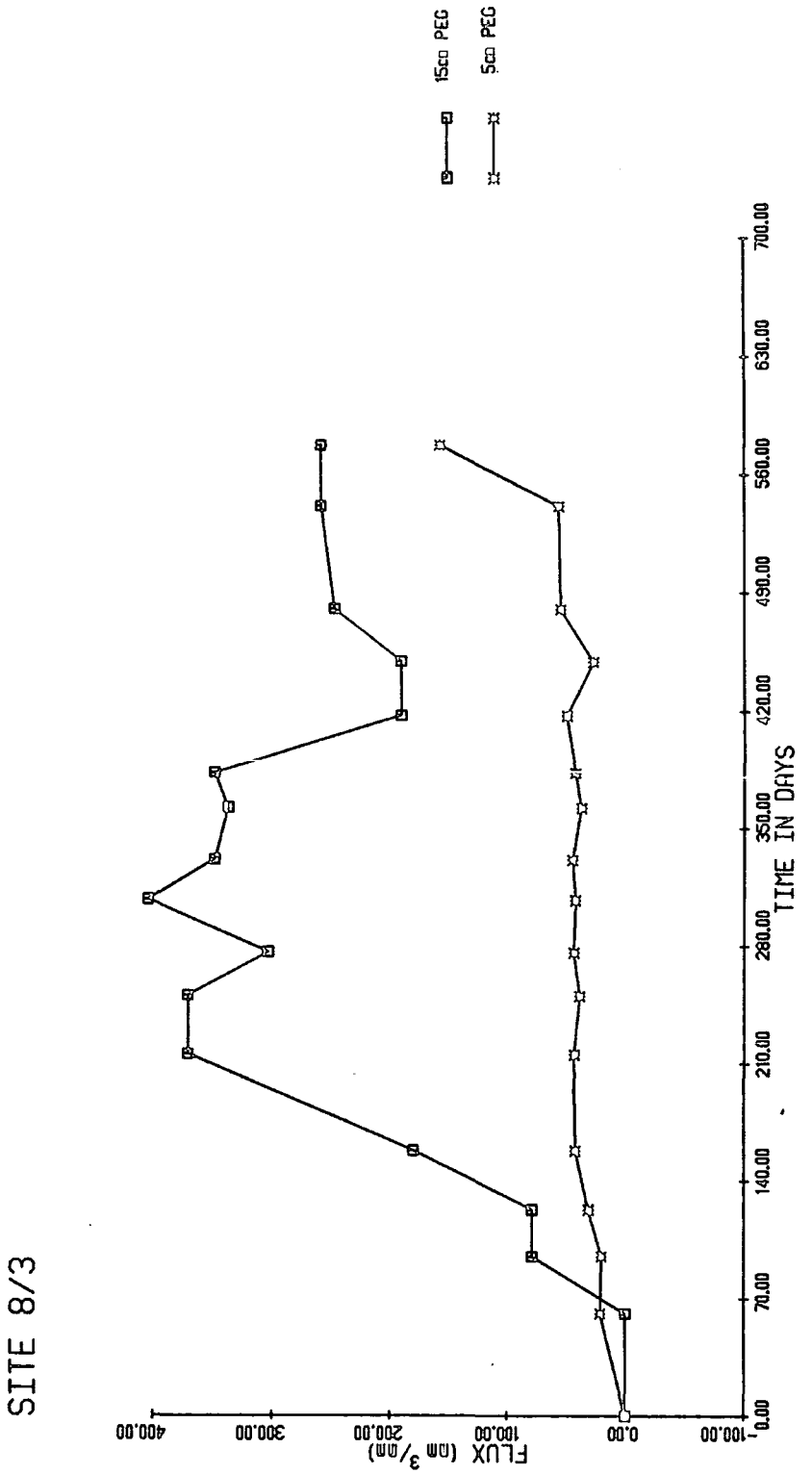
SITE 8/3
15cm PEG
5cm PEG
FLUX (nm 3/nm)
400.00
300.00
200.00
100.00
0.00
-100.00
0.00
70.00
140.00
210.00
280.00
350.00
420.00
490.00
560.00
630.00
700.00
TIME IN DAYS

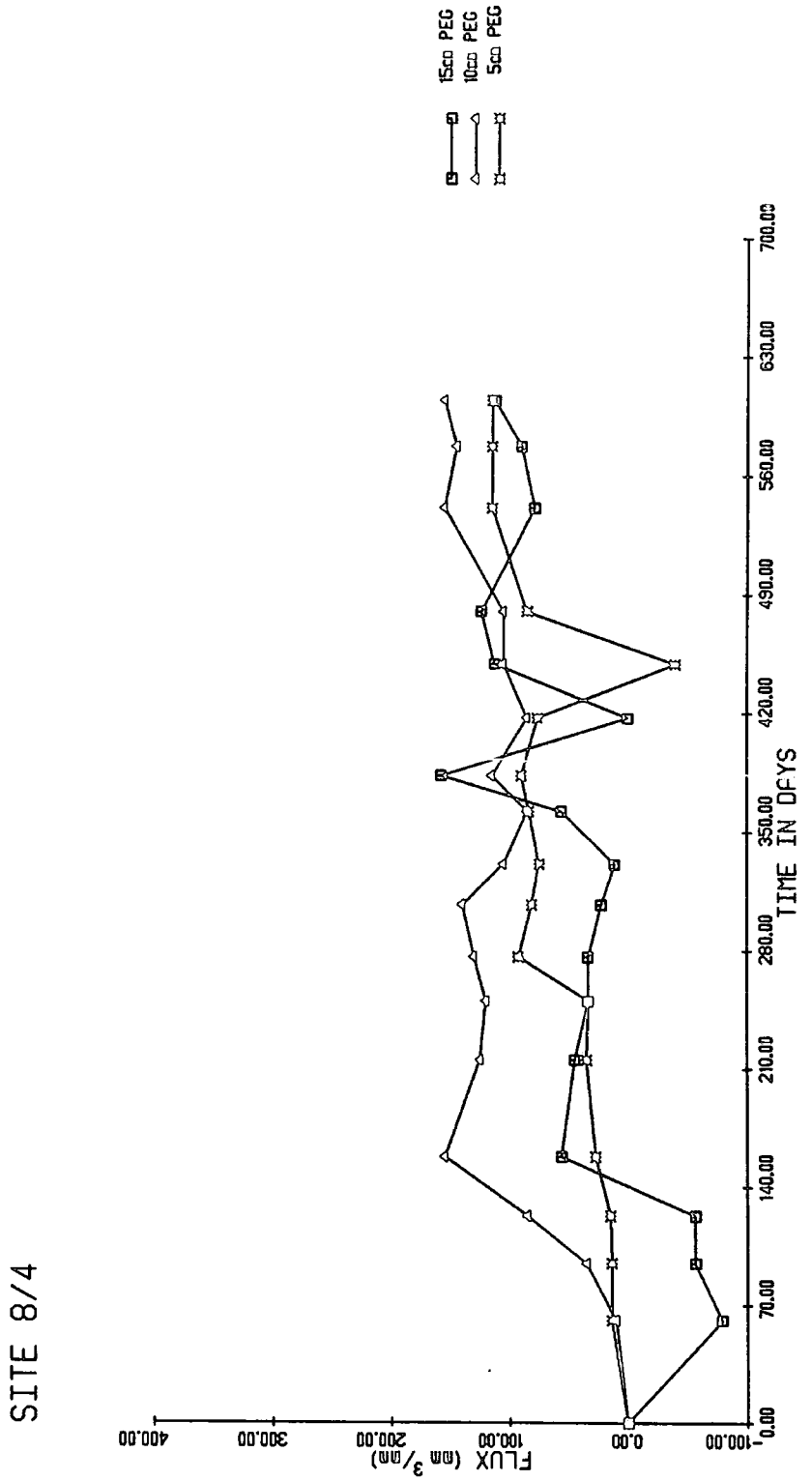
SITE 8/4
15□□ PEG
10□□ PEG
5□□ PEG
FLUX (□□ 3/□□)
400.00
300.00
200.00
100.00
0.00
-100.00
0.00
70.00
140.00
210.00
280.00
350.00
420.00
490.00
560.00
630.00
700.00
TIME IN DAYS

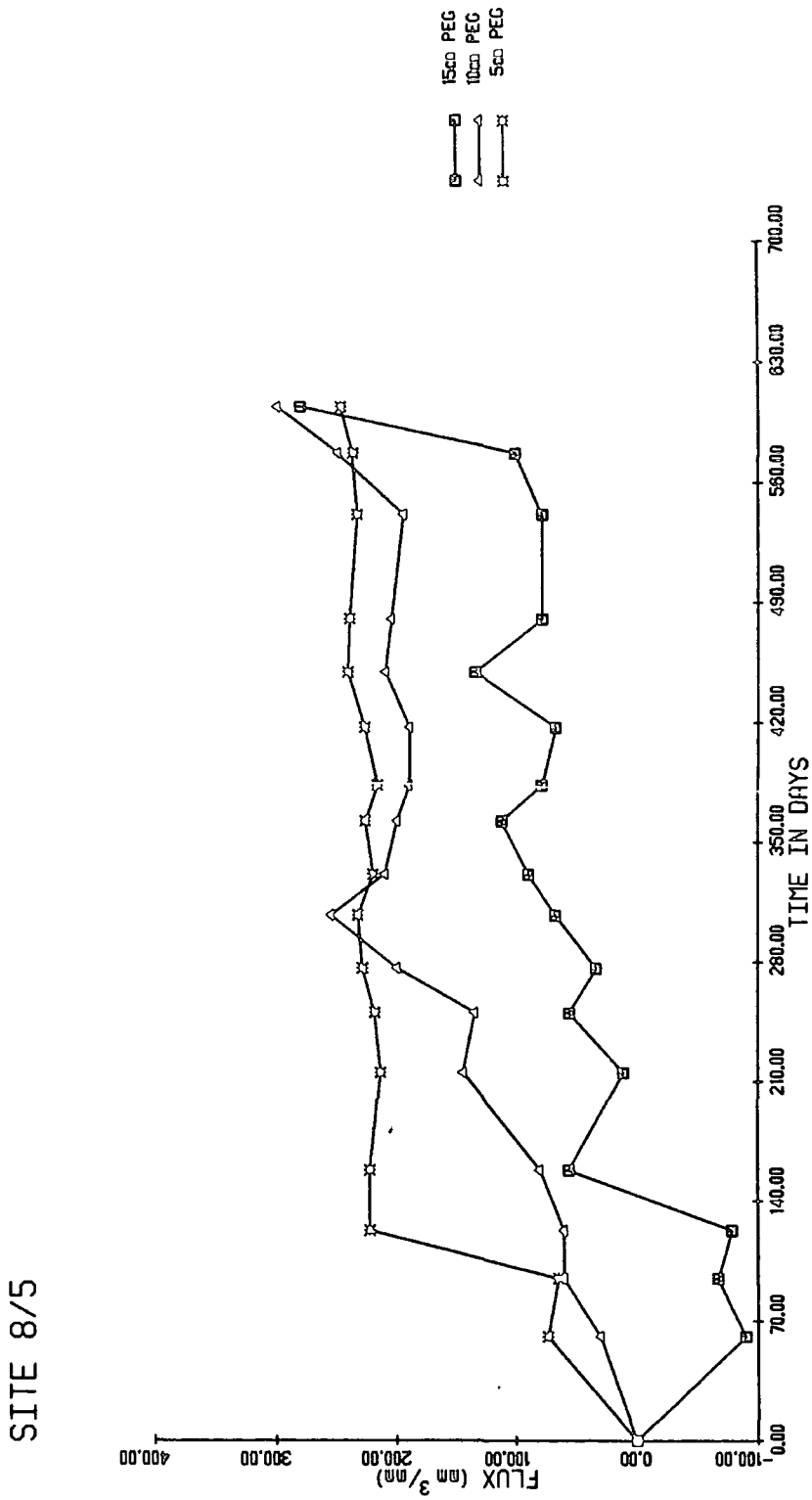
SITE 8/5
15□ PEG
10□ PEG
5□ PEG
FLUX (mm 3/mm)
-100.00
0.00
100.00
200.00
300.00
400.00
0.00
70.00
140.00
210.00
280.00
350.00
420.00
490.00
560.00
630.00
700.00
TIME IN DAYS

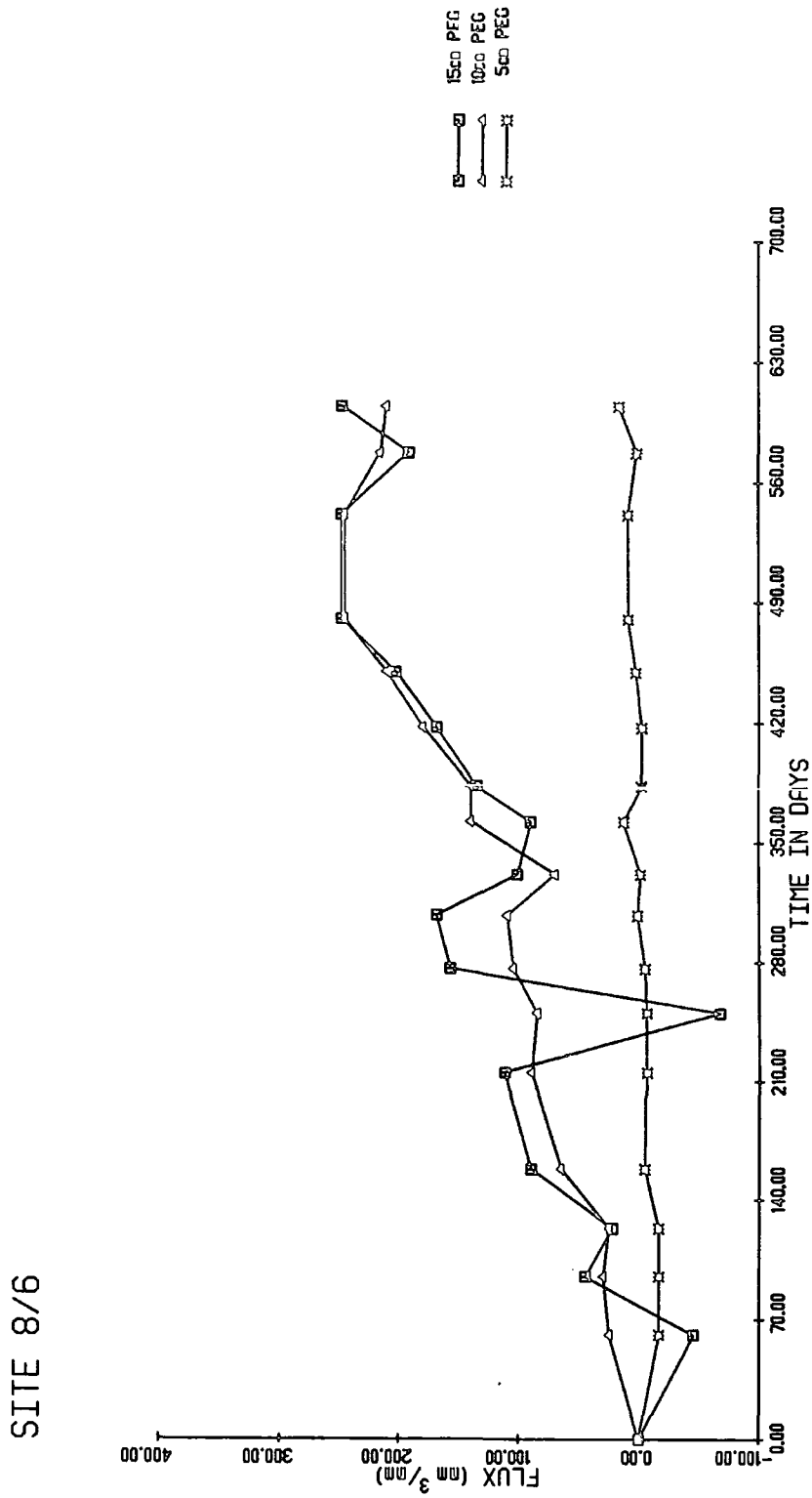
SITE 8/6
15cm PEG
10cm PEG
5cm PEG
FLUX (mm 3/mm)
400.00
300.00
200.00
100.00
0.00
-100.00
0.00
70.00
140.00
210.00
280.00
350.00
420.00
490.00
560.00
630.00
700.00
TIME IN DAYS

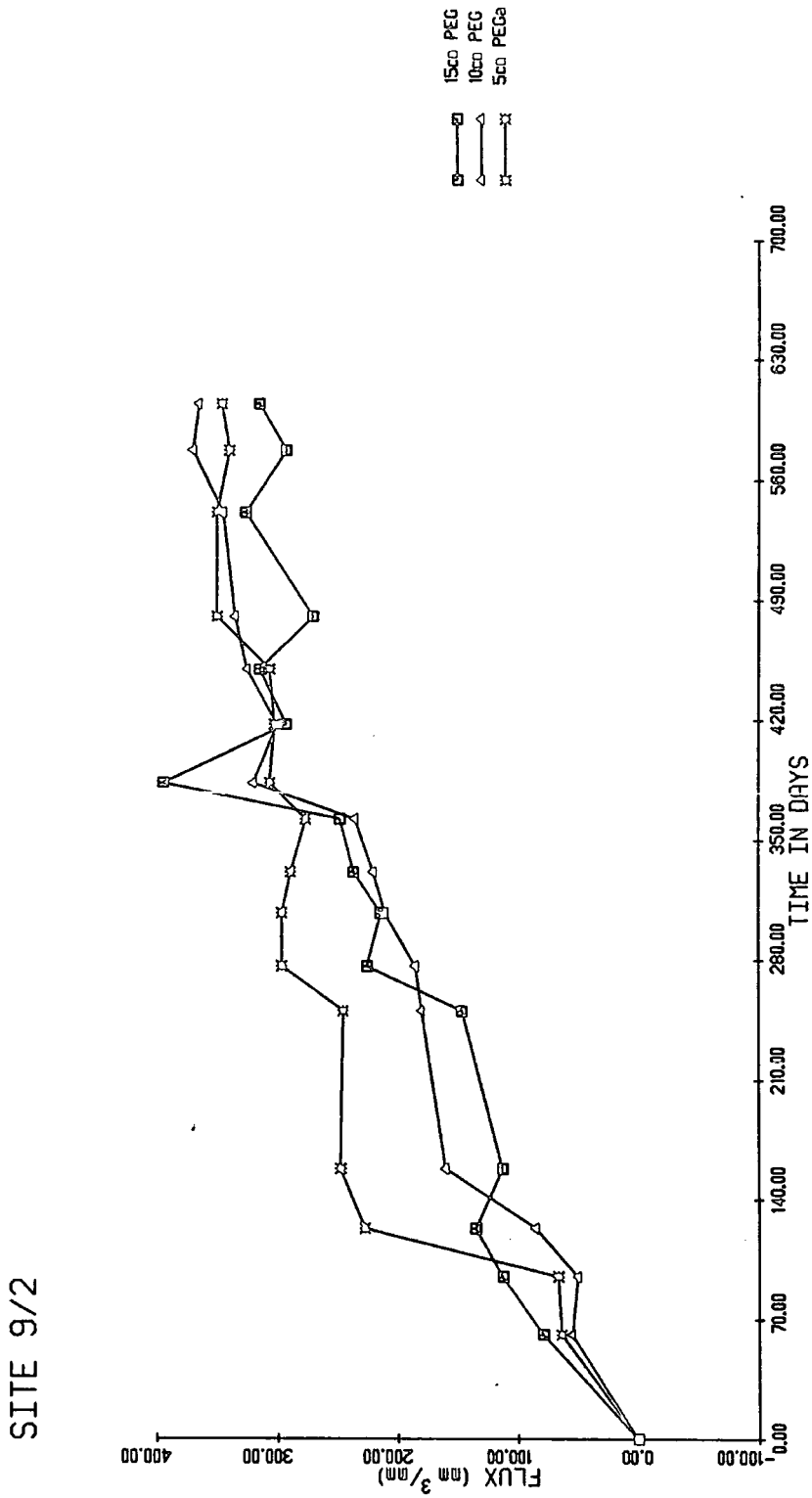
SITE 9/2
15cm PEG
10cm PEG
5cm PEGa
FLUX (mm 3/mm)
-100.00
0.00
100.00
200.00
300.00
400.00
TIME IN DAYS
0.00
70.00
140.00
210.00
280.00
350.00
420.00
490.00
560.00
630.00
700.00

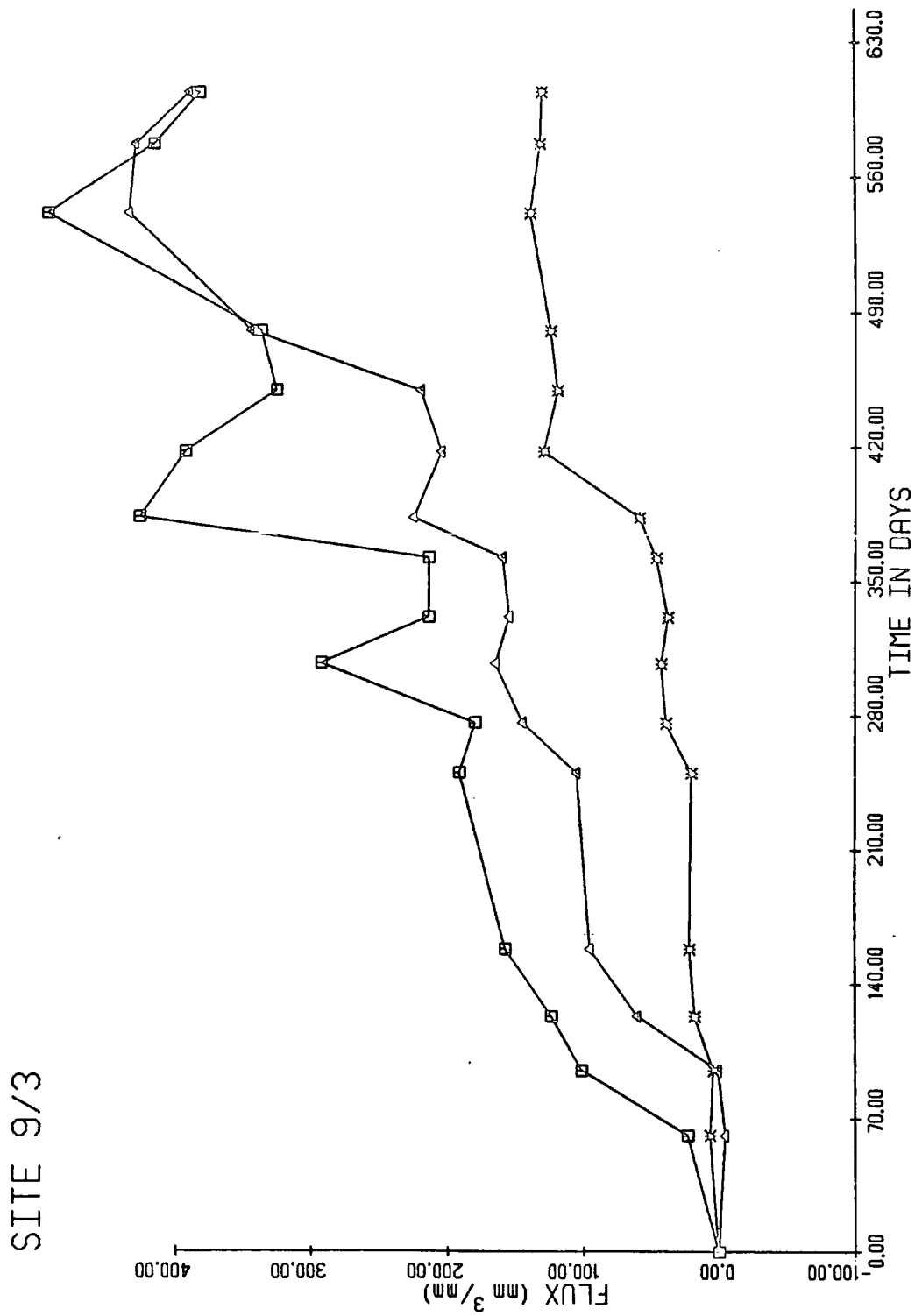
SITE 9/3
FLUX (mm 3/mm)
400.00
300.00
200.00
100.00
0.00
-100.00
0.00
70.00
140.00
210.00
280.00
350.00
420.00
490.00
560.00
630.0
TIME IN DAYS

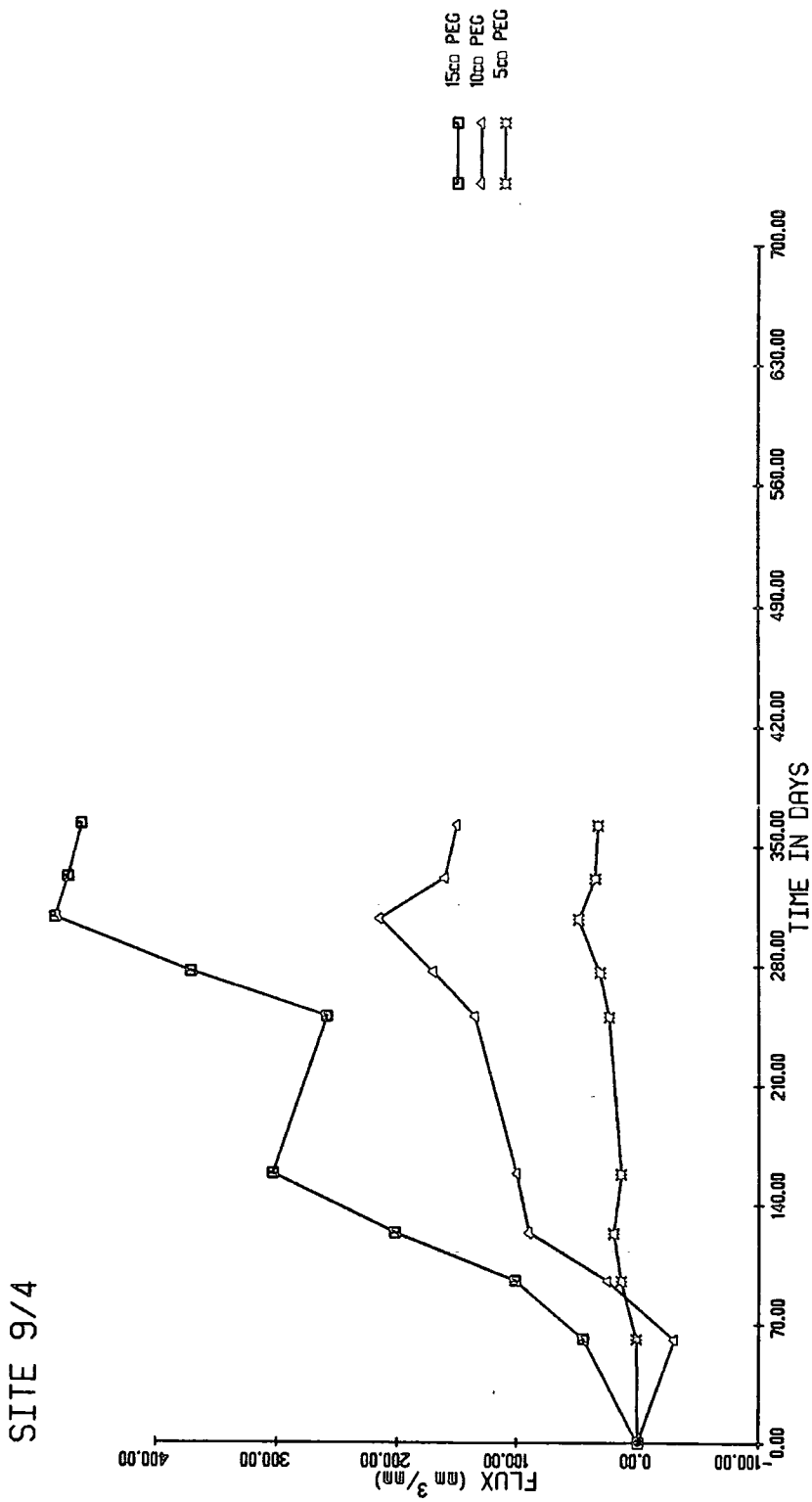
SITE 9/4
15cm PEG
10cm PEG
5cm PEG
FLUX (mm 3/mm)
-100.00
0.00
100.00
200.00
300.00
400.00
0.00
70.00
140.00
210.00
280.00
350.00
420.00
490.00
560.00
630.00
700.00
TIME IN DAYS

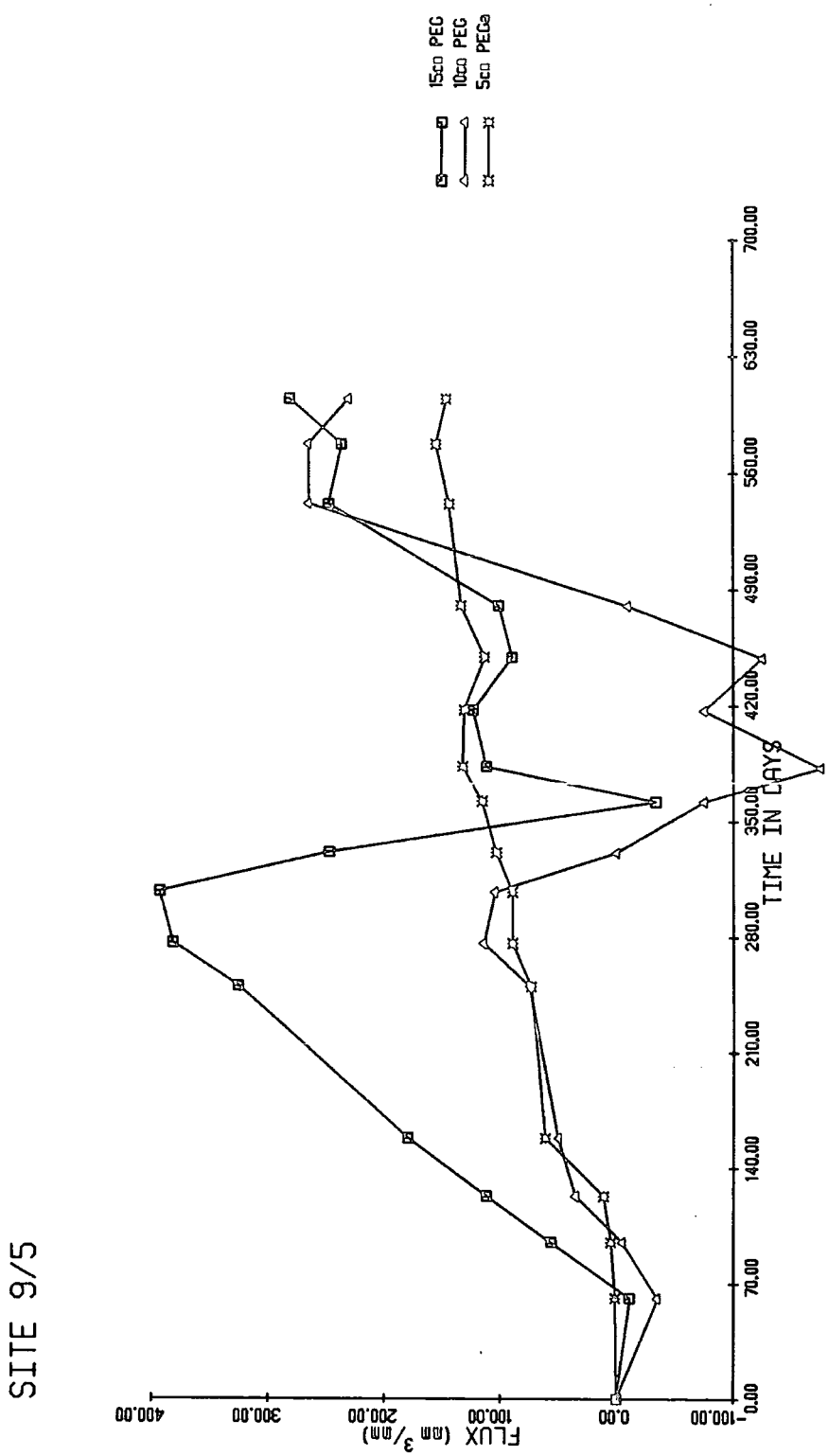
SITE 9/5
15cm PEG
10cm PEG
5cm PEGa
FLUX (mm 3/mm)
400.00
300.00
200.00
100.00
0.00
-100.00
0.00
70.00
140.00
210.00
280.00
350.00
420.00
490.00
560.00
630.00
700.00
TIME IN DAYS

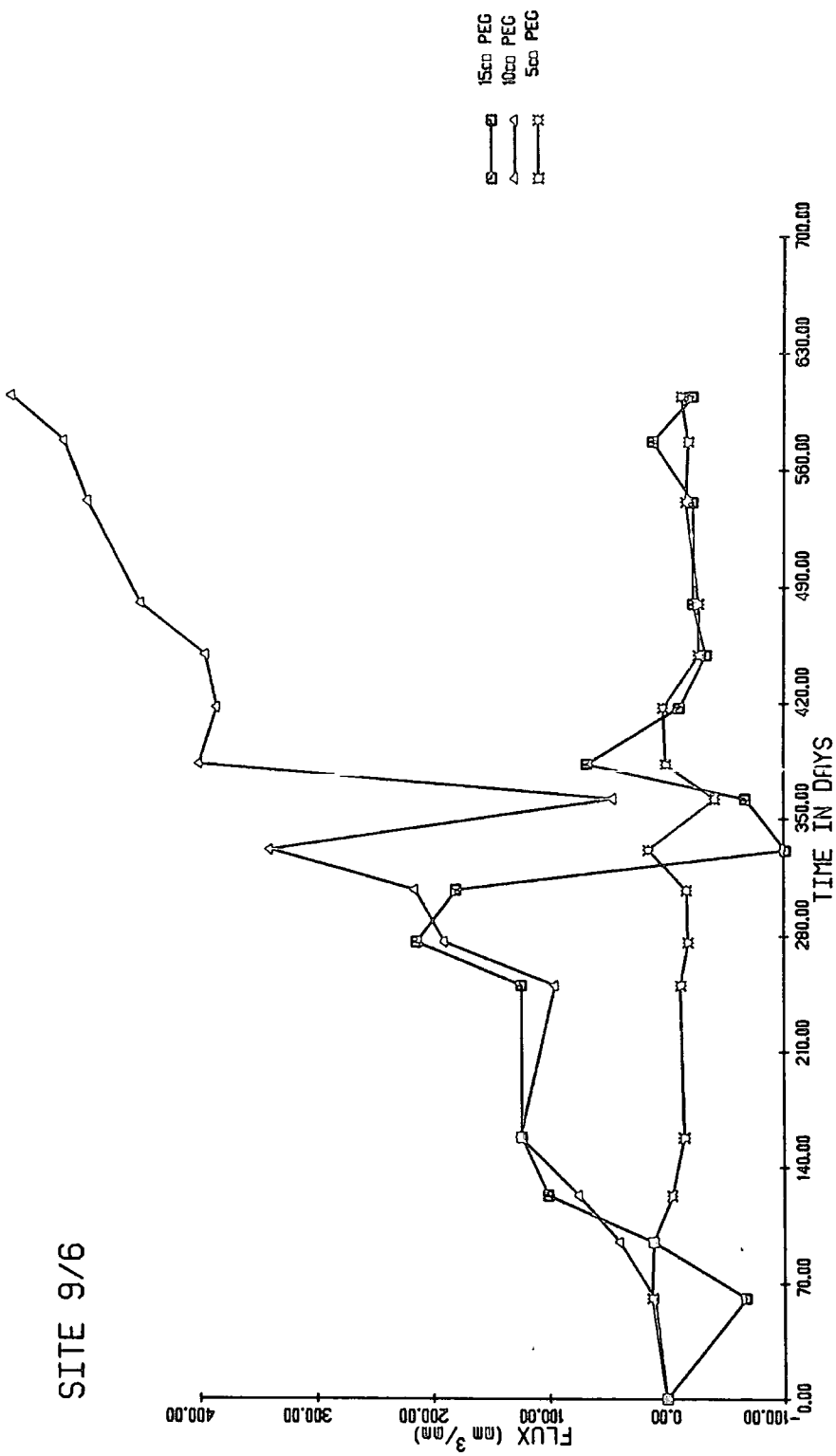
SITE 9/6
15cm PEG
10cm PEG
5cm PEG
FLUX (mm 3/mm)
-100.00
0.00
100.00
200.00
300.00
400.00
0.00
70.00
140.00
210.00
280.00
350.00
420.00
490.00
560.00
630.00
700.00
TIME IN DAYS

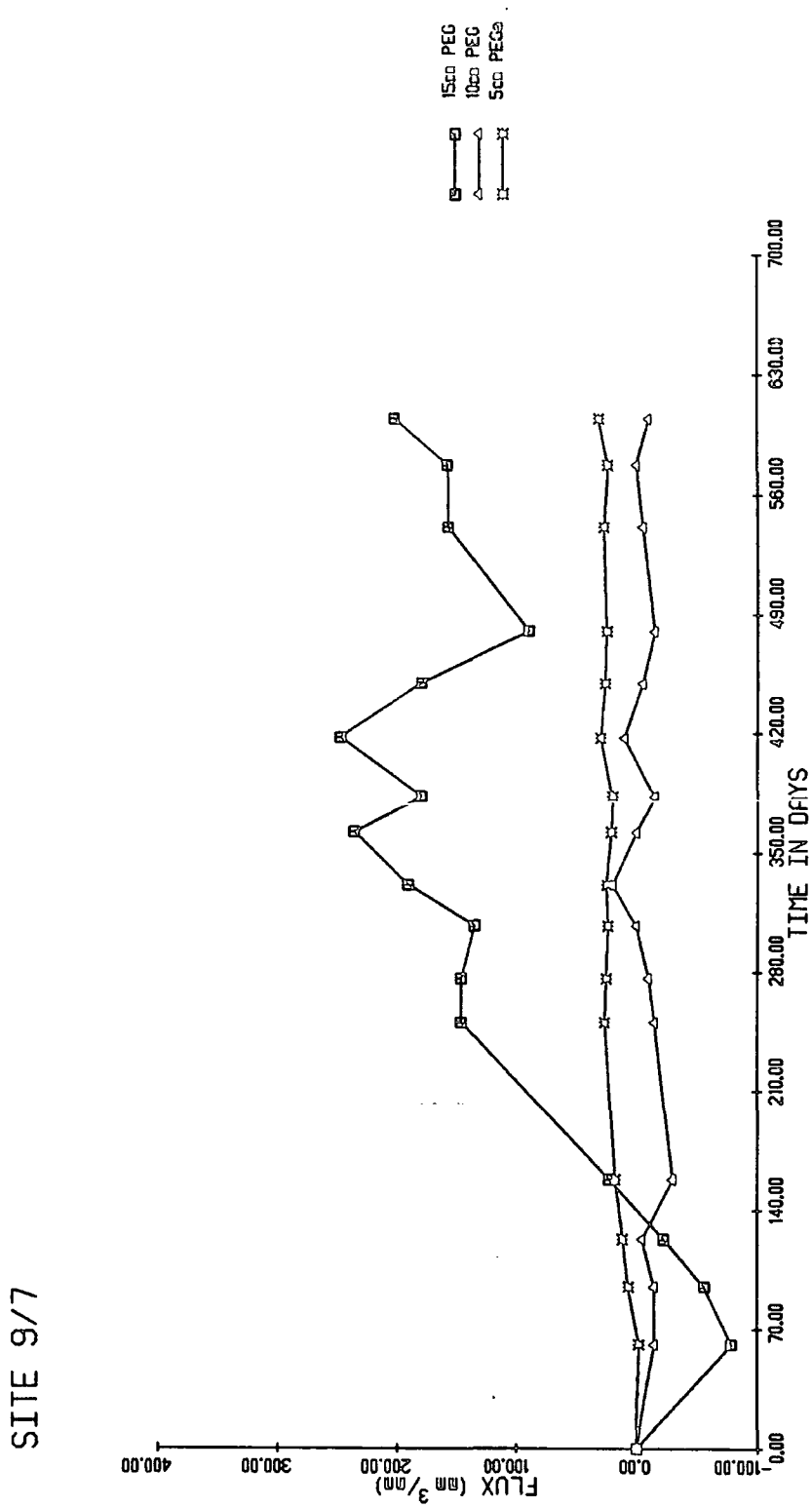
SITE 9/7
15cm PEG
10cm PEG
5cm PEG
FLUX (m 3/m)
400.00
300.00
200.00
100.00
0.00
-100.00
0.00
70.00
140.00
210.00
280.00
350.00
420.00
490.00
560.00
630.00
700.00
TIME IN DAYS

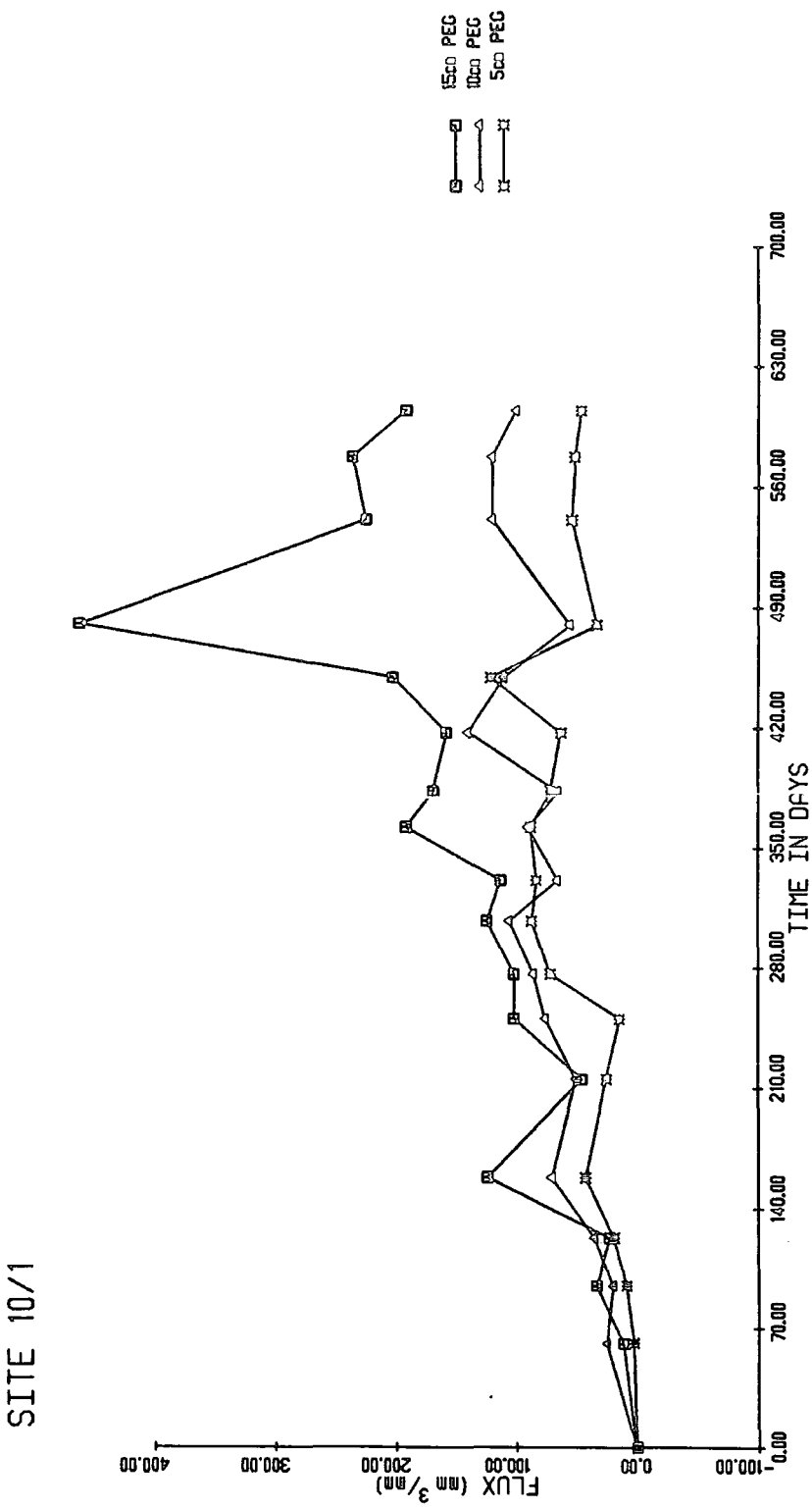
SITE 10/1
15cm PEG
10cm PEG
5cm PEG
FLUX (mm 3/mm)
400.00
300.00
200.00
100.00
0.00
-100.00
0.00
70.00
140.00
210.00
280.00
350.00
420.00
490.00
560.00
630.00
700.00
TIME IN DAYS

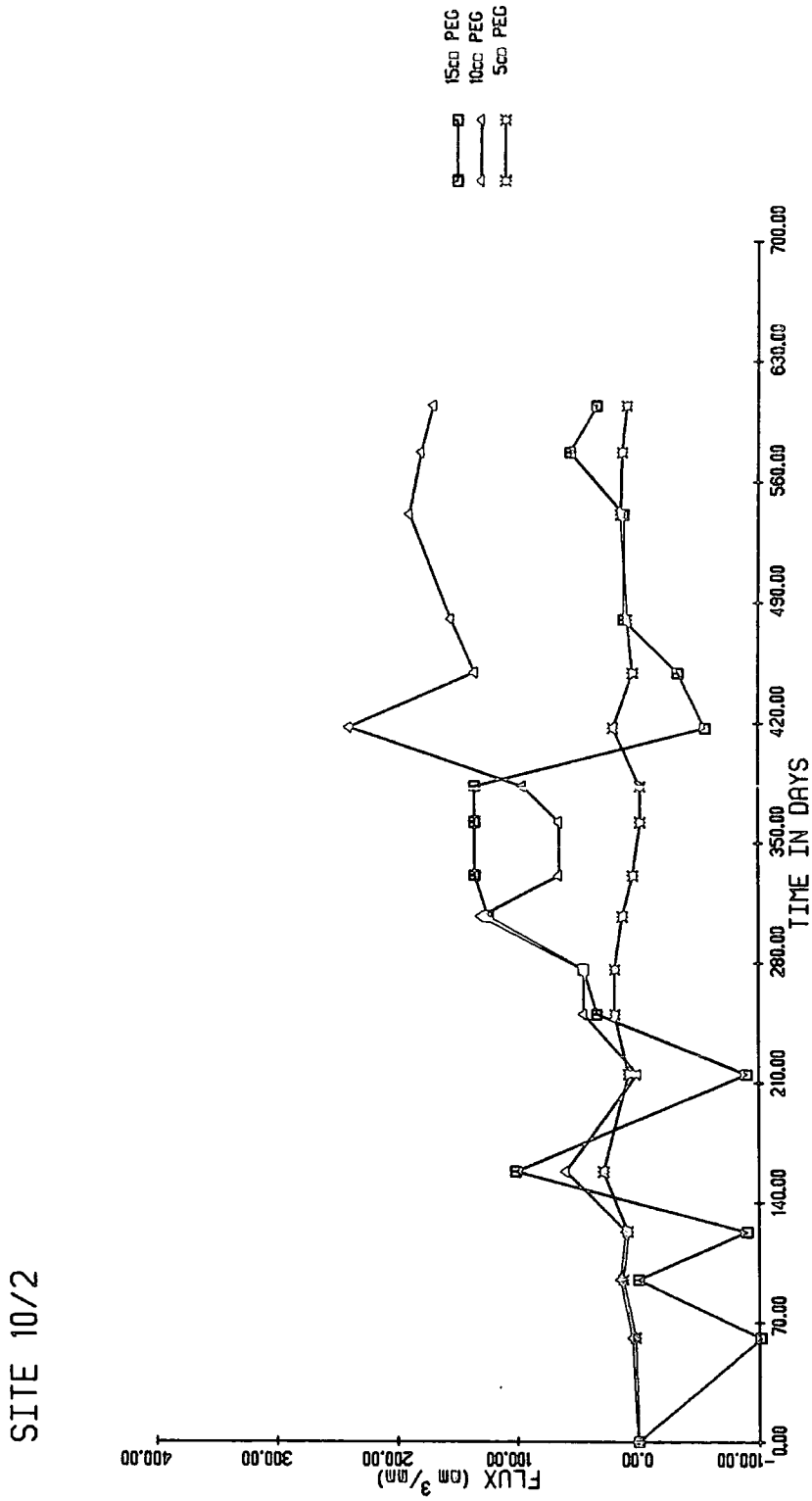
SITE 10/2
15cm PEG
10cm PEG
5cm PEG
FLUX (cm 3/cm)
400.00
300.00
200.00
100.00
0.00
-100.00
0.00
70.00
140.00
210.00
280.00
350.00
420.00
490.00
560.00
630.00
700.00
TIME IN DAYS

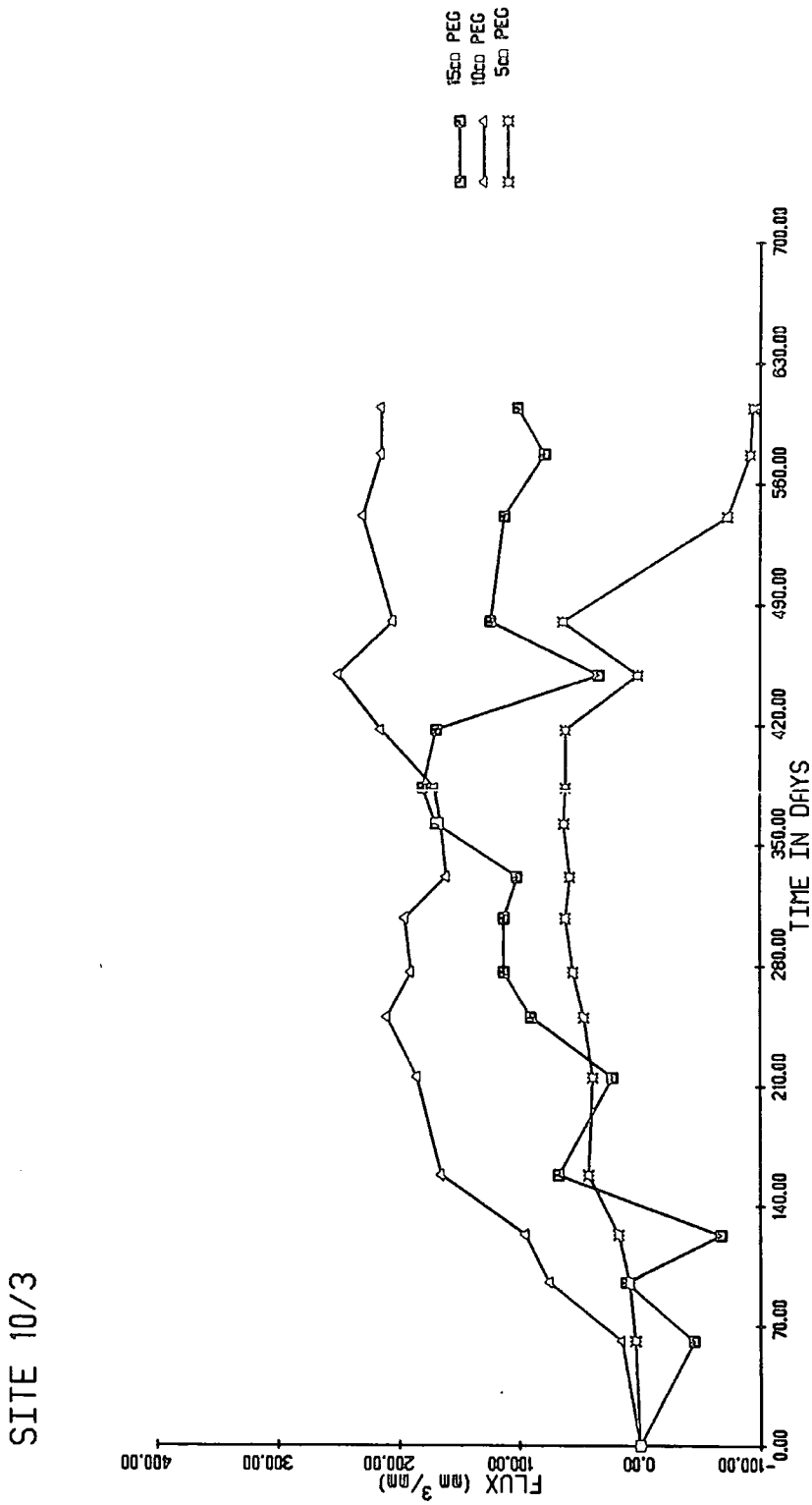
SITE 10/3
15□□ PEG
10□□ PEG
5□□ PEG
FLUX (mm 3/mm)
400.00
300.00
200.00
100.00
0.00
-100.00
0.00
70.00
140.00
210.00
280.00
350.00
420.00
490.00
560.00
630.00
700.00
TIME IN DAYS

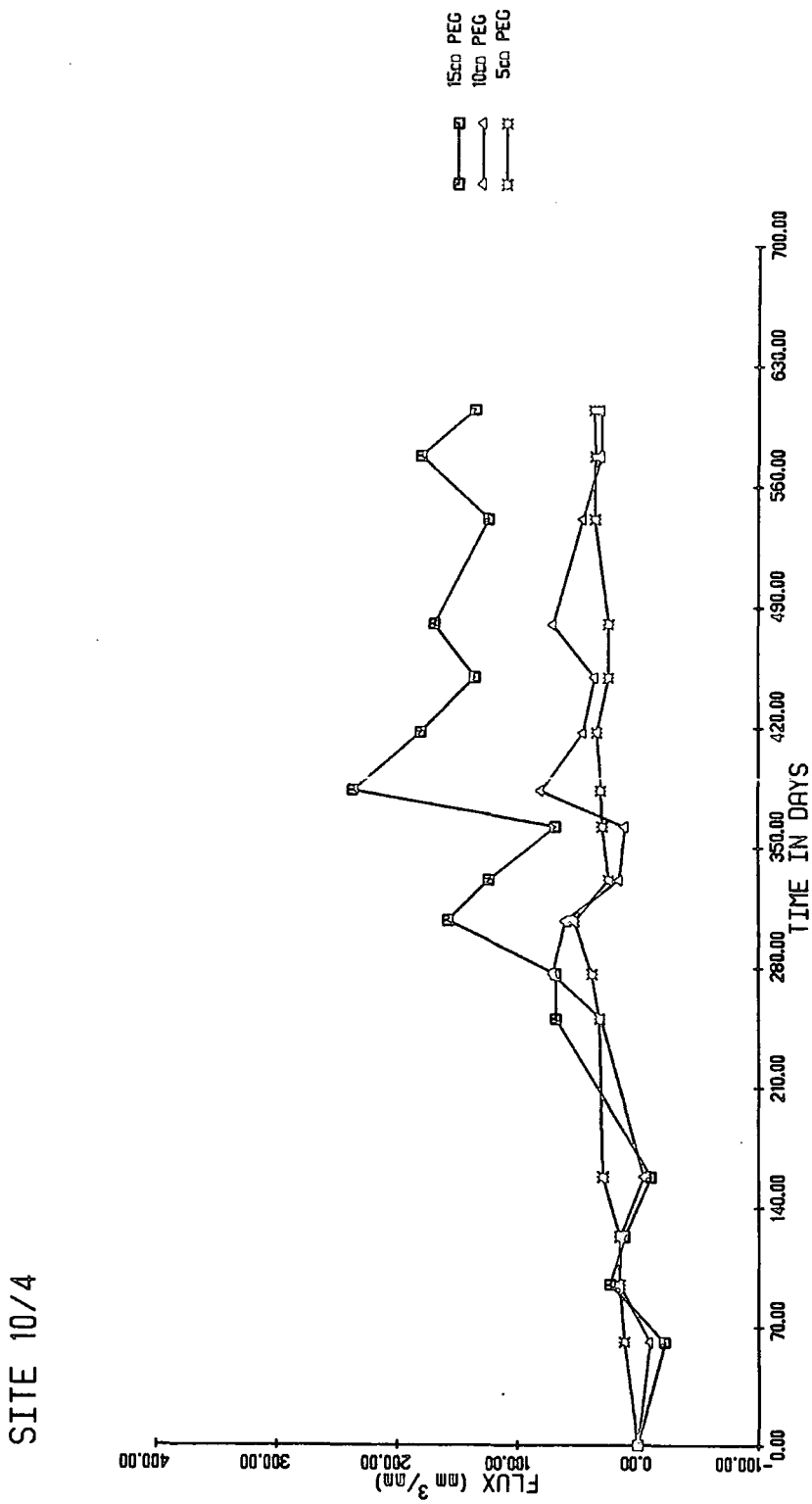
SITE 10/4
15cm PEG
10cm PEG
5cm PEG
FLUX (mm 3/mm)
-100.00
0.00
100.00
200.00
300.00
400.00
0.00
70.00
140.00
210.00
280.00
350.00
420.00
490.00
560.00
630.00
700.00
TIME IN DAYS

SITE 10/5

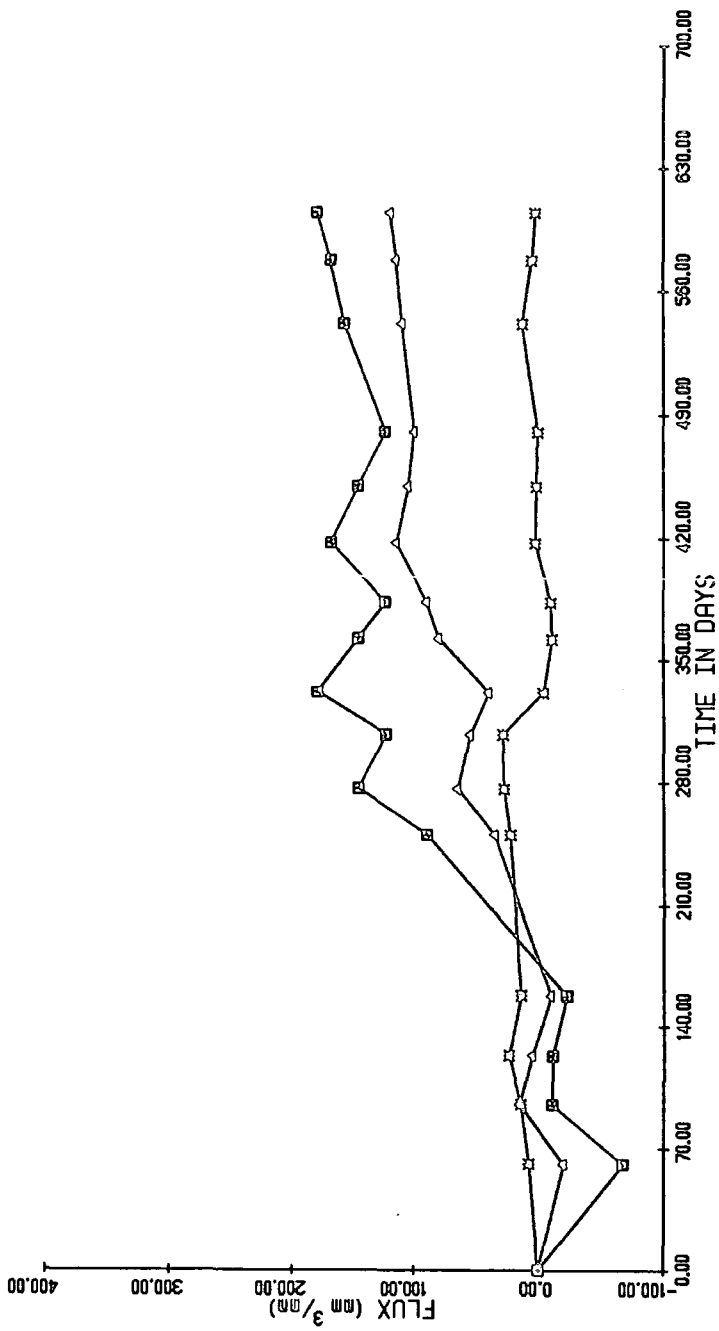
15cm PEG
10cm PEG
5cm PEG
FLUX (mm 3/mm)
400.00
300.00
200.00
100.00
0.00
-100.00
0.00
70.00
140.00
210.00
280.00
350.00
420.00
490.00
560.00
630.00
700.00
TIME IN DAYS

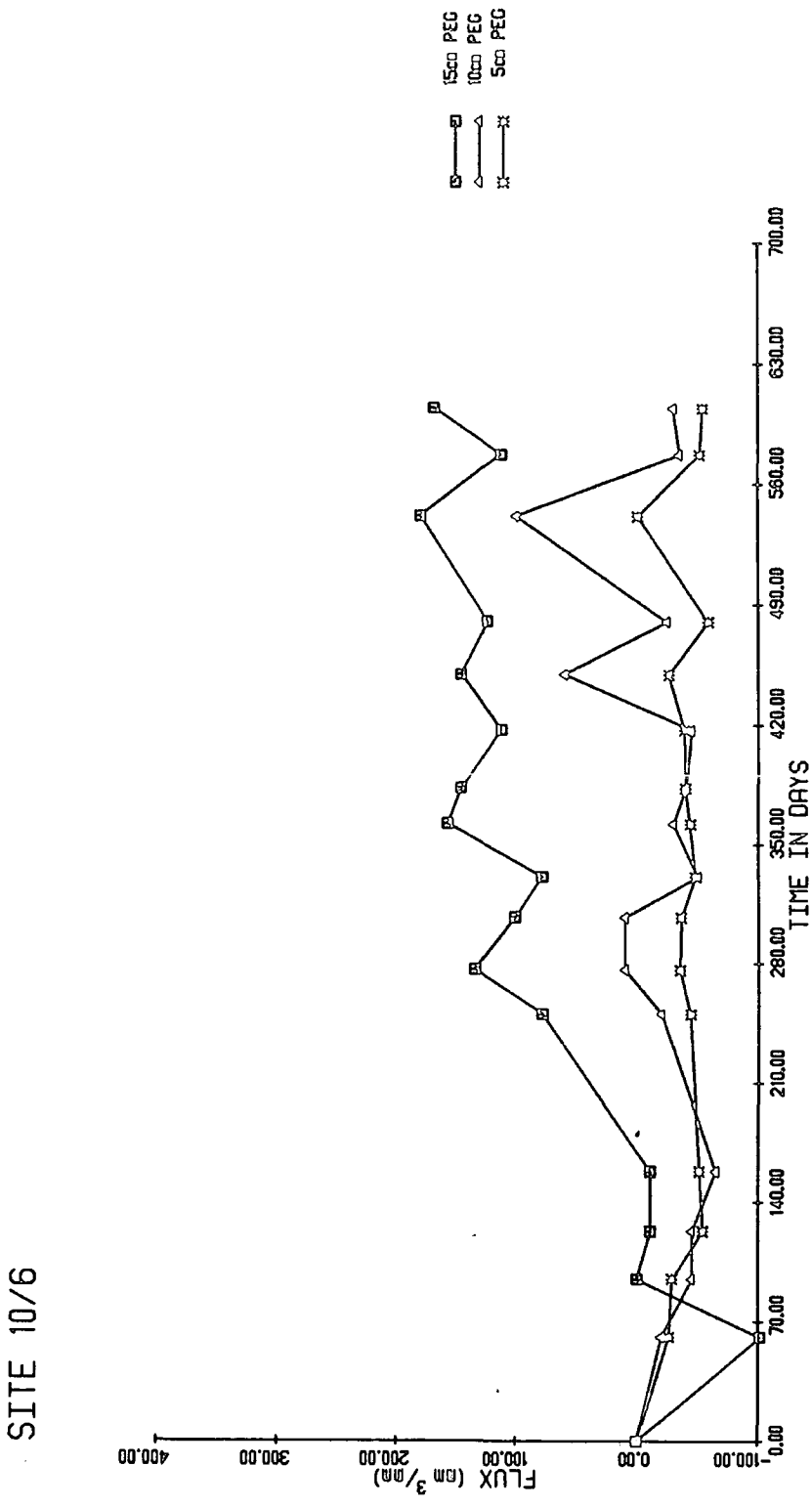
SITE 10/6
15cm PEG
10cm PEG
5cm PEG
FLUX (cm 3/mm)
400.00
300.00
200.00
100.00
0.00
-100.00
0.00
70.00
140.00
210.00
280.00
350.00
420.00
490.00
560.00
630.00
700.00
TIME IN DAYS

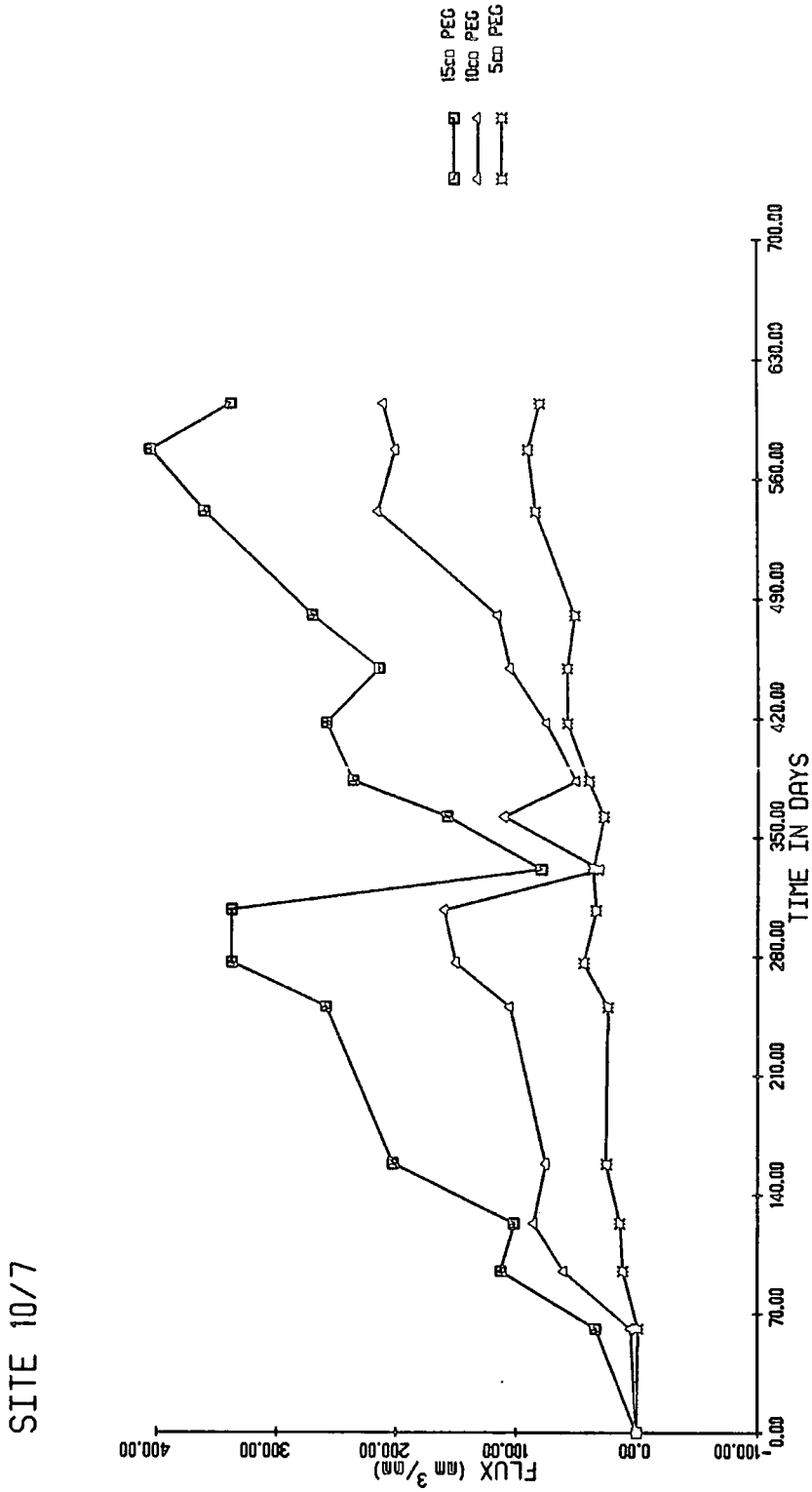
SITE 10/7
15cm PEG
10cm PEG
5cm PEG
FLUX (mm 3/mm)
400.00
300.00
200.00
100.00
0.00
-100.00
0.00
70.00
140.00
210.00
280.00
350.00
420.00
490.00
560.00
630.00
700.00
TIME IN DAYS

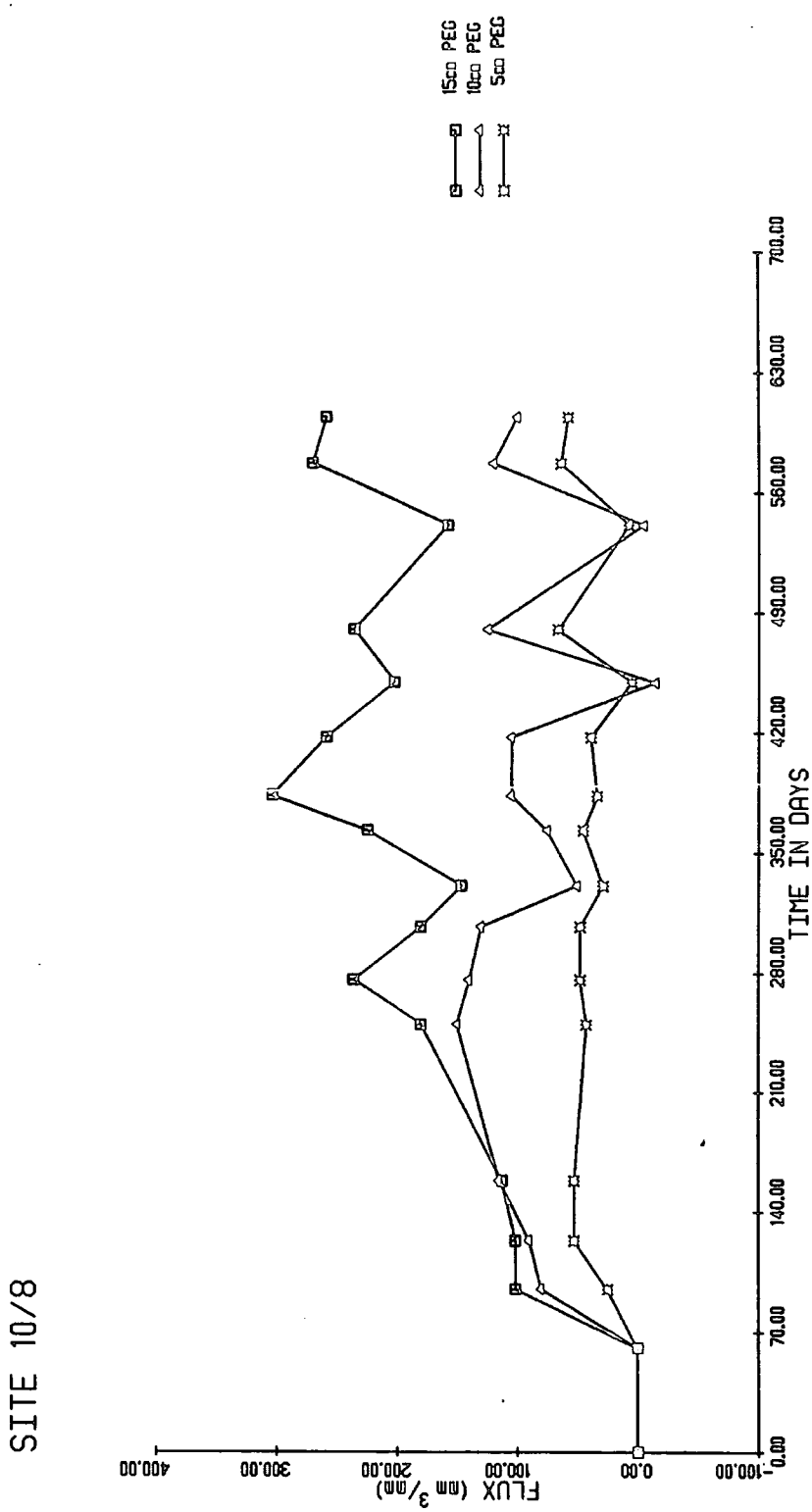
SITE 10/8
15cm PEG
10cm PEG
5cm PEG
FLUX (mm 3/mm)
400.00
300.00
200.00
100.00
0.00
-100.00
0.00
70.00
140.00
210.00
280.00
350.00
420.00
490.00
560.00
630.00
700.00
TIME IN DAYS